

AD-A089 303

FOREIGN TECHNOLOGY DIV WRIGHT-PATTERSON AFB OH F/G 20/7
TRANSACTIONS OF THE ALL-UNION CONFERENCE (2ND) ON CHARGED PARTI--ETC(U)
JUL 80 A L MINTS, A A KOMAR, A A VASIL'YEV
FTD-ID(RS)T-0692-80

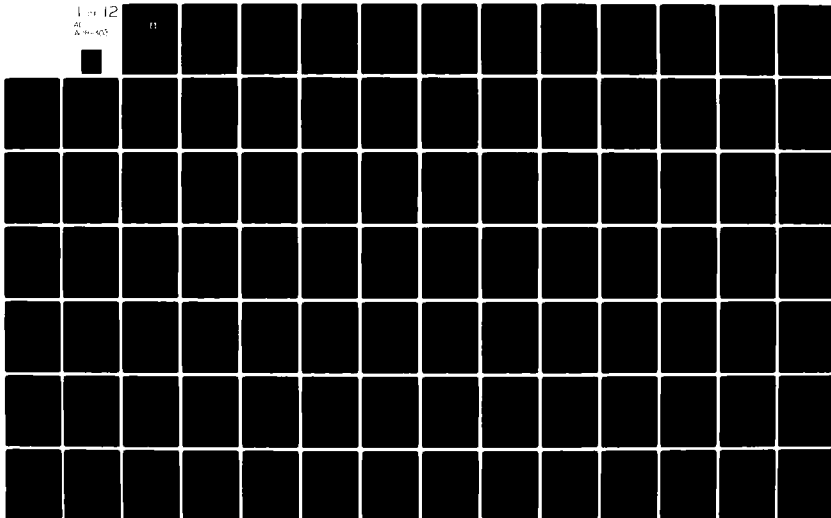
UNCLASSIFIED

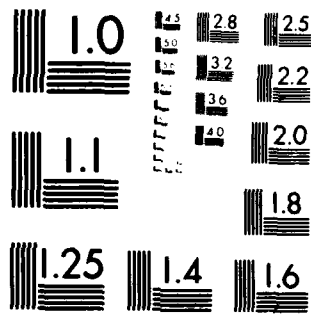
NL

1 of 12

AL
A-10-903

11





MICROCOPY RESOLUTION TEST CHART
NATIONAL BUREAU OF STANDARDS 1963-A

AD A089303

FOREIGN TECHNOLOGY DIVISION



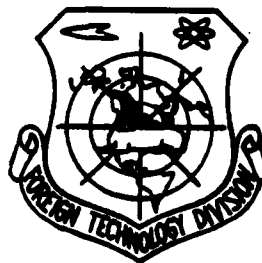
2

TRANSACTIONS OF THE SECOND ALL-UNION CONFERENCE
ON CHARGED PARTICLE ACCELERATORS

(Moscow, 11-18 November 1970)

Vol. I

DTIC
ELECTE
SEP 22 1980
S D E



DDC FILE COPY

Approved for public release;
distribution unlimited.

80 8 25 007

FTD- ID(RS)T-0692-80

UNEDITED MACHINE TRANSLATION

(17) FTD-ID(RS)T-0692-80

(11) 11 JUL 80
18 July 1980

MICROFICHE NR: FTD-80-C-000860

6 TRANSACTIONS OF THE ~~SECOND~~ ALL-UNION CONFERENCE
ON CHARGED PARTICLE ACCELERATORS
(Moscow, 11-18 November 1970), Vol. I, *Volume I*

English pages: 1135

(11) *united machine translation*
Source: Trudy Vtorogo Vsesoyuznogo Soveshchaniya
po Uskoritelyam Zaryazhennykh Chastits,
Vol. I, (11-18 November 1980), Publishing
House "Nauka", Moscow, 1972, pp. 1-273

Country of origin: (USSR) *✓* *PL-243 1742*

This document is a machine translation *N.A.*

Requester: FTD/TQTD

Approved for public release; distribution unlimited

on For

MA&I

cation

By

Distribution/

Availability Codes

Dist.

Avail and/or
special

A

THIS TRANSLATION IS A RENDITION OF THE ORIGINAL FOREIGN TEXT WITHOUT ANY ANALYTICAL OR EDITORIAL COMMENT. STATEMENTS OR THEORIES ADVOCATED OR IMPLIED ARE THOSE OF THE SOURCE AND DO NOT NECESSARILY REFLECT THE POSITION OR OPINION OF THE FOREIGN TECHNOLOGY DIVISION.

PREPARED BY:

TRANSLATION DIVISION
FOREIGN TECHNOLOGY DIVISION
WP-AFB, OHIO.

FTD- ID(RS)T-0692-80

Date 18 JULY 19 80

TABLE OF CONTENTS

U. S. Board on Geographic Names Transliteration System.....	1x
From the Editor.....	4
Introductory Comment of the Chairman of the Organization Committee of the Conference of Academician A. L. Mints.....	10
Salutatory Word of the Vice President of the Academy of Sciences of the USSR of Academician V. A. Kotel'nikov.....	14
Salutatory Word of the Deputy Chairman of State Committee on the Use of Atomic Energy of the USSR I. D. Morokhova.....	16
Session I. Comparative Characteristics of the Accelerators of Different Types From the Point of View of Physical Experiment.....	20
1. Possible Directions of Physical Investigations on the Accelerators of the Nearest Future, by A. A. Komar.....	20
2. Superconducting Cybernetic Proton Synchrotrons to the Energy Into Sotni and Thousands of GES, Which Use as the Injectors Accelerators with the Low Repetition Frequency, by A. L. Mints, A. A. Vasil'yev, E. L. Burstein, Ye. S. Mironov.....	41
3. Contemporary State and Prospects for Stanford Linear Accelerator, by R. B. Nil.....	54
4. Work of Proton Synchrotron to the Energy 70 GES, by Yu. M. Ado, A. A. Zhuravlev, V. I. Zaytsev, A. A. Kardash, K. P. Myznikov, E. A. Myae, A. A. Naumov, V. Ye. Pisarevskiy, O. N. Radin, V. G. Rogozinskiy, A. Ye. Kanimiryan, B. K. Shembel', K. A. Yakovlev.....	112
5. Electron Beam for Experiments in Electronic Cooling, by G. I. Budker, V. I. Kudelaynen, I. N. Meshkov, V. G. Ponomarenko, S. G. Popov, R. A. Salimov, A. N. Skrinskiy, B. M. Smirnov.....	126
6. Possibility of Accelerating the Protons by the Energy Higher Than Rest Energy in the Isochronal Cyclotron, by I. A. Sarkisyan.....	136

Session II. State of the Accelerators of Different Types. Designs of New ones and Reconstruction of the Acting Settings Up.....	144
7. Continuous Microtron FEI (Project), by S. P. Kapits, L. M. Zykin, A. I. Abramov, Yu. Ya. Stavisskiy, V. A. Slobodyanyuk, V. M. Kondratyev, V. P. Marin, A. M. Chernushenko.....	144
8. State of Matters and Prospect for the Development of Electronic Synchrotron DEZI on 7.5 GES, by G. Kumpfert...	155
9. Increase in the Intensity of Proton Synchrotron by the Energy 70 GES by Means of an Increase in the Energy of Injection, by Yu. M. Ado, V. I. Balbekov, A. A. Vasil'yev, F. A. Vodop'yanov, V. A. Glukhikh, A. A. Zhuravlev, V. B. Zalmanzon, Ye. G. Komar, A. A. Kuz'min, V. N. Lebedev, A. L. Mints, N. A. Monoszon, B. P. Murin, E. A. Myae, A. A. Naumov, V. Ye. Pisarevsky, A. V. Popkovich, A. M. Stolov, V. A. Titus, B. N. Shenbel', F. Z. Shiryaev, I. A. Shukevlo.....	192
10. Last Improvements on the Linear Accelerator with the Large Operating Cycle V. Saclay, by F. Netter.....	207
11. Some Questions, Connected with the Acceleration of Deuterons on the Synchrophasotron LVB the J.I.N.R., by G. S. Kazanskiy, A. I. Mikhaylov, G. P. Puchkov.....	221
12. Project of the Circular Synchrotron of the Swiss Institut of Nuclear Research, by D. P. Blazer, G. D. Berber, G. A. Vokkaks.....	230
13. Linear Accelerator of Protons to the Energy 10 MeV in the Collation, by Ye. Dzyur, Ye. Dzyur, V. Grabovski, Yu. Yanushevski, Z. Kozlovski, A. Kukharchik, S. Kulinski, B. Lyudkevich, Z. Mazur, A. Makler, S. Myslinski, T. Nevodnichanski, M. Pakhan, L. Savlevich, Yu. Sur, Ch. Veykhert.....	254
14. New Developments and Improvements of the Technological Systems of Linear Accelerator I-2, by V. A. Batalin, V. I. Bobylev, Ye. N. Danil'tsev, I. M. Kapchinskiy, L. V. Kartsev, A. M. Kozodayev, V. V. Koloskov, R. P. Kuybid, N. V. Lazarev, V. I. Edenskiy.....	265
15. Linear Electron Accelerator to the Energy 2GeV of FTI of AS UkSSR, by V. A. Vishnyakov, I. A. Grishchayev, Yu. I. Dobrolyubov, V. M. Kobezskiy, V. V. Kondratenko, V. I. Myakot.....	273

16. Rapid Booster - Injector of Proton Synchrotron IFVE, by A. D. Artemov, V. I. Balbekov, V. P. Belov, A. A. Vasil'yev, F. A. Vodop'yanov, O. A. Gusev, A. M. Ivanov, Ye. G. Komar, A. A. Kuz'min, B. A. Larionov, I. F. Malyshev, N. A. Monoszon, E. A. Myae, L. L. Pal'mskiy, B. V. Rozhdestvenskiy, A. M. Stolov, Ye. F. Troyanov, V. A. Titus, G. M. Fedotov, P. A. Pefelov, I. A. Shukeylo.....	293
17. Project of the Reconstruction of Proton Synchrotron ITEF, by L. Z. Barabash, A. V. Barkhudyaryan, Yu. A. Bol'shakov, M. A. Veselov, L. L. Gol'din, V. P. Zavodov, P. R. Zenkevich, Yu. M. Zlatov, I. F. Kleopov, V. V. Konstantinov, D. G. Koshkarev, Yu. Ya. Lapitskiy, P. I. Lebedev, K. K. Onosovskiy, L. I. Sokolov, Ye. A. Sysoyev, M. V. Shchelkanov.....	310
18. The pulsed Operations of Microtron FEI, by Yu. Ya. Stavisskiy.....	323
Session III. Ionic and Electronic Sources Direct Voltage Accelerators.....	328
19. Effect of the Conditions of the Selection of Ions from the Source on the Distribution of Phase Density in the Intense Ion Beams, by M. A. Abroyan, V. S. Kuznetsov, N. P. Kuznegova, R. P. Fidel'skaya.....	328
20. Development of the Source of the Polarized Ions, by B. P. Ad'yasevich, V. L. Komarov, V. I. Marasev, V. M. Sokolniks, V. N. Fedorov, B. P. Yatsenko.....	340
21. The Stable Operations of the Work of the High-Voltage Accelerating Tube, by V. P. Yakushev, A. N. Serbinov.....	352
22. Ion Gun with the High Brightness of Base, by N. N. Kutorg, V. S. Sevost'yanova, V. A. Teplyakov.....	362
23. Electron Gun with the Cold-Emission Cathode, by G. G. O. Meskhya, V. N. Yablokov.....	369
24. Electron Gun for Obtaining the Intense Electron Beams, by V. M. Levin, V. V. Rumyantsev, K. P. Rybas, B. N. Telepaev.....	377
25. High-Current Electronic Pulse Direct Voltage Accelerator, by L. N. Kazanskiy, A. A. Kolomenskiy, G. O. Meskhya, B. N. Yablokov.....	390
26. Powerful Nanosecond Oscillator, by L. N. Kazanskiy, B. N. Yablokov.....	404

27. Investigation of Intense Electronic Ones on the Accelerator RIUS-5, by Ye. A. Abramyan, S. B. Wasserman, V. G. Votintsev, V. M. Dolgushin, A. N. Lukin, B. G. Shklyayev.....	416
28. Discharge Through High-Pressure Gase, Initiated by the Beam of Rapid Electrons, by B. M. Koval'chuk, V. V. Kremnev, G. A. Mesyats, Yu. F. Potalitsyn.....	431
29. Aberrations of Space Charge, by Zh. For.....	444
30. Intense Pulsed Operation of Direct Voltage Accelerator, by Yu. Ya. Stavisskiy.....	456
31. Stabilization of the Position of Beam After the Accelerating Tube with the Inclined Field, by A. N. Serbinov, V. P. Yakushev, V. I. Mukhametshin.....	461
32. Adjustment and Operation of the Electrostatic Accelerator EG-1 of FEI in the Pulsed Operation, by V. I. Volodin, A. I. Glotov, N. I. Dudkin, V. N. Kanaki, V. N. Cononov, A. A. Metlev, V. A. Romanov.....	470
33. Electronic Injector with the Circular Gun, by G. A. Babin, A. K. Dezhnev, V. S. Kuznetsov, K. P. Rybas, R. P. Fidel'skaya.....	480
34. Some Special Features of the Work of Cold Cathode with High Pressures of Residual Gas, by G. V. Dolbilov, V. P. Sarantsev, A. P. Sumbayev.....	493
35. Cathode-Ray Source of Polyvalent Ions, by V. A. Al'pert, Ye. D. Vorokbyeve, Ye. D. Donets, V. I. Ilyushchenko.....	502
36. Sources of Polyvalent Ions with the Cathode Sputtering of Work Substance, by Yu. P. Tret'yakov, A. S. Pasyuk, L. P. Kul'kina, V. I. Kuznetsov.....	513
37. Experimental Study of the Parameters of Autoelectronic Gun, by R. M. Voronkov, V. A. Danilichev, B. Yu. Bogdanovich, V. F. Gass.....	530
38. Formation of Powerful Ion Beams by Brush-Type Electrodes, by O. Ya. Savenko.....	538
39. Study of the Work of Plasma Cathodes in the Mode of the Selection of Large Electronic Currents, by G. P. Bazhen, S. P. Bugayev, F. Ya. Zagulov, G. A. Mesyats, D. I. Proskurovskiy, V. G. Shpak.....	546
Session IV. Electromagnets of Accelerators and Their Power Supply Systems. Magnetic Measurements.....	559

40. Methods of Calculation of Magnets in Experiments in High-Energy Physics, by L. Rezegotti..... 559
41. Questions of the Mathematical Simulation of Three-Dimensional Magnetostatic Fields, by N. I. Doynikov, A. S. Simakov..... 599
42. Equipment for the Magnetic Measurements on the Synchrocyclotron of FTI of the AS USSR to the Energy of Protons 1 GeV, by V. A. Yeliseyev, G. A. Riabov, I. I. Tkach..... 612
43. Equipment for the Magnetic Measurements in the Electromagnet VAPP-4, by B. A. Baklatov, V. F. Veremeyenko, M. M. Karliner, E. A. Kuper, B. V. Levichev, A. D. Oreshkov, I. Ya. Protopopov..... 625
44. Formation of Rectangular Current Pulses in the Impact Magnet with the Complex Input Resistance During the Use of Artificial Line, by I. Yu. Beneskiriptov, S. M. Klishevskiy, B. A. Larionov..... 638
45. Magnetic Oscillator for the Formation of Powerful Rectangular Current Pulses in the Inductance, by N. A. Monoszon, B. K. Ratnikov, A. M. Stolov..... 647
46. Special Features of the Construction of the Power-Supply System of the Electromagnet of the Rapid Booster of Proton Synchrotron, by O. A. Gusev, A. I. Konstantinov, A. G. Roshal', F. M. Spevakov, A. M. Stolov, A. A. Tunkin..... 656
47. System of Forming of the Flat Part of the Pulse of the Magnetic Field of Proton Synchrotron IFVE, by Ya. V. Kornakov, V. M. Kofman, G. S. Lyapichev, N. S. Rezchikova, A. G. Roshal', F. M. Spevakova, A. M. Stolov.. 667
48. On the Possibility of Using the Principle of Self-Balanced Field in the Proton Synchrotrons, by I. P. Karabakov, M. A. Martirosyan, Yu. R. Nazaryan..... 681
49. The Magnetic System of F-M Cyclotron with a Three-Dimensional Variation in the Field, by Yu. G. Alenetskiy, S. B. Vorozhtsov, N. L. Zaplatin, L. K. Lytkin..... 693
50. Pulse Generator in Power 1.5-2 GVT on the Magneto Controlled Valves, by L. L. Danilov, V. N. Pankin, G. I. Silvestrov..... 701
51. Electron Analogue of Cyclic Accelerator with the Ultrapowerful Leading Magnetic Field, by A. V. Gryzlov, V. S. Panasyuk, V. M. Ryzhkov, A. A. Sokolov, Ya. M. Spektor, V. M. Stepanov..... 714

52. Use of the Kickers with the Fields 120 kOe in the Unit of the Conversion of Accululator VEPP-3, by T. A. Vsevolozhskaya, T. E. Vecheslavova, L. L. Danilov, V. N. Karasyuk, G. I. Silvestrov, E. M. Trachtenberg.....	726
53. Hydraulic Systems with Electronic Control for Magnets of Beam Output, by V. Kolk.....	740
54. Formation of the Magnetic Cycles of Intricate Shape in the Proton Synchrotron ITEF, by I. F. Kleopov, G. I. Kugushev.....	763
55. Measurement of the Static and Dynamic Parameters of Materials with the Nonrectangular Loop of Hysteresis, by L. Z. Barabash, P. I. Lebedev, L. N. Plyashkevich.....	775
56. To Shaping of Field in the Electromagnets of the Type of "Window Frame", by V. D. Borisov, L. N. Vaulin, N. I. Doynikov, A. S. Simakov, A. S. Sudarushkin.....	779
57. Nuclear Stabilizer of Magnetic Field with the Discrete Stabilization System and Control of Frequency of Autodyne Detector NMR, by Yu. N. Denisov, P. T. Shishlyannikov.....	791
58. Semiconductor Circuit of Control of the Valve Converter of Dubna Proton Synchrotron, by L. N. Belyayev, A. Z. Doroshenko, D. P. Kalmykov, A. A. Smirnov.....	801
59. Calculation of the Three-Dimensional Fields of Iron Free Magnets, by L. R. Zakharov, R. A. Meshcherov, Ye. S. Mironov.....	812
60. Calculations of Iron Free Magnets with "Trick" Windings for Acceleration Technology, by V. G. Davidovskiy.....	819
61. Calculation of Magnetic Field in the Magnets with the Sections, by V. P. Papadichev.....	831
Session V. Collective Methods of Acceleration.....	844
62. Collective Ion Accelerator - New Instrument in Physics of Elementary Particles, by V. P. Sarantsev.....	844
63. Some Questions of the Theory of the Acceleration of Ions by the Scanning of Electron Beam, by A. A. Kolomenskiy, I. N. Logachev.....	860
64. Study Program, Connected with the Development of the Accelerator of Electron Rings in Berkeley, by J. M. Peterson, V. V. Chash, A. A. Garren, D. Keef, G. R. Lambergson, L. J. Laslett, V. A. Perkins, A. M. Sessler....	870

65. Synchronous Emission and Formation of Rings in the Accelerators with Electronic Rings, by K. Pellegrini.....	898
66. State of Works on the Project of the Accelerator of Electron Rings Karlsruhe, by G. Dustman, V. Khaynts, G. Germann, P. Kapp, G. Kraut, L. Shteynbok, L. Tsernial'.....	904
67. Resonances of Connection of Transverse Vibrations of Two Circular Beams, by P. R. Zenkevich, D. G. Koshkarev..	924
68. Progress in the Creation of the Accelerative Section of Ring Accelerator, by N. G. Anishchenko, N. I. Balalykin, V. A. Vasil'yev, Yu. S. Derendyaev, A. G. Zeldovich, N. K. Zeldovich, Yu. V. Muratov, N. B. Rubin, A. A. Sabayev, V. P. Saraitsev, Yu. I. Smirnov, V. G. Shabratov, Yu. A. Shishov.....	933
69. Theoretical and Experimental Studies on the Creation of Intense Waves in the Electron Beams, by G. G. Aseyev, A. P. Klyucharev, G. G. Kuznetsov, N. S. Repalov, B. G. Safronov, N. A. Khizhnyak.....	945
70. To a question about the Acceleration of Ions by Electron Ring in the Decaying Magnetic Field, by I. N. Ivanov, E. A. Perel'shteyn, V. P. Sarantsev.....	957
71. Numerical Investigation of the Radiation Instability of the Charged Relativistic Rings in the Nonlinear Mode, by A. G. Bonch-Osmolovskiy, Ya. P. Zhidkov, V. G. Makhon'kov, V. N. Tsytovich, V. G. Shchinov.....	966
72. Some Questions of the Design of Linear Coherent Heavy-Particle Accelerator to Low Energies, by O. A. Bal'dner, V. A. Vorontsov, S. A. Pukshin, O. N. Popov.....	978
73. Motion of the Charged Relativistic Ring in the Corrugated Magnetic Field, by K. A. Reshetnikova.....	987
74. Calculation of the Phase Volumes of the Electric Ion Clusters and Beams in the Collective Accelerator and Questions of Separation, by M. L. Iovnovich, N. B. Rubin, V. P. Sarantsev.....	993
75. Steady State of Electron Ring in the External Magnetic Field, by S. Budnyan, Ye. Zhidkov, I. N. Ivanov, E. A. Perel'shteyn.....	999
Session VI. Superconducting Elements of Accelerator.....	1007

76. Study Program of Rutherford Laboratory for Superconducting Proton Synchrotron, by N. D. Vest..... 1007
77. The Superconducting Coil Electromagnets with the Iron Screens, by Yu. P. Batakov, N. I. Doynikov, A. G. Zhikhareva, N. A. Monoszon, G. V. Trokhachev, G. F. Churakov..... 1016
78. Some Calculated and Experimental Data on the Development of Synchrotrons with Stationary Field on the Energy 35-350 GES, by N. I. Doynikov, N. A. Monoszon, B. V. Rozhdestvenskiy, Yu. P. Sivkov, A. M. Stolov, G. V. Trokhachev..... 1026
79. Developments for the Cryogenics and the Superconducting Coil Electromagnets, by F. Arendt, Kh. Brekhni, I. Yerb, N. Fessler, G. Khartvig, V. Khaynts, K. P. Yungst, V. Maurer, G. Merle, G. Ris, V. Shauyer, I. Von. Schaewin, P. Tichovski, A. Ulbricht..... 1042
80. Program of Works on the Creation of the Superconducting Coil Electromagnets in Saclay, by G. Bronk..... 1082
81. Development and Investigation of the Combined Conductors with the Thin Superconducting Strands, by A. I. Kostenko, N. A. Monoszon, G. V. Trokhachev..... 1108
82. Calculation of the Losses in the Superconductors and the Kind in the Pulse Magnetic Field, by L. I. Greben', Ye. S. Mironov..... 1119
83. On the Development of Accelerators to the Superhigh Energies with the Superconducting Coil Electromagnets, by R. L. Martin..... 1129

U. S. BOARD ON GEOGRAPHIC NAMES TRANSLITERATION SYSTEM

Block	Italic	Transliteration	Block	Italic	Transliteration
А а	<i>А а</i>	A, a	Р р	<i>Р р</i>	R, r
Б б	<i>Б б</i>	B, b	С с	<i>С с</i>	S, s
В в	<i>В в</i>	V, v	Т т	<i>Т т</i>	T, t
Г г	<i>Г г</i>	G, g	У у	<i>У у</i>	U, u
Д д	<i>Д д</i>	D, d	Ф ф	<i>Ф ф</i>	F, f
Е е	<i>Е е</i>	Ye, ye; E, e*	Х х	<i>Х х</i>	Kh, kh
Ж ж	<i>Ж ж</i>	Zh, zh	Ц ц	<i>Ц ц</i>	Ts, ts
З з	<i>З з</i>	Z, z	Ч ч	<i>Ч ч</i>	Ch, ch
И и	<i>И и</i>	I, i	Ш ш	<i>Ш ш</i>	Sh, sh
Я я	<i>Я я</i>	Y, y	Щ щ	<i>Щ щ</i>	Shch, shch
К к	<i>К к</i>	K, k	Ъ ъ	<i>Ъ ъ</i>	"
Л л	<i>Л л</i>	L, l	Ы ы	<i>Ы ы</i>	Y, y
М м	<i>М м</i>	M, m	Ь ь	<i>Ь ь</i>	'
Н н	<i>Н н</i>	N, n	Э э	<i>Э э</i>	E, e
О о	<i>О о</i>	O, o	Ю ю	<i>Ю ю</i>	Yu, yu
П п	<i>П п</i>	P, p	Я я	<i>Я я</i>	Ya, ya

*ye initially, after vowels, and after ъ, ь, е elsewhere.
When written as ё in Russian, transliterate as yë or ë.

RUSSIAN AND ENGLISH TRIGONOMETRIC FUNCTIONS

Russian	English	Russian	English	Russian	English
sin	sin	sh	sinh	arc sh	sin ⁻¹
cos	cos	ch	cosh	arc ch	cos ⁻¹
tg	tan	th	tanh	arc th	tan ⁻¹
ctg	cot	cth	coth	arc cth	cot ⁻¹
sec	sec	sch	sech	arc sch	sec ⁻¹
cosec	csc	csch	csch	arc csch	csc ⁻¹

Russian English

rot curl
lg log

Page 1.

TRANSACTIONS OF THE SECOND ALL-UNION CONFERENCE ON CHARGED PARTICLE
ACCELERATORS.

(Moscow, 11-18 November of 1970).

Vol. I.

Page 2.

Transactions of the second All-Union conference on charged particle accelerators T. 1 publishing house "Science". 1972.

In the works of the second All-Union conference on charged particle accelerators are placed the materials, which reflect the contemporary state of theory and of accelerators technique. In Soviet and foreign specialists' reports they are described newest accelerators of different types as well as most important systems and elements/cells of accelerators. The transactions of conference are published in two volumes. The first contained reports about the new methods of acceleration, about the use/application of superconducting elements in the accelerators, the survey/coverage of the state of the accelerators of different types and new projects and others.

The materials of conference will be useful for specialists, connected with development and operation of charged particle accelerators.

Organizers of the conference:

Academy of Sciences of the USSR

DOC = 80069201

PAGE 3

State committee on the use of atomic energy of the USSR.

Responsible editor A. A. Vasil'yev.

Page 3.

FROM THE EDITOR.

To the second All-Union conference on charged particle accelerators were represented 175 reports 110 of which were reported on twenty the sessions of conference and special seminars.

In the works are published, with some small exceptions, all represented at the conference reports, and also materials of discussion. The transactions of conference are published in two volumes.

The first volume includes reports of the I-VI sessions of conference.

It is possible to hope that containing in the reports and the discussions useful information will be used by specialists in their daily activity.

A. A. Vasil'yev.

Page 4.

ORGANIZATIONAL COMMITTEE OF THE SECOND ALL-UNION CONFERENCE ON
CHARGED PARTICLE ACCELERATORS.

A. L. Mints (chairman) - the chairman of scientific council for the
problems of the acceleration of the charged/loaded particles OYaT of
the AS USSR.

A. A. Vasil'yev (vice chairman) - the radio engineering institute of
the AS USSR.

Yu. N. Antonov - radio engineering institute of the AS USSR.

V. A. Auslander - institute of the nuclear form of SO AN USSR [
- Siberian Department of the Academy of Sciences of the USSR].

O. A. Val'dner - Moscow physical engineering institute.

O. A. Voynalovich - state committee on the use of atomic energy of
the USSR.

V. A. Glukhikh - scientific research institute of the electrophysical

equipment in. D. V. Efremov.

L. L. Gol'din - institute of theoretical and experimental physics.

I. A. Grish^yev - physiotechaical institute of AS UkSSR.

V. P. Dmitriyevskiy - Joint Institute for Nuclear Research.

S. K. Yesin - Yerevan physical institute.

V. A. Kozlinskiy - state committee on the use of atomic energy of the USSR.

A. A. Kolomenskiy - physical institute in. P. N. Lebedev of the AS USSR.

A. A. Kuz'min - radio engineering institute of the AS USSR.

N. A. Monoszon - scientific research institute of the electrophysical equipment in. D. V. ^Yefremov.

V. P. Sarantsev - Joint Institute for Nuclear Research.

V. P. Semenov - TsNIIAtosinform.

Page 5.

OPERATIONAL PROCEDURE OF CONFERENCE.

11 November, the morning. - The opening of conference. Introductory comment chairman of the organization committee of A. L. Mints's conference Greetings from the AS USSR (Vice President of the AS USSR A. V. Kotelnikov) and from State Committee for the use of atomic energy of the USSR (deputy chairman Goskomitet I. D. Morokhov).

I session - Chairman A. L. Mints. Comparative characteristics of the accelerators of different types from the point of view of physical experiment.

On 11 November, evening is. the II session. - Chairman A. A. Naumov. State of the accelerators of different types, designs of new ones and reconstruction of the acting installations.

On 12 November, morning is. the III session. - Chairman Ye. G. Komar. Direct voltage accelerators. Ionic and electronic sources.

On 12 November, evening is. the IV session. - Chairman N. A. Monoszon. Electromagnets of accelerators and system of their supply.

Magnetic measurements.

On 13 November, morning is. the V session. - Chairman V. P. Sarantsev. Collective methods of acceleration.

On 13 November, evening is. the VI session. - Chairman P. A. Vodop'yanov. Superconducting elements of accelerators.

On 16 November, morning is. the VII session. - Chairman A. A. Kuz'min. Radio electronics of accelerators. Measuring systems of the parameters of beams.

On 16 November, evening is. the VIII session. - Chairman B. P. Murin. Powerful/thick radio engineering devices/equipment and accelerating systems.

On 17 November, morning is. the IX session. - Chairman A. A. Kosomenskiy. Particle dynamics in the accelerators, the accumulators/storage and the installations with clashing beams.

17 November, evening, X session. - Chairman D. G. Koshkarev. Particle dynamics in the accelerators, the accumulators/storage and the installations with clashing beams.

On 18 November, morning is. the XI session. - Chairman L. L. Gol'din.
Targets, separation and transportation of beams. Input and output.

On 18 November, evening is. the XII session. Chairman A. A.
Vasil'yev. Control and direction of accelerators with the aid of the
computers.

Coverage of convention. Final word of chairman Orgkomitet A. L.
Mints.

Page 6.

Introductory comment of the chairman of the organization committee of the conference of academicians A. L. Mints.

Dear comrades and associates, ladies and gentlemen !

On the commission of organizational committee on the convocation of the second All-Union conference on the accelerators of these charged/loaded particle I have an honor to greet you, of gathering in this hall of Moscow house scientists.

To us supplies/delivers/feeds into the specific satisfaction presence at this conference of all chief/leading scientists and engineers of the Soviet Union who deal by study, development and construction of particle accelerators in our country, and also the arrival of many foreign scientists, who politely accepted our invitation to arrive in Moscow and to make reports and communications/reports about their newest works.

This testifies, besides entire other, about the value of our first conference, called in Moscow in 1968. The transactions of this conference were sent out to all its participants. The transactions of

the second conference will be also published and entrusted to its participants.

Missions which the Academy of Sciences of the USSR and the state committee on the use of atomic energy assigned before the organization committee of our conference, include, besides the traditional thematics, also the survey/coverage of the fundamental questions sciences, connected with questions of contemporary nuclear physics and physics of high energy particles.

Reports will be dedicated to both the classical systems of accelerators with the fixed targets, to clashing beams of various kinds, to rings and to collective methods of acceleration. Logically, will be given attention to the use of the phenomenon of superconductivity for the creation of the magnetic fields of high intensity and for reducing the losses in the accelerating structures.

The attentive study of the methods of the investigation of contemporary physics leads to the conclusion that for the newest physical instruments very characteristic is an increase in their sizes/dimensions, complexity and cost/value. Hence and was born winged phrase about the industrialization of contemporary physics. Giant radiotelescopes for studying the extraterrestrial sources of radio emission became the conventional tools of the experiment of the

radio astronomer. In this case it should be noted that the study of distant objects of macrocosm requires not only large, but also precision observation systems, especially in proportion to the shortening of wavelengths in the range of observation. It is also extremely important obtaining the high resolution of all astronomical instruments.

Similar pattern occurs, also, during the study of microcosm - in nuclear physics and in the region of elementary particles.

With the decrease of the studied lengths it is necessary to apply charged particle accelerator everything of high and high energies, i.e., also the giant and simultaneously precision and expensive installations. On the other hand, for the understanding of nuclear physics and different phenomena of microcosm it is necessary to have installations of high resolution.

However, the industrialization of physics does not completely eliminate the creation of new methods and instruments of the sequences in which the fineness of the setting of experiment and the depth of keen vision, and also ingenuity and power of observation of researcher will make it possible to make remarkable works with the relatively simple instruments. As the example let us point out the discovery/opening of the effect of Mossbauer, the discovery of the

effect of Vavilov-Cerenkov, etc.

It is extremely desirable so that and in the field of the creation of charged particle accelerators we could switch over to the more available and less expensive technology.

After the termination of conference is provided for the visit of accelerative centers in Moscow, Serpukhov Dubna and Novosibirsk.

Besides plenary meetings, will be carried out the seminars for separate urgent questions.

Although the visit of the Soviet Union by foreign participants in the conference occurred yearly during the latter/last three years, I hope, that also our this meeting will be useful and interesting.

I warmly desire to you both the successful work at the conference itself and realization of the friendly contacts between the scientists in the lobbies of our conference and during the visit of accelerative centers and institutes in our country.

The second All-Union conference on charged particle accelerators I declare opened.

Page 7.

**SALUTATORY WORD OF THE VICE PRESIDENT OF THE ACADEMY OF SCIENCES OF
THE USSR OF ACADEMICIAN V. A. KOTEL'NIKOV.**

Respected comrades, ladies and gentlemen !

The presidium of the Academy of Sciences of the Union of Soviet Socialist Republics directed to me to greet gathering in this hall of the scientists and specialist-participants in the second All-Union conference on charged particle accelerators.

The Academy of Sciences of the USSR considers science and technology of charged particle accelerators the very important branch of knowledge. As is known, accelerators are the contemporary machines of the knowledge of the structure of matter at all levels, which relate to the microcosm.

In connection with this in the Academy of Sciences of the USSR in 1967 was organized the scientific council for the problems of the acceleration of the charged/loaded particles, which was intended to carry out the coordination of scientific research works, and also a comparative study of principles, which lie at the basis of the

accelerators of light and heavy particles.

Among the numerous tasks the council is obligated once a two years to carry out the All-Union conferences, to which, besides the majority of the specialists, who work in the region of accelerators in our country, arrive the guests from the foreign countries. This fact is allowed, together with the discussion, if one may put it that way, internal questions, to carry out mutual familiarization with achievements and plans/layouts of the Soviet and foreign scientific, working in the region accelerators.

To me it is considered by very advisable that, besides the basic reports at the plenary meetings of conferences, would be conducted the specialized seminars for narrower, more urgent questions. This will make it possible to more deeply discuss the most acute moments of accelerator science and technology to which you dedicated your activity.

On behalf of the presidium of the Academy of Sciences of the USSR and from itself I personally hotly desire the great successes in the work to all participants in the present conference, and also the successful familiarization with the accelerative centers of our country.

Page 8.

SALUTATORY WORD OF THE DEPUTY CHAIRMAN OF STATE COMMITTEE ON THE USE
OF ATOMIC ENERGY OF THE USSR I.D. BOROKHOVA.

Respected Comrades ! Ladies and gentlemen !

It is glad to greet you in our capital which hospitable threw
open to the door of this splendid hall for the specialists, who
dedicated their life to charged particle accelerators !

Accelerators - this is powerful/thick instrument for studying
the structure of material. Word itself "accelerator" reflects the
noble/precious sense of your efforts/forces, your work for the good
of man.

You accelerate the progress of most complicated and most
majestic science - physics. You accelerate the process of knowledge
by man of the concealed/latent in the depths material of the
mysterious essence of things, elementary particles of the material.
With each year is widened our knowledge about the structure of
material.

The prophetic words of the founder of great Lenin's Soviet state: "Electron so inexhaustible as atom, nature it is infinite...", they were filled by the new content.

Inexhaustible the step/stage of the knowledge of microcosm. Is difficult path to the creation of the ordered theory of elementary particles, but it would be generally impossible, if you did not work, were not opened and did not construct giant machines.

In the Soviet Union the Communist Party and the government in every way possible encourage development of accelerative technology. All you, obviously, you know Serpukhov the accelerator of protons which holds the first place in the world on the energy of protons reached. In this year the party and government worthily noted participants in the construction of this unique physical instrument. The Lenin prize and two state prizes are given out to the series/row of the outstanding specialists whom you can see in this hall.

I am glad to congratulate you, expensive laureates, with this acknowledgement of your merits !

Certainly, you, comrades are laureates, you personify the very large collectives of workers, engineers, scientists, who were working it is more than 10 years on development, creation and adjustment of

this physical giant. But in this many-faced labor flow you were the main things, after that to you honor and glory !

The tasks, confronting the accelerative technique of the Soviet country and other countries, are clear and clear: to raise the effectiveness of the acting accelerator facilities; to constantly improve the technical level of accelerators and entire physical equipment, connected with the experimental works; to automate experiments and processing of their results; to search for new ways in the accelerative technology - they are cheaper, more effective. To necessarily better and more fully/totally/completely study foreign experiment, to fasten scientific connections/communications and international collaboration both with the scientists of the socialist countries and with all, who want sparking and it is honest to work with us together, hand to hand, on the most complex problems of high-energy physics.

Our design engineers must especially many forces and time give to economic questions, propose the beautiful and inexpensive solutions, exhibit more than ingenuity and initiative.

Here are present the foreign guests who arrived to our national conference in order to exchange plans/layouts and thoughts.

We await from the guests of friendly criticism and friendly counsels.

State committee on the use of atomic energy from its side will do everything so that our foreign guests' stay in the Soviet Union would be pleasant and useful.

We hope that the situation at the conference will be unconstrained, creative, business.

We desire to all participants in the conference of the successes in the work !

I thank you for the attention.

Page 9.

Session 1.

COMPARATIVE CHARACTERISTICS OF THE ACCELERATORS OF DIFFERENT TYPES
FROM THE POINT OF VIEW OF PHYSICAL EXPERIMENT.

1. Possible directions of physical investigations on the accelerators
of the nearest future.

A. A. Komar.

(Physical institute in. F. N. Lebedev of the AS USSR).

1. Introduction.

1. In connection with conducting at present construction of
several large/coarse accelerators, and also plans/layouts of creation
even of more powerful/thicker accelerator facilities it is of
interest to discuss question about what kind of task advances today's
development of physics of elementary particles and what experiments
in view of this will be placed first of all on new accelerators. In
other words, we want to make the attempt to come to

light/detect/expose the most characteristic and most probable directions of physical investigations on the accelerators of the next years. In this case will be incidentally discussed a question also about conformity in which are found the demands of theory and accelerative possibilities.

During the determination of the character of future physical investigations we logically proceed from the representation about what tasks of considering it important, and what secondary. Since these representations are completely blown by our today's understanding of the properties of elementary particles and their interactions, should be aware in the fact that our conclusion/output and conclusions will carry very preliminary, tentative character. Time can introduce in them essential corrections.

2. Contemporary physics of elementary particles is characterized by sufficiently large quantity of actual data. However, as before, it not in the state to describe them from unity of opinion. Always remains perception, that some essential parts of the information are absent. In the theory of elementary particles in recent years predominates semi-phenomenological, model approach. This approach, as a rule, can pretend to the description of the phenomena only in the limited region of energies or transferred impulses/momenta/pulses (relative to small ones or maximally large) and it does not make it

possible to obtain the complete picture of interaction.

Phenomenological in its essence is the description of masses and quantum numbers of the elementary particles whose quantity all builds up. Phenomenologically are introduced into the theory of elementary particles the symmetries and their disturbance/breakdown. We understand neither origin of these symmetries nor nature of their disturbance/breakdown.

Phenomenological at its basis is very division of interactions into the strong ones, the electromagnetic ones and the weak ones. We do not know, do exhaust they all possible interaction modes, and therefore we just as willingly recently discuss hypotheses about the ultrapowerful ones, the extra weak ones, the semiweak and the like interactions.

In order to overcome this abundance phenomenologism in order to make a selection between different models, and subsequently to pass to the construction of the theory of elementary particles, are necessary new experiments and, first of all, experiments with the higher energies. This confirmation is based not only on that generality, that in this case we will switch over to the study of the smaller distances which can discover to us qualitatively new physics. Entire contemporary experiment and theory push us in this direction,

as we will see below. It is very similar to the fact that the key/wrench to the theory of elementary particles lies/rests at the region of very high energies, so that now the name "high-energy physics accepted" will be completely justified.

We convert/transfer now to the presentation of the most probable directions of the future investigations.

II. Searches of new particles.

As this not strangely will seem, but in spite of the abundance of the already known to physics elementary particles (several hundred), extremely urgent is a question about the searches of new particles. In this case search for the particles of several sharply distinguished types.

1. First of all these are new highly interactive particles from class of particles, known by the name of resonances. These particles compose the large part of the discovered today particles, and their separate groups, apparently, are different steps/stages of the excitation of one and the same system. If this then, it is extremely important to come to light/detect/expose laws in the location of these excitations which would help to more deeply understand the nature of the forces, which control these excitations. Situation here

can be analogous situation in atomic spectroscopy where the empirical laws laid way to quantum mechanics.

Are today known resonances in masses to 3.5 GeV. Available particles, however, it is not sufficient for the establishment of determined regularities.

Page 10.

It is very essential to know how far, with respect to mass, stretch resonance states or their masses they are limited by certain limiting value. In the latter case the accelerators of very high energies will not be required. But in some models appears the linear spin dependence of the square of mass. In order to trace this dependence, will be required proton accelerators all of the increasing energies. Now the searches of new resonances are conducted in Serpukhov and will be doubtlessly they continued on the accelerator in Batavia (USA).

2. Following object for searches - quarks. It is well known that the existence of quarks could explain the appearance of properties, characteristic for SU_3 (unitary) symmetry, in the highly interactive particles. In the presence of quarks it would be more simply come to light/detect/expose laws in the spectra of resonances, it would be

possible to explain quantum numbers of resonances.

Until today quarks are not discovered, and accelerative experiment gives, that the mass of quark most likely more than 5 GeV. But quarks are so tempting an object, that physics soon will not forego the attempts their detection.

With the energy of the protons of order 1000 GeV it would be possible to move searches to $m_q \approx 20$ GeV.

Are recently obtained information, that the quarks are recorded in the process, which is developed with the energy 10^{15} eV in the cosmic rays. (Experiment, true, it is not is not very reliable). So that the searches of quarks, apparently, still for long will remain in the study program on the accelerators, switching on installations with the proton-proton and proton-antiproton beams.

3. One additional long ago unknown object - intermediate vector boson (W). Its detection could introduce substantial changes into our understanding of the structure of weak interactions.

By the way, in this case customary four-fermionic interaction would be not more than a good model for describing the weak processes with the relatively low energies (point of view, which has

sufficiently such adherents!). Lower boundary for the mass of a W-boson according to the different estimations is 2-6 GeV. There are numerous hypotheses in which figure many varieties of intermediate bosons. But they all converge in the fact that a W-boson (or bosons) must be heavy ($m_W > 10$ GeV perhaps even > 30 GeV). In any event for the searches are necessary the accelerators to the very high energies (from 100 GeV it is above). The search of a W-boson will be one of the central tasks in the investigations on the accelerator in Batavia (USA). In the case of failure the searches will be doubtlessly continued on the even larger accelerators.

4. Long time attracts attention of physicists this exotic particle, as monopole (particle, carrying magnetic charge g). In this case $g^2/hc = 137/4$ is great. Based on this, it is possible simply to show that so that the monopole generally would exist in the free state, its mass must be large (not less several GeV, or even 10 GeV). Its searches were thus far unsuccessful. But since it can be very heavy, its searches will continue (in particular, in Batavia). The existence of monopole could explain the quantization of electric charge. Due to the large constant g^2/hc the monopoles were recently used for explaining the nature of strong interactions.

5. Very interesting ones are searches also of such exotic objects as heavy leptons.

In the presence their cur representations about the family of leptons one should subject to radical review.

Are not excluded existence and other, not of the known, until now, to physicists particles, mainly heavy ($m > 10$ GeV). Part of them could decompose into μ -meso and cause some anomalies of their behavior with the energy $> 10^{12}$ eV.

It is shorter, physics they recently exhibit the increased interest in the new particles which could lead to completely new connections/communications in the world of known elementary particles.

III. Checking the locality of theory. Search of length element.

Locality - one of the basic principles, on which rests the contemporary theory of elementary particles. At the same time precisely locality is the reason for divergence in the theory. No departures from the locality, until now, it is discovered. The corresponding limitations to length element (l) comprise:

$l \approx (2 \pm 5) 10^{-15}$ cm. This situation cannot but intrigue physicists and, naturally, that the searches of departures from the locality will be

continued with the high energies and at the smaller lengths. Known in particular that immediate objective is length ℓ_w , connected with weak interactions ($\ell_w = 8 \cdot 10^{-17}$ cm).

1. As the best method of checking locality is usually considered conducting electrodynamic experiments, since sections of corresponding processes can be sufficiently accurately calculated on basis of quantum electrodynamics, local at its basis. All this undoubtedly it is correct, but, as we now will see, there are other methods of checking the locality.

The most effective checking of locality in the electrodynamic processes will be within the next few years carried out on the installations with the clashing electron-positron beams in the reactions of the type:

$$e^- + e^+ \rightarrow e^- + e^+ \quad \text{or} \quad e^- + e^+ \rightarrow \gamma + \gamma.$$

In these processes with the energy of particles in beam ≈ 10 GeV and by the precisions/accuracies of measurements by $\approx 30\%$ it is possible to achieve the border of lengths $\sim 10^{-16}$ of cm. This already very close to ℓ_w

2. Another method of checking locality consists of checking of

dispersive relationships/ratios for processes of scattering (forward) highly interactive particles, for example, for $\nu\bar{\nu}$ - scattering. During the disturbance/breakdown of locality will be disrupted dispersive relationships/ratios. Dispersive relationships/ratios connect the real part of the scattering amplitude ($\text{Re}A$) with the integral on the energy of the total scattering cross-section (σ_{tot}). For their checking one should measure $\text{Re}A(E)$ with sufficiently high energies E and σ_{tot} as function E in possibly the wider interval. Such measurements in 1000-2000 GeV regions will also derive us into the region of lengths $\sim 10^{-16}$ of cm. With further increase in the energy of accelerators the upper limit for ℓ will be reduced $\sim 1/\sqrt{E}$.

One additional method of checking of locality and general/common/total principles of theory is connected with measurement σ_{tot} for particle (σ_{tot}^+) and antiparticle (σ_{tot}^-) on one and the same target, for example hydrogen, with maximally available energy. By examples can serve interactions $\pi^\pm p$, $K^\pm p$, pp and $\bar{p}p$.

Page 11.

The experiments of such are planned/glided in a number of the firsts on all future accelerators. It can happen, that σ_{tot}^+ and σ_{tot}^- with an increase in the energy will not approach one and the same limit. In this case as the test of locality can serve the dependence on the

energy of the relation of the real and alleged parts of the scattering amplitude forward. In this case $\text{Re}A/\text{Im}A \sim \ln E$. In order to trace this sufficiently steady dependence, can be required accelerators with the energy $> 1000 \text{ GeV}$. When $\sigma_{\text{tot}}^+ = \sigma_{\text{tot}}^- \lim_{E \rightarrow \infty} (\text{Re}A/\text{Im}A) = 0$.

3. Supplementary possibilities of checking locality disclose study of behavior of form factors as functions of transferred impulse/momentum/pulse t in space-like and time - similar regions. With the observance of locality these functions must be identical (with $t \rightarrow -t$). For this checking is necessary the combined study of processes of the type

$$\begin{aligned} a) \quad & e^- + p \rightarrow e^- + p, & \stackrel{(1)}{\text{new}} e^- + e^+ \rightarrow \bar{p} + p; \\ & \bar{p} + p \rightarrow e^- + e^+ \\ b) \quad & \pi^- + e^- \rightarrow \pi^- + e^-, \\ & e^- + e^+ \rightarrow \pi^- + \pi^+. \end{aligned}$$

Key: (1) . or.

It is important to emphasize that the investigation of these processes will become actually available on the installations with the clashing electron-positron beams of sufficiently high luminous densities or in the proton machines into hundreds of GeV, possessing beams antiprotons and pions of the required high intensity.

IV. Some questions of dynamics. Testing models.

In the study of dynamics physicists' interests in recent years were concentrated on the region of very high energies. This is connected with the fact that the number of the general considerations of theory, and also available of the physicists models indicate the possibility of the very simple dependences of the sections of different processes on the kinematic variable/alternating (energy, transferred impulse/momentum/pulse), when the values of the latter are very great. Physics of very high energies in a sense can prove to be simpler than physics of average/mean and low energies. The value of energies, with which begins this simplification (asymptotic mode/conditions), at the present moment/torque to indicate difficultly, so that in this point/item is required the aid of experiment. It is possible to only say that at the majority of the cases the asymptotic range lies/rests beyond the limits of our present possibilities. ^{Maybe} ~~to be seen~~ for its achievement they will be required energy into thousand and even tens of thousands of GeV. It is important to emphasize that for the asymptotic range the different models give, generally speaking, the different behavior of sections. Thereby the experiment offers possibilities for the selection of models, the contractions of the circle of the permissible assumptions and thereby runs the path for the construction of singularly correct description, it is possible that the clear understanding of specific character interaction at high energies will help to construct the theory of processes with the smaller energies.

1. For strong interactions in asymptotic range total cross sections of processes, most probable, they become constants. In this case the sections for particle σ_{tot}^+ and antiparticle σ_{tot}^- can be both equal (Pomeranchuk theorem) and equal to each other (see above). Checking this fact is extremely important, and for a long time it will occupy researchers' attention, since the asymptotic range, apparently, lies/rests not closely. We saw also that if $\sigma_{tot}^+ + \sigma_{tot}^-$ there is the large interest in asymptotic behavior $(Re/ImA)_\sigma$. From the positions of the aforesaid, besides the mentioned above processes with π^\pm and K^\pm the mesons, very usefully also the study of the process of regeneration $K_L^0 + p \rightarrow K_S^0 + p$. Its section directly depends on $[A^+(0^0) - A^-(0^0)]^2$.

Different models predict different tendency σ_{tot} toward the limit; into some cases on top, in other on the bottom. In second version σ_{tot} with certain energy must pass through the minimum. All these forecasts need experimental check.

For the differential elastic cross sections in the asymptotic range on E and with relatively small t the sections must take simple form $d\sigma/dt \sim \exp [t/\Lambda(E)]$, moreover the width of cone $\Lambda(E)$ must decrease with the energy (contraction of cone) according to the law

$\Delta(E) \sim 1/\ln E$ OR $\Delta(E) \sim 1/\ln^2 E$. The determination of form of dependence $\Delta(E)$ is of large interest, but it requires experiment in wide energy range.

Elastic scattering with high energies and large t ($t \gg 1$) is controlled by other mechanism. Sections these are small and sufficiently difficult for the study, but it is very interesting, since they correspond to minimum impact parameters. On some models under these conditions must be revealed so-called contact interaction between the nucleons, moreover

$$\frac{d\sigma}{dt}(t \gg 1) = \frac{d\sigma}{dt}(t=0) G^4(t),$$

where $G(t)$ - nucleon form factor.

2. For electromagnetic processes in high-energy region and major momentum transfers in recent years is revealed peculiar special feature/peculiarity, which was called scale invariance. It turned out that the characteristic functions, which describe the highly inelastic electron scattering, S_1 and νW_2 depend only on relation $\frac{2m_p \nu}{t}$ where ν - change in the energy of electron, t - transferred impulse/momentum/pulse, and therefore they are not changed with simultaneous proportional increase ν and t . Checking the scale invariance in the high-energy region will play important role in the study program on the new accelerators. Let us point out moreover that the different models give different behavior and asymptotic behavior

for W_1 and νW_2 . To establish/install then is possible only upon the setting of experiments over a wide range ν and t .

Interesting simple dependences appear in the asymptotic mode/conditions for the total cross section of process of $e^+e^- \rightarrow$ hadrons (in the single photon approximation/approach). Different models give for $\sigma_{tot}(e^+e^-)$:

$$\sigma_{tot}(e^+e^-) \sim \frac{1}{E^2}, \quad \sigma_{tot}(e^+e^-) \sim \frac{1}{E^4 \ln^2 E},$$

$$\sigma_{tot}(e^+e^-) \sim \frac{1}{E^6 \ln^4 E}.$$

Most plausible, apparently, is dependence $\sim 1/E^2$. Its checking is very important, but, unfortunately, it is difficult to thus far indicate necessary for this purpose energy of clashing beams. It can noticeably exceed 10 GeV.

Page 12.

Very simple dependences are noticed at high energies for the processes of the photoproduction of pseudoscalar mesons forward and back/ago:

$$\text{forward} \quad \frac{d\sigma}{dt} \sim \frac{1}{E^2} f_1(t),$$

$$\text{back/ago.} \quad \frac{d\sigma}{du} \sim \frac{1}{E^2} f_2(u).$$

It is important to trace, are retained these dependences with the high energies.

For the photoproduction of vector mesons the experiment gives, that $\frac{d\sigma}{dt} \sim f_3(t)$ and thereby $\frac{d\sigma}{dt}$ does not depend on energy. This property is the manifestation of the hypothesis of the so-called vector dominance, which predicts the nondecreasing section of the photoproduction of vector mesons in the limit of the highest energies. This forecast must be checked with the high energies.

With the hypothesis of vector dominance is connected one additional very interesting forecast. From it it follows that the total cross section for process $\gamma + p \rightarrow$ hadrons does not decrease with the energy and it is equal in the value of 120 μ bar. Space observations show that these it is approximately/exemplarily correct. Now on the turn a precise checking of this confirmation on the accelerators.

3. For weak interactions are also in prospect interesting checkings at high energies. First of all this concerns process $\nu_\mu + N \rightarrow \mu^- +$ hadrons. This process in the type is very close to the highly inelastic electron scattering and in this case also must become apparent scale invariance. For the total cross section of this process it is possible to expect linear increase with the energy of

neutrino. Checking this dependence is very important both from the point of view of experiment and theory. It is essential to know, to what energies will be continued this increase. It is possible to theoretically expect up to $(E_\nu)_{\text{lab}} \approx 10^5 \text{ GeV}$, if we proceed from the model of four-fermion interaction. We already said above in connection with the problem of a W -boson that the structure of weak interaction can be substantially different, and then energy dependencies will be others ($\sim \ln E_\nu$). From the positions of universal four-fermionic interaction continue to retain their value searches $(\bar{\nu}_\mu \mu)(\bar{\mu} \nu_\mu)$ interaction in the process of form $\nu_\mu + Z \rightarrow Z + \mu^+ + \mu^- + \nu_\mu$. The high intensities of neutron beams, which are expected in the large proton machines, can play the here decisive role.

Not are less interesting with the high energies of neutrino checking the precision/accuracy of the retention/preservation/maintaining muon quantum number, rules of selection in the weak interactions and number of other investigations.

V. Problem of μ -meson.

The problem of a difference between μ -meso and electron, which long ago throws call theorists and experimenters, will undergo many-sided attack on the new accelerators. In this case the

significant role can play both the accelerators of the type of "meson-producing cyclotron" with the intense beams of low-energy μ -mesons and new proton accelerators with the sufficiently intense beams of high-energy mesons. Very tempting is the prospect for the creation of storage μ -meson rings.

In the range high-energy in a number of the firsts is assumed the investigation of the highly inelastic scattering of μ -mesons. With the full/total/complete identity of μ -meso and electron the picture of their scattering must be of identical, with the characteristic property scale invariance. From space data it follows that some differences can begin with the approximation/approach to 1000 GeV, where there are indications of the anomalous behavior of μ -mesons. In this point/item are necessary careful quantitative investigations. Very important ones is the study of the process

$$e^- + e^+ \rightarrow \mu^- + \mu^+$$

with as the high as possible energies. Here adjoins the study of scattering of high-energy μ -mesons on the atomic electrons and, if this proved to be possible, scattering e^- on μ^- in clashing beams. All these experiments are aimed at the searches of divergences from the standard electromagnetic properties of such.

With the searches of anomalies in the properties of μ -meso are connected the experiments, aimed at the detection of the heavy

particles, which decompose into the pair $\mu^+ \mu^-$ (see above).

VI. Laws of conservation. Properties of symmetry at high energies.

The laws of conservation (baryon number, strangeness), property isotopic, unitary symmetry, and also discrete/digital symmetries (C, P, T) have established/installed us in the experiments with relatively low energy, and it cannot be previously foreseen, are observed they with the higher energies. Therefore it is expedient to have in mind the setting of experiments in checking of the laws of conservation and properties of symmetry indicated. As yet it cannot be said that the existing situation in physics of elementary particles imperatively requires such checking. But if we recall that all disturbances/breakdowns, found earlier, were always unexpected, then there can be it is worth revealing precaution.

As an example of the processes which could be subjected to investigation, let us point out:

a) for checking strangeness conservation

$$p + p \rightarrow p + \Sigma^+,$$

$$\pi^- + p \rightarrow p + K^-;$$

b) for checking the retention/preservation/maintaining the baryon number

$$\begin{aligned}
 & p+p \rightarrow p+\pi^+, \\
 & p+p \rightarrow \pi^++\pi^+, \\
 & p+p \rightarrow p+\mu^+, \\
 & p+p \rightarrow \mu^++\mu^+;
 \end{aligned}$$

c) for checking T - invariance

$$p+p \rightleftharpoons \pi^++d$$

(observance of detailed balance):

d) for checking C -invariance

$$\begin{array}{lcl}
 \bar{p}+p & \begin{array}{l} \nearrow \\ \searrow \end{array} & \begin{array}{l} \pi^++\pi^- \text{ адроны,} \\ \pi^++\pi^- \text{ адроны} \end{array}
 \end{array}$$

Key: (1). hadrons.

(similarity of the energy spectra of particles and antiparticles):

e) for checking P - invariance the searches of the longitudinal polarization of the protons in pp -scatter.

Page 13.

This enumeration it is far not exhausting. For these all processes today it is not possible to indicate the upper of the boundary of 10 energies to which one should carry out searches. They

must continue increasingly further, unless will appear the considerations, which make such searches excessive.

Everything said above about the possible directions of investigation on the future accelerators indicates that in physics of elementary particles is an an even more sufficient quantity of problems and tasks, which develop by that justified construction and of ever more powerful/thicker machines. The gold pore of physics of elementary particles, apparently, is still in front. Logically limit to further growth of energy of accelerators could place such ideal situation when there would be obtained comprehensive explanation to all known phenomena in the world of elementary particles. But even in this case we must switch over to even higher energies.

2. Superconducting cybernetic proton synchrotrons to the energy into сотни and thousands of GBS, which use as the injectors accelerators with the low repetition frequency.

A. L. Mints, A. A. Vasil'yev, E. L. Burstein, Ye. S. Mironov.

(Radio engineering institute of the AS USSR).

An achievement of energies of order 1000 GeV, necessary for the following stage investigations in high-energy physics, can be carried out both method of the construction of new accelerative complexes over the new areas and by method of the growth of already existing accelerative complexes [1-11].

In the present report are discussed some special features/peculiarities of the accelerative complexes, which consist of the large superconducting proton synchrotron, injection into which is accomplished/realized from the accelerator with the low repetition frequency of the cycles of acceleration. Are given also the estimations of the characteristic parameters of this complex.

The in question in the present report questions arise, when as

the injector in the large ones synchrotron is intended to utilize the proton synchrotron, installed initially for the physical experiment in the region of energies into tens of GeV. It is necessary to note that the ideas of the use of such accelerators, which work with the low repetition frequency of cycles, have long ago appeared; however, in this case the parameters of accelerative complex were distant from the optimum ones. This depended on the fact that the time, required for the accumulation of particles in orbit of large accelerator with the usual non-superconducting magnet due to the large difference in the perimeters of main accelerator and injector-accelerator and rare impulses/moments/pulses from the injector-accelerator, was very large (several minutes). If one considers that due to the limitation of losses in the usual magnet of the "plateau" of the magnetic field, during which is accomplished/realized the conclusion of particles, it cannot be made in the duration of more several seconds, then this accelerative complex will have either the low intensity (during the limitation of storage time), or very large porosity. Both the one and the other led to the fact that proved to be necessary to provide for in the accelerative complex the special circular injector-accelerator, which works with the large pulse repetition frequency. The construction of this booster together with the linear injector-accelerator is it goes without saying independent very complex problem. The successful development of the superconducting cable with thin stranded conductors [12, 13], of the capable of

working with the low losses in the alternating magnetic fields, made it possible again to return to the idea of use of the injector of accelerator with the low pulse repetition frequency.

The use of the superconducting coil electromagnet for the large ring makes it possible to obtain together with the larger value of magnetic intensity (this leads to the decrease of the perimeter of accelerator in comparison with the accelerator with the usual magnet to the same energy) and very large duration of the "plateau" of magnetic field with the maximum energy.

The latter fact makes it possible to have the low duty cycle, which is very important for a large number of physical experiments, even upon consideration of the fact that from the point of view of the decrease of losses on alternating current in the superconducting coil electromagnet and for decreasing the power ^{loss} P_{loss} of the accelerating system the time of acceleration must be largest possible (for the accelerator on 2000 GeV this time can be order 15 s). Thus, the described complex with its superconductive electromagnets and slow-acting ring injector accelerator will have at an extremely low repetition rate (one pulse per one-two minutes) a low duty factor and a relatively high accelerated particle intensity. Specifically, if the length of the "plateau" is equal to the time of accumulation of particles and equal to the sum of the time of rise and decay of the

magnetic field, then the duty factor will be equal to one third and the intensity of particles accelerated to total energy, averaged over the acceleration cycle, will also be equal to one third the intensity of the ring accelerator used as the injector.

Now let us look at the example of the characteristic case, where for injection into a large 2000 GeV accelerator a ring accelerator with an acceleration cycle of 5 s and a perimeter 6 times smaller than that of the main accelerator is used. To fill a large ring 6 acceleration cycles are needed, i.e. 30 s. If we assume that the length of the "plateau" also equals 30 s and that the time of rise and decay of the field constitute 15 s each, then the total length of the cycle equals 90 s. Thus, a very long acceleration cycle is characteristic of such an accelerator complex.

During the time of particle accumulation in a large accelerator an accelerating field with a frequency which may exceed by several times several times (taking into account the phase width of clusters) the frequency of accelerating field during the ejection in the circular injector-accelerator, and the small amplitude, sufficient for guaranteeing the stability region in phase space, which overlaps spread along the impulses/moments/pulses of the injected into main accelerator particles. At the moment of injecting the phase of accelerating fields in main accelerator and

injector-accelerator must be selected so that the next particle momentum would fall to the unfilled another part of the orbit of main accelerator. Since for guaranteeing small radial- phase oscillations in main accelerator is necessary very high harmonic order of accelerating field, then before beginning acceleration, after the capture of all injected particles in the large accelerator, it is necessary to carry out a recapture of particles at the substantially larger frequency of accelerating field. This recapture can be made with the high effectiveness during the use/application of the accelerating system, which ensures the possibility of a steady increase of the amplitude in the process of recapture.

The cost/value of accelerator with the superconducting coil electromagnet due to the high cost/value of the superconducting cable rapidly increases with an increase in the aperture of vacuum chamber. Therefore the decrease of the aperture of vacuum chamber of such accelerators is very important task, even more important than for the accelerators with the usual magnet. For the realization of the small-aperture superconducting accelerator is necessary the use of methods of automatic control by the parameters, which are determining transverse motion of accelerated in this "cybernetic" particle accelerator [14-16].

In this case of beam displacement due to the errors in the

magnetic field they can be compensated by correcting lenses and the transverse sizes/dimensions of electromagnet prove to be small.

At present for the creation of the fluctuating magnets is utilized multicore cable, made from alloy NbTi. The multiple superconducting cable has a diameter of ~ 0.5 mm and operating current in the range of hundreds of amperes and therefore is inconvenient for the direct winding on from it of magnet winding. Preliminarily from this cable is manufactured the "woven strip/film", which consists of tens of multiple thin wires (cables). The important special feature/peculiarity of strip/film is the "transposition" of separate thin wires (cables), which makes it possible for current conductor stable to work in the external and proper magnetic fields.

If we accept the critical density of current for the alloy from NbTi with the magnetic intensity is 65 kOe of the equal to $1.6 \cdot 10^3$ to A/cm^2 , then with the coefficient of 0.2 fillings of winding with superconductor for the aperture of vacuum accelerator chamber 6×6 cm² is required the superconducting winding with internal and outside diameters of by the respectively equal to 7.5 and 13.8 cm. These estimations we used for evaluating the parameters of accelerator to the energy 2000 GeV, of the worker in the described above mode/conditions (see the Table).

During calculations of losses in the superconductor the diameter of these superconducting cores was accepted equal to $3 \mu\text{m}$ - value which can be soon achieved/reached in the future.

From the analysis of given in the table data it follows that the parameters of this accelerative complex are very satisfactory, and the scales of construction completely attained. However, of course, before actual construction the superconducting accelerator with pulsed magnetic field it is necessary to solve a whole series of the engineering and technological problems, connected with the creation of precision electromagnets.

In conclusion we consider it as our long to express appreciation to N. A. Meshcherov and N. K. Kasinskiy, which participated in the discussion of the series/row of the touched upon in the report questions.

Table.

№ пп (a)	(b) Параметр	Обозначение	Значение (d) параметра
1.	Кинетическая энергия при эжекции, Гэв	T_e	2000
2.	Напряженность магнитного поля эжекции, э	H_m	$65 \cdot 10^3$
3.	Средний радиус орбиты, м	R_m	$1,5 \cdot 10^3$
4.	Число бетатронных колебаний на оборот, сек.	Q	32,25
5.	Число периодов магнитной структуры	N_p	120
6.	Длительность инжекции, сек.	t_i	30
7.	Время ускорения, сек.	t_a	15
8.	Длительность плато, сек.	t_p	30
9.	Длительность цикла, сек.	t_c	90
10.	Внутренний диаметр камеры, см	ϕ	6
11.	Вес сверхпроводника, т	W	65
12.	Количество жидкого гелия в криостате, л	V	$55 \cdot 10^3$
13.	Общее тепловыделение в жидкий гелий, вт	P	$8 \cdot 10^3$
14.	Тепловыделение в жидкий гелий на 1 пог.метр магнита (вт/м) в т.ч.:		
	потери в сверхпроводнике;		1,1
	из-за потерь частиц высоких энергий;		0,35
	потери в конструкции из-за токов Фуко;		0,2
	потери по теплоизоляции криостата;		0,15
	теплоприток по вводам		0,3
			0,1

Key: (a). pp. (b). Parameter. (c). Designation. (d). Value of parameter. (1). Kinetic energy with ejection, GeV. (2). Magnetic intensity of ejection, e. (3). Mean radius of orbit, m. (4). Number of betatron oscillations to revolution, s. (5). Number of periods of

magnetic structure. (6). Duration of injection, s. (7). Time of acceleration, s. (8). Duration of plateau, s. (9). Duration of cycle, s. (10). Bore of chamber/camera, see (11). Weight of superconductor, t. (12). Quantity of liquid helium in cryostat, l. (13).

General/common/total heat release into liquid helium, W. (14). Heat release into liquid helium to 1 linear meter of magnet (W/m) in Vol. h.: loss in superconductor; due to losses of high energy particles; loss in construction/design due to Foucault currents; loss on thermal insulation of cryostat; heat-input on introductions/inputs.

Page 15.

REFERENCES

1. Design study for a 300-1000 Bev accelerator. Brookhaven National Lab., 1961.
2. E. L. Burstein, A. A. Vasil'yev, A. L. Mints. Transactions of international conference on the accelerators. Dubna, 1963, M., Atomizdat, 1964, page 67.
3. Report on the Design Study of a 300 GeV proton synchrotron, CERN, AR/Internat. SG/64-15, Geneva, 1964.
4. Cybernetic accelerator of protons to energy 1000 GeV. RAI AN, ed. by Vasil'yev A.A.M., NI 9267-14t, 1967.
5. 200 Bev accelerator design study, UCRL-16000, 1965.
6. National Accelerator Lab, Design Report. Univ. Res. Assoc., 1968.

7. A. L. Mints, A. A. Vasil'yev, E. L. Burstein. Transactions of UP of international conference on the charged particle accelerators high-energy, vol. 1. Yerevan. publ. AN of Arm. SSR, 1970, page 60.
8. P. Cole. Transactions of UP of international conference on the charged particle accelerators of high energies, Vol. 1. Yerevan, publ. AN of Arm. SSR, 1970, page 100.
9. G K Green, Private communication.
10. J B Adams, E J N Wilson. CERN Report of 1970, N 70-60.
11. 300 Gev Project. CERN Courier, 1970, 10, N 6.
12. B H Wilson, C R Walters, I E Lewin, G H Spurway, P F Smith. Rutherford Lab. Preprint RPP/A-73, 1969.
13. A C Barber, P F Smith. Cryogenics, 1969, 9, N 6.
14. E. D. Burstein, A. A. Vasil'yev, A. L. Mints et al. Reports of the AS USSR, 1961, 141, 590.

15. E. L. Burstein, A. A. Basil'yev, A. L. Mints et al. "Atomic energy", 1962, 12, No 3.

16. A. A. Vasil'yev et al. Transactions of UP of international conference on charged particle accelerators high-energy, vol. 1. Yerevan, Izv. AN of Arm. SSR, 1970, page 404.

Discussion.

A. A. Vorobyev. How is the quantity of particles, projected/designed in these installations?

A. A. Vasil'yev. For these parameters about which I spoke, these are - 1/3 the particles, which can be accelerated by circular injector-accelerator. For the existing new complexes this composes approximately/exemplarily 10^{13} particles/s.

Vdovchenko. How were you guided when selecting of intensity?

A. A. Vasil'yev. We were based on those critical currents which are now achieved/reached virtually, with certain extrapolation to the future.

N. S. Dikanskiy. From what considerations was selected the energy?

Indeed already it is known that in Batavia 500 GeV will be achieved/reached in the following year. This energy must be exceeded at least by an order (liveliness in the hall).

A. A. Vasil'yev. On this score there are different points of view. Many of physicists consider that 2000 GeV are of large interest.

F. A. Bodop'yanov. Accelerator on 2000 GeV could have an intensity of the order of 10^{14} particles/s. What sense to utilize an accelerator with a small intensity? Indeed the cost/value of booster does comprise not more than 50/o?

A. A. Vasil'yev. The development of accelerative complexes and designs shows that an achievement of the maximum parameters can be accomplished/realized consecutively/serially in the time both on the energy and in the intensity. In the opposite case the very large capital investments prove to be frozen during the long time. Therefore, apparently, is expedient in the future large accelerators to the superhigh energies to also develop consecutively/serially in the time, after providing this increase in the intensity in the subsequent stages.

3. Contemporary state and prospects for Stanford linear accelerator.

R. B. Nil (Stanford center of the linear accelerators, USA).

I. Statistics of work.

Up to the moment/torque of present conference the two-mile accelerator of the Stanford center of linear accelerators studied about four years. Fig. 1 gives the survey/coverage of registration journal for 16 quarters of work of the accelerator. It is possible to note that within this period the share of the operating time, dedicated to investigations in physics of accelerators, continued to fall, whereas the time of investigations in physics of particles increased. The fraction/portion of the time of planned and unplanned idle times on the whole was lowered; however, it at present achieved the level when further reduction is possible only in the condition for a considerable increase in the planned/glide number of work shifts in the year. The more detailed analysis of work of the accelerator in last two financial years is given in Table 1.

II. Improvements of accelerator.

Today two-mile accelerator achieved the maximum energy (without the load) of 22.1 GeV and maximum average/mean powers of beam 750 kW for the duration of beam burst 1.6 μ s and frequency of repetition 360 pulses/s. Latter/last improvements concern an improvement in the

operating mode with several beams, an increase in the operational flexibility, increase in the beam current, improvement of its stability and energy spectrum. Below some latter/last improvements are described in more detail.

Page 16.

A. Increase in the limiting current of beam.

Loyv, etc. [1] approximately one year ago reported about the achievements on the way of increasing the limiting current of the beam of Stanford two-mile accelerator. By that time (August of 1969) with the aid of the different methods it was possible to raise limiting current to 65 mA. These methods, described completely in the literature [1], in essence consist: 1) of reconstruction and amplification of the system of focusing along the accelerator; 2) from the detuning of three cavities of each of 10- one-foot sections of accelerator for the purpose of systematic frequency shift of transverse resonance (NEH_{11} mode) on 0.2 and 4 MHz. This detuning barely affects longitudinal acceleration in the sections.

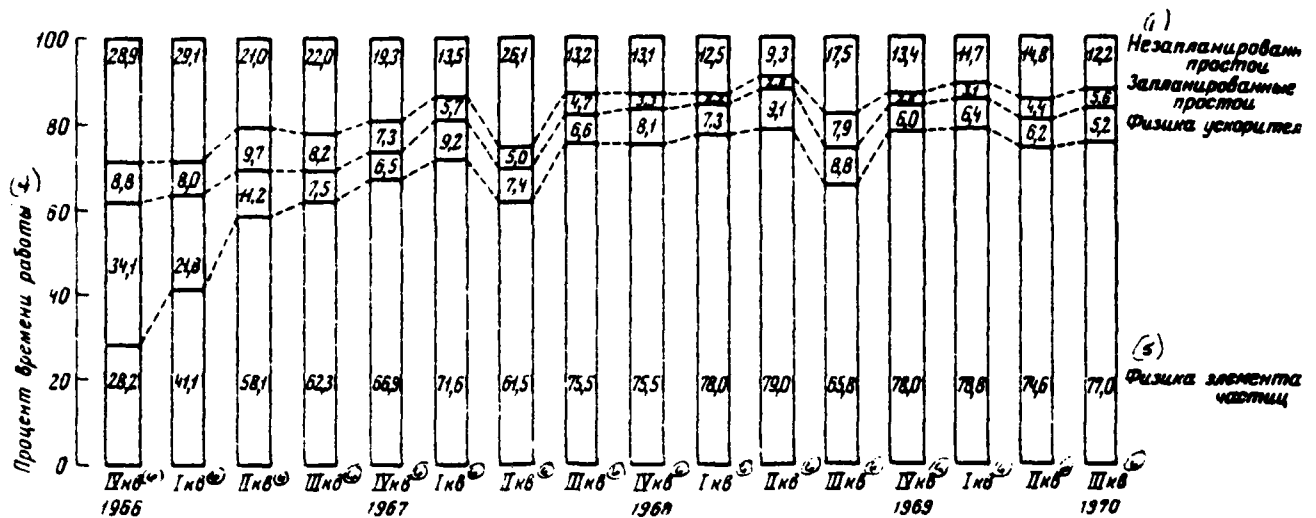


Fig. 1. Compound diagram of work of the accelerator.

Key: (1). Not planned by simple. (2). Planned by simple. (3). Physics of accelerator. (4). Percentage of operating time. (5). Physics of elementary particles. (6). kv.

Table 1. Statistics of work of the accelerator for 1969-1970 financial years and first quarter of 1971.

	1969					1970					1971
	1 кв.	2 кв.	3 кв.	4 кв.	Итого	1 кв.	2 кв.	3 кв.	4 кв.	Итого	1 кв.
<u>А. Часы работы с пучком</u>											
Физика ускорителей	68	121	105	130	424	71	75	98	68	312	59
Физика элементарных частиц	979	1117	1047	1060	4203	531	995	1213	818	3557	880
Всего	1047	1238	1152	1190	4627	602	1070	1311	886	3869	939
<u>Б. Часы прочих работ на ускорителе</u>											
Запланированного простоя	55	49	32	18	154	64	32	48	48	192	64
Незапланированного простоя	258	217	224	208	907	142	173	180	162	657	139
Всего	313	266	256	226	1061	206	205	228	210	849	203
<u>Всего часов работы персонала</u>	1360	1504	1408	1418	5688	808	1275	1539	1096	4718	1142
<u>Б. Часы эксперимента</u>											
Физика ускорителей	153	106	124	259	642	73	79	118	76	346	71
Физика элементарных частиц	2618	4066	2917	2915	12514	1781	3313	3549	2070	10713	2914
Всего часов эксперимента	2769	4172	3041	3174	13156	1854	3392	3667	2146	11059	2985

Key: (1). kv. (2). altogether. (3). hours of work with beam. (4). Physics of accelerators. (5). Physics of elementary particles. (6). In all. (7). hours of other works on accelerator. (8). Planned idle time. (9). Unplanned idle time. (10). Only of hours of work of personnel. (11). Hours of experiment. (12). Only of hours of experiment.

In the latter/last block of 1969 the program of detuning was completed and the limiting current of beam increased to the present level 76 mA. The chronology of the entire program of improvements is given in Fig. 2. The dependence of limiting current on the energy of beam for three stages of adjustment is given in Fig. 3.

Further increase in the limiting current of beam is expected as a result of the introduction/input of pulse quadrupole focusing into the drift sections of the latter 20 of 30 sectors of accelerator. This work, conducted for guaranteeing the possibility of individual optimization to 6 beams, is located at present in the stage of realization and it will be completed approximately through 1 year. By that time is expected an increase in the threshold to 86 mA.

E. New off-axial injector.

Along with the existing coaxial injector recently established/installed the off-axial injector (Fig. 4). New gun with the separate modulator is intended for the redundancy of coaxial injector. At present is utilized the permanent α -magnet, which turns the beam of off-axial gun by approximately 225° . Now there is manufactured the laminar magnet, which will be able to operate on a

pulsed basis with the frequency to 360 imp./s. After completion, approximately toward the end of 1970, system it will ensure the more convenient injection of the alternate beams with different levels of current and pulse durations, without the mutual effects which usually appear during the use of an only gun and modulator.

C. Modulator of the impulses/moments/pulses of short duration for the gun.

In the past year were established/installed the modulator of the impulses/moments/pulses of small duration for the gun ¹, essentially increasing the possibilities of accelerator.

FOOTNOTE ¹. It is developed and constructed by firm "Egerton, Germeshausen and Greer" (EGG), Glendale, state of California.
ENDFOOTNOTE.

Modulator is capable to give on the electron gun impulses/moments/pulses by duration to 5 ns. The pulse separation is regulated from 5 to 100 ns. If necessary can be generated single impulses/moments/pulses.

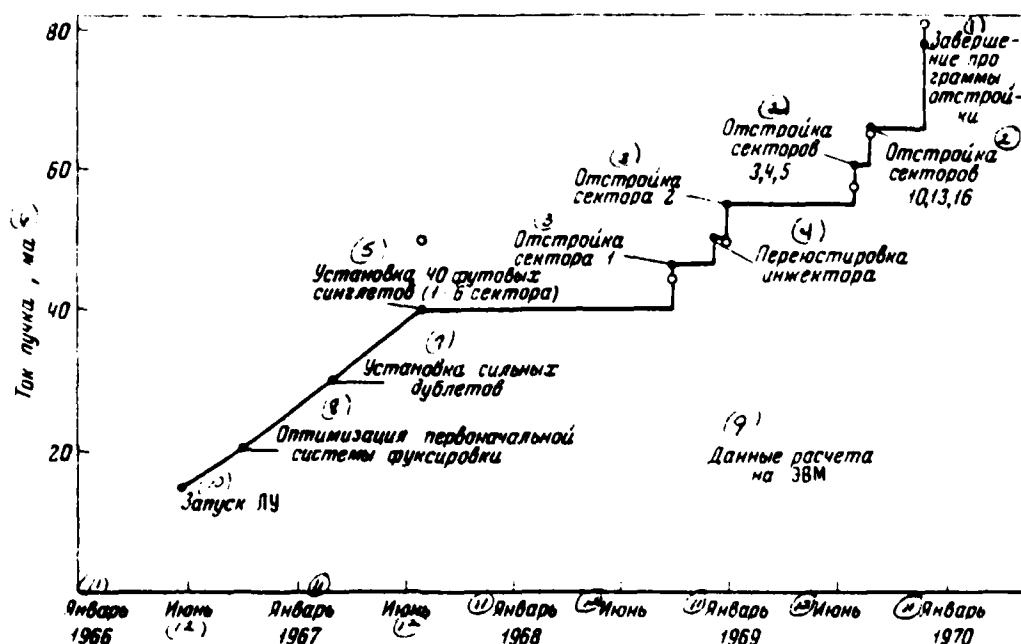


Fig. 2. The limiting current of linear accelerator (for 17 GeV and durations of pulse 1.6 μ s).

Key: (1). Completion of the program of tuning out. (2). Tuning out of sectors. (3). Tuning out of sector. (4). Readjustment of injector. (5). installation of 40 one-foot singlets (1-6 sectors). (6). Beam current, mA. (7). installation of strong doublets. (8). Optimization of initial system of functioning. (9). Data of calculation on computers. (10). Starting of L.U. (11). January. (12). June.

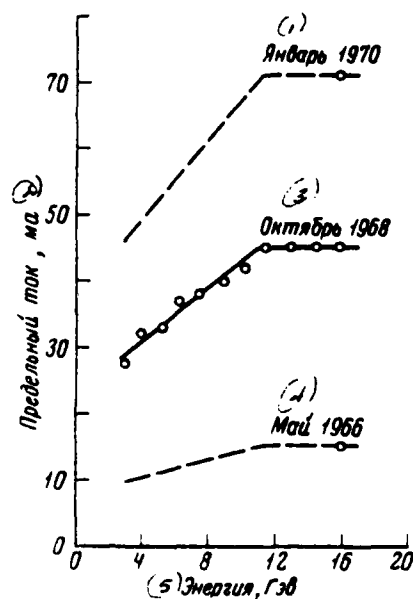


Fig. 3. Dependence of limiting current on energy for three moments of time.

Key: (1). January. (2). Limiting current, mA. (3). October. (4). May. (5). Energy, GeV.

Page 18.

The typical pattern of work of the accelerator with this modulator is given in Fig. 5. With the work with this modulator the limiting current of beam in the milliamperes is equal to 1.25, multiplied by the energy of beam in GeV. For example, with the energy 16 GeV

limiting current in the narrow pulse is approximately 20 mA.

D. Possibility of the interruption of beam.

The installation of the described above modulator of the impulses/momenta/pulses of short duration for the gun increased the control capability of beam and obtaining the intermittent beams. The system of the interruption of beam consists of the group of the resonance deflector plates, situated after the gun, and the second group of the nonresonant deflector plates, situated by approximately the distance of 4 m on the course of beam. Resonance plates are excited with the frequency of 39.667 MHz (72nd subharmonic of the frequency of accelerator 2856 MHz), whereas nonresonant plates are excited with the frequency, adjusted in the range from 5 to 20 MHz. Details are presented in work [1]. The characteristics of beam are given in Table 2. A number of bundles of electrons, passing through the first group of deflector plates at the moment of transiting the stress/voltage through zero and entering into the accelerator, is inversely proportional to peak voltage on the plates. For an example Fig. 6 gives peak beam current, obtained on the slot, which releases 10% of impulse/momenta/pulse, in the dependence on the stress/voltage on the interrupter with the frequency of 40 MHz. The separation of clusters for this case was 12.5 ns (i.e. was accelerated one bundle of electrons of every 36). It should be noted that a number of clusters to the impulse/momenta/pulse varied from 5 to 1 with an increase in the stress/voltage.

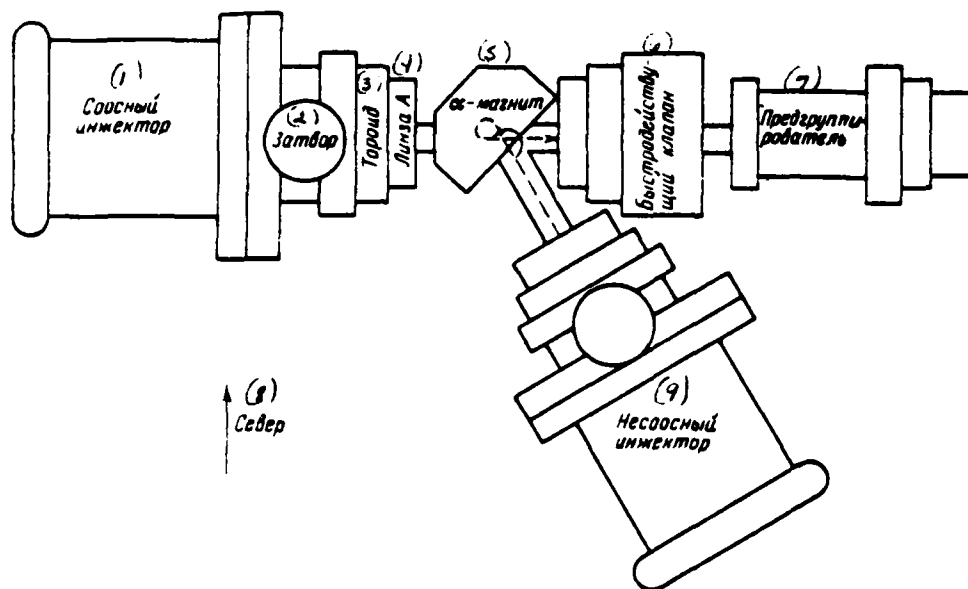


Fig. 4. Diagram of the layout of off-axial injector.

Key: (1). Coaxial injector. (2). Gate. (3). Toroid. (4). Lens. (5). α -magnet. (6). Quick-operating valve. (7). Prebuncher. (8). North. (9). Off-axial injector.

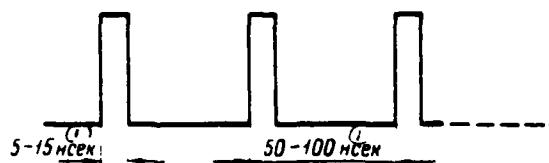


Fig. 5. Diagram of work of the accelerator with modulator of impulses/momenta/pulses of short duration.

Key: (1). ns.

Table 2. Characteristics of the system of the interruption of beam (17 GeV).

Частота пульсации, МГц (1)	Расстояние между импульсами (2)	Максимальный средний ток импульса через 1% - ные щели (3)
40	12,5 нсек (один сгусток/импульс) (4)	~10 ма (5)
40+20	25 нсек (один сг./имп.) (4)	~8 ма (5)
40+20	25 нсек (несколько сг./имп.) (4)	~12 ма (5)
40+10	50 нсек (один сг./имп.) (4)	~2,5 ма (5)
40+6,6	75 нсек (один сг./имп.) (4)	~2 ма (5)
6,8-20 (7) с плавкой регулировкой)	75-25 нсек (несколько сг./имп.) (4)	1-15 ма (5) (9) (ограничивается пушкой)
40+10 + импульсное управляющее смещение (8)	100 нсек (один сг./имп.) (4)	~1 ма (5)
40+10+ импульс на пушку ≤ 50 нсек (11)	Один сгусток (длительностью ~10 нсек) (12)	~10 ⁹ электронов (13)

Key: (1). Frequency of pulsation, MHz. (2). Pulse separation. (3). Maximum average/mean pulse current through 10/o - slots. (4). ns (one cluster/pulse). (5). mA. (6). ns (one cluster/pulse). (7). ns (several clusters/pulse). (8). with continuously variable control. (9). it is limited to gun. (10). pulse control bias. (11). impulse/momentum/pulse on gun ≤ 50 ns. (12). One cluster (by duration ~10 of ns). (13). electrons.

Page 19.

With the low voltages peak current is limited to the phenomenon of the disruption/separation of current, with the the high-emission gun.

E. Improvement of the operating mode with several beams.

It was up to now possibly optimize the conditions of passage and focusing only for one of beams (were possible 6 beams with different by the parameters), accelerated on the Stanford accelerator. Therefore only for one of several conducted experiments usually was obtained beam with the ideal characteristics. In practice the focusing system can be controlled in such a way that the best conditions would be created either for the beams with the high energy or for the beams with the low energy. If the "gradient" of the quadrupole lens (i.e. the speed, with which the current of quadrupoles increases from one clock/module/unit to the next along the accelerator) to control to the best focusing for the beams with the high energy, beams with the energy lower than the specific level fall into the "forbidden band", and do not pass through accelerator. On the other hand, if the "gradient" of quadrupole lenses is made favorable for the beams with the low energy, maximum beam currents with the high energy substantially descend. This fault from Fig. 7, in which is given the dependence of the peak beam current through

cutting out impulse/momentum/pulse of slot of different width on the energy of beam. Are given two groups of the curves: one - for the quadrupoles, optimized to the energy of frame 11 GeV, and another - for the quadrupoles, optimized to the energy of beam 4.5 GeV.

The examined above difficulties, caused by the fact that quadrupoles operate on the direct current, will be solved, when in the sectors with 11 on 30 are established/installed new units of pulse controlling coils and power supplies, and the pulsed sources of the supply of quadrupoles. These devices/equipment which can operate on a pulsed basis with the frequencies to 360 imp./s, make the most individual possible optimization of each accelerated beam. Four sectors are already equipped by pulse blocks/modules/units; remaining blocks/modules/units will be established/installed in the course of the next 16-18 months.

Are set the supplementary devices/equipment, making it possible to carry out the optimization of other characteristics of separate beams, including regulators of pulse delay for 5 sectors, which make it possible to optimize correction on the beam load from one impulse/momentum/pulse to the next, and the sampled-data system of phasing, which ensures the independent phasing for the separate beams.

F. Increase in the effectiveness in the generation of positrons.

The source of positrons is arranged/located in the point, which corresponds of $1/3$ lengths of accelerator (sector 11). This source is called "disk" target; its construction/design allows/assumes rotation so that the beam would fall on different regions of disk. Are possible two operating modes. The first mode/conditions is utilized, when is required the continuous flow of pulses of positrons. In this mode/conditions the disk, made from copper, constantly rotates to avoid excessive increase of the temperature in the isallobaric low in the electron beam. In this case the power of incident beam is limited by the value of 140 kW. Thus, under the typical operating conditions when energy of the incident beam of electrons and beam current are with respect 6 GeV and 60 mA, pulse repetition rates it must not exceed 240 imp./s.

The second mode/conditions is utilized, when it is necessary to accelerate alternate beams of positrons and electrons. In this case disk target remains motionless, as it is proved in Fig. 8. the students committee of electrons they control in such a way that it impinge on target for those impulses/momenta/pulses when it is required the beam of positrons, and was passed by target for those impulses/momenta/pulses when is required electron beam. In this steady state the power of the falling/incident to the target electron

DOC = 80069202

PAGE

68

beam is limited to level 30 kA.

For the band 10/o impulses/acmenta/pulses was obtained the output of positrons 20/o. Fig. 9 gives the graph/diagram of the dependence of the maximum peak current of pcsitrons on the pulse repetition rate for both operating modes.

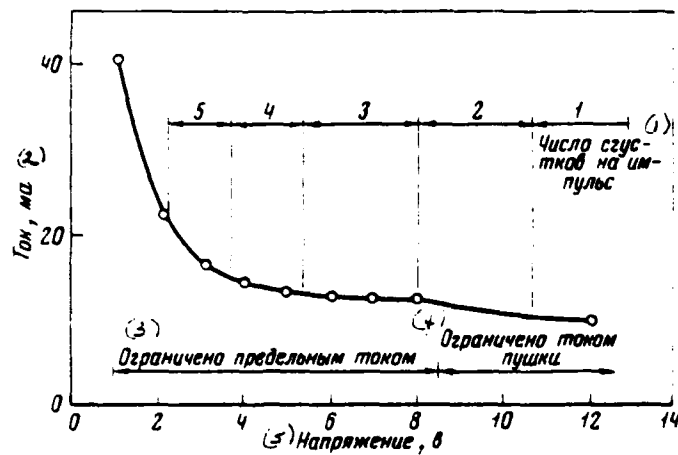


Fig. 6. Dependence of peak beam current on the stress/voltage on the interrupter. Key: (1). Numbers of clusters to the impulse/momentum/pulse. (2). Current, mA. (3). It is limited by limiting current. (4). It is limited by current of gun. (5). Stress/voltage, V.

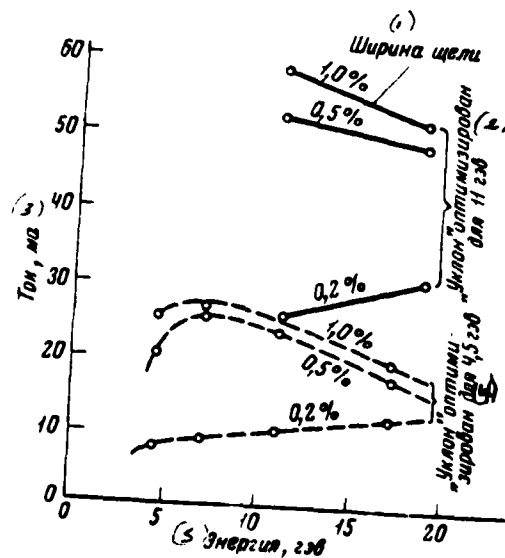


Fig. 7.

Fig. 7. Dependence of peak beam current on energy of three slots of different width.

Key: (1). Width of slot. (2). "gradient" is optimized for 11 GeV. (4). "gradient" is optimized for 4.5 GeV. (5). Energy, GeV.

Page 20.

Were recently carried out the tests, which showed the possibility of the duplication of the output of positrons due to optimization of material and thickness of target. As the new material of target is selected the tungsten. The expected results are shown in Fig. 9.

G. Unification of the halls of control.

Stanford accelerator was initially developed with two halls of the control: one - for accelerator itself (central hall) and one - for the beam-separation system (building of data collection). Entire/all work up to now was accomplished/realized during this dual arrangement/position of controls, and results as a whole were satisfactory. However, for a while it turned out that the effectiveness of formation and beam steering, modulated on the energy, is raised, if all organs/controls, control and the monitoring and measuring instruments are brought together to one place. It is

very probable that will be also achieved/reached the savings due to the decrease of the necessary personnel. After prolonged discussion in the beginning of 1970 was taken the solution about the information of controls into one place which will be they are called the "main hall of control". Location selected the building of data collection. The central hall of control will remain as the auxiliary (in it it will not usually be personnel, besides the personnel of maintenance/servicing, but if necessary for them it will be possible to use).

Each of the available halls of control is equipped with a computer, utilized for checking the blockings, recording of data, adjustment of equipment (magnets of quadrupole lenses) in conformity with the specific requirements for the beam, the inclusion of stand-by klystrons in the case of breakdown of those acting, etc. In the central hall is established/installed computer PDP - 9, while in the building of data collection - computers SIS-925. After unification of signal the control of beam will be transferred between two locations by usual paired leads/ducts. The large part of the remaining signals will be transferred through the line of communications between the computers.

For the savings of place and increase in the operational flexibility in the main hall of control there will be used original

governor [2], named "pushbutton panel". As shown in Fig. 10, the unit of this device/equipment consists of the television screen, on which in the form of rectangular matrix are arranged/located the names controllable/controlled/inspected parameters or devices/equipment. The system of piezoelectric gauges and receivers, arranged/located on the perimeter of screen, determines two orthogonal sets of narrow acoustic beams on the surface of screen. The radiated frequency is about 8.2 MHz. The point of intersection of two-any beams designates the location of the "knob/button" with pressure of which is interrupted/broken acoustic beam and thereby by means of computers SDS-925 is accomplished control. Using the means of the programming of computers, operators can instantaneously reprogram both indication and functions of "knobs/buttons". Thus, one and tighter "pushbutton panel" can be utilized for executing the most diverse control functions.

Work on the association of the halls of control is conducted even now; its completion is planned on 1971.

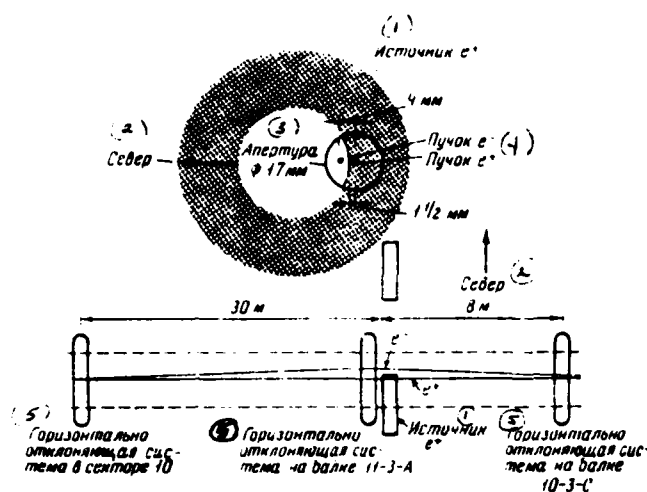


Fig. 3. Diagram of the work of positron source in obtaining of the alternate electronic and positron beams.

Key: (1). Source. (2). North. (3). Aperture. (4). Beam. (5). Horizontally deflecting system in sector.

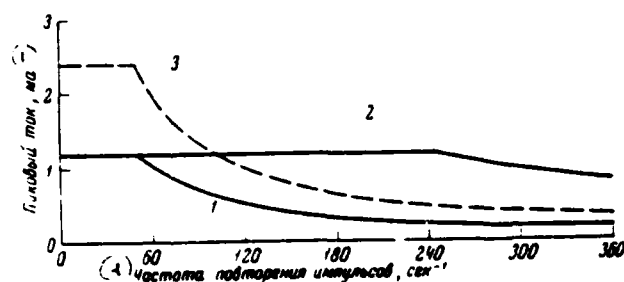


Fig. 9. Dependence of maximum peak current of positrons on pulse repetition rate for two modes of operation (for band of energy 10/0). 1 - in the mode/conditions of the alternate beams; 2 - for the rotary disk; 3 - expected results for the tungsten target.

Key: (1). Peak current, mA. (2). Pulse repetition frequency, s⁻¹.

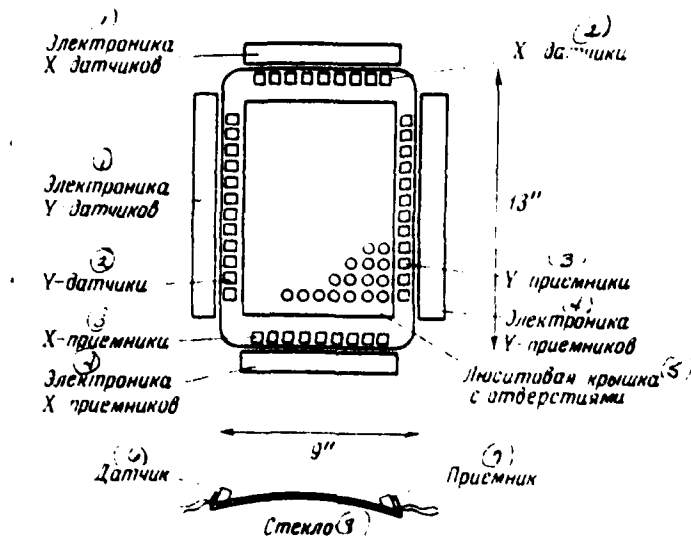


Fig. 10. "pushbutton panel".

Key: (1). Electronics of X-sensors. (2). sensors. (3). receivers. (4). Electronics of Y-receivers. (5). Lucite cover/cap with openings/apertures. (6). Sensor. (7). Receiver. (8). Glass.

Page 21.

III. Experience of operating klystrons.

After approximately 4 years of operation is comprised sufficiently good representation about the characteristics and the service life of powerful klystrons. However, thus far still it is not possible to accurately indicate average life, since the steady-state

mode/conditions in the accelerator is not yet achieved/reached, i.e., in proportion to operation the service life of lamps continues to grow/rise.

Lamps of the initial assembly of accelerator had a peak nominal power of 21 MW and average of 22 kW. Lamps worked with the stresses/voltages of beam ~245 kV, duration of the pulse of ~2.5 μ Sec this to pulse repetition rate 360 imp./s. Is gradually accomplished/realized the plan/layout of an increase in the energy of accelerator by a method of replacing the failed lamps 21 MW by the lamps with a power of 30 MW (see section U. A).

Since the beginning of the work in 1966 through 30 September, 1970, the total duration of the work of klystrons was 4787100 hours. Within this period occurred 302 failures. Thus the accumulated mean time between the failures for the duration of the period indicated was $4787100/302 \approx 15800$ hours. As can be seen from Fig. 11, the accumulated mean time between the failures was retained approximately stable at the level of 15000 hours in last three years. On the contrary, the accumulated average life to the failure increased within the same period from 1060 to 5810 hours and at present it continues to grow/rise.

Fig. 12 gives time allocation of the work of all working on the

accelerator lamps. From the graph/curve it is possible to see that more than 400/o (109) lamps of accelerator served more than 15000 hours. Almost 150/o of lamps studied more than 20000 hours, i.e., from the moment/torque of the beginning of work of the accelerator in 1966. From the analysis of the data about the distribution cut-of-order lamps according to the service lives it is evident that the peak of the distribution of failures falls to relatively low service life: about 250/o cut-of-order lamps served 1000 hours and less.

Characteristics and service life of klystrons are one of the most gladdening results of the work of Stanford accelerator at present. Reached in this region results considerably exceeded preliminary evaluation, made during the design of accelerator.

IV. State of ring.

During September 1970, with the delay by several years, was approved the project of the ring of Stanford accelerator. It is one ring of magnets in which in the aluminum vacuum chamber/camera rotate in opposite directions the electron beams and positrons. The configuration of this ring, named SPEAR (Stanford positron-electronic asymmetric ring), the same as configuration of one of two intersecting rings of the earlier construction/design (see Fig. 13).

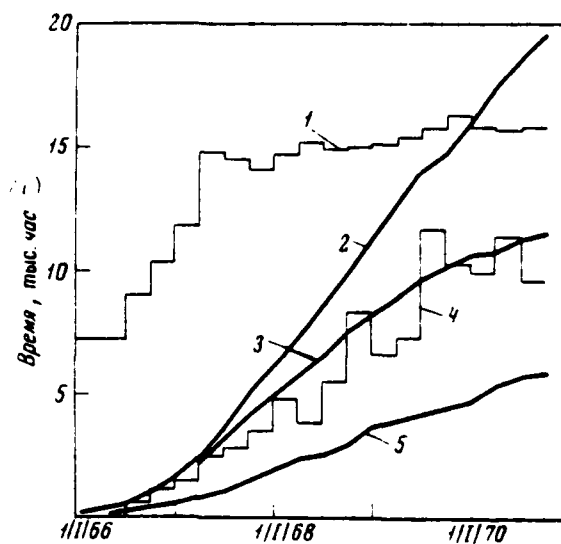


Fig. 11. Statistics of the work of klystrons. 1 - accumulated mean time between the failures; 2 - accumulated operating time to one socket/seat; 3 - mean time of the service of active valves; 4 - average life to the failure; 5 - accumulating average life on failure.

Key: (1). Time, thousand hours.

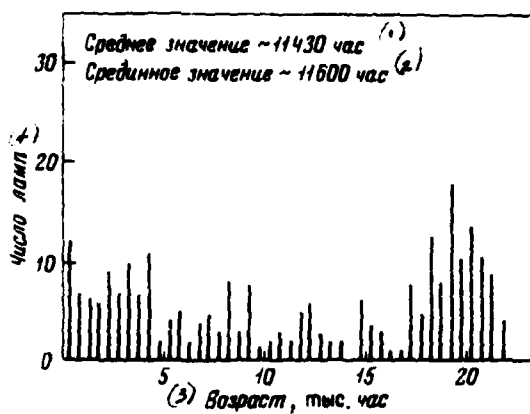


Fig. 12. Distribution of active valves according to operating time on 1 October, 1970.

Key: (1). Average/mean value ~11430 hour. (2). Mean value ~11600 hour. (3). Age, thousands of hours. (4). Number of lamps.

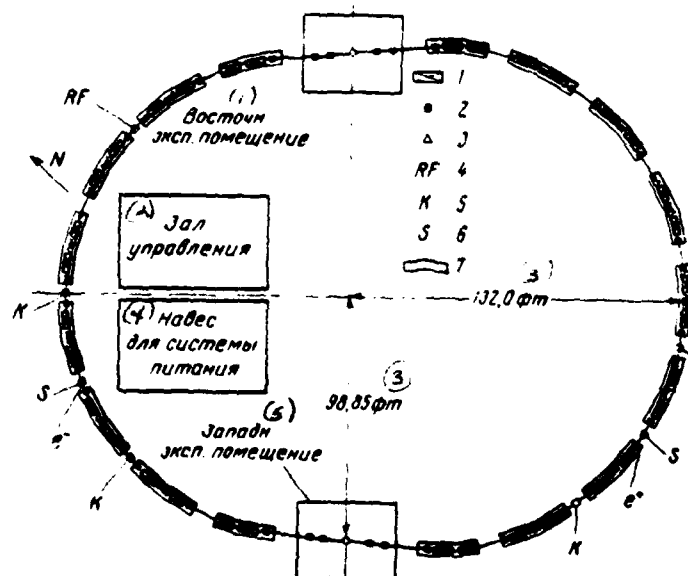


Fig. 13. Diagram of Stanford positron-electronic asymmetric ring (SPEAR). 1 - turning up magnets; 2 - quadrupoles; 3 - sextupoles; 4 - high-frequency resonators; 5 - kickers; 6 - septum-magnets; 7 - moduli/modules.

Key: (1). It is eastern. exp. location. (2). Hall of control. (3). feet. (4). Mounting fixture for power-supply system. (5). Is Western. exp. location.

Page 22.

The expected luminous density (with the energy of each beam 2 GeV) during the collision of particles in the interaction region with the "low beta ones" is $10^{32} \text{ cm}^{-2} \text{ s}^{-1}$.

First energy of ring will be limited by the value of 2.5 GeV, however, after increasing an input power and a number of resonators, it is possible to raise energy to 4.5 GeV. Construction/design allows/assumes also the subsequent installation of the second intersecting ring.

For dealing with the instability, which appeared on the previous rings, are introduced different devices/equipment. They encompass the system of rapid feedback, electrical quadrupole, sextupole and

cctupole lenses.

Each of the interaction regions is arranged/located directly above the volume with a length of 12 m and with a width of 10 m, which ensures under the axis/axis of bundle vertical clearance 3 m. Above the axis/axis of beam also is provided three-meter vertical clearance. In the volume of interaction will be established/installed the equipment, provided for by the experimental program SPEAR.

The cell of the magnetic structure SPEAR with divided functions consist of three quadrupoles and 2 deflecting magnets with the zero gradient. In all are 11 such standard cells and 2 cells of introduction/input, each of which contains 6 deflecting magnets and 9 quadrupoles. Thus, in the ring only of 34 deflecting magnets even 51 quadrupoles. The maximum field of the deflecting magnets is 6.3 kg (with 2.5 GeV), and maximum gradient in the quadrupoles is equal to 590 G/cm. All magnets will be prepared from the sheet rolled steel. In the coils will be used aluminum lead/duct, since experiment of Stanford accelerator showed that the aluminum coils are much cheaper than copper ones.

Particles will be injected into the ring with the energy 1.5 GeV. Since the extent of the orbit of ring comprises 220 m, times of one revolution equally to 0.73 μ s; thus, frequency of the rotation is

equal to 1.36 MHz. High-frequency system operates at a frequency of 42.35 MHz - to 31st harmonic of the frequency of rotation. At first 200 kW (of maximum) high-frequency power will be supplied into one resonator; this will ensure peak radio-frequency voltage 300 kV.

Two-bundle instability, apparently, will make it possible to fill only from 1 to 3 stability region, which are moved on the ring, they are divided between themselves by interval in 24 ns. The injected impulse/momentum/pulse must occupy ~120 or 8 ns. Since the time of one revolution is equal to 0.73 μ s, for the time of each pulse of accelerator by the duration of 1.6 μ s it is possible to fill only 2 groups of regions of stability, divided between themselves by the interval of 0.73 μ s. Fig. 14 depicts typical pattern of injection, when there are two groups of 3 stability regions in each. After each impulse/momentum/pulse of injection it is necessary to 50 ns for damping of betatron and synchrotron oscillations. This limits the speed of the filling with the frequency of 20 imp./s. The time of filling for the electrons and the positrons comprises respectively about 2 and 6 min to the ampere of the circulating beam.

The aluminum vacuum chamber/camera of the ring with a width of 15 and height of 4.4 cm is shown in Fig. 15. Is provided for water cooling for the heat removal, which separates during the absorption of synchrotron radiation. In the chamber/camera will be mixed the

DOC = 80069202

PAGE

8582

special titanium ionic pumps, which with the work will utilize a magnetic field of the magnets or ring. During the preliminary tests of these pumps on nitrogen they were achieved/reached pumping speed of 500 l/s to the meter of pump.

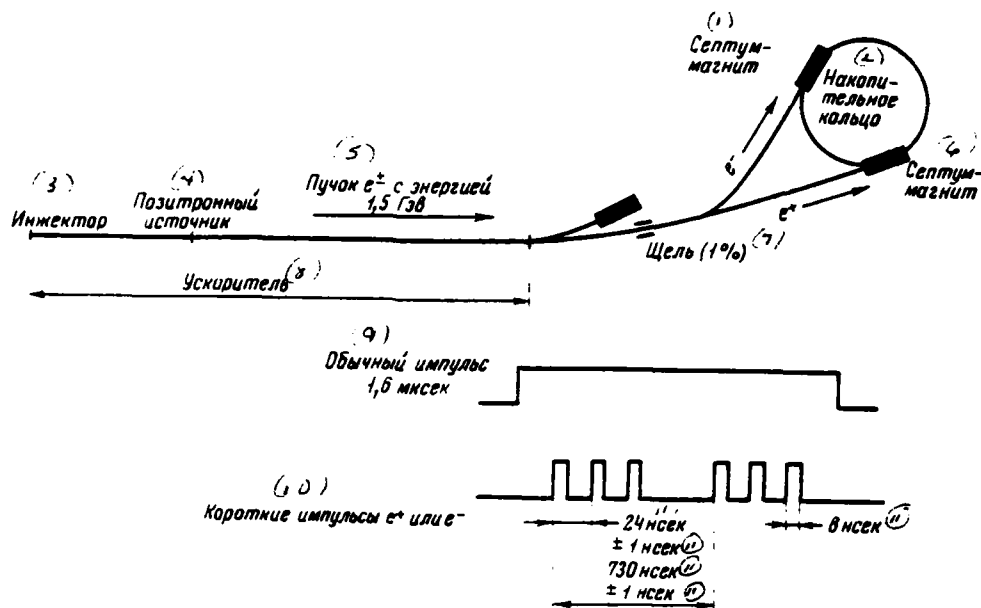


Fig. 14. Diagram of injection into the ring.

Key: (1). septum-magnet. (2). Ring. (3). Injector. (4). positron source. (5). Beam e^+ with energy 1.5 GeV. (6). septum-magnet. (7). Slct. (8). Accelerator. (9). Usual impulse/momentum/pulse 1.6 μ s. (10). short pulses e^+ or e^- . (11). ns.

Page 23.

Are given below the basic parameters of the ring:

A number of rings ... 1 (it is possible to increase to two).

DOC = 30069202

PAGE

84

Sizes/dimensions of ring ... 60x74.

Colliding particles ... \bar{e} and e^+ .

Maximum energy of the particles ... of 2.5 GeV (it is possible to increase to 4.5).

Number of volumes of interaction ... 2.

Luminous density ... of $10^{32} \text{ cm}^{-2} \text{ s}^{-1}$.

Beam current ... 0.5 A (in each beam).

Number of particles in the beam ... 2×10^{12} .

Number of clusters in the beam ... 2.

Distance between the clusters in the time ... 24 ns.

Frequency of hf system ... 42.35 MHz.

Frequency of revolution ... 24 ns.

DOC = 30069202

PAGE 385

Time of the access ... 0.73 μ s.

Number of resonators ... 1.

HF power (maximum) ... 200 kW.

Peak hf voltage ... 300 kV.

Total number of the deflecting magnets ... 34.

Total number of quadrupoles ... 51.

Total pumping speed ... 1.7×10^4 l/s.

Pressure with the beam ... 5×10^{-9} torus.

Time of the filling ... with ϕ sin.

Planned date of obtaining the first beam ... 1972.

More detailed description can be found in the literature [3].
The beginning of the construction of ring is projected/designed in

AD-A089 303

FOREIGN TECHNOLOGY DIV WRIGHT-PATTERSON AFB OH
TRANSACTIONS OF THE ALL-UNION CONFERENCE (2ND) ON CHARGED PARTI--ETC(U)
JUL 80 A L MINTS, A A KOMAR, A A VASIL'YEV

F/G 20/7

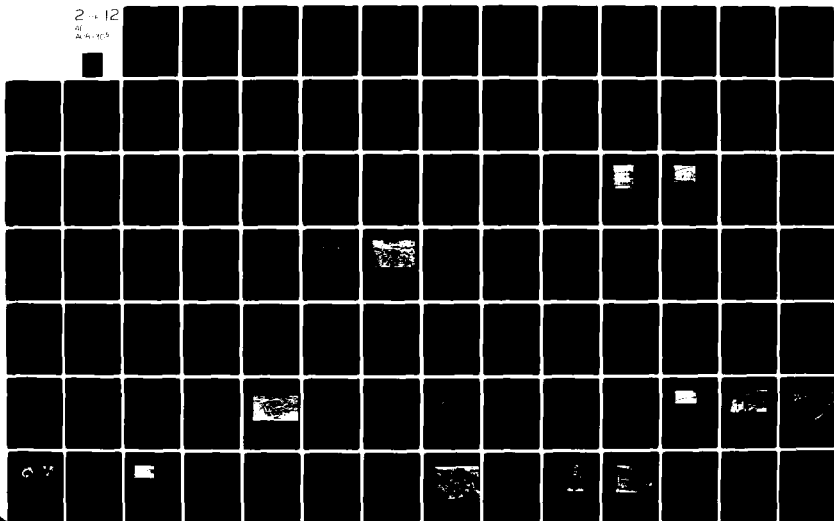
UNCLASSIFIED

FTD-ID(RS)T-0692-80

NL

2 x 12

24 x 36





the latter/last block of 1970, and completion - in 1972.

V. Plans for future.

A. More powerful klystrons.

As it was mentioned in section III, out-of-order 21 MW - klystrons were replaced by more powerful/thicker 30 MW - lamps. At the present time such more powerful lamps equipped 4 sectors of 30. At the existing failure rate for the full/total/complete replacement of less powerful lamps it will be required from 2 to 3 years. This process is not boosted/forced, since from the considerations of savings it is desirable to utilize a full/total/complete service life of the existing lamps before replacing them. Furthermore, it is expedient to obtain a good information about the service lives for several new lamps before carrying out a full/total/complete rearrangement to the work with larger power.

An increase in the power output of klystrons was the consequence: 1) the optimization of drift distances and construction/design of resonators; 2) improvement in the conditions of focusing along the length of lamp even 3) the work of lamps with somewhat more high voltage (265 kV). This increased stress/voltage is located within the possibilities of the modulators of klystrons.

An increase in energy of electrons (in MeV) that called by the field of one klystron, composes approximately/exemplarily $20 \sqrt{P}$, where P - peak power output of klystron, expressed in MW. For the available by 21 MW klystrons (with 50/o of losses in the waveguide between the klystron and the accelerator) an increase in energy is ~90 MeV to the klystron. The corresponding increase in energy for 30 MW of klystrons with the same assumptions will be 107 MeV. With work 240 (from total number 245) klystrons on 30 MW the expected energy of particles (with the low current will achieve ~25 GeV).

B. Possibilities of an improvement in the coefficient of the use of cycle and increase in the energy of beam.

Investigation of the possibility of the alteration of two-mile accelerator in that superconducting (see section V C) unconditionally represent the most ambitious and far going projects of the Stanford center of linear accelerators to the future. However, taking into account that the realization of these plans/layouts will engage 8-10 years (or more), are examined other ideas of improvements, less expensive and requiring are less than the time for the realization. In essence these ideas concern either an improvement in the coefficient of the use of a cycle or an increase in the energy of

accelerator, or increases in both the parameters indicated. The improvements, discussed in this section, utilize the existing technique of accelerators and do not require any fundamental investigations. An improvement in the parameters, of course, will be in this case smaller than for the superconducting accelerator.

1. Increase in coefficient of use of cycle.

For an improvement in the coefficient of the use of a cycle are examined three diverse variants. They all give some decrease of energy of beam. The first and easiest method consists in cycling on one half the modulators $1/720$ seconds after feed to the second half. Injector will work with the repetition frequency 720 imp./s. It is obvious, the coefficient of the use of a cycle in this case will be doubled (i.e. maximum repetition frequency will be 720 imp./s instead of the present of 360 imp./s), but energy of beam twice it decreases (maximum energy will be ~ 10 GeV instead of ~ 20 GeV at present). For the realization of this operating mode are necessary relatively simple changes in the injector, the system of radio-frequency drive, the system of check of the beam and in the system of the pulse deflecting magnets at the end of the accelerator.

The second method of an increase in the duty factor consists in a change in the interior conjugations in the modulator of power

klystron, so as to two existing pulse-shaping circuits would be connected in series, but not in parallel. During the development of the modulators of Stanford accelerator were first provided for the two parallel diagrams of formation for each modulator, since it was not thyatrons, capable maintain full load. Therefore were utilized two thyatrons, each of which commutated one of the parallel diagrams.

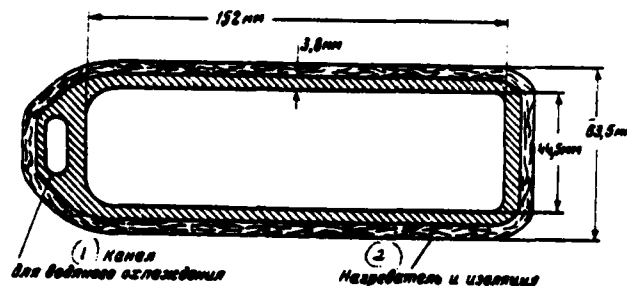


Fig. 15. Section of the aluminum chamber/camera of ring.

Key: (1). Channel for water cooling. (2). heater and insulation/isolation.

Page 24.

Subsequently, when appeared the thyratrons, capable individually to maintain full load, two parallel diagrams began to be commutated by one, more powerful thyatron. Thus, it will not present special difficulties to include/connect both diagrams to consecutively/serially and commutate them with the aid of the available thyatron. As a result will occur the duplication of duration of high-frequency pulse from the klystron (i.e. from 2.5 to 5.0 μ s). Since the time of filling of accelerator is 0.8 μ s, the duplication of the duration of high-frequency pulse will lead to an increase in the coefficient of the use of a cycle 2.5 times. On the other hand, the stress/voltage, supplied to the klystron, descends to

-200 kV, which leads to peak exit power ~12 MW. Energy of accelerator falls into $\sqrt{2}$ once, i.e., to ~14 GeV. The series connection of two diagrams instead of the parallel doubles the impedance of the diagram (i.e. impedance grows/rises from 6 to 12 ohms). This will lead to the disagreement/mismatch between the impedance of diagram and the impedance of klystron, given to the repeated recirculation of beam during many (~120) revolutions until from the modulator of klystron enters following starting (360 amp./s) impulse/momentum/pulse [4].

Using the first method each modulator is supplemented by the second thyatron, identical to the first, as shown in Rich. 17. First thyatron and pulse-shaping circuit are started and the corresponding high-frequency pulse of klystron causes the acceleration of beam in the accelerator. At the end of the accelerator the beam is deflected/diverted on 180° (see upper half of Fig. 18), or on 360° (lower half of Fig. 18), and is supplied to the injector end/lead of the accelerator where it again is deflected/diverted and is injected into the accelerator, passing the second the cycle of acceleration.

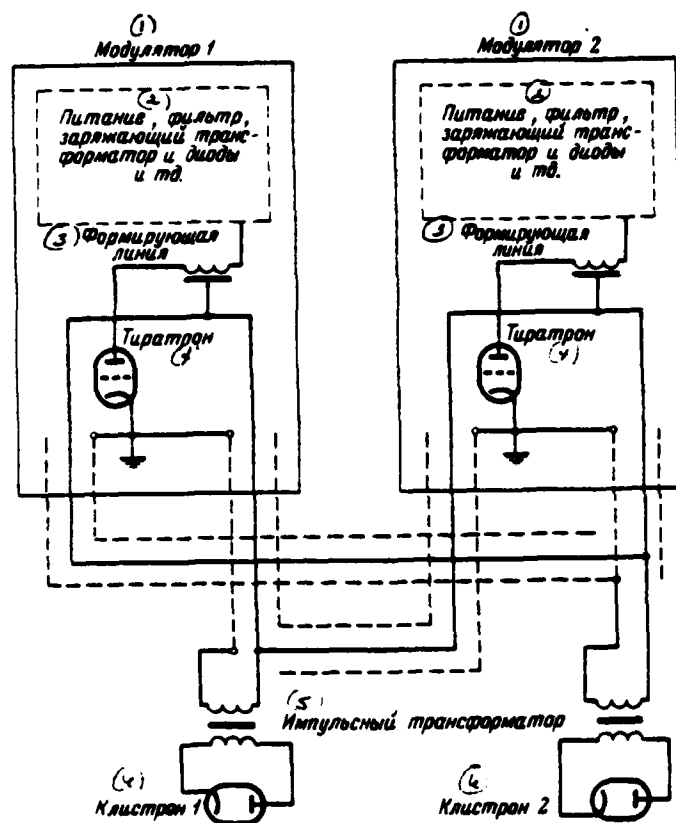


Fig. 16. Diagram of the parallel connection of the pairs of klystrons and modulators for the duplication of duty factor.

Key: (1). Modulator. (2). Supply, filter, which loads transformer and diodes etc. (3). forming line. (4). Thyatron. (5). Pulse transformer. (6). Klystron.

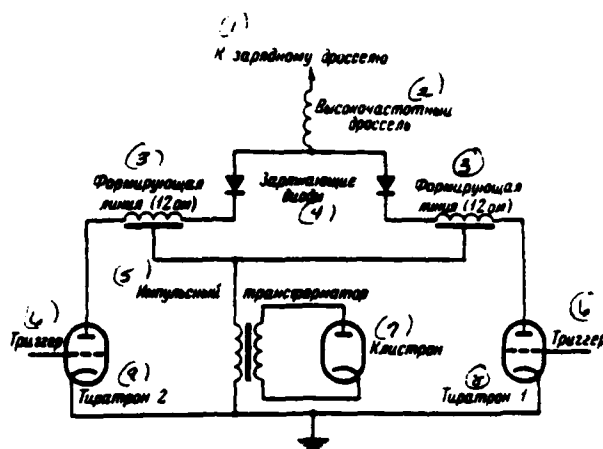


Fig. 17. Modulator circuit, used with first method of increasing energy of beam.

Key: (1). To the charging cacke. (2). High-frequency choke. (3). Forming line (12 ohms). (4). Loading diodes. (5). Pulse. (6). Trigger. (7). Klystron. (8). Thyatron.

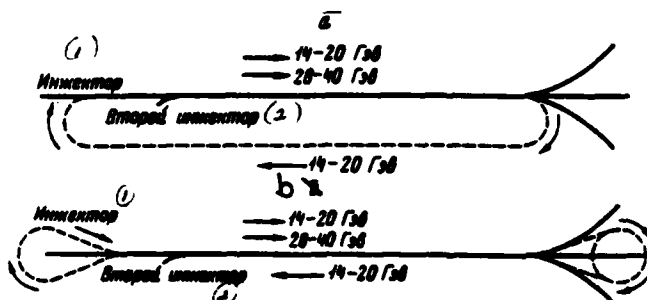


Fig. 18. Two versions of recirculation of electron beam a) system "racetrack"; b) system "two drops".

Key: (1). Injector. (2). Second injector.

Page 25.

Since the time of flight of the path of recirculation is 20 μ s, modulators must again start ~ 20 μ s after the first impulse/momentum/pulse. This is accomplished/realized by a method of the starting/launching of the second thyatron and pulse-shaping circuit at the appropriate moment of time. The voltage pulses, supplied to the klystron, have an amplitude 200 kV, which provides effective power ~ 12 MW. Thus, an increase in energy with the low current with each passage through the accelerator composes ~ 15.8 eV. The energy losses, caused by synchrotron radiation during two rotations on 180° (or on 360°) at the end/lead of accelerator, comprise respectively 0.13 and 0.26 GeV (with the turning radius 50 m). Thus, a total increase in energy with the low current in this recirculating diagram will be 31.5 or 31.3 GeV, depending on type it is selected the deflection system. Load on the beam in some measure will lower these values; for two passages through the accelerator a reduction in the energy will compose 0.07 GeV/nA.

Using the second method the pairs of modulators and klystrons are connected in parallel as in the third method of increasing the coefficient of the use of a cycle, described above (Fig. 16). During

the starting/launching of the first modulator each of two parallel klystrons puts out ~12 MW. Approximately in 20 μ s, after beam finished recirculation, is started the second modulator, and two klystrons put out the second group of high-frequency pulses with a power ~12 of MW. Total increase of energy the same as for the first recirculating diagram.

Third recirculation method assumes the retention/preservation/maintaining electrons in the recirculating ring for the duration of full wave (2.78 ns) between the normal impulses/momenta/pulses of modulators [4]. This means that the system of the transportation of beams must being able hold down/retain beam and preserve its characteristics in the transverse and longitudinal phase space for the duration of this period of time. Since the beam will billeting but lose energy as a result of the radiation/emission on rotation in ends of accelerator, should be provided some method of restoring this energy. This restoration is intended to carry out by means of 4-6 superconducting accelerating sections, supplied each of 20 kW klystron. these sections will be arranged/located on one of the rotations and will work in the mode/conditions of continuous oscillations. Since the klystrons during each impulse/momenta/pulse will put out the total power (~24 MW), a total increase in energy with the low current in this recirculation diagram will compose 31.5 or 31.3 GeV, and dependences on the type of the selected deflection

system. Beam load to a certain degree will lower these values; for two passages through the accelerator a reduction in the energy will compose 0.07 GeV/MA.

Using the second method the pairs of modulators and klystrons are connected in parallel as in the third method of increasing the coefficient of the use of a cycle, described above (Fig. 16). During the starting/launching of the first modulator each of two parallel klystrons puts out ~12 MW. Approximately through 20 μ s, after beam finished recirculation, is started second modulator, and two klystrons put out the second group of high-frequency pulses with a power ~12 of MW. Total increase of energy is the same as for the first recirculation diagram.

Third recirculation method assumes the retention/preservation/maintaining electrons in the recirculating ring for the duration of full wave (2.78 ns) between the normal of pulses of modulators [4]. This means that the system of the transportation of beam must being able to hold down/retain beam and preserve its characteristics in transverse and longitudinal phase space for the duration of this period of time. Since the beam will killeting but lose energy as a result of the radiation/emission on rotation in the ends/leads of the accelerator, should be provided some method of restoring this this energy. This restoration is

assumed to accomplish by means of 4-6 superconducting accelerating sections, supplied each of 20 kW klystron. These sections will be arranged/located on one of the rotations and will work in the mode/conditions of continuous oscillations. Since the klystrons during each impulse/momentum/pulse will put out the total power (~24 MW), a total increase in energy with low current after two passages through the accelerator will be ~40 GeV.

In Table 3 are integrated different discussed above projects, which concern an increase in the duty factor and energy of beam. None of the diagrams moved further theoretical stage. Thus far still there are no detailed estimations of expenditures. Is necessary supplementary investigation in order to determine, do deserve any of these methods of formal review.

C. Reconstruction of accelerator into that superconducting.

For the latter of one-and-a-half year was made investigation [5, 6] of the possibility of the alteration of two-mile accelerator into that superconducting. The basic goal of this program is the achievement of energy of the beam 100 GeV and coefficient of the use of cycle 60/o. With the smaller energies a reduction in the high-frequency losses in the accelerator would make it possible to achieve higher coefficients of the use of a cycle without an increase

in the power of cooling system. For example, with the energy 26 GeV the coefficient of use can achieve 1000/c. Are given below the parameters of the two-mile superconducting accelerator with the energy 100 GeV.

Table 3. The summary table of different diagrams of an increase in the coefficient of the use of cycle and energy of beam.

Назначение (1)	Способ (2)
(8) Увеличение коэффициента использования цикла	(9) 1. Попеременное включение двух групп модуляторов-клистронов с частотой 360 имп/сек (10) 2. Последовательное включение схем модулятора вместо параллельного (11) 3. Два смежных модулятора питают поочередно два смежных клистрона, включенных параллельно
(12) Увеличение энергии пучка	(13) 4. Добавление в модулятор второго тиратрона, включаемого через 20 мксек после первого. Пучок совершает одну рециркуляцию (14) 5. Два параллельно соединенных модулятора-клистрона, как в 3). Пучок совершает одну рециркуляцию (15) 6. Пучок рециркулирует около 120 раз (2,78 мсек) и ускоряется дважды при полной мощности клистрона

Continuation of
Table 3.

Пиковая мощность кlyстро- на, Мвт (3)	Длитель- ность импульса, мксек (4)	Частота слитова- ния им- пульсов пучка, (5) имп/сек	Степень повышения коэффици- ента ис- пользова- ния цикла (6)	Максималь- ная энер- гия пучка при токе 30 ма (7)
21	1,6	720	2	10-11
12	4,8	360	2,5	14-15
12	1,6	720	2	14-15
12	1,6	360	1	23-30
12	1,6	360	1	28-30
24	1,6	360	1	40-42

Key: (1). Designation/purpose. (2). Method. (3). Peak power of klystron, MW. (4). Duration of pulse μ s. (5). Pulse repetition rate of beam, imp./s. (6). Degree of increase in coefficient of use of cycle. (7). Maximum energy of beam with current 30 mA. (8). Increase in coefficient of use of cycle. (9). Alternate inclusion/connection of two groups of modulator-klystrons with frequency of 360 imp./s. (10). Series connection of diagrams of modulator instead of parallel. (11). Two adjacent modulators supply alternately two adjacent klystrons, connected in parallel. (12). Increase in energy of beam. (13). Addition to modulator of second thyatron, included 20 μ s

afterward first. Beam completes one recirculation. (14). Two parallel-connected modulator-klystrons as into 3). Beam completes one recirculation. (15). Beam recirculates about 120 times (2.78 ms) and is accelerated twice at total power of klystron.

Page 26.

Working frequency ... of 2856 MHz.

Length ... of 3000 m.

Linear shunted resistance (?) ... 1.72×10^{13} Ω/cm .

Quality (Q) ... 4.0×10^9 .

Energy (maximum) of ... 100 GeV.

Coefficient of use of cycle ... 1/16.

Peak beam current ... 48 μA .

Average beam current ... 3 μA .

Peak power of the beam ... 4.8 MW.

DOC = 80069202

PAGE 24
191

Average/mean power of the beam ... 0.3 MW.

Number of klystrons ... 240.

The peak power of the klystron ... 20 kW.

Average/mean power of the klystron ... 1.25 kW.

Type of high-frequency system ... Travelling wave with the
high-frequency feedback.

Number of sections of accelerator ... 480.

Length of the sections of the accelerator ... 6 m.

Time of the filling (to 6J.20/0) ... 18 ns.

Scattered in the accelerator power ... 1200 W (4.0 W/m).

Duration of hf pulse ... 0.25 s.

Duration of the beam burst ... 0.24 s.

Interval between hf impulses/moments/pulses ... 3.75 s.

Attenuation factor of accelerator (γ) ... 37.9×10^{-7} neper.

Attenuation factor of feedback (γ) ... 3.7×10^{-7} neper.

Coefficient of bridge (q) ... 0.546×10^4 .

Circulating power P_0 with γ_{max} ... 54.6 MW.

The estimations of expenditures [5] (based on the values of 1969) according to the alteration of Stanford accelerator into superconducting lie/rest in the range from 67 to 79 mln. dollars; total cost/value depends on the feasibility of different versions examined. The cost estimate encompasses 25c/c of unforeseen flow rates and is conducted for the operating frequency of 2856 MHz.

In Stanford are conducted materials research and methods of treatment for the purpose of achievement in the practical constructions/designs of the gradients of 33 MeV/m and small high-frequency losses. At present best of the materials, apparently, is niobium. The connection of components is accomplished/realized by

welding by an electron beam. Welding is conducted from inside of construction/design for obtaining the smoother internal surface. After welding is conducted the etching in the pickle, vacuum annealing by 1600-2000°C, repeated etching and then repeated annealing at a high temperature. Due to the technical limitations are at present prepared and tested only small (for X-range) resonators. Annealing is conducted by induction heating in the quartz vacuum chamber/camera. At present are made installations for welding and treating the resonators of larger size/dimension. They will make possible to connect and to work resonators and short constructions/designs for S - range. The manufactured new furnace will have a heating zone in diameter 5 inches and by the length of 8.5 inches. In this device/equipment it is possible to obtain temperature of 2000°C and pressure 10^{-9} torr.

Measurements for the resonator of X- range for the wave TE_{011} at a temperature of 1.85°K gave value of Q, equal to 3.4×10^9 , and permissible magnetic field ~ 700 G. The recalculation of above-indicated value, $f^{-1/2}$ for the frequency of 2856 MHz proportionally gives value $Q \sim 2.5 \times 10^{10}$. This approximately is 6 times higher than computed value (see above). However, the permissible magnetic field must be brought to ~ 1000 G so that would become possible the work with the calculated gradient of 33 MeV/m.

With the aid of two different programs were made on the computers the calculations of the optimum forms of resonator for the superconducting accelerator. In one of these programs [7] the properties of the structures of waveguide linear accelerators are calculated by the method of functional field expansion instead of the net point method. Another program [8] is the new version on FORTRAN of program LALA [9, 10], comprised in Los-Alamos scientific laboratory. This program is especially convenient for the structures with the standing wave; for the waveguide structures it must be somewhat altered. During the investigation of the optimization of resonators in Stanford was paid special attention to the minimization of the ratios of the peak values of electrical and magnetic fields to the effective ones, since these relations are the basic factors, which are determining the maximum attainable gradients. The obtained as a result of investigations configuration of resonator is shown in Fig. 19. For this construction/design the ratio of peak electric field to the effective is equal to 1.66, and the ratio of peak magnetic to the peak electric field - $31 \text{ G}/(\text{MeV/m})$.

Among other investigations on the superconductivity, made in Stanford, should be noted: 1) the determination of maximum fields and remaining losses; 2) nonlinear effects in the strong fields; 3) the effects of radiation damage; 4) the autoelectric emission; 5) the thermal conductivity of materials even 6) the deformation of

resonators, caused by high-frequency field.

In parallel with the examined above fundamental investigations is constructed the short experimental accelerator, known by the name "Leapfrog" ("leap-frog"). The accelerator "Leapfrog" is a composite part of waveguide resonance ring.

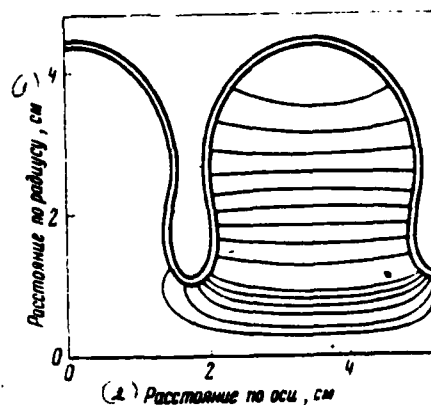


Fig. 19. Form of resonator, which ensures a small relation of maximum electrical and magnetic field and effective.

Key: (1). Radial distance, see (2). Distance along the axis, see

Page 27.

The selection of such construction/design was caused by the fact that the ratio of peak to the effective field for this system to 20-30c/c is lower than in the practical systems with standing waves. The accelerator "Leapfrog", which has the length of 52.5 cm (15 resonators), is depicted within the Dewar container with liquid helium in Fig. 20. With rated current (48 μ A) calculated energy "Leapfrog" is ~ 17 MeV. The beginning of work of "Leapfrog" only with the radio-frequency voltage (stage 1) is planned on the end/lead of calendar 1970. With the successful execution of stage 1 in, 1972,

will be begun the work with beam of Dewar's inside new, horizontal vessel.

REFERENCES

1. G.A. Loew, R.H. Helm, H.A. Hoff, R.F. Kontz, R.H. Miller. Linac beam interactions and instabilities.

Transactions of UP of international conference on the charged particle accelerators of high energies, Vol. 2. Publishing house of AN of Armenian SSR Yerevan, 1970, page 229.

2. D. Fryberger and R. Johnson. Private communication.
3. B. Richter. The Stanford storage ring - SPEAR, Report N SLAC-PUB-780, Stanford Linear Accelerator Center, July, 1970.
4. W.B. Herrmannsfeldt. Internal memorandum, Stanford Linear Accelerator Center (July 13, 1970).
5. Feasibility Study for a Two-Mile Superconducting Study. Stanford Linear Accelerator Center (revised December 1969).
6. P.B. Wilson, R.B. Neal, G.A. Loew, H.A. Hogg, W.B. Herrmannsfeldt, R.H. Helm, and M.A. Allen. Superconducting accelerator research and development at SLAC, Particle Accelerators, July 1970.
7. R. H. Helm. "Computation of properties of traveling-wave linac structures." 1970 Proton Linac Conference, NAL, Batavia, Illinois.
8. W.B. Herrmannsfeldt, R.H. Helm, R.R. Cochran. Electromagnetic and mechanical properties of niobium cavities for a superconducting electron accelerator. 1970 Proton Linac Conference, NAL, Batavia, Illinois.
9. H.C. Hoyt. Rev. Scient. 1966, 37, 755.
10. W.F. Rich and M.D.J. MacRoberts. Report N LA-1219, Los Alamos Scientific Laboratory, September, 1969.

Discussion.

A. A. Komar. There are whether any periods for the translation/conversion of accelerator into the superconducting version with the energy 100 GeV?

R. Nil. The optimistic periods of translation/conversion are approximately 8 years.

A. V. Mishchenko. How frequently the accelerator does go out of order and how much does it during this stay?

R. Nil. Work occurs during three weeks, then one week of preventive maintenance. 80% of time we work with the team.

A. A. Kolomenskiy. Is how the position of matters concerning the translation/conversion of accelerator Mark III on 1 GeV in the superconducting version?

R. Nil. It is assumed that the work on transition must be completed toward the end of the year. For this will be required the displacement of accelerator of one location into another, which is arranged than lower existing. These works have already been begun; in particular, is transferred the equipment, which concerns preliminary acceleration.

A. A. Kolomenskiy. How it is proposed to solve stability problem of beam in the superconducting version of accelerator?

R. the Nile. In the superconducting version it will be necessary to carry out an automatic check of several parameters: first, quantity of reflected energy in the ring of feedback, in the second place, it is necessary to regulate the value of the maximum power, going in the forward direction into the same loop. Then it is necessary to regulate the amount of the power, transferred in this ring of feedback, with respect to the beam. All this will be regulated automatically and simultaneously.

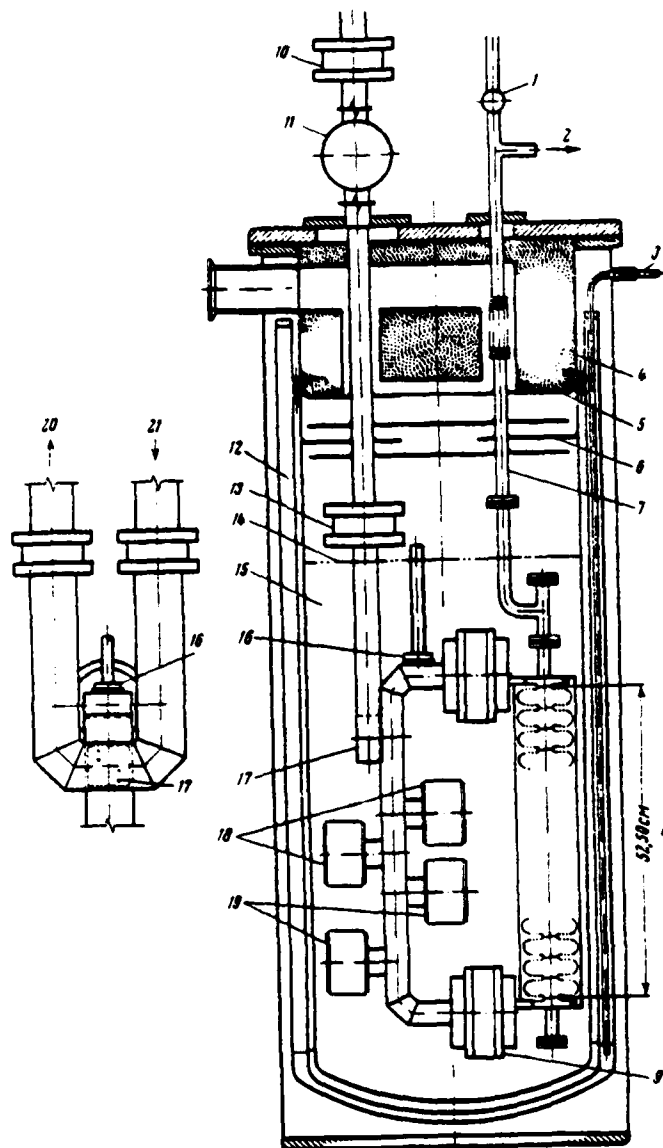


Fig. 20. Accelerator "Isapiroy" in Dewar. 1 - gate; 2 - to manometer; 3 - feed of liquid nitrogen; 4 - sample from the the foam polyurethane; 5, 6 - screens; 7 - evacuation of accelerator; 8-15 -

resonators; 9 - choke joint; 10 - high-frequency window; 11 - evacuation of high-frequency system; 12 - liquid nitrogen; 13 - high-frequency window; 14 - level of helium; 15 - liquid helium; 16 - monitoring instrument; 17 - coupler; 18 - tuning elements; 19 - phase-shifter; 20 - high-frequency load; 21 - klystron.

Page 28.

4. Work of proton synchrotron to the energy 70 GES.

Yu. M. Ado, A. A. Zhuravlev, V. I. Zaytsev, A. A. Kardash, K. P. Myznikov, E. A. Myae, A. A. Naumov, V. Ya. Pisarevsky, O. N. Radin, V. G. Rogozinskiy, A. ~~Y~~ A. Khanchikyan, B. K. Shembel', K. A. Yakovlev.

(Institute of high-energy physics).

The works, conducted on the accelerator, first of all are connected with increase in the reliability of the work of technological systems, creation: the conditions of the simultaneous setting of several physical experiments, with an improvement in the quality of the brought-out beams of particles, with an increase in the intensity of the beam of the accelerated protons. It is communicated below about the basic works, carried out in last year. On certain of them are represented separate reports [1, 2].

Investigations on particle dynamics are conducted in essence for

two sections of the accelerative cycle: a) upon the injection and in the beginning of acceleration; b) in the large fields. The first section is interesting from the point of view of the prospects for an increase in the intensity, and by the second - it is important for the beam shaping with the necessary parameters before its discharge/break on the target and for the conclusion/output of protons from the accelerator.

Investigations in small fields encompassed further works on the correction of orbit and of operating point of accelerator, the study of the effect of different parameters on the characteristics of beam, and also the investigations, connected with an increase in the effectiveness in the synchrotron capture and by space-charge effect with the work of the accelerator with an intensity of 10^{12} protons/pulse is above. For an increase in the capture efficiency was used the method of preliminary beam bunching out of separatrix [3]. In our case this can give an increase in the intensity by 30-40%/o without substantial changes in the mode/conditions of the power-supply system of electromagnet.

Beam bunching was accomplished/realized by displacement of radio-frequency program by the method of introduction to the frequency shift key of the generator of the modulating impulse/momentum/pulse of the duration of 30-80 μ s. The phase

agreement of separatrix with bunches of particles at the moment of the end of the process of bunching was conducted due to the creation of ejection in the radio-frequency program by the duration of 8-10 s. The amplitude of ejection was determined by the value of the necessary phase shift. At the small intensity preliminary bunching gave an increase in the coefficient of capture by 350/o, which coincided with the calculation. From an increase in the current of injection the effect of bunching falls also at the intensities of approximately 10^{12} protons/pulse an increase in the coefficient of capture comprised less than 200/o. The pulse spread of the injected beam was equal to ± 0.25 c/o.

Large program is made on investigation of the passage of parametric resonance 9.5. For the correction of the width of resonance were experimentally tested the diagrams, which correct the 19th harmonic of the distribution of gradient of magnetic field according to the azimuth and the diagrams of the independent correction of resonance bands on α and β [1]. The experimental adjustment of the systems of correction made it possible to raise the maximum value of the intensity of the accelerated beam $\approx 1.2 \cdot 10^{12}$ to $1.5 \cdot 10^{12}$ protons/pulse.

Obtaining high intensity requires the correction of the series/row of the characteristics of magnetic field at the beginning

of the cycle of acceleration [4]. The systematic measurements of the form of equilibrium orbit show, that in proportion to an improvement in the ferromagnetic situation near the accelerator and other reasons the effectiveness of the systems of correction and, in particular, tenth harmonics of field increases. Thus, if the previously [5] introduction to the correction of the tenth harmonic of vertical field component did not lead to the decrease of radial orbit distortions, then at present the fraction/portion of the tenth harmonic composes $\sim 30\%$ in the value of orbit distortion. With the optimum distortion correction of orbit they comprise: on $r - \pm 1,2$ cm, on $z - \pm 0,8$ cm.

Periodic observation of the stability of the position of the blocks/modules/units of circular electromagnet shows that occurs an increase in the strains of basis/base. The basic reasons for the continuous residues/settlings and inclinations/slopes is the displacement of large masses in the region of experimental hall (dismountable concrete shield and heavy technological equipment), and also change of the hydncthermal conditions of ring and adjacent sections. Displacement of the blocks/modules/units of circular electromagnet relative to the designed position (it began of 1967) and caused by this orbit distortions were shown in Fig. 1. As is evident, the greatest changes occurred in the vertical direction where together with orbit distortion in the limits of ± 0.8 cm occurs

the decrease of the aperture of vacuum chamber on 0.6 cm. Apparently, in the very near future the partial adjustment of blocks/modules/units will become necessary.

For the effective use of beams of secondary particles in the physical experiments is required their uniformity on the density for a period of time of conclusion/output. Therefore considerable attention was given to works on an increase in the duration of extracted beam and an improvement in the time/temporary structure. The slow induction of accelerated beam to internal targets is conducted with the aid of the system, which creates local orbit distortion with the use/application of feedback on beam [6]. In order to exclude high-frequency structure, acceleration ceases before the induction of beam to the target. Time of de-bunching approximately 10 ns. The temporary/time heterogeneity, caused by the pulsations of the magnetic field of accelerator, was removed due to an improvement in the frequency characteristics of the system of feedback and power supply. With the passband of feedback loop 3 kHz is suppressed entire spectrum of harmonics, which is present in the field of accelerator. Greatest difficulty presents resonance effect during the induction of beam to the target. Has already been noted [7] that at the end of the acceleration with the beam displacement on a radius intersect the bands of anharmonic resonances of connection/communication. If in the process of induction to the target it is excited by any of these

resonances, then decreases the effectiveness of interaction of the accelerated beam with the target, and appears idle bunching modulation.

Page 29.

This effect is removed either by the method of displacement of beam by a radius into the region, free from the resonances or due to the displacement of operating point with the aid of the system of the correction of gradient. Fig. 2, and shows the time structure of beam under the effect of anharmonic resonance, while in Fig. 2b - the oscillogram of falling of beam to the target during the elimination of this resonance by the correction of gradient. The realization of the measures indicated made it possible to obtain the uniform beams of secondary particles by the duration to 1.3 s with a modulation depth with respect to density not exceeding 10% (Fig. 3). For the experimentation with bubble chambers was put into operation the system, which made it possible to obtain the impulses/moments/pulses of secondary particles by the duration less than 500 μ s [2] and produce the dosage of particles in the chamber/camera. The rapid discharge/break of the accelerated beam to the target is accomplished/realized with the aid of the pulse magnetic deflector, placed in straight section. Current in the deflector is interrupted/broken on the feedback signal after passage through bubble chamber of the prescribed/assigned number of particles.

An increase in the effectiveness in the use of an accelerator was conducted also due to an increase in the number of experiments, conducted in one cycle of acceleration. For this the duration of the flat/plane part of the magnetic cycle was increased to 1.5 s. This made possible if necessary to carry out in one cycle three beam spill to different targets by duration, through 400 ms. Furthermore, in the process of acceleration it is possible to carry out experiments with the thin targets (tape/film or gas), introduced into the circulating beam, and to also utilize a part of the beam for the works in the adjustment of equipment. A maximum number of experiments in one cycle of acceleration reaches five. However, a number of works, which conduct numerical measurements and set of statistics as a rule, does not exceed three.

The range of a change in the level of the flat/plane part of magnetic field corresponds to a change of the energy of particles within the limits of 20-70 GeV. By basic mode of work, however, is mode/conditions with the energy 70 GeV, which corresponds to the level of magnetic field in orbit 12020 e. The field current of electromagnet in this case is equal to 9100 a. The flat/plane part of the field is stabilized with the precision/accuracy ± 4 e. The form of magnetic cycle and the typical arrangement/position of experiments on

it are shown in Fig. 4. With the work of the accelerator on the intermediate energy the duration of cycle is shortened due to corresponding decrease of the time of growth and decrease in the magnetic field. It should be noted that the modes/conditions of the correction of orbit and field gradient are changed with a change in the mode/conditions of work of the accelerator. Thus, upon transfer from the mode/conditions with the energy 70 GeV to the mode/conditions with the energy ≈ 40 GeV betatron frequencies decrease by value $\Delta Q_{x,z} = 0,05 - 0,10$.

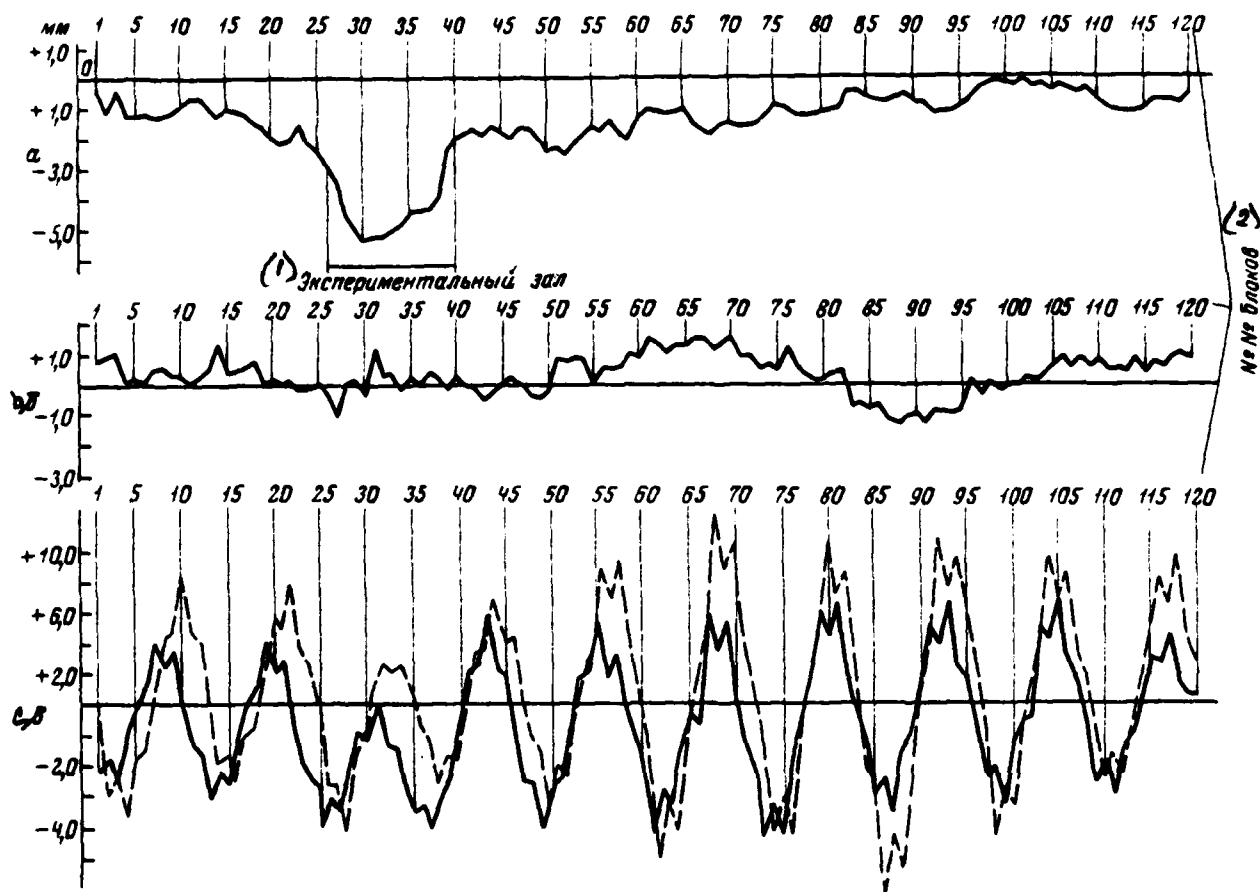


Fig. 1. Displacement of the blocks/modules/units of circular electromagnet. a) on the height; b) in the plan/layout; c) the form of distortion of orbit (dotted line - on the horizontal, continuous - on the vertical line).

Key: (1). Experimental hall. (2). NoNo blocks/modules/units.

Page 30.

At present are conducted works but to the creation of the intermediate plateau of magnetic field, which will make it possible to still raise the effectiveness of the use of an accelerator.

Typical for the accelerator is the four week old cycle of continuous operation with the subsequent two-week cessation for conducting of preventive works, preparation for next experiments and works in the modernization of accelerator. From 22 June, 1969, through 6 June, 1970, the booster duration with the beam was 1024 hours, of them: 82o/o of time were used to the physical experiments and 18o/o to the investigation of accelerator. Idle times within this period composed 14o/o. Average/mean working intensity in the year of work is equal to $7.5 \cdot 10^{11}$ protons/cycle. In the separate performances in conducting the experiments, which require maximum intensity, average/mean intensity reached $9 \cdot 10^{11}$ particles/pulse.

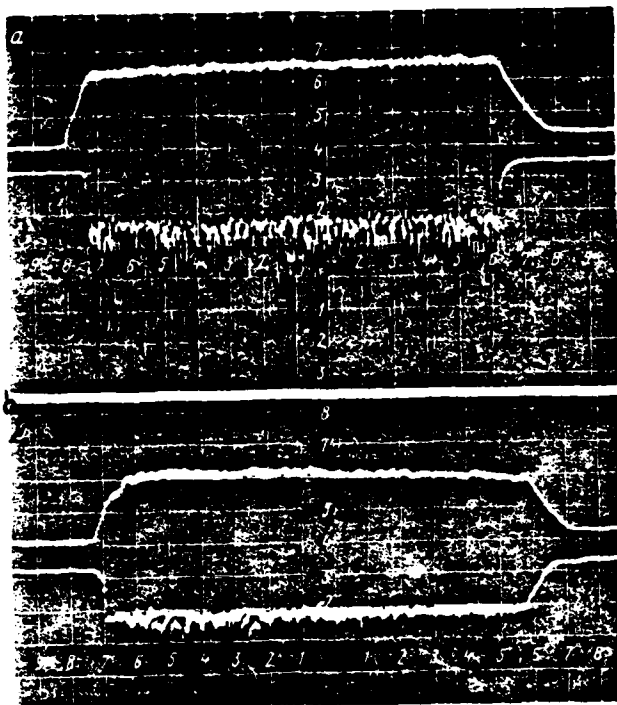


Fig. 2. Oscillograms of the impulse/momentum/pulse of secondary particles. Scanning/sweep of 50 ns/div.

In oscillograms a and b it is given: above - current pulse in the guidance system of beam to the target: below - signal from the monitor of secondary particles. a) under the effect of anharmonic resonance; b) during the elimination of resonance.

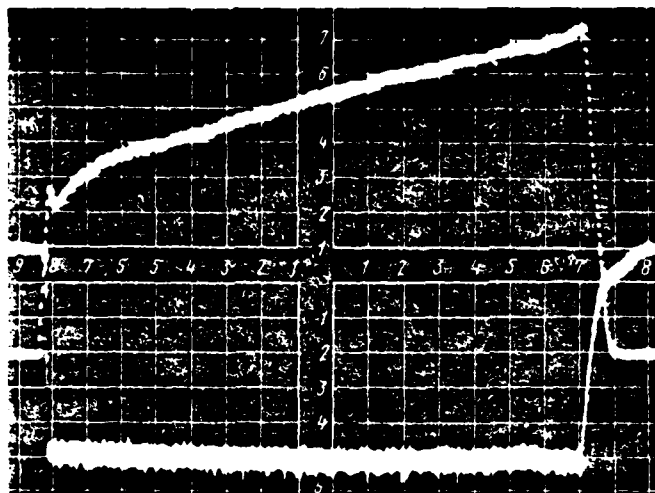


Fig. 3. Oscillogram of the impulse/momentum/pulse of secondary particles.

Below - signal from the detector of secondary particles; above - current pulse in the system of the correction of beam on the target. Scanning/sweep of 50 ns/div.

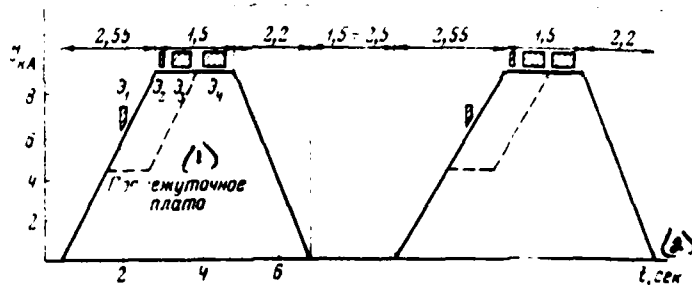


Fig. 4. Diagram of typical mode/conditions of work of the accelerator with energy 70 GeV.

3_1 - adjusting experiments; 3_2 - rapid discharge/break into bubble chamber; 3_3 , 3_4 - experiments in the set of statistics.

Key: (1). noise-resistant plateau. (2). s.

REFERENCES

1. Yu. M. Adoidr. Investigation of the passage of parametric resonance on the accelerator IPVE. This coll., Vol. 1.
2. V. I. Gridasov et al. System of rapid beam release to the target in an accelerator IPVE with an energy of 70 GeV. This coll., Vol. 1.
3. K. Johnsen. Internat. Conf on High Energy accelerators. Brookhaven, 1961, p 194.
4. Yu. M. Ado et al. Preprint IPVE, SKU 69-98, 1969.
5. Yu. M. Ado and E. A. Myayev. "Atomic energy", 27, No 6, 515, 1969.
6. V. I. Gridasov et al. Preprint IPVE, 70-51, 1970.

DOC = 80069203

PAGE 125

7. V. I. Gridasov et al. Transactions UP of international conference on the charged particle accelerators high-energy, that 1. Yerevan, publ. AN ARM of SSR, 1970, page 500.

Page 31.

5. Electron beam for experiments in electronic cooling.

G. I. Budker, V. I. Kudalaynen, I. N. Meshkov, V. G. Ponomarenko, S. G. Popov, R. A. Salimov, A. N. Skrinskiy, B. M. Smirnov.

(Institute of nuclear physics of SO AN USSR [CO AH CCCP - Siberian Department of the Academy of Sciences of the USSR]).

For the realization of oscillation damping of particles in the proton (anti-proton) accumulators/storage G. I. Budker proposed the method of the "electronic cooling" [1] whose essence consists of the following. If in one of straight sections of racetrack of accumulator/storage is created the stationary electron beam, the average speed in which coincides with average speed βc of protons, oscillation of the latter they attenuate with the characteristic time:

$$\tau \approx 10^7 \frac{\beta^4 \gamma^5}{j^2} \theta^3 \text{ сек} , \quad (1)$$

where j - current density in the electron beam in a. cm², γ - ratio of the length of the gap/interval of "cooling" to the perimeter of accumulator/storage,

$$\theta \sim \sqrt{\theta_e^2 + \theta_p^2} , \quad \theta_{p,e} \sim \frac{(v_1)_{p,e}}{v_n}$$

indices p and e relate to the protons and the electrons respectively. The presence of residual gas in the chamber/camera of accumulator/storage superimposes supplementary requirements for the parameters of electron beam [1, 2]:

$$j/\theta_e \geq \frac{10^7 \beta r^3}{\eta} p, \quad (2)$$

where P - pressure of residual gas, torus.

Being steady the size/dimension of the proton beam

$$\theta_p \geq 10^3 \sqrt{\frac{\beta r^3 \theta_e^3}{j \eta}} p, \quad (3)$$

moreover

$$\theta_p \geq \sqrt{\frac{m_0}{M_0}} \theta_e.$$

The study of method is intended to conduct on the ring VEPP-3 of IYAF of SO AN USSR [3] with the energy of protons 200 MeV and electrons 100 keV. Stationary electron beam is introduced into the gap/interval of "cooling" and is derived/concluded from it with the aid of the electron-optical system (Fig. 1), about which it is said below. The basic parameters of electron beam ($W=100$ keV, $j \sim 10$ ($j=1.3$ A/m²), $\theta_e \sim 3 \cdot 10^{-3}$, $P \sim 10^{-9}$ torus) make it possible to obtain $\tau \sim 10$ s. The accelerated protons have $\theta_p \sim 3 \cdot 10^{-3}$. The length of the gap/interval of cooling is 1 m, the perimeter of accumulator/storage 72 m. The general view of the installation of electronic cooling is shown in Fig. 2.

The basic requirement, presented to the electron beam, is the

smallness of the transversing speeds of particles (2). It proves to be that the virtually only method of the compensation for the defocusing actions space charge of beam is its transportation in longitudinal magnetic field [4]. If source of electrons (gun) is placed into the same magnetic field, the transversing speeds, caused by the action of the space charge of beam, give

$$\theta_e \approx \frac{4J}{\rho^2 T^2 c H a}$$

Here a, J - radius of section and beam current. (Use/application of channels with alternating-gradient focusing it does not make it possible to obtain [4] $\theta_e \leq \sqrt{8eJ/\rho^2 T^3 mc^3}$, which comprises for the given above parameters $4 \cdot 10^{-2}$).

For the optical diagram with the source, placed into the magnetic field, natural is the use of optics of pier. The presence of longitudinal magnetic field makes it possible to exclude the defocusing action of arcs opening/aperture. If the length of region Δz on which acts the defocusing radial electric field of the anodes, sufficiently close to value $\lambda = 2\pi pc/eH$ the disturbance/perturbation is small:

$$\theta_e \sim \frac{a}{d} \frac{W}{\Delta z \rho e H} \sin \pi \frac{\Delta z}{\lambda}, \quad (5)$$

where d - distance between the gun and the first accelerator.

Was utilized three-anode gun; distance between the anodes and potential distribution U_i on them were selected on the the

electrolytic bath: $\Delta z = 7$ cm, $U_1 = 45$ kV, $U_2 = 15$ kV, $U_3 = 0$.

Introduction/input and beam extraction from the gap/interval of cooling are conducted in the toroidal magnetic field. So that the "centrifugal" force would not agitate beam, in the sections of introduction/input and conclusion/output is superimposed rotary magnetic field on the order of 20 e.

The heterogeneity of longitudinal magnetic field leads to the disturbance/perturbation of beam. If the region of heterogeneity $\Delta z \ll \lambda$, then

$$Q_e \sim 2\pi^2 \frac{\alpha \Delta z}{\lambda^2} \frac{\Delta H}{H} \quad (6)$$

But if $\Delta z \gg \lambda$, and dependence $\Delta H(z)$ is sufficiently smooth, then

$$Q_e \sim \pi \frac{\alpha \lambda}{(\Delta z)^2} \frac{\Delta H}{H} \quad (7)$$

The windings of longitudinal magnetic field are performed by the cooled copper busbar/tire by section 28×14 mm². The sections of input and output (rotation) of beam are the cuts of torus with the section, greater than the section of the straight/direct sections of solenoid. The necessary uniformity of field ($\Delta H/H \leq 5 \cdot 10^{-2}$, $\Delta z \geq 20$ cm, $\Delta \theta_e \sim 10^{-3}$) is reached by the system of the screens, which untie the magnetic fluxes of solenoids with the different sections.

The adjustment of magnetic system and adjustment of optics guns were checked by the thin electron beam, observed with the aid of sight tube on luminescent screen. Moving screen along axial trajectory and recording the displacement of image Δ , it is possible to rate/estimate the disturbance/perturbation, acquired by beam in the appropriate section

$$\Delta\theta_e \sim eH\Delta / mc. \quad (9)$$

Since the resolution of this method is not better than 0.5 mm, adjustment is necessary to conduct at the values of field about $H=100$ e (precision/accuracy of measurement $\Delta\theta_e \sim 3 \cdot 10^{-3}$); working value $H=1500$ of e.

Experiments with the point beam showed that the magnetic system was made satisfactorily.

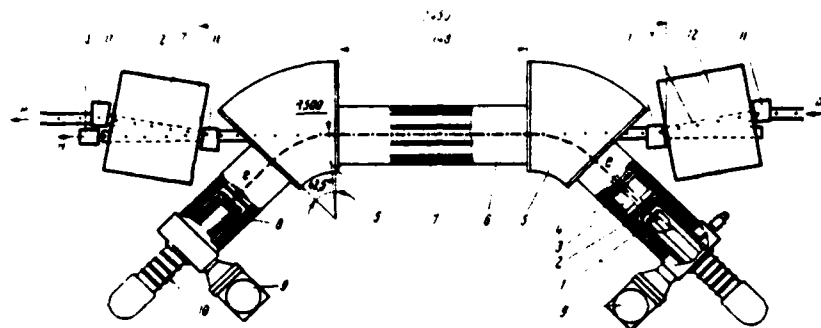


Fig. 1. Diagram of installation of electronic cooling. 1 - electron gun; 2 - anode block; 3 - vacuum chamber with the distributed magnetic discharge pump; 4 - winding of solenoid; 5 - section of rotation; 6 - gap/interval of "cooling"; 7 - vacuum chamber; 8 - collector/receptacle; 9 - magnetic discharge pumps; 10 - carrying insulator; 11 - magnets of the trajectory correction of protons; 12 - quadrupole lenses of accumulator/storage VEPP-3; 13 - counter of the atoms of hydrogen (neutral particles with the energy 200 MeV).

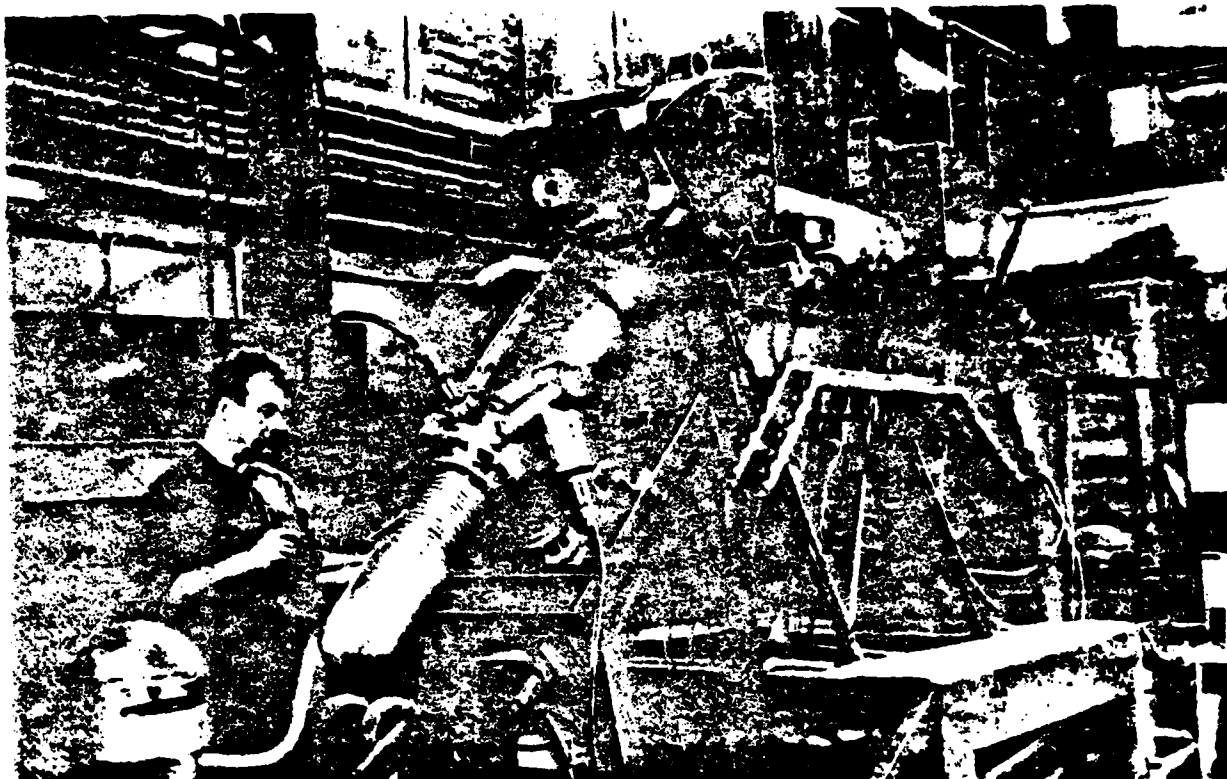


Fig. 2. The general view of the installation of electronic cooling.

Page 33.

Finally, is necessary a good coincidence of the average speeds of electrons and protons [2]. One of the possible sources of this error is instability in the time of energy of electrons. Therefore it is necessary to ensure

$$\frac{\Delta W}{W} \leq \frac{\beta^2 \gamma^2}{\gamma - 1} \theta_e \quad (9)$$

In the selected parameters of installation the reactive power of beam is 100 kW. By the most acceptable resolution of the appearing problem of supply is represented the use/application of a known method of regeneration of the "finishing" electrons.

Experiments in recuperation were conducted on the installation which does not have the sections of rotation [5]. The length of the gap/interval of "cooling" was 2 m. In the mode/conditions of recuperation was obtained direct current $j=1,1$ and with stress/voltage $U_0=100$ kV (field of solenoid 200 e). Less current did not exceed 0.3 mA with the vacuum $5 \cdot 10^{-6}$ torr, potential differences between the cathode and the collector/receptacle 1.3 kV. Thus, the consumed fraction/portion of power composed 1.30/o.

REFERENCES

1. G. I. Budker. "Atomic energy", 1967, 22, No 5, 346.
2. Ya. S. Derbenev, A. N. Skrinskiy. Preprint No 255, IYAF of SO AN USSR.
3. G. I. Budker, I. Ya. Protopopov, A. N. Skrinskiy. Transactions UP of international conference on the charged particle accelerators high-energy, that 2. Yerevan, publishing house AN ARM of

SSR, 1970, page 37.

4. I. N. Meshkov. Blding of intense electron beams, Cand. dissertation, Novosibirsk, 1970.

5. A. I. Arenshtat, G. I. Eudker, I. N. Meshkov, V. G. Ponomarenko, A. N. Skriskiy. Transactions of All-Union conference on the charged particle accelerators, that 2. M., VINITI [All-Union Institute of Scientific and Technical Information], 1970, page 400.

Discussion.

M. Barton. Did achieve you energy of ring 200 MeV?

B. A. Salimov. Final energy of the accelerated protons 200 MeV. Wave energy - 1 MeV. In VEPP-3 the protons they are seized, but it is not thus far accelerated.

A. A. Kolomenskiy. At the equal proton velocities and electrons substantially grows/rises the section recharge (neutralization), and protons are lost. Are such your evaluations of this effect, and how it does affect experiment?

R. A. Salimov. The overcharging of protons on the electrons will be utilized as the method of recording the coincidence of proton and electron beams. Thereby we will see, how good we combined velocity and position of proton and electron beams. According to the estimations it turns out that the time of the disappearance of proton beam due to the recombination at those velocities which we expected, is approximately/exemplarily 150 min, and time of delay - 10 s.

6. Possibility of accelerating the protons by the energy higher than rest energy in the isochronal cyclotron.

I. A. Sarkisyan.

(Radio engineering institute of the AS USSR).

The theoretical and experimental studies of the dynamics of particle motion in the isochronal cyclotrons with a three-dimensional/space variation in the magnetic field, carried out in Dubna [1] and Oak Ridge [2], showed that during the amplitude of radial oscillations into several centimeters (~3.5 cm) and the set with the particle of energy per revolution ~300 keV, internal nonlinear resonance of fourth order ($p = \frac{N}{Q_r} = 4$), caused by the periodicity of the structure of magnetic field virtually it leads to the total loss of beam, and maximum energy of the accelerated protons is limited by the nonlinear resonance $Q_r \cdot 2$. Within the framework of linear theory maximum kinetic energy of protons can be evaluated according to the expression

$$W = E_0 \left(\frac{Q_r}{\sqrt{1 + \frac{3}{2N^2} \left(\frac{\epsilon_1 r}{N\lambda} \right)^2 \sum_{m=1}^{\infty} \left(\frac{\epsilon_m}{m\epsilon_1} \right)^2}} - 1 \right),$$

where E_0 - rest energy of particle; ϵ_1 and ϵ_m - depth of variation of the fundamental and m-th harmonics of field; λ - parameter of Archimedes spiral; r - current radius of acceleration.

In the accelerators with weak axial focusing ($Q_z \sim 0.25$) maximum energy is ~ 810 MeV. Acceleration for radius $Q_z > 2$ together with a considerable reduction in the intensity of the beam (amplitude of radial oscillations several millimeters) [2] meets difficulties with shaping of magnetic field due to the increasing with a radius nonlinearity of middle field and variation in one accelerator. Furthermore, substantially is complicated system conclusion/output from the accelerator and considerably falls its effectiveness.

For the realization of the acceleration of protons in the cyclotron mode/conditions to the energy more than $\sim E_0(Q_z > 2)$ it is proposed to utilize a cascade method of the acceleration, when each previous cyclotron is injector for that following.

Page 34.

In this "cascade isochronal cyclotron the possibility of a considerable increase in the energy is reached due to the selection of the specific frequency band of radial betatron oscillations ω_r in each accelerator. The frequency range in the first, the secondly, the

third and so forth the cyclotrons of the cascade/stage is selected with respect to equal ones to $Q_1 \leq Q_2 \leq \frac{N}{p} - \frac{8}{4} = 2$, $Q_2 \leq Q_3 \leq \frac{N}{p} - \frac{12}{4} = 3$, $Q_3 \leq Q_4 \leq \frac{N}{p} - \frac{16}{4} = 4$ and so forth, where the upper value of frequency in each cyclotron corresponds to internal anharmonic resonance of fourth order ($p = \frac{N}{Q_4} = 4$), which is reached by the appropriate selection of periodicity N . The first cyclotron can be both continuous and circular type (with the external particle injection), that follow all - circular type. The translation/conversion of beam of one accelerator in another is facilitated by the fact that in these cyclotrons for achievement of highly efficient beam extraction it is proposed to utilize resonance connection/communication between the azimuthal and radial motion, which appears on the basis of the mechanism of anharmonic resonance of the fourth order when $Q_4 = 2, 3, 4$ and so forth. Let us point out that in Oak Ridge on the electronic analog P during the careful optimization of the characteristics of beam and leading-out system was achieved/reached the coefficient of beam extraction ~950/o with the aid of anharmonic resonance $Q_4 = 2[2]$. The guarantee of a large radial set per revolution on inside radii of the order of one centimeter makes possible in the circular cyclotrons the use of electrostatic or magnetic pipe with the central plate for the translation/conversion of beam upon the injection.

Table gives the exemplary/approximate parameters of three

accelerators of cascade/stage, which permit implementation of cyclotron acceleration mode of pions before the energy ~ 2.5 GeV. The identification of the parameters of each accelerator was based on the possibility of designing of the required value of middle field and fundamental harmonic in operating region of radii. Here H_0 - magnetic intensity when $v=0$, $v_0 = \frac{E_0}{cH_0}$, r_m and r_k - initial and terminal radii of acceleration, f_0 - frequency of revolution, I - average/mean intensity of emitted beam.

Although upon transfer to the subsequent accelerator in the cascade/stage decreases radial extent of the zone of acceleration $\Delta r = r_k - r_m$, shaping of the required law of middle field with an increase in index n , it is facilitated by a considerable increase in the allowance in the field. This is connected with the approach of the relative particle speed in the beginning and end/lead of the cycle of acceleration and with the possibility of an increase in the set of energy approximately/exponentially by an order in the circular cyclotrons in comparison with the cyclotron with the continuous structure. Thus, in the phase of acceleration $\phi = 30^\circ$ allowance in the field for the first accelerator with 0.4 MeV/revolution composes $\Delta H/H = +1 \cdot 10^{-4}$, for the second and the third with 2 MeV/rev it is respectively equal to $\Delta H/H = \pm 2.2 \cdot 10^{-3}$ and $\pm 5.6 \cdot 10^{-3}$. The estimation of the intensity of beam was based on the strength of internal current in the first cyclotron $I = 500 \mu A$ and the assumption that the

coefficient of beam extraction from the accelerator composes 950/o. Let us note that a considerable increase in the intensity in the isochronal cyclotrons is connected with an increase in axial hardness ($Q_z \approx 1$) [3, 4] and with transition to the high magnetic fields (during the use of superconductivity). In this case average/mean beam current respectively grows/rises approximately/exemplarily to two orders and one orders.

An increase in the energy of protons with the aid of cascade isochronal cyclotron will be determined to a considerable extent by economic considerations, since each accelerator of cascade/stage provides an energy gain of protons approximately/exemplarily to the constant value, equal to 810 MeV. The creation of this high intensity accelerator will make it possible to supply precision experiments in the region of physics of nucleus in the range of energies into several GeV. Thus, with the energy of protons ~ 1.7 GeV the output of pi-mesons will increase 2.3 times in comparison with the output with the energy ~ 800 MeV [5]. Since threshold for the production K^+ - and K^- - mesons on the quiescent proton is equal to with respect 1.5 and 2.5 GeV, then at an energy of several GeV the accelerator examined can become also the high intensity "factory" of k-mesons, competitive with the linear accelerator.

Let us point out that together with the isochronal cyclotron as

first stage of cascade/stage it is possible to utilize the acting and reconstructed (with a variation in the magnetic field) synchrocyclotrons in the range of energies 680-1000 MeV and projected linear accelerators to the energy ~800 MeV.

table.

(1) Номер ускорителя каскада	(2) Параметр ускорителя											
	$H_0, \text{з}$	N	$\lambda, \text{см}$	Q_z	Q_{γ}	$\tau_m, \text{см}$	$\tau_n, \text{см}$	$\tau_k, \text{см}$	ϵ_k	(3) $W, \text{МэВ}$	(4) $M, \text{МэВ}$	(5) $I, \text{мкА}$
(6) Первый	6500	8	8	0,2	$1 \leq Q_{\gamma} \leq 2$	447	0	385	0,281	810	9,88	475
(7) Второй	3000	12	15	0,2	$\sim 2 \leq Q_{\gamma} \leq 3$	1042	902	982	0,501	1650	4,56	450
(8) Третий	1500	16	23	0,2	$\sim 3 \leq Q_{\gamma} \leq 4$	2084	1965	2018	0,687	2500	2,28	425

Key: (1). Number of the accelerator of cascade/stage. (2). Parameter of accelerator. (3). MeV. (4). MHz. (5). μA . (6). The first. (7). By the second. (8). The third.

REFERENCES

1. V. P. Dmitriyevskiy, V. V. Kol'g, N. I. Polunordvinova. Transactions international conf on the accelerators. Dubna, 1963. M., Atcmizdat, 1964, page 833.
2. J A Martin et al. Proc. Intern. Conf. on Sector-Focused Cyclotrons and Meson Factories. CERN, 1963, p 52.
3. V. N. Anosov, A. T. Vasilenko, V. P. Izhelopov, etc. "atomic energy", 1968, 25, 537.
4. M M Gordon. Nucl. Instrum and Methods., 1968, 58, 245.

S. N Metropolis. Phys. Rev., 1958, 110, 204.

Discussion.

Ye. Skhvabe. Are such the possibilities to obtain the range of variable/alternating energies in your project?

L. A. Sarkisyan. On the accelerators for the energy to and above variation of energy to ensure is very difficult. This is connected with the fact that strongly must change the middle magnetic field and its variation. This problem meets with technical difficulties in the realization.

Page 35.

Session II.

STATE OF THE ACCELERATORS OF DIFFERENT TYPES. Designs of new ones and reconstruction of the existing settings up.

7. Continuous microtron FEL (project).

S. P. Kapits, L. M. Zykin, A. I. Abramov, Yu. Ya. Stavitskiy, V. A. Slobodyanyuk, V. M. Kondratyev, V. P. Marin, A. M. Chernushenko.

(Institute of the physical problems of the AS USSR, physical-energetic institute).

Microtrons - resonance cyclic electron accelerators in recent years find an increasing use in nuclear physics investigations also of radiation physics [1, 2]. In the microtron successfully is combined the high monochromaticity of electrons, characteristic to cyclic accelerators, with the large intensity of beam.

There is special interest for the investigations in physics of nucleus in the use/application of continuous duties of accelerators.

Transition from the pulse beam to the the continuous makes it possible to raise the intensity, available for the physical experiment, conducted with the aid of electronics.

Actually/really, in the majority of the cases during the use of a pulse beam the detecting equipment is overloaded during the impulse/momentum/pulse, "stays" between the impulses/momenta/pulses.

The possibility of designing of continuous microtron was shown by one of the authors of present report [5].

Actually microtrons are continuous accelerators (being distracted from the microstructure of beam with the repetition frequency several thousand megahertz, that it until interferes with experiment), and their "pulse use" is caused by a small power of existing SVCh of the generators which can generate the necessary power level only relatively short time.

In proportion to the development of powerful/thick high-frequency continuous oscillators [3] become real and the continuous duties of microtrons.

It is necessary to emphasize that precisely in the microtrons where occurs the multiple traversal of the electrons through

accelerating field of resonator, the realization of continuous duty is most profitable. Actually/really, relative energy loss to the excitation of resonator in the case of microtron is less and n of times of the corresponding value for the accelerators with the single passage (linear accelerators), where n - number of passages. By this fact is explained high effectiveness (efficiency) in the microtrons.

The continuous duty of microtron makes it possible to obtain the high intensities of electrons and γ -rays, important during the radiation-physics investigations.

In this work are examined the fundamental ratings of continuous microtron, planned, in FII on S. F. Kapitsy's proposition on the basis of powerful/thick SVCh of the oscillator of continuous action [3] and magnet of pulse microtron on 30 MeV [4].

Accelerator is designed for obtaining of the steady beam of electrons to 12 MeV with the current of electrons to 2 mA. The overall design of accelerator is given in Fig. 1. System switches on strictly microtron, SVCh oscillator with the high-frequency circuit, cooling system, vacuum system, system of control and inspection of parameters.

1. Microtron. To the accelerator can be attributed the

accelerating cavity, placed into the uniform magnetic field, vacuum chamber, magnetic beam tube and electro-guide for its transportation to the target.

Resonator (Fig. 2) - cylindrical with the flat/plane covers/caps, is calculated for the frequency of 1610 MHz, has the capability of its thin adjustment with the aid of the movable bolt system, on the cover/cap of resonator are arranged/located cathode node/unit (filament cathode from hexaboride of lanthanum), movable cooling diaphragm for absorbing the low-energy electrons, which did not catch into acceleration mode.

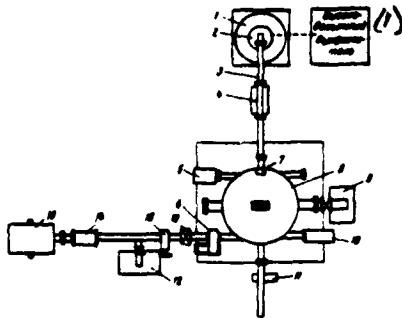


Fig. 1. Block diagram of continuous microtron. 1 - solenoid of magnetron; 2 - magnetron; 3 - wave circuit; 4 - water loads; 5 - mechanism of the adjustment of the frequency of resonator; 6 - drive of magnetic pipe; 7 - resonator; 8 - accelerator; 9 - vacuum aggregate/unit; 10 - gel-installation; 11 - cover lock with the mechanism of balance-start; 12 - vacuum aggregate/unit; 13 - trap of electrons; 14 - external target; 15 - the vacuum seal; 16 - quadrupole lens.

Key: (1). High-voltage rectifier.

Page 36.

Resonator has the branched surface, water-cooled, calculated for the heat release to 150 kW. Is fastened resonator to the wall of vacuum chamber.

Vacuum chamber has cylindrical wall with the extensions for the beam extraction, evacuation, conclusion/output of pilot signals, cooling-water supply, etc. Its covers/caps are polar pole pieces. The sizes/dimensions of chamber/camera make it possible to obtain 14 orbits in magnetic field $H=940$ e. Magnetic field with uniformity 0.10/o is stabilized on the current with precision/accuracy $\sim 10^{-5}$.

For the beam extraction is utilized magnetic pipe from soft iron [4]. Its construction/design is analogous to the constructions/designs of magnetic pipes in the pulse microtrons.

The system electric-guide switches on the focusing lenses, the cooled braking target, trap for the electrons and Faraday cylinder.

2. Magnetron type high-frequency oscillator "nigotron" [3]) is intended to utilize at power output 150 kW. To this power corresponds anode voltage 23 kV and current 3-17.5 A. The supply of "nigotron" is planned to carry out from the adjustable thyatron rectifier, since with a change in current and magnetic field of "nigotron" frequency is changed. Therefore is required voltage regulation of rectifier with precision/accuracy $\pm 0.10/o$. Has the capability of the resonance adjustment of system.

For agreeing SVCh the oscillator with the resonator of

accelerator and for guaranteeing the possibility of steady feed to high-frequency power into the resonator is utilized high-frequency circuit with the divider of power. Ranges of adjustment supplied to the resonator SVCh of the power of oscillator compose 10-90o/o. The power, diverted into the secondary channel of divider, is absorbed in the cooled loads.

A change in connection/communication of the directional coupler is accomplished/realized by a method of introduction to the secondary channel of the dielectric, which changes the propagation constant of electromagnetic wave. As the dielectric is selected ceramics on the basis of oxide of beryllium, which possesses low losses ($\text{tg} \delta \leq 10^{-4}$) with good thermal conductivity, which makes it possible to apply at the high levels VCh of power.

3. Cooling system. Cooling system contains two independent contours/outlines, that switch on heat exchanger, circulating pump, headers and conduit/manifold. As the heat-transfer agent is utilized the distilled water.

The first contour/outline is intended for cooling the elements/cells of high-frequency oscillator, by the second - resonator of microtron, faraday cylinder, braking of targets and traps of electrons.

The maximum power, removed by each contour/outline, reaches 350 kW with the flow rate of cooling water 30 m³/h.

4. Vacuum system. Vacuum system must ensure the greaseless/oil-free evacuation of the chamber/camera of microtron, electro-guide and VCh of circuit to the rarefaction 10^{-6} - 10^{-7} mm Hg. For the evacuation it is proposed to utilize an electric discharge pump.

5. System of control and inspection. System the control also of control makes it possible to check the basic parameters of electron beam (condition and current) and the parameters of the separate nodes/units of installation and to also accomplish/realize remote control of supplies of power, of cooling circuits, of auxiliary and beam current.

System switches on the movable orbital sensor, which uses for measuring the current distribution of beam according to the orbits, sensors for measuring the magnetic field of accelerator, faraday cylinder, pressure sensors and temperature of water at entrance and output of the cooled nodes/units, servodrives of remote control of the nodes/units of accelerator.

In the development of the design of accelerator and to the experimental final adjustment of the separate solutions the large contribution introduced the colleagues of FEI: N. T. Panasik, I. N. Marin, V. A. Kurov, ²⁴~~Z.~~ I. Iyevleva, P. S. Klemyshev, V. I. Puchkov, Ye. S. Afon'kin, colleagues of IFP: V. N. Melekhin, Ye. L. Kosarev, B. S. Zakirov, L. B. Luganskiy: the colleagues of FEI in. V. I. Lenin: V. G. Tatarintsev, M. V. Pavlov, G. I. Kreshishin, and also C. K. Il'inskaya, V. P. Golovenkov, L. M. Fedortsev.

To these all comrades and their associates the authors of report express their deep gratitude.

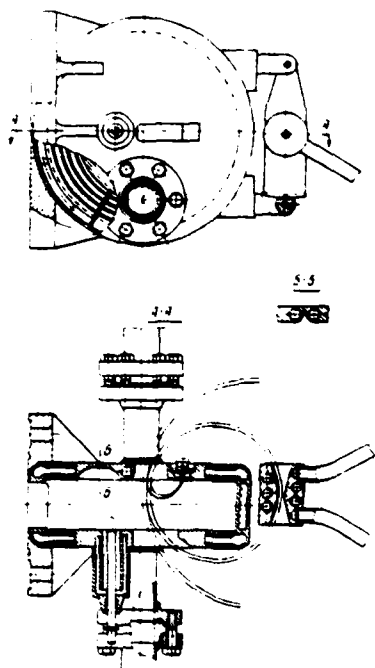


Fig. 2. Resonator of continuous microtron.

Discussion.

A. I. Zykov. Which the power of microtron?

V. A. Slobodyanyuk. 150 kW.

A. I. Zykov. Are such the dimensions of installation?

V. A. Slobodyanok. Diameter of resonator 15 cm, magnet - 1.2 m.

DCC = 80069203

PAGE 154

length of waveguide - 2.5 m, height of "nigotron" - 1 m, diameter -
26 cm.

Page 37.

E. State of matters and prospect for the development of electronic synchrotron DEZI on 7.5 GES.

G. Kumpfert.

(DEZI, FRG).

After the completion of the period of construction, lasting almost five years, beams it was for the first time obtained in the accelerator in 1964. Regular work of the accelerator as the source of particles for the investigations in high-energy physics was begun during October 1964 with intensity 15 of work shifts in the week, and beginning from October 1966 synchrotron it worked continuously, with exception of basic holidays and 4-10- weekly cessation in the year for substantial changes in the synchrotron and the experimental halls. Fig. 1 shows the arrangement/position of the buildings of the complex of accelerator DEZI, in Fig. 2 - the schematic plan/layout of the system of bundles DEZI, and Table 1 gives the hours of work from 1964 through 1969.

Expected operating time on 1970 g approximately the same as in

1969.

Both operation of synchrotron and developments, connected with the programs of improvement, they are accomplished/realized by one and the same colleagues. Advantages this are obvious: on one hand, for the operation, this complicated accelerator as synchrotron, necessary the highly skilled personnel whom it is difficult to find only for the shift work behind the panel; on the other hand, entire experience, acquired in the process of operation, directly is considered in the programs of improvement. At present personnel, who operates accelerator, counts 80 physicists, engineers and technicians.

In the period from 1964 through 1966 before the personnel of synchrotron stood the tasks: to collect work experience on the accelerator, to train operating personnel; to organize preventive works and to introduce technical improvements for the purpose of a reduction in the number of idle times.

The results of this work are given in Table 1, in which is shown a reduction in the number of interlayers.

At the end of 1966 was completed preparation toward the first long-term program of improvements, directed toward an increase in the

intensity and the stability, increase in the energy, improvement in the quality of the concluded electronic and photon beams and further reduction in the number of idle times.

This program was in essence completed in 1968-1969.

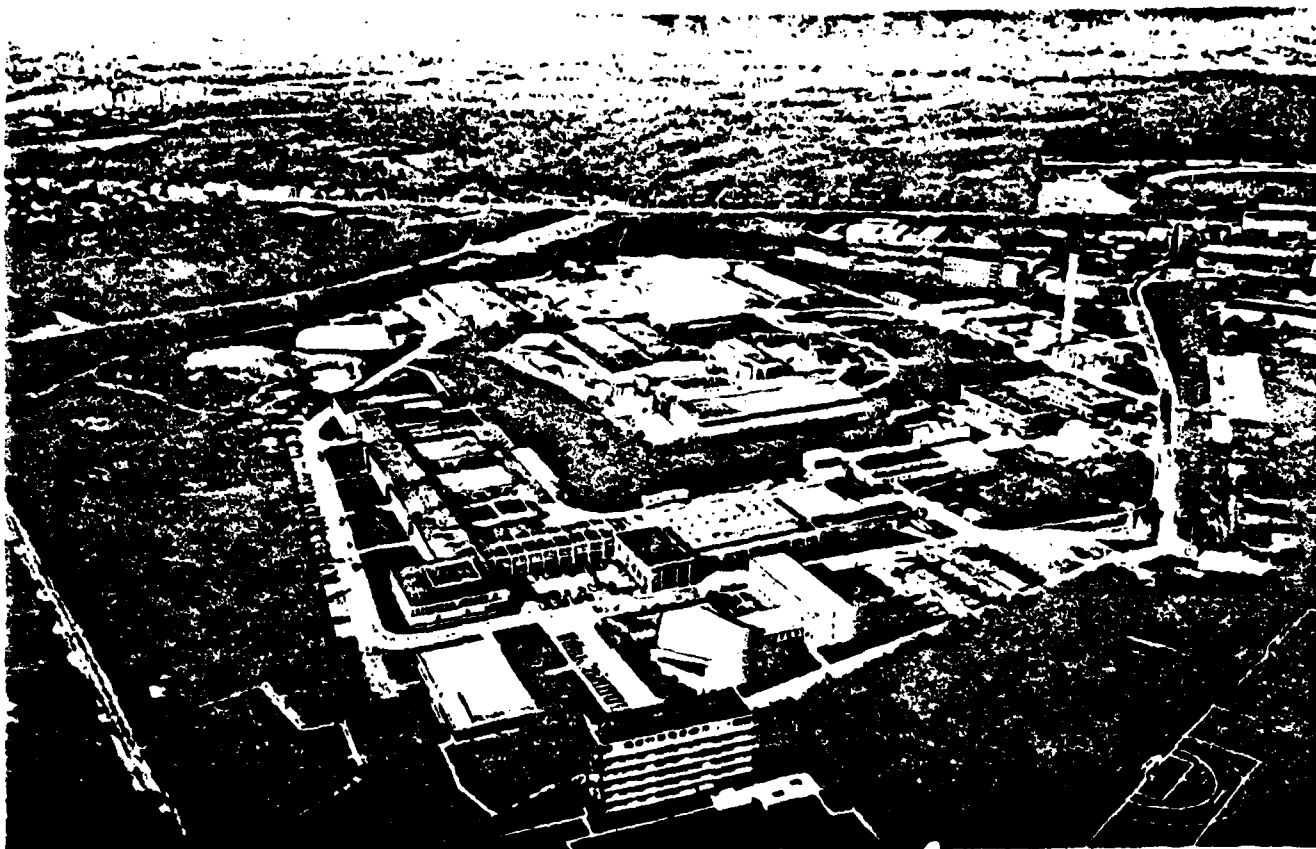


Fig. 1. Arrangement/position of the buildings of the accelerator of "DEZI".

Page 38.

Is given below the summary of the characteristics of accelerator at present:

maximum energy ... of 7.5 GeV.

stability of maximum energy ... $\pm 10/o$ (from one cycle to the next)
 $\pm 20/o$ (long-term).

Repetition frequency ... of 50 imp./s.

Time interval for $\Delta E/E \leq \pm 0.250/o$ with the maximum energy ... of 0.9 ns.

Porosity for high-energy physics ($\Delta E/E \leq \pm 0.250/o$) ... 4.50/o.

Designed intensity ... the average/mean current of circulation 16 mA, either 10^{11} particles per pulse, or 5×10^{12} particles/s/

Optimum values of intensity ... the average/mean current of circulation 18 mA, either 1.13×10^{17} particles per pulse, or 5.6×10^{12} particles/s.

Typical values with the run of job ... the average/mean current of circulation 8-12 mA, either $5-7 \times 10^{11}$ particles per pulse, or $2.5-3.8 \times 10^{12}$ particles/s.

Number of the primary beams ... of 4 photon beams, 2 concluded electron beams.

The quality of the concluded electron beams

intensity ... is maximum of 10^{10} particles per pulse (with the average/mean rotating beam 5 nA).

the emittance ... $E = 2,5\pi$ mm. millirad $E_b^r = 1,5\pi$ mm. millirad.

the time of the conclusion/output ... of 0.4-0.9 ns.

Maximum intensity of the linear accelerator No 1 ... of 180 nA.

However, what was made for obtaining such indices? Let us examine some aspects, connected with the enumerated above programs.

Intensity. Intensity indicated higher approximately is three times higher than the available in the beginning work. The basic reason for this was a large number of changes, introduced into the linear injector-accelerator with the energy 40 MeV.

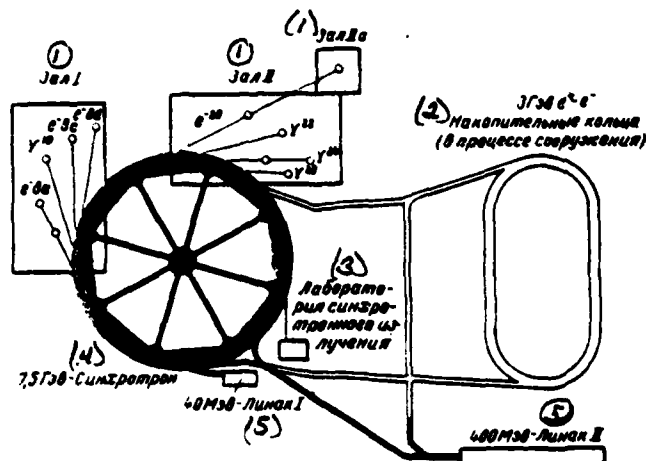


Fig. 2. Schematic plan/layout of the system of bundles "DEZI".

Key: (1). Hall. (2). Rings (in process of outfitting). (3). laboratory of synchrotron from torching. (4). Synchrotron. (5). Linak.

Table 1.

(1) Часы работы	(2) Год					
	1964	1965	1966	1967	1968	1969
(3) Суммарное рабочее время (без остановок и праздников)	-	5075	5855	6816	6968	71
(4) Время остановок (без праздников)	-	2128	1504	1704	1488	12
(5) Профилактика	-	400	508	878	696	7
(6) Рабочее время пучка (без профилактики)	1830	4675	5330	5938	6272	64
(7) Рабочее время на пучке, запланированное для исследований по физике высоких энергий	1009	3487	4228	4833	5745	58
(8) Рабочее время на пучке, реализованное для исследований по физике высоких энергий	767	2592	3460	4387	5137	55
(9) Рабочее время на пучке, запланированное для исследований по ускорителю	821	1208	1119	1105	527	1
(10) Время простоев	(11) часы	-	1206	1012	673	687

Key: (1). hours of work. (2). Year. (3). Total operating time

(without cessations and holidays). (4). Period of stops (without

holidays). (5). Preventive maintenance. (6). Operating time of beam

(without preventive maintenance). (7). Operating time on beam,

planned for investigations in high-energy physics. (8). Operating

time on beam, realized for investigations in high-energy physics.

(9). Operating time on beam, planned for investigations on

accelerator. (10). Shutoff period. (11). hours.

Page 39.

was completely altered the system of injection into the linear
accelerator. New system encompasses new gun with the large service

life, ensuring higher intensity, improved the optical system between gun and section of a 1- linear accelerator, and preliminary grouper at the frequency of 500 MHz. This is - the frequency of acceleration in the synchrotron, whereas linear accelerator works on the 6th harmonic, i.e., at the frequency of 3 GHz. Approximately 75% of accelerated particles depend on the relative phase between the linear accelerator and the preliminary buncher, on one hand, and the synchrotron - on the other hand. Upon the injection is accomplished/realized frequency modulation, moreover only for the short period at the beginning of the cycle of acceleration. Fig. 3 shows improved conditions for acceptance. Moreover, was designed the new system of the transportation of the beam between the linear accelerator on 40 MeV (which we will call accelerator No 1 in order to differ it from the linear accelerator to 400 MeV, named accelerator No 2 and described below) and the synchrotron. The reason for the creation of the new system of the transportation of beam was the radiation damage of magnet and coils of lenses in the old system. However, were also improved dispersion and agreement of envelopes, and are also obtained the best possibilities of a precise centering, which guarantee the clear and well reproducible conditions of injection into the synchrotron.

Fig. 4 depicts the section of gun and preliminary buncher of the linear accelerator No 1, while in Fig. 5 - the channel of the

transportation of electrons in the region of injection. In addition to the mentioned above improvements of linear accelerator and channel of the transportation of electrons, an improvement in the devices/equipment of the measurement of beam and check of magnetic injection field led to an increase in the intensity under the normal conditions for operation. In the straight/direct sections of accelerator were established/installed about 20 sensors for measuring of intensity and displacement, that overlapped the range of intensity measurements from 30 μ A to 300 mA, and provided resolution in the measurements of position of approximately 1 mm.

These blocks/modules/units - inductive type, sensitive to 1 MHz to the structure of the circulating beam, given by the interval of injection (one injection for the revolution).

Fig. 6 and 7 depict block/module/unit in the dismantled/selected and assembled form, Fig. 8 gives an example of signals about the horizontal position along the length of ring upon the injection (displacement of the center of charge as a result of coherent oscillations). Analogous sensors are utilized in the systems of the transportation of beam and between the sections of linear accelerator. In those sections where blocks/modules/units cannot be utilized for lack of space, will be soon established/installed sensors with the high-frequency contours/outlines.

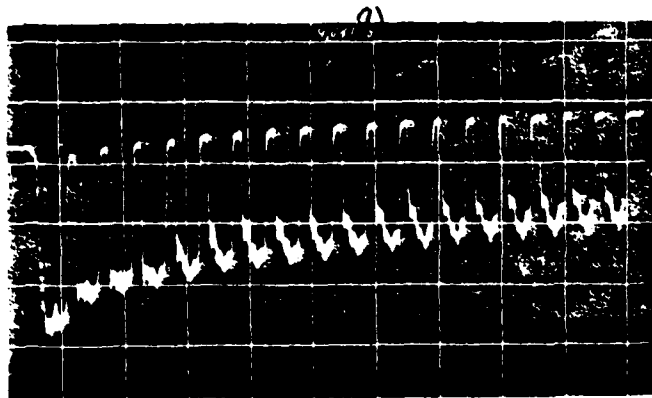


Fig. 3. Losses of particles on the first revolutions.

Key: (1). GeV.

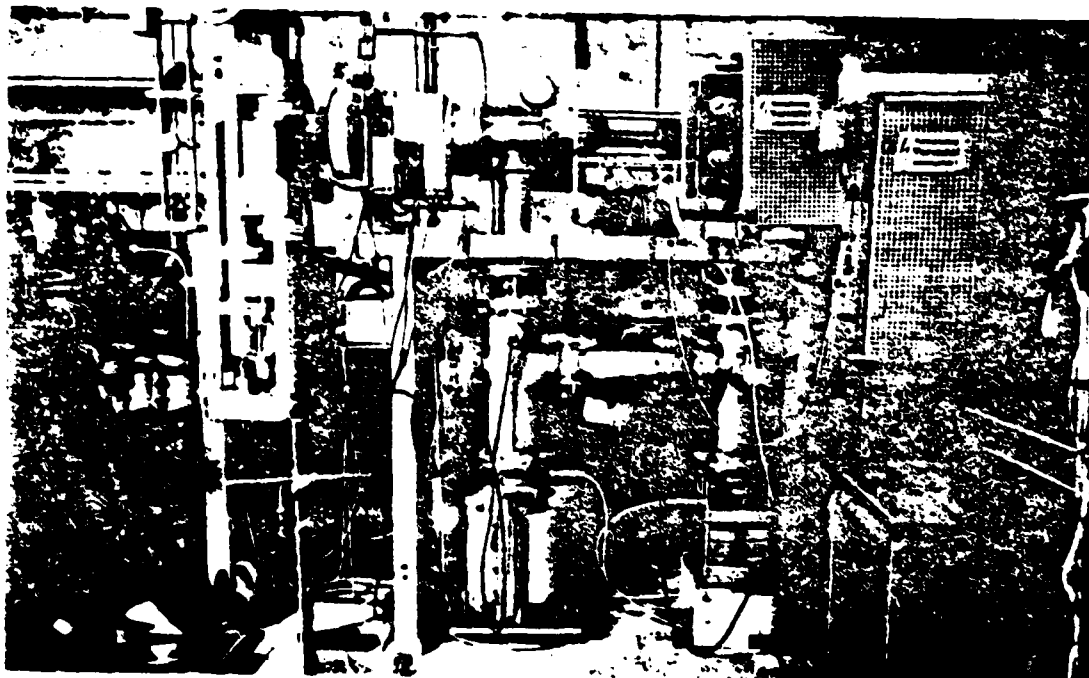


Fig. 4. Electron gun and preliminary buncher of Linak 1.



Fig. 5. Channel of the transportation of electrons in the region of injection.

Page 40.

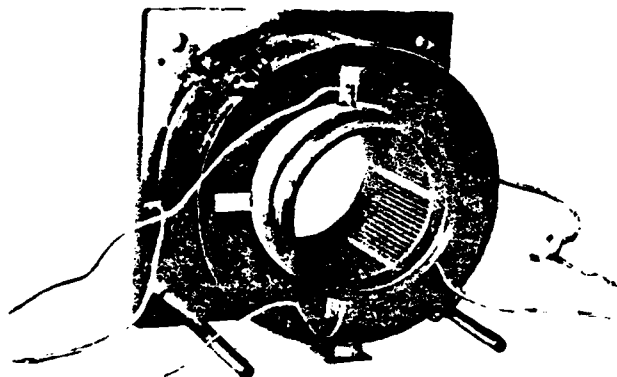


Fig. 6. Sensor of intensity (opened).

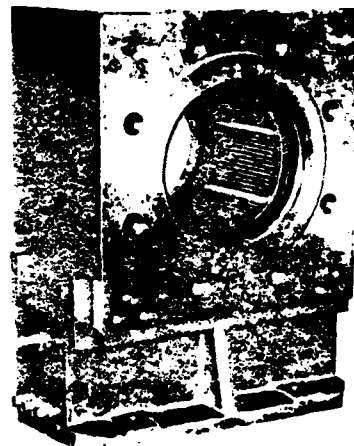


Fig. 7. Sensor of intensity (assembled).

Page 41.

For the correction on the direct current in the field of injection (40 G) are utilized the windings on the pole pieces. With their aid it is possible to introduce horizontal and vertical dipole corrections in the supplement to the usual dipoles, which compensate for a difference in resonant fields in magnets ϕ and ψ . Finally, are quadrupole windings, which make it possible to correct betatron frequencies at the early stages of cycle. Fig. 9 gives an example of

the effect of such corrections.

Should be noted one additional means of an increase in the intensity the data recording system approximately from 200 measuring devices. With the aid of this system the operator follows the undesirable changes in the synchrotron and its components, and it is also intended by the introduced changes, such as beam displacement, investigating the behavior of beam. Fig. 10 depicts the general view of the main console of synchrotron.

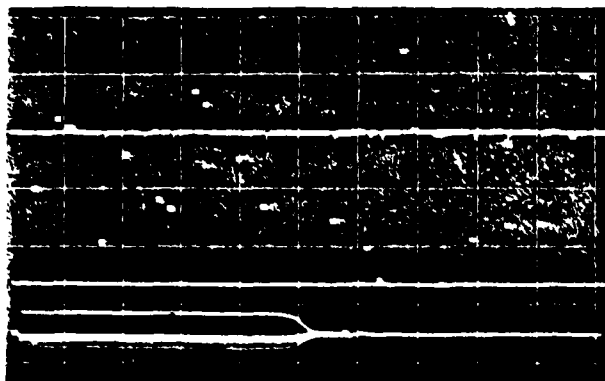


Fig. 8. Horizontal displacements of orbit at 18 points right after injection (upper ray/beam).

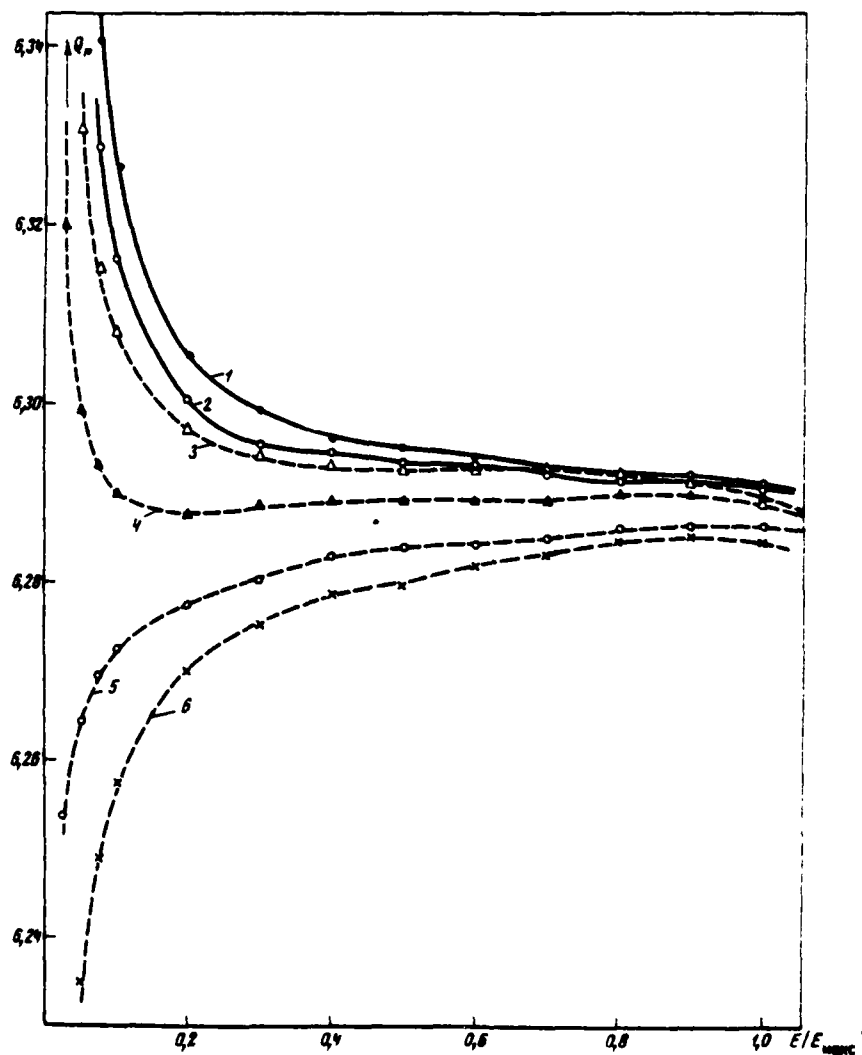


Fig. 9. The effect of quadrupole correction on the betatron frequencies (are utilized pole windings and supply by direct current).

1 - $I_4 D = 50 \text{ mA}$; 2 - $I_4 D = 300 \text{ mA}$; 3 - $I_4 F = 50 \text{ mA}$; 4 - $I_4 F = 100 \text{ mA}$; 5 - $I_4 F = 150 \text{ mA}$; 6 - $I_4 F = 200 \text{ mA}$

Key: (1) . mA.

Page 42.

Increase in the stability. Some most important changes, which ensured the best stability of intensity both from one impulse/momentum/pulse to the next and long-term, have already been mentioned in the preceding chapter, dedicated to intensity. They include new gun, preliminary grasper, with the frequency of 500 MHz, and frequency modulation. Moreover, virtually all electronic devices, which affect the stability of beam in the linear accelerator and the channel of injection, were reconstructed for the target obtainings of the best stability.

Thanks to these technical modifications became attained the long-term stability of circulating current $\pm 50/c$.

The limit of the stability of energy is determined mainly by alternating current of magnets. While direct current is stable with the precision/accuracy of better than 10^{-3} , alternating current, in spite of external and internal reaction circuits in the source, can cause the total oscillation/vibration of final energy to $40/c$. The target of regulation with the feedback is obtaining stable value

at the moment of injection; however since the pulsed source of supply, which feeds for the resonance system of magnet right-angled stress/voltage, it is started from the network/grid 50 Hz (to avoid play between network/grid and cycle of synchronism), phase jumps in the network/grid can cause the instability of the amplitude of the sinusoidal alternating current of magnet.

Increase in the energy. Initially designed energy DEZI was 6 GeV with the possibility of an increase to 7.5 GeV with an increase in the source power of high frequency. This stage was realized in 1968. In the high-frequency oscillator of 2 klystrons they work in parallel, providing the peak power more than 1 MW and average/mean power 300 kW at the frequency of 500 MHz (in the comparison with the values of 400/100 kW for the old generator). Average/mean power is limited to the supply of power of direct current, moreover one lamp gives the average/mean power of 250 kW, what, by the way, is mode/conditions for this lamp during its use in the rings DEZI. The service life of the lamps considerably that were guaranteed; the best lamp it studied about 7000 hours, and operation time from 3000 to 4000 hours is considered normal. Fig. 11 depicts new klystrons. It turned out that besides the alteration of high-frequency oscillator it is necessary to change vacuum system. For the laminar chambers/cameras from the stainless steel and epoxy resin subject in the run of job was the energy 6.25 GeV. As a result of the degassing

(for most part water vapors) under the action of eddy currents and radiations with the energy 6.25 GeV the pressure grew/rose to 5×10^{-6} or even to 10^{-5} GeV. This indicates ionization in the high-frequency resonators with the strength of high-frequency field, necessary for the work with the energy 6.25 GeV. .

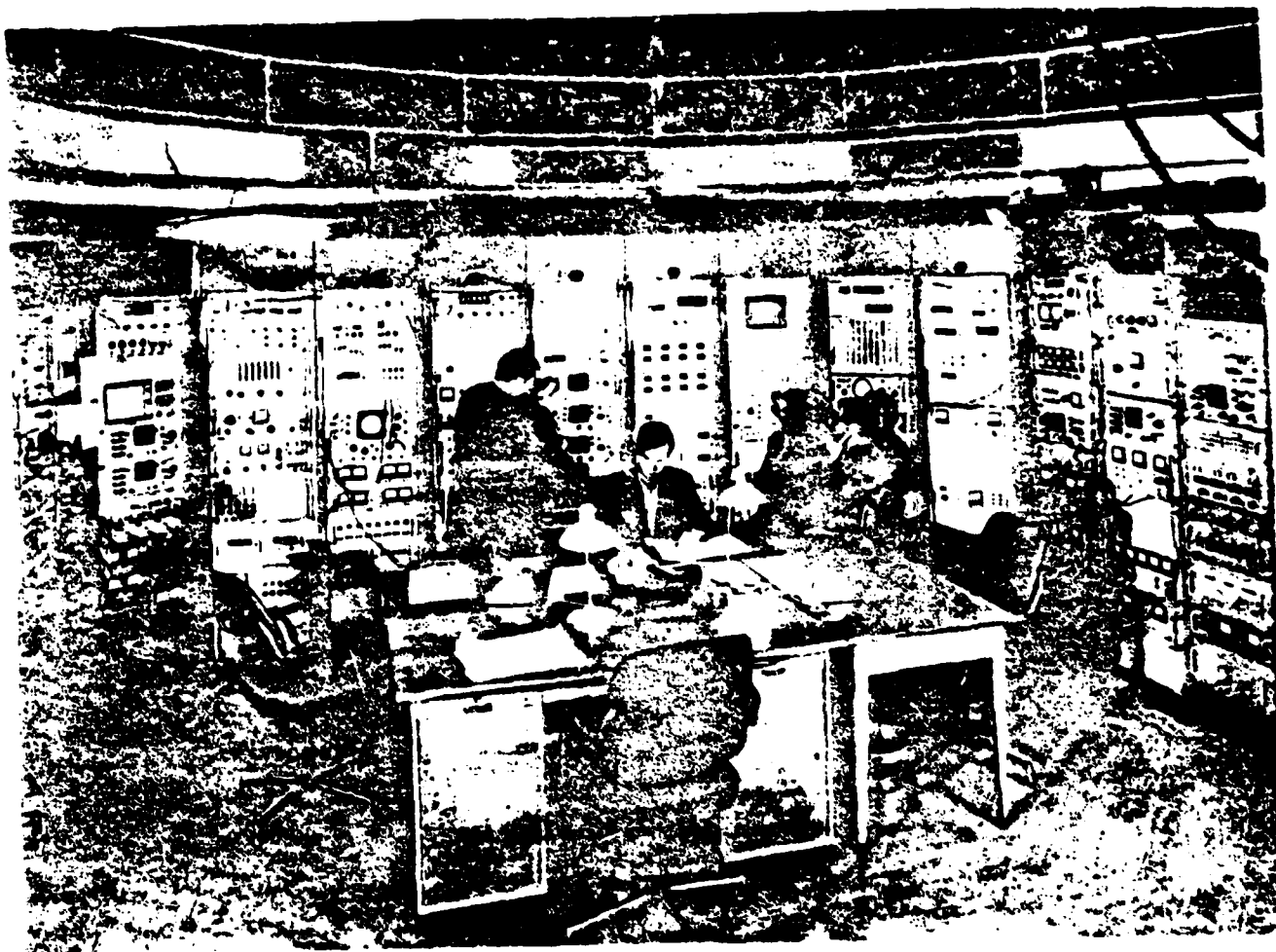


Fig. 10. The general view of the hall of control.

Page 43.

Resolution of problem were ceramic chambers/cameras, each of which was assembled of 14 sublocks with a length of 32 cm with the

metallized edges, to which were soldered small metallic bellows, moreover adjacent bellows were welded between themselves. For these chambers/cameras normal pressure without the special surface treatment and under any operating conditions composes 5×10^{-8} torus, which indicates the resolution of the problem of vacuum. Fig. 12 depicts ceramic can-type chamber for the emerging beam of photons.

The existing limitation of maximum energy of DEZI by the value of 7.5 GeV is not superimposed by technical components, since the magnets and high-frequency supply are capable of working with the energies 7.8-8 GeV. However, as a result of the synchrotron radiation and the connected with it radial betatron oscillations the radial breadth of beam rapidly grows/rises with the energies, which exceed 7.2 GeV. With the energies of above 7.2 GeV the control of the expansion of beam becomes ever more and more unreliable, and with 7.5 GeV beam fills the horizontal aperture of vacuum chamber, constituting in the magnets of radial focusing 12 cm. Is planned/glided additior to the construction/design of the accelerator of the damping magnet, analogous to that used in the Cambridge electron accelerator with the work in the mode/conditions of clashing beams with the energy 3 GeV. This construction/design transforms radial oscillations into the longitudinal ones, as a result of which of damping both types of oscillations.

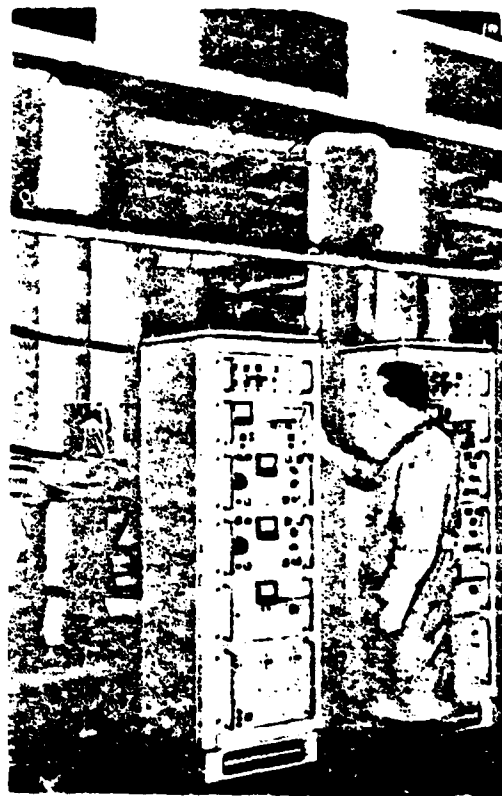


Fig. 11. 500 MHz klystrons to peak power 600 kW and average/mean power of 250 kW.

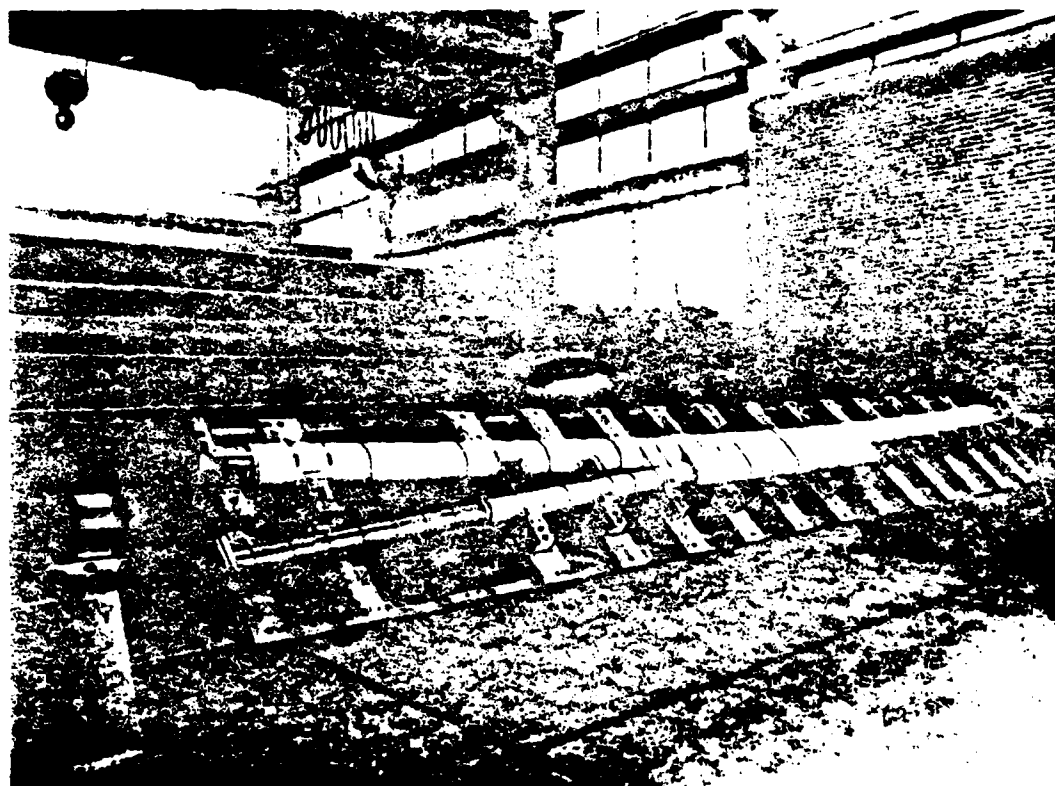


Fig. 12. Ceramic vacuum chamber/camera (for the section of the conclusion/output of photon beam).

Page 44.

If it is necessary to use synchrotron with the "flat/plane apex/vertex" of the current of magnet - the project, described below, this it is impossible to make with the energies of more than 6 GeV, if is not the well working attenuating system.

Characteristic of external beams. For the best control of photon beams are utilized accurately controlled local variations in that closed they are shaved instead of the initially utilized very rough method, consisting of the spiral turning of beam to the target by the method of the simple reduction of the amplitude of high frequency. In order to obtain such divergences of the closed orbit, through four series-connected auxiliary windings they discharge capacitor/condenser, that assures current in the form of half-period of the sinusoid, amplitude and phase of which are adjusted. In the system were introduced different modifications, which ensure the feed of the noncyclic sequences of capacitor discharges for the purpose of the distribution of the impulses/elements/pulses between the users and the latter according to the count, but not in terms of the value, was introduced the system of feedback, which uses as the monitor a photomultiplier, in order to realize not only the Gaussian time distributions of intensity, but also the trapezoidal and rectangular forms of "discharge/break". An example is given in Fig. 13. The basic idea of this method consists in the supplementary distortion of the closed orbit, controlled by feedback signal in such a way that the closed orbit is displaced to the target for the purpose of a reduction in the intensity of rotating beam. Due to the difficulties, connected with the time constant of system and the amplification

within the feedback, is required several dozen cycles of acceleration, until the form of "discharge/break" is managed in accordance with the form, programmed by operator.

The history of the slowly extracted electron beams in DEZI is too vast so that it is in detail to discuss it here.

At first the effectiveness of conclusion/output and the vertical emittance of the concluded beams were worse than expected. Reasons consisted in the resonances of highest orders which passed within the time of conclusion/output. After as a result of complicated measurements and calculations of these reasons explained, the method of conclusion/output at present is modified. It is proposed to change working point in ν_y and ν_z for the accelerator to utilize a diagram with the septum and with the quadrupole and sextupole magnets instead of one current screen. In the preliminary tests the effectiveness was raised to more than 80%, and emittance also corresponds to calculations. Moreover, it turned out that a modification of this diagram can be also utilized for the single-thread conclusion/output.

Plans/layouts for near future. For the synchrotron by new users are 3 GeV e^+e^- the rings, in addition to experiments in high-energy physics, conducted in the large experimental halls. Mainly, in order to obtain the necessary positions, but also for achievement of the

higher intensity of electrons was established, installed new linear accelerator-injector on 400 MeV which thus far is located in the stage of tests, but it will be finished/prepared for the work in the following year. Fig. 14 depicts this sectional accelerator in the tunnel. Table 2 depicts the comparison of designed and preliminary data of the tests of the linear accelerator II. The obtained intensity is located at the level of that expected or for the positrons even considerably above. Besides some equipment problems, will be required for a while for an improvement in the stability; however, in the principle new linear accelerator is already almost ready for the operation. For the investigations on the accelerators a new linear accelerator can be also utilized for the straight/direct injection into the rings. For this use/application the energy of electrons can be increased.

As has already been mentioned, this accelerator will not only in addition to electrons generate positrons, but it will also make possible to obtain the higher intensities than attained ones with the work of synchrotron with the linear accelerator No. 1. This occurs on three reasons: 1) new linear accelerator with the system of preliminary buncher at the frequency of 500 MHz will give approximately two times of more than electrons; 2) energy composes 400 instead of 40 MeV, which indicates field at the moment of injection of approximately 400 G instead of 40 G with only the

AD-A089 303

FOREIGN TECHNOLOGY DIV WRIGHT-PATTERSON AFB OH
TRANSACTIONS OF THE ALL-UNION CONFERENCE (2ND) ON CHARGED PARTI--ETC(U)
JUL 80 A L MINTS, A A KOMAR, A A VASIL'YEV
FTD-ID(RS)T-0692-80

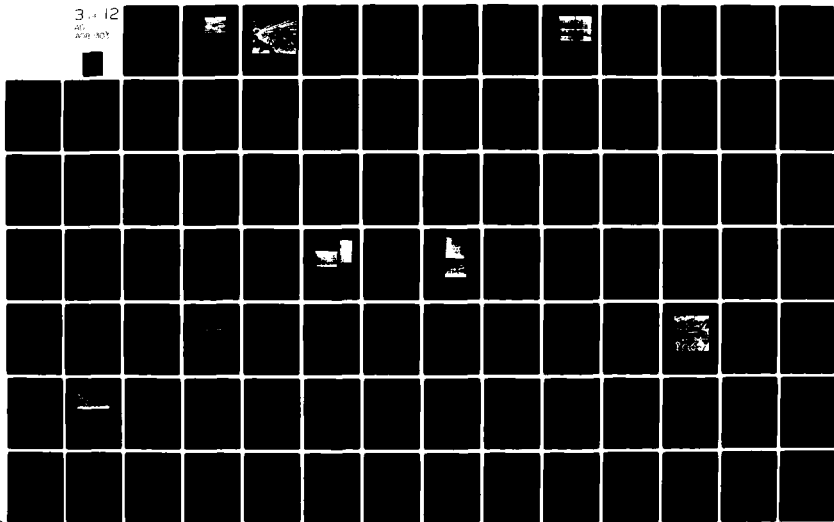
F/G 20/7

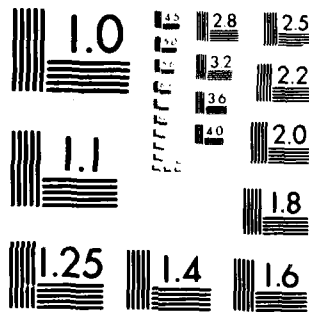
UNCLASSIFIED

NL

3-12

AD-A089 303





MICROCOPY RESOLUTION TEST CHART
NATIONAL BUREAU OF STANDARDS-1963-A

quadruple corrections of the field of injection; 3) with 400 G v at the moment of injection approximately 5 times higher. It indicates a larger increase in energy to the revolution and the respectively smaller problems of beam load, since the created by oscillator high-frequency field in the resonators is above.

From one side, higher intensity is unconditionally very desirable or for the best use of the available booster duration, since for an improvement in the statistics of experiments in high-energy physics. On the other hand, for many experiments, in particular for the experiments with the count, high intensity, in the principle desirable, generally speaking it is problematic - it is possible to remember difficulty with the problems of background and the random coincidences. The probable combat means with these difficulties are improvements in the methods of extraction.

Furthermore, will be changed magnet power supply, in order to obtain the "flat/plane apex/vertex" of the current of magnet, either by the method of adding the fourth harmonic of the frequency of 50 Hz or by the method of feed to the circuit of the half-period of sinusoid.

DOC = 30069204

PAGE

183

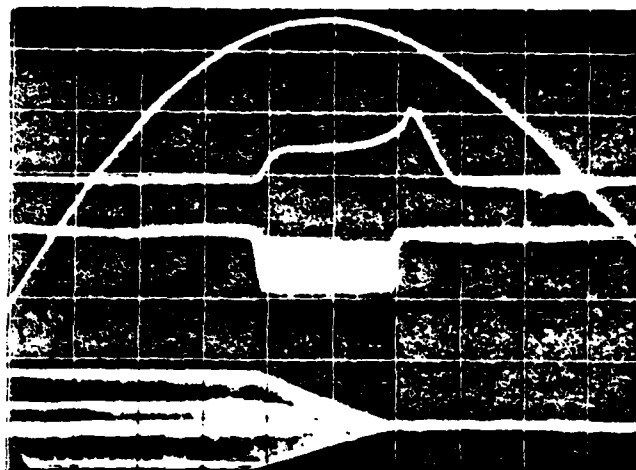


Fig. 13. Generation of photo right-angled beam in the time.

DOC = 80069204

PAGE 184

Page 45.

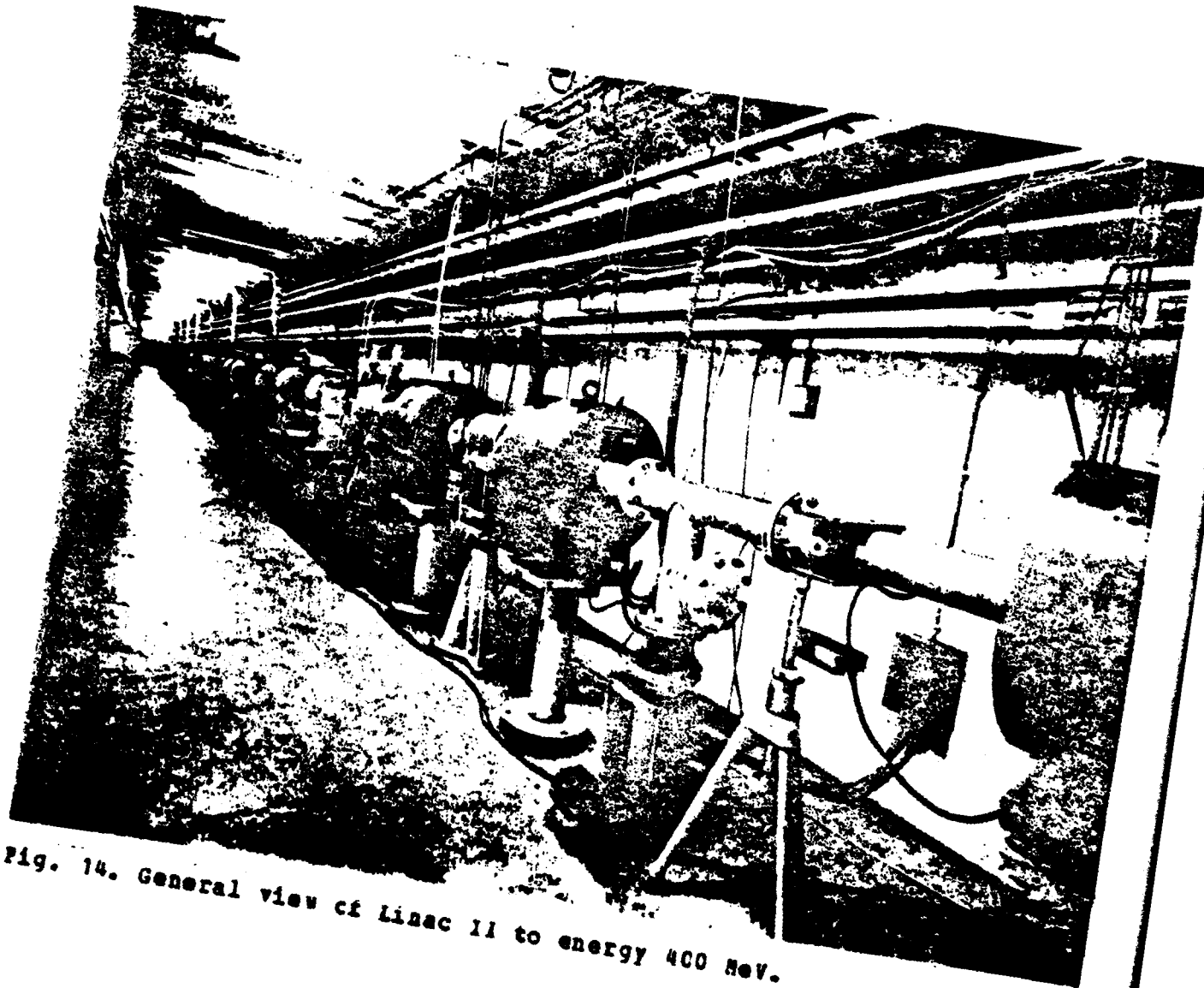


Fig. 14. General view of Linac II to energy 400 MeV.

Table 2.

Характеристика (1)	Проектные (2)	Гаранти- рованные (3)	Измерен- ные (4)	Едини- ца из- мере- ния (5)
(6) Энергия при ну- левом токе	703	647	692	(7) Мэв
(8) Энергия при токе 0,32 а	483	426		(9) Мэв
(9) Энергия при нуле- вом токе на по- зитронном конвер- те	292	269	$\frac{692}{12} \times 5 =$	(10) Мэв
			= 288	
(10) Энергия при токе 0,32 а на позитрон- ном конверте	200	177		(11) Мэв
Мощность при 0,32 а на позитронном кон- верте	64	56		(12) Мвт
(12) Энергия позитронов	410	386	390	(13) Мэв
(13) Позитронный ток на выходе линейного ускорителя	4,16	1,25	3-4	(14) ма
(14) Электронный ток при разбросе энергий в пределах $\pm 1/2\%$ и эмittance 1% см.мрад	240	125	130-160	(15) ма
(16) Позитронный ток при разбросе энергий в пре- делах $\pm 1/2\%$ и эмит- тансе 2% см.мрад	1,04	0,5	1,48	(16) ма

Key: (1). Characteristic. (2). Designed. (3). Guaranteed. (4).
Measured. (5). Unit measurement. (6). Energy with zero current. (7).
MeV. (8). Energy with current 0.32a. (9). Energy with zero current on

positron envelope. (10). Energy with current 0.32 and on positron envelope. Power with 0.32a on the positron envelope. (11). MW. (12). Energy of positrons. (13). Positron output current of linear accelerator. (14). Electronic current with energy dissipation within limits of $\pm 120\%$ and emittance 1 μ see rad. (15). mA. (16). Positron current with scatter of energies within limits of $\pm 120\%$ and emittance 2 μ see rad.

Page 46.

Instead of the available time of the conclusion/output 0.9μ s of energy range $\pm 0.250\%$ about the maximum energy these methods will ensure the time of conclusion/output, equal to 3-4 ns, which means that the porosity for the experiments will be improved approximately 4 times, since repetition frequency will remain as before (50 imp./s). Fig. 15 and 16 give the appropriate forms of the current of magnet. Fig. 17 depicts the current of magnet and the intensity of the of circulating beam during preliminary tests with the energy 1 GeV which were carried out because it was not confidence in the symmetry of magnetic circuit and corresponding three-dimensional/space symmetry of magnetic field at frequencies, different from 50 Hz (unbalanced permittance currents to the earth, traveling waves). New system encompasses the source of power supply 200 Hz, developed together with the groups of synchrotron, energy and

cooling systems on DEZI, and it will be completed toward the end of 1971. As has already been mentioned, for the work in the mode/conditions of flat/plane apex/vertex with the energies of more than 6 GeV it is necessary to provide damping magnet, and unconditionally, is required a supplementary increase in the average/mean power of high-frequency oscillator, in order to compensate losses to the synchrotron radiation in the time of flat/plane apex/vertex.

In conclusion it would like to mention about the problem of instability in connection with the enhanced intensity. Without going into particulars, it is possible to say that not only on DEZI, but also on other electron accelerators the instability of the circulating beam appears already at average/mean intensities 6-12 nA (average/mean current 16 nA for this accelerator corresponds 5×10^{12} particles/s).

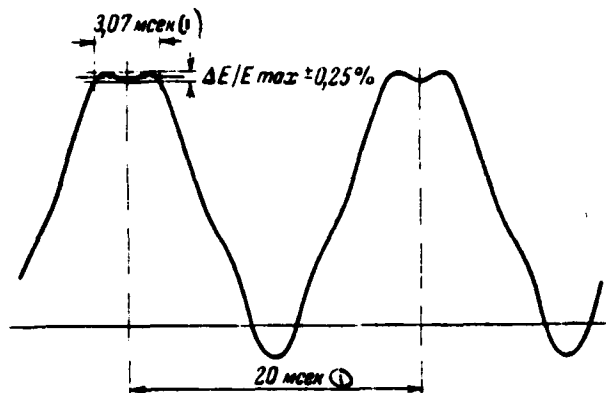


Fig. 15.

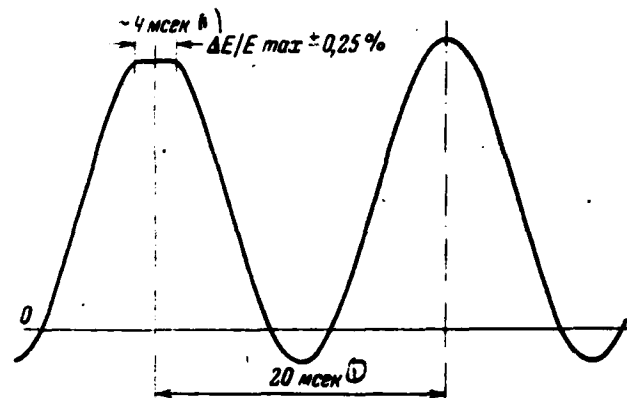


Fig. 16.

Fig. 15. Flat/plane apex/vertex in current of magnet with stress/voltage 50 Hz (100o/o) and stress/voltage 200 Hz (8.45o/o).

Key: (1) . ms.

Fig. 16. Flat/plane apex/vertex with additional impulse/momentum/pulse in the form of half sinusoid.

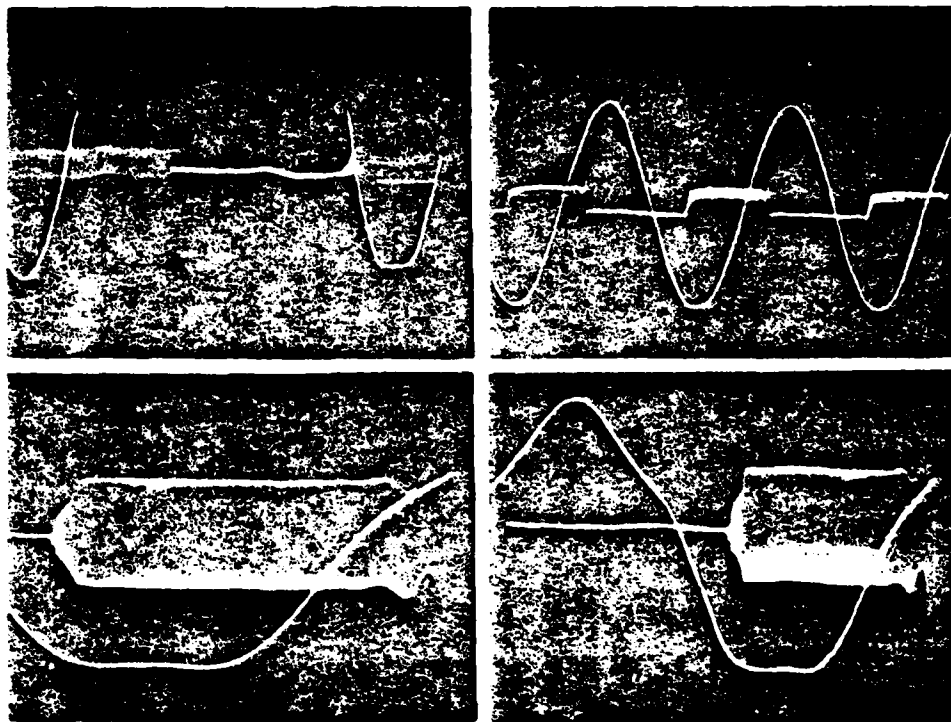


Fig. 17. Current of flat-topped magnet and intensity of beam during the preliminary tests on low energy (~ 1 GeV).

Page 47.

At such relatively low intensities in the chamber/camera still sufficient room, so that upon the acceleration do not appear losses. However, control of conclusion sometimes becomes difficult. Both on DEZI and in other centers are advanced many theories; however, there is no final explanation as yet. Evidently, some phenomena are analogous by certain of the numerous instabilities with which it is

necessary to fight on the rings. Preliminary tests on this synchrotron with the use of a new linear injector-accelerator, during which to the brief time intervals reached the intensities of the circulating beam of more than 50 nA (that approaches 2×10^{13} particles/s), they emphasized the need for further studies since under these conditions of instability they led to the losses of intensity during the acceleration even in the case when into the accelerator was not introduced any experimental target. Thus, besides the theoretical work, continue programs on the creation of the more advanced measuring and research devices, correct as the sensor of the dynamic profile/airfoil of beam, sensors of the group and high-frequency phases: the more advanced data processors for example, by the controlling computer; instrument for the load of high-frequency resonators with high Q for purposes of investigations; high-frequency quadrupoles and additional high-frequency resonators for the independent change in the frequency with the decoupling of the frequencies of beam, instrument for the detection of the highest high-frequency vibration modes, which affect the beam and, etc.

It is obvious, there is no limit to works even on the already existing and regularly working accelerator, if it is necessary to constantly improve it in accordance with the increasing requirements of the groups of experimental high-energy physics. and since the phenomena become ever more complicated, the necessity for the

collaboration between the laboratories, which work in this region, steps of ever of more civicus.

Discussion.

V. I. Kovalenko. What beams at present are derived/concluded from DEZI and what are planned/glided?

G. Kumpfert. In the report is given the general/common/total beam allocation and changes which it is proposed to make. Are derived/concluded 3 electron beams and one photon. It is proposed to derive/conclude additionally positrons and polarized particles.

V. L. Serov. What methods of fight with the beam load?

G. Kumpfert. Synchrotron operates at a frequency of 3 GHz, and prebuncher at the frequency of 250 MHz. We attain precise phase relationship. Furthermore, is applied a variation in the frequency upon the injection. The central frequency of resonator can be reconstructed on 40 kHz, which constitutes 10^{-4} from the frequency, which is utilized in bunchers. Also this is utilized the shunting of resonators. The unloaded resonator has quality on the order of 80000, with the external shunting the quality decreases 5 times.

V. G. Rogozinskiy. Was conducted the warm-up of vacuum chamber in obtaining of vacuum of $5 \cdot 10^{-10}$ torus.

G. Kumpfert. Chamber/camera was made from metallized aluminaceous ceramics. This material can be used for the warm-up. Generally warm-up is not necessary. Without the warm-up is obtained the vacuum $8 \cdot 10^{-10}$ torus.

G. V. Badalyan. In what did consist the alteration of the system of the conclusion/output of electrons?

G. Kumpfert. They improved the agreement envelope of particles with extraction channel during the resonance conclusion/output.

9. Increase in the intensity of proton synchrotron by the energy 70 GZS by means of an increase in the energy of injection.

Yu. M. Ado, V. I. Balbekov, A. A. Vasil'yev, E. A. Vodop'yancv, V. A. Glukhikh, A. A. Zhuravlev, V. B. Zaimanzon, Ye. G. Kozar, A. A. Kuz'min, V. M. Lebedev, A. L. Mints, N. A. Monoszon, B. P. Murin, E. A. Myae, A. A. Naumov, V. Ye. Pisarevsky, A. V. Popkovich, A. M. Stelov, V. A. Titus, B. R. Shentel', P. Z. Shiryaev, I. A. Shukelyc.

(Institute of physics of high energies, scientific research institute

of electrophysical equipment by them. D. V. Efremov, radio engineering institute of the AS USSR).

In the present report are given the results of studying the problem of a sharp increase in the intensity of proton synchrotron IFVE [1]. Are examined only the basic aspects of reconstructions, which are specific in the diagram of an increase in the energy of injection accepted. In more detail about the separate systems and the assemblies of new complex it will be reported in special reports [2-4].

The proposed project is designed for obtaining $5 \cdot 10^{13}$ proton cycle, which corresponds to the average/mean current approximately/exemplarily $1 \cdot 10^{13}$ of prot/s. These parameters were selected on the basis of the following considerations: 1) project must not provide for a considerable change in the basic assemblies and system of biological accelerator shielding; 2) the sizes/dimensions of the accelerated beam must not differ significantly from those existing; 3) accelerator shutdown must not exceed several months.

From the point of view of the permissible Coulomb shift/shear of betatron frequencies the energy of injection into main accelerator must be not less than 1 GeV (Fig. 1), but for weakening of the effect

of anharmonic resonances it is expedient to raise it to 1.5 GeV.

Page 48.

Were examined the injectors of three types: 1) rapid booster, i.e., the synchrotron of a small radius, which works with the high repetition frequency and imprising main accelerator during their several cycles. The diagrams of the work of this injector it is shown in Fig. 2; 2) slow booster, i.e., synchrotron with one or several magnetic paths/tracks and total length and repetition frequency by the same as in main accelerator; 3) linear accelerator.

As a result of the analysis of versions the preference was returned to the rapid booster, major advantages of which are relatively small sizes/dimensions, considerable experience of construction if not by complex as a whole, then all its composite/compound component parts; the absence of the parts, which require the unmastered technical solutions and the new materials. All this makes it possible to hope for the minimum periods of construction, adjustment and starting/launching of new injector. On the other hand, slow booster for the accelerator IPVE would have unacceptably large sizes/dimensions or large number small rapid, and the construction of linear accelerator to the energy 1.5 GeV is knowingly most dear and very complicatedly.

A main deficiency/lack in the rapid booster - the relatively long time of injection into main accelerator - in our case does not have special importance, since without the basic alteration of the power-supply system and basic magnet windings the duration of cycle cannot be made less than 5 s and its increase still approximately/exemplarily on 1 s will lead to a reduction in the average/mean beam current in all to 20%/o. The difficulties, connected with the prolonged circulation of beam in the stationary injection field, also are not insurmountable ones.

Are given below the basic parameters of the new complex of injection and the discussion of the selection of most important ones of them:

intensity in the impulse/momentum/pulse ... $1.7 \cdot 10^{12}$.

Repetition frequency of the cycles ... 25 Hz.

Number of impulses/momenta/pulses of injection into main accelerator ... 30.

Full/total/complete time of injection into main accelerator ...

DOC = 80069204

PAGE 196

1.2 s.

Energy of the protons ... 3.7.5-1500 MeV.

Orbit circumference ... 99.16 m.

Radius of curvature ... 7.87 m.

Magnetic field on the axis ... 1.13-9.55 kOe.

Sizes/dimensions of chamber/camera ... 16x7.4 cm².

Frequencies of the betatron

on a radius ... 3.26.

on the vertical line ... 3.38.

Critical energy (kinetic) ... 1686 MeV.

Frequency of revolution ... 6.63-2.79 MHz.

Multiplicity of radio-frequency ... 1.

Maximum accelerating voltage ... 65 kV.

The natural tendency to make a booster possibly shorter runs, besides the limitations from the side of magnetic field, into the difficulties, connected with the accumulation of a large number of particles on the short path/track. Furthermore, for convenience in the synchronization of booster with main accelerator is required the approximately/exemplarily short relation of their lengths. Based on this the length of booster it was selected equal to 99.16 m, which composes $1/15$ lengths of basic machine. With the multiplicity of radio-frequencies with respect 1 and 30 each cluster, accelerated in the booster, occupies one separatrix of main accelerator for filling of which are required, thus, 30 cycles of injection.

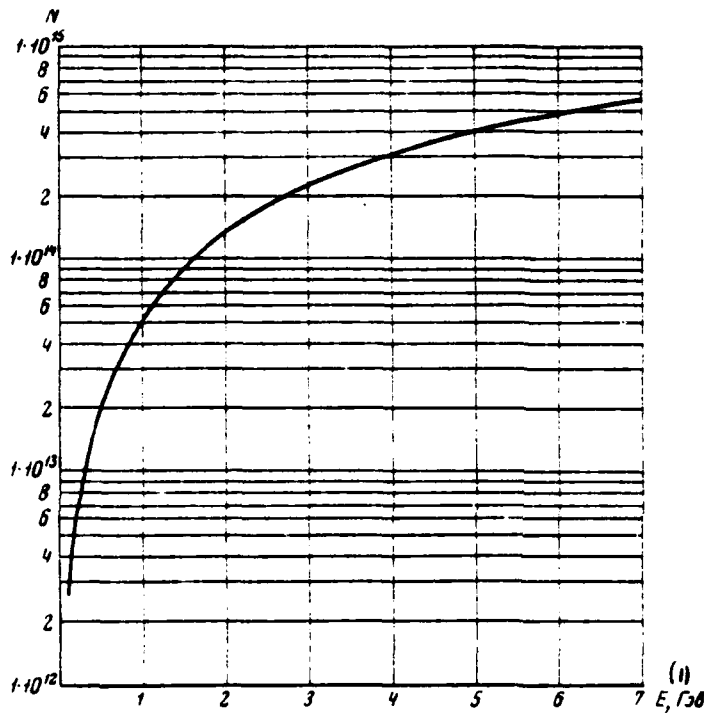


Fig. 1.

Fig. 1. Maximum number of accelerated particles for accelerator IFVE depending on energy of injection.

Key: (1). GeV.

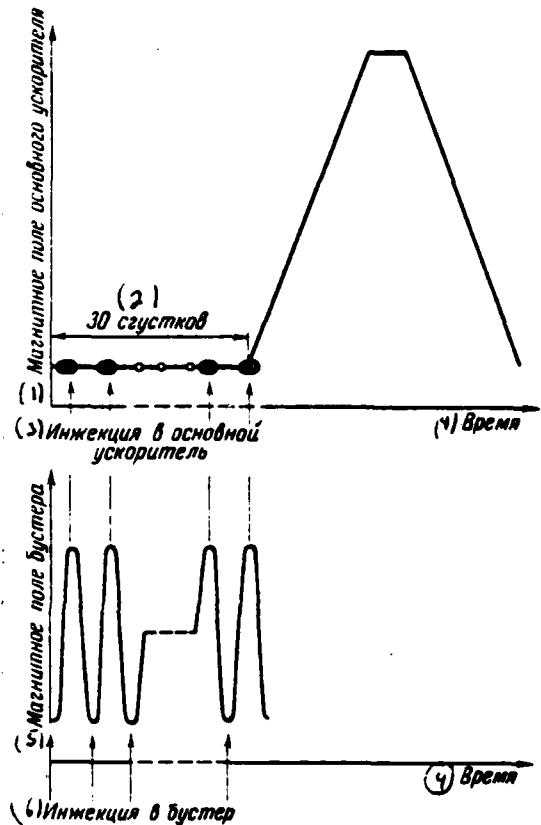


Fig. 2.

Fig. 2. Diagram of work of rapid booster-injector. Above - the cycle

of main accelerator; below - the diagram of the work of booster.

Key: (1). The magnetic field of main accelerator. (2). clusters. (3). Injection into main accelerator. (4). Time. (5). Magnetic field of booster. (6). Injection into booster.

Page 49.

The cluster whose firstly initial length close to 100 m, toward the end of the accelerator in the booster reaches ~25 m and easily placed in the separatrix of main accelerator.

With this method of injection in each cycle of the booster it is must be accelerated $1.7 \cdot 10^{12}$ of particles. Transition to the higher multiplicity of radio-frequency would require a proportional increase in this number and, we conceal that, increases in the amplitude of accelerating voltage.

The frequency of repetition of the cycles of booster is selected as being equal to 25 Hz, and its increase impede the difficulties, connected mainly with the complication of the accelerating system. Consequently, 30--fold injection into the basic machine will last by 1.2 s, which, as already mentioned, comprises less than 20% of time of complete cycle. Accelerating voltage in the booster will be modulated

in the amplitude for achievement of the greatest capture and regulating of the length of clusters upon the injection into main accelerator.

From the considerations of the permissible Coulomb shift/shear of betatron frequencies the energy of injection into booster can not exceed 30 MeV. Its considerable increase is inexpedient, since due to an increase in the particle speed for the accumulation of the same charge will be required larger speed upon the injection. We consider it unfavorable for these reasons to utilize as the injector the existing linear accelerator to the energy 100 MeV. One should also consider that its conversion for the work with the frequency of 25 Hz requires the considerable expenditures of time and resource, and together with the the adjustment of booster this will lead to the prolonged cessation of main accelerator. It is assumed that the existing injector can be preserved in the present form as the stand-by and for the experiments, which do not require high intensity.

Since the necessary parameters of injector for the booster do not exceed the possibilities of the existing linear accelerators of Alvarez's type, for the purpose of the savings of time and resources it was decided for the basis during the design to take the first section of the existing injector, having exit energy 37.5 MeV. With

the current 100 mA and the coefficient of capture $-2/3$ for the accumulation in the booster $1.7 \cdot 10^{12}$ of protons will be required by 3-4 -reverse/circular injection which will be accomplished/realized with the aid of the magnetic inflector and system of the kickers, which create the local distortions of the closed orbit. the accumulation of particles is intended to produce in the radial phase space. The calculations, carried out taking into account the effect of space charge, show that after injection the effective radial emittance of beam will not exceed 44 cm. mrad. This corresponds to emittance of 0.17 cm. mrad with the energy 70 GeV and condition of the adiabatic fading of emittance upon the acceleration.

The magnet of booster consists of 16 periods; the diagram of period is shown in Fig. 3. The selection of structure PCFDCD is caused by the presence of the relatively long gaps/intervals, necessary for positioning/arranging the accelerating devices/equipment, systems water also of the conclusion/output of protons and corrective elements/cells. The parameters were selected in such a way that the critical energy of booster would be above nominal. Were considered also the requirements, which escape/ensue from the special features/peculiarities of the system of single-turn beam extraction which will be accomplished/realized with the aid of the full-aperture kickers.

The timing mechanism of booster and main accelerator must solve three problems: a) the determination of the moment/torque of the conformity of particle momentum to the level of magnetic field in main accelerator; b) the determination of the moment/torque of agreeing the position of cluster with the phase HF of the field of main accelerator; c) the selection of free separatrix. The first two problems are solved by the comparison of frequencies and phases of stresses/voltages in the booster and main accelerator. For agreeing the phases is necessary the "slippage" of frequencies - for this purpose the length of booster to 0.2 exceeds 1.15 part of the length of main accelerator. For the solution of the third problem the signal from the beam is compared with the impulse/momentum/pulse, "cabled" to the phase of accelerating field.

At the designed intensity the effects of space charge in the booster - into that cluster coherent - are insignificant. On the contrary, the Coulomb shift/shear of betatron frequencies in main accelerator is sufficiently great, and, probably, will be required the correction of frequencies for the purpose of the optimization of the position of operating point with respect to the bands of most dangerous resonances. From other expected effects in main accelerator by most essential ones is represented the distortion of longitudinal phase volume near the critical energy and wall instability due to the final conductivity of the material of chamber/camera.

For the introduction/input of protons into main accelerator it is most convenient to utilize the existing place for injection. In this region there is a corresponding free space for constructing necessarily the construction complex. In this case will not be necessary to produce the changes in the arrangement of magnet blocks of main accelerator. Is retained also the possibility of rapid transition not injection from 100 MeV of linear accelerator.

Radiation problem is one of the most essential ones in this project. Calculations and work experience of accelerator show that permissible is scatter $\sim 3 \cdot 10^{12}$ of prot/cycle. This will not require the amplification of the system of biological protection as a whole, with exception of separate places. On the other hand, this means that the effectiveness of conclusion/output must be not worse than 950/o at the maximum intensity. This and even better effectiveness at present is considered as real even for slow conclusion/output [6]. Ground relaying strictly of booster must have a thickness of 7 m.

The arrangement/practice of the new complex of injection in the locality is shown in Fig. 4.

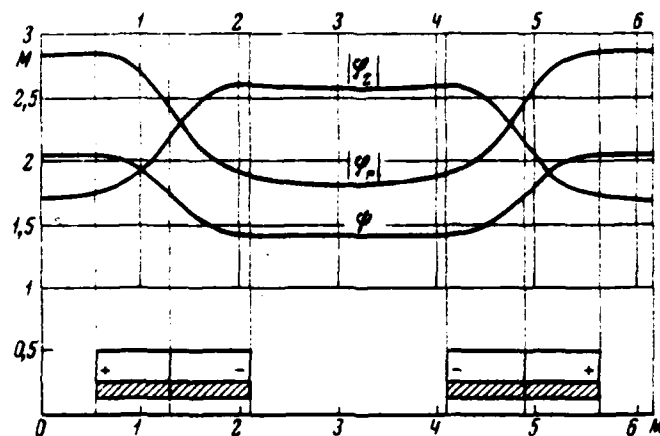


Fig. 3. Period of the magnetic structure of koster.

Page 50.

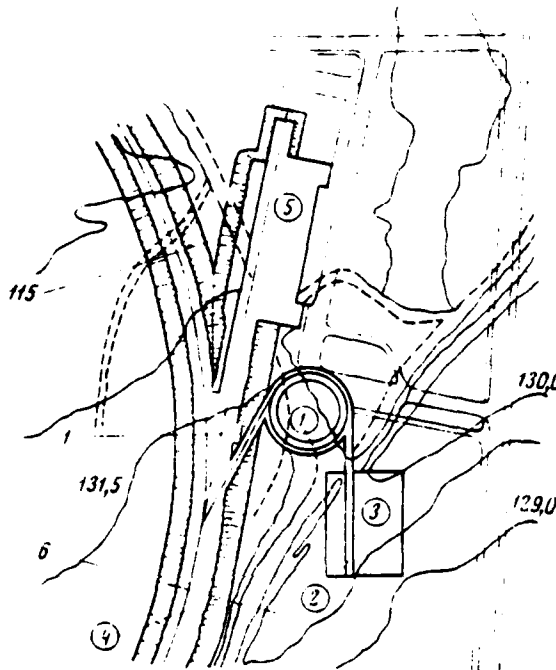


Fig. 4. Plan/layout of arrangement of new complex of injection. 1 - ring of booster; 2 - injector; 3 - laboratory housing; 4 - main accelerator; 5 - existing injector.

REFERENCES

1. Yu. M. Ado. et al. coll. the "Some results of complex adjustment and launching/starting proton synchrotron IFVE to the energy 70 GeV". Atomic energy, 1970, 28, No. 2, page 132.

2. A. L. Artemov et al. Rapid booster - injector of proton synchrotron IFVE. This rev., Vol. 1.
3. P. A. Vodop'yanov et al. New systems of the radio of electronics and control of proton synchrotron IFVE. This coll., Vol. 1.
4. A. L. Mints et al. Injector of the booster of proton synchrotron IFVE. This coll., Vol. 1.
5. I. M. Kapchinskiy et al. On the project of injector for the proton synchrotron to the energy 70 GES - transactions international/inter conf on the accelerators, 1963, M., Atomizdat, 1964, page 462.
6. A. Mashk and K. Simen. System of conclusion/output for the accelerator on 200 GES - The transactions of All-Union Conference on accelerators, Vol. 1. 1968, M., VINITI [ВНИИТИ, - All-Union Institute of Scientific and Technical Information], page 516.

Discussion.

Kh. reich, what assumptions are laid into the calculation of intensity?

E. A. Myae. Calculation was performed through the diagram of Lasslet

taking into account the wall effect of chamber/camera and magnet poles.

Ye. S. Mironov. Which existing size/dimension of beam at the end of the acceleration and what it will be after reconstruction?

E. A. Myae. Now the existence of beam at the entrance 0.17 cm. rad.

10. Latter/last improvements on the linear accelerator with the large operating cycle V Saclay.

F. Netter.

(Saclay, France).

The characteristics and the operational parameters of electronic linear accelerator with the large operating cycle in Saclay are described in the series/row of article [1-4]. Target of present report - to give the survey/coverage of the contemporary state of works. Somewhat larger attention are given to obtaining the beams of positrons and low-energetic/low-energy pions. Report summarizes the work of the numerous personnel of the groups of linear accelerator and nuclear physics.

During 1969 the linear accelerator was used mainly for the tests and the adjustment of the first physical experiments. From January on to August of 1970 of 2000 hour of work of the accelerator were isolated about 1000 hours of useful cluster time for experiments in physics of series/row and elementary particles. The others 50% time fall for the maintenance, the malfunctions of accelerator, the adjustment of the beam of accelerator and to experiments in physics of accelerators. Relatively rare representation of beam experimentally in nuclear physics is connected in essence with the difficulties of obtaining the positron beam. With the work with the electron beam on physical experiments usually fall more than 85% operating time.

At present experience of operating klystrons and high-vacuum lamps is still too small in order to accurately predict the mean life of lamps. Certainly, it is difficult to collect statistics on the system of 15 clystrons and 30 high-vacuum lamps. Furthermore, in the numerous experiments where is required energy 200, 300 or 400 MeV, latter/last klystrons do not work. Therefore only 8 clystrons studied more than 4000 hours with high voltage, of them 3 klystrons - are more than 4500 hour. Within this time was spoiled only one klystron (due to a breakage in the window). Furthermore, two klystrons in the beginning of operation detected anomalous properties that it does not affect statistics from time to time of life. About 20 high-vacuum

tubes studied more than 5000 hour in the heated state. Of all 30 lamps they were spoiled by 2.

Page 51.

At the present time are already carried out or are conducted the following experiments: 1) electronic scattering (e, e'), with coincidences ($e, e'p$) or without the coincidences on the setting up "Roundabout" [3], 2) photoneuclear reactions (in essence $\gamma^0(\gamma, p)$) the formation of pions at a small power level, 4) "neutrino" experiments in checking of the law of conservation of the lepton number (preliminary investigation).

In their present state these experiments require only feeble beams. For example, maximum average/mean intensity in experiments in electronic scattering was 40 μA (current in the impulse/momentum/pulse 40 nA). Therefore it was not the case test on the electronic scattering it was 40 μA (current in the impulse/momentum/pulse 40 nA). Therefore it was not the case test linear accelerator at the average/mean power in the beam of above 100 kW, obtained in 1968. But during October of this year will be established/installed the target of high power for the year will be established/installed the target of high power for obtaining the pions, and for the subsequent scathis is planned/gilded work at the

average/mean power in the beam at the level 100 kW or above.

Contemporary parameters. Electron beam.

Basic parameter of accelerator - energy resolution of electron beam. In order to obtain very narrow energy spectrum for the duration of the entire duration of pulse 10 μ s, was investigated the effect of different factors, such as the smoothness of the top of the impulses/moments/pulses of modulator (variation 20/c) or very small (2 kHz) variations in the pilot frequency of 2999 MHz. In present time it is easy to obtain the spectra with 100% of intensity in energy bite by width 0.5c/c and 80% intensity - in energy bite of 0.30% for the duration of the entire duration of pulse 10 μ s at the repetition frequency 1000 Hz. In energy bite of 0.150% they usually record more than 50% intensity of beam.

Is obtained also the high degree of reproducibility for many days during this adjustment of beam. If we tune linear accelerator by the method of the fine adjustment of the values of the stress/voltage of high-voltage sources, phases of high frequency, currents of the corrective and focusing coils and parameters of the beam-distribution system, then it is possible to immediately obtain beam with the prescribed/assigned fundamental characteristics.

The stability of beam with the continuous operation (24 hour and more) sufficiently good, but for the experiments with the high energy resolution is required to slowly regulate phase of one of the klystrons or pilot frequency in order to ensure permanent intensity in the narrow analyzing slot. For this include the contour/outline of the control the energies, controlled by the intensity of beam which they detect by the ferrite ring, arranged/located after the narrow analyzing slot, utilized in scattering experiments of electrons. As the reference signal is utilized the current, detected before the analysis of beam by another ferrite detector (see figure).

Contour/outline accomplishes/realizes automatic phasing of latter/last klystrons (feeding four latter/last section), if the detected intensity falls below fixture of displacement. However, if linear accelerator is well adjusted, stability itself so high which for obtaining the sufficiently precise system is necessary to regulate displacement at the level, very close to 100%. On the other hand, if linear accelerator is adjusted insufficiently well, this device/equipment is not equivalent to the full/total/complete and precise automatic system of tuning.

Further beam monitoring is accomplished/realized with the aid of the secondary electronic sensors, mounted in the different places. One ring with the central opening/aperture with a diameter of 5 mm is

arranged/located on the end/lead of the latter/last section of linear accelerator and it is very sensitive to any readjustment of the latter/last corrective coils and triplets of the quadrupole lenses, arranged/located by several sections earlier. Minimization of current from this secondary electronic circular sensor - good method of obtaining the accurately directed beam. Other sensors are placed before the slit are corrected with the experimental physical equipment.

High-frequency resonators at the end/lead of each section also are utilized as the detectors of beam which do not give the absolute value of intensity but they make it possible to accurately determine the shape of pulse in the time for the elongation/extent 10 μ s.

Positron beam.

The best current in the impulse/momentum/pulse, obtained at the present time for the beam of positrons with the energy 470 MeV at the end/lead of the linear accelerator, was 36 μ A the inflow of electrons with the energy approximately 80 MeV on the conversion target, equal to 28 nA. This gives conversion factor $1.3 \cdot 10^{-3}$. In energy bite of 10/c it is recorded by 750/c of current, which corresponds to current in the impulse/momentum/pulse 27 μ A. Systematic study of the phase shift between the positron beam and the initial electron beam gives

DOC = 80069204

PAGE ~~4~~ 213

indications about what energy group of positrons selects/takes conversion lens in the first accelerating section (section 7). Magnetic field strength in the conversion lens is limited to insufficient cooling.

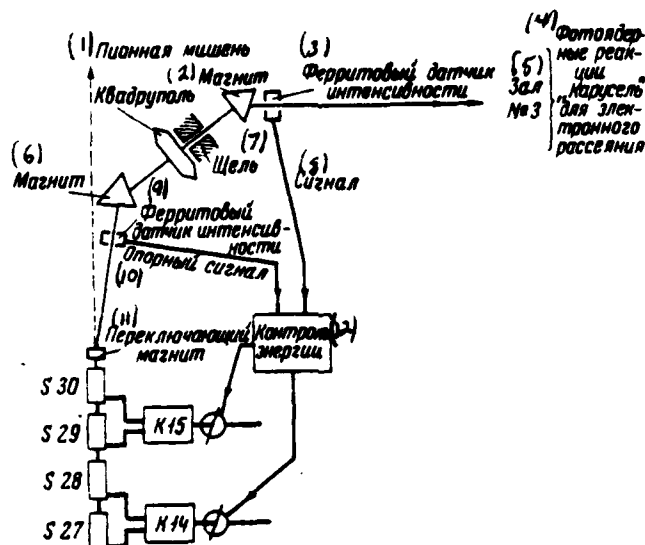


Fig. 1. Location of beams and kernel of the fine adjustment of energy.

Key: (1). Pion target. (2). Magnet. (3). Ferrite sensor of intensity.
(4). Photonuclear reactions "roundabout" for electronic scattering.
(6). Magnet. (7). Slot. (8). Signal. (9). Ferrite sensor of
intensity. (10). Reference signal. (11). switching magnet. (12).
Control of energy.

Page 52

New cooling system, which makes it possible to obtain the field of 1.8 T (18 kOe). It can in future ensure higher coefficient of conversion.

Continuous operation on the high power level necessary for executing the program on the photuclear to reactions, is partially limited by several difficulties:

1) the source of limitations was the instantaneous heating of target. Then the velocity of rotating target was increased from 2 to 3.7 revolutions per second. Nevertheless in a 10- centimeter elliptical trajectory of spot from the beam heating can prove to be excessive due to the very small diameter of spot, precisely, 0.5 mm; therefore it is necessary control current in the electronic focusing triplet of quadrupole lenses during the reduced displacement in order to obtain spot in diameter approximately 1 mm. Certain concern caused also the inequality of the peripheral speed of spot at the ends/leads of the great and minor axes of ellipse. Therefore into the mechanical transmission system of sector were recently introduced the corresponding improvements;

2) the general/constant heating of drift tube and entrance into section 7 due to the development of electronbursts in tungsten target with a thickness of with a of 3 mm is also the source of different disturbances/breakdowns, damage of vacuum, etc. In this place is established/installed new collimator with a good cooling.

If during the short-term tests at end/lead of the linear accelerator was obtained the average/mean intensity of positrons 0.2 μA , then with the continuous operation results were limited to the values of the average/mean current of electrons on the conversion target from 100 to 200 μA .

The typical parameters of positron beam at of long-term work at the large power are given in the table

(1) Энергия позитронов, Мэв	(2) Средний ток позитронов в экспериментальном зале после анализа на шели с $\Delta E/E=1\%$, на	(3) Соответствующий средний ток электронов на конверторной мишени, мкА
40	70	88
300	50	130

Key: (1). Energy of positrons, MeV. (2). Average/mean current of positrons in experimental hall after analysis on slit with $\Delta E/E=10/0$, on. (3). Corresponding average/mean current of electrons on conversion of target, μA .

The decrease of intensity for the beam of positrons with the energy 300 MeV is explained by the increase of emittance.

Up to now the best achievement in continuous operation was

obtaining useful beam of positrons with the energy from 240 to 280 MeV during 71 hours.

The great lifetime of target on the high power level (more than 100 μ A of average/mean electric current on the target) was 130 hours. However, in the future are expected the best results. Furthermore, is studied the possibility of the full/total/complete reconstruction of the source of positrons with the creation of new cooling system. Is investigated also the possibility of the setting up of this source between sections 12 and 13 which corresponds to energy of electrons at the level of approximately 200 MeV.

For improvement and facilitating the control of positron beam in drift space between sections 12 and 13 is established/installed new equipment; the analyzing magnet with the arranged/located after it faraday cylinder gives the possibility to investigate positron beam after acceleration six by sections. In recent measurements with the aid of this new equipment were obtained the positrons with the energy approximately 110 MeV. Are established/installed also the ferrite and resonator sensors, which earlier utilized only for the measurements of large cathode-ray current at the end of each section. The improvement of electronics made it possible to obtain sufficiently high sensitivity in order to measure the positron beam with current in the impulse/moments/pulse 1 μ A.

Obtaining pions.

The new source of pions began to work during January 1970. tests they are carried out only on a small power level of beam (current in the impulse/momentum/pulse 100 μ A - average/mean current 1 μ A). The targets of high power were established/installed during October and tested with the electron beam at the average/mean intensity of 300 μ A and the energy 377 MeV.

The beam-distribution system electron consists of one triplet of quadrupole lenses, which focuses beam to the target which is established/installed at a distance of 150 m after the end/lead of the accelerator; triplet is arranged/located in the middle. More than 90% current of electrons with the energy 400 MeV, which emerge from latter/last sections of linear accelerator, it was possible to focus on the target into the spot 2x5 mm. More accurate results will be obtained on the higher level of current in the impulse/momentum/pulse.

Pions are collected at angle of 120° in the limits of the solid angle of 16 m sterad with maximum momentum acceptance $\Delta p/p=5\%$ in the channel of length 8 m they were detected the pions of very low

energy (20 MeV), but the basic range of the utilized energy corresponds to 50 MeV. The intensity of the beam of muons also has noticeable value.

Construction/design is based on the preliminary measurements, which give intensity 10^5 pions with the energy 50 MeV on 1 μ A of electronic current per second and to the steradian in the momentum range $\Delta p/p = 10\%$.

Real measurements confirmed the estimated value (result somewhat above) of the intensity of pions. Are obtained also very satisfactory results relative to the pollution/contamination of pion electron beam, energy spectrum of pions and their spatial distribution.

Experimental hall is sufficiently great in order to arrange in it two and, possibly, even three systems of the transportation of pions and muons. Is studied the possibility of the setting up of second channel, intended for the muons.

For an increase in the convenience in the operation is made the automatic ^{switching} system of low speed. It will make it possible to alternately guide beam to the pion target and into hall No.3, where is arranged/located equipment for the investigation of photonuclear reactions and setting up "cutoff" for experiments in the

electronic scattering (see figure).

Page 52.

REFERENCES

1. H. Leboutet, G. Azam, F. Netter. J. Phys., 1969, 30, 62, 13.
2. H. Leboutet, G. Azam, F. Netter, C. Tzora. JEEE Trans. on Nucl. Sci., 1969, 16, 299.
3. F. Netter. Proc. 7th Internat. Conf. High energy Accelerators. Yerevan, 1969.
4. L'onde électrique. Special Issue, dec. 1969, 49, 11, 1122.

Discussion.

A. A. Vorob'yev. How does change conversion factor with the energy?

F. Netter. Conversion factor is proportional to energy to 200 MeV.

B. M. Voronkov. Were observed the damages of radiation character in the equipment?

F. Netter. No - with exception of the burn of target converter.

11. Some questions, connected with the acceleration of deuterons on the synchrotron LVE the J.I.N.R.

G. S. Kazanskiy, A. I. Pikhaylov, G. P. Fuchkev.

(United institute of nuclear studies).

In 1968 in high-energy laboratory ICYAI was proposed the method of accelerating of deuterons and α -particles on the synchrophasotron the J.I.N.R. [1]. The basic idea of method consisted of upon transfer of one accelerating system to another (preinjector, linear accelerator, synchrophasotron) velocity of deuterons and α -particles it would be two times less than the proton velocity. In this case it is represented by the possible to utilize the existing systems, if we fulfill following conditions: 1) to lower stress/voltage on the preinjector approximately two times; 2) to decrease with the aid of the special caps/fillings the clearances between the drift tubes of linear accelerator two times; 3) to decrease the stresses/voltages on the inflector plates two times; 4) to accelerate deuterons and α -particles in a synchrophasotron mode in two stages.

The present study examines the synchrophasotron mode of accelerating deuterons and α -particles.

1. Two-stage acceleration for deuterons and α -particles in the synchrophasotron mode.

When the velocity of deuterons and α -particles at the moment of injection is reduced by half in comparison with the velocity of protons, a twofold expansion in the frequency range of the synchrophasotron accelerating system is required. Since the master oscillator and the output stage of the accelerating station they do not provide this range, then it was proposed to accomplish/realize acceleration the synchrophasotron mode/conditions into two stages: I stage - acceleration in the mode/conditions of the second multiplicity in the range of the frequency of accelerating voltage (0.2-1.44) MHz; II stage - acceleration in the mode/conditions of the first multiplicity in the range (0.72-1.44)

MHz.

The necessary law of connection/communication between the frequency of accelerating voltage and the magnetic intensity is formed/shaped with one of the available assemblies of equipment by specially updated for accelerating of deuterons and α -particles.

The first stage of acceleration in the mode/conditions of the second multiplicity terminates in the magnetic field 1300 G, when the frequency of accelerating voltage reaches the limiting value of 1.44 MHz. At this moment it is necessary to carry out transition to the second stage, after changing the accelerating system by the first multiplicity.

In the presence of one accelerating station direct transition from one multiplicity to another is impossible due to the unsteady processes with the rearrangement. Is unsuitable also transition from one multiplicity to another with switched-off, to the transit time, accelerating voltage in the mode/conditions of growing magnetic field, since the duration of unsteady processes with the rearrangement substantially exceeds the lifetime of beam in the chamber/camera (500 μ s after the disconnection of accelerating voltage beam, filling entire azimuth of accelerator, it is displaced on a radius on 25 cm). Most suitable is transition from one

multiplicity to another in the mode/conditions of magnetostatic field. In this case considerably descend the requirements for the duration of unsteady processes with readjustment of the accelerating system.

2. Special features/peculiarities of transition from the first stage of acceleration on the second.

As the basis of transition from one stage of acceleration to another is assumed the principle of repeated capture into the acceleration in the mode/conditions of magnetostatic field [2].

After the translation/conversion of magnetic field into the mode/conditions of "table" (magnetic field is constant) concludes 1 stage of acceleration with the disconnection of accelerating voltage. As a result of the energy spread the beam, which consists initially of two clusters, "being eroded" along the azimuth, is converted in the circular. At this time is accomplished/realized the rearrangement of the law of connection/communication to the first multiplicity, and the output circuit of the accelerating system by the frequency of 720 kHz.

After this rearrangement is accomplished/realized repeated capture in the acceleration of the circular beam by a reclosing of

accelerating voltage with the subsequent transition from magnetostatic field to growing and accelerations to the II stage of up to the maximum energy.

Page 54.

Although, as show calculations, into the second stage of acceleration it is possible to take 80% of intensity of the beam, accelerated toward the end of 1 stages, the part of the beam will be lost upon transfer of magnetic field on I will shade branch. These losses depend mainly on the character of a change in the magnetic field on the transition, the value of its pulsations and value and character of a change in the amplitude of accelerating voltage. In the optimum case, utilizing mode/conditions of preliminary phase bunching [3], after transition it is possible to obtain about 60% of intensity of the beam, accelerated toward the end of 1 stages.

3. Experimental results.

During September 1969 on the synchrotron the J.I.N.S. were carried out experiments in acceleration of deuterons. In these experiments was not placed the task of obtaining the maximum intensity of deuterons, but was pursued the target of obtaining the data about the character of losses to the I stage of acceleration,

capture efficiency into the II stage and about the losses with the transition of magnetic field to the growing branch. Such data were necessary in order subsequently to take measures, which remove the effect of different factors on the losses of intensity upon the acceleration of deuterons.

Investigations showed difference in the character of losses in the initial section upon the acceleration of protons and deuterons. If upon the acceleration of protons the interval of losses stretches during the build-up of field to 500 G, then upon the acceleration of the deuterons of loss occur in entire 1 stage. This difference is characterized by the larger losses of deuterons on the residual gas due to smaller two times of kinetic energy of injection and by its slower increase upon the acceleration.

In Fig. 1 Presentation of the oscillogram of the intensity of deuteron beam with the acceleration in 1 stage and the initial section of the II stage (magnetic field is constant). From the oscillogram it follows that into the II stage it is seized by 70% of intensity of the beam, accelerated toward the end of 1 stages. This oscillogram is taken with included diagram of the depression of pulsations on the "table" of magnetic field. In the presence of pulsations are observed the large losses of intensity, obliged to the resonant step-up of synchrotron oscillations which it is difficult to

bridge due to the contradictory requirements for the amplitude of accelerating voltage. Insignificant losses at end of I stages occur as a result of the large pulsations of magnetic field upon transfer into the mode/conditions of "table" (diagram of the depression of pulsations is included after the transition of magnetic field into the mode/conditions of "table" and is turned off/disconnected before the transition to the growing branch).

Fig. 2 shows the oscillogram of the intensity of beam in the II stage of acceleration (Fig. 2a) and the radial position of beam (Fig. 2b) in the I and II stages. The sharp losses of intensity appear upon transfer of magnetic field on I will shade branch. These losses occur, apparently, as a result of " " of equilibrium phase jump, since after engagement of the diagram of the depression of pulsations magnetic field first decreases on 5 G, and only then it begins to grow/rise (see the oscillogram Fig. 3). The character of a change in the amplitude of accelerating voltage while conducting of these experiments is illustrated by the oscillogram Fig. 4.

The use/application of a system of the depression of coherent phase oscillations [4] although decreases the losses upon transfer of magnetic field to the growing branch, not in this measure, in which it should be expected. Obviously, are too great " " of equilibrium phase jump on the transition and is too weak appears coherence in the formed/shaped beam in the beginning of the II stage.

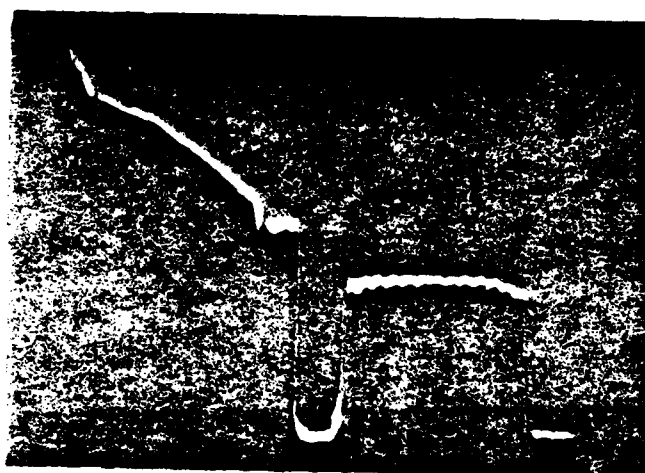


Fig. 1.



Fig. 2.

Fig. 1. Oscillogram of intensity of deuteron beam upon acceleration to I and nacale II stages.

Fig. 2. Oscillograms of signals of intensity upon acceleration of deuterons on II stage (a) and radical position of beam to I and II stages (b).

In conclusion the authors consider it their pleasant duty to express appreciation to A. M. Baldin, I. N. Semeryushkina, N. I. Pavlov, L. P. Zaiov'yev, V. I. Mircz, K. V. Chekhlov, to L. N. Belyayev for the permanent attention to the work, and also the collectives of the divisions of Radiotechnical, Elektrotekhniches and Sinkhrofazotron for the active assistance in the experimentation.

REFERENCES

1. Yu. D. Beznigikh, L. P. Zinov'yev, A. I. Mikhaylov, V. I. Moroz, G. S. Kazanskiy, N. I. Pavlov. Preprint the J.I.E.E. 9-4214, Dubna, 1968.
2. G. S. Kazanskiy, A. I. Mikhaylov. Preprint IOYAI 2795, Dubna, 1966.
3. G. S. Kazanskiy, A. I. Mikhaylov, N. B. Rutin, A. P. Tsarenkov. "atomic energy", 1965, Vol. 18, iss. 6, page 555.
4. G. S. Kazanskiy, A. P. Tsarenkov. Preprint IOYAI 2491, Dubna, 1965.

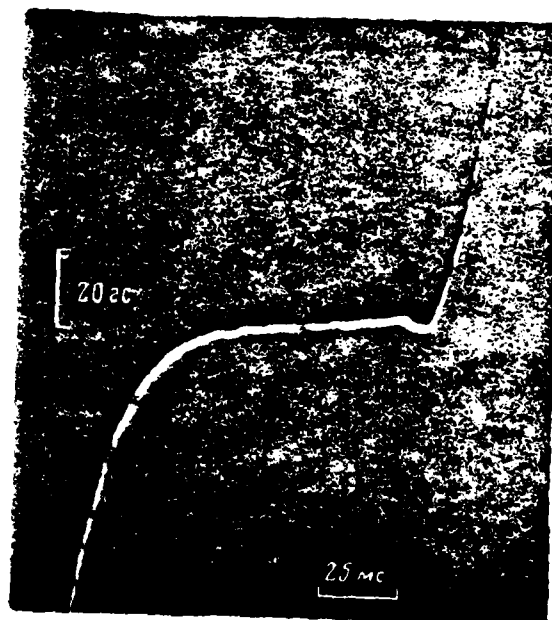


Fig. 3.

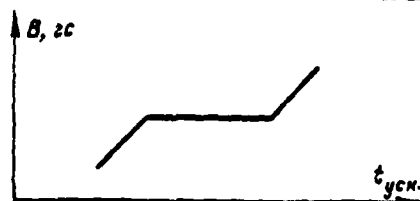


Fig. 4.

Fig. 3. Character of change in magnetic field on "table".

Fig. 4. Character of change in amplitude of accelerating voltage on I and II stages.

12. Project of the circular synchrotron of the Swiss institute of nuclear research.

D. P. Blazer, G. D. Gerber, G. A. Villaks.

(SIN, Switzerland).

Introduction.

SIN - abbreviated, reduced name of the Swiss institute of nuclear research. This institute obtained status of the branch of Swiss federal technological institute in 1968. In combination with the projected accelerative laboratory near Willingen, in 35 km to the northwest of Zurich, SIN to 1973 will allow contemporary experimental installations to the Swiss universities and other research groups.

DCC = 80069204

PAGE

231

At present the large part of the operating personnel works in the temporary/time location in a Zurich-Cerlikon.

Description of accelerator.

The basic designation/purpose of accelerator consists in the creation of large flows π^- and μ^- mesons with the aid of the proton beam with the energy approximately 600 MeV and the intensity of 100 μ A [1].

end section.

Page 56.

Accelerator is the two-stage combination of avf cyclotron (72 MeV) and circular cyclotron (590 MeV) with the separate magnets (Fig. 1). Both accelerators work isochronally at the frequency of 50 MHz [2].

Injector cyclotron. In order to obtain the accelerator, suitable for the wide experimental program, it was decided to utilize as the injector multiparticle cyclotron with the adjustable energy.

Avf cyclotron has the diameter of poles 2.45 m, one-quant system, alternating magnetic field and continuously changing frequency in the limits from 4.7 to 17 MHz, which provides the acceleration of the beams of different particles to the energies, given in Table 1.

Accelerator has the axial injection of the polarized protons and deuterons. During 250/c of time these beams they will utilize for experiments in nuclear physics in the individual section of experimental hall. After the passage of arc of 110° in the analyzing

magnet their energy resolution will comprise $\Delta E/E-10^{-4}$ (full/total/complete width on the half height).

As the injector for the high-energy step/stage this cyclotron will operate at the frequency of 50 MHz, which is third harmonic of the frequency of revolution of particles in the cyclotron. In this mode/conditions it will create proton beam with the energy 72 MeV with an intensity of 100 μA with the energy spread of less than 0.30/o and with the emittances of less than 30 mm. mrad. Will be undertaken special measures for the optimization of central region, symmetry of magnetic field (4 sectors) and system of conclusion/output, in order to ensure the guaranteed beam with the given above parameters (Fig. 2).

Contract to the construction of this accelerator was signed by firm "Phillips Oland" in the fall of 1968. Some basic elements/cells are located in the stage of construction and production.

The circular cyclotron. Proton beam with the energy 72 MeV is introduced into the ring which possesses the following basic characteristic special features/peculiarities, which facilitate obtaining the beams of high intensity with the intermediate energy: the separate magnets with small clearances, which ensure a small middle field and sufficiently strong axial focusing; a sufficiently

large energy gain per revolution, created by separate high-frequency resonators to very high voltages.

In this device/equipment are provided the conditions for a good control and the qualitative conclusion/output of steady beam with the high characteristics.

The circular cyclotron (Fig. 3) has 8 C-shaped magnets by azimuthal width of $\sim 18^\circ$. The pole gap decreases from 9 to 5 cm in the range of radii from 200 to 460 cm. Sectors must be spiral, since the focusing is only due to a step-like change in the magnetic field insufficient with the energies in question. Of the considerations of lighter and more effective working/treatment for the poles was selected the form of circular arcs, which ensures helical angle of $\sim 32^\circ$. Field in the limits of pole grows/rises with an increase in the radius from ~ 15 to 20.6 kg with the final energy 590 MeV (Fig. 4). The system of weak-current polar cases against the bundle will provide the necessary corrections fields. Vacuum chamber made of the stainless steel is connected directly with the magnet poles by elastic welded joint. Different sections of vacuum chamber contain sensors, collimators, devices/equipment for injection and beam extraction.

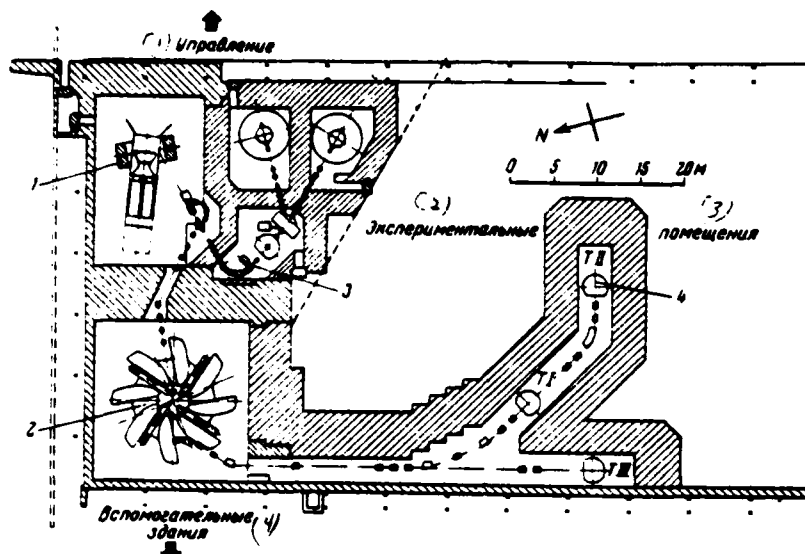


Fig. 1. The layout of accelerator SIN and experimental halls: 1 - injector cyclotron with the variable/alternating energy; 2 - the circular cyclotron for the protons with the energy 590 MeV; 3 - beam hole with the variable/alternating energy, including 110° analyzing magnet; 4 - target T I, T II and T III for the secondary beams (π , μ - mesons, neutrons, polarized protons); the moving concrete blocks for the protection of experimental hall, the channels of bundles and target.

Key: (1). Control. (2). Experimental. (3). Locations. (4). Auxiliary buildings.

Page 57.

The technical characteristics: the diameter of poles - ~ 2.5 m; a maximum radius of beam - ~ 1.1 m; a quantity of spiral sectors - 4; isochronal field - 0.4-1.6 in s/m^2 ; cyclotron frequencies - 1.6-17.1 MHz; voltage frequency on the dees - 4.7-17.1 MHz, 50.8 MHz (third harmonic of the mode of injection); dee voltage - 70 kV; beam extraction - precessional; the effectiveness of conclusion/output - 70%; the source also of ions - internal; internal with the preliminary acceleration α ; external, axial injection; are possible the sources of the polarized particles.

Table 1. Injector cyclotron (development of first "Phillips").

Частица (1)	(2) Интервал энергии, Мэв	(3) Интенсивность, мка	Эмиттансы x, z (4) мм, мрад, норм. при энергии 50 Мэв	Разброс по энергии (5)	Относительная длительность импульса (микроструктура), % (6)
Режим инъекции при 50,8 МГц (7)	72 ± 1	> 100	≤ 30	≤ 0,3%	3 - 5
Режим переменной энергии (8)					
p	10 - 75	25	≤ 30	≤ 0,3% ~ 100 кэв (9)	1,5 - 1,4
d	10 - 65	25	≤ 30	≤ 0,3% ~ 100 кэв	1,5 - 1,4
α	20 - 130	15	≤ 30	≤ 0,3% ~ 100 кэв	1,5 - 1,4
He ³	15 - 160	15	≤ 30	≤ 0,3% ~ 100 кэв	1,5 - 1,4
Тяжелые ионы (10)	0,6 - 10 Мэв на нуклон (11)	2	≤ 40	≤ 0,5% ≥ 100 кэв	1,5 - 1,4

Key: (1). Particle. (2). Energy range, MeV. (3). Intensity, μ A. (4). Emittances x, z mm, mrad, n. with energy 50 MeV. (5). Energy spread. (6). Relative duration of beam burst (microstructure), o/o. (7). Mode/conditions of injection with 50.8 MHz. (8). Mode/conditions of variable/alternating energy. (9). keV. (10). Large ions. (11). MeV to nucleon.

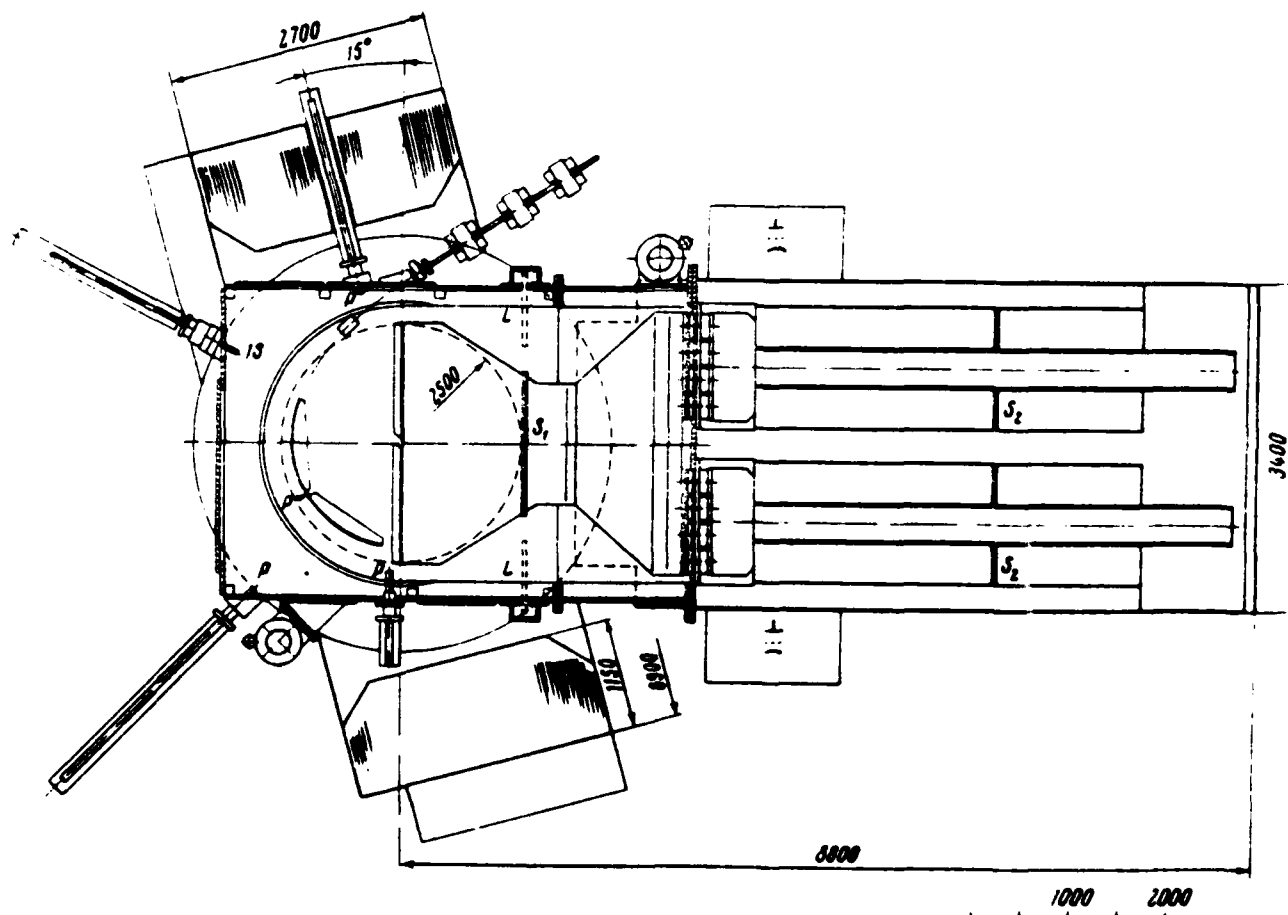


Fig. 2. Construction/design of injector cyclotron. s_1 - HF short for 50 MHz; s_2 - moving HF short for the frequencies between by 4.6 and 17.1 MHz; Is - ionic source; P - testers.

Page 58.

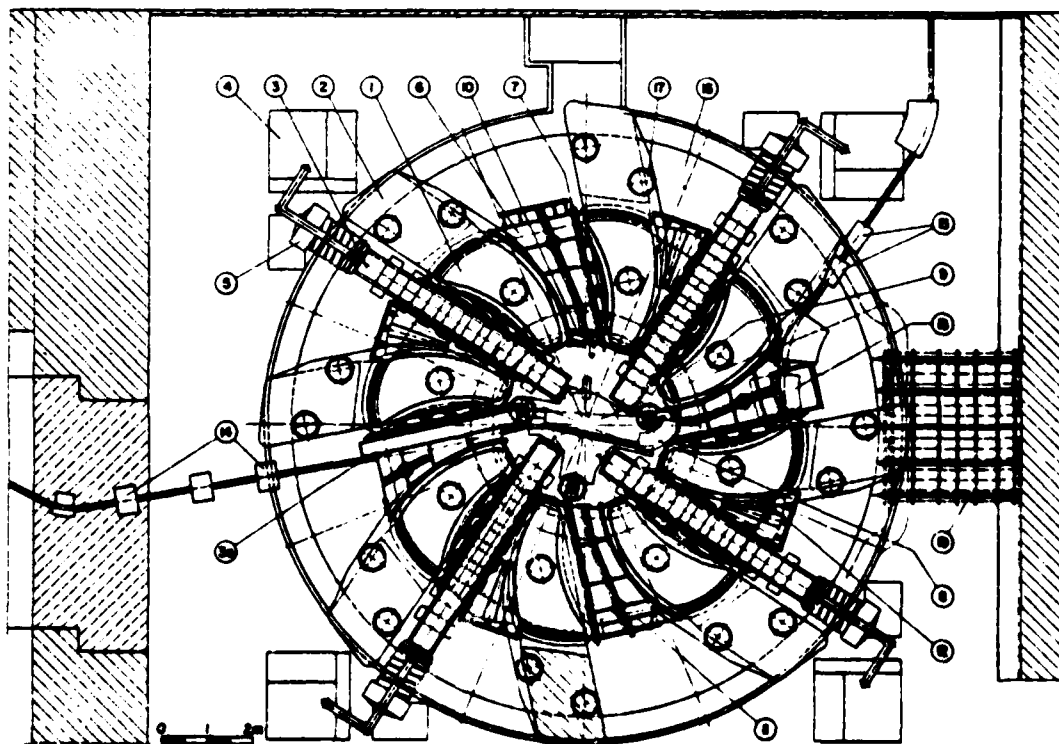
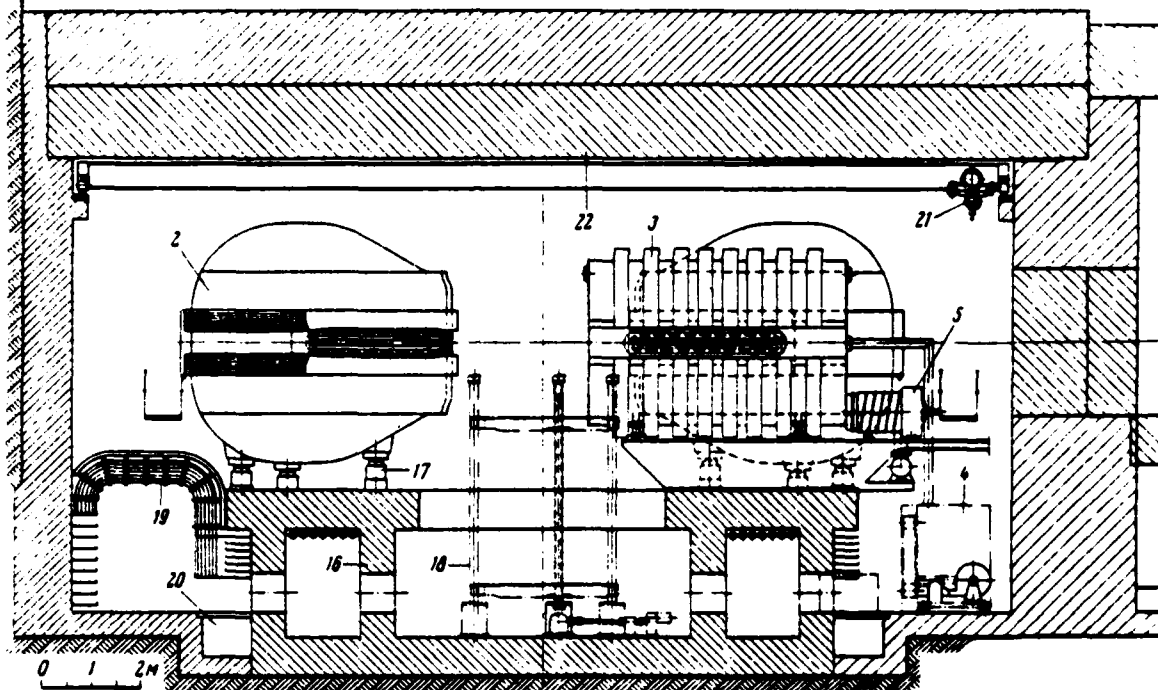


Fig. 3. Construction/design of the circular cyclotron. 1 - pole of sector magnet; 2 - framework of sector magnet; 3 - RF resonators 50 MHz; 3a - place for 150 MHz RF of resonator; 4 - RF oscillator on 250 kW; 5 - high-vacuum pumps; 6 - free sections of vacuum chamber; 7 - pressure-operated devices for the vacuum seals; 8 - magnet for the injection, 94°; 9 - magnetic injection channel, 3 kg; 10 - electrostatic inflector; 11 - electrostatic deflector; 12 - magnetic focusing and controlling element/cell for the deflected bundle; 13 - leading-out magnet with septum 2 cm by winding; 14 - focusing elements/cells for 72 MeV of beam; 15 - focusing elements/cells for 590 MeV of beam; 16 - concrete circular foundation; 17 - adjustable jacks for the magnets; 18 - supporting gear for the equipment in the center of accelerator; 19 - cables; 20 - channel for the ducts with the cooling water; 21 - small auxiliary tap/crane; 22 - domain/blast furnace concrete blocks.

Page 59.

Four high-frequency resonators with a width of 40 cm in the direction of beam, by the length of 530 cm in the radial direction and by the height of 330 cm with the accelerating gap with a length of 15 cm create each stress/voltage of approximately 500 kV of the frequency of 50 MHz, which is the sixth harmonic of the frequency of

revolution of particles in this accelerator. They are excited by separate high-frequency oscillators by the power of 250 kW, connected with one well stabilized master oscillator. Electronic circuits provide control of stress/voltage and phase.

Beam is injected into median plane through 90- degree deflecting magnet the nit after which is arranged/located magnetic pipe of injection, and it is placed in equilibrium orbit, utilizing the corrective channel. Since on a radius of injection occurs the full/total/complete separation of orbits, the losses of beam can be made negligible.

For an energy gain per revolution on the order of 1.5 MeV near a radius of conclusion/output the critical spacing is 6 mm, growing/rising to ~8 mm at the point of conclusion/output. In this region the amplitudes of the incoherent radial oscillations of beam will have value on the order of 3-4 mm. For the system of conclusion/output, which is of the electrostatic channel to the intensity/strength of field 50 kV/cm septum with a thickness of 0.1 mm and length of 120 cm, magnetic focusing elements/cells, mixed further on the ring on 45°, and the deriving/concluding septum magnet, displaced on the ring by 90°, the calculated effectiveness of conclusion/output exceeds 90%/c (table 2).

Vacuum chamber is prepared partially from the stainless steel and partially from alusium. Separate sections can be connected either with the aid of metal multiplexing or with the aid of the inflatable plastic elements/cells, stable to the effect of radiation. Since the pollution/certamination by oil of the surfaces of high-frequency resonators, apparently, limits the maximum attainable stress/voltage, it is proposed to utilize a combination of turbomolecular pumps and titanium sorption pumps, directly coupled with the resonators.

Technical characteristics: radii of poles - 1.9-4.6 m; radii of beam - 2.1-4.5 m; a quantity of spiral sectors 8 (separate magnets); isochronal field - 0.6-0.9 V.s/m²; hill field - 1.46-2.06 V.s/m²; the field flutter - 1.05; maximum helical angle - 35° (neg) frequency of axial betatron - 0.95-0.75; frequency of radial betatron - 1.1-1.7; frequency of cyclotron - 8.47 Hz; the adjustment of resonators - 50.8 MHz (sixth harmonic); an increment in energy per revolution - ~1.7 MeV; beam extraction - when $Q_r \sim 1.1$; the effectiveness of conclusion/output $\rightarrow 90\text{c/c}$ (theory); the injection of beam - into median plane with 72 MeV; the circular vacuum chamber/camera: bore - 3.5 m, outside diameter - 9.2 m; the outside diameter of magnet yoke 15 m; the height of magnet - is 4.9 m; the weight (full/total/complete) ~2000 of t; the required power; magnets - ~650 kW, resonators - ~600 kW; the full/total/complete required power - ~1.5 MW.

Table 2. The circular cyclotron (development SIN).

(1) Частица	(2) Интервал энергии, Мэв	(3) Интенсивность, мкА	(4) Эмиттанс мм.мрад	(5) Разброс по энергии	(6) Относительная длительность импульса пучка (мик- роструктура)
(7) Р при 50,8 Мгц	~ 590	~ 100	10	0,3%	3-5%

Key: (1). Particle. (2). Energy range, MeV. (3). Intensity, μA . (4). Emittance x, z of mm. mrad (5). Energy spread. (6). Relative duration of beam burst (microstructure). (7). with 50.8 MHz.



244

244

Page 60.

State of the construction of accelerator. It is possible to consider that the construction of the basic elements/cells of the circular accelerator is passed successfully. Are prepared tests of prototypes of the following important elements/cells of accelerator: sector magnet with the geometry of poles, which corresponds to energy 590 MeV (initially 520 MeV); high-frequency resonator on 50 MHz in scattered power 150 kW; high-frequency oscillator on 50 MHz, 250 kW; the section of vacuum chamber, connected with the magnet pole without the multiplexing; the code/unit of vacuum evacuation of section, which contains turbomolecular pumps and titanium sorption pump (by productivity of 10000 l/s); the deriving/concluding magnet to 16 kg, which has the two-centimeter septum winding (insulation/isolation from oxide of aluminum).

Is made prototype of the section of fine-adjustment winding with insulation/isolation from oxide of aluminum.

At present the majority of the elements/cells of accelerator released into the production.

About 650/o of budget of the construction of accelerator (common cost/value of 43 mln. Swiss francs) are transmitted on the contracts

into the industry.

Dynamics of beam and construction/design of magnet. The solution to change final energy of accelerator from 520 to 590 MeV was accepted after obtaining of good results on prototype of the magnet (divergence from the isochronal field with 590 MeV less than 0.2c/c) and after careful analysis of the conditions of beam extraction with the increased energy, carried out Joho [3].

Before the working treatment to the field of the coils of all magnets they were finished before obtaining of the required geometry (corresponding final energy 590 MeV) of the pole of two magnets which at present are accumulated on the test bench (Fig. 5).

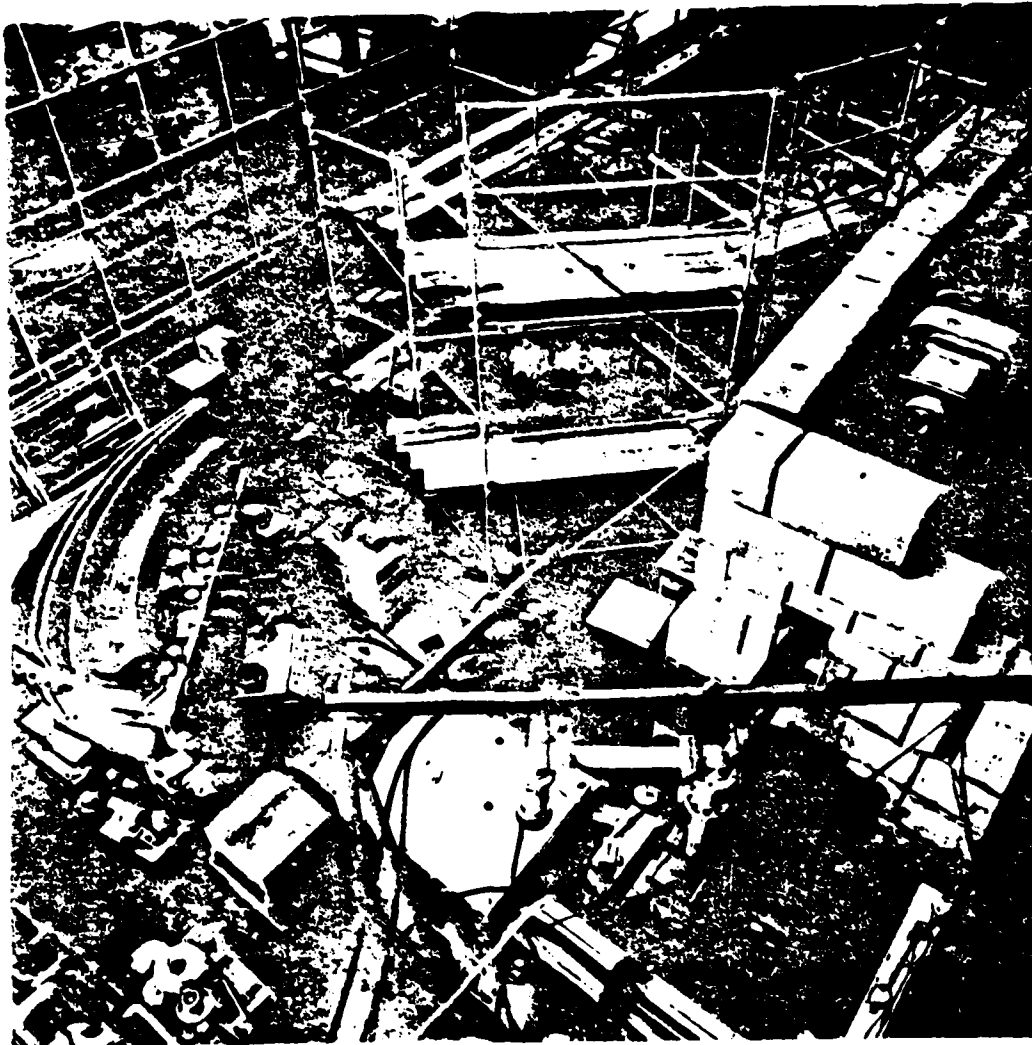


Fig. 5. Temporary/time test bench. Upper left angle - prototype of sector magnet in the location with air conditioning; to the left - the prototype of vacuum chamber with the magnetic poles; from below to the right - 250 kW, 50 MHz- generator, connected with the

prototype of resonator (after the concrete shield); above in the center - assembling section for the assembly of the second magnet.

Page 61.

High-frequency system. Probably, the most significant success is the starting/launching of the high-frequency power-supply system on 250 kW, prepared in conformity with the specifications of institute by firm "AEG - Telefunken." The system, which contains recently developed by firm tetrode YL [491] with the water cooling, easily separates/liberates the high-frequency power of 250 kW on the equivalent load. To prototype of resonator are transferred about 140 kW of high-frequency power, which corresponds to peak voltage of approximately 600 kV on the frequency of 50 MHz. Under conditions for stable operation it is possible to support stress/voltage from 400 to 450 kV. Bischoff, etc. [4] showed that the finish of internal surfaces is very important for maintaining of the necessary stress/voltage and elimination of high-frequency discharges.

State of the program of construction.

The construction of buildings is passed in accordance with the graph/curve. The main experimental hall (85x48 m) can be will be completely conducted under the roof in this year.

At present in the operational building and in the official building, arranged/located in the neighborhood with the experimental evil, is established/installed technical equipment (energy and cooling) (Fig. 6).

Graph/curve provides for the assembly of accelerator in the period with years 1971 or 1973.

Secondary beams.

In order to support at the accelerators the reasonable level of the induced activity, secondary beams are intended to obtain in essence on external targets.

At present [5] are studied the constructions/designs of target systems and systems of the transportation of secondary beams.

Table 3 gives the expected intensities of typical experimental beams.

table 3. Secondary beams.

(1) Частица	(2) Энергия, Мэв	(3) Интенсивность, сек	(4) Примечания
p + 10%	590(±3)	$3 \cdot 10^{10}$	(5) 6 г/см^2 , 10^6 , $3 \cdot 10^{-3}$ стерад (6)
n + 33%	450±30	$1 \cdot 10^7$	(5) 3 г/см^2 , 27^0 , $2 \cdot 10^{-3}$ (6) стерад, 20 (7) мка
n	580±2	$3 \cdot 10^8$	(5) 1.7 г/см^2 , $2 \cdot 10^{-4}$ (6) стерад, 20 (7) мка
π^+	150±3	$2 \cdot 10^8$	(5) 9 г/см^2 , 10 м , $6 \cdot 10^{-3}$ (6) стерад, 100 (7) мка
π^-	150±3	$2 \cdot 10^7$	
μ^-	60±10	$1.5 \cdot 10^8$	(8) на 100 см^2 Соленоида (9)
μ^-	(10) остановленные	$2 \cdot 10^5$ (11) (12) сек, -1	(12) 10 м, ϕ 15 см, 50 кг

Key: (1). particle. (2). Energy, MeV. (3). Intensity, s^{-1} . (4).

Notes. (5). g/cm^2 . (6). sterad. (7). μA . (8). cm. (9). Solenoid.

(10). Stopped. (11). (g. s^{-1}) (12). see 50 kg.



Fig. 6. Area of construction SIN near Williger (August 1970).

REFERENCES.

1. J.P. Blaser, H.A. Willax, H.T. Gerber et al. The SIN Ring Cyclotron Project. High-Energy Physics and Nuclear Structure, Plenum Press, 1970, p. 556.
2. H.A. Willax. Status Report on SIN. Internat. Cyclotron Conf. Oxford, September, 1969.
3. W. Lohr. Extraction of a 590 MeV Proton Beam from the SIN Ring Cyclotron. SIN-Report TM-11-OB, May, 1970.
4. B. Bishof, J.P. Blaser, P. Lanz, U. Schryber. Pendel vervielfachung von Sekundarelektronen. SIN-Report IM-04-15. February, 1970.
5. J.B. Blaser, H.F. Gerber. Internat. Conf. on Electron Scattering and Nuclear Structure. Status Report on the SIN Cyclotron Facility. October 24, 1970.

Discussion.

L. A. Sarkisyan. Are such the values of the parameter of the spiral of Archimedes and the amplitude of fundamental harmonic and why is selected weak helicity?

Kh. Villaks. We apply not Archimedes spiral, but with certain change.

Low helicity is selected in connection with the fact that the coefficient of flutter is more than one.

A. A. Vorobyev. Which the diagram of automatic control of accelerator?

Kh. Villaks. Will be used multiplex system. Initially computer will be utilized only for the recording of data. Then for the control of some parameters (for example, by the parameters of the focusing lenses). After several years of operation and gaining of experience will be used full/total/complete automatic control of accelerator.

Ye. Skhvabe. Name/call basic data of the system of conclusion/output.

Kh. Villaks. Electrostatic device/equipment with a length of 120 cm and by intensity/strength of field 50-60 kV/cm. Angle of deflection ~ 7 of mrad. Then will cost quadrupoles and septum - magnets with 2-centimeter winding. Before the electrostatic channel there will be established the system of thin wires for measuring the profile/airfoil of beam.

Ye. Skhvabe. Which the precision/accuracy of the maintenance of

phase?

Rh. Villaks. 2-3°.

E. K. Shembel'. Which maximum gradient of HF field in the rescnator with the stable operation? Which the frequency of sparking?

Rh. Villaks. The average value of intensity/strength - 30 kV/cm. The frequency of sparking was not measured.

Xe. d. ~~Donets~~ Donets. Which the expected intensity of the beam of the polarized protons?

Rh. Villaks. During the scattering on the carbonic/carbon target $\sim 10^{11}$ 1/s. During the use of an external source $\sim 10^{12}$ 1/s, and will how much be at the output, it is unknown.

13. Linear accelerator of protons to the energy 10 MeV in the collation.

Ye. Dzyur, V. Grabovsk^í, Yu. Yanushevsk^í, Z. Kozlovsk^í, A. Kukharchik, S. Kulinsk^í, B. Lytchevich, Z. Mazur, A. Makler, S. Myslinsk^í, T. Nevodnichansk^í, B. Pakhan, I. Savlevich, Yu. Sur, Ch. Veykhert.

(Institute of nuclear research, Sverck, Poland).

The described accelerator was designed and constructed with its own forces in the center of nuclear research in the collation about Warsaw. Accelerator was constructed for conducting of fundamental and practical investigations in the region of nuclear low-energy physics.

In the accelerator was utilized the accelerating structure of Alvarez's type with $L_n = \beta_n \lambda$ and $g_n/L_n = \text{const} = 0.25$. This structure was checked by numerical calculations with the aid of the modified method of Martini-Warner. The selected parameters of the focusing channel of accelerator are compromise between maximal value of acceptance in the phase space and the technically permissible values of field gradients in the quadrupole lenses. Obtained compromise value $\cos \mu$ for the system PDDF equal to 0.45. The values of transverse acceptance and emittance are equal to with respect 100 and 30 mm. mrad.

Injector is a usual accelerator of Cockcroft-Wolton's type with the high-frequency ion source. The duration of beam burst can be regulated in the limits from 100 to 1000 ns. Accelerator tube of injector consists of 14 sections. The average/mean gradient of

accelerating field is equal to 0.55 V/m . The quality of beam 515 keV can be measured with two reactely/distance controlled systems of slots, with faraday cylinders and with magnetic-induction meters of current. For beam matching with the entrance of accelerator serve two triplets of quadrupole lenses and two pairs of the corrective coils.

The copper resonator, loaded with 40 drift tubes, is placed in the steel vacuum container. Each drifting tube it is supported at the axis/axle of resonator by two rods.

The quadrupole lenses, placed within the drift tubes, are supplied by direct current by the value of 150-250 A. The windings, wound by copper tubes, are cooled by water. Gradient of magnetic field in the quadrupole lenses is measured from 4985 G/cm at entrance do of 928 G/cm at the output of resonator. Resonator has 12 plates of tuning, 4 of them it is possible remotely/distance to regulate during the work of machine.

The power-supply system of high frequency consists of three oscillators of power, strongly connected with the resonator, and of one generator-exciter. In the oscillators are established/installed tetrodes EIMAC 4W 2000Ca.

The duration of pulse HF is equal to 1000 μ s. The pulse repetition frequency is synchronized with the network/grid and may vary abruptly in the limits from 1.5 to 12.5 imp./s. The distribution of the electric field along the axis/axle of accelerator was measured according to the perturbation method. After equalization is obtained the distribution with the changes, lying in limits of $\pm 5\%$.

The system of vacuum evacuation consists of two vapor-oil diffusion pumps and traps, cooled by liquid nitrogen. Entire system is prepared in the workshops of institute. Pressure in the vacuum container is approximately $4 \cdot 10^{-7}$ mm Hg.

First accelerated beam from the accelerator was obtained on 15 January 1970. Work on an improvement in machine parameters continues. At present the current of the accelerated beam (June 1970) is equal to about 400 μ A (with the current of injector 6 mA) without the buncher.

Are given below the parameters of the accelerator:

exit energy..... 9.7 MeV.

Resonance frequency..... 193.25 MHz.

Number of drift tubes..... $40 + 2\frac{1}{2}$.

Energy of injection..... 515 keV.

Synchronous phase..... -30° .

Transverse acceptance..... 100 mrad.

Focusing system..... FDDF, $\cos \mu = 0.45$.

Length and diameter of rescatterer..... $l = 5524$ mm, $2r = 1077$ mm.

Quality..... $Q = 58000$.

Duration of pulse HF..... 1000 μ s.

Pulse repetition frequency..... 1.5; 3.1; 6.2; 12.5 imp./s.

Power HF in the impulse/momentum/pulse..... 700 kW.

Average intensity/strength of accelerating field..... 2.24 MV/m.

Pressure in the resonator..... $4 \cdot 10^{-7}$ mm Hg.

Theoretical works in essence concerned questions of the dynamics of the proton beam and calculations of the resonance structure of accelerator. Numerical calculations were conducted in machine GIER. For this purpose were written corresponding programs in language ALGOL, and are also transferred into this language and were adapted to the possibilities of this machine other existing programs. The analysis of phase and transverse particle motions in the accelerator made it possible to accurately determine its phase and transverse acceptance and emittance. Are calculated the parameters of the system of the strong focusing FIDF or accelerator, and also the parameters of the systems, which agree the conclusion/output of injector with the entrance of accelerator and its output with the analyzing magnet.

Is developed program for calculating of electromagnetic fields and natural frequencies of the resonators of linear accelerators. This program is the variety of methods of Martini and D. Warner and makes it possible in future to decrease the machine time and the storage capacity, necessary for the calculations. The idea of modification lies in the fact that all operations/processes of integration and differentiations, necessary in the process of count, is done by analytical method in those fields of the resonator where the fields are described by analytical expressions. This is

especially useful during the calculation of eigenvalue κ^2 , calculated cyclically in the iterative process of count.

Integrals take the form

$$\int \tau c_l(\lambda_m \tau) c_k(\lambda_n \tau) d\tau, \quad k=0,1,$$

and are expressed by combinations functions $c_l(\lambda_m \tau), c_k(\lambda_n \tau)$, where c_l, c_k - Bessel function (usual or modified), λ_m, λ_n - some parameters, which depend on the geometry of resonator.

Therefore it is possible to avoid numerical integration in the entire upper region of the resonator (it is more than 10000 points).

The launching phase of accelerator, counting from the moment/torque of the termination of the measurements of the parameters of HF of structure to the moment/torque of obtaining the beam, it lasted very for long, since it was connected with many difficulties, in essence, with weak material and setting base, which was found at the disposal of collective. Main stages of this period: 1) the control of the system HF of supply for obtaining the correct joint-operation mode of all oscillators, the ensuring high efficiency. The preliminary functional check of oscillators was conducted with dummy load; however, final adjustment became possible

only with the work on finished HF structure under conditions of high vacuum; 2) transition through the "barrier" of resonance discharges; 3) the achievement of the intensity/strength of accelerating field, which corresponds to acceleration level, without the breakdowns, or only with the random breakdowns; 4) the acceleration of proton beam, the optimization of the work of injector on 515 keV and the focusing channel.

Basic difficulties: 1) the emergencies in the system of HF caused mainly by overvoltages in the circuits/outlines and damages of the insulating elements/cells; 2) emergency in the vacuum system and the periodic incidence/impingement of oil or water into the volume of resonator; 3) the difficulties with the elimination of resonance discharges, connected with the materials of electrodes (usual copper, not non/without-oxygen), the incidence/impingement of organic (oil vacuum system), and with the "slow" system HF of supply; 4) the breakdowns during the long time at the high level, also connected with the materials of electrodes and with the vacuum conditions.

During the discharges in the resonator they were given by observation through inspection windows in housing. One from the windows, arranged/located at the angle of vacuum envelope, it gave the possibility to control the entire system of drift tubes and their rods. Therefore we could follow the emergence of discharges and

determine their location. The checking of the phenomena, which occur in the vacuum, was performed by the mass of accelerator. With its aid was determined the spectrum of residual gases under varied conditions for work.

In the beginning of the process of starting/launching the resonator was supplied by the continuous wave of a small power for accelerating the process of removal of gas from the surfaces of electrodes and for the preliminary formation of their surfaces. The transition through the region of resonance discharges is completed with the supply of structure generators, which with the full load excites in the resonator the strength of field in the clearances of approximately 0.25 mV/cm.

Page 64.

The transition of the region of resonance discharges was made difficult due to the low speed of the build-up of field; therefore it was necessary so "form/shape" the surfaces of electrodes in order to decrease the secondary-emission coefficient to the sufficiently low level. Effective method proved to be work of oscillator with the increased repetition frequency. discharges appeared alternately with different strengths of field, beginning from 7 to 120 kV/cm. On the whole the observed levels of field will agree well with the

theoretical forecasts for the sizes/dimensions of the clearances, available in the structure. They are burdensome and prolonged were discharges at the lowest level. At discharges at the high levels corresponded, as a rule, brightness in the region of tubes. After serious vacuum emergencies and hit of a considerable quantity of oil into the resonator, aging/training did not completely give results. In such cases was necessary the flushing of the internal surfaces of resonator.

After outages of accelerator (without the opening of vacuum envelope) again appeared resonance discharges, which entailed the need for "aging/training". "breakdown" between the drift tubes they appeared on the level of field 0.7 from the threshold value of the intensity/strength of accelerating field. The reduction of impulse/momentum/pulse with 1000 μ s to 300 μ s did not affect a number of breakdowns. At first breakdowns appeared at the pulse apex, and with the subsequent impulses/momenta/pulses, also at the front. With the schematic of timer device/equipment is connected the dividing circuit of repetition frequency for the work with the frequency of 0.3 s and 0.1/s. Is provided for also the possibility of the manual blocking of launching/starting the oscillators of power. Before the emergence of the breakdown between the tubes, which accompanied the bright brightness, is observed on the faces of drift tubes the numerous foci ("asterisks"). Gradually reached all high levels of

field and possibility of work with the high repetition frequencies.

In the case of the emergence of a small leak in the system of water cooling and incidence/incingement into the resonator of water vapor was observed a considerable decrease in the disruptive level of field.

After obtaining of the first accelerated beam was carried out checking energy of the accelerated protons by the method of measuring the path/range of beam, brought out into the air. At present is prepared the setting up of buncher and conducting the precise measurements of the parameters of beam with the aid of the analyzing magnet.

14. New developments and improvements of the technological systems of linear accelerator I-2.

V. A. Batalin, V. I. Ectylev, Ye. N. Danil'tsev, I. M. Kapchinskiy, L. V. Kartsev, A. M. Kozdaev, V. V. Kolcskov, B. P. Kuybid, N. V. Lazarev, V. I. Edemskiy.

(Institute of theoretical and experimental physics).

Introduction.

The construction/design of linear accelerator (LU) I-2, experiment of its adjustment, and also putting into commission as the injector of the proton synchrotron (PS) of ITEP were described in the literature [1-3]. During three years work LU provides exit pulse current of approximately 100 mA, that makes it possible to have at the output PS the intensity $4-6 \cdot 10^{11}$ protons per pulse. Duration of beam current LU of 30 μ s, the stability of the current strength from one impulse/momentum/pulse to the next 8-10%/c. The width of the energy spectrum of particles on the longitudinal impulse/momentum/pulse comprises at the output of LU ± 0.60 /c (on the half height). LU work 11 months in the year by three-week continuous

cycles with the weekly gaps/intervals for the preventive works. Idle times LU with respect to the planned operating time composed 3.5o/c from 4741 hour into 1968 and 2.5c/c of 4520 hours into 1969. The basic reasons for idle times were connected with that carried out 3-5 times by the replacement of cathode in the ionic source of preinjector, by the exchange of oscillator tubes and thyratrons, and also by the occurred disturbances/breakdowns of the correct mode/conditions of vacuum evacuation. The contribution of remaining technological systems to the total rest period is insignificant.

It is interesting to note that in spite of the use/application of oil-vapor evacuation and the high value (to 140 kV/cm) of the strength of fields in the clearances in 4 years of continuous operation of LU vacuum envelope was revealed not to time. The consequences of those had the place into 1967-1969 two vacuum emergencies with the incidence/impingement of oil vapors into the resonators was possible to overcome by prolonged (to 70 hours) HF aging/training. For preventing such cases on the forevacuum main lines are established/installed the high speed gates.

Work of LU from the alternately changing by duration pause between the impulses/acmenta/pulses.

Essential reserve of an increase in the effectiveness in the use

FS ITEP was revealed by proposition accelerate proton beam to the energy 150-200 MeV (for the medical targets) during the pause of basic cycle. The realization of this proposition required from LU of the frequency doubling of injection for the alternately changing duration of spacings between pulses, which is 0.8 and 3.2 s. Basic modernization underwent the system of the high-voltage power supply of preinjector. The modulator of peak transformer IT-800 had the necessary supplies according to the power for the work with the frequency to 1 Hz; however, due to the incomplete charge of storage capacitance (time constant more than 0.3 s) and nearness of operating stress/voltage IT-800 to the permissible value, was required a strict periodicity of starting/launching.

Page 65.

This limitation was taken with the aid of the antihunting circuit of voltage across capacitors of modulator. Stabilization with precision/accuracy $\pm 0.1\%$ is accomplished/realized by the three-phase thyristor diagram which is connected with the primary windings of step-up power transformer [4]. The introduction of this diagram substantially (from ± 0.5 to $\pm 0.3\%$) lowered the instability of energy of injection.

The frequency doubling of work LU required also increase in the

power of the stabilizer of charging voltage in the modulators of the system HF of the supply (lamps of the type GMI-9C were replaced on GMI-2B). During last year LU in essence it worked in this new mode/conditions.

Second channel of beam extraction LU.

LU I-2 can give the beam (on the average) of 1 times per second: therefore has the capability into the time interval of 3.2 s. between the impulses/moments/pulses or the injection of normal and "medical" cycle PS to utilize additionally 2 impulses/moments/pulses LU for the experiments with the proton beam, accelerated to the energy 25 MeV, or for measuring the parameters of beam.

Location for the work with the beam is located on axis/axle LU directly beyond the first rotary magnet of the ion guide, which links LU with PS. In all on this ion guide are utilized four rotary magnets, their windings are connected in series and are supplied by direct current. Achromaticity of the system of the rotation of beam makes it possible to significantly lower requirements for the stability of current. Therefore the logical at first glance solution to replace the first rotating magnet with pulse and to include it only by the period of the transmission of beam in PS was rejected due to the difficulty ensure the register of the values of the amplitude

of pulse field in the first and the stationary field in the remaining three magnets. setting up it is direct at the output of LU of the supplementary kicker which would make it possible to pass beam on the side from the first rotary magnet, it was impossible due to the closeness of the location of the remaining elements/cells of ion guide. Thus, most advisable solution proved to be the pulse demagnetizing of the first rotary magnet to the period of the transmission of beam (30 μ s) into the laboratory location. Pulse field is created by a 6- loop loop, introduced together with laminated polar tips inside vacuum chamber of the first rotary magnet. The brass walls of vacuum chamber serve also as the screen, which prevents the appearance of overvoltages in inducing windings, supplied by direct current. Stationary field in this magnet has virtually the same configuration, as with the continuous pole pieces, so that achromaticity of the system of the rotation of beam proves to be preserved. With the transmission through the pulse loop of current of approximately 15 kA the magnetostatic field in the beam region completely is compensated and beam passes through the magnet without the divergence. The tests prototype of pulse loop confirmed the possibility of the multipurpose use of a beam of LU. At present is conducted work on the introduction/input of this system into the operation.

Second channel of beam extraction of LU is equipped by

chambers/cameras for observation by pulse quadrupole lenses with the aperture 70 mm on the ferrites and the correctors on the transformer iron. By the selection of the values of pulse beam currents was carried out through the channel and brought out in the atmosphere.

Increase in the reliability of operation and reduction in the cost/value of operation of LU.

Considerable portion of operating costs of LU compose flow rates to powerful/thick vacuum lamps and thyratrons, the real service life of which in the large measure determines also the reliability of the work of machine. An increase in the power of the excitation of the final stages on the lamps GI-27A allowed (without a change in the power output) to somewhat lower the filament voltage of these expensive lamps, which increased the period of their service from 1000 to 4000 hours. A reduction in the filament stress/voltage of roentgen kenotrons V1-C3/70 in the modulator IT-800 to 13 in increased the period of their service more than 10 times. The frequent reason for cessation of LU was the need of exchanging the thyratrons TR1-85/15 in the modulators HF of system. These thyratrons ceased to be cut off after 400-500 hours of pulsed operation with the currents to 1000 a. It turned out that the deionization time of the thyratrons, which work under these conditions, considerably exceeds certified/rating value and increases during the operation. The

delay/retarding/deceleration of the process of the charge of the forming line by 700 μ s (with the aid of the choke/throttle with the inductance 5 H) weakened/attenuated the effect of this phenomenon and the real service life of thyratrons in the modulators increased to 2-3 thousand hours. Subsequently it turned out that the cases when the thyatron, which mastered 2-3 thousand hours, is not closed after operating pulse, occur sufficiently rarely - 1-2 times in the grids. The arrangement of diagram, which in such cases automatically disconnects by 0.1-0.2 s rectifier, made it possible to utilize thyratrons of more than 5 thousand hours.

For the enlistment of the attention of person on duty in the case of breakdown in the resonators are developed the diagrams, which react to the slope/transconductance of the drop of the envelope of HF impulse/momentum/pulse.

Improvements in the system of vacuum pumping, introduction of booster pumps BN-3 between the fore pumps and the high-vacuum aggregates/units, and also the replacement of ejector nozzles on pumps NBT to the steam-jet ones made it possible to decrease the acceleration time of LG. After the week of preventive works (not connected with the allowance of the atmosphere into the jacket) the evacuation of resonators for the introduction/input of HF power occupies only 3 hours.

DOC = 80069205

PAGE 222

REFERENCES.

1. PTE, 1967, No 5, 9-10.

2. Transactions of international conf on high-energy accelerators.
Cambridge, 1967, page 1 - 1, 1 - 30.

3. PTE, 1969, No 6, 14.

4. PTE, 1970, No 4.

Page 66.

15. Linear electron accelerator to the energy 2 GeV of FTI of AS UkSSR.

V. A. Vishnyakov, I. A. Grishchayev, Yu. I. Dchrolyubov, V. M. Robezskiy, V. V. Kondratenko, V. I. Myakot.

(Physico-technical institute of AS UkSSR).

Linear electron accelerator was constructed in Kharkov physiotchnical institute of AS UkSSR in 1965, and from this time it successfully works on the wide study program in nuclear physics and physics of accelerators.

Accelerator represents the enormous complex of the systems, from the mounted work of each of which depends the pcssibility of performing work. The overall diagram of accelerator is shown in the figure.

Accelerator consists of 49 accelerating sections in long on 4.8 m. Each section is excited from the separate powerful/thick klystron amplifier. Klystrons with exit power to 20 MW in turn, are excited with the aid of the thermostatically controlled waveguide from the main master oscillator with high frequency stability. The impulse/momentum/pulse of high voltage by the duration of 2.5 μ s on the cathode of klystron is created by pulse modulator on the forming line with the thyristor commutators. Electron beam is formed/shaped in the injector, which accelerates particles to 4.5 MeV, which uses the accelerating structure with permanent phase wave velocity. The axisymmetric magnetic field is created by solenoid. On basic part of the accelerator is used the system of quadrupole lenses and diaphragms, which ensures the creation of the phase channel of a small width and beam shaping with a small emittance. The overall length of the accelerating system is 240 m. It is logical that for the normal operation is necessary the display system of position, intensity and beam shape. As such systems are utilized the span magnetic-induction position detectors and current, retractable screen- flags, covered with the layer of phosphor, image on which is examined with the aid of the television systems. For the correction of the position of beam is utilized the system of the corrective coils.

At the output of accelerator the beam falls into formation

system. The system of beam shaping makes it possible to generate on the target "pure/clean" electronic, positron and photon beams. The basic parameters of these beams are shown in Table 1.

Positron beam is obtained on the converter, established/installed in the 9th section where with the incidence/drop on the tantalum target of electrons with the energy of 250 MeV is formed electron-positron cloudburst. With corresponding change in the phase of accelerating field the remaining part of the accelerator accelerates positrons.

Photon beams are formed on the thin radiators, then they are cleaned in the clean-up systems. Because of a small emittance of the output beam on our accelerator successfully works the system of obtaining the polarized quasi-monochromatic photons. Photons are formed due to coherent interaction of electrons with the crystal of diamond.

For the time, passed from the starting time of accelerator, its many systems are perfected and improved. This affected the resultant performance characteristics of accelerator. Table 2 shows a change in the basic parameters of accelerator for 4 q. and for the first half of 1970.

Table 3 shows changes in the operating characteristics of accelerator for the same time. Sufficiently characteristic numeral is the flow rate of electric power per the hour of experimenter's work.

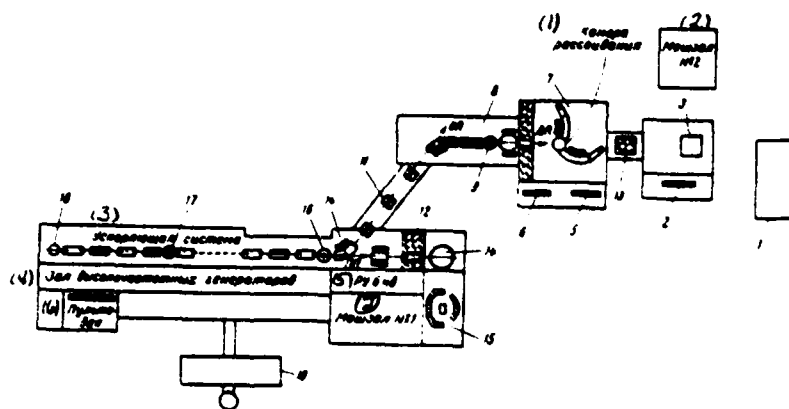


Fig. 1. The diagram of linear electron accelerator to the energy to 2 GeV: 1) cryogenic housing; 2) control panel of bubble chamber; 3) hydrogen bubble chamber; 4) the hall of spectrometers; 5) physicists' panel; 6) the panel for conclusion/output; 7) protection; 8) the hall of beam shaping; 9) photon targets; 10) the deflecting magnet; 11) quadrupoles; 12) protection; 13) is saw that retracting; 14) experimental hall on the straight/direct bundle; 15) central accelerator frequency; 16) photon target; 17) positron target; 18) electron source; 19) ventilation ducting; PP - straight line of bundles; OP - once turned beam; EP - twice turned beam.

Key: (1). Chamber of scattering. (2). Equipment room. (3). Accelerating system. (4). Hall of high-frequency oscillators. (5). kv. (6). Console.

Page 67.

Table 1. Parameters of Kharkov linear electron accelerator to the energy to 2 GeV (as of 1970).

(1) Параметр	(2) Единица измерения	(3) Значение параметра
(4) Пучок электронов		
(5) Энергия	(6) Гэв	0,4-1,8
(7) Энергетический разброс на уровне 0,5 макс.	%	1
(8) Средний ток на выходе ускорителя (макс)	(9) мка	1
(10) Импульсный ток на выходе ускорителя (макс)	(11) ма	20
(12) Длительность токового импульса	(13) мксек	1,2-1,4
(14) Частота посылок максимальная	(15) имп/сек	50

(16) Размеры пучка (диам.) на выходе ускор.	мм
(18) Средний ток на мишени спектрометра	(17) мка
(19) Размеры пучка на мишени спектрометра	мм
(20) Длительн. имп. тока на мишени спектрометра	(21) мксек
(21) Стабильность положения пучка на мишени спектрометра в течение 8 часов	мм
(22) Стабильность тока на мишени спектрометра в течение 8 часов	%
(23) Расходимость тока на мишени спектрометра	(24) рад. (25) Г/В
(27) Количество отклонений секций в час зашито при 35-45 работающих секциях	(26) откл. час
(29) Уровень фона от пучка электронов в помещении мишени	(30) мкр/сек

AD-A089 303

FOREIGN TECHNOLOGY DIV WRIGHT-PATTERSON AFB OH
TRANSACTIONS OF THE ALL-UNION CONFERENCE (2ND) ON CHARGED PARTI--ETC(U)
JUL 80 A L MINTS, A A KOMAR, A A VASIL'YEV

F/G 20/7

UNCLASSIFIED

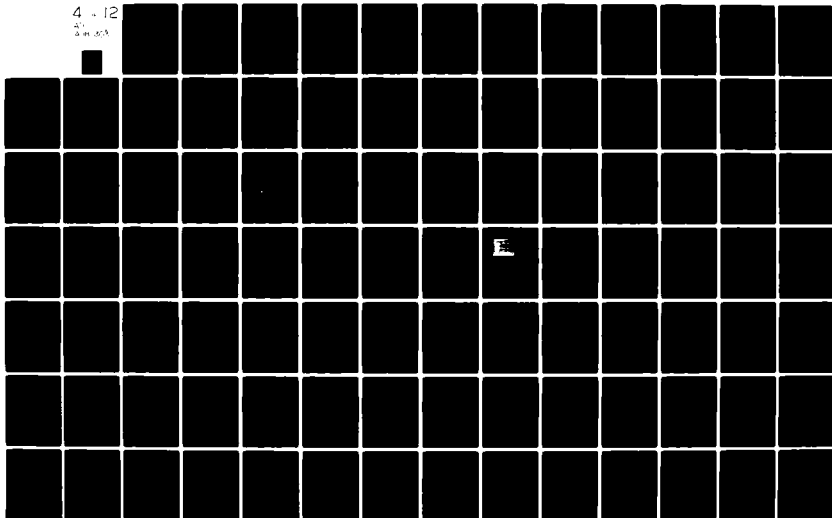
FTD-ID(RS)T-0692-80

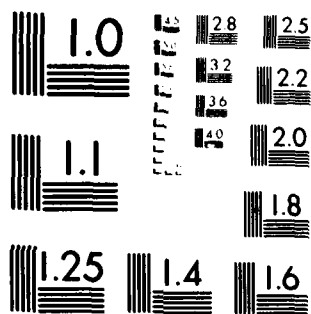
NL

4 - 12

4-12

4-12





MICROCOPY RESOLUTION TEST CHART
NATIONAL BUREAU OF STANDARDS-1963-A

Table 1., Continued.

(31) Пучок позитронов на выходе ускорителя

(32) Энергия	(33) Гэв	1,2
(34) Энергетический разброс на уровне 0,5 I макс.	%	1,5
(35) Размеры пучка	мм	4
(36) Угловая расходимость по горизон- тали	(37) рад.	$1 \cdot 10^{-3}$
(38) по верти- кали	(39) рад.	$1 \cdot 10^{-4}$
(40) Интенсивность пучка	(41) част/сек	$5 \cdot 10^9$
(42) Отношение интенсивности по- зитронов на выходе ускорителя к интенсивности электронов на конверторе	-	$2 \cdot 8 \cdot 10^{-4}$
(43) Фотонный пучок на выходе ускорителя		
(44) Интенсивность	(45) экв. фот. сек	$1 \cdot 10^{10}$
(46) Угол коллимирования	(47) рад.	$5 \cdot 10^{-4}$
(48) Фон	%	(49) менее 1
(50) Поляризованный квазимонохроматический пучок фотонов		
(51) Энергия фотонов	(52) Гэв	1,2
(53) Полная интенсивность фотонов	(54) экв/мкм	$1 \cdot 8 \cdot 10^{11}$
(55) Поляризация при $\lambda/\lambda_0 = 0,3$	%	40
(56) Расходимость пучка	(57) рад.	$10^{-3} + 10^{-4}$
(58) Угол коллимирования	(59) рад.	$3 \cdot 8 \cdot 10^{-4}$
(60) Точность отсчета угла по гониометру	(61) сек.	10
(62) Толщина мишени (алмаза)	(63) см. рад.дл.	$\frac{0,2}{1,5 \cdot 10^{-2}}$

Key: (1). Parameter. (2). Unit measurement. (3). Value parameter. (4). Electron beam. (5). Energy. (6). GeV. (7). Energy spread at the level 0.5 I max. (8). Average/mean output current of accelerator (swing). (9). μA . (10). Pulse output current of accelerator (swing). (11). mA. (12). Duration of make pulse. (13). μs . (14). Frequency of messages maximum. (15). imp./s. (16). Sizes/dimensions of beam (diam.) at output of accel. (18). Average/mean current on target of spectrometer. (19). Sizes/dimensions of beam on target of spectrometer. (20). Prolonged pulse of current on target of spectrometer. (21). Stability of position of beam on target of spectrometer for 8 hours.

(22). Stability of current on the target of spectrometer for 8 hours. (23). Divergence of current on target of spectrometer. (24). rad. (25). horiz. (26). vert. (27). Quantity of cutoffs/disconnections of sections in hour of that seen with 35-45 operating sections. (28). dev./h. (29). Background noise level from electron beam in place of target. (30). $\mu kr. s$. (31). Beam of positrons at output of accelerator. (32). Sizes/dimensions of beam. (33). Angular divergence. (34). on horizontal. (35). on vertical line. (36). Intensity of beam. (37). part./s. (38). Ratio of intensity of positrons at output of accelerator to intensity of electrons on converter. (39). Photon beam at output of accelerator ¹.

FOOTNOTE ¹. It relates to the electron beam: $E=1400$ MeV, $I sr.=0.5$ μA , $\Delta E/E=40\%$ at the level 0.1 I max, $\phi_{beam} = 0.6$ cm. ENDFOOTNOTE.

(40). Intensity. (40a). equiv. [act./s. (41). Angle of collimation.
(42). Von. (43). it is less. (44). Polarized quasi-monochromatic beam
of photons. (45). Photon energy. (46). Total intensity of photons.
(47). equiv./min.
(48). Polarization with. (49). Divergence of beam. (50). Angle of
collimation. (51). Accuracy of reading of angle in goniometer. (52).
s. (53). thickness of target (diamond). (54). cm/rad. length.

Page 68.

Because of the improvements, introduced into the modulators, to an
improvement in effectiveness and reliability of operation the flow
rate of electric power was reduced with 5.42 MW of hours in 1966 to
3.25 MW of hours in 1969. Is visible a systematic increase in the
indices of accelerator.

Should be noted basic improvements and improvements, made for
this time on the accelerator.

At first of work in 1965 on the accelerator was discovered the
phenomenon of the shortening of current pulse, connected with the

excitation in the accelerating system NEM-11 of wave by the flying beam. The large length of the accelerating system, the permanent structure of sections and high quality contributed to the development of instabilities and limited output current of accelerator $0.3 \mu\text{A}$. For eliminating this phenomenon we established/installed in the beginning of the accelerator of section with the sections/cuts on the disks, divided into 5 subsections. In conjunction with an improvement in the focusing this raised the maximum accelerated current.

Improvement on the modulators - the equalization of flat/plane part - and an improvement in the stability of excitation system they led to an essential improvement in the energy spectra. The introduction of narrow phase channel, additionally decreasing the spectrum, substantially improved the emittance of beam at output of accelerator.

Is made the large complex of works on an increase in the reliability of the systems of accelerator, and at present the general/common/total flow of failures on to systems is lowered to the low values. The total the flow of failures on the average in 5 months of 1970 composes 0.1 failure/hour of work along all systems and additionally 0.06 failure/hour on all modulators. At the same time, it is probable, the way of small improvements, beginning from some moment/torque, it will prove to be barely effective.

Table 2. Changes in some parameters of linear electron accelerator on 2 GeV in 1966-1970.

(a) Параметр	(b) Единица измерения	1966	1967	1968	1969	(c) 1970 за 5 месяцев
(1) Диапазон рабочих энергий фактический	(2) Гэв	0,4-1,6	0,4-1,4	0,4-1,6	0,4-1,5	0,4-1,4
(3) Энергетический разброс на уровне 0,5 максимума	%	6-8	2-4	1,5-2	1-2	0,5
(3) Энергетический разброс на уровне 0,1 максимума	%	-	-	4-6	2-3	1-2
(4) Предельный импульсный ток	(4a) ма	12	15	15	25	25
(5) Предельное значение среднего тока на выходе ускорителя	(4a) мкА	-	0,8	0,8	1,3	1,3
(7) Эмиттанс (90% частиц)	(4a) мм мрад.	-	-	0,47	0,47	0,17
(8) Поперечные размеры пучка на выходе ускорителя	мм	6-8	6-8	4-5	4-5	4-5
(9) Длительность импульсного тока на мишени спектрометра	(10) мксек	-	0,3-0,5	0,5-0,8	0,8-1,0	0,8-1,0
(11) Количество отключений клистронов в час (среднее значение)	(12) откл./час	2-4	1-3	1-2	1-2	1-2

Key: (a). Parameter. (b). Unit measurement. (c). 1970 in 5 months.
(1). Range of working energies actual. (2). GeV. (3). Energy spread at the level of I maximum. (4). Maximum pulse current. (4a). mA. (5). Limiting value of average/mean output current of accelerator. (6). μ A. (7). Emittance (90% of particles). (7a). mm mrad. (8). Transverse sizes/dimensions of beam at output of accelerator. (9). Duration of pulse current on target of spectrometer. (10). μ s. (11). Quantity of cutoffs/disconnections of klystrons in hour (average/mean value). (12). dev./hour.

Page 69.

In connection with this reason - but to raise a question about the path of most advantageous change of the characteristic of accelerator in the future. In this case it is possible to discuss different stages, including very removed at the time. As the basic essential points it is possible to isolate the following groups of factors: a) the improvements in the parameters of beam at the fixed/recorded moment of time, connected with an improvement in the stabilization of high-frequency fields and form of clusters both during the impulse/momentum/pulse and from one impulse/momentum/pulse to the next; b) an improvement in the accelerating system for the purpose of an increase in the limiting current, being limited by the effect of

the explosion of beam, an improvement in the full-load saturation curves of sections; c) an increase in the duration of current pulse and connected with this increase in the duration of the pulse of high-frequency field; d) the creation of new cnes and the improvement of the operational systems of snapping of the accelerated beam.

The enumerated works virtually can be accomplished/realized without prolonged accelerator shutdowns, in this case it is logical that the cost/value and the later expense of these all works is different.

Achievements recently on the accelerator of the value of energy spread $\pm 0.15\%$ on the half-height of the spectrum due to the creation of narrow channels show that by this method it is possible to obtain still essential advance. It is easy to show that, if we ensure frequency stability of high-frequency field not worse than $5 \cdot 10^{-6}$, the phase width of cluster of approximately 0.5° and the stability of high-frequency field at the level 0.05% , it will be possible to obtain the full/total/complete spectra not worse than 0.1% . For achievement of this it is necessary to improve the master oscillator, to introduce the stabilization system of the pulse apex of modulators, to remove noises in the klystrons and to inject new effective injectors.

An improvement in the accelerating system can go in two directions: the setting up of the instead of acting sections of sections with the cross-shaped sections/cuts with the magnetic fields, created by solenoids, and setting up in the initial part of the accelerator of 10-20 sections with the permanent gradient, also with the solenoids. These actions must increase limiting current to 100-150 mA.

Table 3. Operational indices of the work of linear electron accelerator on 2 GeV from 1966 through 1970.

(1) Наименование работ	1966	1967	1968	1969	(2) 1970 за 5 месяцев
(3) Расчетное (планируемое) время работы (полное)	3670 час ⁽⁴⁾	5241 час ⁽⁴⁾	5068 час ⁽⁴⁾	4406 час ⁽⁴⁾	3298 час ⁽⁴⁾
(5) Время работы на исследовательские программы, в том числе	1900 час ⁽⁴⁾	3250 час ⁽⁴⁾	3248 час ⁽⁴⁾	3263 час ⁽⁴⁾	2777 час ⁽⁴⁾
физика ядра	960	2226	2571	2937	2242
физика ускорителя	940	1024	677	326	535
(6) Время на исследования в % к расчетному времени работы (фактически)	52,5	62	64	74	84
(7) Полное время работы ускорителя с пучком	3004	4703	4805	4144	3077
(8) Продолжительность работы ускорителя между остановками на профилактические работы	4) 6 суток	4) 6 суток	4) 6 суток	4) 6 суток	4) 25-30 суток
(9) Время, затрачиваемое оператором на изменение энергии на мишенях на 50% (в среднем часов)	6-8	3-6	2-3	1-2	1-1,5

Key: (1). Designation of works. (2). 1970 in 5 months. (3). Calculated (planned/glide) operating time (full/total/complete). (4). hour. (5). Operating time to research programs, including physics of nucleus physics of accelerator. (6). Time to investigations in o/o to estimated time of operation (actually). (7). Production time of accelerator with beam. (8). Operating time of accelerator between cessations on preventive works. (9). days. (10). Time, spent by operator on change in energy on targets to 50c/o (on the average of hours).

Page 70.

The only deficiency/lack in the sections with the constant gradient is an increase the time of filling of section electromagnetic field. In connection with this one of the most efficient factors of an increase in the average/mean current of accelerator is an increase in the duration of the pulse of klystrons and gun.

At present virtually of 2.5 μ s the impulse/momentum/pulse of klystron in the overall "window", which ensures the best parameters of beam, it remains only 1-1.3 μ s, since 0.8 μ s departs on the filling of waveguide with field and still several the tenths are expended on the insufficiently good synchronization and the unsatisfactory

duration of the flat/plane part of the impulse/momentum/pulse of klystrons. In connection with this an increase in the duration of the pulse of high-frequency field to 10 μ s, increasing power on the klystron 4 times, virtually 8-10 times will increase average/mean current. However, naturally, for this it is necessary to conduct the replacement of all modulators of klystrons. After the replacement of the modulators of the first sections and amplification of power engineering of accelerator further replacement of modulators can it is conducted on the operating accelerator. Finally, the creation of the new systems of formation in the new and old halls will make it possible to in the best way utilize working hours. A number of our new systems includes the introduction of the "jumping" photon targets, which makes it possible to conduct simultaneously works on the photons and the electrons in two halls.

Perfection of optics in formation system and improvement in the power-supply systems of magnets will make it possible to actually generate beams in the area whose diameter is not more than 1 mm.

The basic parameters of accelerator after accomplishment of all outlined measures are shown in Table 4.

It seems to us that with an increase in the power of beam increasingly essential will be manifested the effect of the

reliability of systems and ease of control on the possibilities of experiment. Therefore considerable attention must be given to questions of the overall automation of control of accelerator. It is possible to assume that the proposed path is not maximum. Probably, due to the improvement of the stabilization systems and high-frequency supply even now to actually pose the problem of obtaining on the accelerator of our type of electrons with the energy spread is not more than 10^{-4} with the high high-frequency efficiency.

Table 4. Parameters of Kharkov linear electron accelerator.

(1) Параметры		(2) Данные 1970 г.	(3) Данные пос- ле реализа- ции всех программ
(4) Энергия электронов, максимальная	(5) Гэв	1,3	$2,0^{-1}$
(6) Ширина спектра на уровне 0,5 I макси- мальный	%	0,5	0,1
(7) Ток импульсный, максимальный	(8) мА	25	100
(9) Частота посылок, максимальная	(10) Гц	50	100
(11) Длительность им- пульса тока	(12) мксек	1,3	8,5
(13) Ток средний рабочий	(14) мкА	1,3	50
(15) Мощность пучка	(16) кВт	1	100
(17) Поперечные размеры пучка	мм	5÷8	1
(18) Расходимость, мак- симальная	(19) рад.	10^{-4}	10^{-5}
(20) Скачки по току		15000	1200
(21) Длительность ВЧ импульса на уровне 0,9	(22) мксек	2,2	10
(23) Длительность импуль- са возбуждения	(24) мксек	5	30
(25) Рабочее давление в ускоряющей системе	(26) торр	10^{-6}	10^{-7}
(26) Время непрерывной работы до остано- вки на профилактику	(27) час	150	600
(27) Полезное время ра- боты с пучком в год	(28) час	3200	4200
(28) Возможность одно- временной работы на пучке нескольких групп		(29) Будет обеспе- чена в комп- лекс с новыми залами	(30) Нет
(31) Надежность работы ус- корителя	%	90	(32) Лучше 90% в среднем за год

Key: (1). Parameters. (2). Data of 1970. (3). Data after execution of all programs. (4). Energy of electrons, maximum. (5). GeV. (6). Width of spectrum at the level 0.5 I maximum. (7). Current (pulse, maximum). (8). mA. (9). Frequency of messages, maximum. (10). Hz. (11). Duration of current pulse. (12). μ s. (13). Current average/mean worker. (14). μ A. (15). Power of beam. (16). kW. (17). Transverse sizes/dimensions of beam. (18). Divergence, maximum. (19). rad. (20). Duty factor with respect to current. (21). Duration of hf pulses at the level 0.9. (22). Duration of pulse of excitation. (23). Time of continuous operation to cessation to preventive maintenance. (24). torr. (25). Time of continuous operation to cessation to preventive maintenance. (26). hour. (27). Good time with beam per annum. (28). Possibility of simultaneous work on beam of several groups. (29). It will be provided in complex with new halls. (30). No. (31). Reliability of work of the accelerator. (32). It is better than 90c/o average in year.

FOOTNOTE 1. During the replacement of 50 sections to the new ones.
ENDFOOTNOTE.

REFERENCES

1. V. I. Beloglazov, Yu. M. Bazayev, A. K. Walter et al. Linear accelerator on 2 GeV of FTL of AS UkSSR. "Atomic energy", 1968, 24.

2. L'accelerateur lineaire d'Orsay et ses possibilites actuelles. L'Onde Electrique, 1969, 49, fasc. 7, 723

Page 71.

16. Rapid booster - injector of proton synchrotron IFVE.

A. D. Artemov, V. I. Balbekov, V. P. Belov, A. A. Vasil'yev, F. A. Vodop'yanov, O. A. Gusev, A. M. Ivanov, Ye. G. Komar, A. A. Kuz'min, E. A. Larionov, I. P. Malyshev, N. A. Monoszon, ^E/₂ A. Myae, L. L. Pal'mskiy, B. V. Rozhdestvenskiy, A. M. Stolov, Ye. P. Troyanov, V. A. Titus, G. M. Fedotov, P. A. Pefelov, I. A. Shukeylo.

(Scientific research institute of the electricophysical equipment in. L. V. Efremov, institute of high-energy physics, radio engineering institute of the AS USSR, state union design institute GKAE).

In the present report are given some designed considerations by construction of the basic systems of rapid booster - the injector whose development was the result of studying the general/complex/total problem of a sharp increase in the intensity of proton synchrotron IFVE [1]. Some questions, which relate to the separate systems of booster, are in detail described in reports [2, 3].

The high intensity of the accelerated particles ($1.7 \cdot 10^{12}$ protons per pulse at the repetition frequency of 25 hertz) with the

limited (~100 m) perimeter determines constructive solutions and operating modes from the efficient systems of booster.

The selection of magnetic structure POPDCD with 16 elements/cells of periodicity and acceptance, which corresponds to the acceptance of main accelerator, is caused by the minimal sizes of the cross section of magnet and by the length of gaps/intervals (1.1 and 2 m) between the units, sufficient for positioning/arranging 10 accelerating stations, the equipment of the introduction systems and conclusion/output, correction, monitoring, etc. The hardness of magnetic system is maxima for C-shaped magnets without the neutral poles. For convenience in input and output of particles the frameworks of all units are turned inside the ring. The wide intervals between those defocusing to semiblocks they are preferable both for the system of conclusion/output and for the more optimum cross section of the clusters of rescatters.

Due to the effect of space charge at the large intensity will be comparatively large the scatter of frequencies of the betatron. Fig. 1 shows the lines of resonances and the possible positions of the region within which are located the frequencies of betatron at the moment of the cycle when the scatter of frequencies is maximum. The repeated intersection of anharmonic resonances can increase the transverse sizes/dimensions of beam to end of the acceleration in

comparison with the calculated ones. This will lead to the losses of particles upon the injection into main accelerator or during the conclusion/output from it. Therefore to the straggling of the nonlinearity of the magnetic field of booster are presented stringent requirements [4].

In the interval of the variation in the magnetic field 1.33-9.55 kg the basic source of nonlinearity can be the nonlinearity on the ends/faces of units and in the region between the focusing semiblocks whose contribution grows/rises at the relatively small length of units. It is proposed experimental-design method to compensate for these nonlinearity in entire operating range of fields by the special selection of profiles/airfoils on the ends/faces and between the semiblocks.

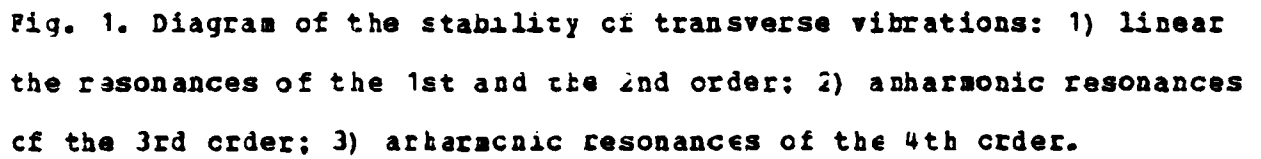
Another source of nonlinearity can be metallic vacuum chamber/camera. At present are examined two possible versions of the chamber/camera: from aluminaceous ceramics (Al_2O_3) and the thin-walled corrugated chamber/camera from the nickel alloy with the high specific resistance (Fig. 2).

Ceramic chamber/camera satisfies all requirements, but relative to it is expensive. Metallic chamber/camera from the seamless pipe with a thickness of 0.25 mm in height of corrugation 6 mm and

steps/pitches 3 mm is satisfactory from the point of view of the attenuation of field and heating, but it is not thus far found a constructive solution for the expanded sections of chamber/camera on the input and the output from the booster. Is feasible the combined version of vacuum chamber.

Together with the correction only some of the components of field, which usually emerge beyond the permissible limits in proton synchrotrons, and the correction, connected with the selection of the optimum modes/conditions of booster, probably, it will be required linearity correction of magnetic field for the purpose of the decrease of the force of some anharmonic resonances. For these purposes are provided for the corrective elements/cells with the identical implicit-pole magnetic circuits, the characterized by excitation windings (dipoles, quadrupoles, sextupoles, and octupoles). Their replacement can be conducted without the deterioration in vacuum.

With the current of linear accelerator 100 ^A mA [5] and the effectiveness of injection and capture by 60-70% for obtaining the intensity 1, 7, 10^{12} protons and the impulse/momentum/pulse it is sufficient 3-4 - reverse injections.



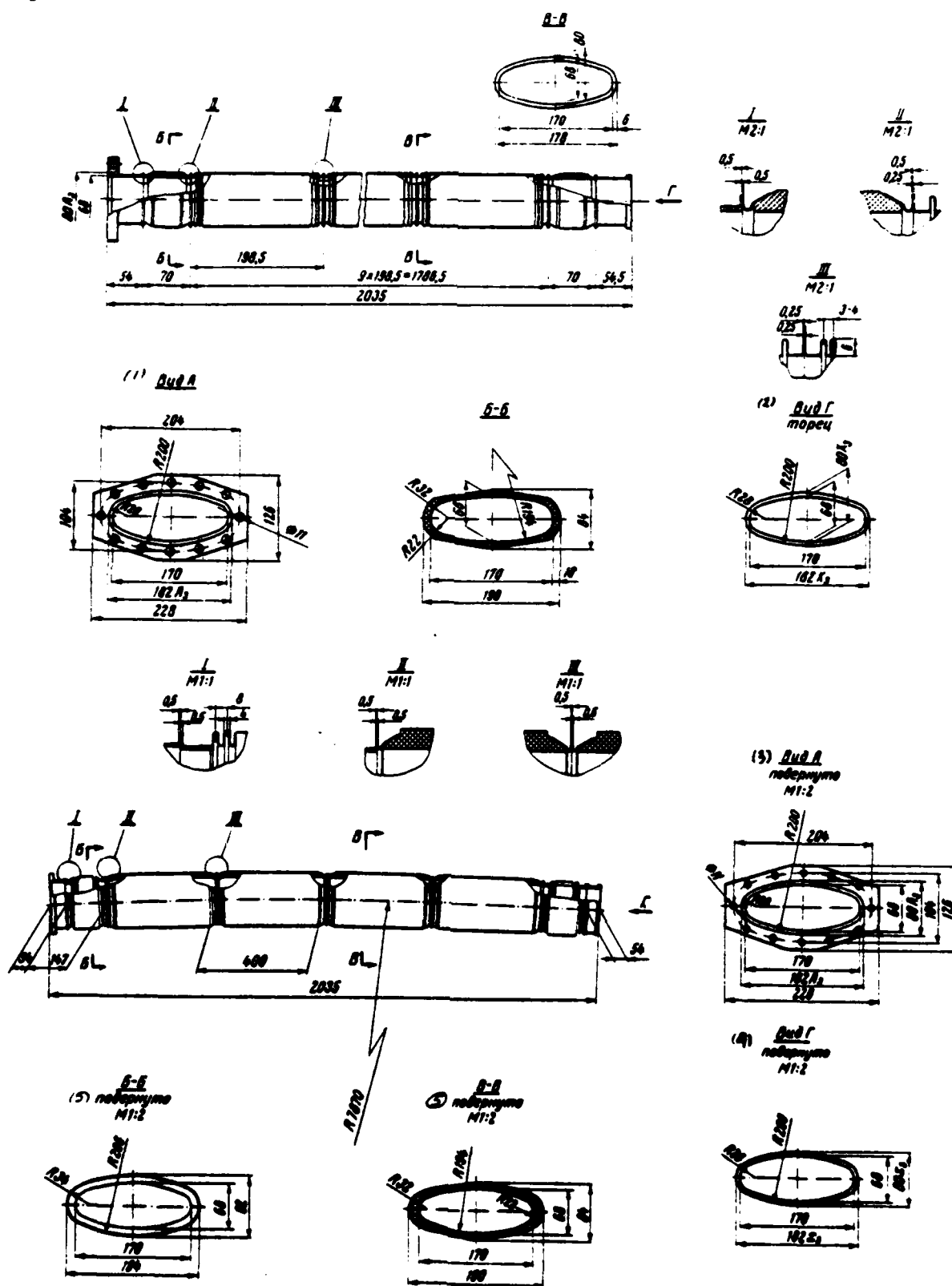


Fig. 2. Section of vacuum chamber.

Key: (1). View. (2). View G end/face. (3). View A is turned M1:2.
(4). it is turned. (5). is turned.

Page 73.

Is theoretically developed the resonance diagram of the introduction/input of beam into the phase space of radial betatron oscillations ($Q_r = 3.5$ upon the injection), that involves the changing in the time local distortion of equilibrium orbit. The introduction/input of launching/starting with the exitance, mismatched with the acceptance of booster; makes it possible to bridge the region of the strongly nonlinear fields of the focusing on a radius units. Local distortion of orbit and change in the frequency of betatron for the period of injection proposes to use by ferrite magnets and lenses with the single-turn excitation windings. For the purpose of the decrease of the effect of space charge on the effectiveness of injection is assumed maximum filling of chamber/camera in the vertical direction. With this more effectively is utilized elliptical cross section of chamber/camera.

The acceleration of protons is intended to accomplish 10

accelerating stations (2 of them - stand-by), which involve the reconstructed resonators. Rearrangement in the frequency is accomplished by the magnetic biasing of the ferrite, filling the resonators. The accelerating station consists of two coaxial cavities, excited on the TEM wave and operating in the antiphase to one clearance. The frequency range of accelerating voltage 0.83-2.79 MHz with multiplicity 1 is close to the frequency range of main accelerator [3]. The maximum amplitude of accelerating voltage of 65-70 kV/rev. corresponds the maximum of N. Coordination of the radial size/dimension of separatrix with the pulse scatter it is provided by the reduction of the amplitude of accelerating voltage upon the injection to 1.5 kV/rev. Calculated capture efficiency composes 620/o. In concen. of the cycle of acceleration by a change in the amplitude of accelerating voltage is regulated the longitudinal size/dimension of cluster. For the purpose of weakening the load of resonators by beam with modulation of stress/voltage it is proposed to use the noncofhasal supply of rescnators.

The conclusion of particles from the booster - single-thread; cluster; brought out from the booster, fills one separatrix of main accelerator. The diagram of conclusion/output is traditional for the proton synchrotrons: at the end of the cycle of acceleration equilibrium orbit locally is distorted in the radial direction and beam with the aid of the full-aperture ferrite impact magnets is

thrown into the deflecting septum-magnet, located in the maximum of orbit distortion.

An essential special feature/peculiarity of the devices/equipment of the commutation of beam on the input into the booster and the output from it, and also during the introduction/input into main accelerator is the mode of their operation with the repetition frequency 25 Hz. All equipment components must provide not less than 10^6 activations without the replacement. The breaking stress to which can be calculated at present switching elements/cells, which form lines, etc., is 50 kV. With the required fronts 80-150 ns impact are magnetic necessary to divide in the section (12-16 sections in impact magnet during the introduction/input into main accelerator). Have limitations on the current and switching elements/cells (hydrogen thyatron - to 3000 A). However, an increase in the total number of elements/cells leads to a decrease in the reliability of entire system. Furthermore, the inductance of introductions/inputs and magnets become commensurable. At present are studied the possibilities of the improvement of the complex articles for their use in this mode/conditions (oil filling of cables, stabilization of the parameters of thyatrons, etc.), the uses/applications of the small strip forming lines, are developed/processed low-inductance coaxial introductions/inputs and resistors.

The electromagnet of booster consists of 32 units (Fig. 3). The construction/design of units in essence is analogous to the electromagnets of the electron synchrotrons (Fig. 4). The excitation of electromagnet is sinusoidal with the magnetic biasing. Is examined [2] the possibility of exciting the electromagnet by nonsinusoidal current in order to decrease the maximum speed of field change and, consequently, also power of the accelerating stations.

Unit consists of 5 straight/direct glued/cemented made of sheet steel ^E~~42~~ of packets. The pole of extreme packages they are rounded on the ends/faces. Steady transition from the focusing semiblock to that defocusing is made in the average/mean package. This magnetic structure makes it possible to decrease heating steel on the ends/faces of unit and in the transient field, to decrease the effective nonlinearity in the distribution of magnetic field, to stabilize effective lengths in entire range of fields and according to the results of the measurements of magnetic characteristics in the pilot model to correct before beginning mass production the relationship/ratio of the lengths of semiblocks by the method of mixing along the azimuth of the dividing line of semiblocks without a change in the length of packages. The excitation winding of unit consists of four sections on 16 turns, included in parallel.

Transposition is accomplished/realized on 2 units. Armature coils are coiled from the square copper tube with section $13.5 \times 13.5 \text{ mm}^2$ with hole for cooling water $\varnothing 6 \text{ mm}$. In this case certain increase in the ohmic losses on alternating current is compensated by simplicity and reliability of construction/design.

By project is provided for the possibility of the work of main accelerator both with the injection from the linear accelerator I-100 and from the booster.

Fig. 5. shows the mutual location of booster and main accelerator.

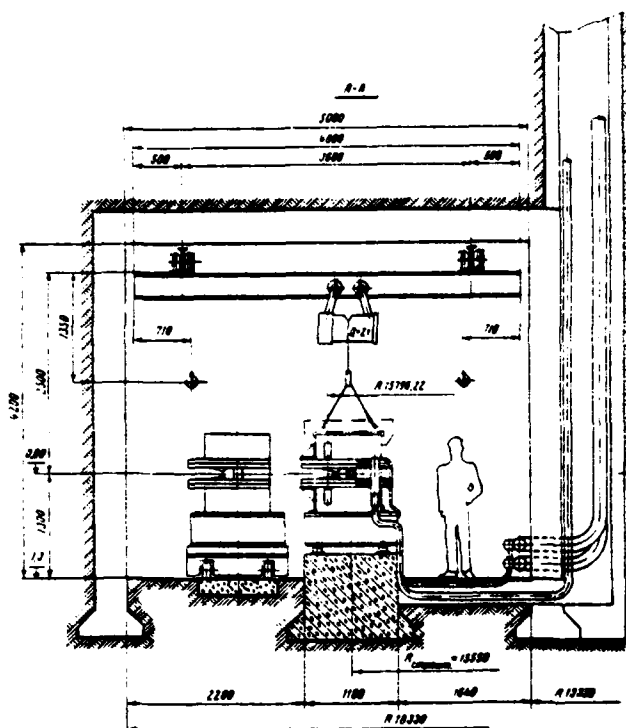


Fig. 3. Section of the tunnel of booster.

Page 74.

Basic parameters of the booster:

Energy of the protons of 37.5-1500 MeV.

Intensity in the impulse/momentum/pulse $1.7 \cdot 10^{12}$.

Repetition frequency of the cycles of 25 Hz.

Orbit circumference of 99.16 m.

Radius of curvature of 7.87 m.

Frequencies of the betatron

on a radius 3.26.

on the vertical line 3.38.

Frequency of revolution 0.83-2.79 MHz.

Multiplicity of radio-frequency 1.

Maximum accelerating voltage 65-70 kV.

A number of accelerating stations 8+2 it is stand-by.

Number of elements/cells of periodicity 16.

Number of units 32.

DCC = 90069206

PAGE 306

Magnetic structure

FCEDCE.

Range of a change in the magnetic field in orbit
kg.

of 1.13-9.55

Length of unit on iron

1.545 m.

Weight of the electromagnet

320 t.

Aperture of vacuum chamber

6.8x16 cm².

Pressure in the chamber/camera of booster

2.10⁻⁷ torr.

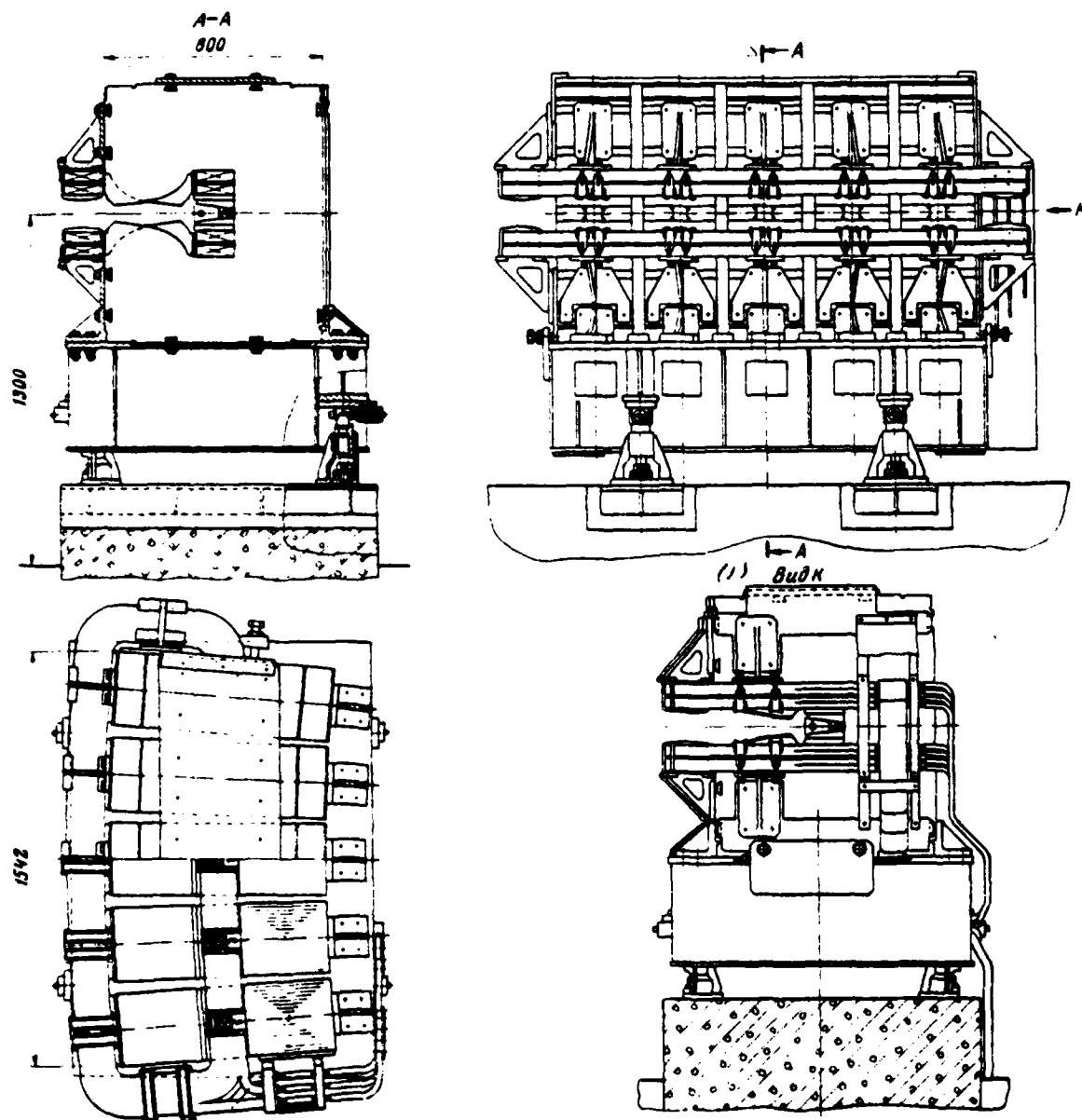


Fig. 4. Unit of electromagnet.

Key: (1). Form.

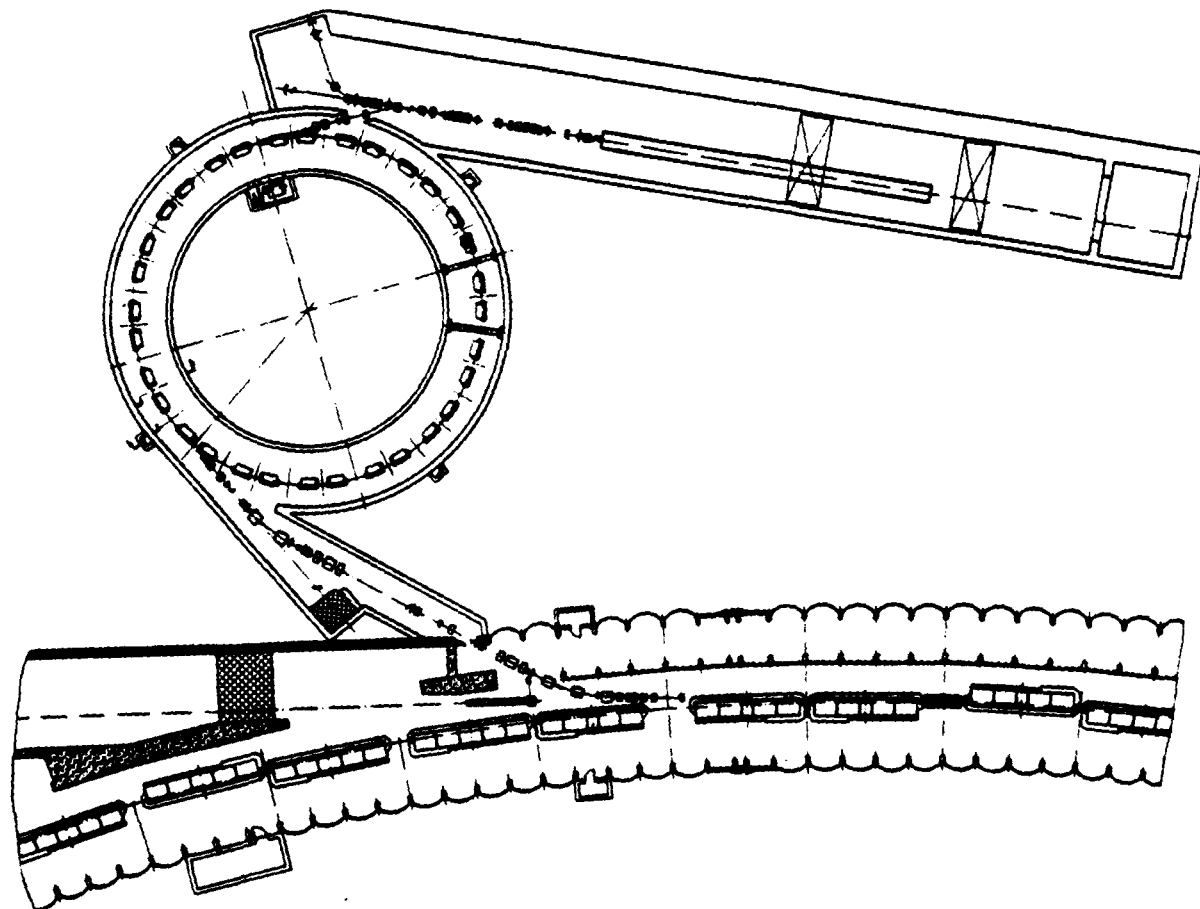


Fig. 5. Booster and section of introduction/input into main accelerator.

REFERENCES

1. Yu. M. Ado, V. I. Balakov et al. Increase in the intensity of

proton synchrotron by the energy 70 GeV by means of an increase in the energy of injector. This coll., Vol. I.

2. O. A. Gusev et al. Special features/peculiarities of the construction of the power-supply system of the electromagnet of rapid booster. This coll., Vol. I.

3. F. A. Vodop'yanov et al. New systems of radio electronics and control of proton synchrotron IFVE. This coll., Vol. I.

4. V. I. Balbekov, I. A. Shukeyic. Some effects of space charge in the booster in main accelerator IFVE. This coll., Vol. I.

5. A. L. Mints et al. Injector of the booster of proton synchrotron IFVE. This coll., Vol. I.

Page 75.

17. Project of the reconstruction of proton synchrotron ITEP.

L. Z. Barabash, A. V. Earkhudyaryan, Yu. A. Bcl'shakov, M. A. Veselov, L. L. Gol'din, V. P. Zavodov, P. R. Zenkevich, Yu. M. Zlatov, I. P. Kleopov, V. V. Kcrstantinov, D. G. Koshkarev, Yu. Ya. Iapitskiy, P. I. Lebedev, K. K. Cncsovskiy, L. I. Sckolov, Ye. A. Sysof, ^{ver} M. V. ^{ch} Shelkancv.

(Institute of theoretical and experimental physics).

Target of reconstruction.

The reconstruction of proton synchrotron ITEP [1] pursues the following targets: 1) readjustment of magnetic system in order to create the sections, fitted out for the highly efficient conclusion/output initial particles, and the conclusion/output of particles from internal targets at angles close to zero; 2) an increase in the energy of protons from 7 to 10-11 GeV; 3) an increase in the frequency of cycles from 15 to 24 in min. A disadvantage in the present structure of accelerator is the absence of straight sections, fitted out for the conclusion/output of particles. After

reconstruction in the structure will appear two long (2.4 m) gaps/intervals in each period of magnetic system (Fig. 1). The afterward second of these gaps/intervals usual F - unit with the framework, placed outside the ring, it will be replaced by the closed unit, altered from D unit (Fig. 2). Because of this in three consecutive magnets, which follow after the second long gap/interval, the frameworks prove to be turned inside the ring. This structure of magnetic system will make it possible by simple means to carry out a highly efficient (at will - slow or rapid) conclusion of the proton beam, accelerated before full/total/complete energy, which now is impossible. From such gaps/intervals it is easy to also carry out a conclusion of secondary particles, generated on internal target. In this case from one target it will be possible to simultaneously derive several beams of secondary particles one of which will emerge at angle, close to 0° . The conclusion/output of secondary particles from another gap/interval can be accomplished at angle approximately 13° , i.e., approximately/exemplarily in the manner that now is conducted the "universal conclusion" of secondary particles.

Page 76.

An increase in the energy of beam to 11 GeV will make it possible to expand the field of resonances, available for the investigation on the accelerator, and gives the possibility to produce works with the antiprotons and the antineutrons which are now formed insufficiently effectively because maximum energy of particles

the too close to oscillation point of antinucleons.

An increase in the frequency of cycles is more than one and a half times, by itself represents important task, since dialing rate of statistics during the physical experiments is proportional to the frequency of cycles. As is known, an increase in the frequency of cycles usually proves to be considerably more usefully than an increase in the intensity of beam.

The proposed reconstruction is the necessary first step/pitch, without which is impossible further modernization of accelerator. The second step/pitch of modernization will be the conclusion/output of proton beam into the special - proton - housing, calculated for the work with the primary beam and the short-lived particles, generated in the housing itself, next to the experimental installations. The conclusion/output of primary beam into the available experimental hall becomes after reconstruction completely feasible, but it will be hardly advisable due to the difficulties with the protection.

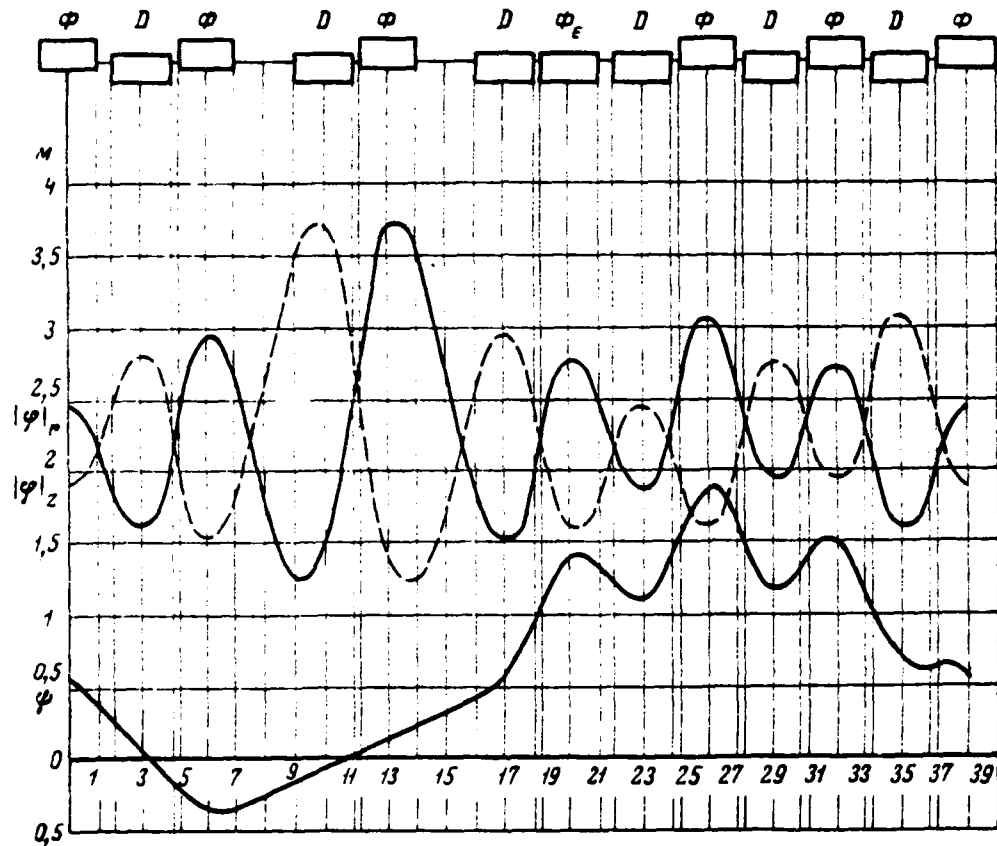


Fig. 1. Magnetic structure.

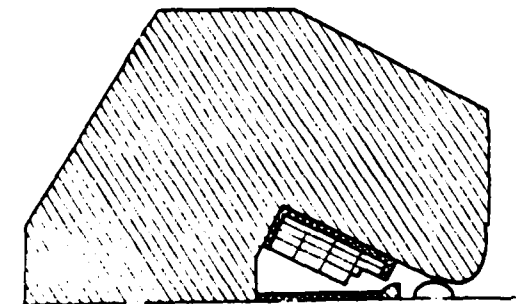


Fig. 2. Magnet of type "E".

Page 77.

Thus, reconstruction not only raises the frequency of cycles and energy of protons, but also exceeds proton synchrotron ITEP into the contemporary accelerator with the convenient output and the input of particles and is opened the way for future modernization.

Structure of magnetic system.

The magnetic structure of the working new accelerator contains 112 magnet blocks, from which 98 are C - by units and 14 X - units. X - boost clusters do not have a field on the axis and are quadrupole lenses. C - units as focus, so also turn beam. Of 98 C - units 56 they defocus beam on a radius (L - units), and 42 - they focus (F - units). All 14 X - units focussed beam on a radius. Magnet blocks are established/installed on the special plates/slats, making it possible to move units with the adjustment. Plates/slats are sealed in into the reinforced concrete ring, which forms the foundation of magnetic system.

The period of magnetic structure after the rearrangement (see Fig. 1) contains 12 magnet blocks; 6 focusing and 6 defocusing. Of

twenty gaps/intervals, belonging to each period, two are long (2.4 m), two - extended (0.6 m), one normal (0.45 m) and seven short (0.304 m).

Two long gaps/intervals together with their dividing pair of units form minus-single matrix/die, which ensures undisturbed transition from the previous magneto-optical channels, containing 10 units, to the following such to channel.

One of the units of each period - the first focusing unit, which goes after the second long gap/interval, is done the closed type. Turned inside the framework these units do not interfere with the conclusion of particles of the accelerator. The closed units are manufactured from existing L - boost clusters, among which are excess, while F - units are not sufficient.

Accelerator chamber is retained previous, but it is shifted/sheared into the region of large fields. This shift of chamber/camera decreases the ratio of the gradient of magnetic field to the value of field and necessary in order to decrease the hardness of focusing (number of oscillations for the revolution). Decreased the hardness of focusing must be to preserve smooth envelope of betatron oscillations in the presence of long straight sections. The shift of chamber/camera to the side of large fields brings,

Furthermore, to an increase in the middle field, and it means and maximum energy of accelerator with the same maximum coil current of magnets. Withdrawal from magnetic system X - units does not affect maximum energy of accelerator, since these units do not have a field on the axis. At the same time removal/distance X - units decreases the inductance of ring (by 140/o) and is decreased its resistance (almost doubly). The decrease of the impedance of magnetic system contributes to an increase in the number of cycles.

Here it must be noted that the frequency of cycles in the present accelerator is limited by not so much magnetic system (and by the power of feeder), as by ineffectiveness of the accelerating system on span tubes. The replacement of these tubes by resonators and the decrease of the impedance of magnetic system make it possible to raise the frequency of cycles from 15 to, at least, twenty four.

An increase in the frequency of cycles and energy of accelerator leads to the need for increasing an energy gain on the revolution from ≈ 4 to ≈ 15 keV. This increase is provided by the replacement of the existing accelerating system on drift tubes to the resonator accelerating system.

In this case appears the possibility of failure of the formation of magnetic cycle with permanent rate of rise of the field.

The latter fact offers the possibility of replacing the existing power-supply system of the magnet of accelerator with the electromagnetic conversion unit to the supply directly from the power system.

Besides simplicity and larger reliability this power-supply system makes it possible to work with the permanent frequency, which in turn, strongly simplifies the task of filtering the field to area of magnetic cycle, necessary for a good work of all systems of slow beam extraction.

Let us compare some characteristics of accelerator before and after reconstruction. The maximum of the modulus/module of the function of floquet after rearrangement somewhat increases and it reaches 3.72 (to rearrangement 2.91), but amplitude Ψ - function virtually is not changed. An increase in the modulus/module of the function of floquet leads to the decrease of those permitted the amplitude of betatron oscillations, which decreases the acceptance of chamber/camera. One should, however, note that after the rearrangement of machine the maximum value of the modulus/module of the function of floquet for the radial direction attains in F - unit of minus-single matrix/die, i.e., in that place where Ψ - function

is equal to 0.2 m. In the remaining units the modulus/module of the function of floquet does not exceed 3 (see Fig. 1).

In the working new accelerator the maxima of the function of floquet and γ - function coincide. This fact partially compensates the losses, connected with an increase in the amplitude of the function of floquet. The at the same time Coulomb limit of the intensity of accelerator after rearrangement decreases and will compose $1 \cdot 10^{12}$ instead of $1.6 \cdot 10^{12}$ with the energy of injection 25 MeV. As will be shown below, this decrease of practical value does not have.

After the rearrangement the accelerator will have the best characteristics for the particles, differing with respect to the impulse/momentum/pulse from the nominal. Let us point out first of all, that the coefficient, which is determining the dependence of frequency of betatron on the impulse/momentum/pulse, proves to be after rearrangement one and a half times less than now (11 instead of 16). The decrease of this coefficient will allow particles longer to remain in the chamber/camera with interaction with the target, which raises the output of secondary particles. Furthermore, in this case is expanded permissible variations of particles on the impulse/momentum/pulse during the injection. This scatter composes now $\pm 2.2 \cdot 10^{-3}$ and will increase after the reconstruction of machine

to $\pm 5 \cdot 10^{-3}$.

The intensity of beam in the accelerator at present is limited due to an insufficient quantity of protons in the necessary interval $\Delta p/p$ in the beam, going from the linear accelerator. To decrease $\Delta p/p$ in the beam contributes debuncher, but this scatter nevertheless rejects by excessive, and the percentage of the seized particles - it is insufficient to large ones (300/o). The high Coulomb limit of the existing accelerator therefore cannot be used. After the rearrangement of accelerator the percentage of the seized particles substantially will increase and the intensity of beam, in spite of certain reduction in the Coulomb limit, it will increase.

Page 78.

Systems of correction.

In the proton synchrotron IIEP are three types of the corrective windings: the supplementary windings, placed on magnet yoke, the windings, placed on surface magnet poles, and the windings, wound around the neutral pole. The first serve for the correction^{of} 13 and 14 harmonics of the magnetic field distortions, which are now the most dangerous, the second - for the correction of frequencies of the betatron, for eliminating the coupling of oscillations, and the third - for the distortion correction of orbit in the vertical direction.

After the reconstruction of accelerator the corrective windings, placed on magnet yoke, are retained. By them, after the appropriate changeover, it will be possible to amend the 9th and eighth harmonics of the distortions of the vertical component of magnetic field. As already mentioned above, pole windings after the reconstruction of accelerator will be distant. Hardly has sense to retain and the windings, wound around the neutral pole. The functions of pole windings will perform the corrective magnetic lenses, placed in the long and increased gaps/intervals. Experience of operating accelerator showed that for obtaining a good intensity it is necessary in the field of injection to produce the correction of field from many parameters. At the same time at the end of the cycle of acceleration for obtaining the effective conclusion/output it is necessary (and apparently, sufficiently) to have the capability to correct frequencies of betatron in the limits of the whole cage/cell of frequencies, i.e., in limits $\Delta Q_1 \approx \pm 0.5$; $\Delta Q_2 \approx \pm 0.5$. At present we do not have possibilities for so strong a correction of frequencies at the end of the cycle, but it is desirable to obtain it after reconstruction.

In accordance with what has been said we intend to place in the gaps/intervals two systems of the corrective elements/cells. One system consists of 16 quadrupole lenses (one pair each on superperiod). This system provides the correction of the frequencies

of betatron oscillation/vibrations, and also 16th harmonic of gradient during entire cycle of acceleration. Parameters of the lenses: the length of 25 cm, the maximum gradient of 750 oersteds/cm, aperture - 110 mm. The windings of lenses must provide for to washing both direct current and by current of saw-tooth form. For the correction of field in the beginning of cycle are provided for special multipurpose magnetic lenses in a quantity of 16 pieces. These lenses can be made in the form of the cut of circular duct from the ferromagnetic material with a length of 30 cm in thickness approximately 5-7 mm. Each lens must have 3 types of the windings, arranged/located from inside of duct. In this case each winding has its law of arrangement within the duct. The first winding must create the uniform radial magnetic field (law of coil/winding $\cos \phi$). It serves for the correction of the closed orbit in the vertical direction. The second type of windings creates quadrupole field in the axes/axles, turned on 45° relative to the adopted system of coordinates. This target serves for correction of connection/communication of frequencies. Type of coil/winding $\cos 2\phi$.

The third winding is intended for the correction constant component quadratic nonlinearity of magnetic field. The conductors of this winding are placed within the lens according to the law of $\cos 3\phi$.

REFERENCES

1. D. G. Koshkarev, Ye. K. Tarasov. Designed considerations about the reconstruction of proton synchrotron ITEP. Reports on international/inter conf on the accelerators. USA, Cambridge, 1967.

18. The pulsed operations of microtron FEI.

Yu. Ya. Stavisskiy.

(Physical-power institute).

Microtron group of FEI (A. I. Abramov, G. N. Anikin, V. T. Vasin, N. A. Klintsov, Yu. Ya. Stavisskiy, V. F. Filyayev, Yu. M. Choporov) is developed, fluffed and is operated about three years pulsed microtron on 30 MeV for neutron spectrometry on the time of flight and photonuclear investigations.

In essence the construction/design of microtron FEI is analogous to the constructions/designs of 30-MeV of microtrons of IFP of the AS USSR [1] and the Joint Institute for Nuclear Research [2]. Colleagues of these institutes, especially S. P. Kapits, V. N. Melekhin and I. E. Mator rendered essential assistance in the launch procedure of accelerator.

The special feature/peculiarity of microtron FEI is the use/application of nonretunable resonator with cooled covers/caps [3] and the use of a power-supply system of magnetron on the basis of rigid modulator. The use/application of the nonreadjustable resonator

with the cooled covers/caps made it possible to increase substantially the reliability of its operation and service life. The developed methods of a precise production of resonators and monitoring of their parameters ensured the possibility of their use/application with the virtually nonreadjustable 10-centimeter magnetrons (frequency control was accomplished/realized by a method of changing the magnetic field in the magnetron, which makes it possible to vary frequency in the limits of altogether only ~ 3 of megahertz [3]).

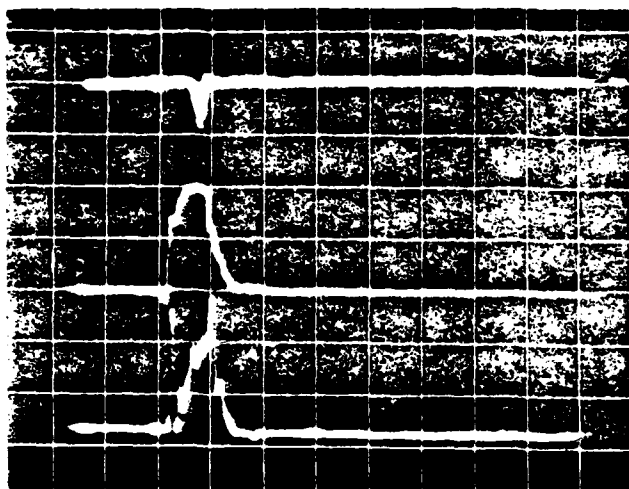
The use of a rigid vacuum-tube modulator of large power for the supply of magnetron allowed to carry out the new modes/conditions of work of the accelerator, which are of interest for the series/row of neutron experiments, in particular for the analyses of neutron spectra from (γ, n) - reaction near the threshold (see for example, 4). The vacuum-tube modulator, duration and the pulse repetition frequency of which smoothly they are varied over wide limits, makes it possible to obtain the narrow pulses of the accelerated electrons and high repetition frequencies.

Page 79.

For the investigations (γ, n) - reactions near the threshold is necessary the energy of electrons 10-12 MeV. With this energy the

minimum duration of the pulse of the accelerated electrons (without the loss of peak intensity) is ~ 50 ns (see figure). Prolonged experiments were conducted at the repetition frequency ~ 3 kHz, duration of pulses ~ 100 ns, currents in the impulse/momentum/pulse ~ 80 - 90 mA. For the beam extraction of the electrons of energy 12 MeV the resonator was shifted/sheared inside the magnet with the aid of the waveguide inset.

An improvement in the conditions of cooling the elements/cells of resonator will allow, apparently, to increase substantially the intensity of beam in a similar mode/conditions and to approach according to average/near characteristics $M \sim \sqrt{\tau}$ the powerful/thick linear accelerators during a good energy resolution, characteristic to microtron (~ 30 keV). In any case, accelerative limitations lie/rest considerably above: into the short-term the experiments, limited by the heating of the elements/cells of resonator, we obtained pulse currents to 500 mA for the duration of 50-100 ns and at the repetition frequency ~ 8 kHz.



Form of the current pulse of modulator.

Upper curve - the current of target, average/mean - current, cathode, lower - reflected by resonator of SRF wave. One division on the horizontal - $0.5 \mu\text{s}$.

REFERENCES

1. Microtron. coll. of articles edited by S. P. Kapitsy. Publishing house "Science", 1965.
2. V. D. Anan'yev et al. Microtron ANP the J.I.N.E. Preprint J.I.N.R., 9-3283, 1967.

3. G. N. Anikin et al. Resonator of microtron FEI and its agreement with the SHF generator, SRF oscillator. Preprint FEI-149, 1969.
4. Bollindzher. (γ , n) - spectroscopy near on the horns. Washington conf on technology of retrich cross sections, 1966.

Page 80.

Session III.

Ionic and electronic sources direct voltage accelerators.

19. Effect of the conditions of the selection of ions from the source on the distribution of phase density in the intense ion beams.

M. A. Abroyan, V. S. Kuznetsov, N. P. Kuznetsova, R. P. Fidel'skaya.

(Scientific research institute of the electrophysical equipment im. L. V. Efremov).

Phase volume of ion beam is determined in essence by conditions of the selection of ions from the source. For the solution of the problem of increasing the phase density in the intense beams it is necessary to, first of all, establish/install connection/communication between the distribution of phase density in the beam and the conditions of the selection of ions from the plasma of source. The redistribution of phase density and the change in the

configuration of phase volume, which occur in real beams [1], do not make it possible to unambiguously interpret the effect of the conditions of selection with a change of distributing the phase density in the beam section, distant from the source. The measurement of the distribution of phase density in immediate proximity of the surface of plasma is extremely difficult and hardly at present possibly.

In our investigations according to the measured distribution of phase density in certain beam section, distant from duoplasmatron type source [2], numerically were calculated the distribution of phase density f , of the configurations of transverse phase volume and density distribution of current for the beam section, close to the surface of plasma. For the calculation was utilized the method of the numerical solution of the system of equations of the self-consistent field for function f , described in works [1, 3, 4].

For measuring the transverse phase volume was applied the modification of the known method of four slits [5].

Were investigated three groups of tasks with the varied conditions of the selection of ions. The parameters of the modes of operation of ionic source for these cases are given in the Table.

The results of measurements and calculations of the distribution of the phase density and other parameters of beam for the first group of the tasks (see the Table) are transferred in Fig. 1.

Номер задачи (1)	Ток пучка I, a (2)	Магнитная индукция B, mT (3)	Ток разряда I_p, a (4)	Вытягивающее напряжение U, kV (5)	Яркость пучка, B ($a/m^2 \cdot rad^2$) $\times 10^8$ (6)
1	1,5	0,33	55	60	4,8
2	I	2,0	0,33	92	6,1
3	2,4	0,33	200	60	8,4
1	1,1	0,85	55	30	3,7
2	II	1,2	0,85	40	5,3
3	1,3	0,85	55	50	5,8
1	1,2	0,33	92	30	5,1
2	III	1,8	0,52	92	7,6
3	1,8	0,85	92	30	9,7

Key: (1). Number of task. (2). Beam current. (3). Magnetic induction, V, MP. (4). Current of discharge. (5). Extraction voltage u , kV. (6). Brightness of beam V ($A/m^2 rad^2$) $\times 10^8$.

Page 81.

In this case changed the density of plasma and the shape of surface of emission with the aid of a change in the current of the discharge in the source. Fig. 1 gives density distribution of current and projection of transverse phase volumes for several beam sections, and also envelopes of the investigated beams. Calculated envelopes correspond to the data of visual observations and to the estimations

of the sizes/dimensions of beams in source according to the image on the photographic film.

The configuration of transverse phase volume and density distribution of current uniquely determine the shapes of surface of plasma. The qualitative character of the configurations of the emitting plasma surfaces for the investigated cases is given in Fig. 3. Are there for the comparison depicted some simplest configurations of plasma surface, usually utilized in the qualitative examination of the selection of ions from the plasma.

In Fig. 2 it is evident that the real surface of plasma is complex surface with the variable radius of curvature. The curvature of this surface can have different sign. In these cases, as is evident in Fig. 2, the extracted beam has complicated multiple-speed structure.

the bow configuration of the projection of phase volume (Fig. 3c) corresponds to plasma surface with the curvature, which decreases from the edges to the center (is possible sign change of curvature), and to beam with saddle-shaped density distribution of current.

The zigzag configuration of the projection of phase volume (Fig. 3b) corresponds to plasma surface with the curvature, which increases

from the edges to the center, and to beam with funnel-shaped density distribution of current. Are possible the more complicated cases (Fig. 3a).

As can be seen from the given results (see Fig. 1), distribution of phase density and configuration of the projection of transverse phase volume significantly change upon transfer from one beam section to another.

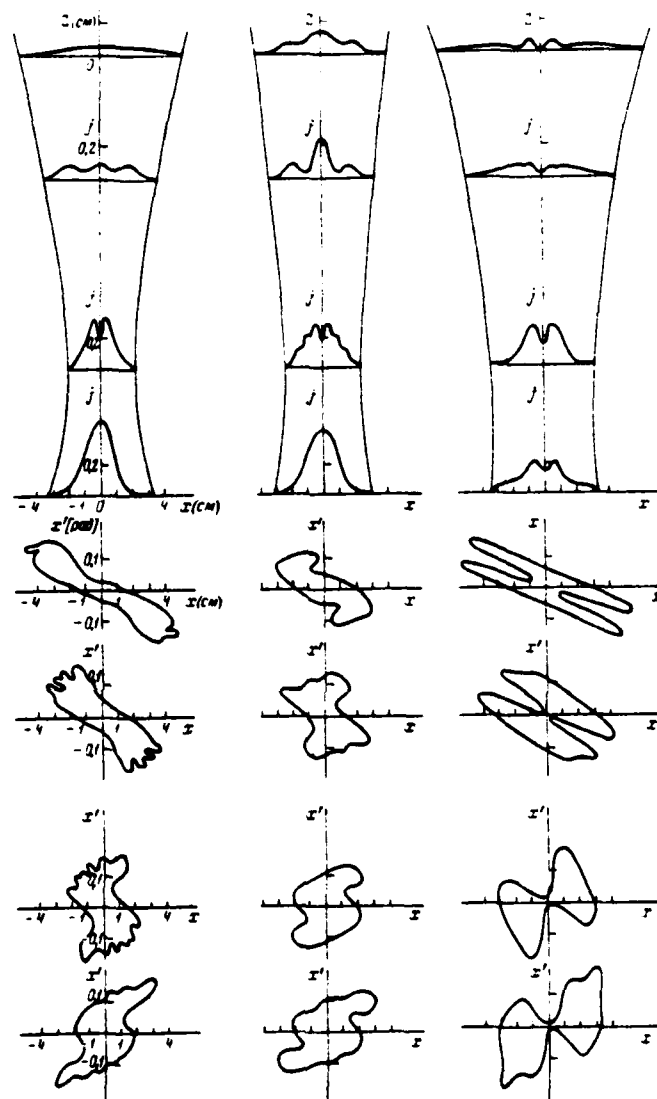


Fig. 1. Enveloping, density distributions of current and projection of the phase volumes of beams at the different values of the current of discharge in the source.

Page 82.

Invariant upon transfer from one beam section to another is the dependence of beam current I on the four-dimensional phase volume. Furthermore, this dependence characterizes the brightness of beam, or the current density in the phase volume, which is the most important stream conditions of the charged/loaded particles.

Fig. 3 gives dependences $I(V_e)$ for all investigated cases. Fig. 3, and corresponds to the different values of the current of discharge at the constant values of the remaining parameters of source. In this case change both density the plasma and the form of plasma surface. An increase in the brightness of beam with an increase in the current of discharge is connected with an increase in the density of plasma. However, as has already been spoken, here due to the distortion of plasma surface deteriorates the configuration of the projection of phase volume, which brings, in spite of an increase in the brightness, to an increase in the effective phase volume of beam.

Fig. 3b corresponds to a change in the extraction voltage; in this case changes only the configuration of the surface of plasma. Therefore at the high values of extraction voltage the brightness of beam falls due to the large distortion of the emitting plasma

surface.

Fig. 3c corresponds to a change in the magnetic field, which compresses the discharge in the duoplasmatron. Since in the extraction region of ions magnetic field is absent, the increase of the brightness of beam in this case is less sharply than with an increase in the current of discharge.

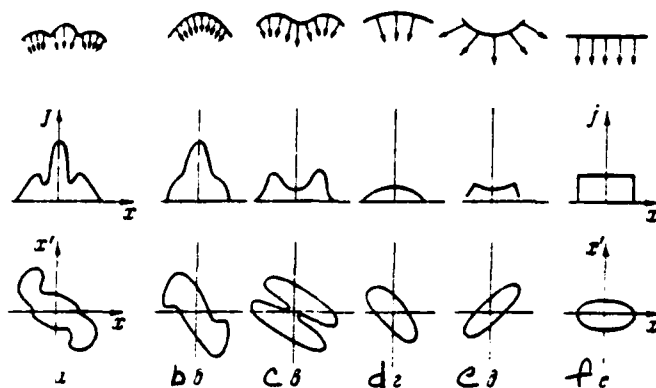


Fig. 2. Forms of plasma surface, density distribution of current and projection of the phase volumes of beams during the different modes of operation of source.

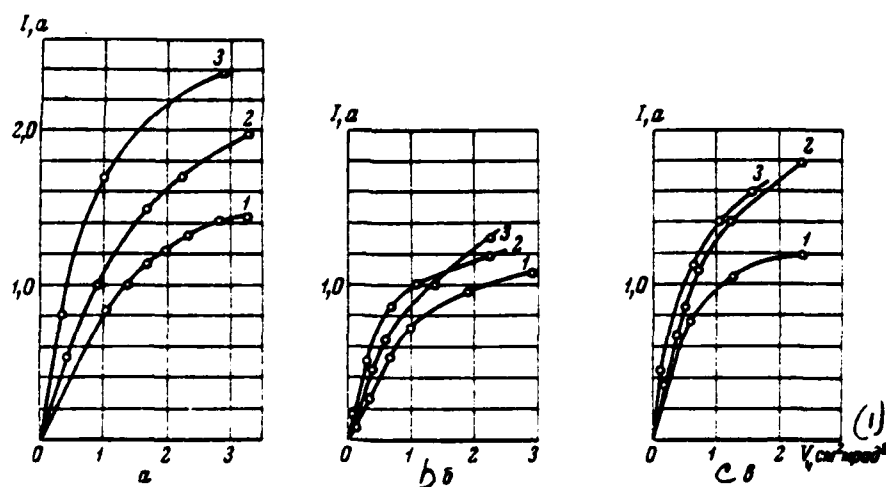


Fig. 3. Dependence $I(V_d)$ a) with change in current of discharge; b) with change in extraction voltage; c) with change of magnetic field in source.

Key: (1). $V, \text{cm}^2 \text{rad}^2$.

REFERENCES.

1. V. S. Kuznetsov et al. Investigation of the redistribution of phase density in the real charged particle beams with the aid of the numerical calculations. Transactions of All-Union conference on the charged particle accelerators, Vol. 2. M., 9-12 October, 1968. M., VINITI [- All-Union Institute of Scientific and Technical Information], 1970, page 419.

2. M. A. Abroyan, V. L. Kazarov. coll. "electrophysical equipment", iss. 1, M., Atomizdat, 1963, page 119.

3. V. S. Kuznetsov. ZhTF, 1967, 37, 5, 932.

4. V. S. Kuznetsov, E. E. Fidel'skaya ZhTF, 1968, 38, 10, 1756.

5. N. P. Ivanov, Yu. P. Sivkov, A. I. Solnyshkov, coll. "electrophysical equipment", iss. 4. of M., Atomizdat, 1966, page 3.

Discussion.

I. A. Soloshenko. Did change the value of phase volume with the

distance from the source or only configuration?

M. A. Abroyan. Four-dimensional phase volume was retained, configuration changed.

A. L. Mints. As you explain in the second figure the unusual behavior of curves in comparison with first and third figures the latter go regularly, and on the average/mean graph/curve by curved 2 and curve 3 they intersect.

M. A. Abroyan. With a change in the extraction voltage changes the form of ardent emitter. Upon transfer from 30 kV to 50 kV the form of plasma emitter, obviously, passes through the optimum.

Ye. Regenshtreyf. Is invariant the dependence of current on the four-dimensional phase volume in the case of different phase distributions?

M. A. Abroyan. Yes, this dependence is invariant for different distributions, including for Gaussian-the Maxwellian.

Zh. for. What extraction voltage and what geometry you did utilize?

DOC = 30069207

PAGE

~~33~~ 339

M. A. Abroyan. Extraction voltage varied from 30 kV to 50 kV.
Was applied the expander with a diameter of 100 mm.

Ye. Regenshtreyf. In all whether cases the beam was axially
symmetrical?

M. A. Abroyan. Yes, beam was axially symmetrical in all cases.

Page 83.

20. Development of the source of the polarized ions.

E. P. Ad'yasevich, V. L. Komarov, V. I. Marasev, V. M. Sokolniks, V. N. Fedorov, B. P. Yatsenko.

(Scientific research institute of the electrophysical equipment im. L. V. Efremov).

Ye. K. Zavoyskiy's proposition about obtaining nuclear polarized auto-sources of hydrogen and deuterium with the pickup of the polarized electron by ion [1], according to our estimations, made it possible to hope for the creation of the source of the polarized particles (IPCh) - the protons of deuterons, tritons and ions He³ - with intensity on the order of hundreds of microamperes [2]. However, number of questions required experimental check. One of them - the transportation of ion beam through the long dielectric channel - in the principle was solved, when through the pyrex tube with a length of 500 mm with the opening/aperture the diameter of 9 mm carried out the ion beam of hydrogen with the current 3 mA with the energy 40 keV. Was constructed the experimental source of the polarized "fast" atoms of the deuterium the principle of operation of which was shown in Fig. 1.

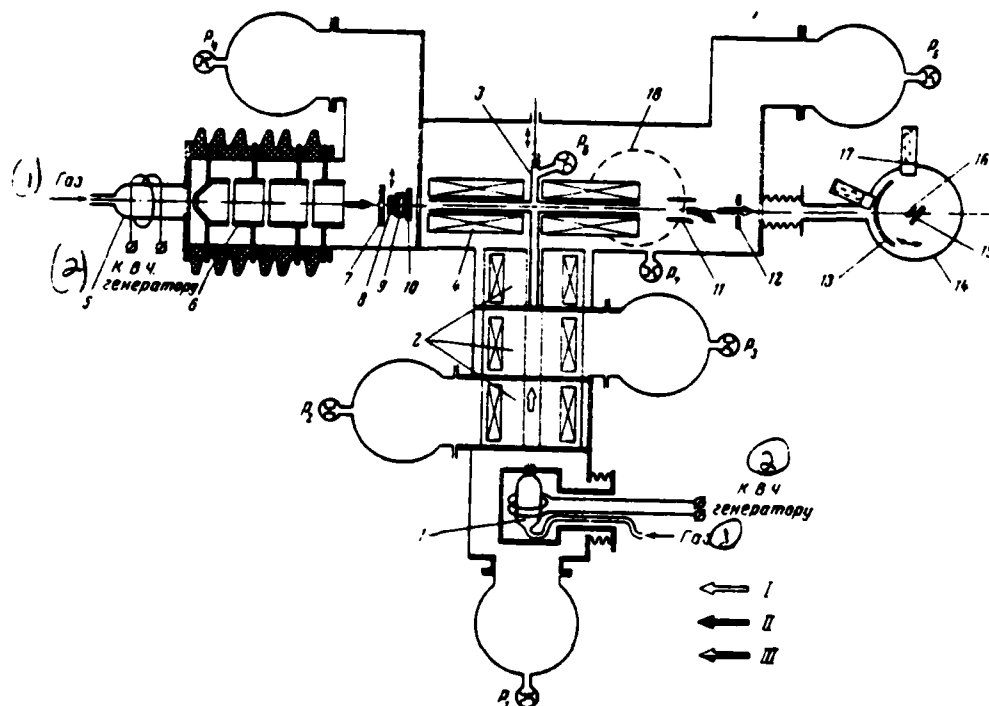


Fig. 1. The schematic diagram of the experimental source of the polarized fast atoms of action 1 - radio-frequency dissociator with the micro-collimator; 2 - four-terminal magnetic lens; 3 - T-shaped pyrex tube; 4 - solenoid; 5 - radio-frequency ion source; 6 - electrostatic unipotential lens; 7 - diaphragm; 8 - movable meter of the current of ion beam; 9 - circular thermionic cathode of electron gun; 10 - anode of electron gun; 11 - electrostatic capacitor/condenser; 12 - diaphragm; 13 - movable diaphragm; 14 - chamber casing of reactions; 15 - zirconium-tritium target; 16 - meter of beam current; 17 - sensors of radiation/emission; 18 -

nitric-titanate pump; P_1, P_2, \dots, P_7 - pressure sensors; I - beam of slow atoms; II - charged particle beam; III - beam of fast atoms.

Key: (1) - Gas. (2) - To V.C. to oscillator.

Page 84.

Atomic beam with 100c/o of electronic polarization, shaped with four-terminal magnetic lenses, enters in T-form the pyrex tube, placed into the strong magnetic field of solenoid. Due to a difference in the entering and outgoing streams of atoms in the T-shaped tube is created the increased concentration of the polarized on the electronic spin atoms. Ion beam from the radio-frequency ionic source, shaped with electrostatic single-potential lens, with the energy 40 keV are passed through T-form tube and with the pickup of the polarized electron is formed the beam of "rapid" atoms polarized on the electronic spin. For the compensation for space charge of ion beam in T-form tube it is injected electron beam with the energy 1 keV. The tensor polarization F_{33} is achieved at the adiabatic conclusion/output of atomic beam from the magnetic field of solenoid. Estimations showed that for the undistorted field of solenoid the condition of adiabaticity for the atom of deuterium is observed up to the energy in 2 MeV. With the flow of the atoms $3 \cdot 10^{15}$ of atoms/s and the ion beam in 75 μ A is obtained the atomic beam in 2.2 equivalent

μA with $P_{33}=0.07\pm 0.03$. So low a value of value P_{33} is caused in essence, by two reasons: first, by high intensity of atomic beam from the neutralization of ions (capture of electron) on molecules and atoms of residual/remnant vapors and gases; in the second place, the activity of the surface of tube to the processes of the depolarization of the atoms of gas target during the bombardment of surface with the part of the ions of beam. With an increase in the intensity of the passing ion beam P_{33} it falls (Fig. 2).

Further progress of this type IPCh is connected with the considerable decrease of the scatter of ions on the speeds and with the reduction of the concentration of unpolarized atoms in the beam by an order of magnitude.

The analysis of the advances in the field of creating IPCh indicates that in the near future, obviously, the most interesting source will remain the source of polarized particles based on the separation of the components of the fine structure of the atoms in a highly heterogeneous magnetic field of multiterminal networks with the subsequent ionization.

magnetic field of multiterminal networks with the subsequent ionization.

In NIIEFA together with IAE is developed/processed standard IPCh for the electrostatic generators with the overcharging (EGP), for the cyclical accelerators of the type cyclotron, P-M cyclotron, linear accelerator. As the basis of standard IPCh is accepted the source of the polarized protons and deuterons with the induced transitions between the superfine structure levels of atomic beam in magnetic field [3]. The calculated parameters of the developed/processed modifications IPCh are given in the table.

Are developed two constructions/designs of the system of the induced transitions: No 1 - for the atoms of deuterium, No 2 - for the atoms of hydrogen. Is developed/processed the third system - universal - for deuterium and hydrogen. Each of three systems consists of two regions of transitions in the "weak" magnetic field and one region of transitions in the "strong" magnetic field. All three systems with two regions of the induced transitions consist of of four types of transitions and three types of magnets.

Are developed/processed three types of the ionizers: two - in the strong magnetic field, axial to atomic beam (one of them plasma), and one in weak field - type of cylindrical diode [4].

Modification of IPCh for EGP (Fig. 3) has charge-exchange target, which represents the flow of the atoms of cesium or mixture of sodium and potassium, shaped with nozzle and which gives the effectiveness of overcharging to 250/o, ion-optical system for the agreement with the input lens of accelerator tube EGP the filter of wire for the assignment on the physical target of the necessary direction of the polarization of ions relative to their impulse/momentum/pulse (0, $\pm 45^\circ$, $\pm 90^\circ$, $\pm 135^\circ$, $\pm 180^\circ$) and the separations of the associated ions. Ionizer, target, ion-optical system into the filter of wire are located under the potential approximately 100 kV. Energy of beam from IPCh is regulated to 100 keV by this potential. In Fig. 3 chamber/camera and magnet of the

source of negative ions are expanded/scanned by 90° relative to the axis/axle of injection in EGF.

Modification IPCh for the cyclic accelerators (Fig. 4) is developed/processed with the system of bunching of the ions of beam, which makes it possible to raise the intensity of the beam, seized into acceleration mode, not less than 6 times. As the basis of the system of bunching is accepted the equipment, developed in NIIÉPA for neutron generators [5].

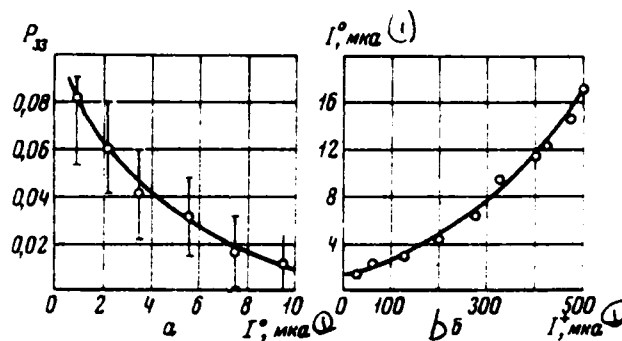


Fig. 2. Dependence of the tensor polarization P_{33} on the current of neutral atoms U^0 (a) and the current of neutral particles U from the current of ion beam (b).

Key: (1) . μA .

(1) Род ионов	(2) Ток пуч- ка, мкА	(3) Энергия пучка, кэВ	(4) Варианты систем ин- дуцированных переходов					
			№ 1		№ 2		№ 3	
			В	Т	В	Т	В	Т
(5) Водород								
H ⁺	4	10	-	-	+1	-	+1	-
H ⁻	0,8	100	-	-	+1	-	+1	-
(6) Дейтерий								
D ⁺	4	14	+1/3	+1	-	-	+1/3	+1
D ⁻	0,8	100	+1/3	+1	-	-	+1/3	+1

Note. C - vector polarization P₃, T - the tensor polarization P₃₃.

Key: (1). Kind of ions. (2). Beam current, μA . (3). Energy of beam, keV. (4). Versions of systems of induced transitions. (5). Hydrogen. (6). Deuterium.

Page 85.

In connection with the special features/peculiarities of the geometry of channel for the injection through the magnet pole of cyclotron and F-M cyclotron, the conditions of bunching of beam and the requirements for the electrostatic mirror for the rotation of beam in the center of accelerator the beam of the polarized ions must have to the rotation an energy of about 100 keV. Before the rotation it

DGC = 30069207

PAGE

~~28~~ 347

brakes to the energy 15 keV, after which is conducted bunching of beam.

At present in the stage of assembly and adjustment is located the mock-up of the source of the polarized particles, on which will be finished all elements of the modifications of standard IPCh.

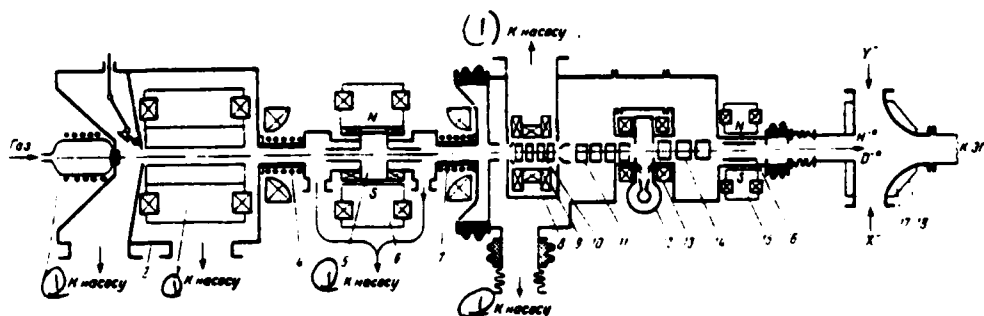


Fig. 3. Schematic diagram IFCa for EGP. 1 - dissociator; 2 - chamber/camera IPCh; 3 - six-pole magnet; 4 - system of the induced transitions in the weak field; 5 - resonator; 6 - magnet; 7 - system of the induced transitions in the weak field; 8 - chamber/camera of ionizer; 9 - magnetic coils; 10 - electrodes of ionizer; 11 - system of electrostatic lenses; 12 - charge-exchange target; 13 - magnetic coils; 14 - unipotential electrostatic lens; 15 - magnet of the filter of wine; 16 - electrodes of the filter of wine; 17 - chamber/camera of the rotary magnet of the injector of negative ions; 18 - rotary magnet of the source of negative ions.

Key: (1). To the pump.

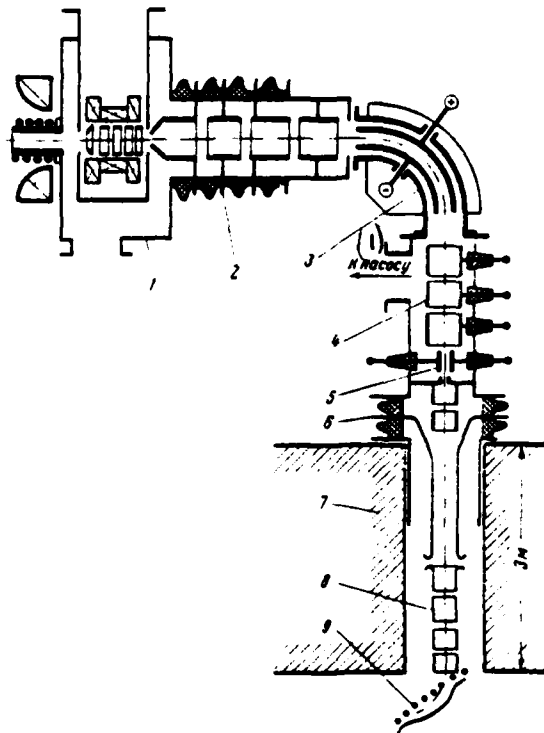


Fig. 4. Schematic diagram of the source of the polarized particles for the cyclic accelerators. 1 - source of the polarized ions; 2 - focusing system; 3 - filter of wine; 4 - focusing system; 5 - plate for the high-frequency divergence of beam; 6 - focusing and accelerating electrostatic system; 7 - framework and magnet pole of accelerator; 8 - braking system and bunching of ion beam; 9 - electrostatic mirror for the rotation of ion beam.

REFERENCES.

1. Ye. K. Zavoyskiy. ZhETF [- Journal of Experimental and Theoretical Physics], 1954, 32, page 408.

2. B. P. Adnyasevich, V. L. Komarov, B. F. Yatsenko. Source of the polarized electrons. Is author's certificate., No 212397. Bulletins of invention and trade signs, 1968, No 9.

3. R. Beurtey. Rapport CEA-E-2366. Saday, 1964.

4. G. A. Vasilev, E. A. Gladkov. Nucl. Instrum. and Methodes, 1968, 58, p 303.

5. M. I. Avramenko. L., Cand. dissert. 1969.

Discussion.

R. Martin. How you did measure the polarization of protons?

V. L. Komarov. The polarization of protons we did not measure. There does not exist the satisfactory methods of measuring the polarization with this low energy, eliminating Stern-Gerlach's method.

G. I. Kir'yanov. Within what limits did change the asymmetry of

DOC = 90069207

PAGE

~~27~~ 351

the distribution of α -particles in the reaction deuterium-tritium
with a change in the polarization of deuterons?

V. L. Kamaev. Asymmetry of the distribution of α -particles
changed to 110/o.

Page 86.

21. The stable operations of the work of the high-voltage accelerating tube.

V. P. Yakushev, A. N. Serbinov.

(Physical-energetic institute, Chelninsk).

The disturbance/breakdown of the nominal voltage distribution according to the electrodes of tube due to the hit on them of the part of the charged particle beam can carry unstable building up character [1], especially with smallest accelerating voltage also in the tubes with the inclined field. The region of stable operation and character of transition into the unstable mode/conditions is conveniently analyzed with the aid of the static volt-ampere characteristics of the separate gaps/intervals with the beam, which compose tube and system of formation. The stability of mode/conditions depends on the form of the general/common/total characteristic of tube and on external characteristic of the oscillator of accelerating voltage.

Without taking into account secondary particles the

characteristics are located directly by the method of the consecutive calculation of gaps/intervals, beginning from the ionic source. As the parameter is taken the current, which crosses the divider of tube from the oscillator of accelerating voltage. The current of divider determines stress/voltage on the first gap/interval, with which are calculated the sizes/dimensions of beam and the part of it, which falls to the output electrode of gap/interval. Current to the electrode is added to the initial current of divider. Summed current flows/occurs/lasts over following resistance and is determined stress/voltage on the second gap/interval. So are calculated all gaps/intervals. As the final result is located the dependence between the stress/voltage on the tube and the current which it consumes from the oscillator, i.e., volt-ampere characteristic. The account of secondary particles will require the series/run of successive approximations.

Fig. 1 gives characteristics for three typical cases: 1 - beam falls to the electrodes, but there are no secondary particles; 2 - beam falls to the electrodes and are caused secondary particles; 3 - beam do not disrupt voltage distribution. Characteristic 3 is absolutely stable; characteristic 1 has unstable regions on the stress/voltage (it is antilogous on the stress/voltage); characteristic 2 has unstable regions on the current and the stress/voltage. Let the characteristic of oscillator correspond to

curved 4 (for example, cascade generator). Then, heaving stress/voltage, abruptly we pass from the point C into the point E, from the nonoperative region into the worker: instantly appears beam at output of tube. Decreasing the stress/voltage, cannot be been dropped/omitted lower than point D (it is the boundary of stable operation) - further follows transition abruptly into point A, into the nonworking region: beam at output of tube disappears. Straight line 5 corresponds to external characteristic of the electrostatic generator whose abrupt transitions are observed for characteristic 2 and are absent for the tube with the characteristic.

For the determination of the currents, which fall to the electrodes, in the approximation/approach of linear fields is convenient the model of bundle in the form of the superposition of the series/row of microcanonical beams [2]. By the selection of a sufficient number of beams it is possible to how conveniently draw nearer design model the real beam. Taking into account the stability it is frequently sufficient two-three beams.

The approximation of real beam by design models is shown in Fig. 2. Experimental points are obtained on the high-frequency ionic source for electrostatic oscillator [3], they show the dependence of the fraction/portion of beam on the angular solution/opening. The beam current 120 μ A, energies of particles it was changed in the

DOC = 80069207

PAGE

355

interval of 2-12 keV.

Change in the optical properties of accelerating system and effect of space charge lead to the distribution of points in certain region, which can be restricted by two limit approximating broken lines, which correspond to two models.

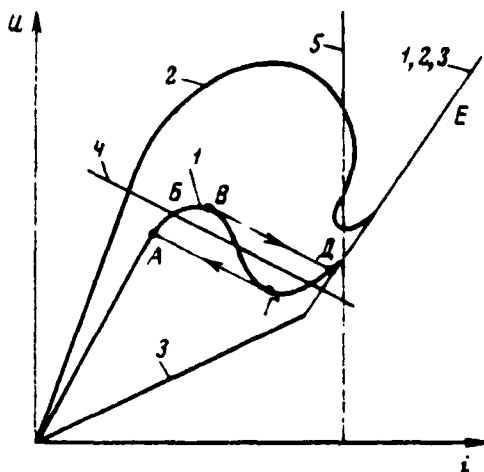


Fig 1.

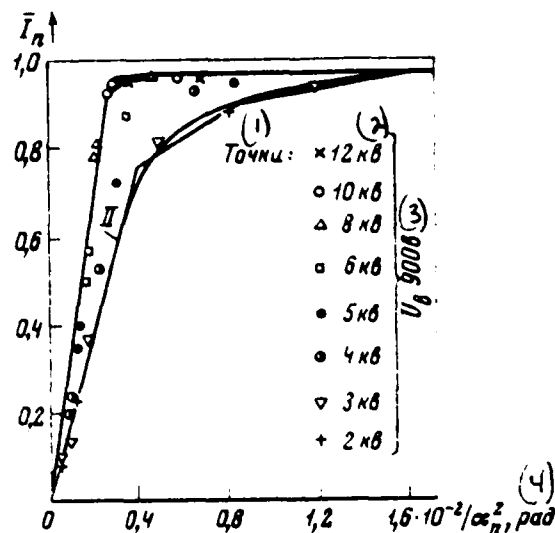


Fig. 2.

Fig. 1. Statistical velt-ampere characteristics of accelerating tubes with beam and analysis of stability.

Fig. 2. Approximation of real beam by design model.

Key: (1). Points. (2). kV. (3). V. (4). rad.

Page 87.

Linear dimensions were taken with the supply on the basis of the size/dimension of the channel of the extraction of ionic source.

With the microcanonical beam it is possible to find simple analytical expression to volt-ampere characteristics for the propagated gap/interval with the uniform field. To such calculated element/cell it is possible to bring together some parts of the real accelerating tube: a) the separate gaps/intervals of the accelerating tube, which consists of the series/row of the accelerating sections, divided by the sections of drift; b) the sections of tube with the uniform field, divided by diaphragms with the reduced passage openings; c) sections to the place of the greatest divergence of beam in the tube with the inclined field, etc. In these all cases is possible the incidence/displacement of the part of the beam to the latter/last electrode of section. Depending on concrete/specific/actual conditions the characteristics are essentially different. If the input energy of particles is strictly proportional to the stress/voltage of section, then only in one case (but most frequently encountering in the real tubes), when beam is not limited to input electrode and the size/dimension of beam in the section of latter/last electrode is much greater the size/dimension of beam in the crossover, equivalent resistance of gap/interval proves to be negative, but characteristic is unstable. The characteristics of sections for different cases are depicted in Fig. 3.

The procedure of calculation of stability limit was checked on a

comparatively complicated tube with the inclined field on the small accelerator on 200 kV. Tube contains 4 accelerating clearances (three of them inclined); the length of the active part of the tube 480 mm, the opening/aperture on the electrodes with a diameter of 20 mm [4, 5]. The design models of bundle were undertaken, according to Fig. 2. Optimistic estimation gave the values of 49 kV, pessimistic of 109 kV. The experimental value of 75 kV is located between these values. Were determined stability limits with respect to the individual parts of the tube: the entrance of tube, the second electrodes of the first and second accelerating gap; as a result were obtained values of 67; 68 and 115 kV respectively. Is most close to the total calculation the third case, because in the region of this electrode beam has maximum size. This section of tube actually defines the boundaries of stability for the entire tube. The simultaneous incidence/incingement of beam other electrodes is manifested little.

The diagram of auto-focusing [6] (particles enter into tube with the energy, which corresponds to a voltage drop across high-impedance resistance from the course of the current of divider) is very convenient, especially for the tubes with the inclined field. However, it can become the reason for instability with the smallest operating stresses/voltages when the part of the beam will fall to the input electrode of tube. This instability can be removed, if instead of resistance to use servo rectifier [7] whose exit

stress/voltage varies in proportion to the current of divider and virtually it does not depend on the current, which falls to the input electrode of tube.

The volt-amperes characteristics of tubes with the beam for the accelerators EG-1 and EG-2.5 are shown in Fig. 4. Both tubes with the inclined poor; ionic sources and entrances into the tube identical. Accelerator EG-1 works with resistance, while accelerator EG-2.5 - with the servo rectifier and with the limiting diaphragm at the entrance of tube, which does not make it possible for beam to fall to the electrodes of tube. On the accelerator EG-1 with the stress/voltage of approximately 1 keV and below operating mode becomes unstable: beam first appears at the output of tube, then it disappears, which is accompanied by the spontaneous kicks of stress/voltage on the accelerator. On the accelerator EG-2.5 the beam remains stable and well focused up to the smallest stresses/voltages (200 kV); however, the current strength, beginning with 900 keV, decreases.

The disturbance/breakdown of stability in the usual accelerating tubes is connected with the defocusing of beam, and in the tubes with the inclined field with the defocusing and especially with the mixing of beam, so that it cannot traverse the tube. Therefore in the tubes with the inclined field the phenomena of instability become apparent much more strongly, especially with the considerable divergences of trajectory from the normal.

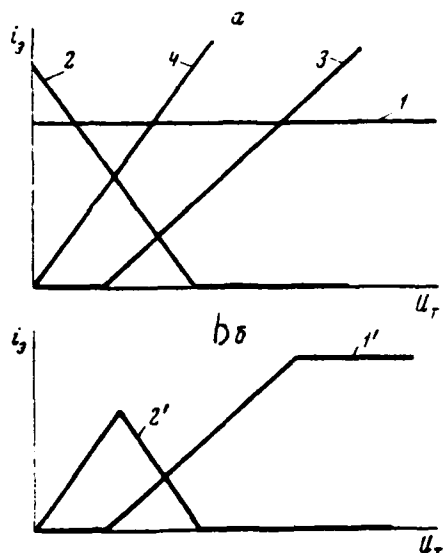


Fig. 3.

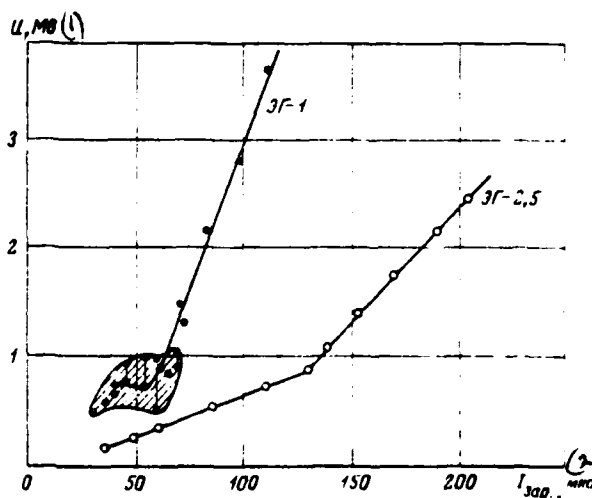


Fig. 4.

Fig. 3. Volt-ampere characteristics of sections with uniform field. 1 - the size/dimension of beam in the region of output electrode is close to size of crossover; 2 - size/dimension of beam much more than the size/dimension of crossover; 3 and 4 - the same, but beam is limited to the input diaphragm (a); 1', 2' - the same, but beam begins to be limited to the input diaphragm when stress/voltage is lower than the specific value (b).

Fig. 4. Diagrams of stability of tubes of accelerators EG-1 and EG-2.5.

Key: (1). mV. (2). μ A.

Page 88.

REFERENCES.

1. V. P. Rkusev, A. N. Serbinov. PTE, 1970, No 1.
2. I. M. Kapchinskiy. particle dynamics in the linear resonance accelerators. M., Atomsizdat, 1966.
3. V. a. of novels, A. N. Serbinov. PTE, 1963, No 1, page 27.
4. A. N. Serbinov et al. PTE (in the press/printing).
5. A. N. Serbinov, V. P. Yakushev. Are author's. certificate, No 246713. Bulletins of inventions. and trade signs, 1969, No 21, page 67.
6. A. V. Almazov, F. P. Myitsev. PTE, 1964, No 5, page 43.
7. A. N. Serbinov, V. P. Yakushev, V. A. Nikitin. PTE, 1969, No 6, page 211.

22. Ion gun with the high brightness of beam.

N. N. Kutorg, V. S. Sevcst'yanova, V. A. Teplyakov.

(Institute of high-energy physics).

The theoretical and experimental study of axially symmetrical beam [1, 2] made it possible to calculate and to design the ion gun with the high brightness of beam, employed by injector into the accelerator with the focusing high-frequency by field [3]. During the development of gun special attention is given to simplification in its construction/design, to increase in reliability and time of failure-free operation, to a reduction in the required power.

In order to decrease the dependence of the maximum parameters of beam on any kind of the errors in the geometry of gun, it was decided to form/shape beam by that by weakly diverging. This means that the given perveance of gun must not be more than 0.015 [1]

$$p = \frac{1}{2\pi e \sqrt{2 \frac{e}{m}}} \frac{I}{U^{3/2}} \left(1 + \sqrt{2} \frac{I_2}{I} + \sqrt{3} \frac{I_3}{I} \right), \quad (1)$$

$$\frac{1}{2\pi e \sqrt{2 \frac{e}{m}}} = 1.3 \cdot 10^6,$$

where I - current of the proton component of beam; I_2, I_3 - ion

currents H_2^+ and H_3^+ respectively; U - stress/voltage of gun.

The normalized emittance of beam the less, the less the radius of plasma boundary in the expander of source [2]

$$\epsilon = 2R_k \sqrt{\frac{2T_e}{Mc^2}} \approx 2 \cdot 10^{-4} R_k, \quad (2)$$

where R_k - radius of plasma boundary, T_e - temperature of ions on plasma boundary, eV.

The perveance of the gun or pier, which forms the beam of a permanent radius, is equal to

$$P = \frac{2}{9} \frac{R_g^2}{d^2}, \quad (3)$$

where R_g - radius of beam at output from the gun; d - distance between the plasma boundary and the puller electrode. Therefore the prescribed/assigned current or energy of protons at the output of gun completely determine its geometry.

According to the conditions of injection into the initial part of the accelerator the energy of injection must be not less than 100 keV, the current of proton beam - not less than 200 mA, and the emittance of beam - is not more than 10^{-4} rad cm. The crossover of the bundle with a diameter of 1 cm must be located in the first clearance of accelerator. The gun, which satisfies the stated requirements, now works.

In this gun of ionic the source of the type of von Ardenne's duoplasmatron [4] works in the mode/conditions of nonindependent arc discharge. Arc current is limited and stabilized by the emission of tantalum cathode. The source of arc voltage 200 V has negligible internal impedance, so that the arc easily it would be ignited, and dynode of source during the discharge was found under the floating potential, potential 100 V is supplied to dynode through the diode.

Gas inlet into the source is accomplished/realized by the diamagnetic pulse valve, analogous in the operating principle described in [5].

Accelerating voltage on the source is supplied from the small peak transformer. Its high-voltage winding is performed by dual lead/duct, which allows to conduct network power to the power supply units of ionic source without the supplementary insulating transformer.

Beam focusing is accomplished/realized by a pulse short magnetic lens with the maximum magnetic field. Vacuum $2 \cdot 10^{-7}$ torr is created in the gun with the aid of the orbitron of special construction/design. Orbitron is simple structurally/constructurally and consumes power on the order of 300 W at average/mean pumping speed to 3000 l/s with 10^{-5} torr. The resource/lifetime of its work

is approximately 800 hours.

Entire/all electronics of gun is made on the semiconductors and has high reliability with prolonged continuous operation.

The described source with the pulse gas inlet and with entire electronics of supply and control already two years is in operation on preinjector I-100 and IFVE. Operating experience showed that the time of the reliable work of the cathode of source is not less than 1000 hour, electronics - not less than 5000 hour, valve - it is more than 10^6 impulses/moments/pulses.

Figure gives the construction/design of the ion gun, which has the following parameters of beam: energy of ions 100 keV; the current of proton beam 200 mA; the maximum perveance of gun 0.016; the emittance of beam $0.06 \cdot 10^{-3}$ rad cm; the crossover of bundle is located at a distance of 8 cm from the focusing lens.

Page 89.

The current of gun in the range 0-200 mA is smoothly regulated by a change in the cathode glow. The duration of current pulse 10 μ s with the fronts is not more than 2 μ s. The stability of the apex/vertex of pulse is not worse than $\pm 50\%$.

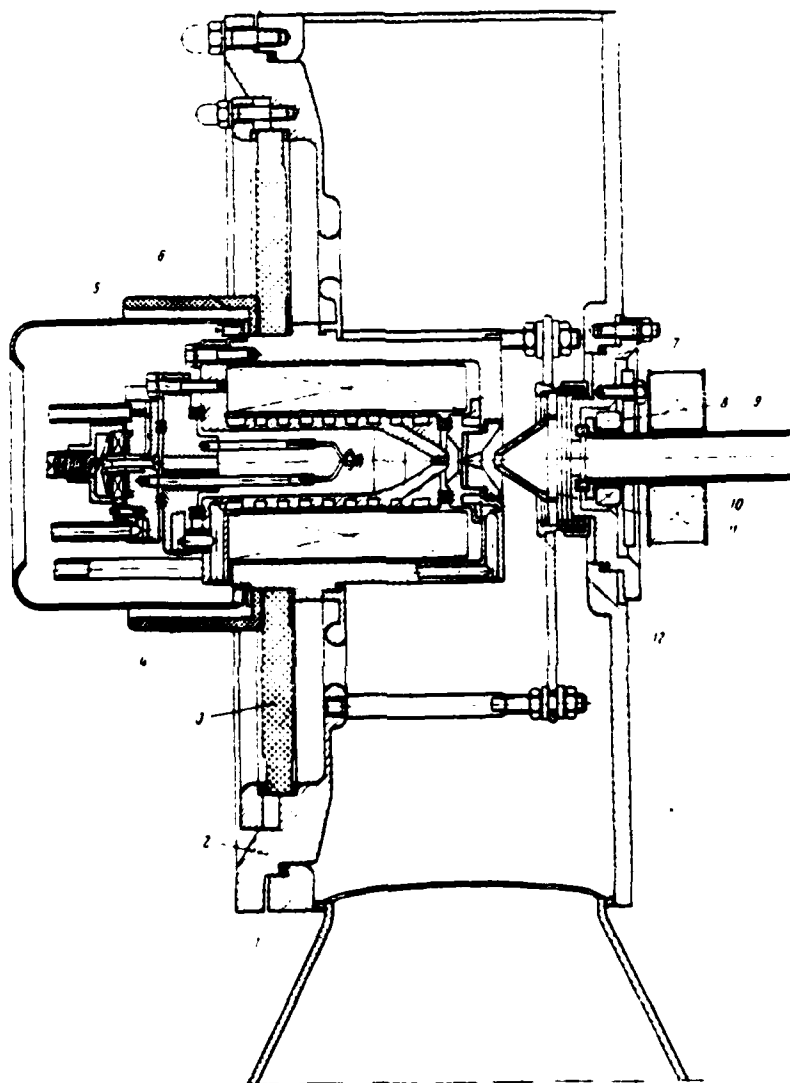


Fig. the construction/design of ion gun. 1 - vacuum container; 2 - ring of insulator; 3 - ceramic insulator; 4 - insulator from the fiberglass; 5 - screen of source; 6 - ionic source; 7 - flange of ion guide; 8 - induction current-sensing device; 9 - ion guide; 10 -

magnetic lens; 11 - puller electrode; 12 - expander of source.

REFERENCES.

1. V. A. of over-all housings. PTE, 1968, No 6, page 13.
 2. V. I. Derbilov, V. A. Teplyakov. PTE, 1969, No 1, page 21.
 3. I. M. Kapchinskiy, A. P. Maltsev, V. A. Teplyakov. On the project of the linear accelerator of protons from the lowered/reduced by energy injection and high intensity of beam. Reports on UP of international conference on the charged particle accelerators. Yerevan, 1969.
 4. M. Ardenne. Tabellen der Elektronenphysik, Ionenphysik, und Ultramikroskopie, Bd. 1, 2, Berlin, 1956.
 5. J. Marshall. In coll. "physics of hot plasma and thermonuclear fusions". M., Atomsizdat, 1959, page 290.
- Discussion.
- Yu. D. Beznogikh. was involved source to the duration of operating pulse of more than 10 μ s?

V. A. Teplyakov. Source on the preinjector works with the duration of pulse 40 μ s. Source in the preliminary experiments worked in the continuous duty; therefore from the point of view of thermal loads it can work with any pulse duration. Source with the pulse gas inlet can work by impulses/moments/pulses with the duration up to several ten microseconds.

G. I. Kir'yanov. 1. What form valve was used in gun? 2. Did investigate you composition of ion beam?

V. A. Teplyakov. Source works with diaphragm type valves in dosing volume 6-10 mm³. The dosing volume, filled with hydrogen with 2-3 atm., is connected with the source to the period of order of tens of microseconds. 2. Yes, mass composition of beam is known. With an increase in the arc current the share of proton component grows/rises. Two hundred milliamperes of proton current in focused beam at output of ion guide are obtained with 260 mA of total current from the gun.

Page 90.

23. Electron gun with the cold-emission cathode.

G. G. O. Meskhya, B. N. Yanickov.

(Physical institute im. P. N. Lebedev of the AS USSR).

The successes, achieved in recent years in the field of the generation of powerful/thick electron beams by the nanosecond of duration, make it possible to hope for the possibility of further use of such beams in the accelerative technology. However, the obtained now beams have the poor monochromaticity, one of reasons for which is the poor agreement of the oscillator of nanosecond impulses/momenta/pulses and electron gun. Furthermore, very construction/design of electron gun exerts a substantial influence on the high-voltage impulse/momenta/pulse, supplied to the field emission cathode.

Fig. 1 gives the equivalent schematic of the guns, utilized at present [1, 2]. From the diagram it is evident that already very construction/design of the high-voltage insulator of gun must be selected in such a way that the distortion of the

impulse/momentum/pulse of nanosecond duration would be minimum. On the other hand, the requirement of more uniform potential distribution along the insulator creates definite difficulties in satisfaction of preceding condition.

Actually/really, it is known that a potential drop in the first section from the high-voltage end/lead of the insulator is determined by the self-capacitance of section C and by capacity/capacitance to the earth C_0 [3]

$$\Delta V_1 = \left(\sqrt{\frac{C_0}{C}} - \frac{C_0}{2C} \right) V_0,$$

where V_0 - the total voltage, supplied to the insulator.

Ideal ones in the sense of agreement should be counted the case when $C_0 \approx C_{nos}$ - linear capacity/capacitance of the supplying line. However, the technical realization of this condition is in practice unrealizable in the construction/design of the guns, utilized at present.

Use in the accelerators of the type in question as the insulating medium of dielectric with large ϵ significantly decreases the dimensions of setting up. But use in the accelerators with this filling of gun examined above becomes generally impossible due to a sharp increase of capacitance to the earth C_0 .

In developed in our laboratory accelerator ESU-1 (stress/voltage 2-3 MV, current 30 kV) as the insulating medium is utilized the glycerin - liquid dielectric with $\epsilon \approx 40$. The construction/design of gun for this accelerator, shown in Fig. 2, makes it possible to avoid the difficulties about which it was mentioned above.

High-voltage insulator is made in the form of the matched vacuumtight transition from the coaxial line, filled with glycerin, to the vacuum coaxial line. The angles of the generatrices of insulator and radial deflection terminal to the axis/axle of accelerator are selected by such that the ratio of the linear inductance L_1 to the linear capacitor C_1 in the section with the insulator would be equal to the relation of these values in the supplying coaxial line. The presence in construction/design of diaphragming ring 3 and supporting disk 4 makes it possible by the appropriate selection of their form to attain virtually uniform potential distribution along the insulator.

The study of the construction/design of insulator in the electrolytic bath confirmed the correctness of the selected construction/design. Fig. 3 depicts the pictures of electric field with the various forms of the diaphragming ring and supporting disk.

The presence in system of dielectric with large ϵ and c by sufficiently high conductivity made it possible to avoid the partitioning of insulator and to simplify technology of production.

The length of insulator over surface of ~ 30 of cm was selected by such form, in order to the maximum gradient of electric field on the vacuum side, as by least durable to the electrical breakdown, it did not exceed 100 kV/cm.

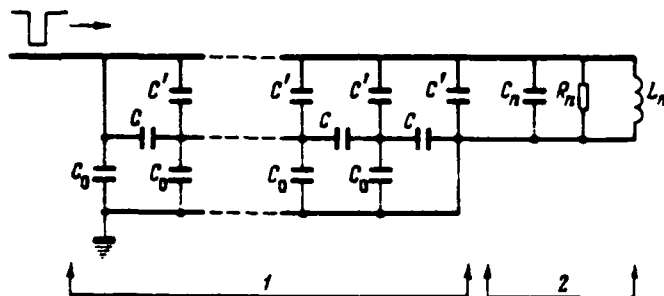


Fig. 1. Equivalent schematic of gun. C - capacitance of the unit of the length of insulator; C_0 , C' - capacitance of the unit of the length of insulator to the earth and to the high-voltage electrode respectively, C_n , R_n , L_n - the components of the impedance of gun.

Page 91.

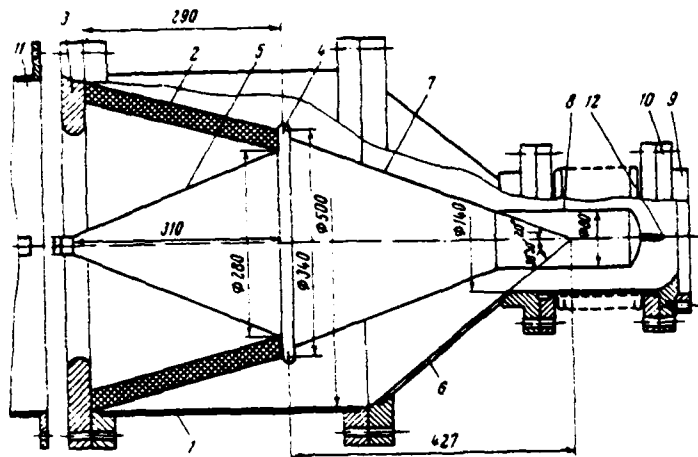


Fig 2. Schematic of gun. 1 - external screen; 2 - high-voltage insulator; 3 - diaphragming ring; 4 - supporting disk; 5 - sleeve; 6 - external cone; 7 - female cone; 8 - cathode holder; 9 - anode; 10 - anode holder; 11 - supplying line; 12 - cathode.

AD-A089 303

FOREIGN TECHNOLOGY DIV WRIGHT-PATTERSON AFB OH F/G 20/7
TRANSACTIONS OF THE ALL-UNION CONFERENCE (2ND) ON CHARGED PARTI--ETC(U)
JUL 80 A L MINTS, A A KOMAR, A A VASIL'YEV

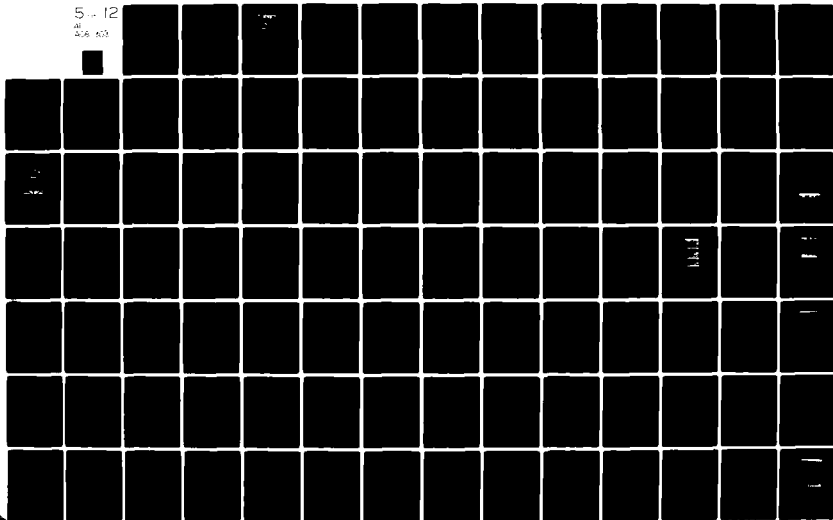
UNCLASSIFIED

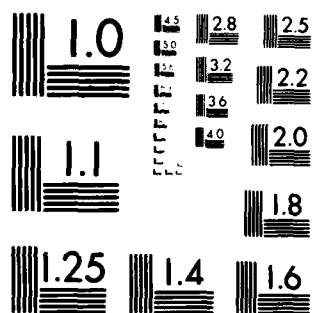
FTD-ID(RS)T-0692-80

NL

5-12

AD
208 503





MICROCOPY RESOLUTION TEST CHART
NATIONAL BUREAU OF STANDARDS 1963 A

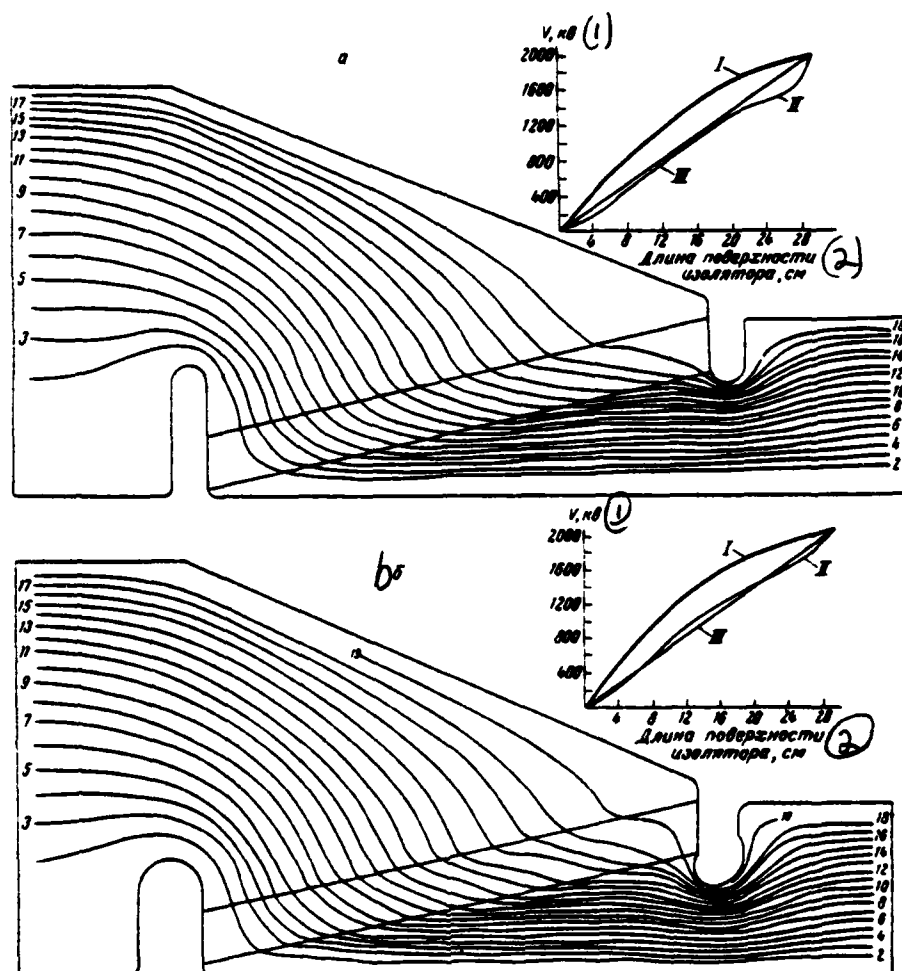


fig 3. Pictures of electric field with the various forms of diaphragm ring and supports of disk. I - over the surface of insulator in the glycerin; II - over the surface of insulator in the vacuum; III - even distribution.

Key: (1). kV. (2). Length of surface of insulator, cm.

Page 92.

The construction/design strictly of electron gun allows for the possibility of the control of an anode-cathode distance and change in the number of tungsten needles - autoemission cathodes. This will make it possible to attain maximally possible by this method of agreeing the oscillator of high-voltage pulses and load whose role performs electron gun.

For the experimental functional test of the described construction/design of gun is prepared the model into 1/3 full sizes (Fig. 4). The investigations, carried out on this model, confirmed the correctness of the selected construction/design and its efficiency.

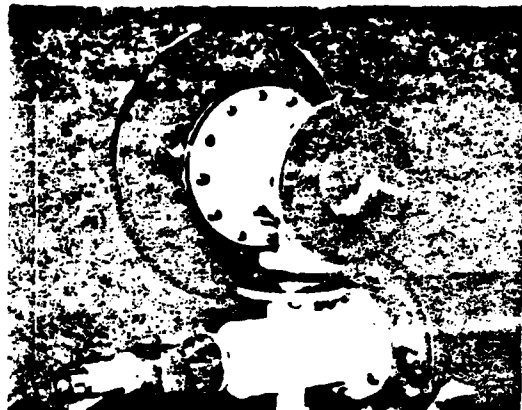


Fig 4. The appearance of the model of electron gun.

REFERENCES.

1. S. E. Graybill, S. V. Nablo. IEEE Trans. Nucl. Sci., 1967, NS-14, N 3, 782.
2. T. H. Martin. IEEE Trans. Nucl. Sci., 1969, NS-16, N 3.
3. K. A. Krug. Bases of electrical engineering, Vol. 2. Gosenergoizdat, 1932.

24. Electron gun for obtaining the intense electron beams.

V. M. Levin, V. V. Rumyantsev, K. E. Rybas, E. N. Telepaev.

(Scientific research institute of the electrophysical equipment in L. V. Efremov).

In recent years grew considerably the necessity for the intense electron beams (with current on the order of 1 kA in the impulse/momentum/pulse with the perveance $10 \cdot 10^{-6}$ a/b^{3/2}) for the accelerative, thermonuclear and other areas of technology. For obtaining the intense electron beams it is utilized the plasma of spark discharge [1], autoelectronic cathodes [2, 3] and thermoelectronic cathodes [4, 5].

To the electron beams, obtained from the plasma of spark discharge, is characteristic the considerable instability of amplitude of current. The electron beams, obtained with the use/application of autoelectronic cathodes, are also characterized by a comparatively high instability of the amplitude of current (15-20%/o) and by the large divergence of beam (more than 2.2 it erased), caused by the sharp heterogeneity of electric field in point

[6]. Appear large complexities with the focusing of the nonhomocentric electron beam, obtained during the use of a cathode with many points.

The electron beams, obtained from the thermionic cathode, with reasonably selected optics are characterized by the high stability of current and low transverse components of the speed of electrons - order of thermal ones. Usual optics of pier makes it possible to obtain electron beams with the perveance not more $3 \cdot 10^{-6} \text{ a/b}^{3/2}$ [7]. If opening/aperture in the anode is tightened by grid or is supplied intermediate grid electrode, the possibilities of these guns substantially will increase. In the three-electrode, to gun grid unconditionally it will unconditional work in the more light duty than the mesh anode, but the conduct of third electrode complicates the construction/design of gun and makes the angular characteristics worse of beam.

The circular electron guns of pier [8] and magnetron guns [9] provide obtaining, electron beams with the perveance it is more $10 \cdot 10^{-6} \text{ a/b}^{3/2}$, but they possess the known deficiencies/lacks, which impede their use/application in the accelerative technology. Now to us it is considered by most advisable to utilize guns of pier with the recticular anode. But at the current density in the plane of grid 100 A/cm, stresses/voltages 300 kV, duration of pulse 100 ns and

frequencies of messages 5 1/s surface/skin layer turned to the cathode, toward the end of the impulse/momentum/pulse is heated to the temperature, close to the melting point of tungsten; this superimposes one of the basic limitations on the possibility of gun.

Working conditions of thermionic cathodes in the guns, intended for the use in such electrophysical installations as the accelerators, very heavy. In connection with this to the cathode is presented the series/row of the specific requirements: 1) cathode must region by the stable emission of more than 50 A/cm² at a pressure of residual gas $5 \cdot 10^{-6}$ torr and operating stress/voltage 100 kV; 2) the emissive power of cathode must not deteriorate with a short-term increase in the pressure to $5 \cdot 10^{-6}$ torr; 3) the emissive power of cathode must not substantially decrease after the repeated stay of cold cathode in the atmosphere air. Operating temperature of cathode must not exceed $\sim 1000^{\circ}\text{C}$, since otherwise with the large sizes/dimensions of cathode it is difficult to attain the identical temperature of the surface of cathode, i.e., the uniform density of emission. Furthermore, high operating temperature and connected with this high expenditure of power complicate the construction/design of gun and is decreased its reliability.

Page 93.

From the cathodes used on the emissive power and the resistance to poisoning only cathode from hexaboride of lanthanum satisfies to that indicated) to requirements, but for obtaining the large current density (it is above 50 A/cm^2) these cathodes it is necessary to heat to temperature of 1700°C [5].

In NIIEFA it was developed the pressed porous oxide-nickel cathode with a diameter of 50 mm with the spherical emitting surface, which satisfies all requirements indicated above.

Fig. 1 gives the curves of the dependence of the current density of emission on the pressure of residual gas with the anode voltage, equal to 100 kV, and different temperatures of cathode.

From curves 1-3 evident that with an increase in the pressure the emission current at first decreases, reaching minimum value at a pressure $8 \cdot 10^{-6}$ - $1.5 \cdot 10^{-5}$ torus, and then it increases, almost reaching its initial value at a pressure $1 \cdot 10^{-4}$ torus. At a temperature of cathode of 2930°C emission current does not depend on

the pressure of residual gas in the measured interval of pressures ($1.5 \cdot 10^{-6}$ - $4 \cdot 10^{-6}$ torus). At a temperature of 2970°C current density of emission in the mode/conditions of space charge is 110 A/cm^2 . After the quintuple stay of cathode in the atmosphere of air of the noticeable decrease of emission it was not observed.

Were developed two versions of electron gun with the pressed porous oxide-nickel cathode. In both versions is used the high-wave glass insulator, designed for the stress/voltage 350 kV. The first version of gun, depicted in Fig. 2, has an insulator with a length of 150 mm and is intended for the work in oil. The second version has an insulator with a length of 345 mm and is intended for the work in the air. Electron gun can work both in the vertical and in the horizontal positions. In the horizontal position in the second version of gun the divergence of cathode node/unit from the axis/axle, during the heating to operating temperature, does not exceed 0.3 mm. The construction/design of cathode node/unit makes it possible to regulate the position of cathode on the focusing electrode and to perform full/total/complete dismantling and assembly of cathode unit.

Degassing and activation of cathode is conducted after the assembly of gun on the special bench or in the accelerator at a pressure of residual gas not more $5 \cdot 10^{-6}$ torus during 10 hour.

The power, necessary for heating of cathode to operating temperature of 970°C , comprises only 500 W, i.e., the effectiveness of cathode on the intense heat comprises 1-2 A/W. Cathode has identical temperature all over surface in limits of accuracy of measurement, provided by a pyrometer of the type OPPIA-017 ($\pm 10^{\circ}\text{C}$).

The investigations of divergence of beam with the current 200a were conducted with the aid of the fluorescing screen by the voltage on the cathode of gun relative to the anode 100 kV. The crossover of bundle is located at a distance of 45 mm from the grid of the anode. Diameter of beam in the crossover 28-32 mm. The perveance of beam in this experiment comprises $6.3 \cdot 10^{-6} \text{ A/V}^{3/2}$. Based on this perveance, is possible to expect that with the voltage 300 kV from this gun can be obtained beam current about 1000a in the impulse/momentum/pulse.

By the decrease of distance cathode - the anode and by a change in the curvature of the grid of anode electrode the perveance of beam was increased of $11 \cdot 10^{-6} \text{ A/V}^{3/2}$ and with the voltage 200 kV was obtained the current in the beam, equal to 1000a. The measurement of the diameter of beam in the crossover in this experiment was not made.

The results of the conducted investigations make it possible to make a conclusion about the possibility of producing the stably

working thermionic cathodes in diameter to 100 mm, with the current density of emission to 100 A/cm² and the full current to 8000a. On the basis of such cathodes is real the production of two-electrode electron guns with the mesh anode to the currents to 4000a (for the duration of pulse on the order of 0.1 μ s, of periodicity of order $2 \cdot 10^{-4}$, with the voltage 200-300 kV) and the three-electrode guns to the currents to 7000-8000a.

The authors note the participation of A. K. Dezhnev and G. N. Karimov in the design development of electron gun and are expressed appreciation to G. P. Shelkuncov for valuable advice and P. M. Zheltova for the participation in the experiments.

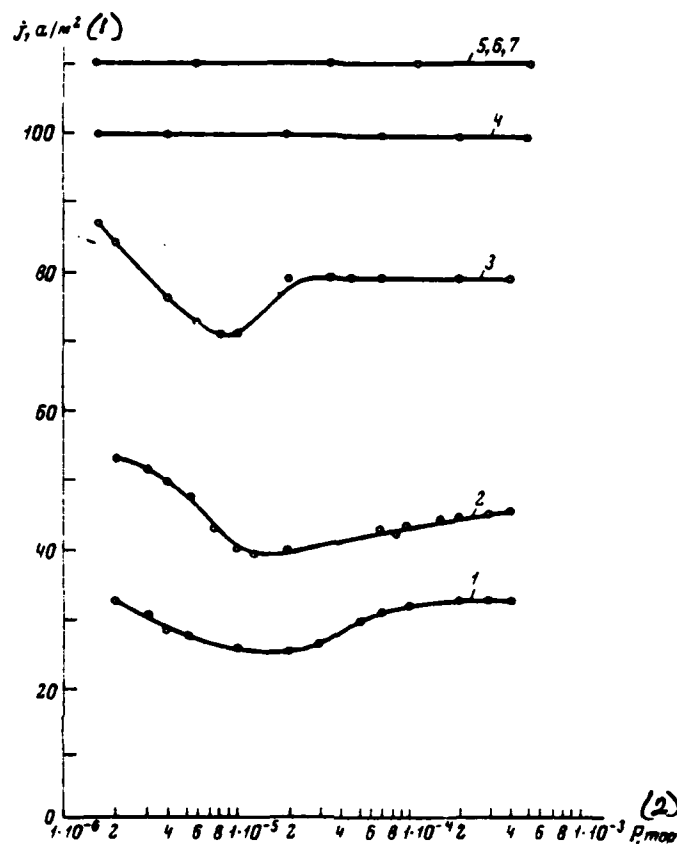


Fig. 1. Dependence of the pulse current density of emission on the pressure of residual gas for different temperatures of the pressed porous oxide-nickel cathode with the anode voltage 100 kV. 1 - 830°C; 2 - 870°C; 3 - 900°C; 4 - 930°C; 5 - 970°C; 6 - 1010°C; 7 - 1055°C.

Key: (1) - A/m^2 . (2) - t_{crus} .

Page 94.

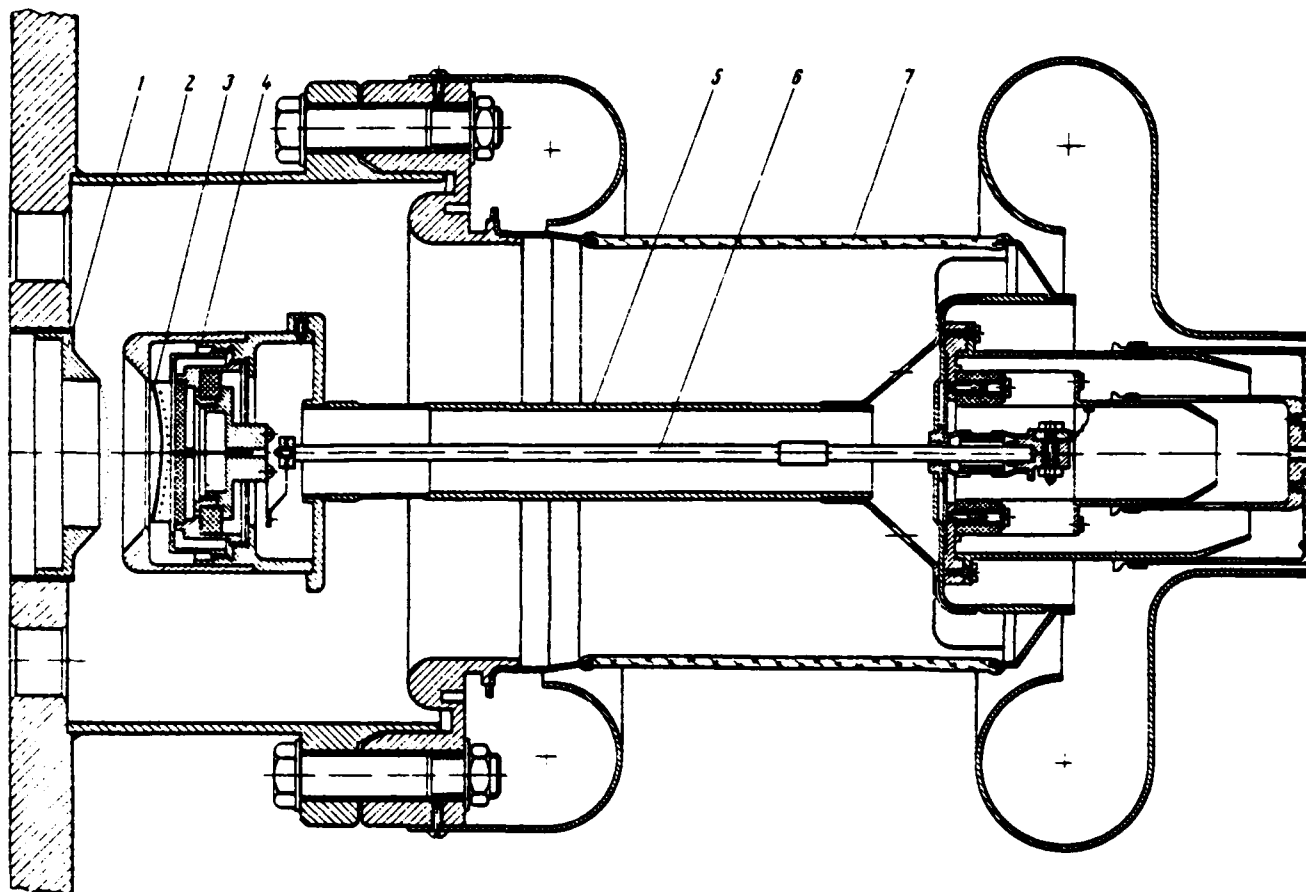


Fig. 2. General view of electron gun. 1 - anode; 2 - anode branch pipe; 3 - cathode; 4 - focusing electrode; 5 - cathode stock/rod; 6 - conductor; 7 - high-voltage glass insulator.

REFERENCES

1. I. V. Kozhukhov et al. FTE, 1966, No 1, page 139.
2. R. I. Garber et al. FTE, No 1, page 196.
3. I. D. Ventova et al. Report on XIV All-Union conf in emissive electronics, 11-16 May, 1970, Tashkent.
4. Jack W. Beal, N. C. Christofilos, R. E. Hester. IEEE Trans. on Nucl. Sci., 1969, NS-16, N 3.
5. V. I. Perevodchikov et al. Ukrainian republic conf on electr. optics and its uses/applications, dedicated to a 100-year-anniversary from the birthday of V. I. Lenin, 22-26 September, 1969.
6. V. N. Shrednik, E. N. Popov. Report on XIV All-Union conf in emissive electronics, 11-16 May, 1970 Tashkent.
7. I. V. Alyamovskiy. Electron beams and electron guns. M., "Soviet radio", 1963.
8. Ye. G. Todd, T. E. Bryuer, N. B. Cramer. The 4th international congress for instruments SVCh. Shvenigen, Holland, 3-7 November, 1962.

9. A. Kh. Beck, Kh. L. Natrass. Sverigen, Holland, SVCh, 3-7 November, 1962.

Discussion.

M. V. Karpov. Which service life of your gun?

K. P. Rybas. The service life of gun, determined by the service life of cathode, is 300 hours. During this time the filament emission descends to 300/c.

Ye. Regenshtreyf. It was utilized flowing your calculations the theory of laminar or unilaminar flows?

K. P. Rybas. In our calculations was utilized the theory of laminar flows. Experimental data coincide sufficiently well with the calculated ones.

V. G. Bagramov. Was removed/taken the dependence of the current density of emission on the pulse duration? Which the pulse duration in your case?

K. P. Rybas. The dependence of the current density of emission on the pulse duration was not studied. The pulse duration in cur

experiments was 100 ns.

V. I. Perevodchikov. was studied the volatility of the material of cathode and the effect of vaporization products on dielectric strength of gap.

K. P. Rybas. The speed of vaporization of the material of cathode was not investigated. The decreases of dielectric strength of gap/interval cathode-arcs during the work of gun was not observed.

Page 95.

V. F. Gass. Is required the making more active of cathode after the allowance of the atmosphere?

K. P. Rybas. The making more active of cathode after the allowance of the atmosphere is necessary. It should be noted that after the first allowance of the atmosphere the emissive power of cathode grows/rises by 5-100%.

V. I. Perevodchikov. How is determined the service life of cathode?

K. P. Rybas. The service life of cathode is determined by

DOC = 80069208

PAGE 389

decrease with the time of the recovery rate of free alkali-earth metals from their oxide, as a result of which decreases the emissive power of cathode.

25. High-current electronic pulse direct voltage accelerator.

L. N. Kazanskiy, A. A. Kicimenskiy, G. O. Meskhy B. N. Yablokov.

(Physical institute im. P. N. Lebedev of the AS USSR).

In recent years is vigorously developed the new scientific direction, connected with obtaining and using pulse electron beams [1, 2]. They will find use in many regions of physics, chemistry, biology and different applied regions. During the development of electronic high-current accelerator in FIAN we had in mind pursuance of research on physics of intense relativistic electron beams in the vacuum and media, and also the acceleration of ions due to the collective interaction with the intense electron beams.

The requirements for the parameters of electron beam, determined by the intended targets, not the same, and at the development of electronic high-current accelerator (ESU-1) we decided to dwell on the average parameters: energy of electrons 2-3 MeV, current 30-50 kA, the duration of pulse ~30-50 ns. In this case was taken into consideration the almost full/total/complete absence of experiment of the construction of similar installations and the extreme deficiency of effective areas. After the detailed examination of possible

diagrams ESU we stopped at the electronic high-current accelerator with coaxial type dual formulating line, filled with dielectric with the high dielectric permeability. Line is charged by resonance form by surge generator (GIN) for the time of order $5 \cdot 10^{-7}$ s and is commutated by the single-gap multi-spark discharger which works in the compressed gas. At the output of the dual forming line (DFL) is connected the transforming line (TL) with the transformation ratio ~ 1.5 , loaded to field emission type electron gun (Fig. 1).

Selection as the filler of the line of dielectric with high value ϵ was determined by the following considerations:

1. The power which can be removed/taken from the line

$$P \sim E^2 \sqrt{\epsilon}.$$

Since the maximum permissible strengths of field in all liquid dielectrics at our range of the duration of charge are approximately/exemplarily identical and lie/rest in the region 200-300 kV/cm, the use/application of dielectrics with high value ϵ makes it possible to obtain from the same volume several times large power.

2. Use/application of dielectrics with large ϵ makes it possible to sharply reduce length of installation, which in our case has high value.

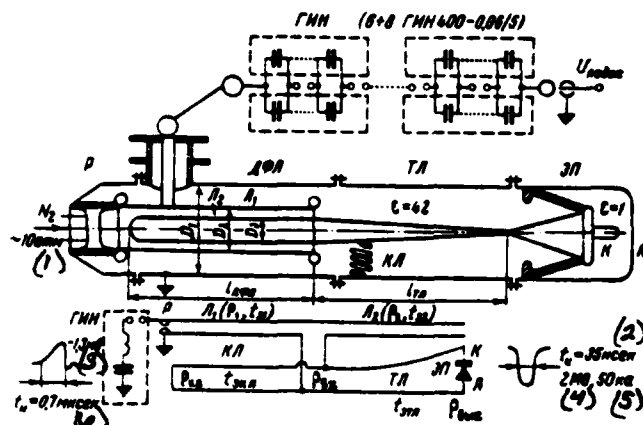
3. Use/application of dielectrics with large ϵ makes it possible to utilize transforming line of small length and to lower charging voltage DFL.

After the careful study of the high-frequency properties of different dielectrics (water, alcohols, different types of glycerin) we stopped at the technical glycerin as having sufficiently good frequency properties over a wide range of frequencies and ensuring the acceptable shape of pulse.

The selection of coaxial construction/design of DFL was determined by the fact that in contrast to the track construction/design, in it is provided the full/total/complete screening of fields by the grounded external electrode, edge effects in it are substantially less and the agreement of all elements/cells of accelerator to more easily fulfill. However, coaxial geometry has a number of deficiencies/lacks. The shape of the pulse of voltage, generated by DFL, has ideal form, if wave impedance of both lines is equal. However, in this case maximum electric intensities in the lines prove to be substantially dissimilar

$$\frac{E_{\max}}{E_{\min}} = \frac{R_{\min}}{R_{\max}} = \exp\left(-\frac{2\sqrt{\epsilon}}{60}\right),$$

where R_{\min} and R_{\max} - radii of internal and average of electrodes,
 $z = z_{\max} = z_{\min}$ - line characteristic.



Key: (1). atm. (2). ns. (3). mV. (4). MV. (5). kA. (6). μ s.

Page 96.

With different impedances of lines the impulse/momentum/pulse will be accompanied by the sequence of spurious pulses (Fig. 2). The amplitude of these spurious pulses with the commutation of domestic circuit $u_n = u \left(\frac{2Z_n - Z_{\text{imp}}}{2Z_n + Z_{\text{imp}}} \right)^n$, where u - voltage of main impulse. In the case of equal maximum intensities/strength in the lines the relation of the wave impedance

$$I_{\text{он}}/I_{\text{нар}} = \exp\left(\frac{U}{ER_{\text{он}}}\right),$$

where u - voltage on the line; E - maximal strength of field and R_{em} - radius of internal electrode.

The case of the equal impedance of lines and the case of equal intensities/strength limit the region in which should be selected the geometric parameters of the dual forming lines (Fig. 3). The parameters of installation of ESU-4 and its model ESU-0 (see below) are given in the table. Charge is accomplished/realized by a resonance form from surge generator. Use in DFL of polar dielectric with the small specific impedance ρ leads to the need for taking into consideration of loss in the dielectric in the process of charge. If we restrict the energy losses ten times by percentages of the energy, stored up into GIN, then the minimum frequency of charge

$f \geq 4.16 \cdot 10^{13} / \epsilon \rho$. For glycerin $\epsilon \approx 40$, $\rho \approx 1.5 \cdot 10^8$ Ω/cm and $f_{\text{min}} \approx 0.7$ MHz. In our case for the charge of DFL proved to be convenient to utilize 6-8 standard GINs Serpukhov condenser/capacitor plant GIN-40C-0.06/5 with the impact stress 400 kV and impact capacitance 12 nF, connected into two parallel columns on three or four consecutively/serially. As showed experiments, multiple operation of GINs it is possible to attain, connecting; the in parallel each step/stage of each of GIN. Structurally/constructurally this is performed with the aid of the single column, in which are assembled all gaps, which work in the atmosphere of nitrogen at a pressure 3 atm.

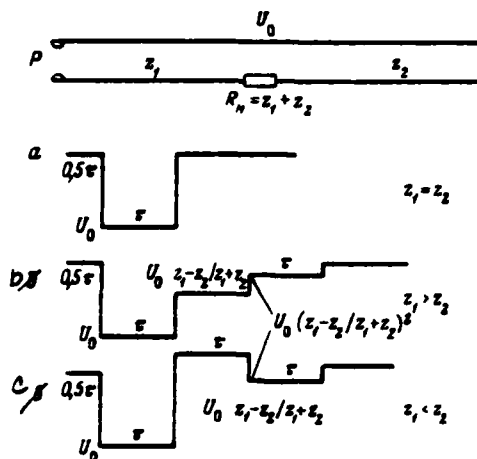


Fig. 2. Impulse shaping in the dual forming line with different relationships/ratios of the wave impedance of its lines.

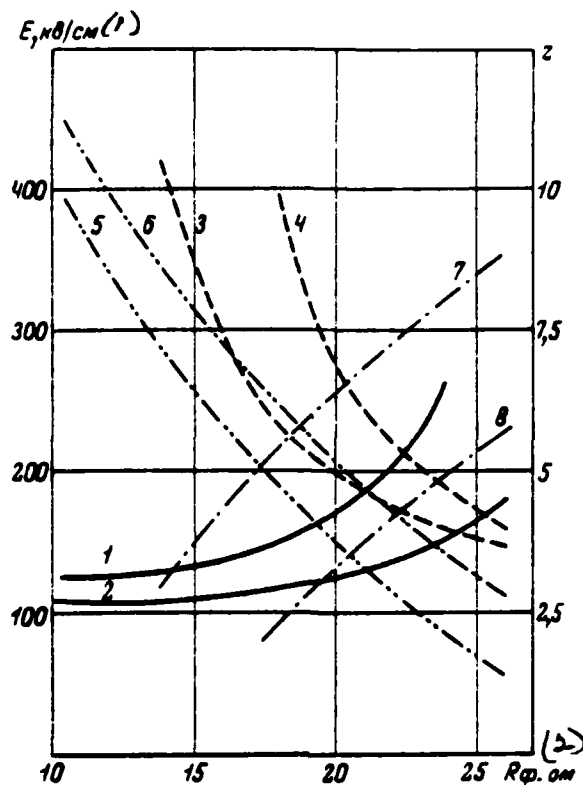


Fig. 3. Intensity/strength of field in the lines and wave impedance depending on the geometry of the lines

1 - E_H при $D_1 = 80$ см; 2 - E_H при $D_1 = 70$ см; 3 - E_{bH} при $D_3 = 20$ см; 4 - E_{bH} при $D_3 = 28$ см; 5 - $Z_{нар}$ при $D_1 = 80$ см; 6 - $Z_{нар}$ при $D_1 = 70$ см; 7 - Z_{bH} при $D_3 = 20$ см; 8 - Z_{bH} при $D_3 = 28$ см

Key: (1). kV/cm. (2). cm. (3). with.

	ЭСУ-0	ЭСУ-1
(1) Энергия, Мэв	0,8	2,0
(2) Ток пучка, ка	20	50
(3) Длительность импульса, нсек	35	40
(4) Режим работы	(5) Однoчные импульсы	
(6) Генератор импульсных напряжений (ГИН)		
(7) Число ГИН-400-0,08/5	4	6-8
(8) Ударное напряжение, Мв	0,8	1,2-1,6
(9) Ударная емкость, нф	12	8-6
(10) Индуктивность, мкгн	5	7-10
(11) Двойная формирующая линия (ДФЛ)		
(12) Диаметр электродов D_1, D_2, D_3 , см (см. рис. 1)	41; 19; 9;	60; 20; 10
(13) Длина, см	80	90
(14) Импеданс внутренней линии, см	7	6,5
(15) Импеданс внешней линии, см	7	3,5
(16) Зарядное напряжение, Мв	0,5-0,8	1,3-1,5
(17) Максимальная напряженность, кв/см	250	200
(18) Трансформирующая линия (ТЛ)		
(19) Входной импеданс, ом	14	10,3
(20) Коэффициент трансформации	1,46	1,65
(21) Длина, см	90	150
(22) Электронная пушка		
(23) Импеданс, см	30	30
(24) Число игл	1-5	1-5
(25) Вакуум, мм.рт.ст.	10^{-7}	10^{-7}

Key: (1). Energy, MeV. (2). Beam current, kA. (3). Duration of pulse, ns. (4). Operating mode. (5). Single impulses/acmenta/pulses. (6). Surge generator (GIN). (7). Number. (8). Impact stress, MV. (9). Impact capacitance, nF. (10). Inductance, μ H. (11). Dual forming line

(DFL). (12). Diameter of electrodes D_1, D_2, D_3 , cm (see Fig. 1).
(13). Length, see (14). Impedance of domestic circuit, Ω m. (15).
Impedance of outline, Ω m. (16). Charging voltage, MV. (17). Maximum
intensity/strength, kV/cm. (18). Transforming line (TL). (19). Input
impedance, Ω m. (20). Transformation ratio. (21). Length, Ω m. (22).
Electron gun. (23). Impedance, Ω m. (24). Number of needles. (25).
Vacuum, mm Hg.

Page 97.

For the experimental check of the principles, placed as the basis of accelerator ESU-1, is assembled small installation-model ESU-0 to the energy 600-800 keV (Fig. 4). In this model the line characteristics are identical and equal to 7 chms. Is commutated outline with the aid of the spark discharger, filled with nitrogen at a pressure 4-7 atm. On this installation are checked the different types of gaps (axial and radial), of distortion of impulses/momenta/pulses due to the charge inductance, the transformation of impulses/momenta/pulses and the construction/design of electron gun.

The development of gun for the line, filled with dielectric with high value ϵ , is complex problem. The usually utilized construction/design of gun [1, 2] does not make it possible in the

case of transition into the vacuum from the medium with large ϵ to obtain good agreements with the oscillator of nanosecond impulses/moments/pulses due to a sharp increase of the reactive component of the impedance of gun. Furthermore, it is difficult to obtain uniform potential distribution along the high-voltage insulator. Therefore we carried out special study on the creation of the gun, capable of working in the medium with large ϵ .

As a result is developed the construction/design of gun (Fig. 1), which provides simultaneously sufficiently good agreement and distribution of potential along the high-voltage insulator. The presence in system of dielectric with a comparatively large conductivity makes it possible to avoid the partitioning of insulator, which substantially simplifies its production.

As the electron source it is utilized from 1 to 5 tungsten needles in radius of bending ~ 0.1 mm, prepared with the method of electropolishing from wire $\phi 2-3$ mm. Is provided for the possibility of a precise change in anode-cathode distance for the control of the impedance of gun.

Construction/design, calculations and study of nanosecond oscillator and gun in greater detail are examined in the separate reports.

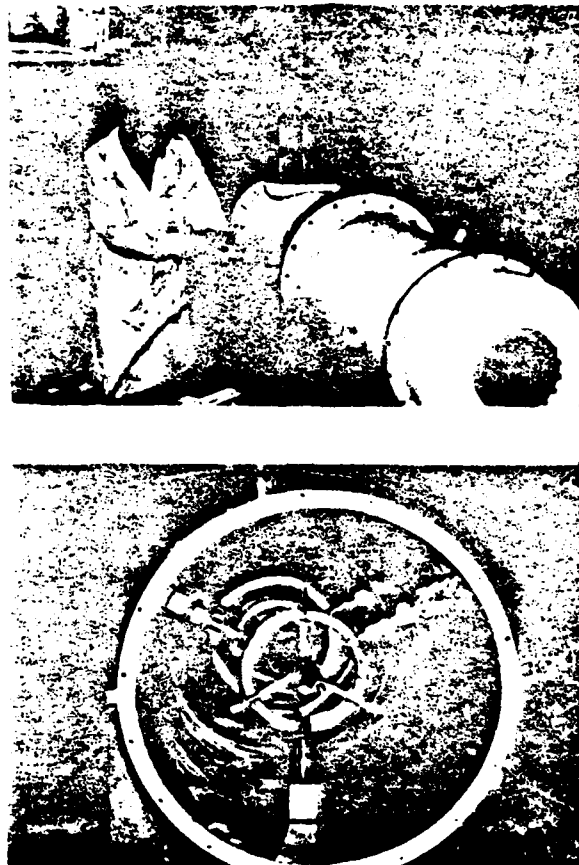


Fig. 4. Model of electric high-current accelerator ESU-0. a) general view; b) the internal part of the line from the side of load.

REFERENCES

1. S. E. Graybill, S. V. Nablo. IEEE Trans. on Nucl. Sci., 1967, NS-14, No 3, p. 782.

2. T. H. Martin. IEEE Trans. on Nucl. Sci., 1969, NS-16, No 3, p. 59.

Discussion.

A. A. Vorobyev. Did not test you to utilize in your devices/equipment water?

B. N. Yablokov. The use/application of water in the dual forming lines is possible with the very good quality of water (specific impedance $\geq 10^6$ to ohms cm). However, work with this water is very complicated. It is difficult to preserve good qualities of water in the metallic volumes. In this case the line must be equipped with the continuously operational system of the ion-exchange decontamination. Furthermore, during the use of water line to the duration of pulse on the order of 40 ns becomes short and with voltage on the order of 1 MeV its diameter becomes compared with the length. This line is converted into the capacitor/condenser.

V. G. Bagramov. How is provided the operational stability of multi-spark discharger/gap?

B. N. Yablokov. As yet we did not obtain the multi-spark work of discharger/gap. However, we hope that with a sufficient power in the

sparks and the diversity of the igniting sparks in the space it will be possible to attain the multi-spark work of discharger/gap. Now sparks break down with the precision/accuracy of better than 2 ns.

Page 98.

S. B. Vassermaya. Why you do consider that the subdivided tube is more complicated than one-piece/entire, and from what material it is proposed to manufacture one-piece/entire insulator?

B. N. Yablokov. Insulator of gun is made from the fiberglass. To groove insulator in one part in our case is possible, and this is simpler than to collect/compose it from the series/row of rings.

Yu. P. Vakhrushin. Which dielectric strength of glycerine in your operating modes?

B. N. Yablokov. According to our data, the breakdown of glycerin in the areas of electrodes $\sim 10^4$ cm² begins with the intensities/strength of field 230-250 kV/cm.

V. Hines. Which emittance of gun?

B. N. Yablokov. We yet did not measure the emittance of gun.

Work with it recently was begun.

V. L. Komarov. What value of electronic current you did obtain on the model?

B. N. Yablokov. On the preliminary measurements the current strength comprises 500a.

V. G. Bagramov. What type the transforming line?

B. N. Yablokov. exponential type transforming line. In more detail about this is speech in the following report.

26. Powerful/thick nanosecond oscillator.

L. N. Kazanskiy, B. N. Yablokov.

(Physical institute im. E. N. Lebedev of the AS USSR).

1. General/common/total description.

Oscillator is intended for the supply of the field emission electron gun (EP) of setting up ESU-1 by single impulses/moments/pulses with the following parameters:

Voltage ... 2 MV.

Current ... 50 kA.

Duration of the pulse ... 35 ns.

Duration of the front (shear/section) ... 10-12 ns.

The generation of output pulse is accomplished/realized on known diagram [1, 2] with the use of dual forming of lines (DPL) [3], which is charged by resonance method from Arkad'eva-Marx's oscillator

(GIN) .

FOOTNOTE 1. In the foreign literature DFL is known by the name Elumlein. ENDFOOTNOTE.

However, oscillator has some peculiarities associated with the tendency to maximally decrease the dimensions of setting up.

First, is utilized liquid polar dielectric with the high dielectric permeability - glycerin ($\epsilon = 42$). In the second place, impulse/momentum/pulse DFL transforms itself for decreasing the voltage of charge DFL. Thirdly, discharger/gap of DFL is connected between the grounded electrode and the high-voltage electrode at the point where to the latter is injected from GIN. This location facilitates control of discharger/gap and provides "reference" of GIN from EP and DFL after the commutation of the latter.

Fundamental oscillator circuit is given in Fig. 1. DFL 1 consists of two lines L_1 and L_2 , connected on the entrance of the transforming line (TL), which is made in the form of the steady exponential transition (see this coll., page 60, Fig. 1). The charge of line L_2 is accomplished/realized through the spiral short-circuited line (K1). All elements/cells of oscillator, with exception of GIN, have coaxial performance, which makes it possible

to utilize the grounded electrode as the screen and to decrease the edge effects.

2. Identification of parameters and calculation of oscillator.

With the energy, given up into the beam of $\sim 3.0-3.5$ kJ in the impulse/momentum/pulse, the energy, accumulated in DFL taking into account the disagreements/mismatches and the losses, must compose $W_{\Sigma} \sim 5$ kJ. Voltage DFL relative to voltage on EF is determined by identification of parameters TL. If TL and DFL are filled with identical dielectric $\epsilon_{\Delta\Phi n} = \epsilon_{TL}$, then the length of these lines they are connected with relationship/ratio [4]

$$l_{TL}/l_{\Delta\Phi n} = 2t_3/\tau = (\ln K)^2/(\Delta U/U), \quad (1)$$

where t_3 - delay TL; K - transformation ratio of voltage; $\Delta U/U$ - taper of pulse apex at the output of TL. Accepting $\Delta U/U = 0.1$ and $l_{TL}/l_{\Delta\Phi n} \approx 1$, we will obtain $K = 1.4$. Thus, voltage DFL must be 1.4 MV, and capacitance $C_{\Delta\Phi n} \approx 5000$ pF.

For an increase in the pulse power the duration of pulse (τ) and output resistance of DFL ($Z_{\text{вых}} = Z_1 + Z_2$) should be selected as small as possible

$$p = \frac{W}{\tau} = \frac{U^2}{Z_1 + Z_2}. \quad (2)$$

Here Z_1 and Z_2 - wave impedance of L_1 and L_2 . However, their decrease is limited by the permissible duration of pulse edges and by the

inductance of discharger/gap (L_p). Accepting $t_0 \leq 0.2\tau$ and taking into account that $t_0 \approx 2.2 L_p/Z_1$, we obtain with $z_1 = z_2 = z$

$$\tau > 11 L_p / Z_1 = 4.7 (W/L_p)^{0.5} u^{-1}. \quad (3)$$

Hence it follows that with \sqrt{H} value which hardly it is possible to decrease with $u > 10^6$ V, $L_p > 2 \cdot 10^{-8}$ ns and $z > 7$ ohm.

Page 99.

The selection of dielectric DFL and its geometry, i.e., the relation of the diameters of coaxial electrodes $\alpha = D_1/D_2 = D_2/D_3$ is made from the condition of maximum specific energy content (W/V) with the given ones $z_1 = z_2$.

FOOTNOTE 1. Equality the wave impedance of L_1 and L_2 in the principle is not necessary, but it is necessary for the full/total/complete agreement of DFL with the load. ENDFOOTNOTE.

The electric strength of all dielectrics was initially assumed/set by identical. Utilizing known relationships/ratios, for the coaxial lines it is possible to obtain

$$W/V = \frac{60}{\pi c} \frac{\epsilon^2}{Z^2} \frac{(\ln \alpha)^3}{\alpha^4} = \text{const} \frac{(\ln \alpha)^3}{\alpha^4}, \quad (4)$$

where V - full/total/complete volume of DFL. Maximum energy content is obtained when $\alpha_{\text{opt}} \approx 2.12$, and optimum dielectric permeability

$$\epsilon_{\text{opt}} = (60 \ln \alpha_{\text{opt}} / Z)^2. \quad (5)$$

For our oscillator they were selected $\alpha=2.12$ and glycerin ($\epsilon=39-45$).

It is interesting to note that with the prescribed/assigned wave impedance of DFL is a specific optimum dielectric permeability of its filling dielectric. For the illustration let us give the following example: for $Z_1=Z_2=7$ ohms and $r=35$ ns the volume DFL to 200/o is more during the use of water in comparison with the glycerin with the equal maximum electric intensities.

On the basis of the given above considerations it is designed and prepared the model of oscillator, the parameters and basic dimensions of which they are given in Table 1. For the model are prepared the dischargers/gaps DFL of two types: radial and axial (Fig. 1). Dischargers/gaps are trigatrons with 6-10 igniting for guaranteeing the multi-spark mode of operation [5].

The charge of GIN is assembled of four standard GIN-400-0.06/5. Serpukhov plant: two parallel columns on 2 pieces in each consecutively/serially.

3. Investigations.

Were measured in the range 0.1-100 MHz dielectric permeability ϵ and quality $Q \approx 10^5$ of glycerin, water and alcohols (Fig. 2). Was investigated the passage of narrow pulses (10-50 ns) through the lines, filled with these dielectrics. The best characteristics they possess the thoroughly cleaned with water ($\rho > 10^6 \Omega/\text{cm}$), glycerin has acceptable data, if is permitted the duration of fronts ~10-12 ns.

Was simulated the process of charge of DFL for the selection of the optimum parameters R_L ($Z_{k0} = 110 \text{ ohm}$, $t_3 = 17 \text{ ns}$, $L_{k0} = 1.9 \text{ } \mu\text{H}$) and the estimation of prepulse voltage on EP. The process of charge is checked on the model (Fig. 3): maximum voltage of DFL composes ~120% from total charging voltage of GIN, voltage on EP during charge <10% from the voltage of operating pulse.

Table 1.

(1) Узел генератора	ДФЛ	ТЛ
(2) Диэлектрик	(3) Глицерин ($\epsilon = 42,5$)	
(4) Емкость, пф	5000	900
(5) Волновое сопротивление, ом	14	14-30
(6) Коэффициент трансформации	-	1,46
(7) Длительность резонансного заряда, мксек	0,8	-
(8) Длительность импульса, нсек		35
(9) Диаметр электродов, см	9; 19; 41	9; 16; 41
(10) Длина, см	85	100
(11) Максимальная напряженность поля при зарядном напряжении 1,4 Мв, кв/см	420	600

Key: (1). Node/unit of oscillator. (2). Dielectric. (3). Glycerin. (4). Capacitance, pF. (5). Wave impedance, ohm. (6). Transformation ratio. (7). Duration of resonance charge, μ s. (8). Duration of pulse, ns. (9). Diameter of electrodes, cm. (10). Length, cm. (11). Maximum strength of field with charging voltage 1.4 MV, kV/cm.

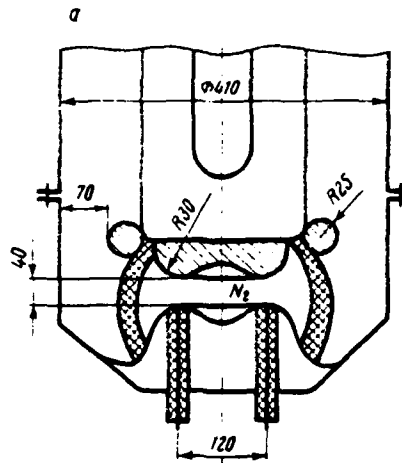


Fig. 1. Fundamental oscillator circuit.

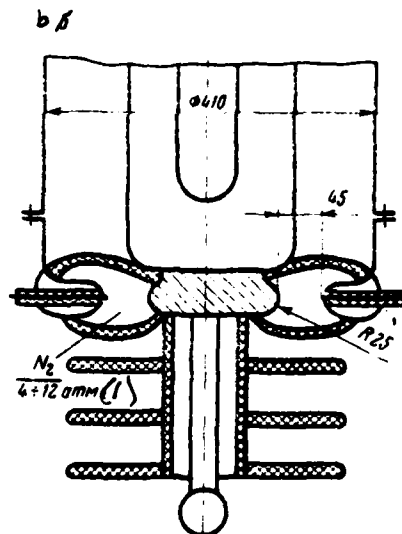


Fig. 2. Discharger of dual forming line of axial (a), radial (b) types.

Key: (1). atm.

Page 100.

Results of measuring the inductance of dischargers from a number of sparks, which were being initiated by thin wires $\phi 1.5 \text{ mm}$, of are shown in Table 2. Are obvious need the guarantees of multi-spark work of discharger and advantage of radial discharger.

During model tests for the electric strength charging voltage on DFL was raised to 600 kV. Breakdowns in the discharger were not observed at pressure N_2-4 by the atm. (discharger was tested on 10 atm.).

With 600 kV at the second maximum charging voltage there were the breakdowns in the glycerin on the end/face of DFL ($E=230 \text{ kV/cm}$).

Is at present initiated the production of basic oscillator ($U_{A\phi n}=1.4 \text{ MV}$; $U_{gn}=2.0 \text{ kV}$). The maximum strength of field in it is selected with $\sim 200 \text{ kV/cm}$, outer diameter DFL is 600 mm and its wave impedance to $z_1=3.8 \text{ ohm}$ and $z_2=6.5 \text{ ohm}$.

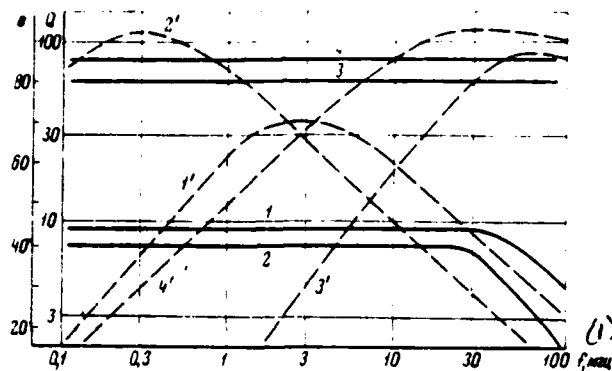


Fig. 3. Frequency dependences of dielectric permeability ϵ_1 (solid lines) and quality $Q=1/\tan\delta$ (dotted lines). 1.1' - technical glycerin ($\rho=1.7 \cdot 10^6$); 2.2' - glycerin " " ($\rho=60 \cdot 10^6$); 3.3' - distilled water ($\rho=10^6$); 4.4' - thoroughly purified water ($\rho=10^6$); ρ - volumetric impedance [ohm·cm].

Key: (1) . MHz.

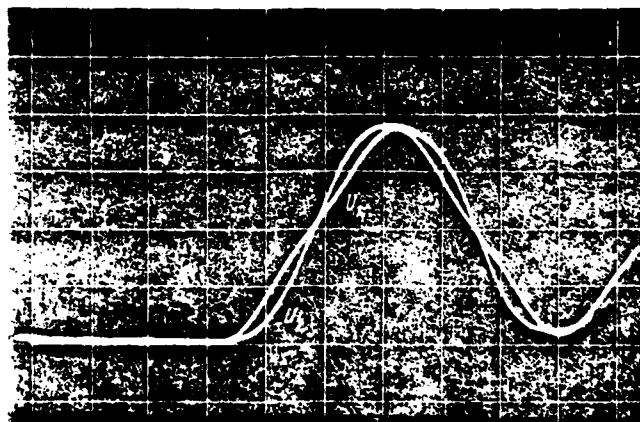


Fig. 4. Charging voltages on lines of DFL V_1 on L_1 and V_2 on L_2 . Scale on the horizontal $0.2 \mu s/cm$, on the vertical line $200 kV/cm$.

Table 2.

(1) Число каналов	1	2	3	4	5	6
(2) Радиальный раз- рядник, зазор 4,5 см	60	28	17	12	11	9,5
(3) Аксиальный раз- рядник, зазор 4,0 см	75	40	32	29	26	24

Key: (1). Number of channels. (2). Radial discharger clearance 4.5 cm. (3). Axial discharger clearance 4.0 cm.

REFERENCES

1. W.T. Link. IEEE Trans. on Nucl. Sci., 1967, NS-14, N 3, p. 777.
2. T. H. Martin. IEEE Trans. on Nucl. Sci., 1969, NS-16 N 3, p. 59.
3. Ya. S. Itskhokya. Pulsers. M., "Sov. radio", 1959.
4. I. Lewis and F. Puls. Milli-microsecond pulse technique. IL, 1956.
5. R. Buser et al. Electronics, 1968, 72, p. 74.

Discussion.

A. A. Vorobyev. How I understood. You does interest microsecond range?

L. N. Kazanskiy. The charge of the forming line is accomplished/realized during 0.4-0.6 μ s, the duration of the output pulse, which enters the electron gun, 30-50 ns at the level 0.5 of amplitude.

V. G. Davydovskiy. What efficiency of system you expect to obtain? How many impulses/elements/pulses in the unit of time can give system?

L. N. Kazanskiy. Efficiency relative to the energy, stored up in GIN must compose with approximately 500/o. Repetition frequency is determined by those utilized GINs (GIN - 400-0.06/5). Maximum frequency - 2 imp./min.

ge 101.

. Investigation of intense electronic ones on the accelerator
US-5.

. A. Abramyan, S. B. ^Wasserman, V. G. Votintsev, V. M. Dolgushin,
N. Lukin, B. G. Shkly^Yaev.

nstitute of nuclear physics of SC AN USSR [Siberian
partment of the Academy of Sciences of the USSR]].

The accelerator RIUS-5, intended for obtaining the beams of
lativistic electrons in the short (40-50 ns)
pulses/moments/pulses with the currents to 30 kA, was constructed
d launched in the institute of nuclear physics of SO AN USSR in
69 [1].

During last year was conducted the work on the improvement of
e construction/design of accelerator and the investigation of the
rameters of beam. At present all assemblies and systems of
celerator stable work with the voltage of high-voltage oscillator
8 MV and the voltage on accelerator tube to 5 MV. Pulse repetition
te - one per minute (with the work with the issue of beam in the

atmosphere).

Accelerator is made on commission for installations up of such type diagram: the source of high voltage, which leads high-voltage capacitance, discharger - peaking circuit with the ignition, accelerator tube with the cold cathode. As the source of high voltage is used the pulse generator on the coupled circuits (transformer of T). Insulating medium - mixture of eargas (sulfur hexafluoride) and nitrogen in relation 1:1 at a total pressure 15 atm. The schematic diagram of accelerator is shown in Fig. 1. The description of construction/design and work of setting up is given in [1].

In the report are described new construction/design and special features/peculiarities of the work of subdivided accelerator tube and dewatering outlet with the longitudinal magnetic field, and are also given the results of studies of the series/run of parameters and characteristics of the accelerated beam.

Accelerator tube and dewatering outlet.

Accelerator tube (Fig. 2) consists of the insulating rings, made from fiberglass and divided by electrodes of duralumin with rubber gaskets joints. Total number of sections - 13, the length of tube of approximately 75 cm. The construction/design of tube is made

according to the type of the dismountable tubes, which successfully work in the pulsed accelerators with thermoemission cathode [2] with the microsecond pulses of voltage. In accordance with A. Watson's recommendations [3] from the vacuum side the surface of insulator is made conical. The geometry of tube as a whole was selected on the electrolytic bath in such a way that voltage distribution according to the sections would be close to the uniform.

As noted above, tube successfully works with the voltages on it to 5 MV. However, there is no full/total/complete confidence in the fact that the materials accepted and the geometric forms of insulating rings and metal electrodes are optimum. Are at present initiated studies of dielectric strength of different in the material, the sizes/dimensions and the geometry sections on the high-voltage (to 1 MV) nanosecond bench.

The necessary condition for the normal work of accelerator tube is, as usual, its preliminary aging/training. The attempt to conduct aging/training tube in the operational conditions by the method of a gradual increase in the voltage did not yield positive results: the effect of aging/training was absent. The energy, isolated in this case in the channel of discharge, composes ~1 kJ (with the voltage of the generator ~3 MV) and, apparently, it is excessively great. The successful aging/training of tube is realized with parallel

connection of sections and upon their connection to the high-voltage electrode of oscillator. In this case the energy, isolated in the channel of discharge, does not exceed 10 d. Aging/training tube in the accelerator directly proves to be possible because of the fact that the voltage of the generator is easily regulated virtually from zero. Of this consists one of the advantages of pulse generator on the coupled circuits in comparison with Marx's oscillator.

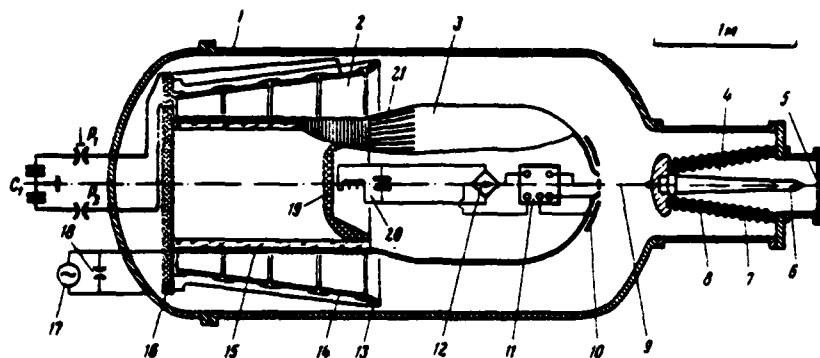


Fig. 1. The schematic diagram of setting up. 1 - boiler; 2 - transformer; 3 - high-voltage electrode (conductor); 4 - accelerator tube; 5 - delivery port (anode); 6 - cathode; 7 - insulator; 8 - electrode of tube; 9 - discharger-peaking circuit; 10 - capacitive voltage-divider; 11 - unit of ignition; 12 - rectifier; 13 - electrode; 14 - primary winding; 15 - secondary winding; 16 - insulating basis/base; 17 - oscillator of the supply of ignition; 18 - shunting discharger; 19 - electrode of capacitive protection; 20 - oscillatory circuit; 21 - "transparent" part of the conductor; C_1 - capacitor bank; P_1 and P_2 - air dischargers

Page 102.

The prepulse voltage, aimed in the accelerative gap/interval (because of the capacitive division) of up to functioning of a discharger-peaking circuit (Fig. 3), can lead to the vacuum breakdown

across gap, which, as a rule, affects the geometry and other parameters of beam. For preventing the vacuum breakdown across gap in the prepulse stage we accepted measures k for a reduction in the value of the aimed prepulse voltage, so for an increase in dielectric strength of accelerative gap/interval.

For the purpose of the decrease of potential, aimed, to the high-voltage electrode of 9 tubes (Fig. 2), the latter is displaced into the depth of housing 1, in this case the clearance of a discharger-peaking circuit 9 (Fig. 1) increases. For agreeing the electrical strength of a discharger-peaking circuit with the strength of the high-voltage clearance of oscillator is utilized point 10 (Fig. 2). The value of the aimed voltage on the tube composes $\sim 2.5\sigma/c$ of the high voltage of the generator.

The dewatering outlet of tube, shown in Fig. 2, makes it possible to arrange/locate window 5 at the considerable distance from the emitter with the sufficiently high electric intensities on the cathode. The longitudinal magnetic field, formed by solenoid 6, smoothly builds up in the value to 3-4 kg and it further remains approximately permanent up to delivery port. The divergent from the cathode bundle becomes then parallel. This dewatering outlet has essential advantages before it is usual by exhaust system (see Fig. 1). The size/dimension of beam on the anode can be easily regulated;

dielectric strength of gap/interval in the prepulse stage noticeably grows/rises, impeding breakdowns (the "disruptions/separations" of the induced on the tube voltage); processes on the anode, caused by the bombardment with electron beam, more weakly they affect a reduction in the impedance of gap/interval a cathode-anode; the insulator of tube considerably better is shielded from the becoming dusty by the metal, which flies from the anode.

The first tests of dewatering outlet with the longitudinal building up magnetic field passed successfully.

Results of the measurements of the parameters of beam.

The typical oscillograms of the impulses/moments/pulses of accelerating voltage and current (exhaust system usual) are shown on Fig. 4. With air-gap clearance an emitter-anode 4 cm the voltage of the generator 8 MV of the amplitude of the beam current and accelerating voltage compose 50 kA and 3.5 MV. Energy of beam in the impulse/momentum/pulse, measured by the calorimeter, placed after the foil, is equal to 3 kJ.

The changes, which occur in the accelerative gap/interval in the period of the passage of electron beam, explain the higher values of current in middle and end/lead of the impulse/momentum/pulse in

comparison with the current in the beginning of impulse/momentum/pulse with the same voltages. Maximum voltage on the gap/interval is achieved through 15 ns since the beginning of the impulse/momentum/pulse, and it is possible, apparently, to consider that up to this moment/torque the characteristics of beam still are determined only by the emissive properties of cathode and by the geometry of accelerative gap/interval. The values of beam current with maximum accelerating voltage in the range $U_m = 1 - 4$ MV is well approximated by the dependence

$$j_m = k U_m^{5/2},$$

where k - coefficient, depending on the geometry of gap/interval, emitter and material of the latter.

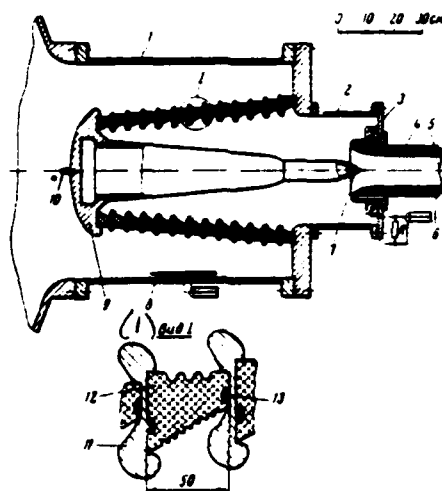


Fig. 2. Accelerator tube and dewatering outlet. 1 - housing; 2 - vacuum chamber; 3 - Rogovskii's band; 4 - housing of dewatering outlet; 5 - delivery port; 6 - solenoid; 7 - emitter; 8 - sensor of voltage on the tube; 9 - high-voltage electrode of tube; 10 - point; 11 - electrode of tube; 12 - insulator; 13 - sealer.

Key: (1). Form.

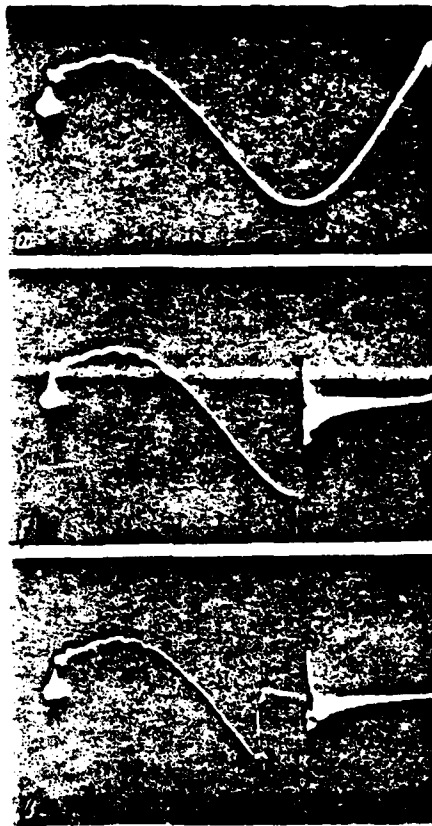


Fig. 3. Voltage on accelerator tube during entire cycle of the work of installation . a) a discharger-peaking circuit did not operate/actuate; b) discharger operated/actuated (was visible voltage surge on the tube); c) in the prepulse stage it occurred the "disruption/separation" of voltage (breakdown of vacuum gap/interval). Scanning/sweep - 5 ns/cm.

For the emitter made of the stainless steel whose form is shown in Fig. 5b, with air-gap clearance to the anode 4 cm $k=2.240 \cdot 10^{-12}$ A/V². It should be noted that the finish of the surface of emitter and the form of edges (sharp/acute or blunted) noticeably value k do not affect.

Fig. 5 shows the cross sections of electron beam on the anode with maximum accelerating voltage in the impulse/momentum/pulse for different emitters. The circular form of beam section from the conical emitter is well known. Expected on this basis/base halving of beam on the circular edge and possibility of changing the diameter of beam due to the inclination/slope of edges were confirmed during the investigation of the emitters whose form was given in Fig. 5b and c. The configuration of beam sections was observed on the glass plates which were placed after the aluminum filters, which passed only the electrons of maximum energies. With the increase of energy of electrons the diameter of beam decreases.

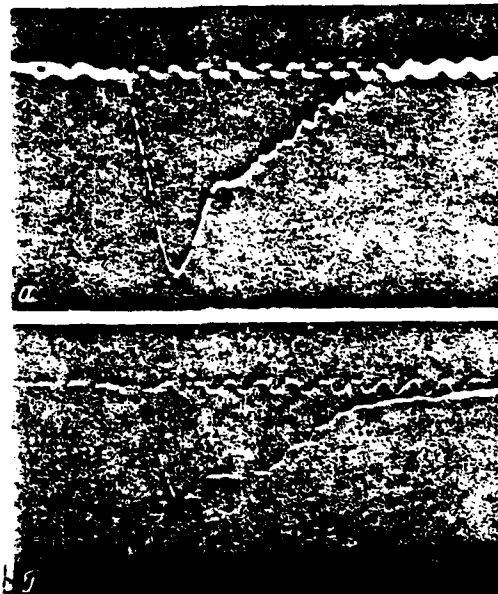


Fig. 4. Shape of the pulses of accelerating voltage (a) and current (b) of beam. Markers - 100 MHz.

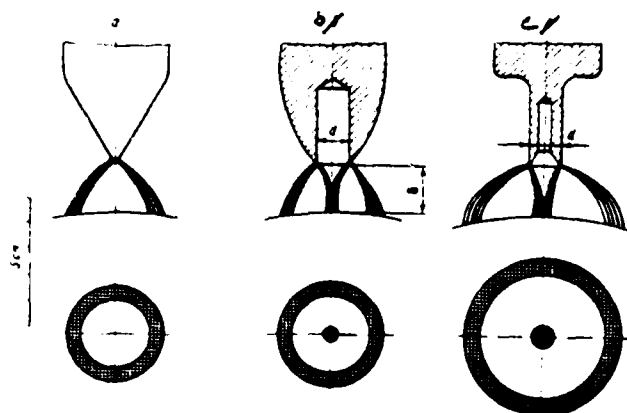


Fig. 5. Electron paths and beam shape on anode for different emitters. Energy of electrons $W_0 = 1 + 1.5$ MeV, $\delta = 2$ cm; $d = 1.2$ cm

REFERENCES

1. Ye. A. Abramyan et al. Reports of the AS USSR, 1970, 192, No 1, page 76.

2. Ye. A. Abramyan, S. B. Wasserman. "Atomic energy", 1967, 23, iss. 1, page 44.

A. Wilson. J. Appl. Phys., 1967, 38, N 5, p. 2019.

Discussion.

A. N. Lebedev. 1. In what region of energies was observed law of $5/2$ and what magnetic field strength it was utilized for conclusion/output? 2. How proper field of beam, and with what current were conducted experiments? 3. Which maximum current for energy 5 MeV was obtained on this gun?

S. V. Wasserman. 1. Law of $5/2$ was observed in region of energies from 1 to 3.5 MeV. Field built up along the axis/axle of bundle to 4 kg. 2. Experiments were conducted with currents to 20 kA. Magnetic field strength beam, unfortunately, I do not remember. 3. With energy

5 MeV current was about 30 kA.

A. A. Vorobyev. How does differ current from impulse/momentum/pulse to the impulse/momentum/pulse and which the duration of the continuous work of this setting up, determined by thermal condition?

S. B. Wasserman. Scatter from one impulse/momentum/pulse to the next in limits of 50/o. Since machine works with the repetition frequency of 1 times per minute, then a question about the thermal overloads it did not appear.

I. M. Royfe. From what material of production tube? Do not intend you to decrease the duration of frict?

S. B. Wasserman. For the insulating rings is utilized the fiberglass. Electrodes are prepared from the dural. Front into present time is equal to 15 ns, and for our purposes there is no need for it shortening.

B. N. Yablokov. What delay time between the impulse/momentum/pulse of trigatron and main discharge on the tube?

S. B. Wasserman. Delay time was not measured, but the stability of functioning good.

N. V. Pleshivtsev. 1. Are such geometric dimensions of cathode and its material? 2. Did work you in mode/conditions with voltage of less than 1 MV?

S. B. Wasserman. 1. Cathode is prepared from stainless steel and is cone with different angles. Usually angle - 60° and length - 3 cm. Point had a rounding. 2. No, they did not work.

K. V. Khodataev. What fraction/portion of energy does take away beam in comparison with the energy, stored up in the battery?

S. B. Wasserman. In the maximum rating energy of the battery of 10 kJ, on the high-voltage electrode - 7 kJ, in the beam - 3 kJ.

Page 104.

28. Discharge through high-pressure gas, initiated by the beam of rapid electrons.

B. M. Koval'chuk, V. V. Kremnev, G. A. Mesyats, Yu. F. Potalitsyn.

(Institute of optics of the atmosphere SC AN USSR).

In work [1] it was shown that for eliminating channeling the discharge through gas at a high pressure it is necessary before beginning discharge to have many initiating electrons, distributed by cathode or volume of gap/interval. In [2] for this purpose it was proposed to utilize a beam of rapid electrons. Let us examine this possibility in more detail.

Let there be the gas-filled gap with a length of d with the electric intensity E_0 and by pressure of gas p . If from the side of cathode into it enters uniform electron beam by section s , with the current density j_0 and energy W (Fig. 1), then, by disregarding secondary processes on the cathode and by taking into account impact ionization and electron drift, we will obtain the equation of continuity for the electrons

$$\frac{\partial \rho(x,t)}{\partial t} + \frac{\partial \rho(x,t)v(x,t)}{\partial x} = \alpha(x,t)v(x,t)\rho(x,t) + \psi(t). \quad (1)$$

To account for the effect of space charge we will use the equation of Poisson

$$\frac{\partial \mathcal{E}(x,t)}{\partial x} = \frac{\rho_+(x,t) - \rho_-(x,t)}{\epsilon_0}, \quad (2)$$

where $\rho_-(x,t)$ and $\rho_+(x,t)$ - density of the electron charge and ions in the gap/interval; $v_-(x,t)$ and $\alpha(x,t)$ - drift velocity and coefficient of impact ionization; ϵ_0 - dielectric permeability of vacuum;

$\mathcal{E}(x,t)$ - strength of field in the gap/interval,

$$\psi(t) = j_s(t) n_0 p \sigma_{cp}; \quad (3)$$

$n_0 = 3.6 \cdot 10^{16} \text{ 1/cm}^3 \cdot \text{torr}$; σ_{cp} - middle ionization cross section, cm^2 ;
 p - gas pressure in the gap/interval, torus. Boundary and initial conditions

$$\rho_-(0,t) = 0, \quad \rho_-(x,0) = 0. \quad (4)$$

Values $v_-(x,t)$ and $\alpha(x,t)$ are determined by the intensity/strength of field $\mathcal{E}(x,t)$, and the latter by a voltage drop across gap/interval $U(t)$. Value $U(t)$ is determined from the equation of Kirchhoff. In the case of the discharge to the gap/interval of capacitance C

$$U(t) = U_0 - \frac{1}{C} \int_0^t I(t) dt, \quad (5)$$

while in the case of the discharge of line with the wave impedance of Z

$$U(t) = U_0 - RI(t), \quad (5)^1$$

where $i(t)$ - the current through the gap/interval.

In general the solution of system of equations (1), (2), (5) is difficult; therefore let us introduce some limitations. Assuming that at any moment of time $\frac{\partial \psi}{\partial x} = 0$, the solution of equation (1) taking into account conditions (4) leads to the current through the gap/interval:

$$i(t) = \frac{v_-(t)S}{d} \int_0^d dx \int_0^t \psi(t') \exp \left[\int_{t'}^t \alpha(t'') v_-(t'') dt'' \right] \times \left[x - \int_{t'}^t v_-(t'') dt'' \right] dt'. \quad (6)$$

If for the duration of electronic flux τ_e and length of gap/interval d are observed the conditions

$$\tau_e \ll t_p, \quad \int_0^{t_p} \alpha(t) v_-(t) dt \gg 1, \quad (7)$$

where t_p the time of discharge build-up then from (6) for the current in the discharge circuit we will obtain

$$i(t) \approx \frac{N_0 e v_-(t)}{d} \exp \left(\int_0^t \alpha(t'') v_-(t'') dt'' \right), \quad (8)$$

where $N_0 = \frac{\sigma_{ep} n_0 p S}{d} \int_0^{t_p} j_0(t') dt'$. This process of an avalanche-type increase in the current was examined by us in [1, 2]. Let us pause now at other case when

$$\tau_e \approx t_p \quad \text{and} \quad \int_0^{t_p} \alpha(t) v_-(t) dt \ll 1. \quad (9)$$

Key: (1). and.

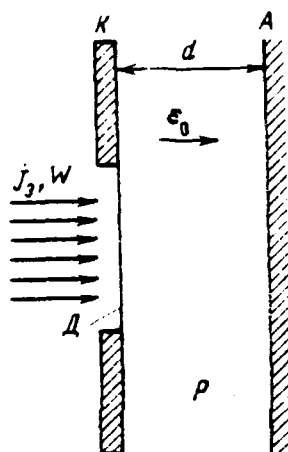


Fig. 1. Design diagram of commutator. A - anode; K - cathode;
D - diaphragm.

Page 105.

If a potential difference between the cathode and the anode is such, that $U_0 = E_0 d < U_{cr}$ (U_{cr} - static breakdown voltage), then with the observance of conditions (9)

$$\int_0^{t_p} v_-(t) dt \ll d. \quad (9')$$

Conditions (9) and (9') mean that the impact ionization by electrons can be disregarded/neglected and that the length of electron drift is much lower than the length of gap/interval.

Under condition (9), taking into account that $v_-(t) = K_0 \frac{U(t)}{pd}$, the solution of equation (6) for the discharge of capacitance leads to the current in the contour/outline

$$i(t) = U_0 \lambda \exp\left(-\frac{t^2 \lambda}{2C}\right), \quad (10)$$

while during the discharge of the line

$$i(t) = \frac{U_0 \lambda t}{1 + R \lambda t}, \quad (10')$$

where $\lambda = \frac{n_0 K_0 \sigma_{cp} l_0}{d}$, $i_0 = j_0 S = \text{const.}$ - beam current of the initiating electrons, when $t < t_0$ and $i_0 = 0$ with $t > 0$.

Formulas (10) and (10') were obtained under two conditions: constancy along the gap/interval of the intensity/strength of field $E = E(t)$ and ionization cross section $\sigma = \sigma_{cp} = \text{const.}$

The effect of space charge on the strength of field along the gap/interval was taken into consideration during the solution of system (1) and (2) by the method of successive approximations. During the calculation a voltage drop in the commutator is accepted by constant and equal to U_0 . As the zero approximation the strength of field in entire gap/interval was taken by constant. In this case solution (1) when $\psi(t) = \text{const}$, $\alpha(t)v_-(t) \approx 0$ takes the form

$$\rho_-(x, t) = \psi \frac{x}{v_-} \quad (11)$$

with

$$0 < x < v_-^{(0)} t;$$

$$\rho_-(x, t) = \psi t. \quad (12)$$

when $v_-^{(0)} t < x < d$. Equation (4) taking into account (11) and (12) has a solution

$$\begin{aligned} \varepsilon_{0 < x < v_-^{(0)} t} = & -\frac{U_0}{d} - \frac{\psi t v_-^{(0)} t}{2 \varepsilon_0} \left(1 - \frac{v_-^{(0)} t}{6d} \right) + \\ & + \frac{\psi t v_-^{(0)} t}{\varepsilon_0} \left(\frac{x}{v_-^{(0)} t} - \frac{x^2}{2 v_-^{(0)2} t^2} \right); \end{aligned} \quad (13)$$

$$\varepsilon_{v_-^{(0)} t < x < d} = -\frac{U_0}{d} + \frac{\psi t v_-^{(0)2} t^2}{6 \varepsilon_0 d}. \quad (14)$$

Under condition (9') by field change in basic part of gap/interval ($v_-^{(0)} t < x < d$) with the short times t negligible, and in region ($0 < x < v_-^{(0)} t$) for simplicity it is accepted

$$\varepsilon_{0 < x < v_-^{(0)} t} \approx -A_1 + B_1 x, \quad (15)$$

where

$$A_1 = \frac{U_0}{d} \left(1 + \frac{\psi v_-^{(0)} d}{2 \epsilon_0 U_0} t^2 \right), \quad B_1 = \frac{\psi t}{2 \epsilon_0}.$$

Solution (1) in the first approximation, taking into account the field by formula (15) takes the form:

$$x = \omega d e^{-t^2} (t e^{t^2} - t_0 e^{t_0^2}); \quad (16)$$

$$\rho = \frac{2 \sqrt{\pi} \epsilon_0 U_0}{d^2 \omega} e^{t^2} [\operatorname{erf}(t) - \operatorname{erf}(t_0)], \quad (17)$$

where $t = t \frac{\sqrt{K_0 \psi}}{2 \sqrt{p} \epsilon_0}$; $\omega = \frac{2 \sqrt{K_0 \epsilon_0} U_0}{\sqrt{\psi p} d^2}$; t_0 - parameter, which is changed within limits of $t=0$ with change x within limits $0 - v_-^{(0)} t$. The voltage drop near the cathode is obtained as the integral of the solution of equation (2) in the second approximation/approach, i.e., taking into account (16) and (17)

$$U_K \approx U_0 \omega \left(2t - e^{-t^2} \int_0^t e^{\xi^2} d\xi \right). \quad (18)$$

Assuming/setting $\frac{U_K}{U_0} \ll 1$ from (18), we have

$$\frac{U_K}{U_0} \ll \frac{2 K_0 U_0 t}{p d^2} \approx \frac{2 v_-^{(0)} t}{d}. \quad (19)$$

It is not difficult to see that condition (19) is identical to condition (9'). This means that with satisfaction of condition (9') it is possible not to consider the effect of space charge in the cathode on the course of current in the gap/interval. In this case when $v_-^{(0)} t \ll d$ we have

$$j/j_0 \ll n_0 p d, \quad (20)$$

i.e. a limitation to the gas amplification factor of current in the

gap/interval.

Checking predicted losses was accomplished/realized by a method of the comparison of the parameters of current pulses at the discharge of the non-inductive capacitor/condenser with a capacitance $C=3.5 \cdot 10^{-9}$ f on the gas-filled gap with a length of $d=8$ mm with the calculation according to formula (10). From (10) it follows that the amplitude of pulse

$$i_m = U_0 \sqrt{\frac{\lambda C}{e}}, \quad (21)$$

where e - Napierian base, and pulse duration on the half-height

$$t_u \approx 1,6 \sqrt{\frac{C}{\lambda}}. \quad (21')$$

Substituting value λ from (10'), we will obtain

$$\frac{U_0}{i_m} = 1,65 \sqrt{\frac{d}{n_0 K_0 \sigma_{cp} i_3 C}}, \quad (22)$$

$$t_u = 1,6 \sqrt{\frac{Cd}{n_0 K_0 \sigma_{cp} i_3}}. \quad (22')$$

Electron beam with current $i_3 \approx 10^3$ a was formed/shaped with the aid of nanosecond direct voltage accelerator [4] with the field emission multitip cathode, to which was supplied the voltage pulse with amplitude $U=300$ of kV, duration $t_0 \approx 35 \cdot 10^{-9}$ s and front $t_f \approx 3 \cdot 10^{-9}$ s.

In the discharge gap being investigated the electrons fell through the diaphragm from the titanium foil with a thickness of 50 μm .

After passage through the foil maximum energy of electrons in the beam descends on $\Delta E \approx 80$ the keV [5], and the current of electrons, measured after diaphragm with the aid of the faraday cylinder, comprised $i_e = 100$ μA .

Fig. 2 gives the characteristic oscillograms: electronic current, which passed through the foil to the discharge gap (Fig. 2a); discharge current with the autobreakdown of gap/interval static breakdown voltage in the absence of electronic current (Fig. 2b); the commuted current, initiated by electron beam, at pressures 1; 6 and 12 atm. (Fig. 2c-e) respectively.

Fig. 3 depicts the experimental dependences of the amplitude of commuted current on the applied in the discharge gap voltage with the direct current of electrons $i_e = 100$ μA for the different pressures (Fig. 3a) and the experimental dependences of the amplitude of commuted current on the pressure in the discharge gap with the different voltages (Fig. 3b). With a change in the pressure from 3 to 15 atm. the experimental value of ratio $\frac{U_0}{U_M} \approx 2.2 \pm 0.2$ ohm. The pulse duration on the half-height barely depended on pressure p and voltage U_0 and was 22-26 ns.

For the comparison of experimental data with the calculated ones it is necessary to know values K_0 and ϕ_{cp} . In the experiment value \mathcal{E}/p was changed in limits (0.5-10) of V/cm·torr. For this range \mathcal{E}/p according to the data, given in [3] for nitrogen, $v = 0.5 \cdot 10^8 (\mathcal{E}/p)^{3/4}$, consequently, $K_0 = 0.5 \cdot 10^8 (\mathcal{E}/p)^{-1/4}$.

Dependence $\phi(W)$ for nitrogen is given in Fig. 4 [5]. Is here given the dependence product pd on energy of electron W which shows, what is necessary minimum energy of electron W , so that it would cross the gap/interval the d pressure of nitrogen p . Under conditions for our experiment product $pd = (0.2-1) \cdot 10^4$ torr.cm, $W \approx 200$ keV, therefore, $\phi_{cp} \approx 3.8 \cdot 10^{-13} \text{ cm}^2$.

After substituting in (22) and (22') used in the experiment values U_0 , ϕ_{cp} , d , C and \mathcal{E}/p , we will obtain that $\frac{U_0}{U_M} \approx (7.05 \pm 10.2) \text{ ohm}$, and $2.4 \cdot 10^{-8} \text{ s} < t_u < 3.5 \cdot 10^{-7} \text{ s}$. Certain disagreement with the experiment, apparently is caused by inaccuracy in determination ϕ_{cp} . Value ϕ_{cp} will be substantially above, if we consider the contribution to resulting quantity ϕ_{cp} , caused by electrons with low energies which are formed with the passage of the beam through the foil and through the gas.

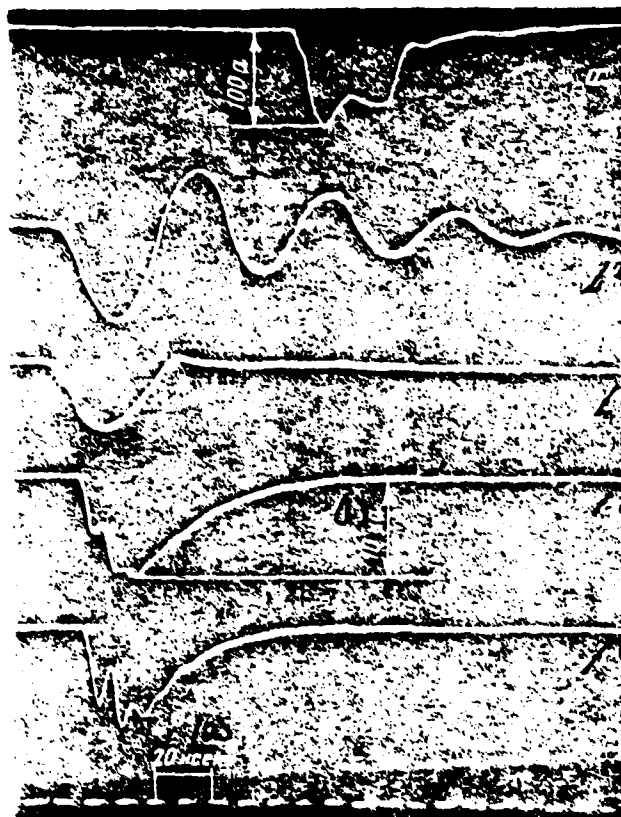


Fig. 2. Oscillograms of the electronic (a) and discharge (b-e) currents.

Key: (1). kA. (2). ns.

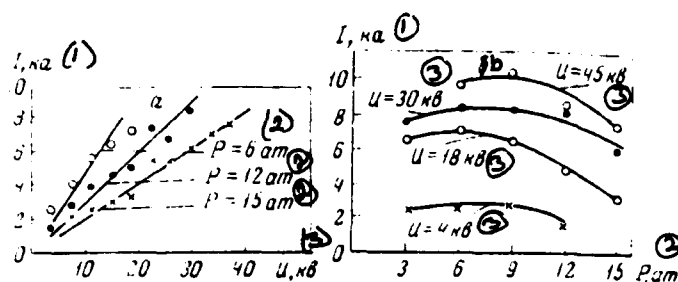


Fig. 3. Experimental dependences $\alpha - I_m = f(U_0)$ with constant $U_0 = 100 \text{ V}$ for different P ; $\delta - I_m = f(P)$ with the the different U_0 .

Key: (1). kA. (2). atm (tech). (3). kV.

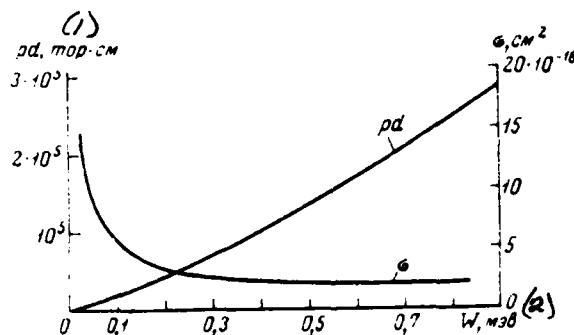


Fig. 4. Dependences $\sigma = f(W)$ and $pd = f(W)$

Key: (1). torr·cm. (2). MeV.

REFERENCES

1. G. A. Mesyats. Dr. dissert. Tomsk, 1966. G. A. Mesyats et al.

ZhTF, 1969, 39, No 1, page 75.

2. B. M. Koval'chuk et al. Reports of the AS USSR, 1970, 191 v. 1.

3. G. Reter. Townsend ionization and by probe in the gases. M., publishing house "Mir," 1968.

4. G. A. Mesyats et al. PTE, 1969, No 2, page 102.

5. Alpha-, beta- and gamma- spectroscopy, Vol. 1. Edited by K. Sieghahn. M., Atomizdat, 1969.

Page 107.

29. Aberrations of space charge.

Zh. For.

(Saclay, France).

When in 1964 was developed/processed preinjector "Saturn" to 750 keV, special attention was given to the guarantee of constancy of the optical properties of beam from the ionic source to the output of tube. For this optical system must be as possible more linear. For obtaining the linearity of the forces of space charge, at least in the region low energies of beam, was first of all investigated ionic the source for the target eliminate the effect of aberrations of space charge in the region of conclusion/output and was achieved/reached almost uniform density on the output of source. In this case for executing calculating the beam focusing was made the assumption about the linearity of the forces of space charge after the region of conclusion/output. Since was conducted the optimization

of electrostatic lens from the parameter of aberrations, assumption indicated above could be considered justified.

Experimental results with the energy 750 keV showed that although was obtained almost calculated emittance (ϵ, ϵ'), density differed from that measured by the output of source and near the axis/axle of bundle was failure/dip/trough.

It was established, installed, that density distribution depends mainly on extraction voltage. Although the quality of beam was sufficient to high ones for the injection into the linear accelerator, it was decided to investigate in the digital form the effect of a heterogeneous space charge in this preinjector.

Preinjector on 750 keV.

Given preinjector was already described [1]. Let us give only voltage distribution along the axis/axle where it is possible to isolate three regions: the extraction region, focusing and acceleration (see Fig. 1A).

Voltage distribution can be optimized in such a way as to obtain at the output of accelerator tube the contraction of beam in the free from the aberrations focusing system. Calculations were carried out

for the beam 100 mA. The measured emittance at the output of source, numbered to the beam 100 mA, is 1.2×10^{-6} mrad.

Initial forecasts theory and experimental results.

Fig. 1a, depicts envelope of particles; emittance (ϵ, ϵ') , obtained as a result of initial calculations, it is given in Fig. 1b.

The direction of the initial velocity of particles and axis/axle are given plane; therefore it is possible to calculate only action in plane (ϵ, ϵ') .

Fig. 2a, depicts the emittance of beam, experimentally measured at a distance of 1.7 m from the ionic source. Experimental emittance (ϵ, ϵ') was measured with the aid of the openings/apertures, agitated according to the diameter of beam and ensuring the pencils which are analyzed by means of lead-collector/receptacle, arranged/located at a distance one meter on the course of beam. Recording the current of the lead/duct of collector/receptacle gave density curves and emittance. As can be seen emittance it is compared with the calculated; whereas density is heterogeneous and strongly it differs from the initial (see Fig. 2b).

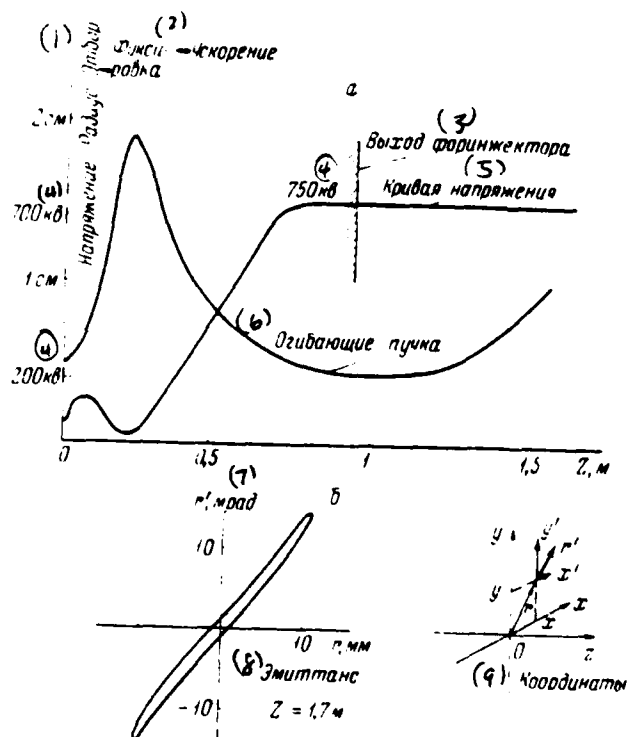


Fig. 1. Characteristics of the preinjector: a) $U(z)$ and $v_n(z)$; b) the calculated emittance.

Key: (1). Voltage Radius Selection. (2). fixing-acceleration. (3). output of preinjector. (4). kV. (5). Voltage curve. (6). Envelope of particles. (7). mrad. (8). Emittance. (9). Coordinates.

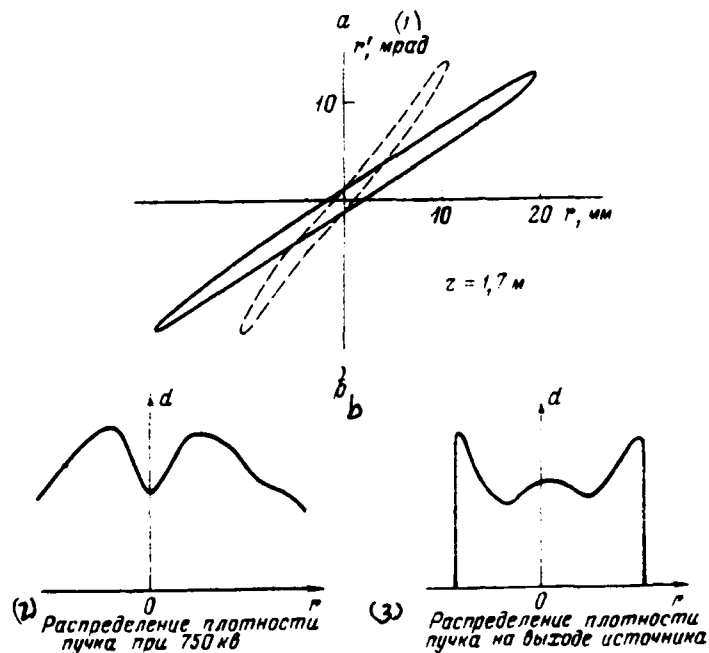


Fig. 2. Experimental characteristics of the beam of preinjector a) emittance; b) density distribution.

Key: (1). mrad. (2). Density distribution of beam with 750 kV. (3). Density distribution of beam at output of source.

Page 108.

New calculations of space charge.

In order to include/connect the nonlinear effects of space

charge, with the aid of the program, written in 1960, was traced the path of 325 particles. Recently program was modified in order to trace 2000 particles for the same machine time [2].

As the coordinates of position and speed in the program are utilized by x , y , x' and y' , so that, eliminating neglects of the longitudinal effect of space charge, with calculation was not done any special assumptions. Initial values were taken at the end of the region of pier and in the initial theory. Experiments showed that, regulating the stress/voltage of pier and the polarization of the block/module/unit of expanding the plasma, succeeds in obtaining Gaussian, flat/plane or with the indentation in the distribution center in the density of beam according to the section.

Calculations were carried out for several initial distributions, which approach experimental ones. Initial region emittance was supported by the constant: 1.8×10^{-6} mrad for 100 mA.

Numerical results.

First of all, it is necessary to note that envelope of particles virtually on depends on initial distribution according to (x, y) . In the second place, results are almost not depended also from the initial distribution according to (x', y') .

Therefore will be given results for three real types of spatial distributions: flat/plane, Gaussian and with the indentation in the center.

Fig. 3 gives distributions within and outside the preinjector. It is evident that in the case of flat/plane and even in the case concave initial distribution can arise the indentations in the region where was made the measurement of emittance for the energy 750 keV. If distribution curve carries Gaussian character, it is possible to obtain peak.

Fig. 4 gives the curves $E=f(l)$ (E - the emittance, obtained by projection of volume (x, x', y, y')) but for the concave or flat/plane distribution (200/o for 950/c of beam); however, it is more noticeably in the case of Gaussian distribution (750/o).

Discussion and conclusion/output.

1. From Fig. 3 and 4 it is evident that depending on selected section Gaussian initial distribution gives at output of preinjector concave distribution or peak of density.

This can be explained as follows: let A and B, combined since the origin of the coordinates x , x' be two the pencil (see Fig. 5a). Straight line OAB is distorted by the nonlinear effect of space charge. Consequently, when beam enters into lens, A and B they are arranged/located, as shown in Fig. 5b; calculation shows that the density of beam in this section is smoothed. The effect of lens consists in increase in x for negative x and in decrease of x' for positive x . In Fig. 5, in it is possible to see the new form of emittance after the passage of the beam through the lens.

In accelerator tube the emittance drifts, as shown in Fig. 5d. It is easy to see that during the correct selection of section the density can have an indentation on the axis/axle. Thus, high density on the axis/axle after source generates due to aberrations of space charge beam with the cavity inside.

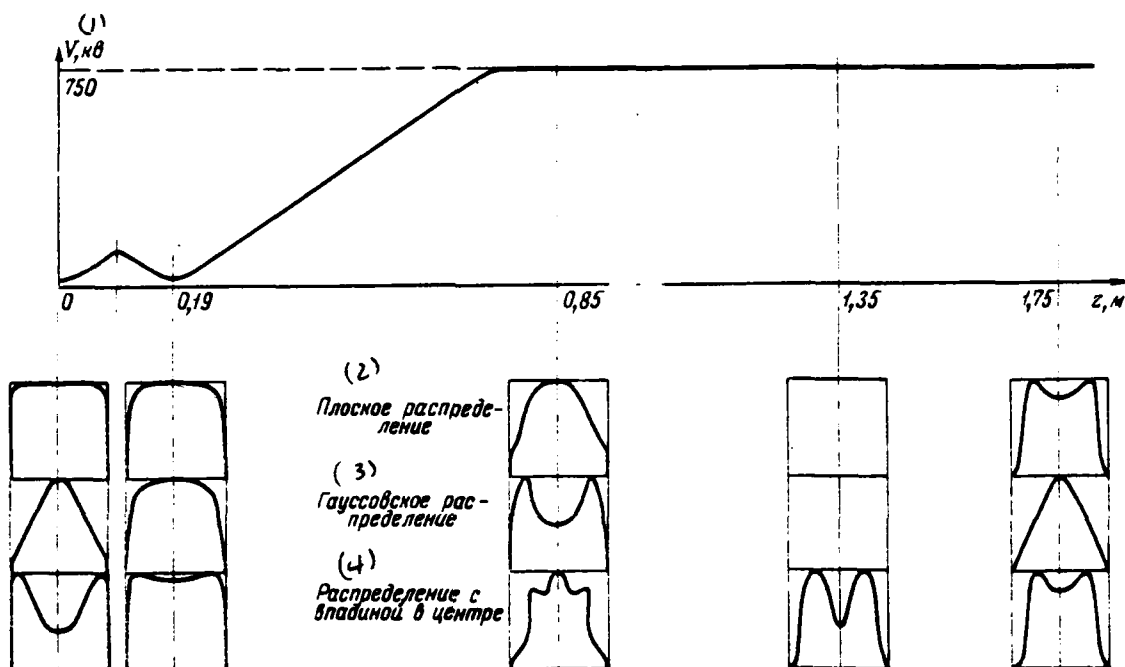


Fig. 3. Density distribution of beam within and after the output of preinjector.

Key: (1). kV. (2). Flat/plane distribution. (3). Gaussian distribution. (4). Distribution with indentation in center.

Page 109.

2. Even in the case of uniform initial density beam at output of preinjector has on axis, axis somewhat less density. This density distribution is unstable. Dr. Lapstoll' [3] indicated the

theoretical possibility of obtaining the stationary beams in the permanent focusing systems; however hardly it is possible to generalize theory to the electrostatic lenses, used in this preinjector.

3. Was given trajectory calculation in short tube where particles at first are accelerated to final energy, and then they are focused by magnetic triplet. For the Gaussian distribution were obtained analogous results.

4. It is obvious that aberrations of space charge which make beam that more diverging through lens, increase effect of aberration of lenses, since larger quantity of particles is found at large removal/distance from axis/axis. Consequently, the effects of aberration of space charge and lenses are summarized, distorting the density of beam.

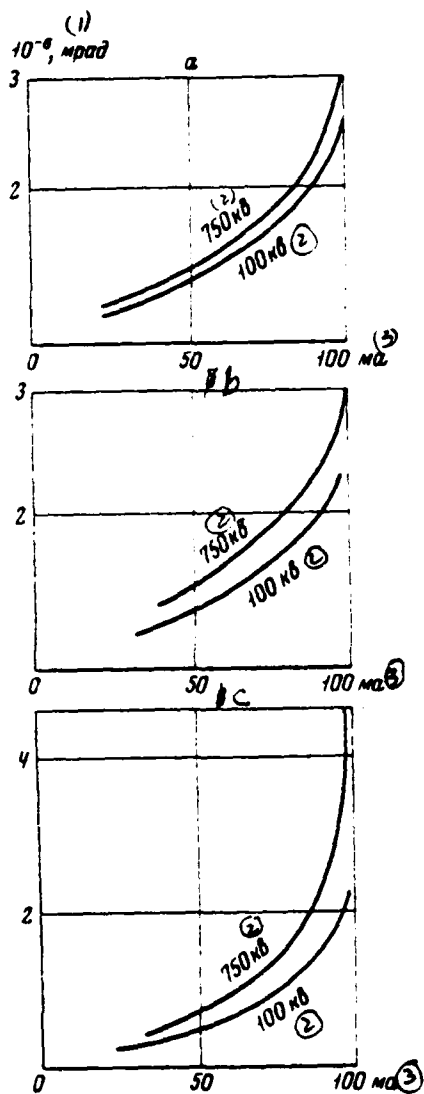


Fig. 4.

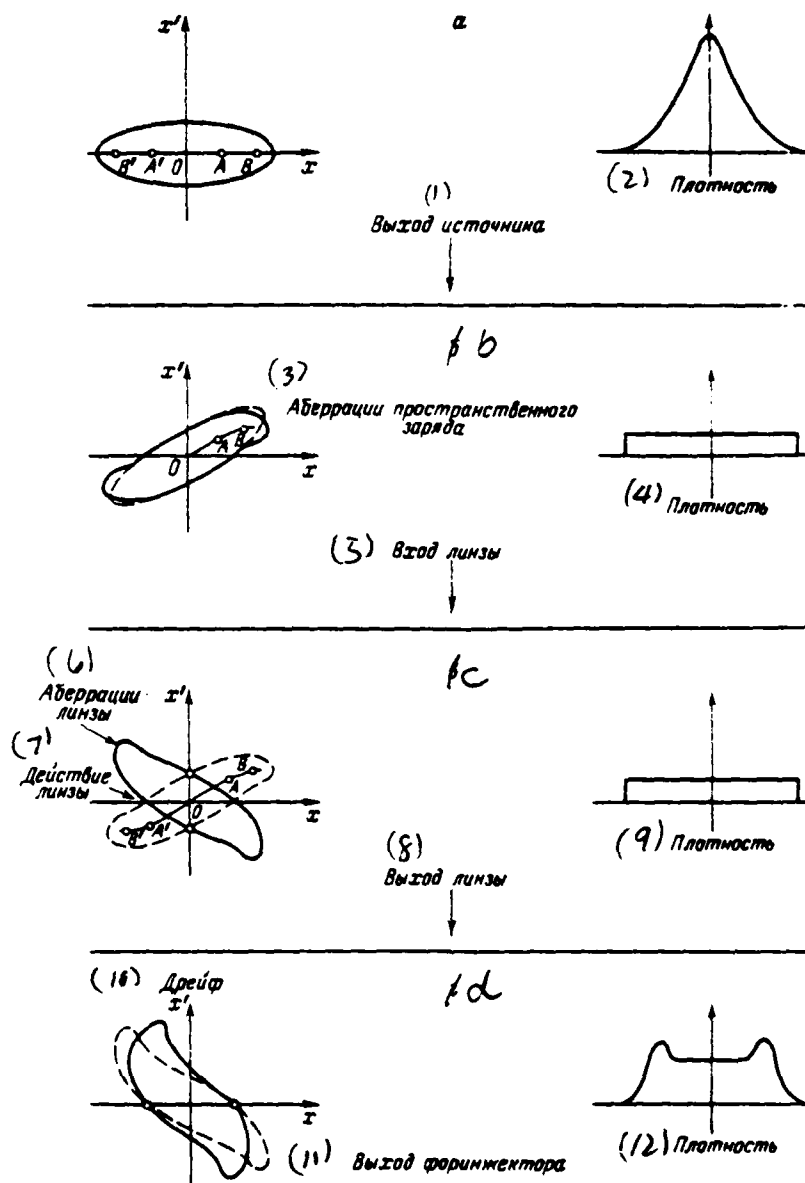


Fig. 5.

Fig. 4. Dependence $E=f(I)$ for the entrance of the focusing lens (100 kV) and the output of preinjector (750 kV) a) flat/plane initial distribution; b) initial distribution with the indentation in the center; c) Gaussian initial distribution.

Key: (1). mrad. (2). kV. (3). mA.

Fig. 5. Emittance and density distribution of beam in different sections of preinjector.

Key: (1). output of source. (2). Density. (3). aberrations of space charge. (4). Density. (5). entrance of lens. (6). aberrations of lens. (7). Action of lens. (8). output of lens. (9). Density. (10). Drift. (11). output of preinjector. (12). Density.

REFERENCES

1. I. Faure. The new Saturne injector status report on the 750 keV preinjector. Proceedings of the 1968 proton linear accelerator conference, Brookhaven, 1968.
2. P. Tanguy. CERN MPS LIN 70-1.
3. P. Lapostolle, B. Lapostolle. CERN-ISR-300/LI 69-43.

Page 110.

30. Intense pulsed operation of direct voltage accelerator.

Yu. Ya. Stavisskiy.

(Physics-energetic institute, Chniinsk).

In recent years in the investigations in physics of slow, intermediate and fast neutrons had extensive application the pulsed sources of neutrons on the basis of accelerators - linear electronic, synchrophasotrons, isochronal cyclotrons [1]. All these sources are characterized by the high average/mean neutron intensities (to $2 \cdot 10^{13}$ N/s), which have the wide energy spectrum, which stretches to tens of mega-electron-volts. There is special interest in use in the pulsed operations of the accelerators of the protons of the direct action (the electrostatic accelerators), making it possible to obtain the sharply limited neutron spectra, up to the noncenergetic ones, that open the wide circle of supplementary possibilities in the experiment. Unfortunately, the existing pulsed sources on the basis of direct voltage accelerators (see, for example [2]) they are characterized by relatively low average/mean intensities and considerably are inferior in terms of the quality factor $M = \bar{J}/\tau^2$,

where \bar{J} - average/mean neutron intensity.

Were made the estimations of the possibility of the realization of the intense pulsed operation of direct voltage accelerator (with the average/mean current of protons to 2 mA).

For the basis were accepted the cascade generator of the physical-energetic institute (Obninsk), developed by NIIIEPA im. D. V. Efremov whose design parameters provide for obtaining the continuous ion current of protons to 5 mA with the energy to 2.5 MeV (are at present in the alignment procedure obtained currents to 0.6 mA and stress/voltage to 2.2 MeV, stability on the stress/voltage 1 keV).

The advantages of cascade generator, together with the high average/mean current, are large powers for the supply of injector (10 kW) and possibility of oil cooling on the high-voltage side, which virtually removes/takes the appropriate limitations during the creation of powerful/thick injector.

During the estimations were examined the elements of the systems whose parameters were achieved/reached in the known works (ionic source of the type duoplasmatron to the current ~10 mA [3], accelerator tube kg-2.5, the system of magnetic grouping Mobile [4]).

The diagram examined provides for the interruption of the ion current of source (10 mA, 100 ns), klystron grouping before the acceleration (50 mA, 20 ns), additional grouping in accelerator tube (60 mA, 17 ns) and magnetic grouping on the target (~1a, 1 ns) with the neutralization of the volume charge of the cluster (see figure). Are carried out the evaluations of the effect of space charge on the radial and longitudinal sizes/dimensions of cluster in the process of its formation and passage through the accelerating and grouping system.

Comparative characteristics of the pulsed source of neutrons on basis kg -2.5, linear electron accelerator and isochronal cyclotron are given in the table.

459

(1) Ускоритель	Длительность импульса τ , нсек (2)	Частота повторения, Гц (3)	\bar{f} нейтр. сек (4)	(5) Эффективность	
				$M = \bar{f} k^2$	$M = 10,05 - 0,5$
(6) Линак	9	720	$26 \cdot 10^{12}$	$3,2 \cdot 10^{28}$	$3,2 \cdot 10^{27}$
(7) ИЦ Карlsruhe	1	$2 \cdot 10^4$	$2 \cdot 10^{13}$	$2 \cdot 10^{31}$	$5 \cdot 10^{29}$
КГ-2,5-И	1	$0,2 \cdot 10^6$	$2 \cdot 10^{12}$	$2 \cdot 10^{30}$	$2 \cdot 10^{30}$ 6

Key: (1). Accelerator. (2). pulse duration, τ , ns. (3). Repetition frequency, Hz. (4). neutr. s. (5). Effectiveness. (6). Linak. (9). ITS Karlsruhe.

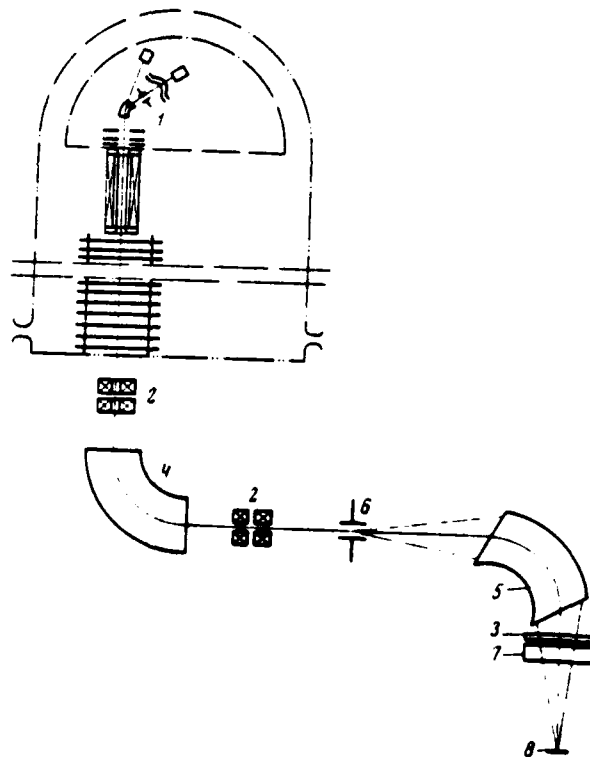


Fig. Diagram of installation CK-2.5-И. 1 - injector; 2 - quadrupole

DCC = 80069209

PAGE 17 460

lenses; 3 - astigmatic lens; 4 - analyzing magnet; 5 - Mobley grouping magnet; 6 - system of scanning/sweep of beam; 7 - neutralization system; 8 - target.

REFERENCES

1. Seminar for intense neutron sources. Santa-fe, September, 1966. PS 660925.
2. R. Maclin et al. Phys. Rev., 1964, N 136, B695.
3. L.J. Christensen, E.I. Zaharis. Rev. Scient. Instrum., 1966, 37, N 11.
4. K. Tsukada et al. Nucl. Instrum and Methods, 1966, v.39, p. 249.

Page 111.

31. Stabilization of the position of beam after the accelerating tube with the inclined field.

A. N. Serbinov, V. P. Yakushev, V. I. Mukhametshin.

(Physics-energetic institute, Chbinsk).

The use/application of the contemporary accelerating tubes with the inclined field requires the trajectory corrections of beam at output of tube [1]. In the smaller measure, but it is also necessary certain correction and in the perpendicular direction, mainly due to exchange or wear of the system of the extraction of ionic source in the process of work. Usually the correction is conducted automatically with the aid of the electronic devices and the feedback on the beam, i.e., is accomplished/realized the stabilization of the position of beam [2, 3].

On the accelerator IG-2.5, which works on the tube with the inclined field, is used the stabilization of the position of beam at output into the magnetic analyzer in two mutually perpendicular directions. Corrector has one pair of plates which deflects/diverts

beam in the "transverse" direction (i.e. in the direction of the inclination/slope of the electrodes of tube), and two pairs of the plates, which displace beam in parallel in the "longitudinal" direction (in the plane of magnetic analyzer). The length of deflector plates is 200 mm, the clearance between them is equal to 48 mm. The "longitudinal" pairs of plates are located from each other at a distance of 580 mm; between them is placed the pair of "transverse" plates. Corrector is arranged/located immediately after the accelerating tube. At a distance of 1650 mm from corrector and 300 mm from the entrance into the magnetic analyzer are established/installed four measuring sector plates, which form slots for the passage of the beam: 4 mm for "longitudinal" direction and 6 mm for the "transverse". From the plates is removed/taken the feedback signal. Due to the presence of magnetic quadrupole lens after magnetic analyzer the stabilization of the position of beam on measuring plates simultaneously provides the stabilization of the position of beam on the target.

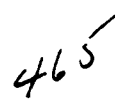
Electronics of both channels of stabilization is carried out identically. Fig. 1 shows the schematic diagram of differential amplifier and exit high-voltage cascade/stage, which feeds deflector plates. Limits of regulating for the beam with the energy 2.5 MeV are $\pm 4.8 \cdot 10^{-3}$ rad in "transverse" direction and ± 3.7 mm in the "longitudinal"; in the frequency of approximately/exemplarily 100 Hz.

General/common/total factor of amplification of entire system of approximately 25.

Fig. 2 depicts the regions of the permissible particle trajectories for of the "transverse" and "longitudinal" directions in the plane of the output of the accelerating tube with the energy 2.5 MeV. Region 3 relates to the plane of measuring plates with the smallest factor of amplification of system, which still provides the use of an amplitude range of device/equipment (5 for the "transverse" channel and 2.8 for the "longitudinal" with the energy 2.5 MeV); it characterizes the possible scatter of trajectories after measuring plates. With an increase in the amplification factor the linear component of region 3 decreases in so many cases. Thus, the use/application of stabilization of the position of beam expands the permissible region of trajectories at the output of the tube (this depends on corrector's amplitude range) and narrows the region of the scatter of trajectories in the plane of measuring slot at the entrance into the magnetic analyzer (depending on the general/common/total factor of amplification of entire automatic control system).

The device/equipment of stabilization makes it possible to measure the disturbance/perturbation of the trajectory of bundle with null method. An example of those observed during the work of the

accelerator of the static divergences of beam is given in Fig. 3: 1 - "longitudinal" even 4 - a "transverse" increase in the beam; straight lines are taken with a consecutive increase in the energy; the region: 2 - "longitudinal" even 3 - "transverse" mixings are obtained during the observation of the position of beam during the long time (approximately/exemplarily 3 sciths), when accelerator worked on the physical experiment with different ones of intensity and energy of beam without the replacement of the system of the extraction of ionic source.



465

465

465

465

beam by the tube with the inclined field and about the adjustment of magnetic analyzer.

Fast divergences of the position of beam are shown in Fig. 4a, and b. Against the general/constant/total background sharply are separated/liberated the greatest divergences which follow with the period of revolution of charging belt, i.e., after 0.27 s. In the "transverse" direction the rapid divergences do not exceed ± 1.5 mm, in the "longitudinal" ± 0.07 mm. In this case the energy of beam was equal to 1.1 MeV, but beam current on the target was 50 μ A.

The stabilization system of the position of beam successfully is operated on the accelerator BG-2.5 of more than a year, it is reliable, facilitates control of accelerator, does not require the interference of operator in entire range of energies 0.5-2.5 MeV. The use/application of stabilization of the position of beam increased the reliability of work of the accelerator as a whole, appeared the possibility to continue normal operation during the considerable displacement of frame at the output of tube, was eliminated need in this labor-consuming operation/process as the adjustment of magnetic analyzer after the replacement of the system of the extraction of ionic source. Appeared the possibility to constantly measure the beam displacement thus to follow the state of ionic circuit and to utilize this information for the adjustment of magnetic analyzer.

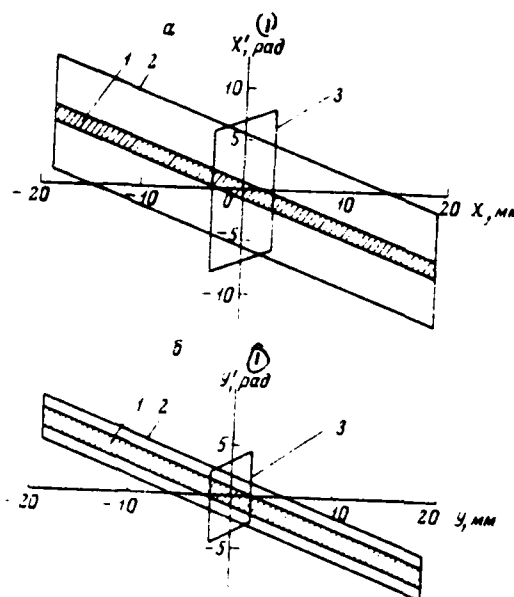


Fig. 2. Regions of the trajectories of bundle a) "transverse" direction; b) "longitudinal" direction. The permissible regions at the output of tube; 1 - without the stabilization of position; 2 - with stabilization of the position of beam; 3 - greatest region of the scatter of trajectories after slots.

Key: (1). rad.

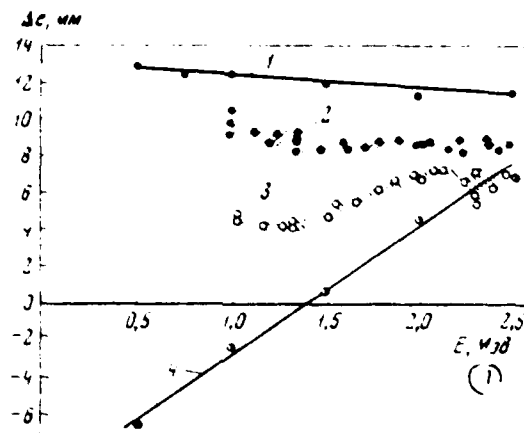


Fig. 3. Static divergences of beam after accelerating tube with inclined field.

Key: (1). MeV.

4-9

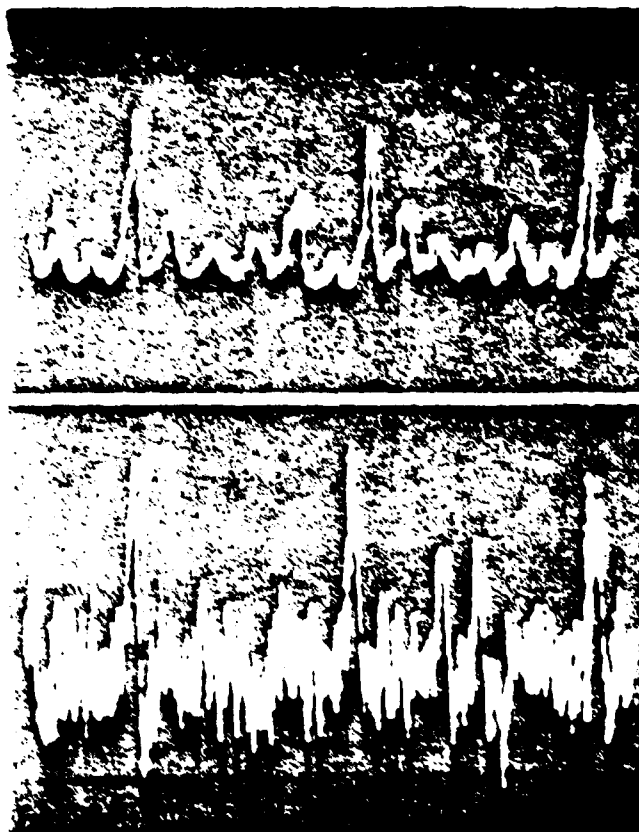


Fig. 4. Oscillograms of the rapid oscillations of beam a) "transverse" oscillations; b) "longitudinal" oscillations.

REFERENCES

1. A. N. Serbinov, V. I. Romanov. Accelerating tube with the inclined fields for the electrostatic accelerator. Author's. cert. No 177569. Bulletins of invent. and brands, 1965, No 1.
2. A. L. Evans, K. Johnson, Rev. Sci. Instrum., 1967, 38, No 10, p. 1911.
3. Richter, E. Exper. Tech. Phys., 1968, XVI, No 1, p. 8-17.

AD-A089 303

FOREIGN TECHNOLOGY DIV WRIGHT-PATTERSON AFB OH
TRANSACTIONS OF THE ALL-UNION CONFERENCE (2ND) ON CHARGED PARTI--ETC(U)
JUL 80 A L MINTS, A A KOMAR, A A VASIL'YEV
FTD-ID(RS)T-0692-80

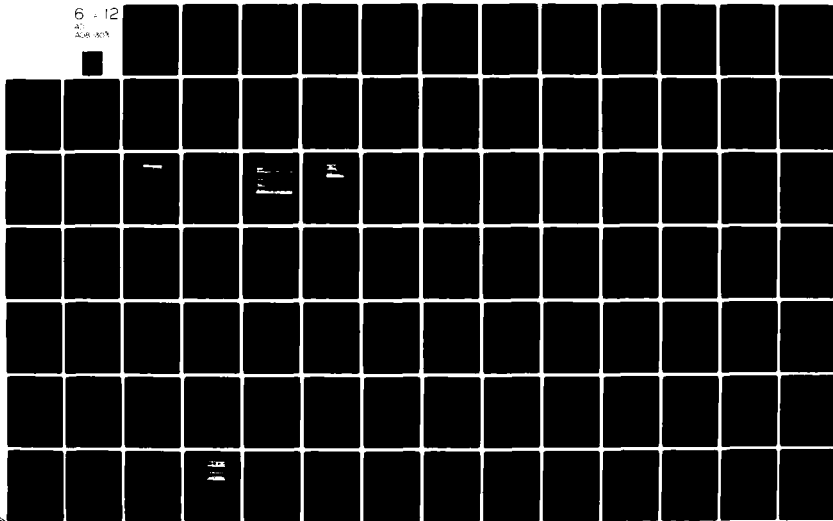
F/G 20/7

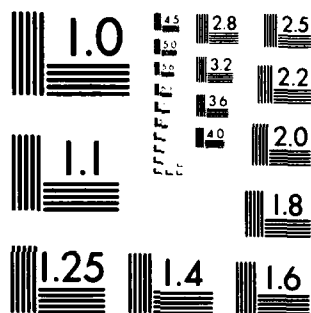
UNCLASSIFIED

NL

6 - 12

AD
208 207





MICROCOPY RESOLUTION TEST CHART
NATIONAL BUREAU OF STANDARDS 1963-A

Page 113.

32. Adjustment and operation of the electrostatic accelerator EG-1 of FEB in the pulsed operation.

V. I. Volodin, A. I. Glotov, M. I. Dudkin, V. N. Kanaki, V. N. Cononov, A. A. Metlev, V. A. Hcasncv.

(Physics-energetic institute, Charkov).

For the experimentation in to nuclear physics with the use of the time-of-flight method in the region of neutron energy of the order of kiloelectronvolt was developed pulse ionic source and was realized the translation/conversion of the electrostatic accelerator EG-1 into the pulsed operation.

Pulse ionic source.

Pulse ionic source consists of high-frequency ionic source, system of the formation of ion beam, system of interruption and correction of the position of beam on the diaphragm and electric power supply (Fig. 1) [1].

Formation system of ion beam was unipotential three-electron lens. The shaped ion beam had in the crossover a diameter of approximately 2 mm (for the ion current of approximately 1.5 mA and energy of ions 30 keV).

The interruption of ion beam was accomplished/realized on the tantalum diaphragm with the opening/aperture 2x2 mm, located in the plane of the focus of the forming system at a distance of 370 mm from the ion source. Before the diaphragm were established/installed two mutual perpendicular pairs of the deflecting plates with a length of 50 mm, to which were supplied permanent potentials for the correction of the position of beam on the diaphragm and right-angled surge voltage. The interruption of beam with the aid of the pulse rectangular stress/voltage allowed, in accordance with the requirements of experiment, it is independent to change over wide limits repetition frequency (to 700 kHz) and duration of the pulses of ion current (15-500 ns).

The oscillator circuit of the high-voltage square pulses of the stress/voltage, which was being utilized for the interruption of ion beam, is represented in Fig. 2. Oscillator made it possible to obtain the voltage pulses with the amplitude of 1 kV, with the duration of flat/plane apex/vertex 20-500 ns and repetition frequencies to 700 kHz with minimum porosity 20.

472

The minimum calculated duration of the pulses of ion current, determined by the velocity of the displacement of beam in the aperture plane and by the value of the front of the build-up/growth of the deflecting voltage (not more than 5 ns) for the data of the parameters of beam and geometry of the system of interruption was 10-12 ns. The total power, which was being consumed by the system of interruption, was 150 W.

The supplies of the rectifiers of pulse ionic source it was accomplished/realized from two insulated from each other of converters of the type GSA-1a (220V, 500 Hz, 750 VA).

Transportation of ion beam.

For conducting the physical experiments it was necessary to change energy of accelerated ions H_1^+ from 1.7 to 3.3 MeV.

The solution of this problem met the series/row of difficulties, since the crossover of ion beam should have been fixed/recorded at the level of the diaphragm of the system of interruption, and energy of the emerging from the source ion beam could not be changed over wide limits to avoid the decrease of ion current.

The hf ion source made it possible to obtain ion current H_i^+ of more than 1 mA with the flow rate of hydrogen of approximately 3.5 cm³/h. The high-frequency discharge in the quartz discharge chamber was excited by oscillator (100 MHz) with a power of 280 W.

Therefore the agreement of the optical properties of ionic source and accelerating tube was conducted a change in the distance of "P" [2] from the diaphragm of the system of interruption to the first working electrode of the accelerating tube. Within small limits the agreement could be conducted by a change in the energy of the entering the accelerating tube ion beam with the aid of a change in the electrode potential before the entrance into the accelerating tube.

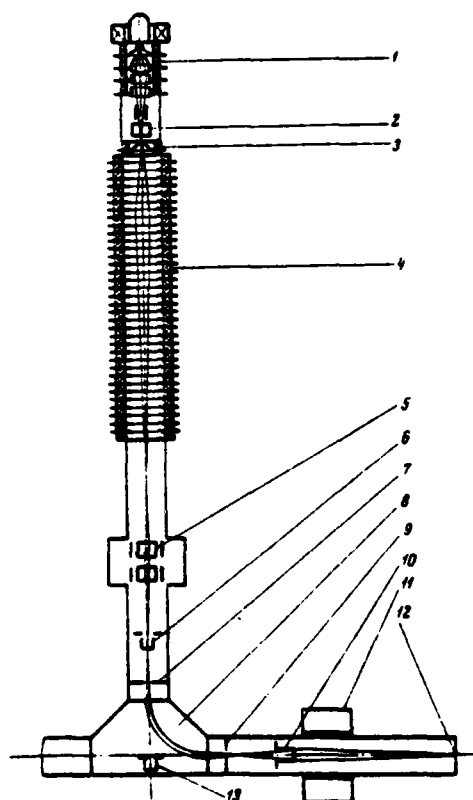


Fig. 1. Ion-optical system of accelerator EG-1 with the pulsed operation. 1 - ionic source and system of formation; 2 - system of interruption and correction of the positions of beam; 3 - dynode; 4 - accelerating tube; 5 - doublet of electrostatic quadrupole lenses; 6, 10, 13 - current-collecting devices; 7, 9 - slotted instruments; 8 - magnetic analyzer; 11 - doublet magnetic quadrupole lenses; 12 - target.

As a result of the fact that the accelerating tube gave considerable linear magnification in the sizes/dimensions of ion beam upon the entrance into the magnetic analyzer, after the accelerating tube was set the doublet of the electrostatic quadrupole lenses, with the aid of which was provided the satisfactory passage of the beam through the magnetic analyzer.

The calculation of system the doublet of quadrupole lens-magnetic analyzer [3, 4] was carried out in such a way that the crossover of ion beam would be arranged/located after the magnetic analyzer. Quadrupole lens was designed so that its location between the vacuum aggregate/unit and the accelerating tube would not reduce the speed of evacuation of the latter.

Visual monitoring of ion beam was accomplished/realized with the aid of the quartz targets, arranged/located on the distances of 1400 mm before magnetic analyzer and 1000 mm - after it.

The sizes/dimensions of the observed after analyzer beam did not exceed 5x15 mm.

For the beam shaping in the physical target, which was being located at a distance of approximately 3 m from the magnetic analyzer, was used the doublet of magnetic quadrupole lenses.

476

Conclusion/output of ion beam to the target.

The observation of the nonanalyzed ion beam was accomplished/realized at the quartz target before the magnetic analyzer. The control of mode of the operation of ionic source and system of the interruption of beam was supervised of form and value of the impulses/moments/pulses of ion current on the quartz target with the aid of oscillograph C1-8. On the oscilloscope face were observed the impulses/moments/pulses with the ratio of amplitudes 20:3:3, which corresponded to ions H_1^+ , H_2^+ , H_3^+ .

The evaluation of the effectiveness of the agreement of the optical properties of ionic source and accelerating tube was conducted according to the observed sizes/dimensions of ion beam and in the value of the impulses/moments/pulses of proton current.

After conducting of the measurements of the parameters of ion beam on the quartz target before the magnetic analyzer ion beam was formed/shaped with electrostatic quadrupole lenses first on the maximum average/mean ion current on the target, arranged/located in magnetic analyzer 13 (Fig. 1), and then on the maximum average/mean ion current H_1^+ on the quartz target after analyzer. Then proton beam

was focused by magnetic lens to the physical target.

Obtained results.

The amplitude of pulses of proton current, which was being measured on the physical target directly with the aid of oscillograph C1-11 and by the method of value measurement of the periodicity of impulses/moments/pulses and average/mean proton current, had a value to 1 nA.

The measurements of the duration of the pulses of proton current conducted with the aid of the time-of-flight method on Irina of the peak of γ -rays from reaction $\text{Li}^7(p,\gamma)\text{Be}^8$, showed that the minimum pulse duration was 15 ns with the amplitude of pulses 700-800 μA and pulse repetition rates to 700 kHz. Maximum duration of the pulses of proton current - 500 ns.

Fig. 3 depicts typical time/temporary neutron spectrum from reaction $\text{Li}^7(p,n)\text{Be}^7$ (thickness of target ~ 100 keV, the excess of energy of the protons above the threshold of reaction ~ 16 keV).

The relative content of ions H_1^+ from the ionic source composed more than 80% service life of of ionic source of approximately 1000 hours.

The translation/conversion of accelerator EG-1 into the pulsed mode made it possible to begin from the end/lead of 1969 the conducting of physical experiments with the use of the time-of-flight method. Are at the present time carried out the preliminary measurements of value of σ_{F}^{239} in the region neutron energy 20-100 keV.

In conclusion the authors express appreciation to Yu. Ya. Stavisskiy, on the initiative and with permanent support of whom was carried out this work, and to entire operational personnel of accelerator EG-1, who took active part in adjustment of accelerator for the pulsed operation.

References.

1. В.И. Володин и др. Результаты испытаний импульсного высокочастотного источника для ускорителя ЭГ-1. Доклад на рабочем совещании по наносекундной технике времени пролета. Обнинск, 1969.
2. M.M. Elkind. Rev. Scient. Instrum., 1953, 24, p.129.
3. Г.Р. Рик. Масс-спектрометрия. М., Атомиздат, 1963.
4. M.L. Bullock. Amer. J. Phys., 1955, 23, N 5, p.264.

479

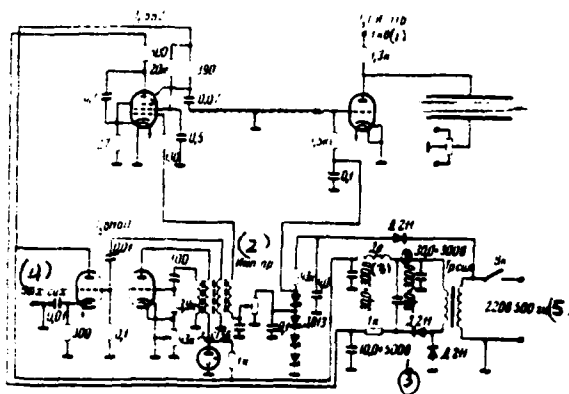


Fig. 2. Oscillator circuit of the high-voltage square pulses of stress/voltage.

Key: (1). kV. (2). Pulse rect. (3). V. (4). Cut. sikh. (5). Hz.

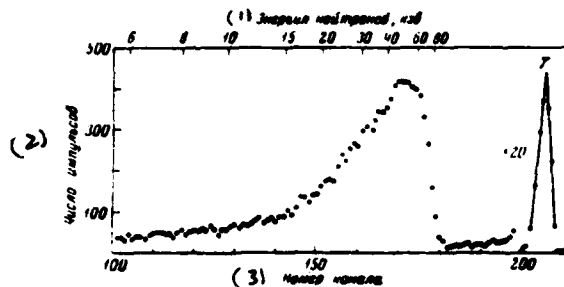


Fig. 3. Time/temporary neutron spectrum from reaction Value of channel 4.6 ns.

Key: (1). Neutron energy, keV. (2). Number of impulses/monenta/pulses. (3). Number of channel.

Page 114.

33. Electronic injector with the circular gun.

G. A. Babin, A. K. Dezhnev, V. S. Kuznetsov, N. P. Sybas, B. F. Fidel'skaya.

(Scientific research institute of the electrophysical equipment in. L. V. Efremov).

The purpose of this work is the investigation of the electronic injector, intended for the introduction/input of circular electron beam into the ion beam, which passes along the axis of injector.

Circular beam has a series/row of advantages before the continuous: 1) the perveance of circular beam by an order exceeds the perveance of continuous cylindrical beam [1, 2]; 2) the introduction/input of circular electron beam into the ionic to more easily carry out, than introduction/input of continuous cylindrical beam.

In connection with this was investigated the electronic injector in which are included the circular gun, which emits circular electron

beam on a radius to its axis/axis, and spherical capacitor/condenser SK, simultaneously focusing and turning electron beam at an angle of of 90° . The general view of electronic injector is given in Fig. 1.

The circular electron beam, which moves between the electrodes SK, has two radii of curvature: R - radius of curvature over arc of which moves the electron beam (mean radius SK), $(R_0 - R \sin \theta)$ - the mean radius of tubular bundle. In the latter/last relationship/ratio θ - the angle of rotation of beam, calculated off the beginning of SK (from the side of the anode). With $\theta=0$ the mean radius of tubular bundle is equal to R_0 .

Calculation was conducted for the thin-walled electron beam, i.e., for the case when $R_0 - R \gg \Delta r$, where Δr - thickness of beam.

Current per the unit of length in the circumference of ring it is equal to

$$i(\theta) = \frac{I}{2\pi(R_0 - R \sin \theta)}, \quad (1)$$

where I - the full current of beam.

The equation of action of the electrons of thin-walled circular beam in SK can be with a sufficient approximation/approach written analogously with the equation of strip/tape beam in the field of cylindrical capacitor with radii of electrodes of R_1 and R_2 , by

assuming that the current strength by the unit of the length of ring in this beam grows/rises in proportion to the rotation of frame in accordance with expression (1).

Then the equations of motion of boundary beam electrons can be written as follows:

$$\frac{d^2 r_1}{d\vartheta^2} = \frac{2}{r_1} \left(\frac{dr_1}{d\vartheta} \right)^2 + r_1 + C_1 (Dr_1^3 + 2\pi\rho r_1^5), \quad (2)$$

$$\frac{d^2 r_2}{d\vartheta^2} = \frac{2}{r_2} \left(\frac{dr_2}{d\vartheta} \right)^2 + r_2 + C_2 (Dr_2^3 + 2\pi\rho r_2^5), \quad (3)$$

where

$$D = \frac{U_{CK} - \pi\rho[(r_1^2 - r_2^2) + 2r_1^2 \ln \frac{r_1}{r_2} - 2r_2^2 \ln \frac{r_2}{r_1}]}{\ln \frac{R_2}{R_1}},$$

$\rho = \frac{i(\vartheta)}{v_{cp}(r_1 - r_2)}$ - density of space charge; r_1 and r_2 - radii of the trajectories of boundary beam electrons; v_{cp} - the average speed of electrons; U_{CK} - stress/voltage between the electrodes SK; U_k - stress/voltage, applied between cathode and anode of circular gun; $C_{1,2} = \frac{1}{2r_{0(1,2)}^2 U_k \cos^2 \alpha_{0,1}}$ - constants, which depend on initial radii of beam $r_{0,1}$, $r_{0,2}$ and angle of divergence of beam at the entrance SK $2\alpha_{0x}$.

In the computer were carried out numerical calculations in the following parameters of injector: $S_0 = 20$ mm, $R_1 = 15$ mm, $R_2 = 13$ mm, $U_{CK} = 500$ V, $U_k = 1750$ V, $I = 250; 500; 750$ mA.

Fig. 2a, gives the thickness of circular beam as function of

angle of rotation θ for three values of the beam current, parallel at the entrance in SK, and for the strength of current with which it is possible to disregard the action of space charge. From Fig. 2a it is evident that with the increase of currents from the value with which the action of space charge can be disregarded/neglected, to the currents with the large charge the focus at first is displaced from $\theta=67$ to $\theta=90^\circ$, and with further increase in the currents it decreases to 30° .

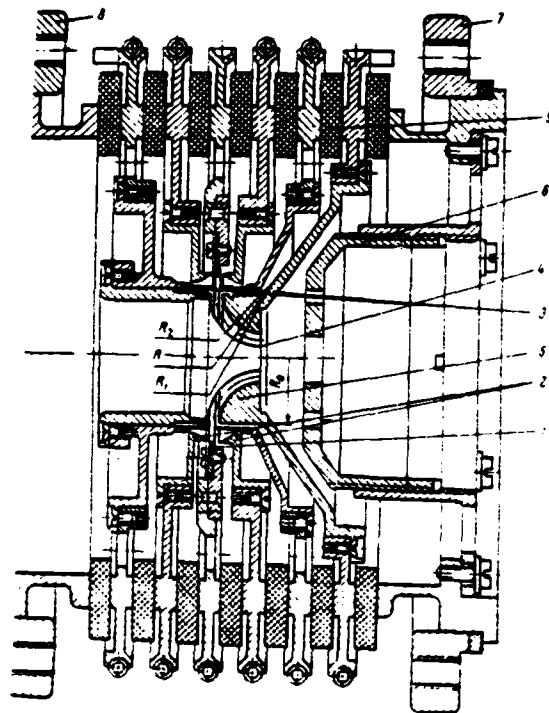


Fig. 1. General of electronic injector with the circular gun. 1 - circular cathode with the emitting coating from berber of lanthanum; 2 - internal electrode; 3 - anode; 4 - internal electrode of spherical cathode (SK); 5 - external electrode of SK; 6 - magnetic screen; 8 - flange; 9 - ceramic insulator.

Page 116.

Fig. 2. The dependence of the thickness of beam Δr on the angle of rotation: different angles of divergence of $2\alpha_{0m}$ at the

entrance in SK. In these all cases during the rotation in SK at an angle of $\theta=90^\circ$ is obtained parallel tubular beam.

Results of experiments.

The investigation of electronic injector was conducted in vacuum chamber at a pressure of residual gas not more $5 \cdot 10^{-5}$ torus. In the chamber/camera there was a movable dual collector/receptacle, which could be moved along and across the beam without the deterioration in vacuum. Collector/receptacle consisted of the basic collector/receptacle in center of which was the opening/aperture the diameter of 0.5 mm and supplementary collectors/receptacles, fastened/strengthened with the aid of the insulators behind the basic collector/receptacle opposite the opening/aperture. By basic collector/receptacle was measured the full current of beam minus the insignificant part of the current, which passed through the opening/aperture in it. With the aid of the supplementary collector/receptacle was made the measurement of density distribution of current according to the beam section.

In Fig. 3 is shown the electrical circuit of supply and measurement of the currents of electronic injector.

The given in Fig. 3 diagram does not permit directly measuring

the beam currents, which fall to the internal and external electrodes SK, due to the secondary-electronic emission from the internal electrode.

For determining the currents on the electrode SK by the measured currents I_2 and I_3 it is possible to utilize the following expressions:

$$I_4 = \frac{I_2}{\sigma - 1}; \quad (4)$$

$$I_3 = I_1 - \frac{\sigma}{\sigma - 1} I_2; \quad (5)$$

$$I_3 = I_3 - \frac{1}{\sigma - 1} I_2, \quad (6)$$

where I_4 - beam current to the internal electrode SK; I_3 - beam current to the external electrode SK.

When the electron beam of circular gun entire goes to the internal electrode, i.e., $I_3=0$, which occurs when $U_{CK}=0$, from expressions (5) and (6) let us find

$$\sigma = \frac{I_1}{I_2}. \quad (7)$$

Value, obtained from (7), close to value σ for the material of electrodes SK (tantalum).

Fig. 4 gives beam current I_4 on the basis collector/receptacle, and also beam currents to the internal and external electrodes of the spherical capacitor I_4 and I_3 in the function of stress/voltage U_{CK} . Maximum current flow of electron beam composes 800/c.

Fig. 5 gives the curves of density distribution of current according to the beam section, measured at a distance of 30, 60 and 90 mm from the output from the spherical capacitor. As can be seen from Fig. 5, at a distance of 30 mm the beam has well expressed circular form with the thickness of ring on the half the height of the amplitude of current, equal to 3 mm. In proportion to removal/distance from the injector in the beam occurs the redistribution of current and beam is converted into the continuous cylindrical, moreover the full/total/complete diameter of beam increases insignificantly, which is probable, it is caused by the presence of ion focusing.

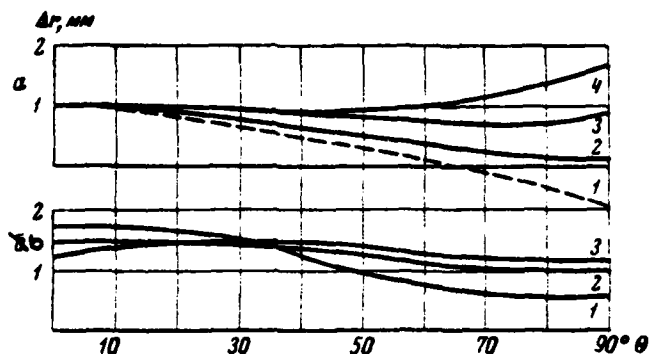


Fig. 2. Trajectory of the boundary particles of electron beam in the spherical capacitor. a) beam upon the entrance in SK parallel ($\alpha_{bz}=0$), 1 - beam current $I_n=0$; 2 - $I_n=250$ mA; 3 - $I_n=500$ mA; 4 - $I_n=750$ mA; b) beam with the different angles of divergence α_{bz} upon the entrance in SK in the beam current $I_n=500$ mA, 1 - $\alpha_{bz}=0$; 2 - $\alpha_{bz}=0.038$; 3 - $\alpha_{bz}=0.056$

489

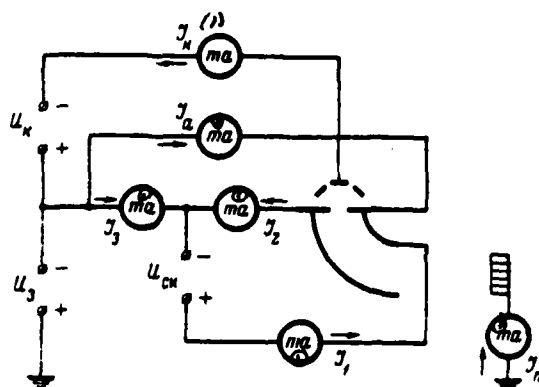


Fig. 3. Electrical circuit of electronic injector.

Key: (1). mA.

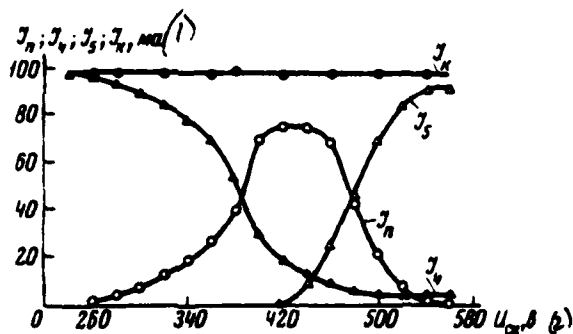


Fig. 4. Emission current I_k , removed from cathode, beam current I_n , beam current to internal electrode SK I_s , beam current to external electrode SK I_v , in function of stress/voltage U_{CN} with $U_K = 1000$ V in constant duty with $R_0 = 20$ mm, $R_1 = 15.5$ mm; $R_2 = 12.5$ mm.

Key: (1). mA. (2). V.

Page 117.

Thus, calculated method showed that the circular beam with the zero angle of divergence at the entrance into the spherical capacitor has a focus during the rotation to the angle θ , which changes over a wide range from 30 to 90° depending on the perveance of beam.

The results of experiments showed that in the circular beam during the removal/distance from the injector in the absence of magnetic field occurs the considerable redistribution of current, as a result of which the beam is converted in the continuous without a considerable increase in the maximum/overall diameter of beam.

Similar type electronic injector can be used in cyclic accelerators [3], and for certain treatment/processing - in direct voltage accelerators where the basic advantage of this injector lies in the fact that the cathode is shielded from the ion bombardment of high energies.

In conclusion the authors consider it their pleasant duty to express appreciation V. D. Lukinykh for the great assistance in conducting the experiments.

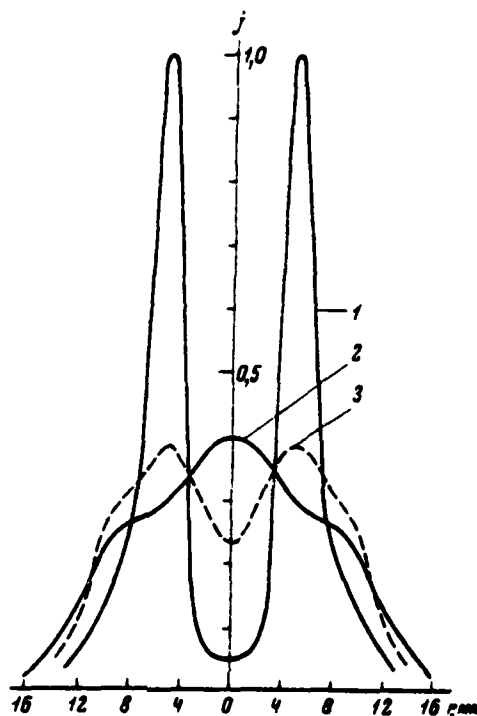


Fig. 5. Curves of density distribution of current according to the beam section in the constant duty with $U_k = 1000$ v, $R_0 = 20$ mm, $R_1 = 15.5$ mm, $U_{ch} = 20$ v, $I_n = 60$ mm, $R_2 = 12.5$ mm

1 - at a distance of 30 mm from the output of their spherical capacitor; 2 - at a distance of 60 mm; 3 - at a distance of 90 mm.

REFERENCES

1. Ye. G. Todd, G. R. Eryuer, M. B. Cramer. Sheveningen. The 4th international congress for the SHF instruments, 3-7 September, 1962.

DOC = 80069209

PAGE ~~55~~ 492

2. I. V. Alyanovskiy. Electron beams and electron guns. M., "Soviet radio", 1966.

3. G. I. Dimov. Bulletin of highest edcnl. instit., Physics, 1957, 1 pages 65.

34. Some special features/peculiarities of the work of cold cathode with high pressures of residual gas.

G. V. Dolbilov, V. P. Sarantsev, A. P. Sumbayev.

(Joint Institute for Nuclear Research).

Recently, in connection with the problems of the controlled thermonuclear fusions and new methods of accelerations, is amplified interest in a question of obtaining intense electron beams. The possible methods of solution of this task is the use/application of so-called field emissive diodes [1] and systems of straight/direct discharge or linear plasma betatron [2-4].

In the present work is investigated the behavior of point cathode with the high pressures of residual gas. The schematic of experimental installation is depicted in Fig. 1. Square-wave generator 1 in the operating modes being investigated had the low internal impedance, determined by register $R_1 \ll 4$ ohm. The duration of the pulse of stress/voltage was regulated by delay factor of controlling discharger/gap P_2 of pulse. Voltage on cathode 2 was checked the means of the active divider R_2-R_3 ; current in the system

was measured by Rogowski loop 3 and by coaxial shunt R_m . Pressure in cathode chamber/camera 4 and glass discharge tubes 5 with diameter of 12 mm and with a length of 30 cm was regulated by flow regulator 6. Working gas - helium. As cathode served the tungsten wire with a diameter of 0.5 mm. Any preliminary working of cathode it was not conducted. On other end/lead of discharge tube is arranged/located collector/receptacle 7, in which there was a narrow channel with a diameter of 3 mm and with a length of 10 mm. The energy spectrum of the electrons, which passed through this channel into high-vacuum chamber/camera 8, was investigated by electrostatic analyzer 9. Furthermore, were made the calorimetric measurements of the energy, isolated in collector/receptacle 7.

Fig. 2 gives oscillographs of the voltage on the cathode and the current from the faraday cylinder 10. The latter corresponds to the maximum of the function of energy distribution (see Fig. 3).

Page 118.

The oscillograms Fig. 2 are obtained at a pressure in the chamber/camera $\sim 5 \cdot 10^{-3}$ torr and durations of the pulse of voltage 400 ns. It is evident that the current of energetic/energy electrons appears after 200 ns after the inclusion/connection of voltage. Delay in the appearance of a current depends on pressure in the cathode

chamber/camera and decreases with the increase to 10^{-2} torus is inversely proportional to pressure. The amplitude of the current, taken from collector/receptacle 7, increases with an increase in the duration of the pulse of voltage and the pressure increase in the chamber/camera, and it is changed under our conditions from 10 to 10^3 A. The calorimetric measurements of the energy, isolated on the collector/receptacle, showed that the basic share of current was caused by energetic/energy electrons.

The function of the distribution of the electrons, which penetrate into chamber/camera 8, according to the energies is given in Fig. 3; voltage on the cathode 60 kV.

Fig. 1a depicts another version of discharge chamber. Cathode 2, short glass tube with 5 and heliow cylindrical anode 11 with the section/cut of lengthwise generatrix for observation of beam are placed into the volume with the adjustable pressure, the photographs of beam are given in Fig. 4, a-d. The beam, directed along the axis of system, drifted within the anode up to the distances to 30 cm. (see Fig. 4a) and it was upset to Faraday's cylinder 12 (Fig. 4aCh). Beam deflected from the axis/axis, was not upset to the anode, but it continued to drift, being reflected from the internal walls of the anode (Fig. 4b), or it was upset to Faraday cylinder (Fig. 4c). As working gas served helium. Photographs correspond to pressure in

chamber/camera $\sim 10^{-2}$ torr. The gas-focused beam in the transverse magnetic field behaved analogously with electron beam in the vacuum. Fig. 5 gives the photograph of beam in the field of the permanent magnet, arranged/located outside the chamber/camera. Energy of electrons, evaluated along the trajectory of bundle, comprises to the maximum of the function of energy distribution (see Fig. 3).

With the divergence of beam by external magnetic field on the axis of system for magnet there is noted the flow of the accelerated ions. Were recorded helium ions with the energy, by an order which exceeds energy of electrons. The amplitude of ion current reached by pore 10^2 a.

In conclusion it must be noted that the behavior of the electron beam, obtained from the point cathode at the elevated pressures of residual gas, in many respects is similar to the behavior of electron beams in the plasma, investigated in works [1-5].

497

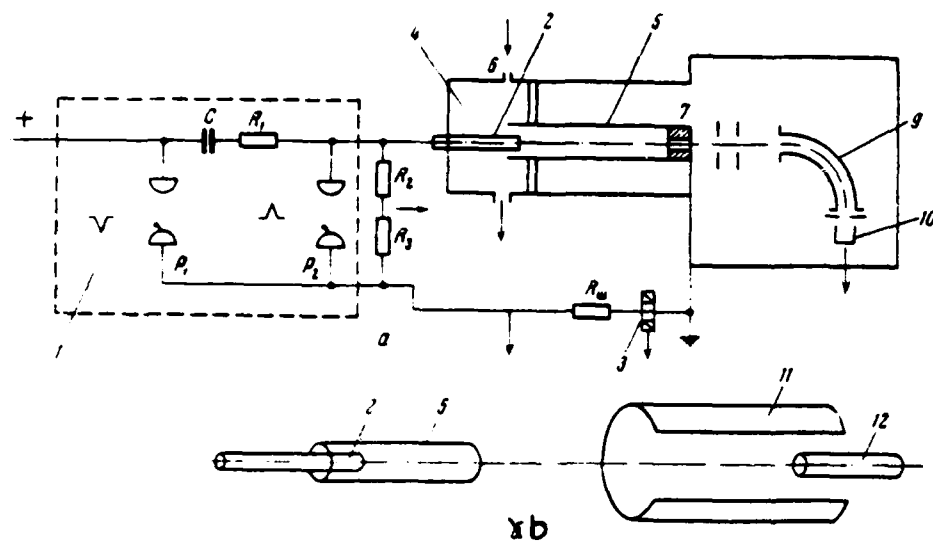


Fig. 1. Experimental installation. a) diagram; b) one of the versions of discharge chamber.

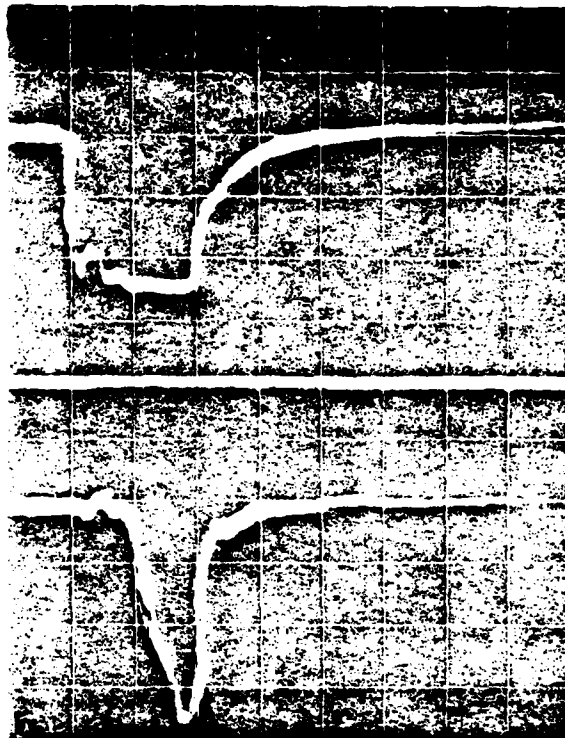


Fig. 2. Oscillograms of voltage on cathode (a) and current from the faraday cylinder (b). Sweep length 200 ns to the division.

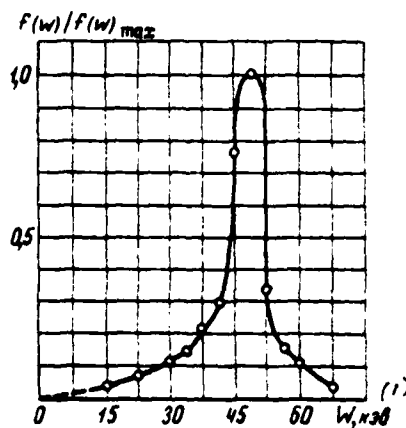


Fig. 3. Distribution of electrons, which penetrate into high-vacuum

DOC = 80069209

PAGE

~~57~~ 499

chamber/camera, according to energies. Voltage on the cathode - 60
kV.

Key: (1). keV.

Page 119.

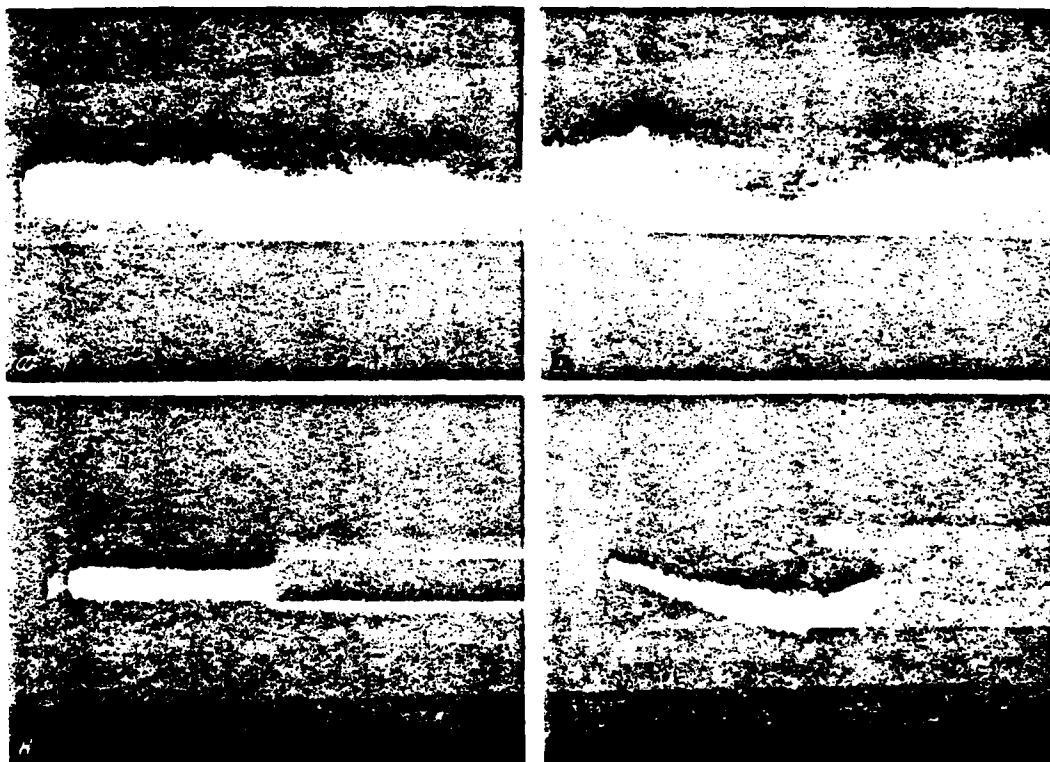


Fig. 4. Photographs of beam, which drifts within cylindrical anode.

501



Fig. 5. Photograph of beam in the transverse magnetic field.

REFERENCES

1. W.T. Link, Electron beam from 10^{11} - 10^{12} watt pulsed accelerators, IEEE Trans. on Nucl. Sci., 1967
2. A. B. Boya and E. M. Beykerudel'. ZhTF, 1961, 31, iss. 9, page 1127.
3. A. I. Karchevskiy et al. ZhETF [- Journal of Experimental and Theoretical Physics], 1970, 58, iss. 4, page 1131.
4. Ye. I. Lutchenko, Ya. B. Paynberg et al. ZhETF, 1969, 57, iss. 5, page 1575.
5. A. A. Plyutto et al. "atomic energy", 1969, 27, iss. 5.

35. Cathode-ray source of polyvalent ions.

V. A. Al'pert, Ye. D. Vetrobyev, Ye. D. Donets, V. I. Ilyushchenko.

(Joint Institute for Nuclear Research, laboratory nuclear reaction).

Introduction.

The urgent at present problem of the acceleration of superheavy ions (to uranium inclusively) can be solved by the development of the source of high(ly)-charge ions. Thus, for instance, for the large cyclotron of the laboratory of the nuclear reactions of the J.I.N.R. are required uranium ions with charge $+38$ - $+40$, and after its reconstruction into the accelerator in diameter of poles 4 m the required charge of ions will be lowered to $+24$. It is customary to assume that the available plasma sources of large ions cannot ensure the ion beams of such high charges. Therefore in many laboratories is conducted work on the development of the new types of the sources of high(ly)-charge ions [1-6].

Here are set forth the basic principles of the so-called cathode-ray source of polyvalent ions, being developed in the laboratory of the nuclear reactions of the J.I.N.S. Are examined the constructions/designs of experimental installations and the results of the investigations, carried out with their aid [7-11].

Method of ionization.

In the process of consecutive ionization can be achieved/reached the necessary charge of ions z , if is provided corresponding to this charge value of the product of the density of the flow of the ionizing electrons j to the period of interaction τ . It is obvious that

$$j\tau = \sum_{i=0}^{z-1} \frac{1}{\sigma_{i-i+1}},$$

where σ_{i-i+1} - ionization cross section of the positive ion of charge. For the approximate computation of the necessary values it is possible to use, for example, the relationship/ratio for σ_{i-i+1}

from work [12]

$$\sigma_{i-i+1} = \frac{C}{E_0 I_{i-i+1}} \ln \frac{E_0}{I_{i-i+1}},$$

where E_0 - energy of electrons; I_{i-i+1} - ionization energy of the ion of charge i ; C - constant.

Fig. 1 shows dependence of Z on values j with E_0 - the keV for uranium ions. From the figure follows that $Z=38$ corresponds $i=10^{20}$ cm⁻², i.e., in the use even of such high current densities of electron beam as 100 A/cm², the time of interaction must reach tenths of a second.

The such long times of interaction it is possible to provide, utilizing an effect of the natural sagging of electric potential in the continuous electron beam, caused by its negative space charge.

The negative space charge of electron beam quite widely is used for an increase in the ionization probability; beginning from the early works of Plumlee [13], and at present in the works of Redhead [14-17]. However, for obtaining of intense beams of highly charged ions it is hardly expedient to apply steady-state operating conditions, during which occurs the continuous admission of the atoms of work substance into the electron beam and the continuous extraction of ions under conditions for virtually full/total/complete space-charge neutralization of electrons by the space charge of ions.

To this target more corresponds the following method of operation [7]. In the space of ultrahigh vacuum is created the extended electron beam with an initial current density of j_0 . At the moment of time t_0 , for the short time interval Δt into the beam is introduced determined the time interval Δt into the beam it is introduced the specific number of positive univalent ions of work substance. The distribution of electric potentials along the axis/axle of bundle is such, that its terminal sections are plugs for the positively charged/loaded particles. Further at the moment of time t_1 , which can follow directly $t_0 + \Delta t$, the current density of electron beam increases to j_1 . In this case the amplitudes of the radial oscillations of those seized into the space of electronic ion

beam decrease. For the time from t_1 to t_2 occurs the ionization of the atoms of work substance to the necessary charge Z .

In this case, naturally, positive space charge increases, which leads to an increase in the amplitude of the radial oscillations of ions. A quantity of atoms of work substance and a multiplicity of ionization Z are selected by such that the amplitudes of oscillations at moment/torque t_2 would not exceed initial amplitudes at moment/torque t_0 . At the moment of time t_2 potential of one of the terminal sections of beam is made constantly (or periodically) by negative with respect to the potential of entire beam. In this case the ions leave trap in the axial direction and they can be used for the analysis or the acceleration. Process is repeated repeatedly. Fig. 2a shows the capture of ions into the electron beam, Fig. 2, b-g - method of the introduction/input of atoms into the beam of the building up density and conclusion/output of ions to the analysis and in Fig. 2d schematically depicts installation for the realization of the processes of those mentioned above.

Experimental installations IEL-1 and IEL-2 and results of measurements.

For testing the method of ionization examined was prepared the experimental installation IEL-1 (ionizer of cathode-ray) [8-11].

Electron gun with micro-perveance 0.95 is arranged/located within the shielded solenoid with the maximum magnetic intensity of approximately 4 kOe. Cathode from hexaboride of lanthanum rests on the tantalum disk in diameter of opening/aperture 2.5 mm. For guaranteeing the necessary emission is used the electronic preheating of cathode. At a distance of 2.5 mm from the cathode is located anode diaphragm in diameter of opening 3 mm. Further it is arranged/located drifting the tube, which is of five isolated/insulated sections in length 20, 20, 60, 20 and 20 mm respectively. In the wall of next-to-last section is an oblong hole of rectangular form, along which is arranged/located the spiral of the vaporizer/evaporator of work substance.

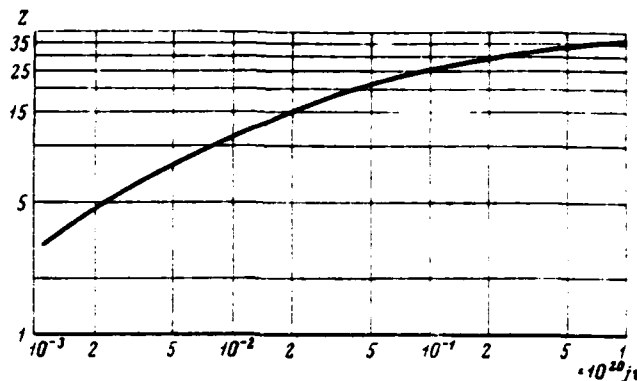


Fig. 1. Dependence of the multiplicity of ionization Z on the value of the product of the density of electron beam j (electron/cm²·s) to the period of interaction τ (s).

Page 121.

The latter/last section of the drift tube rests on the magnetic of bands, directly after which is established/installed the electronic collector/receptacle of cylindrical form. Is coaxially with the electronic collector/receptacle arranged/located ionic collector/receptacle or accelerating electrode of mass spectrometer on the time of flight.

The electrons, emitted by cathode and accelerated with anode potential, by intense magnetic field are formed/shaped into the beam which after the passage of drift tube and output from the magnetic field is recorded by electronic collector/receptacle.

The ions, which appear in the region of electron beam, can be held there, either be derived/concluded in the axial direction in the ionic collector/receptacle or for the analysis of the time of flight. For this are utilized the corresponding potential distribution in the sections of drift tube. The diagram of electrical supply provides the constant component of electronic current through IEL and powerful/thick current pulses with the voltage to 6 kV with the duration to 100 ns.

For guaranteeing the closing of ions in the region of electron beam in the latter/last section of drift tube are supplied pulses of the positive polarity whose parameters they can vary in the necessary limits.

Source works under conditions of ultrahigh vacuum.

The experiments, carried out on the installation IEL-1, showed that the method of ionization is realized. From the residual gas are obtained the ions to O^{+8}, N^{+7}, C^{+6} inclusively, and furthermore during the addition into the electronic atomic beam of gold are obtained ions to Au^{+19} .

After this was prepared second experimental installation (IEL-2) of considerably larger length (1 m) with the improved introduction system of work substance into the electron beam (see Fig. 2) and the considerably larger density of electronic current.

The first experiments, carried out on this setting up, showed that in the electron beam can be accumulated the ionic charge to 10^{11} elementary charges and it is brought out without the losses along the beam.

The calculations, based on the obtained experimental results, show that on the setting up IEL-2 upon transfer to the pulsed operation with the porosity, close to the unit, they can be obtained, for example, ion currents $Au^{+19}, U^{+24} \sim 10 \mu A$. The delivery/procurement of ions into the space between the dees of cyclotron can be realized along the electron beam.

One should indicate another possibility of using the ionizer of the type IEL, namely, for obtaining the large pulse currents of the polarized particles, for example, for the synchrocyclotron. Calculation shows that in the electron beam for the time between the cycles of capture it can be accumulated to 10^{12} polarized protons, the time of their conclusion/output from the beam can not exceed 50 μs . This, thus, is equivalent to the source of the polarized protons, which works in the continuous duty with intensity $\sim 2-3$ of mA.

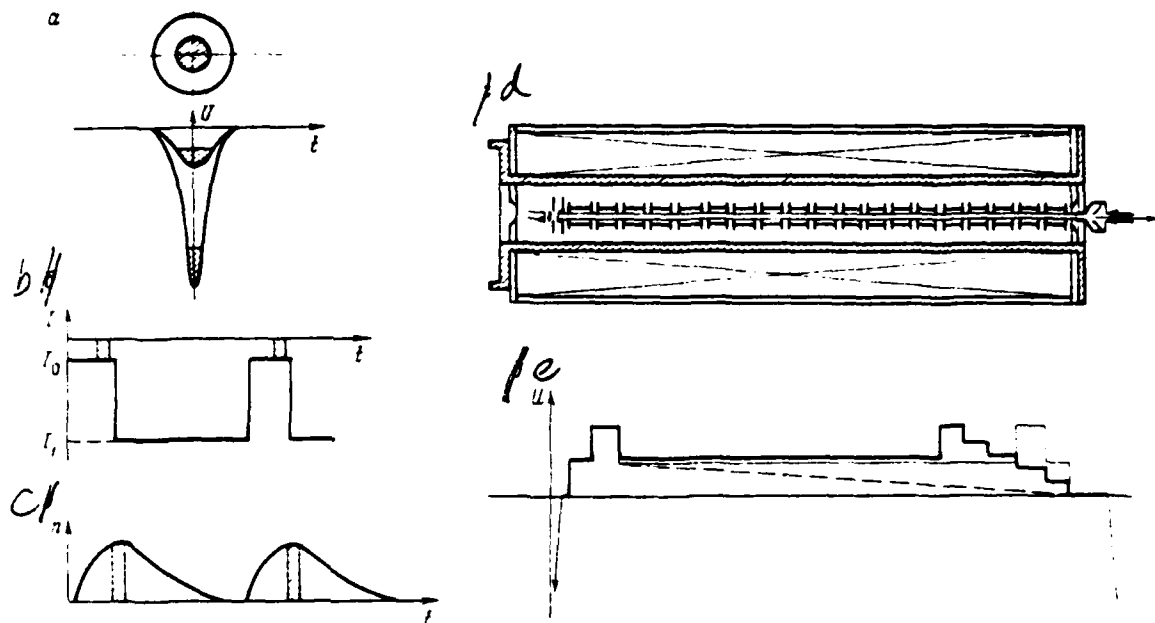


Fig. 2. Diagrammatic representation of the basic elements of installation IBL (d), the capture of ions into the electron beam (a), method of the input of the atoms of work substance into the electron beam and the output of ions to analysis (b-e).

REFERENCES

1. J.D. Paugherty, I. Grodzins, G.S. Janes, R.H. Levy, Phys. Rev. Letters, 1968, 20, 359.
2. J.D. Paugherty, J.E. Eninger, G.S. Janes, R.H. Levy, IEEE Trans. on Nucl. Sci., 1969, NS-16, N 3, 51.
3. V. V. Apollonov, Yu. A. Bykovskiy, I. N. Degtyarenko, V. P. Yelesin, Yu. P. Kozyrev, S. M. Sil'nov. Letters ZhETF, 1970, 11, 377.

4. T.H.Stix, Phys. Rev. Letters, 1969, 23, 1093.
5. T.H.Stix, Phys. Rev. Letters, 1970, 24, 135.
6. H. Postma, Phys. Letters, 1970, 31A, 196.
7. Ye. D. Donets. Authors cert. No 24886C. Bulletin of inventions, and brands, 1969, No 24.
8. Ye. D. Donets, V. I. Ilyushchenko, V. A. Al'pert. Preprint of J.I.N.R. 7-4124. Dubna, 1968.
9. Ye. D. Donets, V. I. Ilyushchenko, V. A. Al'pert. Preprint of J.I.N.R. 7-4469, Dubna, 1969.
10. Ye. D. Donets, V. I. Ilyushchenko, V. A. Alpert. Report at 1 international conference on the ionic sources. Saclay, 18-20 June, 1969.
11. Ye. D. Donets, V. I. Ilyushchenko, V. A. Al'pert. Theses of the reports of 1st All-Union conference on physics of electronic and atomic collisions. Riga, publishing house "Zinatne", 1969, page 52.
12. G.S.Jones, R.H.Levy, H.A.Bothe, B.L.Feld. Phys.Rev., 1960, 115, 925.
13. R.H. Pammel, Rev. Scient. Instrum., 1957, 28, 830.
14. P.A. Redhead, Canad. J. Phys., 1967, 45, 1791.
15. P.A. Redhead, S.Feser, Canad. J.Phys., 1968, 46, 867.
16. P.A. Redhead, S.Feser, Canad. J.Phys., 1968, 46, 1905.
17. P.A. Redhead, Canad. J.Phys., 1969, 47, 2119.

Page 122.

36. Sources of polyvalent ions with the cathode sputtering of work substance.

Yu. P. Trét'yakov, A. S. Pasyuk, L. P. Kul'kina, V. I. Kuznetsov.

(Joint Institute for Nuclear Research, laboratory of nuclear reactions).

The development of the source of multicharged ions with the cathode sputtering of work substance had as a goal to enlarge the assortment of the ions, obtained from the arched ion source with heating cathode [1.2].

The gas-discharge source of multicharged ions (m. z. i.) with the hot-cathode, in which is used arched discharge with the oscillation of electrons, during the the rainbow discharge with the oscillation of electrons, into course the number of years is used on cyclotrons of the laboratory of the nuclear reactions of the J.I.N.R. This source is most effective of the known sources m. z. i.

However, its use is limited to the elements, which have the gaseous connections/compounds (or connection/compound with the high vapor pressure in normal conditions.

For obtaining the polyvalent ions from the solid connections/compounds we developed source n. z. i. with the supply of working substance by cathode sputtering [3].

Construction/design of source.

The construction/design of source and its work are clear from Fig. 1. Source works in the magnetic field Cyclotron. Cathode 7, preheated by electronic flux with thread 6, emits the electrons which oscillate between the cathode and cooled anticathode 17, which are located by potential of cathode. Electronic flux ionizes the gas, which enters discharge chamber 16 (it is the anode) through channel 5 on tube with 9 of the stainless steel, as a result of which appears arched discharge. Electrode 13 of the pulverized work substance, fixed on cooled copper holder 12, is located under the negative potential. Under the action of the bombardment with the accelerated ions of plasma the electrode atomizes. Knock-on particles fall into the discharge and are ionized. The nourishment of cathode, anticathode and thread of source was achieved on the usual diagram of the nourishment of source n. z. i. [4]. The pulverized electrode was

connected to minus of the separate adjustable rectifier through the ballast resistance which in the sum with the internal impedance of rectifier was ~90 ohms. Maximum stress/voltage of rectifier 3 kV, current - 2a. The positive pole of rectifier was grounded through the non-inductive impedance by the value of 10 ohms from which was removed the oscillograph is the current pulse of electrode.

This construction/design of source has the following advantages: Into the discharge can be given the refractory substances with any melting point and the evaporations, which do not have gaseous connections/compounds.

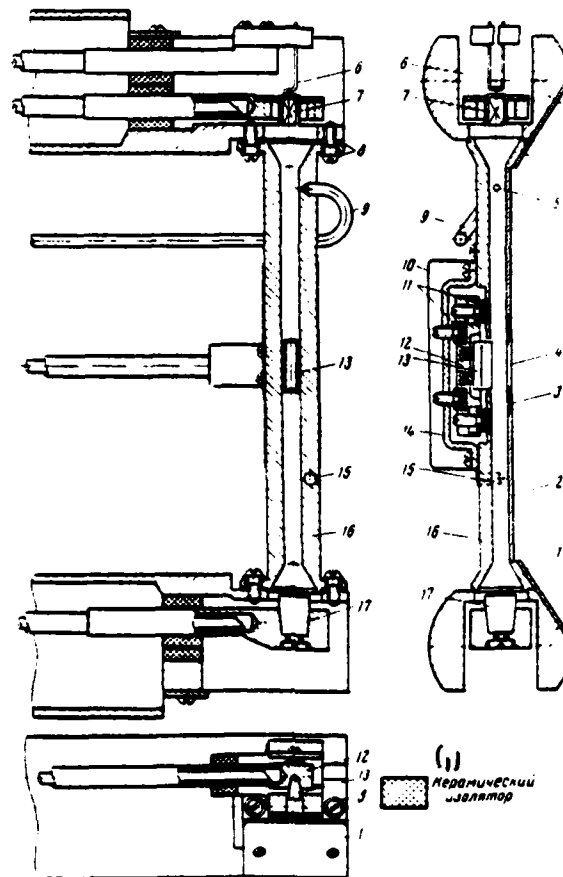


Fig. 1. Construction/design of the source of polyvalent ions with the cathode sputtering of work substance.

Key: (1). Ceramic insulator.

The dispersion of working substance of the ions of plasma occurs only during work impulse/momentum/pulse of source; in the pauses between the impulses/momenta/pulses the electrodes are not pulverized. The result of this is a decrease in the flow rate of substance with the larger porosity of impulses/momenta/pulses and the retention/preservation/maintaining dielectric strength of accelerating gap.

The autonomous nourishment of the pulverized electrode from the adjustable rectifier makes it possible to carry out the precise independent dosage of entering into the discharge of the atoms of work substance.

The arrangement/position of the pulverized electrode in the region of the emissive slot of source and the continuous feed of auxiliary gas lead to the localization of work substance (in the form of neutral particles and ions) in the place of the extraction of ions. Gas ions predominantly are located out of the region of the location of electrode. Therefore obtained from the source the ion current of work substance exceeds the ion current of auxiliary gas and composes 60-90o/o of the total current (see the Table).

For the purpose of a decrease in flow rate of substance with the work on calcium and zinc is developed the source with the hot

discharge chamber, heated by working discharge [5]. In this source discharge chamber 16 and its front/leading wall 2 are prepared from the stainless steel, insert/bushing 3 with emissive target 4 is prepared from the molybdenum. Chamber/camera is heat-insulated from the cooled stocks/rods with the aid of titanium washers 8. The temperature of chamber/camera is monitored by chromel-alumel thermocouple, placed into the nest of 15 chambers/cameras. The holder of atomized electrode is stopped up on insulators 11 between the rear wall of discharge chamber and clamp 14 of stainless steel. The position of the pulverized face of electrode relative to the post of discharge is regulated by screws/propellers. The parts of the setting up of electrode with enclosed casing 10 for averting the losses of substance. Molybdenum plates 1 will seal chamber/camera and stocks/rods from the fusion by the current of the secondary electrons which are knocked out from anode by ion beam.

Source is tested on the stand of ionic sources [2, 6] and on the cyclotron U -300 of the laboratory of nuclear reactions. With the work on stand the ions by extraction voltage 15-22 kV through emissive target by the size/dimension 1x15 mm. The separation of ions according to the charge to mass ratio was achieved in the uniform magnetic field by an intensity/strength 4 kOe with the rotation of beam on 180°. In the same field worked the source. Emissive target of source on the cyclotron had a size/dimension

2.5x12.5 of mm.

Results of experiments.

During the tests of source the stress/voltage on pulverized electrode was supplied after establishment of the mode/conditions of arched discharge on the gas (argon, or xenon) and operating temperature of discharge chamber. Type of gas was selected so that the relation charging to mass (Z_0/A) of its ions would not coincide in possibility Z_0/A of material ions of electrode, i.e., it did not interfere to measure magnitude of currents of these ions.

The voltage-current characteristics of gap/interval the pulverized electrode-anode during the constant mode/conditions of arc are given in Fig. 2.

Presence in the discharge of the material of electrode could be seen with respect to a change in the color of the discharge. Electrode during the work it was pulverized in essence on the face, in direction of the discharge.

(1) Рабочее вещество (2)		Ток ионов рабочего вещества по зарядностям в йм-пульсе, ма									(3) Сумма токов ионов рабочего вещества (7) ма % общего тока		Вспомогательный газ (4)	Режим источника (в импульсе) (5)			
z (6)	символ	1	2	3	4	5	6	7	8	9	(7) ма	% общего тока	(4)	U _d , в	I _d , а	U _{эл} , в	I _{эл} , а
12	Mg	18,4	84,9	31,8	3,0	0,4	0,08	0,005			140	77	Ar	660	7,5	520	2,0
13	Al	22,0	59,1	20,0	3,4	0,25	0,04				105	100	He	300	8,2	980	1,9
20	Ca	3,0	23	22	14	4,5	1,0	0,18	0,035		66	60	He	600	9,5	540	1,2
22	Ti	17,7	32	26,8	12,5	4,7	1,6	0,25*	0,04		95	60	Ar	400	15,2	930	3,4
29	Cu		29,8	31,7	35,3	26	6,8	1,9			150	70	Ar	540	10,0	400	2,3
30	Zn		69,8	54,7	29,34	9,49	3,95	0,76	0,2	0,024	168	93	He	400	7,5	560	1,6
42	Mo		24	24,8	23,3	16,8	9,4	2,0	0,4		100	90	He	380	9,5	940	1,8
73	Ta				11,4	18,9	12,5	8,4	3,0		54	65	Ar	470	9,8	970	1,5
74	W			20	17,1	13,1	6,8	3,3	0,7	0,12	61	65	He	380	9,0	980	1,4

Note. Here U_d - voltage of the arc of the discharge in the impulse/momentum/pulse; I_d - discharge current in the impulse/momentum/pulse; $U_{эл}$ - voltage on the pulverized electrode during the impulse/momentum/pulse; $I_{эл}$ - current to the pulverized

electrode in the impulse/momentum/pulse.

Current is shown approximately, precision determination prevented the imposition of peaks T_i^{7+} and N^{2+} .

Key: (1). Work substance. (2). Ion current of work substance on charges in impulse/momentum/pulse, mA. (3). Sum of ion currents of work substance. (4). Auxiliary gas. (5). Mode/conditions of source (in impulse/momentum/pulse). (6). symbol. (7). mA. (8). of total current.

Page 124.

By the intensity of the spectral lines of the radiation/emission of atoms and ions of the atomized substance is determined a relative change of the concentration of work substance in discharge with potential change on the electrode. Spectra were obtained with the aid of the quartz spectrograph ISP-28. In these experiments/experiences the flow of auxiliary gas, voltage and arc current remained constant. Under such conditions the intensity of line will be proportional to the concentration of corresponding particles [7]. The relative intensity of the spectral lines of calcium, copper and zinc almost linearly grows/rises with an increase in the voltage on the pulverized electrode. Were obtained also the spectrograms, which give

idea about the distribution of atoms and ions of calcium according to the height of the plasma column in the source. The results of the microphotometric working/treatment of spectral lines

CaI 8537.46Å, CaII 8508.03Å, and CaIII 8502.68Å are carried out in Fig. 3, from which it is evident that the location of neutral atoms and ions of calcium limited by the height by the location of the pulverized electrode. In the source with the hot discharge chamber the width of the distribution curve of the intensity of calcium lines according to the height somewhat more than in the source with the cooled discharge chamber. But also here the zone of the propagation of calcium is considerably less than the height of the post of discharge.

It is possible to assume that the ions depart to the walls of discharge chamber more rapid than to the cathode and anticathode along the magnetic field. This phenomenon is connected/bonded, probably, with the "anomalous diffusion" of the plasma of the positive column of discharge across the magnetic field, which can be caused by low-frequency plasma oscillations.

On the stand were measured the ion currents of different charge nine strongly differing in the atomic weight and the structure of metals - from magnesium to the tungsten. The pulverized electrodes were prepared from the technical material, special measures for purification it is not accepted. length of work

impulse/momentum/pulse of source was 1 ns, pulse frequency - 100 Hz. The diagram of the currents of the polyvalent ions of calcium, written down by writer EPP-09, is represented in Fig. 4. The results of the measurements of currents from the source with the cooled discharge chamber are given in table (are shown summed currents in the impulse/momentum/pulse of all isotopes of the element being investigated).

Were obtained output curves of the polyvalent ions depending on the parameters of the discharge in the source. The dependences of the current of polyvalent ions of zinc from the potential on the pulverized electrode they were shown in Fig. 5.

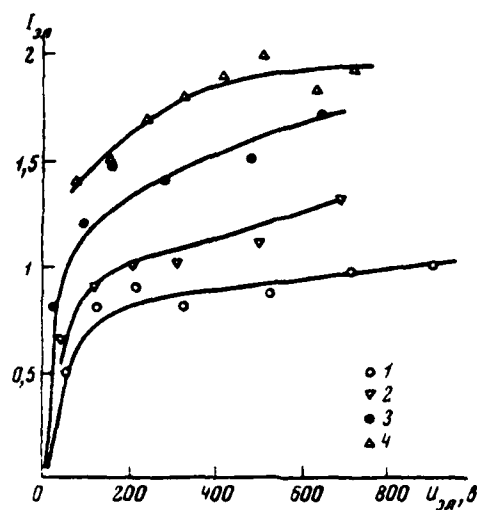


Fig. 2. The voltage-current characteristics of gap/interval the atomized electrode-anode.

(1) Обозначение	(2) Материал электрода	Ток дуги, (3) а	(4) Напряжение дуги, в
1	Ca	5	750
2	Ca	9	700
3	Ca	15,5	670
4	Zn	6	600

Key: (1). Designation. (2). Material of electrode. (3). Current of arc, A. (4). Voltage of arc, V.

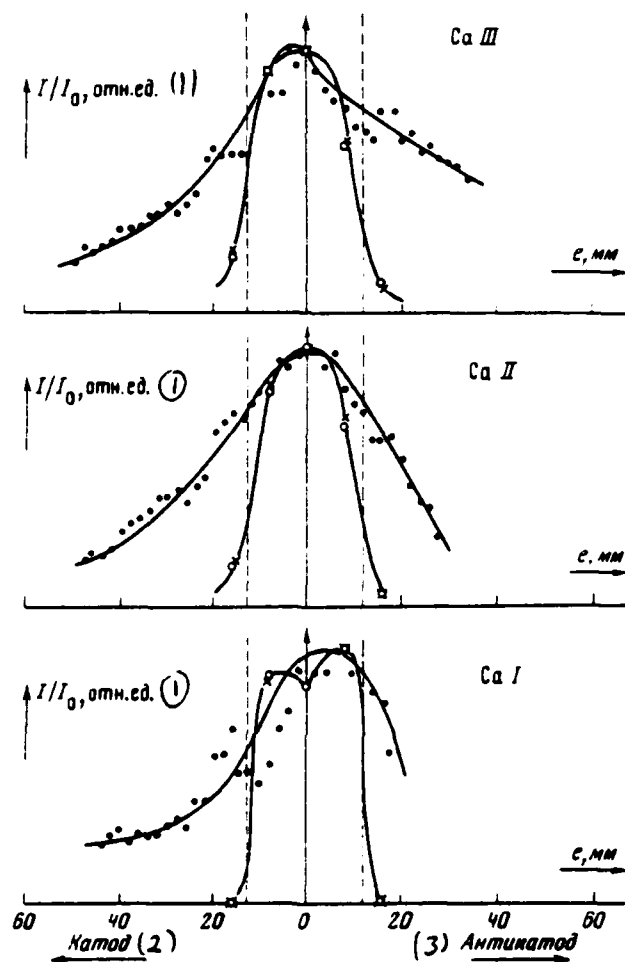


Fig. 3. Change in the relative spectral line strength of atoms and ions of calcium along the gas-discharge chamber/camera. 1 - dispersion of calcium in the cooled chamber/camera, supply of auxiliary gas (xenon) into the region of cathode; 2 - dispersion of calcium in the cooled chamber/camera, simultaneous supply of xenon into the region of the cathode and anticathode; 3 - dispersion of

calcium in the hot chamber/camera. Dotted line showed the boundaries of the pulverized electrode.

Key: (1). rel. un. (2). Cathode. (3). Anticathode.

Page 125.

Arc current and voltage on it remained constant. A change in atom concentration of the atomized substance so affects output n. z. i. as a change in the feed rate of gas into the discharge chamber.

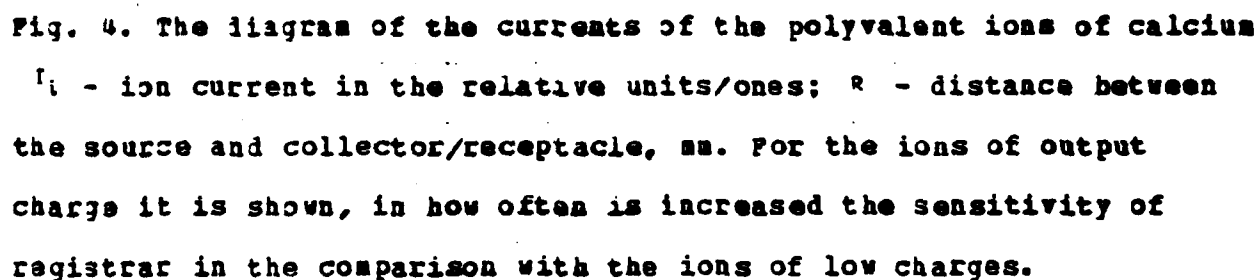
The dependences of output n. z. i. on current and voltage of arc at the constant values of other parameters did not differ in the nature of curves from the same dependences, measured with the work of source on gases [2].

On the cyclotron U-300 were accelerated seven- and eight - charge ions of calcium. Average/mean ion current Ca_{40}^{7+} on a radius of 100 cm was 3 μA , ion current Ca_{40}^{8+} 0.4 μA . Source with the fixed/recorded position of the pulverized electrode from calcium on the cyclotron U-300 worked 5-6 hours without a significant decrease in the intensity of the ion beam of calcium.

During the work on the stand of source with the cooled discharge

chamber the electrode consumption from calcium was approximately 100 mg/h, from zinc - 150-200 mg/h. Heating discharge chamber made it possible to shorten the consumption of drops and zinc by an order in comparison with the source with the cooled discharge chamber. Expenditure/consumption of calcium in this source constituted 11 mg/h, zinc - 17-20 mg/h.

In the bench tests the source with the hot discharge chamber worked for 8 hours without electrode travel, then electrode was removed/taken for the weighing. Electrodes were used repeatedly, but after each weighing holder approached a discharge chamber for the setting up of electrode to optimally the position.



Key: (1). rel. un.

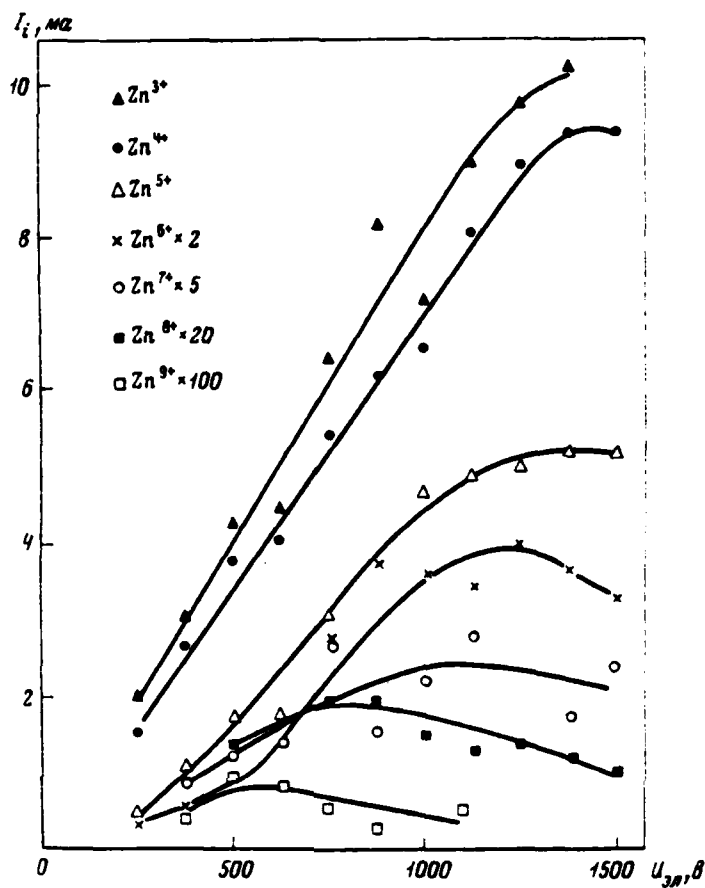


Fig. 5. dependence the current of the polyvalent ions of copper and zinc from the voltage on the pulverized electrode. Mode/conditions of the discharge: $U_A = 600$ V; $I_A = 9$ A.

Page 126.

REFERENCES

1. P. M. Morozov, B. N. Makov, M. S. Joffe. The "atom energy", 1957, 2, 272.
2. A. S. Pasyuk, Yu. P. Tret'yakov, S. K. Gorbachev. "Atomic energy", 1968, 24, 21.
3. Yu. P. Tret'yakov, A. S. Pasyuk, L. P. Kul'kina, V. I. Kuznetsov. Preprint of J.I.N.R., R7-447, Dubna, 1969.
4. A. S. Pasyuk, I. A. Shelaev, Go Tsi-Tsyan', Yu. P. Tret'yakov. PTE, 1963, No 5, 23.
5. A. S. Pasyuk, Go Tsi-Tsyan', Yu. P. Tret'yakov. Preprint of J.I.N.R., 1523, Dubna, 1963.
6. L. P. Kul'kina, A. S. Pasyuk. ZhTF, 1966, 36, 726.
7. Yu. P. Tret'yakov, L. P. Kul'kina, V. I. Kuznetsov, A. S. Pasyuk. Preprint the J.I.N.R., R7-5004, Dubna, 1970.
37. Experimental Study of the parameters of autoelectronic gun.

R. M. Voronkov, V. A. Danilichev, B. Yu. Bogdanovich, V. F. Gass.

(Radio-technical institute of the AS USSR, Moscow physical engineering institute).

In the works of U. P. Dike [1] and M. I. Yedinson [2] were noted the very advantageous conditions for the work of autoelectronic cathode in SVCh field. The studies, which were being carried out by V. P. Gass [3], they showed expediency and prospect of use of autoelectronic gun with SVCh by nourishment as the injector of linear electron accelerator. In this work are given the description of device/equipment and the results of measuring parameters of the beam of the autoelectronic gun, intended for the injection of electronic clusters with phase width of $30+40^\circ$ and energy 300-400 keV into accelerating section with a constant phase speed, equal speed of light and with the strength SVCh of field of approximately 100 kV/cm.

The construction/design of gun is shown in Fig. 1. Resonator 1, calculated for the length 16.5 cm, is prepared from copper of brand MB., their own of Q-factor of approximately 6000. With the aid of flexible wall 2 the resonance frequency can be reconstructed in limits of $\pm 5\%$. Autocathode 3 is prepared from the tungsten wire of high cleanliness and is fastened/strengthened in the resonator so that it is possible to temper by forward current to temperature of

1000-2000°C. Points in radius of bending 6-10 μm were manufactured with electrochemical etching in the 10% solution of KON.

For decreasing the divergence of electron beam is used the focusing system, formed by coils 4 and 5 and magnetic circuit 6. On the output from the anode opening/aperture, which has the diameter of 12 mm, the beam is intercepted by the cylinder of Faraday 7 with the water cooling.

Vacuum evacuation was achieved by two electric discharge pumps. One of them type "Nord 10" is connected with the cavity of resonator by short branch pipe, and by the second of the type "Nord 100" - with the input waveguide by section 120x57 mm. During the first experiments the pressure in the resonator was in limits $(2-5) \cdot 10^{-6}$ torus. Before beginning work was produced tuning resonator and agreement to $K_{SVN}=1.1$.

Block diagram of device is shown in Fig. 2. A klystron amplifier of the type 15015 worked with the duration of pulse 5.5 μs and repetition frequencies of pulses 7 Hz.

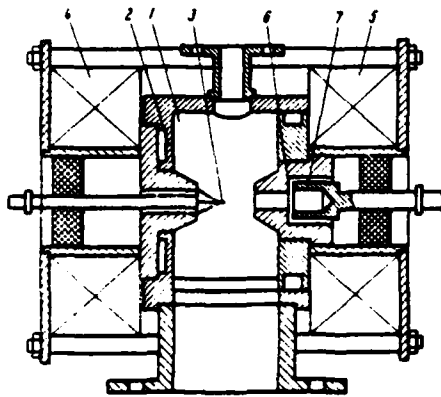


Fig. 1.

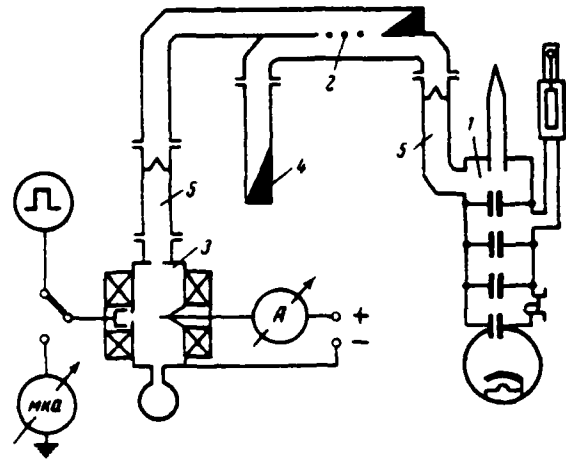


Fig. 2.

Fig. 1. Construction/design of gun. 1 - resonator; 2 - flexible wall; 3 - cathode; 5, 4 - coil; 6 - magnetic circuit; 7 - Faraday cylinder.

Fig. 2. Block diagram of setting up. 1 - klystron; 2 - the directional coupler; 3 - gun; 4 - water load; 5 - window.

Page 127.

Its output power was regulated in the limits of 2-15 MW. With aid of directional coupler 2 100% of power it was sent for gun 3, and major portion of the power was absorbed by water load 4, replacing the entrance of the accelerating section. The plumbing, filled with

nitrogen under the pressure 5 atm, is isolated from the vacuum of klystron and gun by ceramic windows 5.

Fig. 3 shows the curve of a change in the intensity/strength of focusing magnetic field H along the length l of gun, taken/removed by instrument IMI-3 with the remote cathode and the faraday cylinder. As the reference point of length is accepted the rear wall of resonator.

Fig. 4 gives family of curves, which show the dependence of the pulse value of beam current J_b , falling to the cylinder of Faraday, from the currents in focusing coils (J_k - current in the coil on the cathode, J_ϕ - current in the coil on the cylinder of Faraday). Curves are taken with SHF power, introduced into the gun, $P_{\text{in}} = 1.05$ MW. The measured value of average/mean current was recounted into the pulse value through the porosity, equal to 28500. Upper knee of curve, apparently, is explained by the fact that practically all electrons, emitted by cathode, begin to penetrate anode-with the opening/aperture of gun to the Faraday cylinder.

Fig. 5 shows the dependences of the pulse beam current J_b and medium energy of electrons ϵ on input SHF of power P . The medium energy of electrons was determined by the method of dividing the average/mean power, by defined beam on the Faraday cylinder, to the

average/mean beam current. The average/mean power of beam was measured by calorimetric method with the calibration according to the replacement scheme.

For obtaining the preliminary idea about the stability of the parameters of gun in time and about possible life of autocathode was carried out the girder/drive of gun during the workday (about 7 hours). During the girder/drive approximately one in the hour it was produced measurements J_0 and ϵ , whose data were given in Fig. 6. In these measurements the average/mean power of beam was determined calorimetrically with the running water without the calibration on the diagram of replacement that, possibly, led to somewhat high values ϵ in comparison with the data of Fig. 5. Taking into account the low accuracy of measurements, it is possible to consider it J_0 and ϵ during the girder/drive practically unchanged.

All measurements were carried out with one autocathode, which studied on the whole more than 20 hours. Maximum value J_0 , which was being controlled the time of testing, was equal to 1.3 and (average/mean current - 46 μ A). With the inspection of cathode under the microscope after the development of the gun of noticeable changes in its geometry it is not discovered. During the repeated setting up of cathode into the gun its parameters remained practically constant.

The authors express gratitude to G. A. Rudintsev for the aid in organization of the technology of the production of autocathodes, and also to A. F. Ivanov for the fulfillment of complex and fine limit work on the assembling of gun and setting up for its study.

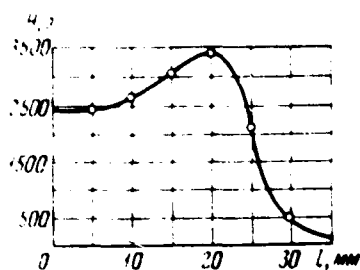


Fig. 3.

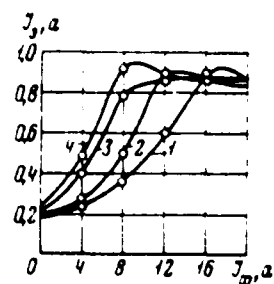


Fig. 4.

Fig. 3. Change in strength of focusing magnetic field N along the length l of gun.

Fig. 4. Dependence of beam current J_b on current in focusing coil on Faraday cylinder J_ϕ at different values of current J_k in coil on cathode: 1 - $J_k = 2$; 2 - $J_k = 10$ A; 3 - $J_k = 20$ A; 4 - $J_k = 25$ A.

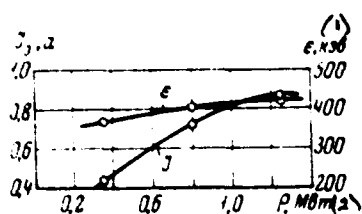


Fig. 5.

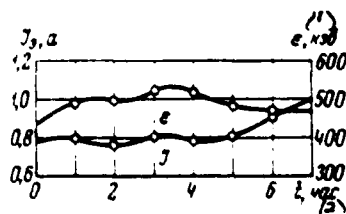


Fig. 6.

Fig. 5. Dependence of beam current J_b and medium energy of electrons ϵ on input SHF power P .
Key: (1), keV. (2), MW.

Fig. 6. Change in beam current J_b and medium energy during

girder/drive.

Key: (1). keV. (2). hour.

REFERENCES

1. W.P. Dyke. IRE Trans, 1960, Mil-4, 1, 38.
2. M. I. Melinson, M. A. Gor'kov. / "Radiotekhnika i elektronika", 1961, 4, 2, 336.
3. V. N. Gass. In the coll. "Uskoriteli" [accelerators], issue 4. M., Atomizdat, 1962, p. 22.

Page 128.

38. Formation of powerful/thick ion beams by brush-type electrodes.

O. Ya. Savenko.

(Institute of nuclear physics of SO AN USSR [CO AN CCCP) - Siberian Department of the Academy of Sciences of the USSR)).

The ion current, formed/shaped from the plasma with the system of usual electrodes, is limited usually to the space charge of beam. For decreasing the influence of the effect of space charge by us was used electrodes in the form of two fine mesh grids [1-3]. The first grid was found under the positive potential of plasma, the second grid was grounded. Distance between cells was much more than the size/dimension of cell and much less than the diameter of grid fabrics/beds. Therefore this system forms/shapes almost parallel ion flow. The second grid, as a rule, was connected with the metal tube,

in which, because of the overlap/allowance of aza, were created the conditions for almost full/total/complete space-charge neutralization of beam. Therefore the effect of space charge occurred only in the small volume of intergrid gap/interval. In the optimum mode/conditions of beam shaping the plasma did not penetrate the intergrid gap/interval: plasma "was resolved" by electric field near the first grid at the depth of the order of the sizes/dimensions of cell (Fig. 1). The terminal radius of the curvature of boundary of plasma, the heterogeneity of electric field near the cells of the first grid cause divergence of beam. For the evaluation of this effect were used the brush-type electrodes in the form of parallel nickel wires in diameter 0.05 mm and step/pitch 0.25 mm. The diameter of the fabric/bed of grids was changed from 8 to 37 mm, the distance between the grids was about 4 mm. In assence were investigated the proton beams in which of this effect was detected according to the distribution of intensity in beam H^- , H^0 and H^+ . Fig. 2 gives the distribution of intensity in the ion beam H^- in the direction lengthwise (unbroken curve) and across (dashed curve) to the direction of filaments first grid. Detector is arranged/located at a distance about the meter from the place of beam shaping, the initial diameter of beam - 8 mm. As it follows from this figure, the divergence, caused by the field of the first grid, is commensurated with the isotropic part of the divergence and is approximately 0.015 radians. The anisotropic part of the divergence weakly depends both

on the current in the beam and on interelectrode voltage, but strongly it depends on intergrid distance. The isotropic part of the divergence of beam (caused, apparently, by the thermal energy dissipation of protons, selected/taken out of the plasma) in the optimum mode/conditions does not depend on the conditions for beam shaping.

The selected by us method of space-charge neutralization with use of a gas target gives, apparently, almost full/total/complete space-charge neutralization of beam in the space after the second grid. This assertion illustrates Fig. 3, in which is shown the dependence of proton beam current on the selection of protons from the plasma at different pressures of hydrogen in the tube. From the figure one can see that at pressures of above $4 \cdot 10^{-3}$ mm Hg up to proton currents 1 and remains the linear dependence of the strength of ion current from the selection of ions from the plasma (unbroken curve). The diameter of beam is equal to 37 mm. Calculations give, that the degree of the undercompensation of this beam was not more than 0.10/o. However, if we decrease the gas pressure in the tube to 10^{-3} mm Hg, then proton current sharply decreases, the linear dependence of current in the beam on the value of the selection of protons from the plasma will disappear (dashed curve in Fig. 3). Rough estimate according to these effects gives the value of undercompensation $\sim 0.50/o$.

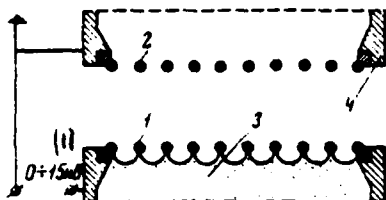


Fig. 1.

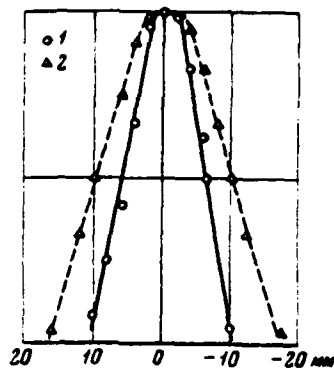


Fig. 2.

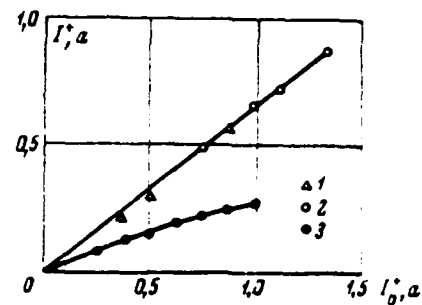


Fig. 3.

Fig. 1. Brush-type electrodes. 1 - first grid; 2 - second grid; 3 - plasma; 4 - metal tube.

Key: (1). kV.

Fig. 2. Distribution of intensities H^- across beam. 1 - along the direction of the threads of the first grid; 2 - across the direction of the threads of the first grid.

Fig. 3. Dependence of proton current in beam on selection of protons from plasma. 1 - gas pressure in the tube $1 \cdot 10^{-2}$ mm Hg; 2 - gas pressure in the tube $4 \cdot 10^{-3}$ mm Hg; 3 - gas pressure in the tube $1 \cdot 10^{-3}$ mm Hg.

Page 129.

Apparently, for the different gases the mechanism of compensation is unequal. This it indicates, for example, the different nature of current to the tube depending on the kind of the ions: for the proton beam the current to the tube is positive and roughly equal to a difference in the proton input current and at the output of tube, and in transit through the tube of ion beam N^+ current to the tube is negative and only by order of value it coincides with a difference in the input and output ion current $N^+ [3]$.

Main disadvantage in the brusa-type electrodes is their low mechanical strength with respect to the breakdown of intergrid gap/interval. Therefore brush-type electrodes require the thorough aging/training of the second grid. Aging/training was conducted as follows. With the voltage in intergrid gap/interval 200-400V the system works until the percentage of breakdowns decreases to 40-50. After this voltage it rises to 3-5 kV. If through several ten impulses/moments/pulses (duration of pulse 200 μ s, repetition frequencies 0.2 s^{-1}) breakdowns across gap disappear, it is possible to consider that the process of aging/training is finished. Usually aging/training new grid lasts 2-4 hours. In the process of aging/training the second grid is covered/coated with dark film and the coefficient of second emission from it falls 2-3 times (with 5-8

kV). Therefore it is possible to assume that the process of aging/training consists in the sharp decrease of second electron emission, which is the reason for the breakdown of intergrid gap/interval. Possibly, the decrease of second emission is connected/bonded both with the change in the nature of the emitting surface and with development of local electric fields on the threads of the second grid, which impede supply to it of fast ions.

With the formation of ion beams were used extensively gas targets [3]. Therefore was additionally investigated delay/retarding/deceleration ionized by gas in the tube. Fig. 4 shows one of the dependences of the speed loss of particles on the logarithm of the ratio of the intensities of flow of particles at the entrance and the output from the tube. Last value is proportional to the gas pressure. From these results it is evident that at optimum pressures of gas ($3-6 \cdot 10^{-3}$ mm Hg) the energy loss of particles is not more than several ones electronvolt.

The typical dependences of proton current in the beam, formed with grids in diameter of fabric/bed 37 mm, on the value of intergrid voltage are shown on Fig. 5. Three different curves answer the different values of the selection of protons from the plasma - 0.4, 0.6 and 1A. The motion of graphs is qualitatively explained as follows. From the point 1 plasma from the plasma source reaches to

the second grid and therefore beam is not formed/shaped; in the interval 1-2 boundaries of plasma with an increase in the voltage are moved from the second grid to the first - the defocusing influence of the second grid and plasma boundary decreases, and current grows/rises. At point 2 plasma reach the first grid; further weak growth of current in the beam is connected/bonded, apparently, with the decrease of influence on the divergence of beam of its space charge. Maximum currents, obtained by us with use of brush-type electrodes, which follow: current H^+ -1.2 but, current He^+ -0.5 but, current N^+ -150 mA, current Ar^+ -70 mA.

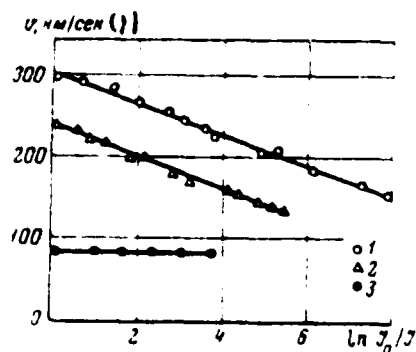


Fig. 4.

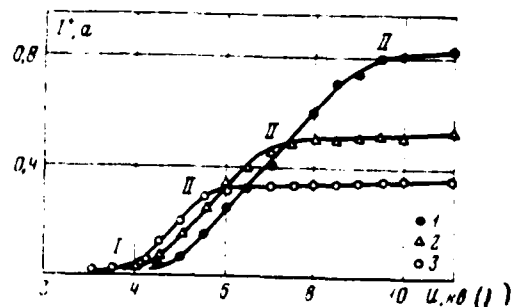


Fig. 5.

Fig. 4. Dependence of speeds of ions at output from tube on degree of their scattering on gas targets (J_0 - particle flux at entrance into tube; J - at output from tube). 1 - ion flow N^+ , which pass turn hydrogen gas target; 2 - ion flow N^+ , passing through the argon gas target; 3 - flow of ions Ar^+ , passing through the argon gas target.

Key: (1) . km/s.

Fig. 5. Dependence of proton currents in beam on intergrid voltage. 1 - the selection of protons from the plasma - 1A; 2 - selection of protons from the plasma - 0.6A; 3 - selection of protons from plasma - 0.4A.

REFERENCES

1. G. I. Dimov, Yu. G. Kononenko, O. Ya. Savchenko, V. G. Shamonovskiy. ZhTF, 1968, 38. 997.
2. G. I. Dimov, O. Ya. Savchenko. ZhTF, 1968, 39. 2002.
3. O. Ya. Savchenko. ZhTF, 1970, 40, 305.

Page 130.

39. Study of the work of plasma cathodes in the mode/conditions of the selection of large electronic currents.

G. P. Bazhen, S. P. Bugaev, F. Ya. Zagulov, G. A. Nesyats, D. I. Proskurovskiy, V. G. Shpak.

(Institute of optics of the atmosphere SO AN USSR, institute of nuclear physics with by Tomsk polytechnic institute).

For creating the powerful/thick electron accelerators with the currents in beam 10^6 - 10^8 and serious value has the development and the study of heavy current pulse cathodes. Usually for these purposes are adapted bolt [1], multi-needle-shaped [2] and plasma cathodes [3]. The authors of works [1, 2] consider their cathodes as field emission. It is possible to show that these cathodes as field

emission. It is possible to show that these cathodes also are plasma.

The appearance of plasmoids on the surface of metallic cathode for the first time have discovered we during a study of the kinetics of vacuum breakdown [4]. It was shown that by the reason for the formation of plasmoids (cathodic torches, KP) is the explosion of micro-points on the surface of cathode as a result of resistance heating field emission current [5]. The time lag of the explosion of micro-points is very critically to the strength of field and in the fields $\sim 10^6$ V/cm is $\sim 10^{-8}$ s. In works [1] the value of the maximum intensity/strength of field $E > 10^6$ V/cm. One should expect that KP appear already on the pulse edge of voltage.

Simultaneously with the advent of KP begins an increase in the current in gap/interval [4]. This current is caused by the emission of electrons from the front extended KP [5]. If the pulse duration of voltage is less than the time of closing gap/interval by plasma, then is possible obtaining the impulses/moments/pulses of electronic current. There is reason to believe that this circumstance is the basis of obtaining large electronic currents in works [1-3].

For the understanding of the mechanism of the emission of electrons there is the greatest interest a study of the parameters of plasma KP, of speed of the expansion of torches and in a study of the

conductivity of vacuum of gap with KF.

Average/mean by the volume particle concentration is the plasmod

$$\bar{n}(t) = \frac{M(t)}{m_0 (vt)^3}, \quad (1)$$

where $M(t)$ - the mass of the entering the torch metal; m_0 - mass of atom; v - speed of the dispersion/divergence of plasma.

The entering of metal into the torch was determined by the method of photographing point cathode in the electronic or optical microscopes before and after action on the vacuum gap/interval by the pulses of the voltage of the specific duration. With a radius of the apex/vertex of opening is more than $10 \mu\text{m}$ mass M grows proportional to length of impulse/momentum/pulse (Fig. 1), which indicates the continuity of the entering of metal into the cathodic torch.

The speed of the dispersion/divergence of plasma KF was determined by the speed of the expansion of the boundary of glow $U_{c0}[4]$ and motion of the boundary of emission $U_{s1}[6]$. It turned out that $U_{c0} \approx U_{s1} \approx 2 \cdot 10^8 \text{ cm/s}$ for W, Cu, Mo and Al little changes in the course of time and weakly it depends on the applied voltage. Theoretical estimations/estimates/evaluations show that after time $\sim 10^{-9}$ of s the plasma KF becomes noncolliding for the inelastic processes and heating by its through current becomes unessential.

If on the boundary plasma - vacuum is electric field $E=0$, then motion of KP can be presented as the adiabatic dispersion/divergence of gas sphere into the void. In this case the speed of the motion of the leading edge of plasma will be written down in the form

$$v = \sqrt{\frac{4\gamma}{\gamma-1} \eta \xi}, \quad (2)$$

where $\gamma = C_p / C_{v,\xi}$ - specific heat of sublimation of metal; η - degree of superheat which in experiments in the rapid explosion of conductors composes 2-5 [7]. If $\gamma = 5/3$, then $v \sim (1-2) \cdot 10^5$ cm/s for the investigated by us cathodes.

From (1) it follows that for the case, represented in Fig. 1, mean concentration \bar{n} for the time from 5 to 20 ns falls from $2 \cdot 10^{17}$ cm $^{-3}$ to $5 \cdot 10^{15}$ cm $^{-3}$ (with $\alpha = 1$ mm). The temperature of electrons in KP was determined according to the ratio of the intensities of lines with the aid of the monochromator with the photoelectric prefix/attachment with the temporary/time resolution $\sim 5 \cdot 10^{-9}$ s. Through 20 ns after development of KP its value was 4.5 eV for cathode of Al.

on our opinion, the output of electrons from the metal in KP was caused by thermo-self emission under the action of electric field on the boundary a metal-plasma, that appears as a result of the

separation of the charges of plasma (Debye field E_d). For that found from the experiment of current density $i_k \sim 2 \cdot 10^5$ A/cm² value

$E_d \sim 5.2 \cdot 10^7$ V/cm (for mho). Taking into account that $E_d \sim 1.25 \cdot 10^{-5} (nT)^{1/2}$ and assuming/taking $T = 8 \cdot 10^4$ K (Fermi temperature for mho) we obtain concentration on the surface of cathode $n \sim 10^{20}$ cm⁻³, which is completely actual, since $n = 10^{18}$ cm⁻³.

Let us examine now the current flow of electron in gap in the front of plasma - anode.

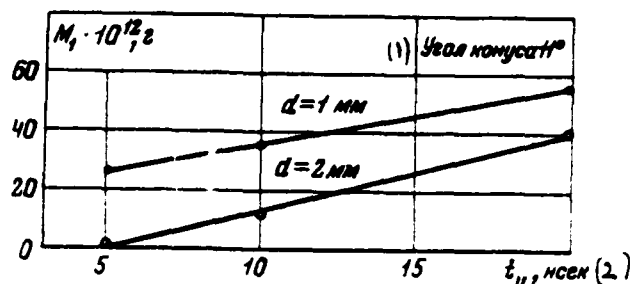


Fig. 1. Dependence of the mass of metal M , which comes the cathodic torch from the pulse duration for the molybdenum point (α - length of gap/interval).

Key: (1). Angle of taper. (2). ns.

Page 131.

If we the area of emission of torch present in the form $S(t) = \pi v^2 t^2$, and distance is the front of plasma - anode in the form $x(t) = d - vt$, then started of the limitation of current by the propagation of charge we have

$$i(t) = \frac{4}{9} \epsilon_0 \sqrt{\frac{2e}{m_0}} \frac{U_i^{3/2}(t) \pi v^2 t^2}{(d - vt)^2} \kappa \left(\frac{vt}{d - vt} \right), \quad (3)$$

where κ - correction, which considers the action of field in the case of limited emitting area $U_i(t)$ - voltage on the gap/interval. From (3) it follows that the perveance of electron beam is the function of relation $vt/d - vt$:

$$\frac{i(t)}{U_i^{3/2}(t)} = p \left(\frac{vt}{d - vt} \right). \quad (4)$$

The results of an experimental study of perveance are given in Fig. 2. The validity of Langmuir's law under these conditions is confirmed by the fact that the experimental points are arranged/located in general curve.

The given results make it possible to formulate the conditions of obtaining the impulses/momenta/pulses right-angled of electronic current. From (3) it follows that the slope/transconductance of the build-up/growth of current is determined by the rate of growth in the emitting area. Since the speed of dispersion/divergence of KP does not exceed $2 \cdot 10^6$ cm/s, increase in the slope/transconductance of current can be achieved/reached by the use/application of a multitip system with the simultaneous explosion of points, or by the use of the sliding discharge on the dielectric. The possibility of obtaining large electronic currents from the plasma of the incomplete discharge with the dielectric in the vacuum for the first time have shown we in [8]. The discharge current through the dielectric in the incomplete stage grows with increase in ϵ of dielectric. Therefore was investigated the emission of electrons from the plasma of the creeping discharge of titanate of barium ($\epsilon = 1500$) in the system of electrodes, given in Fig. 3a. The velocity of propagation of glow on dielectric (Fig. 3c) composes $U = 10^7$ cm/s and approximately it coincides with the speed of the expansion of the region of emission. Penetration of plasma into the depth of gap/interval occurs with speed

$v_1 \approx 2 \cdot 10^7$ of cm/s. The plasma near of point develops as a result of destruction and ionization of vapors of dielectric under the action of the current of self emission from the point. The flow of discharge current is ensured by the charging of the dynamic capacity/capacitance, formed by the gap/interval between the plasma, which moves along the dielectric, and by the layer of silver 2 (Fig. 3d), substituted to the dielectric.

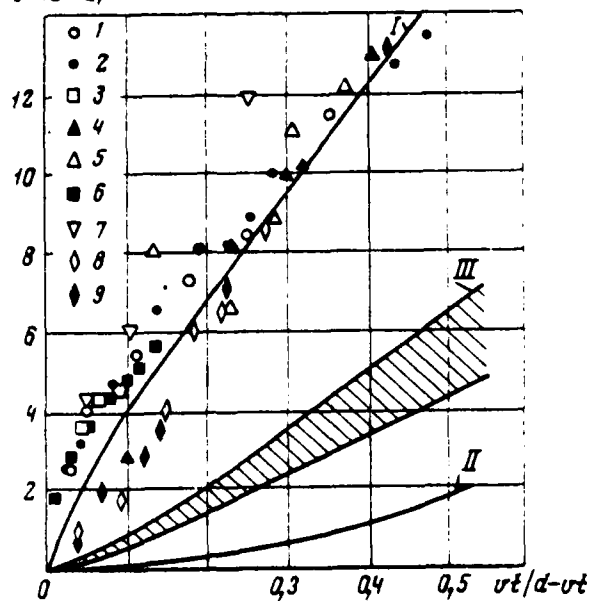
$P \cdot 10^6 a/V^{3/2}$ 

Fig. 2. Dependences $p(vt/d - vt)$, built for $v = 2 \cdot 10^8$ cm/s. 1 - experiment; II - calculation according to (3) for $K=1$; III - calculation according to (3) with K on [6]

Обозначения :	d, см	U, кв
1	0,08	27
2	0,1	20
3	0,2	11
4	0,2	160
5	0,2	100
6	0,32	35
7	0,4	100
8	0,4	80
9	0,6	180

Key: (1). symbols.

555

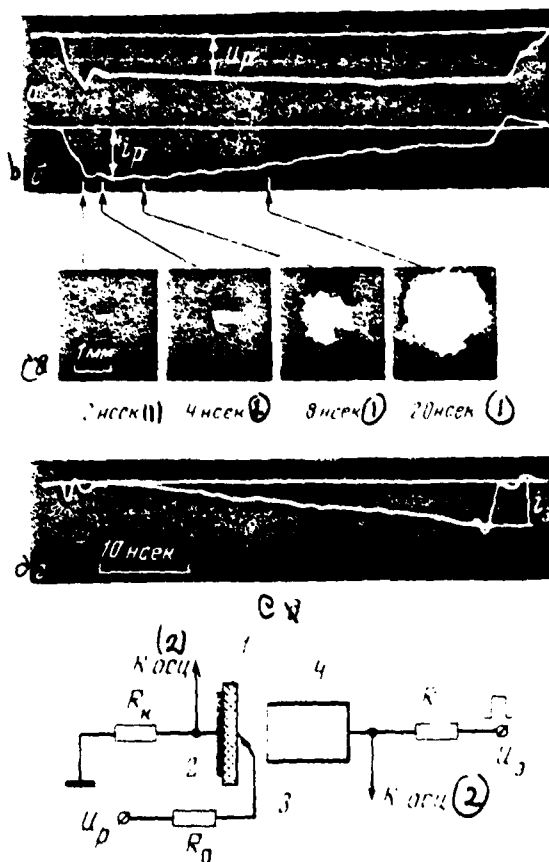


Fig. 3. Oscillogram of voltage of discharge (a), current of discharge (b), photograph of discharge figures (c), emission current from the plasma of discharge (d), schematic diagram (e). 1 - dielectric; 2 - electrode; 3 - needle; 4 - extractor; $R_K = R_0 = 75$ ohm; $R_0 = 56$ ohm; \wedge ohm.

Key: (1) . ns. (2) . osc.

Since current of discharge through dielectric and area of discharge figure increase with an increase in the discharge voltage, then emission current from the plasma also grows. This is distinctly evident from the graph/diagrams of the dependence of the perveance of electron beam from the plasma about parameter $\frac{V_c}{d-V_{it}}$ (Fig. 4). By a change in the discharge voltage it is possible to regulate the perveance of the electronic flux, selected/taken from the cathode. The advantages of the sliding discharge were realized in developed by us controlled plasma cathode [9].

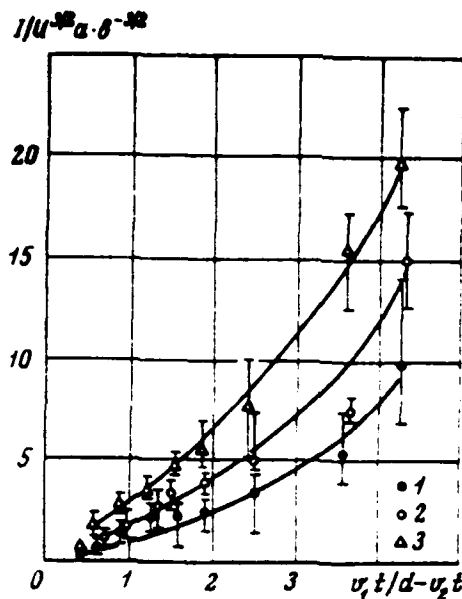


Fig. 4. The graph/diagram of the dependence of the perveance of electronic flux from the plasma on parameter $v_1 t / d - v_2 t$ (d - the length of gap/interval, t - time) 1 - $U_p = 0.5$ kV; 2 - $U_p = 1$ kV; 3 - $U_p = 1.5$ kV.

REFERENCES

1. S.E. Graybill, S.V. Nablo. IEEE Trans. on Nucl. Sci., 1967, NS-14, N 3, p. 782, см. также Rev. Scient Instrum., 1969, 40, N 11, p. 1413.
2. F.M. Sharbonnier et al. IEEE Trans. on Nucl. Sci., 1967, NS-14, N 3, p. 789.
3. M. Andrews et al. Laboratory of plasma studies. Cornell Univ., N.Y., LPS18, July, 1969.
4. S. P. Bugaev et al. ZhTF, 1967, 37, No 12, p. 2206.
5. S. P. Bugaev et al. DAN of USSR, 1969, 186, No 5, p. 1067.

6. G. A. Mesyats, D. I. Proskurovskiy. Izv. of the highest edcnl. Inst. physics, 1968, No 1.
7. Sb. "Electrical explosion of conductors". M., publishing houses "Mir", 1965.
8. S. P. Bugaev, G. A. Mesyats. ZhTF, 1967, 37, No 10, p. 1855.
9. S. P. Bugaev et al. Izv. of the highest edcnl. Inst. physics, 1968, No 1.

Page 133.

Session IV.

ELECTROMAGNETS OF ACCELERATORS AND THEIR POWER SUPPLY SYSTEMS.
MAGNETIC MEASUREMENTS.

40. Methods of calculation of magnets in experiments in high-energy physics.

L. Rezegotti.

(CERN).

In experiments in high-energy physics are utilized the magnets of several different types. Majority of them relates to two types: the magnets, which lead beam, designation/purpose which lies in the fact that to guide and to focus beams, and the analyzing magnets which serve for determining the impulses/momenta/pulses of the charged/loaded particles from the curvature of their trajectories in the magnetic field. In the case of experiments on clashing beams the

magnets, arranged/located in the point of intersection of beams, can perform both functions. Different tasks of more special character are performed by the magnets which remove the charged/loaded particles from beam, by magnets for the polarized targets, by magnets, utilized in the experiments with the precession of spin, magnetic horns, which ensure the concentration of secondary particles with different impulses/momenta/pulses. Some of the magnets, utilized for the transportation of beam, satisfy the special requirements, which concern three-dimensional/space field pattern and time behavior of their work (magnets with the shielding partition and pulsed magnets in the delay lines).

Starting point during the design of magnet is, obviously, the account of the special requirements, connected with its designation/purpose. For example, spatial distribution of the field of magnet for bubble chamber is three-dimensional or at best possesses rotational symmetry; however, the high values of the strength of field and the accessibility of space in the magnet is more important requirements; than the uniformity of field. On the contrary, in the case of the magnet of accelerator necessary field pattern in the plane, perpendicular to the axis/axle of bundle, must be sustained very accurately; however in the majority of the cases of the disturbances/perturbations, created by edge effects, are almost unessential or they can be compensated taking into account the

integrating properties of launching/starting high energy particles, thanks to which the task is reduced to the two-dimensional.

During the determination of the basic parameters of magnet should be considered also the total cost/value of system, which involves besides the cost/value strictly of magnet also the cost/value of the supplies of power, cables, cooling system, and also running costs and maintenance/servicing. These considerations can play the decisive role during the determination of current density in the windings of magnet and its overall sizes/dimensions. In the case of the kickers important factor is also the stored up magnetic energy. Finally, it can prove to be necessary to determine the amount of elastic strains and deformations, which appear in the system during the maximum mode/conditions.

This work is dedicated to the methods of calculation of fields when the basic parameters of magnet are already determined. Primary attention will be turned to the magnets for the transportation of beam, in which a precise execution of prescribed/assigned field pattern is especially important.

For such magnets we deal concerning the two-dimensional task, since, if we are distracted from the connected with the edge effects limitations, field distribution in all perpendicular ones of the

axis/axle of pencil of planes must be identical. From the equations of Maxwell for the statistical magnetic field it follows that field in magnet gap it is possible to obtain from the scalar potential V , which satisfies relationship $\nabla^2 V = 0$. For purposes of optics of electron beams it is useful to present this potential in the plane, perpendicular to the axis/axle of bundle, in the form of Fourier series in the polar coordinates

$$V = -\sum_{n=1}^{\infty} a_n \rho^n \sin(n\theta + \theta_n), \quad (1)$$

whence it is possible to directly obtain the following expressions for the components of the field:

$$\begin{aligned} B_\rho &= -\mu_0 (\partial V / \partial \rho) = \mu_0 \sum_{n=1}^{\infty} n a_n \rho^{n-1} \sin(n\theta + \theta_n); \\ B_\theta &= \mu_0 \left(\frac{1}{\rho}\right) (\partial V / \partial \theta) = \mu_0 \sum_{n=1}^{\infty} n a_n \rho^{n-1} \cos(n\theta + \theta_n). \end{aligned} \quad (2)$$

Unknown field distribution can be determined, after assigning the values of coefficients a_n and θ_n in different terms. Coefficient a_1 corresponds to the field of dipole, a_2 - to field of quadrupole, coefficient a_n - to field $2n$ - multipole.

Page 134.

The most important problem lies in the fact that to find the current distribution (for the iron free magnet) or currents and iron cores (for the magnet with iron), which create the necessary configuration of magnetic field in the clearance.

For some simplest field patterns are known the solutions of direct problem. For example, in the absence of iron the clean field of dipole is obtained in the opening/aperture, which is the region of overlapping two identical conductors of elliptical cross section, that have the uniform and equal current densities of opposite sign and arranged/located, as shown in Fig. 1^a. If two ellipses overlap at the right angle, and clearance is formed purely quadrupole field (Fig. 1b) [1].

Purely dipole field is formed also in the clearance between two rectangular conductors, conducting equal and opposite currents, limited by the flat/plate parallel surfaces of two iron poles with the infinite magnetic permeability. This field pattern, which obtained the name of the field of w-shaped magnet, is accomplished/realized in particular in the magnets with the shielding partition which are utilized in the systems of ejection or for splitting of beam (Fig. 2 and 3). Another example of purely dipole field is the so-called dipole of Ussatetter [2], formed by the imposition of two identical w-shaped magnets whose axes/axles form angle of 90° (Fig. 4). In this case the value of induction on the surface of poles is only $B/\sqrt{2}$, and field in the clearance can reach 3T without saturation of iron.

Purely quadrupole field is obtained in the rectangular clearance between four conductors of the corresponding sizes/dimensions with the uniform current density, included in rectangular iron box with the infinite magnetic permeability (quadrupole of Panovskiy, Fig. 5 [3]).

Other configurations of the conductors and the iron can be obtained of that examined above as a result of the filling with iron by the infinite magnetic permeability of entire space, external with respect to the closed contour/outline, perpendicular to the lines of flow. Utilizing this method M. Mcrpurgo [4] designed and constructed a very compact quadrupole magnet, which surrounds the elliptical aperture (Fig. 6 and 7).

Although the analytical examination of the enumerated above tasks is strict, the use of iron as the medium with the infinite magnetic permeability is approximation/approach (by virtually completely satisfactory at the densities of flow, which reach 1.5T, where $\mu_{Fe} > 1000\mu_0$).

Another approximation/approach which sometimes is utilized for the semiconductors, lies in the fact that are examined the

surface/skin currents. Surface/skin current distribution in the cylindrical layer, which surrounds the circular opening/aperture which is necessary for the creation in this clearance of the field of multipole order $2n$, is described by the sinusoidal function of angle of $n\theta$.

Calculated field distribution can be represented in the form of step function, which can be constructed from the intervals with the permanent linear current density. Examining K of steps/stages to the quadrant of the variable/alternating $n\theta$, R. Beth [1] proposed the method which makes it possible to remove all harmonics fraction up to the harmonic with the number $4K+1$. In practice it proves to be sufficient to be restricted to three or four steps/stages, since basic assumption about the small thickness of the current-carrying layer proves to be already sufficiently poor approximation/approach.

R. Beth's method was used for designing the dipole and quadrupole superconducting coil electromagnets in Brookhaven national laboratory [5]. Dipole magnet was the layer of the superconducting winding with a thickness of 12.7 mm on the circular cylinder with a diameter of 50 mm (see Fig. 8).

The actual thickness of windings is considered in the formula, proposed for designing the superconducting coil electromagnets in the

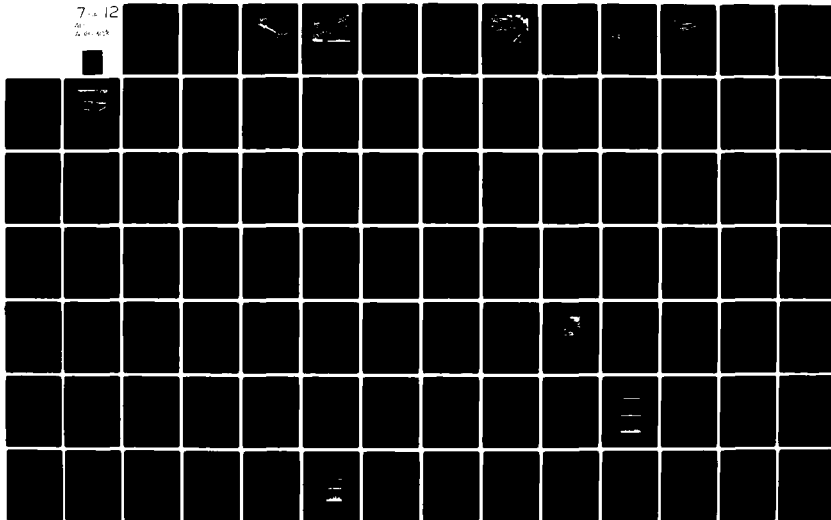
AD-A089 303

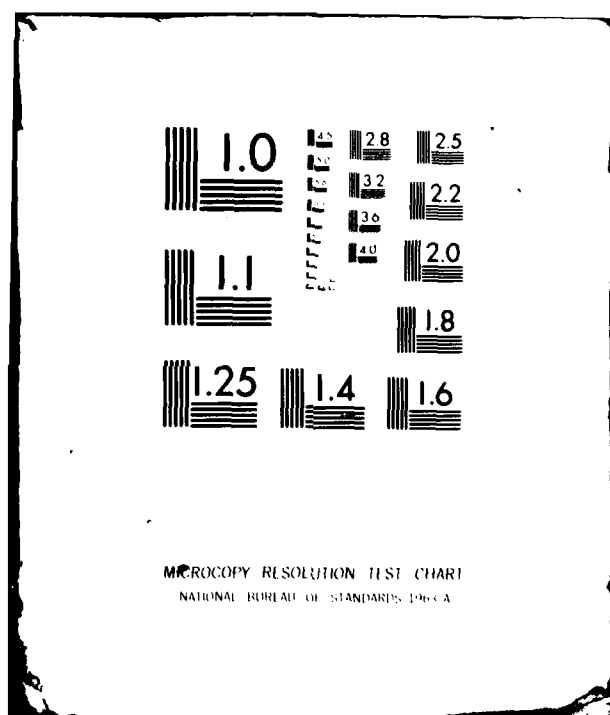
FOREIGN TECHNOLOGY DIV WRIGHT-PATTERSON AFB OH F/G 20/7
TRANSACTIONS OF THE ALL-UNION CONFERENCE (2ND) ON CHARGED PARTI--ETC(U)
JUL 80 A L MINTS, A A KOMAR, A A VASIL'YEV
FTD-ID(RS)T-0692-80

UNCLASSIFIED

NL

7-12
10
11-12





work of Esner, Deutsch and Iselin [6] (Fig. 9). They utilized expansion in the series/row of vector potential A of the two-dimensional field, created at point $P(\rho, \psi)$ infinitesimal current element with density j , arranged/located at point $Q(r, \varphi)$ and perpendicular to the plane of the cross section in question:

$$\left(\frac{1}{r} \frac{d^2 A}{dr d\varphi} - \frac{\mu_0 j}{2\pi} \left(\sum_{k=1}^{\infty} \frac{1}{k} \alpha^k \cos k(\varphi - \psi) - \ln r \right) \right). \quad (3)$$

Integral over entire cross section of winding can be written in the polar coordinates, which facilitates the selection of geometry and current densities with which the coefficients for any number of terms, which correspond to different harmonics to zero. This method was equal used during the design of the superconducting quadrupole magnet in CERN (Fig. 10).

The effect of the cylindrical iron screen, which surrounds iron free magnet, can be calculated, examining the images of current elements relative to cylindrical surface, when the density of flow in the iron screen is sufficiently great and its magnetic permeability it is possible to consider it infinitely large.

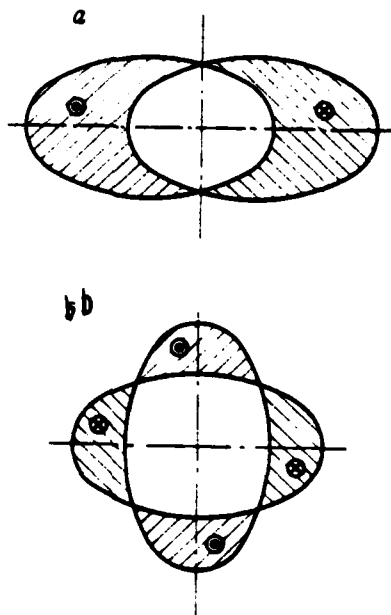


Fig. 1. Field pattern during the intersection of two identical elliptical conductors: a) dipole magnet; b) quadrupole magnet.

DCC = 90069211

EAGB

568

Page 135.

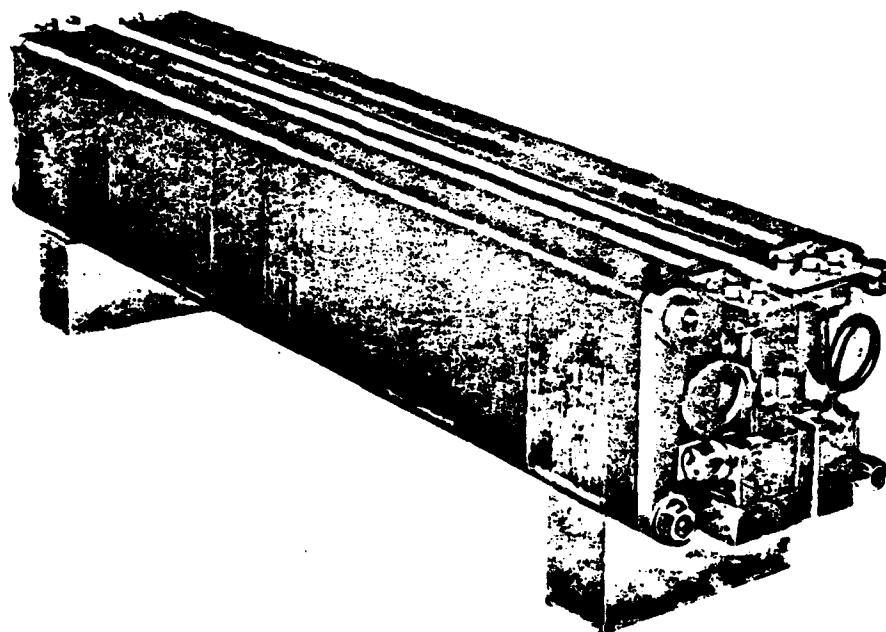


Fig. 2. Pulse septum-magnet for system of ejection of proton synchrotron of CERN.

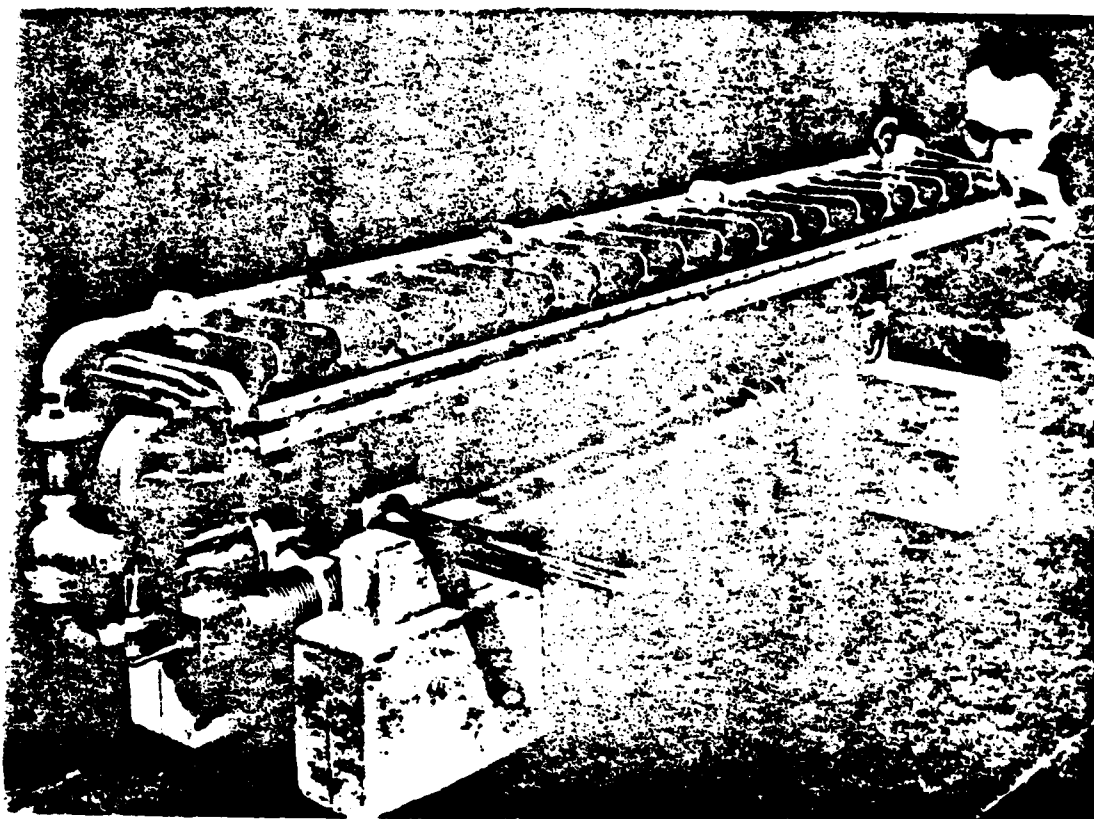


Fig. 3. Dc septum- magnet for splitting/fission of beam.

Page 136.

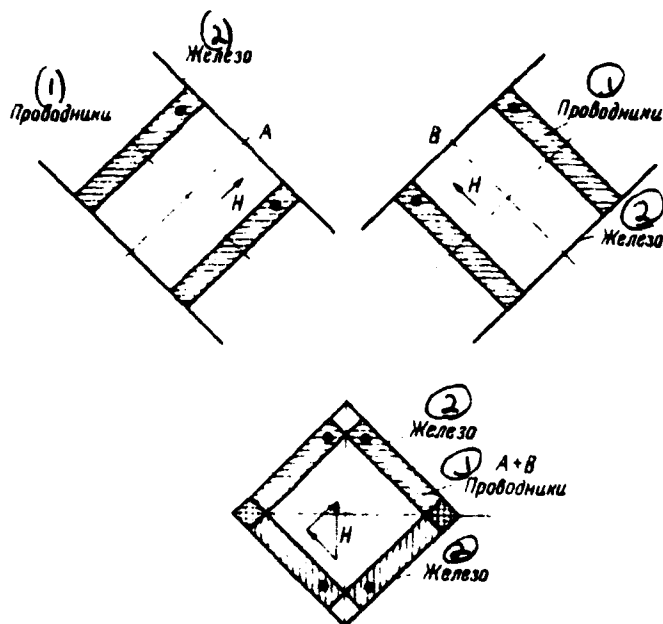


Fig 4. Diagram of dipole of Unstetter.

Key: (1). Conductors. (2). Iron.

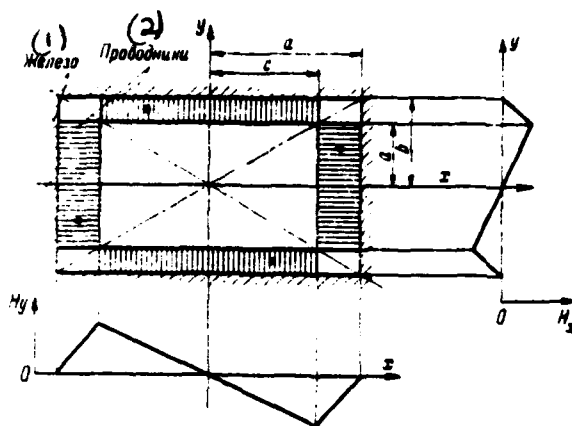


Fig. 5.

Fig. 5. Diagram of quadrupole of Fanovskiy.

Key: (1). Iron. (2). Conductors.

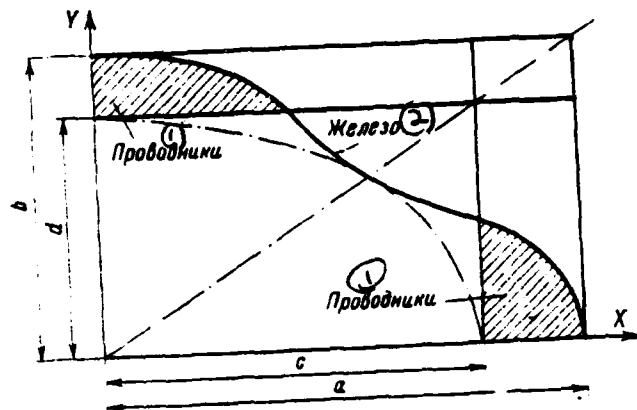


Fig. 6.

Fig. 6. Diagram of quadrupole of Mscrpurge.

Key: (1). Conductors. (2). Iron.

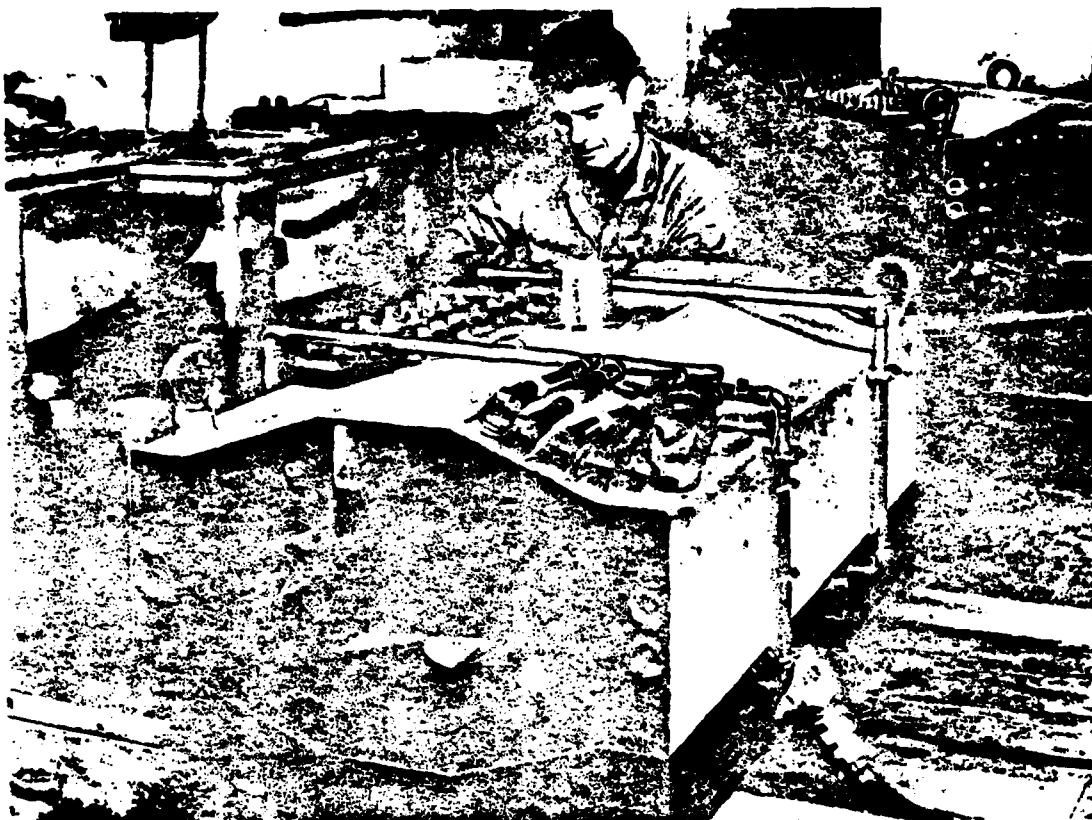


Fig. 7. Large aperture of quadrupole of Morpurgo.

Page 137.

During the production of magnets practical considerations frequently make it necessary to differ from ideal geometry and to utilize the constructions/designs which possess technological or economic advantages from the point of view of the possibility of their realization with the required precision/accuracy.

The analytical solutions frequently require high current densities, which proves to be unfavorable economically, taking into account the cost/value of supply and cooling. Therefore general/common/total tendency lies in the fact that to form/shape field pattern in most important sectors of iron-cored magnets due to imparting of the corresponding shape of surface of poles.

In the majority of the cases as the first approximation is utilized the assumption about the infinitely large magnetic permeability of the iron and for determining the shape of surface of poles they calculate magnetic constant field curves, which must be obtained. Then is calculated the effect of currents and they introduce the appropriate corrections with the aid of the shims, the auxiliary windings or a change in the profile/airfoil of poles.

Within the framework of the hypothesis of equipotential poles for the establishment of conformity between the families of the equipotentials, which correspond to different configurations, it is possible to utilize a method of conformal mapping, so that, knowing the form of poles, which gives single field pattern, to find the form of poles, which gives complex field distribution.

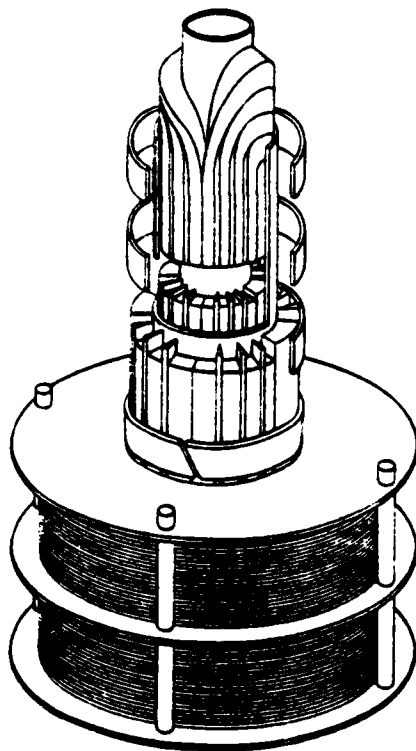


Fig. 8.

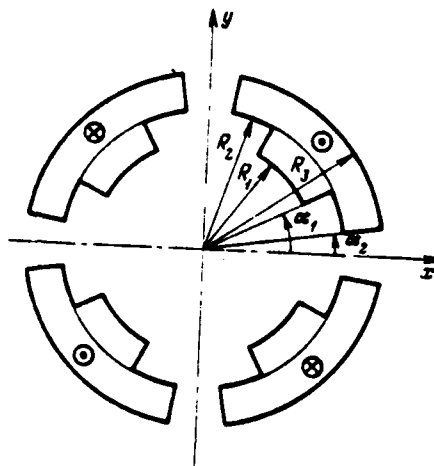


Fig. 9.

Fig. 8. Superconducting dipole of BNL.

Fig. 9. Diagram of quadrupole.

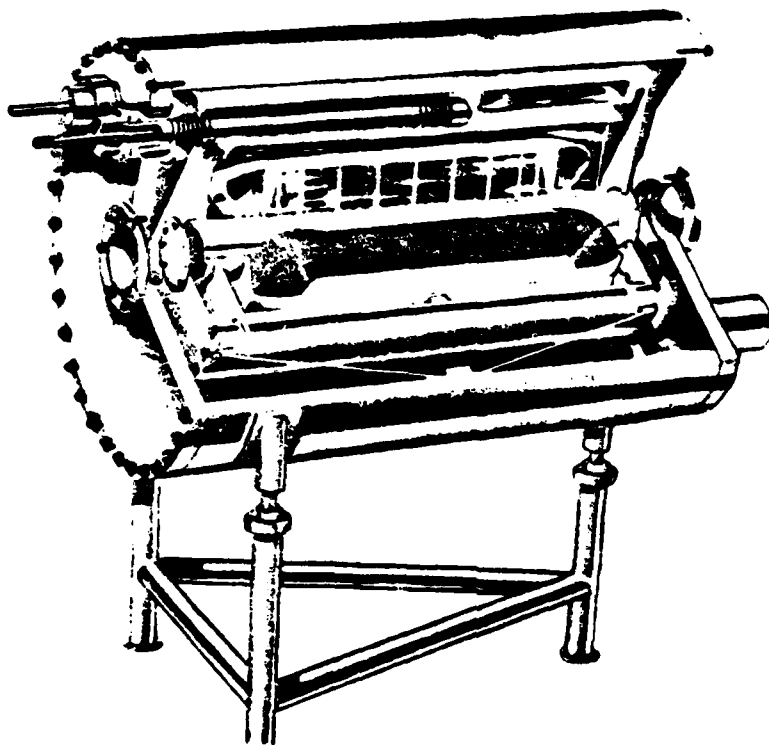


Fig. 10. Superconducting quadrupole.

Page 138.

This method proved to be especially useful during the design of magnets, combining different functions, for the strong-focusing accelerators. This method was used also for calculating the form of edges/fins or ends/leads of the poles, moreover in the calculation of the form of edges/fins or ends/leads of the poles, moreover in the calculations was utilized the condition of the constancy of the

density of flow in some contours/outlines for the purpose of obtaining the contours/cttlines, in which is absent local saturation [7].

As a most contemporary example of the use/application of a method of conformal mapping for designing the form of poles can serve the glorious magnet of the intersecting rings in CERN [8] (Fig 11). Used conformal mappings are shown on Fig. 12, 13.

The adjustment of field distribution frequently can be provided with the aid of the pole windings. The necessary currents of these windings with a good precision/accuracy can be rated/estimated on the basis of assumption about infinitesimal thickness of the current carrying layer, calculating the change in the magnetic potential along the surface of pole, which would correspond to the necessary multipole terms in field distribution.

As a result of the complicated combination of all mentioned above physical, technological and economic considerations the final stage of the design of magnet is unavoidably the solution of the reverse problem, i.e., the calculation of field pattern, created by this configuration of currents and iron.

In the case of iron free magnets this problem is solved

directly, since it is singular, what is necessary for this, the straight/direct integration of Laplace's first law.

The programs of calculations for TSVM [digital computer], which foresee this integration, were comprised, for example, for determining the form of the field of special iron free magnets for the investigations on the thermonuclear fusion (see Fig. 14) [9-11].

When is present iron in the form of core with the poles as in the majority of usual electromagnets, or the type of framework or screen, closing magnetic flux, as for instance, in the superconducting coil electromagnets, field pattern in the principle can be calculated, after considering the contributions of the elementary dipoles, which appear as a result of the magnetization of iron.

The local intensity of magnetization of any element of volume of iron is the function of the local strength of field and can be obtained from the curve of primary magnetization; however this field is in turn, the function of the intensity of magnetization of all other elements/cells of iron. Therefore at each step/pitch of iterative process must be solved full/total/complete system of equations. During the solution of the usual tasks, connected with the calculation of magnets, such calculations require so large a storage

capacity, that they prove to be impracticable with exception of the simplest cases.

The enormous majority of the calculations of the fields of iron-cored magnets is accomplished/realized with the aid of the relaxation methods. Because of the use of contemporary TSM, which possess the vast memory and high speed, these methods provide this speed and precision/accuracy of calculations, that almost completely extruded/excluded other traditional analog methods.

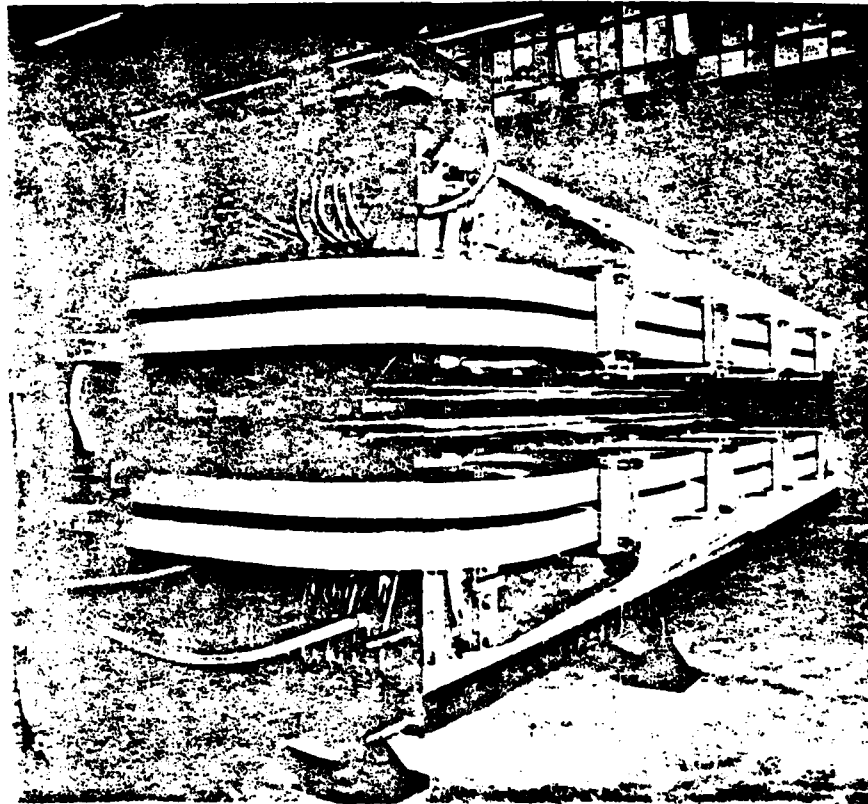


Fig. 11. Short unit of the magnet of the intersecting rings.

Page 139.

The configuration of iron and current distribution are utilized with the formulation of boundary conditions during the solution of the equations of Maxwell for the static magnetic field. In this case it is proposed that relationships/ratios $B=B(H)$ and $\mu=\mu(B)$ are single-valued and are determined by the curve of the initial

magnetization of iron, i.e., they disregard hysteresis and residual/remanent magnetization. Induction B can be obtained from the vector potential, determined by equality $B = \text{rot} A$. Under assumptions presented above relative to connection/communication between values B and H simultaneously are solved relative to A , B and μ the following equations:

$$\text{rot} \left[\left(\frac{1}{\mu} \right) \text{rot} A \right] = J; \quad B = \text{rot} A; \quad \mu = \mu(B). \quad (4)$$

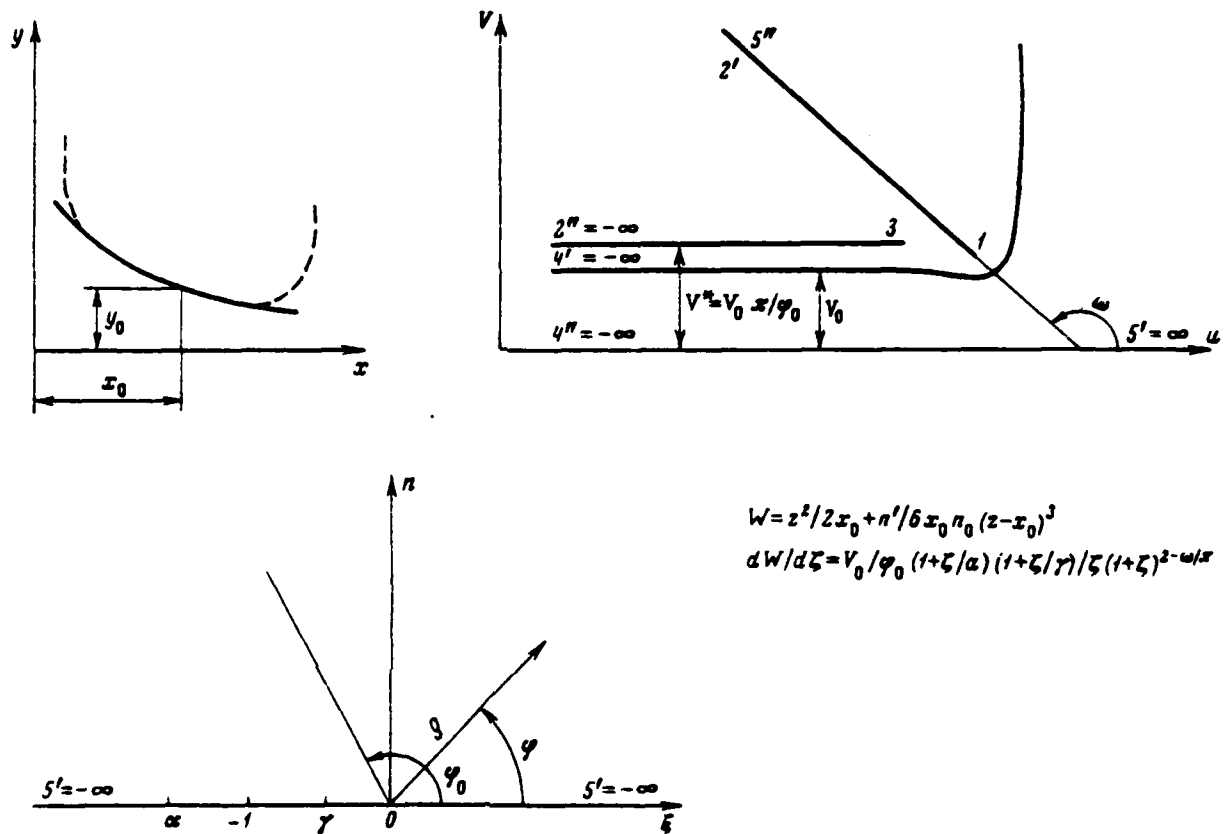


Fig. 12. Conformal conversions, utilized during the calculation of the profile/airfoil of the magnet of the intersecting rings.

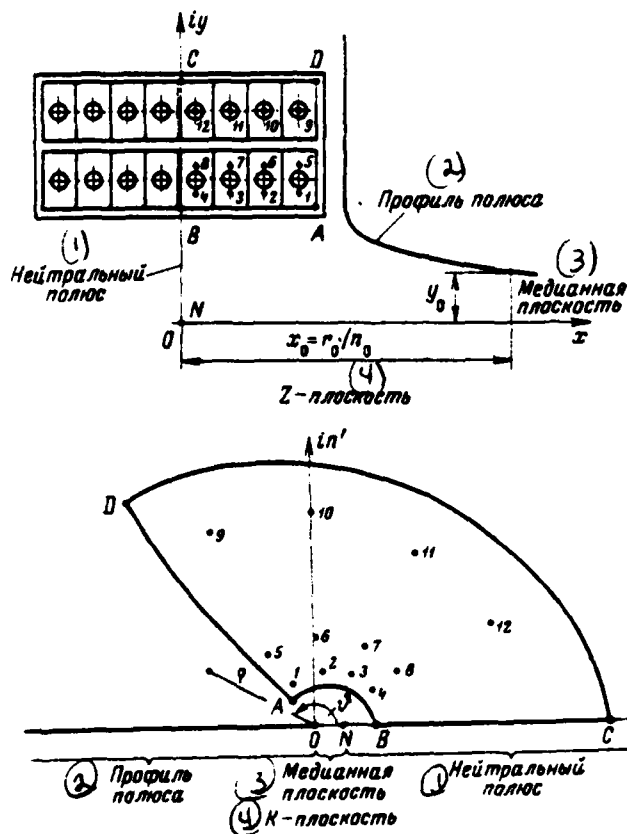


Fig. 13.

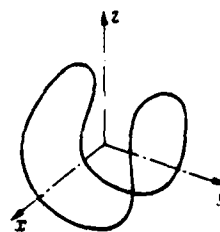


Fig 14.

Fig. 13. Conversions for winding of magnet of intersecting rings.

Key: (1). Neutral pole. (2). Profile/airfoil of pole. (3). Median plane. (4). plane.

Fig. 14. Diagram of unwinding type "joint of tennis ball".

Page 140.

1) Relaxation methods in the case of two-dimensional tasks. The calculation methods and appearing in this case practical difficulties are best to demonstrate at the two-dimensional case, for which were comprised several machine programs. In this case it is assumed that value J has only one different from zero components J_z and is calculated field distribution in the plane (x, y) . Then vector potential has only one different from zero components A_z , which under condition $\text{div } A = 0$ must satisfy the relationship/ratio:

$$\frac{d^2 A}{dx^2} + \frac{d^2 A}{dy^2} - \frac{1}{\mu} \frac{d\mu}{dx} \frac{dA}{dx} - \frac{1}{\mu} \frac{d\mu}{dy} \frac{dA}{dy} = -\mu J_z \quad (5)$$

It is easy to see that in this case a difference in the vector potentials for two points is proportional to magnetic flux between these two points.

For the solution of problem the region in question is covered/coated with the calculated network of corresponding configuration, and equations in the partial derivatives are replaced by equations in the finite differences which must be satisfied at all points of network. In existing programs for the calculation on TsVM is utilized either the network, consisting of the rectangular cells, position and sizes/dimensions of which are fixed/recorded, or the network, which consists of the triangular elements/cells which are constructed for each particular task in accordance with

examined/considered the configuration they have available in such a way that the outer boundaries and the dividing lines, approximately depicted as the polygons, usually would be arranged/located on network lines.

Direct calculation by relaxation method on TSVM with the use of equation for the vector potential requires a large number of iterations, which is connected with the method of the expression of boundary conditions for A. However, in spite of relative complexity, machine programs of the solutions of equations for the vector potential are of known interest as a result of the single approach to the examination tasks as a whole. The programs of this type were comprised and they are utilized, for example, at Stanford University [12], and the radiation laboratory of Lawrence in Berkeley [13], by the authors [14], and also in Dubna [15].

The program of radiation laboratory "TRIM" can serve as an example of the use of a triangular calculated network. During its use it is necessary to begin from the determination of the geometry of task, after subdividing the region in question on the subregion with the uniform properties of material or the uniform distribution of currents. Further in each such region program constructs the calculated network, which consists of the triangles which can be equilateral or rectangular, depending on input data. TSVM provides

the graphic indication of network that it makes it possible for operator to introduce all necessary corrections taking into account the obtained results. The selection of network is conducted by the trial-and-error method and is the decisive factor on which depends the success of calculations.

Coincidence of network lines with the outer boundaries of the region in question and the interfaces assures considerable simplification of writing of difference equations for such boundaries and simplicity in the assignment of boundary conditions. However, with the work with this program calculated network can contain smaller number of points, than during the use of a program with the fixed/recorded rectangular network, since for each point in 2D TSVM must be stored the larger quantity of information. During the construction of network are required the special precautionary measures, since the strong distortions of the form of triangles or their imposition it is possible to lead to the erroneous results. Fig. 15 gives an example of the network, obtained during the use of a program "TRIM" for calculating the magnet with the field gradient.

In another group of programs for the solution of two-dimensional problems by relaxation method are separately and alternately examined the regions of coils with air gap and iron. In this case they attempt to utilize the advantage that in the majority of the in practice

interesting cases the sufficiently precise first approximation can be obtained, counting magnetic permeability of the iron as infinite, for which in similar programs during calculations of the region of coils and air clearances is utilized the modified scalar potential, which on initial stage of calculations can be considered constant on the surface of iron.

For this purpose is introduced the auxiliary vector M (Fig. 16), which is determined by equality $\text{rot} M = J$.

Then equation $\text{rot} H = J$ is written in the form $\text{rot}(H - M) = 0$. Further vector $(H - M)$ can be considered as the gradient of the scalar potential V^* , whence we have

$$H = \text{grad} V^* + M. \quad (6)$$

Since magnetic permeability is permanent and uniform, we have also $\text{div} \vec{H} = 0$, whence

$$\nabla^2 V^* = -\text{div} M. \quad (7)$$

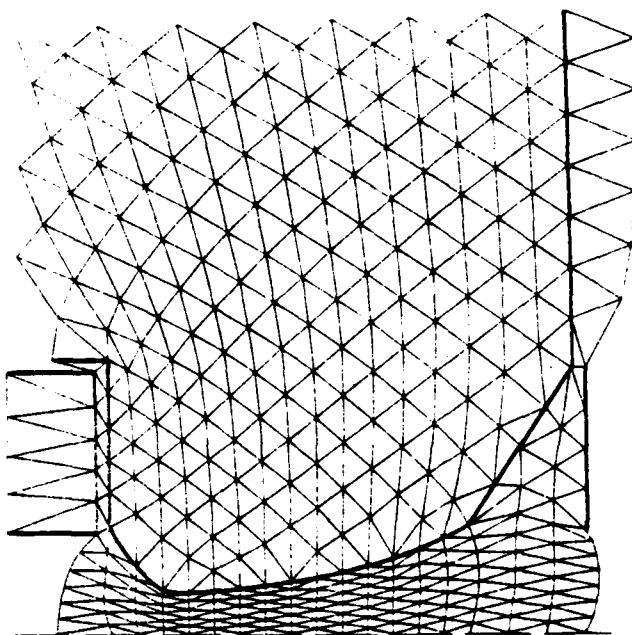


Fig. 15. Example of the calculated network TRIM.

Page 141.

In the case of two-dimensional task one of the components \bar{M} can be arbitrarily placed equal to zero (for example, $M_y=0$), then M_x is determined by the equality

$$M_x = \int J dy + c, \quad (8)$$

and boundary conditions for the modified potential V^* can be easily determined, integrating equation (7) for the interface of the regions of iron and air with the coils.

After the solution of equation for by the V^* , relaxation method obtained designs magnetic flux for interface between the air and the iron, which gives boundary condition for calculating the vector potential in the region, filled with iron. Further are performed calculations in this region in process of which are determined the vector potential, magnetic induction and magnetic permeability at each point of network. First vector potential A calculates at all points, assuming/setting magnetic permeability of constant; then find components inductions B as the partial derivatives of vector potential A , and values B are found from the tables. The further described procedure is repeated with the new, refined values of magnetic permeability. This iterative process is repeated until changes in magnetic permeability become less than certain assigned magnitude. In conclusion are calculated differences in magnetomotive force between different points of the contour/outline, formed by iron. The values of the latter are utilized then for refining the strengths of the currents and scalar potential V^* on the interface iron - air which are utilized in the following cycle of calculations in the region, filled with air and coils.

The separate examination of the regions of iron and windings provides the considerable decrease of a number simultaneously of the points in question and the savings of working storage, since data for one of the regions can be retained in the lasting memory when are

performed calculations for another region, and vice versa.

R. Perin and S. Van der Meer in CERN developed the program "MARE", which utilizes in the calculations alternately vector and scalar potentials [16]. This program was applied, in particular, during the design of the magnets of all types for the intersecting rings in CERN. In order to ensure the sufficiently precise calculations of field pattern in the most important regions of clearances, calculations were repeated with the consecutive decrease of mesh sizes. For example, the values of gradients for the basic magnets were calculated with the precision/accuracy, best $2 \cdot 10^{-3}$, which corresponds to the error in the relative values of field $2 \cdot 10^{-3}$. For the comparison Fig. 17 gives the calculated and measured divergences of gradient from the nominal values for F- magnets of intersecting rings [17]. Two curves, shown in the figure, correspond to middle field and field in the saturation.

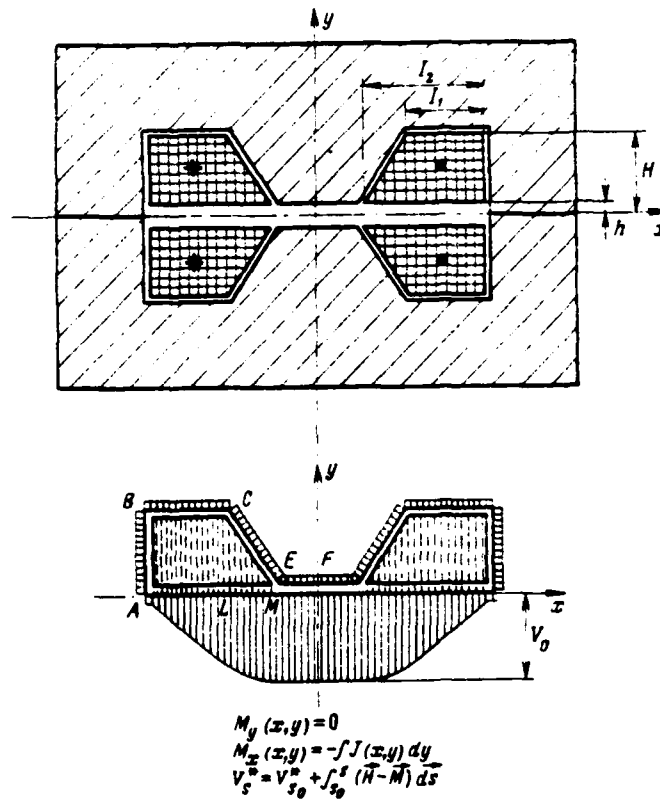


Fig. 16. Form of the modified scalar potential for the magnet with the conical poles.

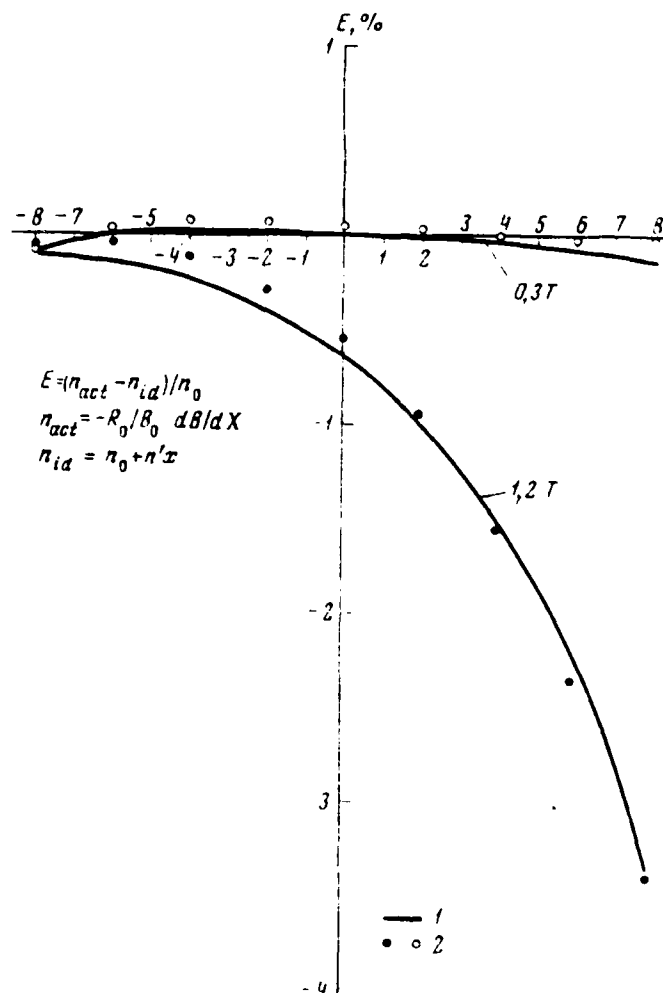


Fig. 17. The calculated and measured values of the error for gradient in the magnets of intersecting rings 1 - calculation; 2 - experiment.

Page 142.

One of the particular classes of the tasks which can be solved

with the aid of the two-dimensional programs, are tasks with rotational symmetry, when field is the function only of radial and axial coordinates. Corresponding equation for the vector potential, written in cylindrical coordinates and which has the form

$$\frac{\partial^2(\tau A)}{\partial r^2} + \frac{\partial^2(\tau A)}{\partial z^2} - \left(\frac{1}{r} + \frac{1}{\mu} \frac{\partial \mu}{\partial r}\right) \frac{\partial(\tau A)}{\partial r} - \frac{1}{\mu} \frac{\partial \mu}{\partial z} \frac{\partial(\tau A)}{\partial z} = -\mu J, \quad (9)$$

it can be solved analogously with usual equation for the two-dimensional task in the Cartesian coordinates.

2) Relaxation calculations in the three-dimensional case. Ideal for designer of magnets would be the calculated program, which makes it possible calculate all three components of magnetic field at any point during the prescribed/assigned three-dimensional current distribution and iron. As far as is known to the author, this full/total/complete program thus far yet there does not exist. The attempts to create this program were done and they continue at present; however, they are encountered with the serious practical difficulties (mainly exaggerated machine time and necessity for too large a storage capacity).

As in the two-dimensional case, in resolving entire task it is possible to utilize only a vector potential or only scalar potential with the sections/cuts, which correspond to currents. It is possible

to assume that in the first of these methods will arise the same difficulties, connected with boundary conditions, as with the solution of two-dimensional problems. Second method was used by R. Christian and M. Foss [18, 19]. The author [18] communicates that he obtained good results for the magnet of bubble chamber in which the iron plays the role of the framework, which closes magnetic flux, and also for the screens of system with Helmholtz's coils, and considerably less satisfactory results in other cases. It revealed/detected that, if air gap out of the iron framework is not considered in the calculations, iterative procedure does not converge.

S. Caeymaex in CERN made the attempt to find the method of the solution of three-dimensional problems with the use of two potentials, following the general/common/total idea, placed as the basis of program MARE [20]. Up to now it successfully overcame the first stage in which it is assumed that magnetic permeability of iron is infinitely great. In its program MINI-A are utilized the modified scalar potential and the calculated network, which consists of the parallelepipeds. At each point of network the equation in the partial derivatives is approximately replaced by the difference equation, which contains the values of function into four nearest adjacent points (on two points on each axis/axle). In the calculations consecutively/serially are utilized the sets of three of the adjacent

planes of three-dimensional lattice, that that in the working storage TsVM simultaneously must be stored data only for three adjacent planes.

As an example it is possible to refer to the calculations, which were being carried out for the magnet of the intersecting rings of CERN. Was utilized the network, which consists of ~124000 points (49x55x46). On TsVM CDC-6600 the solution was obtained in 25 min. Magnet itself and entire/all region of calculations is schematically shown in Fig. 18.

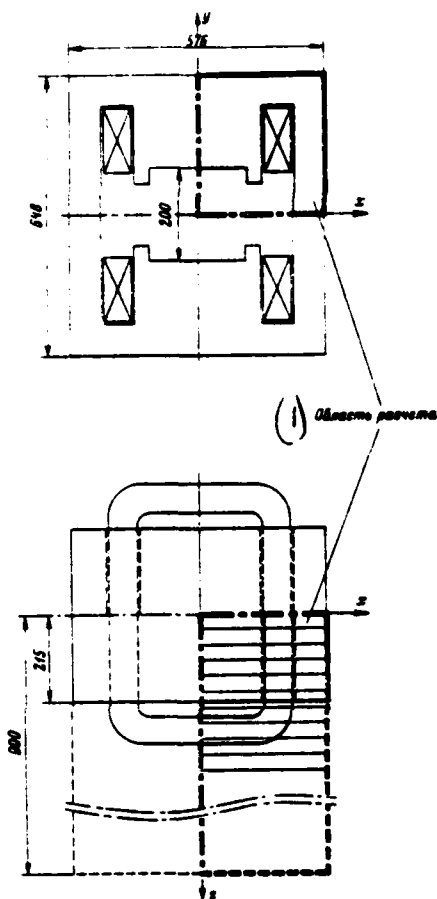


Fig. 18.

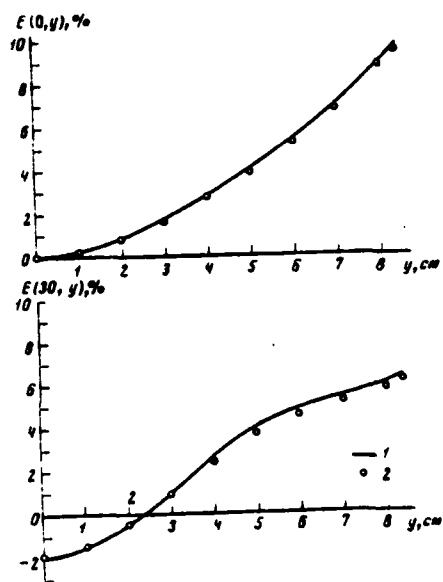


Fig. 19.

Fig. 18. Schematic of magnet with radial field of intersecting rings.

Key: (1). Region of calculation.

Fig 19. Calculated and measured errors for amount of turning up force

of magnet with radial field of intersecting rings. 1 - calculated values; 2 - measured values.

Page 143.

Fig. 19 for the comparison gives the calculated and measured values of the turning up force of magnet, which has Gaussian spatial distribution. It is evident that these values differ not more than on $5 \cdot 10^{-4}$.

At present it is developed/processed to program MIMI-1 for calculating the vector potential in the iron.

REFERENCES.

1. R.A. Beth. Proc. 1968 Summer Study on Superconducting Devices at Brookhaven. Report BNL 50155, 1968, 3,p.843.
2. K. Lebb, H.H. Umstätter. Report CERN, 1966, 66-7.
3. L.N. Hand, W.K.H. Panofsky. RSI, 1959, 50, p.927.
4. M. Morpurgo. Report CERN, 1965, 65-34.
5. R.B. Britton. Proc. 1968 Summer Study on Superconducting Devices at Brookhaven. Report BNL 50155, 1968, 3, p.893.
6. F. Deutsch. CERN Internal Report MPS-Int., 1967, MA 67-9.
7. W. Hardt. "DESY". Bericht A 1.5, 1959.
8. R. Perin. CERN Internal Report AR/Int., SG 64-12, 1964.
9. W.A. Perkins and J.C. Brown. J. Appl. Phys., Nov., 1964.
10. M. Larkin. Report CIM-R 31- H.M.S.O., 1964.
11. A.A. Halacay, G. Clark, J. Dunks. Proc. 2nd Internat. Conf. on Magnet Technol., Oxford, 1967, p.61.
12. E.A. Taylor. Proc. Internat. Sympos. on Magnet Technol. Stanford, 1965, p.208.
13. A.M. Winslow. Proc. Internat. Sympos. on Magnet Technol. Stanford, 1965, p.170.
14. J.S. Colonias, J.H. Dorst. Proc. Internat. Sympos. on Magnet Technol. Stanford, 1965, p.188.
15. S.B. Vorozhtsov, L.T. Zakamskaya, N.L. Zaplatin. J.I.N.R. Report. Dubna, 1970.
16. R. Perin, S. Vander Meer. Report CERN 67-7, 1967.
17. S. Caeymaex, R. Perin, L. Resegotti. CERN Report, ISR-MA 70-04, 1970.
18. R. Christian. Proc. 2nd Conf. on Analysis of Magnetic Fields, Reno 1969, Univ. Nevada. Engineering Report, 1969, N 26, p.44.
19. M.H. Foss. Proc. 2nd Conf. on Analysis of Magnetic Field, Reno 1969, Univ. Nevada. Engineering Report, 1969, N 26, p.51.
20. S. Caeymaex. Proc. of the 3rd Internat. Conf. on Magnet Technol., Hamburg, 1970; CERN Internal Report ISR-MA 70-19, 1970.

Discussion.

Ye. S. Mironov. Is how the operating speed of the computer, in

which were done the calculations of field taking into account the saturation of iron?

L. Peren. Not it is clear that you call the operating speed of machine. We utilized machine SDS-6600.

V. G. Davidovskiy. In the present report were examined the methods of calculation of magnetic fields with the prescribed/assigned configuration of conductors and iron. However, large interest are of the methods of the determination of the forms of the windings with the permanent current density, which create the required field in the circle or the ellipse in the unshielded system or in the system with the current or iron screening.

If is prescribed/assigned the formed/shaped in the circle (ellipse) field, then field in the metal is determined by a precise analytical expression joining which with the expansion of applied field in the series/row in terms of the multipoles, it is possible to accurately determine by numerical method the unknown boundary of conductor when in the iron of screen $\mu \rightarrow \infty$, without resorting to net point method. This considerably economizes the memory of machine and speeds up count.

41. QUESTIONS OF THE MATHEMATICAL SIMULATION OF THREE-DIMENSIONAL MAGNETOSTATIC FIELDS.

N. I. Doynikov, A. S. Simakov.

(Scientific research institute of the electrophysical equipment in. L. V. Yefremov).

In this communication/report is set forth and is discussed the procedure of calculation of three-dimensional/space magnetostatic fields for the isotropic media, based on finite-difference approximation of the variational and integral forms of Maxwell equations relative to the vector and modified scalar of potentials.

1. Expedient to construct finite-difference equations relative to three-component vector potential $A(x, y, z)$ on the basis of condition of minimum of integral

$$\Phi = \int_{(V)} [q(B^2) - 2VA] dv, \quad (1)$$

in which A satisfies prescribed/assigned values on external boundary of the region. Function $q(B^2)$ is proportional to magnetostatic energy and is connected with magnetic permeability μ with the relationship/ratio

$$g' = \frac{1}{\mu} = \frac{dg}{d(B^2)}, \quad (2)$$

$$B = \text{rot } A, \quad (3)$$

3 - current density; integration is done over entire volume of field.

Page 144.

The chosen method of the determination of the finite-difference equations is not only; however, with this approach most clearly is revealed/detected the physical sense of the obtained expressions.

For the rectangular network (Fig. 1A) difference analogue of integral (1) can be written in the form

$$\Phi \approx \sum_{i,j,k} \left[g(B_{i+\frac{1}{2},j-\frac{1}{2},k+\frac{1}{2}}^2) - 2(J_{i,j,k}^x A_{i,j,k}^x + J_{i,j,k}^y A_{i,j,k}^y + J_{i,j,k}^z A_{i,j,k}^z) \right] h_x h_y h_z, \quad (4)$$

in which through $J_{i,j,k}^x, J_{i,j,k}^y, J_{i,j,k}^z, A_{i,j,k}^x, A_{i,j,k}^y, A_{i,j,k}^z$ are designated the components of the current density and vector potential in node/unit i, j, k , and through $B_{i+\frac{1}{2},j-\frac{1}{2},k+\frac{1}{2}}^2$ - value of the square of induction in the center of cell 1. If first-order derivatives of the unknown functions in formula (3) are replaced with central differences for the average/mean between the nodes/units points, then the unknown system of the finite-difference equations we obtain

during the minimization of sum (4):

$$f_{i,j,k}^x = \partial\Phi/\partial A_{i,j,k}^x = 0, \quad f_{i,j,k}^y = \partial\Phi/\partial A_{i,j,k}^y = 0, \quad (5)$$

$$f_{i,j,k}^z = \partial\Phi/\partial A_{i,j,k}^z = 0.$$

Let us note that expressions (5) can be found also from the integral form of the equations of Maxwell with the circuit/bypass of points $(i \pm \frac{1}{2}, j, k), (i, j \pm \frac{1}{2}, k), (i, j, k \pm \frac{1}{2})$ along the contours/outlines whose planes are perpendicular to the appropriate axes of the coordinates (Fig. 1 it shows the contour/outline of circuit/bypass PQMN of point $(i + 1/2, j, k)$).

The solution of the systems of nonlinear equations (5) is accomplished/realized on the computers by the method of consecutive over-relaxation similarly to works [1, 2].

Based on the example of the task about the effect of nonlinear cube on external uniform field (Fig. 2a shows the first octant of the studied region on boundaries of which it was disregarded by the effect of cube on the applied field) was checked the correctness of computational algorithms, were determined the intervals of the parameter of the consecutive over-relaxation, which ensure the stable convergence of iterative process.

The time of the execution of one cycle (cycle - the correction

of three components of potential in all calculating mesh points) according to the program, written in the input language Fortran, was 10 s on the computers BESM-6 for the region, shown in Fig. 2a. In this case for determination A_x, A_y, A_z with the satisfactory precision/accuracy were required ~40 cycles. The given in Fig. 2b results of calculation give only correct qualitative picture and do not pretend to the precision/accuracy in view of a small number of nodes/units in the studied region (Fig. 2a).

2. Upon classical setting of boundary-value problems of magnetostatics calculation of field is complicated by presence of current carrying regions. This is connected with the vortex/eddy properties of the magnetic field for describing which is applied three-component vector potential. Its most relief calculated difficulties become apparent during the analysis of three-dimensional/space fields in the curvilinear boundaries.

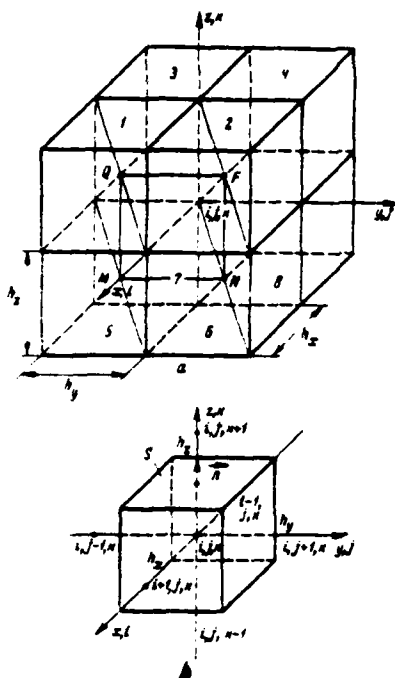


Fig. 1.

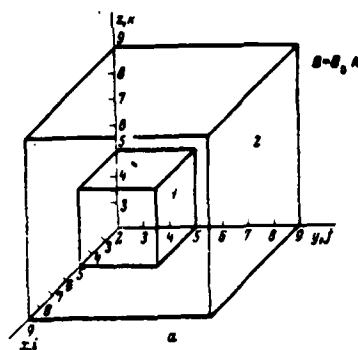


Fig. 2.

Fig. 1. To conclusion/output of finite-difference equations.

Coordinates of the points: $M: i+\frac{1}{2}, j-\frac{1}{2}, k-\frac{1}{2}$; $N: i+\frac{1}{2}, j+\frac{1}{2}, k-\frac{1}{2}$; $Q: i+\frac{1}{2}, j-\frac{1}{2}, k+\frac{1}{2}$; $F: i+\frac{1}{2}, j+\frac{1}{2}, k+\frac{1}{2}$

Fig. 2. On the calculation of the components of potential a) the first octant of the region in question: $1 - \mu = \mu(\bar{E}) = a + B^2/c + B^2$, $a=25600$, $c=16$; $2 - \mu=1$. b) distribution $B_z(x,y,z)/B_0$ along the lines, parallel to the coordinate axes:

$$\begin{aligned} 1 - x = \frac{1}{2}h, y = \frac{1}{2}h, z = \nu\tau; \\ 2 - x = \nu\tau, y = \frac{1}{2}h, z = \frac{1}{2}h \end{aligned}$$

Page 145.

However, the solution is possible substantially to simplify, after raising simultaneously precision/accuracy with the numerical solution of task, if we use the modified scalar potential $V(x, y, z)$ whose description for the two-dimensional fields in linear media ($\mu=1$) is contained in works [3-6].

In this communication/report is constructed the modified scalar potential in the general/common/total (three-dimensional) form for the isotropic media.

Let the magnetic intensity be determined by the expression

$$H = \text{grad } V + P. \quad (6)$$

Then from the equation of Maxwell

$$\text{rot } H = J \quad (7)$$

it follows that vector P must satisfy the relationship/ratio

$$\text{rot } P = J, \quad (8)$$

but from

$$\text{div } B = 0 \quad (9)$$

with

$$B = \mu H \quad (10)$$

and the known vector P it is obtained equation for the determination of potential V :

$$\operatorname{div}(\mu \operatorname{grad} V) = -\operatorname{div} \mu P. \quad (11)$$

In the case $\mu = \text{const}$ expression (11) is simplified and takes form [4]

$$\Delta V = -\operatorname{div} P. \quad (12)$$

The given reasonings, obviously, are valid also for the arbitrary dependence $B(H)$. On the geometric interface of heterogeneous media according to expressions (6) and (10) we have

$$V_1 = V_2, \quad (13)$$

$$\mu_1 \left(\frac{\partial V_1}{\partial n} + P_n \right) = \mu_2 \left(\frac{\partial V_2}{\partial n} + P_n \right), \quad (14)$$

while at infinity

$$\operatorname{grad} V = -P. \quad (15)$$

During the conclusion/output of relationships/ratios (13) - (15) was utilized the continuity of vector P . For the majority of virtually interesting tasks vector P can be constructed so that on the interface of heterogeneous media it will be equal to zero. It does not represent the work to consider also surface/skin currents.

With prescribed/assigned tangential component of field H_τ on bounding surface boundary values V_s (Dirichlet condition) it is located by the integration of relationship (6).

As vector P it is possible to select any particular solution of equation (8). In accordance with selection P will change values V_s

and conditions (14), (15). In the Cartesian coordinate system vector F can be selected as follows:

$$p_x(x, y, z) = \frac{1}{2} \left[\int_{z_0}^z J_y(x, y, t) dt - \int_{y_0}^y J_z(x, t, z) dt - \int_{x_0}^x d\eta \int_{y_0}^y \frac{\partial}{\partial t} J_y(x, t, \eta) dt \right], \quad (16)$$

$$p_y(x, y, z) = \frac{1}{2} \left[\int_{x_0}^x J_z(t, y, z) dt - \int_{z_0}^z J_x(x, y, t) dt + \int_{z_0}^z d\eta \int_{x_0}^x \frac{\partial}{\partial t} J_x(t, y, \eta) dt \right]; \quad (17)$$

$$p_z(x, y, z) = \frac{1}{2} \left[\int_{y_0}^y J_x(x, t, z) dt - \int_{x_0}^x J_y(t, y, z) dt \right], \quad (18)$$

where lower integration limits x_0 , y_0 , z_0 are permanent. If $J_z = 0$, then components (16)-(18) can be written in the simpler form:

$$p_x(x, y, z) = \int_{z_0}^z J_y(x, y, t) dt, \quad p_y(x, y, z) = - \int_{z_0}^z J_x(x, y, t) dt, \quad p_z = 0. \quad (19)$$

In plane-parallel case ($J_x = J_y = 0$) it has [3-5]:

$$p_x(x, y) = - \int_{y_0}^y J_z(x, t) dt, \quad p_y = 0, \quad p_z = 0. \quad (20)$$

In the cylindrical coordinate system vector F is constructed analogously.

This reception/procedure can prove to be useful also with the solution of the problem about the determination of vector by its vortex/eddy and disagreement [7].

Applying the law of conservation of flow to surface of S (see

Fig. 1.b), it is easy to obtain the finite-difference equations whose solution is accomplished/realized on the computers by the method of consecutive over-relaxation [1, 2, 5].

Let us illustrate the possibilities of the described procedure based on the example of the calculation of the end field of a magnet of the type of "window frame" without taking into account the effects of the saturation of the magnetic circuit (from that presented it is clear that there can be also considered the effects of saturation). Fig. 3 depicts the studied region in the divisions of square network. For simplification of computational program the geometry of coil on magnet end is approximated by rectangular fractures. Computational program is written in the input language Fortran, for obtaining the results with the acceptable precision/accuracy on the computers BESM-6 it was required by 40-50 min. From the comparison curves in Fig. 4, 5 it follows that the calculated and experimental data for distributions B_z/B_0 and B_x/B_0 coincide satisfactorily.

In the case of the separate examination of linear and nonlinear saturated regions can be considered by the known [4, 5] method of successive approximations with the use of that of respectively modified of scalar and vector potentials.

In conclusion let us note that the procedure presented can prove

to be highly useful during the design of electromagnets.

The authors express sincere gratitude to the colleagues of
NIIÉPA V. D. Borisov and L. N. Vaulin for the granting of the given
magnetic measurements.

Page 146.

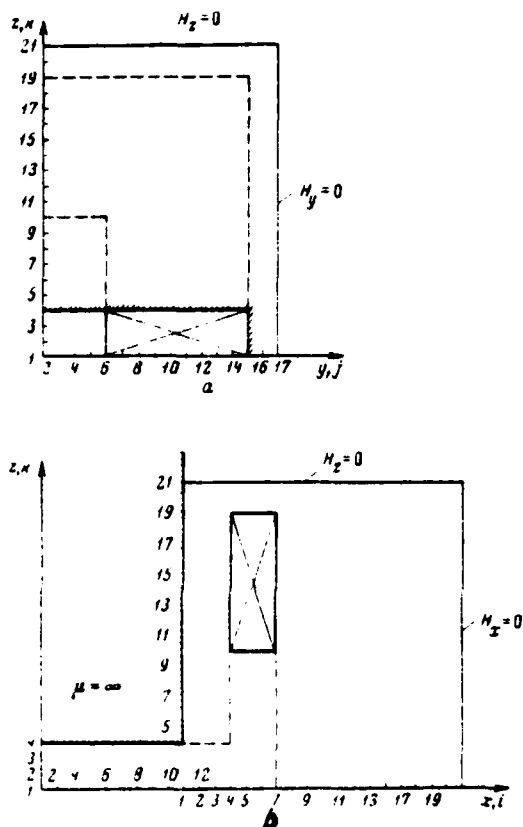


Fig. 3.

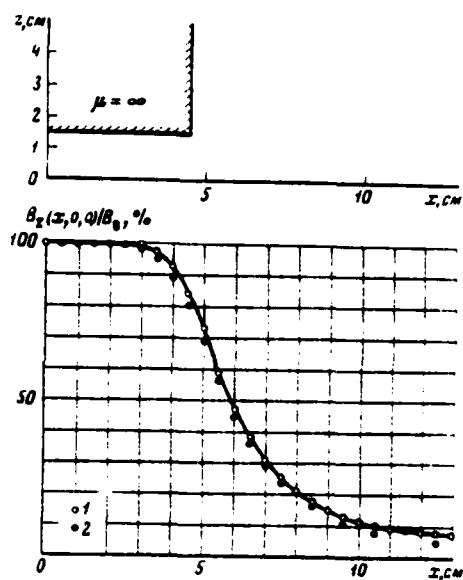


Fig. 4.

Fig. 3. Studied region. a) fourth of the cross section of magnet in the divisions of square network with the step/pitch $h=0.5$ cm; b) the part of the longitudinal section (with a density of $y=0$) of magnet in the divisions of the quadrupoles of network ($h=0.5$ cm). Dotted line showed the simplified for the calculation geometry of coil on the

end/face.

Fig. 4. Distribution $B_z(x, 0, 0)/B_0$. 1 - calculation data when $M=\infty$; - 2 - experimental data with $B_0=6$ kg (E_0 - in the field at the center of the clearance of electromagnet).

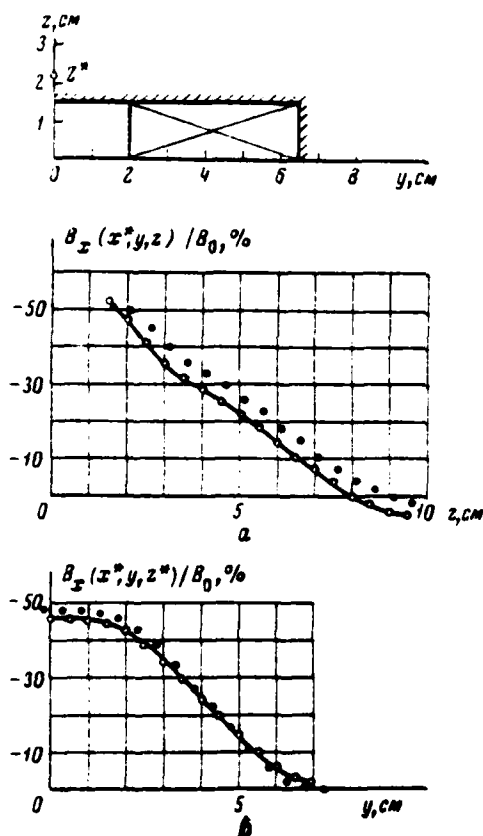


Fig. 5. Distributions $B_x(x^*, 0, z)/B_0$ (a) and $B_x(x^*, y, z^*)/B_0$ (b) ($x^* = 0.7$ - distance from the end surface of magnetic circuit).

REFERENCES.

1. P. Concus. Proc. Internat. Sympos. on Magnet Technol., Stanford, 1965, p.164.
2. N. I. Doynikov, A. S. Simakov. ZhTF, 1969, 39, page 1463.
3. M.S.Livingston, J.P. Blewett. Particle Accelerators. McGraw Hill, N.Y., 1962, p.253.
4. R.Perin, S.Van der Meer. CERN 67-7, ISR Div., 1967.
5. N. I. Doynikov, A. S. Simakov. Transactions of All-Union conference on charged-particle accelerators. M., VINITI, 1970, 1, 319.
6. M. Kumagai. Japan. J. Appl. Phys., 1969, v.8, N 7, p.961.
7. N. Ye. Kochin. Vector analysis and beginnings of tensor calculus. M., "Science", 1965.

Discussion.

V. A. Papadichev. There are whether the methods of the rapid estimations of field with small changes in the parameters of magnet, or each time it is necessary to check version anew?

N. I. Doynikov. There are no such methods, it is necessary to carry out entire calculation anew.

Page 147.

42. Equipment for the magnetic measurements on the synchrocyclotron of PTI of the AS USSR to the energy of protons 1 GeV.

V. A. Yelisseyev, G. A. Siabov, I. I. Tkach.

(Physiotechnical institute im. A. F. Joffe of the AS USSR).

Large volume of the measured magnetic field, stringent requirements for the precision/accuracy of shaping of ground field of 7-meter synchrocyclotron and fields in the system of output led to the necessity of creation of precision magnetometer equipment and automation of the process of measurements. Developed for this purpose complex of instruments consists of the nuclear magnetometer (YAN), the meter of the position of median surface (IMF), precision magnetometer of Hall (PKH) and automated coordinate system (KS) with the unit of control and printed digital output.

Nuclear magnetometer with the automatic frequency control [1]

makes it possible to take a reading of field, without resorting to adjustment after the setting up of sensor into the point with the prescribed/assigned coordinates. Entire measured range of field 17-20 kg overlaps with one sensor. Error of measurement $3 \cdot 10^{-3}$. For the measurements in the fields with the heterogeneity of 20-80 G/cm is applied the compensation for gradient. Extension block/module/unit with the self-excited oscillator and the preamplifier (Fig. 1), carried out on the planar-electrode tubes, is located in the measured field. The length of coupling cable is equal to 40 m. The signal frequency of nuclear resonance is measured by electronic frequency meter Ch -4 and together with the coordinates of measuring point is printed on the strip/film by device/equipment TsPM-1.

The meter of the position of median surface is carried out on the basis of the vertically oriented pickup of Hall [2], which measures radial component B_r . The Hall pickup is arranged/located in the massive copper cylinder, suspended/hung from thin caprone filament (Fig. 2). Massive cylinder provides the vertical orientation of sensor and the effective attenuation of mechanical oscillations due to the eddy currents. An inaccuracy in the vertical orientation of sensor is removed by the method of the subtraction of the results of measurements in the initial position of sensor and in the position, turned relative to vertical line on 180° . The coordinate of median surface ($B_r=0$) is located by interpolation of values B_r of

those measured at two points according to the vertical line near the median surface. With this method of determining the position of median surface sufficient to produce relative measurements and IMP it is actually "zero-adjustment instrument". In this case there is no need in a good stabilization of the feed current of sensor, temperature stability and in the calibration of the sensitivity of the Hall pickup. Therefore were utilized the Hall pickups from n-6e with temperature stability of $0.20/0/1^{\circ}\text{C}$, but with sensitivity $\sim 100 \mu\text{V/G}$, which ensured the measurement of value B_z by digital voltmeter R-339 with the precision/accuracy 1 G without the use/application of an amplifier.

The measurements of nonuniform fields with the gradients $>80 \text{ G/cm}$ were made with the aid of the magnetometer with the thermostatically controlled Hall pickup. The construction/design of tester MKh is given in Fig. 3. Within the tester is maintained temperature of $37 \pm 0.1^{\circ}\text{C}$ with the aid of the adjustable preheating at a temperature of environment of $20 \pm 10^{\circ}\text{C}$. For the equalization of temperature gradients the internal volume of tester is flooded by oil. Temperature detector is the impedance from the copper wire with a diameter of 0.05 mm, connected with alternating-current bridge with the frequency of 1 kHz. The electrical block diagram of thermostat is given in Fig. 4.

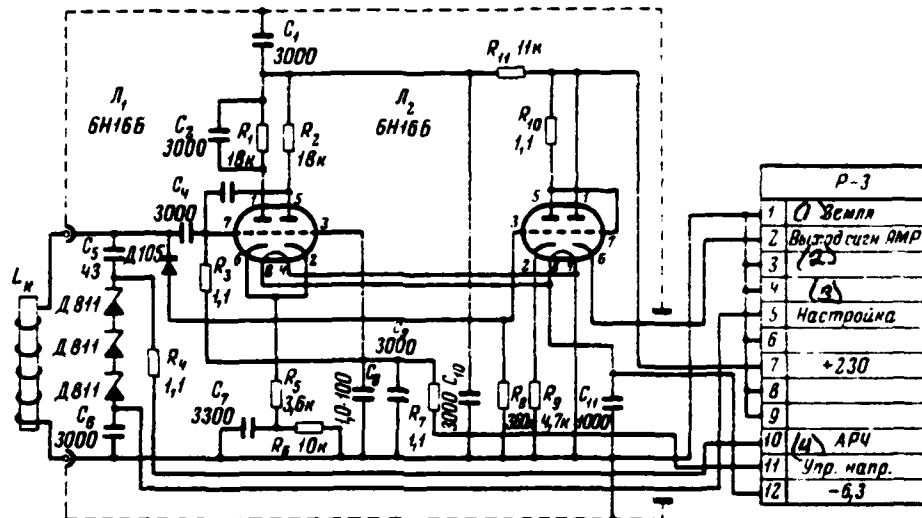


Fig. 1. Diagram of the extension block/module/unit of nuclear magnetometer.

Key: (1). Ground. (2). Output sign. (3). Adjustment. (4). Cont. pulse.

Page 148.

For the supply of the Hall pickups was applied the stabilizer, which ensures work on two ranges of the current: 50-200 mA with the load 1-2 ohms and 5-20 mA with the load 100-200 ohms. Precision/accuracy of the stabilization of current 10^{-4} . Stabilizer is carried out on the diagram with the conversion of constant stress

into the variable/alternating. As the converter is utilized integral interrupter IP-1G. Standard resistance, IP-1G and supporting/reference stabilizer tube D818Ya are placed into the thermostat, in which is maintained temperature of $60 \pm 0.5^\circ\text{C}$. The block diagram of stabilizer is given in Fig. 4. Calibration of MKh was conducted with the aid of YaM, an error of measurement MKh $3 \cdot 10^{-4}$. Hall voltage is measured by digital voltmeter B-339 and together with the coordinates is printed on the strip/film.

Coordinate system with the unit of control [3] makes it possible to automate the process of the measurements: to remotely/distance install sensors into measuring point, to start meters, to print coordinates and results of the measurements by device/equipment TsPM-1. Basis of KS is five-meter beam/gully with the rotational axis in the center of magnet. Radial coordinate is assigned by the displacement of measuring carriage along the beam/gully, azimuthal - by rotation of beam/gully; z - coordinate of tester IMP is assigned mixing of tester relative to carriage. Displacements over R and θ - to coordinates are conducted by engines of the nonmagnetic materials, for which the measured field is stator. Azimuthal coordinate is set by the two-channel servo system with the coefficient of reduction from the fine selsyn to rough of 50:1. The rotation of beam/gully is conducted by the actuating mechanism, carried out from the stray field, with the aid of the shaft with a length of 5 m. The setting up

DCC = 80069212

PAGE

6/7

of carriage on a radius is produced at discrete/digital points with the step/pitch 80 mm. For the measurements in the system of the conclusion/output where there was required the decrease of the step/pitch of measurements, was utilized the carriage, which makes it possible to move sensors relative to carriage to the length of 150 mm with the minimum step/pitch 1 mm.

PAGE

618



Key: (1). Form on arrow/pointer A.

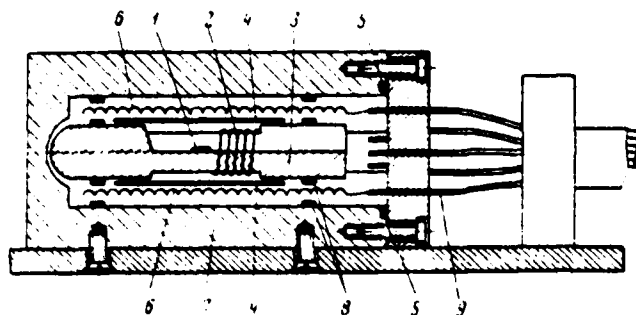


Fig. 3.

Fig. 3. Tester of Hall's magnetometer. 1 - Hall pickup; 2 - winding of thermometer; 3 - copper basis/base; 4 - heat-insulating packing; 5 - rubber gasket; 6 - heater; 7 - housing; 8 - packing; 9 - electrical leads.

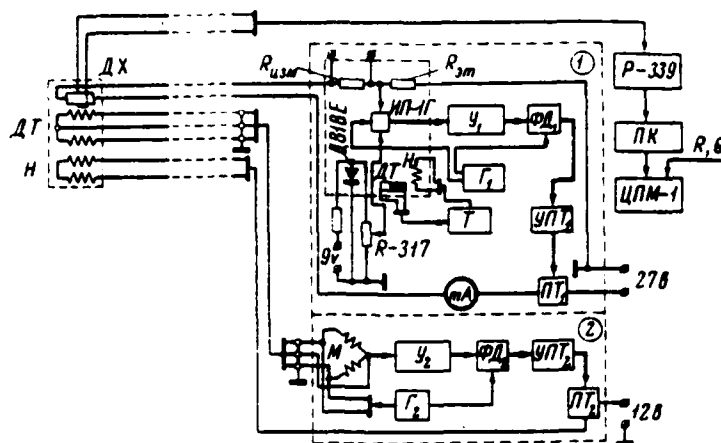


Fig. 4. Block/module/unit is the diagram of Hall's magnetometer: 1 - current regulator; 2 - thermostat of tester; 3 - thermostat of current regulator; ДХ - pickup of Hall of the type Kh511, U - amplifier; ФД - the phase discriminator; Г - oscillator; УПТ - dc amplifier; ПТ - passage transistor; ДТ - temperature sensor; Н - heater; Т - control of the thermostat of stabilizer; Р-339 - digital voltmeter; ПК - converter of code Р-339; ЦПМ-1 - printer; Р-317 - potentiometer; IP-11 - integral interrupter.

Page 149.

Range of displacement over the vertical line 150 mm with the step/pitch 25 mm. The points of measurement along the azimuth are distributed evenly, a number of measuring points can be equal to 100,

50, 25, 20 or 10. The precision/accuracy of the setting up of the coordinates of sensors comprises on radius and height of 0.1 mm, along azimuth of 0.1°. Control of shift on all coordinates, the position display of sensors (R , θ , z), the starting/launching of meters and printed digital output are conducted by the unit of the control whose block diagram is given in Fig. 5. The position of sensor on each of the coordinates is determined by the bidirectional counter, which counts a number of points by a number of closings/shortings of key/wrench, which occur with the passage of measuring point. YAM measurements can be conducted automatically according to the previously selected program. Rate of the automatic measurements of YAM on radius 15 measurements per minute, along the azimuth - 25 measurements per minute (in the measurements at 100 points). Rate of the measurements by Hall's magnetometers - 140 measurements in the hour. Measurements are conducted by one operator from the panel, distant on 20 m from the measured field. After the introduction of series of changes, connected with cooling of the sensors of YAM, IMF and engines, which are located in magnet gap, appeared the possibility to use equipment for the control measurements of the topography of field with the vacuum in accelerative chamber/camera [4].

Measuring complex is very effective with shaping of ground field of synchrocyclotron. With its aid was possible to shape the field of

seven-meter synchrocyclotron with the relative amplitude of the fundamental harmonic $\leq 2 \cdot 10^{-6}$ and the divergence of median plane from the the geometric mean ≤ 1 cm. With its aid were also shaped the fields of magnetic pipe and regenerator in the highly efficient system of conclusion/output [5, 6].

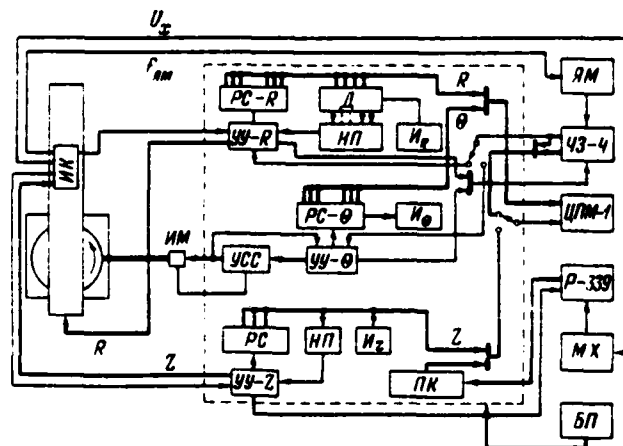


Fig. 5. Block diagram of the control unit. BS - bidirectional counter; D - decoder; NP - setting field; I - indication; UU - block of the logic of control of displacement; USS - servo-amplifier; IM - the actuating mechanism of servo system; IR - measuring carriage; BP - power supply unit; YAM - nuclear magnetometer; MKh - Hall's magnetometer; TsPM - 1 - printer; B-339 - digital voltmeter; ChZ-4 - electronic frequency meter; PK - converter of code B-339.

REFERENCES

1. I. I. Tkach. Nuclear magnetometer with the automatic tuning. Preprint of FTI, 039, L., 1967.
2. M. K. Abrosimov, V. A. Yeliseyev, G. A. Riabov. Instrument for the measurements of the position of nodular surface. Preprint of

FTI, 040, L., 1967.

3. N. K. Abrosimov, V. A. Yeliseyev, G. A. Biabov, I. I. Tkach. Instruments and technique of experiment, 1968, No 6, page 217.

4. N. K. Abrosimov, V. A. Yeliseyev, I. A. Petrov, G. A. Biabov, I. I. Tkach, N. N. Chernov. Magnetic measurements on the synchrocyclotron of FTI with the vacuum in the accelerative chamber/camera. Preprint of FTI, 131. L., 1968.

5. N. K. Abrosimov, D. G. Alkhazov, S. F. Dmitriev et al. Synchrocyclotron of FTI of the AS USSR to the energy of the accelerated protons 1 GeV. Report on international conference on the charged particle accelerators. Yerevan, 1969.

6. N. K. Abrosimov, V. A. Velchenkov, V. A. Yeliseyev, G. A. Biabov, N. N. Chernov. The conclusion/output of the proton beam of the synchrocyclotron of FTI of the AS USSR to the energy of protons 1 GeV (see this coll., Vol. 1).

43. Equipment for the magnetic measurements in the electromagnet VAPP-4.

B. A. Baklakov, V. P. Veremeyenko, M. M. Karliner, E. A. Kuper, B. V. Ievichev, A. D. Oreshkov, I. Ya. Protopopov.

(Institute of nuclear physics of SO AN USSR [Siberian Department of the Academy of Sciences of the USSR]).

In connection with the large volume of the magnetic measurements of the electromagnet of proton-antiproton accumulator/storage VAPP-4 in the institute of nuclear physics (Novosibirsk) was developed and prepared the improved measuring equipment, in which for measuring the magnetic field are utilized the Hall pickup, the distributed on operating region sections of magnet. The use/application of a commutator on the field-effect transistors and the use of a direct coupling with the computers made it possible to sharply increase the operating speed of system in comparison with the system, described in work [1].

Page 150.

As the measuring elements/cells are utilized the Hall pickups,

developed in SKB IPAN of the USSR (Leningrad). The standard characteristics of sensors are given below:

Sensitivity of sensors with the operating current, $\mu\text{V/Oe}$... 10-15.

Operating current, mA ... 160.

Temperature sensitivity index, $\text{c/c}/^\circ\text{C}$... 0.01-0.03.

Input and output resistance, ohm ... 1-3.

Emf of nonequipotentiality with operating current, μV ... ≤ 100 .

Temperature coefficient of emf of nonequipotentiality, $\mu\text{V}/^\circ\text{C}$... 1-2.

Effective area of sensor, mm² ... 1.5x0.5.

These sensors are characterized by a small drift of emf of nonequipotentiality and its weak quadratic dependence on the tangential component of magnetic field [2]. The calibration of sensors is conducted in the special calibration magnet whose field is stabilized with the aid of the nuclear magnetometer with the precision/accuracy not worse $\pm 10^{-4}$.

The sensor unit of Hall is carried out analogously with that described in work [1]. Ten sensors measure the vertical component of magnetic field (two series/rows on 5 sensors), two sensors - radial. Besides them, into the block are installed the thermistors, signals from which are utilized in the computers for the introduction of temperature correction, which made it possible to forego the thermostatic control.

The block diagram of measuring system is shown in Fig. 1, and its general view - in Fig. 2.

The Hall pickups are connected in series and are supplied from one source of stable current with the lasting instability less $\pm(2-3) \cdot 10^{-4}$. The oscillator circuit of current is isolated/insulated and has a small capacity/capacitance with respect to the earth/ground and the power line (200 pF).

The sensor unit of Hall is moved within the chamber/camera of electromagnet on accurately carried out guides. The motion of block is accomplished/realized continuously with the aid of the screw/propeller in long approximately 4 m with which is mechanically connected the light sensor of longitudinal coordinate. Precision/accuracy of the determination of coordinate ± 0.1 mm. The shaper of light sensor puts out synchronizing pulses through 1 cm of the path, passed by sensor unit.

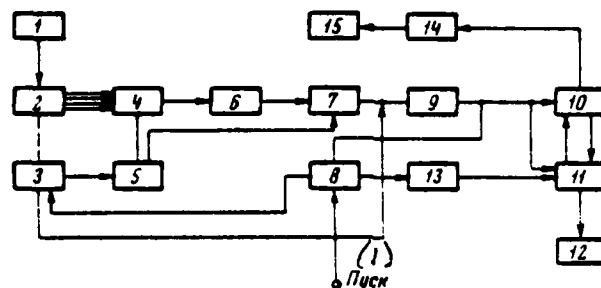


Fig. 1. The block diagram of the measuring system: 1 - current generator; 2 - sensor unit of Hall; 3 - block of displacement and measuring the coordinate; 4 - commutator; 5 - programmer; 6 - dc amplifier; 7 - digital voltmeter; 8 - block of initial data; 9 - code converter; 10 - computer "Minsk-22"; 11 - buffer; 12 - magnetic recorder; 13 - control unit of recording; 14 - code converter; 15 - electrical typewriter.

Key: (1). Launching/starting.

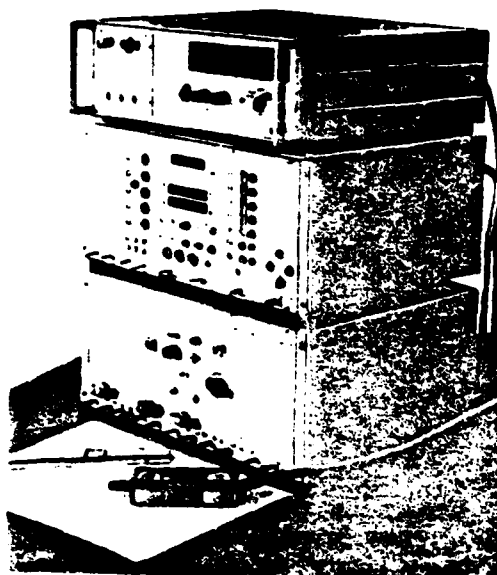


Fig. 2. Measuring system.

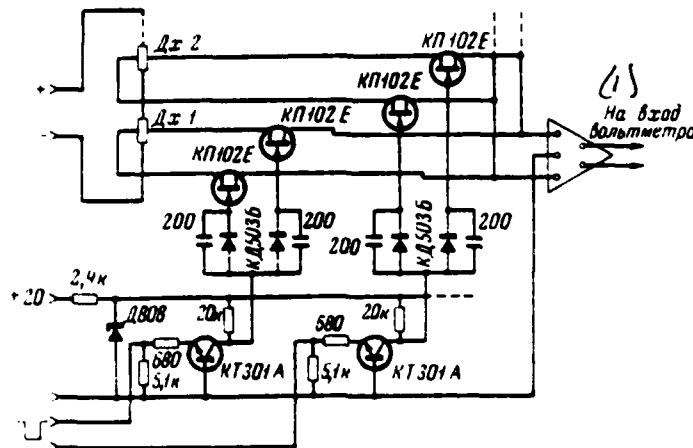


Fig. 3. Diagram of commutator on the field-effect transistors.

Key: (1). To the entrance of voltmeter.

Page 151.

The start of any sensor (DKh1, DKh2 and so forth in Fig. 3) is accomplished/realized during closing/shorting of two keys/wrenches on the field-effect transistors KP102Ye. Field-effect transistor is opened, when the voltage between the source and the gate is equal to zero, and it is closed, when voltage on the gate relative to source more or is equal the potentials of cutoff, equal to usually 2-3 V. Control of channel accomplishes/realizes the commutating cascade/stage on the transistor KT301A, potential on

collector/receptacle of which can take two values: $\pm 8; 0.6$ V. The collector/receptacle of the commutating transistor is connected with the gates of two field-effect transistors by the silicon diodes KD503B, shunted by the capacitances/capacitances of 200 pF which serve for accelerating the changeover. This diagram of control of keys/wrenches makes it possible to support at the gate of the open transistor zero potential relative to source (acode/conditions with the floating gate).

The voltage drop, which appears because the currents of the gates of the closed transistors in other channels flow/occur, last over the triggered key/wrench, makes the accuracy worse of measurement, but with the identical impedances of the pair of keys/wrenches in the open state and identical currents of gate occurs the compensation for these voltages. Therefore field-effect transistors were selected into the pairs with the identical impedances in the open state and identical currents of gates. The selected transistors have the following characteristics: the current of gate in the closed state is not more than 10^{-9} A, the impedance of key/wrench in the open state is not more than 3 kilohms, in that closed - not less than 10^{10} ohms. The symmetry of the diagram of commutator decreases the cophasal focusing/induction from the network/grid. For decreasing the commutation interferences is provided for the channel, which short-circuits the entrance of

amplifier at the moment of changeover on 2000 μ s. The assembly of commutator is produced on the glass, Textolite and teflon for the exception/elimination of leakages.

The temperature drift of difference emf, which appears due to the imbalance of the currents of gates and impedances of keys/wrenches, is equal to 0.1-1 μ V/ $^{\circ}$ C in the working temperature range of 10-30 $^{\circ}$ C.

Scale dc amplifier is carried out on the diagram "modulator-amplifier-demodulator" with the transformation of signal on the field-effect transistors KP102Ye. The use/application of field-effect transistors in the modulator made it possible to obtain small temperature (~ 2 μ V/ $^{\circ}$ C) and time/temporary (~ 6 μ V in 8 hour) of the zero drift amplifiers. For obtaining the high input resistance (this is necessary, since the triggered key/wrench on the field-effect transistor it has comparatively high impedance) and stable amplifier gain is included by the crossed feedback (Fig. 4). This feedback proved to be possible because of the fact that the entrance of amplifier balance (weakening the cophasal signal of amplifier without the feedback 120 dB) and source of signal was not grounded. Amplifier is balanced in such a way that input resistance is equal to 30 M Ω . The instability of amplification factor in the working temperature range is not more $3 \cdot 10^{-4}$. Time constant of

amplifier on the order of 1 μ s.

For decreasing the electromagnetic focusing/induction the conductors, that connect the Hall pickups with the amplifier, are interwoven, and entire/all diagram is shielded. Focusing level, led to the entrance of amplifier, is 20-30 μ V, but its effect decreases because the starting/launching of digital voltmeter is synchronized with the network/grid.

The measured by voltmeter V2-22 voltage in the form of the parallel binary decimal code enters the converter of the code which transforms the code into the parallel-series for the transmission in MOZU [core storage] of computer. Duration of transmission of one numeral in the form of the five-digit parallel code - 60 μ s. For the setup and gauging works is provided for the work for perforator PP-20. Furthermore, is possible the recording of the results of measurement for the tape recording strip/film. With the work directly on computers (without the magnetic recorder) is provided for the possibility of using the teletype channel of computers for data input into the machine, the controls of the program of processing measurements and operational obtaining of information about the course of measurements.

The automatic cycle of measurements in one section of

electromagnet includes the recording of zero of amplifier upon the shortened/shorted out entrance, consecutive request of 12 sensors, testing the amplifier gain and current of sensors, control of the temperature of sensor unit, recording of the value of the current of electromagnet. Control of channels and digital voltmeter accomplishes/realizes a programmer. The beginning of cycle is determined by synchronizing pulse from the sensor of longitudinal coordinate.

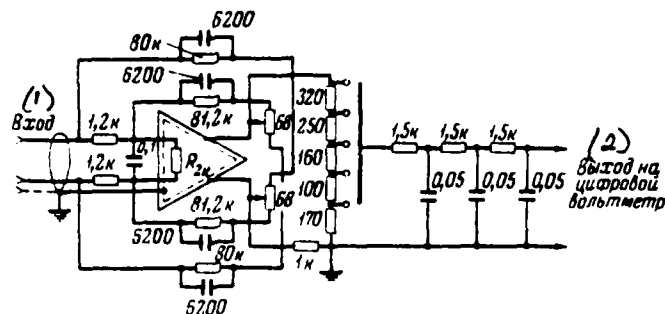


Fig. 4. Amplifier of direct current with feedback.

Key: (1). Input. (2). Output to digital voltmeter.

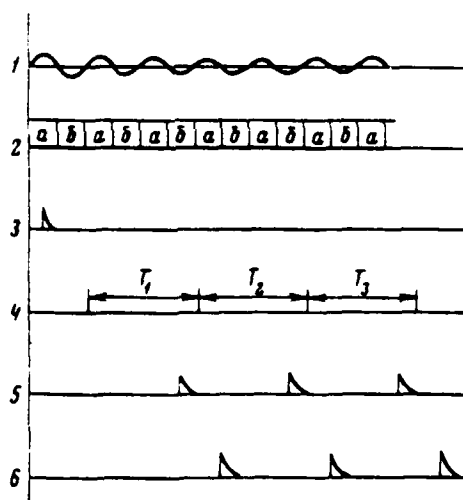


Fig. 5. Temporary/time performance record of system with frequency of 25 Hz: 1 - power line 50 Hz; 2 - performance record of digital voltmeter, a) time of measurement, b) storage time of measured voltage; 3 - trigger pulse of cycle of measurements; 4 - diagram of changeover of channels, T_1 - time, during which is connected first

channel T_2 - time when is connected second channel and so forth; 5 - trigger pulses of voltmeter; 6 - trigger pulses of code converter.

Page 152.

The time of one measurement is equal to 40 μ s, the time of measurement in one section (i.e. the duration of cycle) - 640 ns. Measurement is made without the cessation of the sensor unit which passes the path with a length of 0.5 cm in the complete cycle. Fig. 5 shows the time performance record of system with the frequency of 25 Hz. The work of system is synchronized with the frequency of power line. Are provided for the modes/conditions of external manual and automatic starting/launching. At the moment of the beginning of cycle in the computers is sent the value of the coordinate of sensor unit.

Before beginning the measurements by the block of initial data in the computers are sent following data: the standard code, which indicates the beginning of next measurement; the number of measurement; the number of magnet; the date of measurement; the cipher of the operator, which generates measurements; stand-by information.

Because of the fact, that during the cycle of measurements in one section of electromagnet in the computers will be brought in values

of zero and amplifier gain, and also current of the Hall pickups, significantly descend requirements for the lasting stability of these parameters.

Resultant error in this measuring system does not exceed $\pm(3-5) \cdot 10^{-4}$.

REFERENCES

1. B. A. Baklakov, M. M. Karliner, E. V. Levichev, A. S. Medvedko, I. Ya. Protopopov. Device/equipment for the precision measurements of magnetic field in the electromagnet of accumulator/storage. Transactions of All-Union conference on the charged particle accelerators. M., 9-16 October 1968. Vol. 1. M., VINITI, 1970, page 674.
2. B. A. Baklakov, M. K. Karliner, E. V. Levichev, A. S. Medvedko, I. Ya. Protopopov. Use/application of Hall pickups for the precision measurements of magnetic field. Preprint of IXAF of 9-70 AS USSR, Novosibirsk, 1970.

44. Formation of rectangular current pulses in the impact magnet with the complex input resistance during the use of artificial line.

I. Yu. Beneskiptov, S. M. Klistevskiy, B. A. Larionov.

(Scientific research institute of the electrophysical equipment in. E. V. Efremov).

Conducting a whole series of experiments on the contemporary accelerators requires the creation of the systems of the pulse commutation of the beams, which ensure the highly efficient conclusion/output of part or entire accelerated beam. One of the basic elements of this system is the impact magnet which provides the necessary angular deflection of beam, moreover field in magnet opening for the effectiveness of conclusion/output 100% must build up to the nominal value ides zero for the time smaller than the time/temporary interval between adjacent bunches, i.e., for the time of order 10^{-7} s, for the duration of pulse $\sim 5 \cdot 10^{-8}$ s.

In known systems [1, 2] as the kicker is used the magnet, which is delay line with the impedance, equal to the impedance of the forming line. For the formation of trailing edge of pulse in the

diagrams indicated is utilized the special discharger/gap, which short-circuits the entrance of the transmitting cable directly before the termination of impulse/momentum/pulse from the forming line.

In spite of simplicity of the diagram of formation and good parameters of the formed/shaped impulse/momentum/pulse, diagram with the magnet of the type of delay line has a number of the deficiencies/lacks, basic from which is the excessive structural/design complexity of magnet, especially during the low-resistance performance.

Considerably simpler by the construction/design is a magnet of the type of the lumped inductance which was for the first time used in the system of rapid conclusion/output in Brockhaven [3]. However, in the proposed in Brockhaven diagram of formation the parameters of the impulse/momentum/pulse, formed in the magnet, are considerably inferior to the analogous diagrams of formation during the use in them of a magnet of the type of delay line. Furthermore, this diagram does not provide the possibility of the formation of trailing edge of pulse.

The deficiencies/lacks indicated are resolved in the diagram, shown in Fig. 1.

By the correct selection of corrective capacity/capacitance C_k it is possible to obtain with the permissible ejection at the pulse apex Δi leading impulse front t_ϕ not worse than during the use of a magnet of the type of delay line.

For the diagram in Fig. 1 the leading impulse front of current in the inductance is determined by the expression:

$$t_\phi = \frac{2\tau\tau'}{\sqrt{8\tau\tau' - (\tau + \tau')^2}} \left(\frac{\pi}{2} + \arctan \frac{\tau - 3\tau'}{\sqrt{8\tau\tau' - (\tau + \tau')^2}} \right), \quad (1)$$

where

$$\tau = \frac{L_M}{R_M}; \quad \tau' = R_M C_k,$$

but the relative ejection of the current above conservative value $\frac{\Delta i}{j}$ is found from the equation:

$$\frac{\Delta i}{j} = \sqrt{\frac{\tau'}{\tau}} \exp \left[-\frac{\tau + \tau'}{\sqrt{8\tau\tau' - (\tau + \tau')^2}} \left(\frac{\pi}{2} + \arctan \frac{\tau + \tau'}{\sqrt{8\tau\tau' - (\tau + \tau')^2}} \right) \right]. \quad (2)$$

Page 153.

For the assigned magnitude of ejection $\frac{\Delta i}{j}$ the necessary value of the corrective capacity/capacitance and the corresponding rise time can be found from the graph/curve, obtained according to formulas (1) and (2) for the most interesting range of values $\frac{t_\phi}{\tau}$ and $\frac{\Delta i}{j}$ (see Fig. 2). In principle, if line (Fig. 1) forms symmetrical square pulse, then rise/leading and trailing edges of pulse of current in magnet L_M will be equal. However, the real

shapers - artificial line or distributed-parameter line due to the presence of ohmic losses form/shape the impulse/momentum/pulse whose trailing edge is considerably worse than the front/leading.

In connection with this for the formation of trailing edge of pulse into the diagram is introduced the short-circuiting discharger/gap K_2 , with series-connected with it inductance L_2 , which represents by itself several ferrite rings, put on to the lower electrode of discharger/gap. Sizes/dimensions and brand of ferrite rings are selected so that the current of saturation of ferrite would compose 5-10% of the basic current, and the current of the ignition of discharger/gap must somewhat exceed this value. Inductance L_2 in the unsaturated state is selected equal to (5-8) L_m . During the supplying to the lower clearance of discharger/gap K_2 of the igniting impulse/momentum/pulse inductance L_2 is saturated also with the subsequent breakdown of the basic discharge gap of discharger/gap K_2 the forming line short. Up to the moment/torque of the arrival of the echo signal (time is determined by the length of the transmitting cable and it is usually 0.5-1.0 μs) current in discharger/gap K_2 is close to zero, inductance L_2 is in unsaturated state, the input resistance of circuit $K_2 L_2$ is great in comparison with the input resistance of the forming line and the attached echo pulse, after passing the forming line, is absorbed by impedance of R_1 .

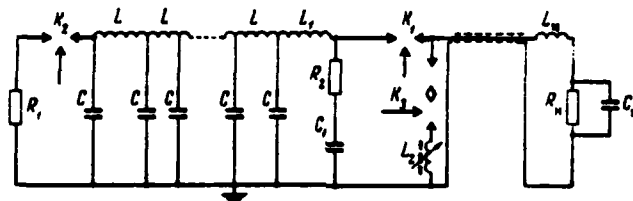


Fig. 1. Diagram of formation with the absorbing inductance in the circuit of the short-circuiting discharger/gap. LC - cell of the forming line; K_1 - basic discharger/gap; K_2 - discharger/gap, which controls the pulse duration; K_3 - short-circuiting discharger/gap; L_2 - saturating inductance in the circuit of discharger/gap K_3 ; L_1 , C_1 , B_2 - managing cell; R_1 and R_N - absorbing and load resistance; C_k - corrective capacity/capacitance; L_m - impact magnet.

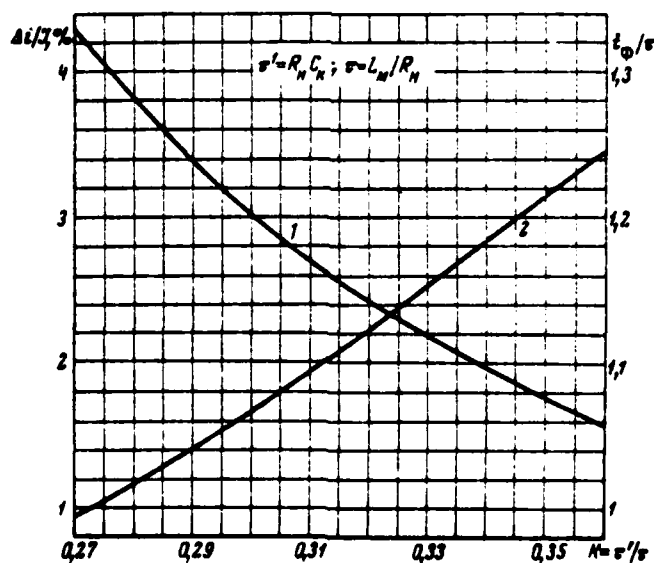


Fig. 2.

DOC = 80069212

PAGE

643

Fig. 2. Graph/diagram of dependence of selection (1) and pulse edge (2) on value of corrective capacity/capacitance.



Fig. 3. Oscillogram of the voltage pulse from the forming line. Scale of the oscillogram time marks of 0.2 μ s.

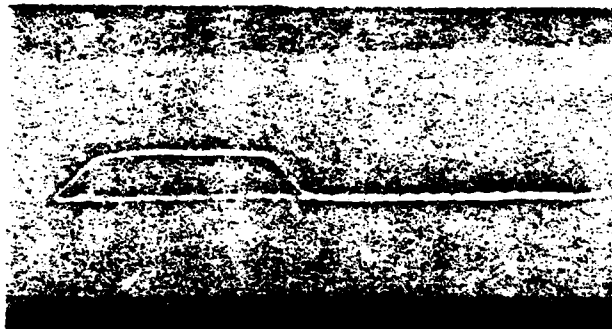


Fig. 4. Current oscillogram in magnet with inductance in circuit of discharger/gap. Scale of the oscillogram time marks of 50 ns.

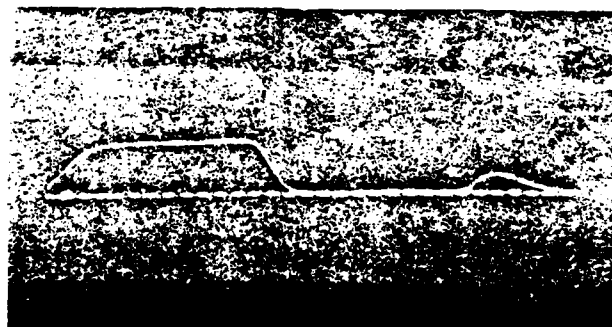


Fig. 5. Current oscillogram in magnet without inductance in circuit

of discharger/gap. Scale is the method of the time of 50 ns.

Page 154.

The conducted theoretical and experimental investigations showed that with value indicated above of inductance L_2 and trailing edge of pulse from the forming line, which does not exceed the dual delay time of the transmitting cable, the echo signal in magnet -10/o of the basis, while in the diagram without inductance L_2 the echo signal reaches value 40o/o from the basis. The system described above was virtually realized in connection with the development of the system of the rapid output of channel B for the accelerator IPVE.

Diagram is calculated for the following parameters: working voltage 50 kV, the impedance of the forming line - 4 chas, currents in the magnet $6.25 \cdot 10^3$ A, pulse edges - 150 ns. The forming line consists of 40 cells. The capacitor of cell is formed by 18 series-connected sections, by which are the capacitors IM-50-3 with the changed construction/design of conclusion/output. Stray inductance of the capacity/capacitance of the cell of order $8 \cdot 10^{-9}$ H with the inductance of cell $0.6 \cdot 10^{-6}$ H. In the managing cell $L_1 C_1 R_2$ are used the capacitors of the type KVI-3.

As the commutating elements/cells K_1 , K_2 and K_3 are utilized the

coaxial controlled 4-cta dischargers/gaps, which work on the compressed gas. Time jitter of activation of dischargers/gaps is not worse than ± 10 ns.

Fig. 3 gives the oscillogram of the voltage pulse from the forming line, while on Fig. 4 and 5 - current pulse in magnet L_m with the inductance in the circuit of discharger/gap K_2 and without it.

As can be seen from the given oscillograms, introduction to the diagram of inductance L_2 virtually removes the echo pulses in impact magnet L_m .

REFERENCES

1. H. Van Breugel, J. Goni, E. Kuiper. Pulse generators for delay line deflectors, NPA/INT, 65-28, 1965.
2. B. Kuiper, S. Milner. The new "Bare" kicker magnet of the CPS fast ejection system. NIA/INT, 67-10, 1967.
3. E. B. Forsyth, C. Lasky. The fast Beam extraction system of the Alternating Gradient Synchrotron. N Y, BNL 910 (5-979) Upton, 1965.

45. Magnetic oscillator for the formation of powerful/thick rectangular current pulses in the inductance.

N. A. Monoszon, B. K. Fatnikov, A. M. Stelov.

(Scientific research institute of the electrophysical equipment in. D. V. Efremov).

For the rapid conclusion/output of the part of the beam from the synchrotron is required the impulse/momentum/pulse of magnetic field with the fronts, which do not exceed the time/temporary gap/interval between bunches of particles, the stepped diagram of beam extraction [1] allowing/assuming the oscillations of field in the work of that magnet to $\pm 50\%$ of the amplitude of pulse [2].

One of the possible solutions of stated problem is described in [3], where for the impulse shaping with the steep/abrupt decrease in the impact magnet of the type of delay line is utilized artificial line with the short-circuiting discharger/gap. However, with this method of the formation of square pulses supply voltage is twice higher than the voltage, applied to the magnet. Furthermore, magnet is very complicated construction/design. Therefore continues the

search of the solutions, which make it possible to utilize an impact magnet of the type of inductance.

The formation of rectangular current pulses in the inductance on the basis of the use of nonlinear properties of ferromagnetic square-loop materials of hysteresis makes it possible to decrease supply voltage, to simplify the system of rapid conclusion/output and, therefore, to raise its reliability.

Simplest diagram with the nonlinear elements/cells is the oscillatory circuit in which the capacitor of capacity/capacitance C_0 is discharged for inductive load L_m through the choke/throttle, magnetized by current $I_1 = -I_2 N_2 / N_1$, where N_1 - number of turns of inducing winding of choke/throttle, $I_2 N_2$ - ampere turns of control winding, and sign "minus" shows that the current of magnetic biasing in the direction is opposite to current in the working circuit. If the toroidal core of choke/throttle is prepared from the ferromagnetic square-loop material of hysteresis and current I_1 such more than saturation current I_s , then in the working current circuit will build up to the ascent/torque of time t_ϕ , beginning from which choke/throttle it is reversed magnetism. With the partial magnetic reversal of choke/throttle will be shaped rectangular impulse/momentum/pulse with the duration of plateau $\tau_{on} = 2C_0 U_c / I_1$, where U_c - voltage across capacitor at the ascent of time t_ϕ . The

condition of the partial magnetic reversal of choke/throttle can be presented in the form $I_1 L_M \tau_{na}/t_0 = 8N_1 S B_s$, where S - section of core,

B_s - saturation induction, and the amplitude of oscillation of current in plateau of impulse/accentum/pulse to determine according to formula $\Delta i \approx U_c \sqrt{C_3/L_M}$, where C_3 - equivalent capacity/capacitance of choke/throttle. Data of relationship/ratio are valid when ferromagnetic material corresponds to the selected operating frequency of oscillations $f_0 \approx 1/2\pi \sqrt{C_3 L_M}$.

Page 155.

Diagram with one nonlinear choke/throttle provides oscillating process with the square pulse for the required positive half-wave of current and sinusoidal form for the negative half-wave. For the formation of single square pulses it is necessary that the negative half-wave of current would not pass through inductive load L_M and its energy would be absorbed on effective resistance of R . This task can be solved, if load is separated/liberated with the aid of the magnetized peak transformer IT , in primary circuit of which is connected the attenuating choke/throttle.

Fig. 1 gives the schematic diagram of the generation of single rectangular current pulses in the inductance. In this diagram chokes/throttles L_1 and L_2 are intended for the formation of the

flat/plane part of the current pulse of the necessary amplitude. Choke/throttle L_3 serves for the reduction of the amplitude of the current of negative polarity in the load to the value, which does not exceed the saturation current of choke/throttle L_3 . The attenuating choke/throttle L_4 , which smooths oscillations in plateau of impulse/momentum/pulse, plays the role of tilt key. The impulse/momentum/pulse of positive polarity is passed in essence through the saturated choke/throttle L_4 , and negative polarity - through resistance of R . Cable is intended in order to remove the serviced discharger/gap from the zone of radiation.

Throttle control is accomplished/realized from two power supplies. Low-power direct-current circuit supports cores in the saturated state. Powerful/thick pulsing circuit creates the current of sinusoidal form whose duration is determined by the permissible change in the current at the pulse apex in the time interval for shaping right-angled of operating pulse. Capacitor bank of the pulsing circuit of control is isolated by high frequency from the control windings of chokes/throttles L_1 and L_2 with the aid of the transformer whose magnetic circuit is collected from iron. In the control circuits are also connected the chokes/throttles of the decoupling of contours/outlines L_{p1} and L_{p2} .

For decreasing the value of the equivalent capacity/capacitance

of transformer IT is preferable the construction/design, which has two one-layers winding from the flat/plane busbar/tire, arranged/located above each other. For the given construction/design of windings equivalent capacity/capacitance will be $C_2 = C_{12} + C_{10}$, where C_{12} - capacity/capacitance between the windings, and C_{10} - capacity/capacitance between the winding and the core. The capacity/capacitance between the windings is equal to zero, if transformation ratio $k=1$ [4]. The capacity/capacitance between the winding and the core will be smallest, if we core insulate from the zero potential and to increase the thickness of isolation between the core and the winding. An increase in the thickness of insulation/isolation between the core and the winding leads to the increase of the inductance of chokes/throttles in the saturated state and the corresponding decrease of the pulse steepness. The instantaneous value of current in the inductive load at the pulse edge for case of $k=1$ takes the form

$$i_2 = \frac{U_0}{\rho} \frac{4}{1-\eta} \exp\left[-\frac{1+\eta}{2} \frac{t}{T}\right] \operatorname{sh} \frac{1-\eta}{2} \frac{t}{T},$$

where U_0 - charging voltage of capacitor; ρ - wave impedance of the transmitting cable; $\eta = L/C_0 \rho^2$, $T = L/\rho$; $L = L_M + L_{H2}$, L_{H2} - total inductance of the saturated chokes/throttles, scattering of transformer, etc. When $\eta \approx 0.41$ the current will achieve value U_0/ρ , equal to the current of cutoff (magnetic biasing) I_2 of choke/throttle L_2 for time $t_0 = L/\rho$.

The experimental investigations of oscillating processes in the contours/outlines with the nonlinear elements/cells were conducted for the diagram without the attenuating choke/throttle. As the toroidal cores of chokes/throttles and peak transformer was utilized the ferrite 100NN. The sizes/dimensions of core were $\phi 30 \times \phi 56 \times 12,5$ mm. Inducing windings had 6 turns.

Circuit parameters following: $C_0 = 0.1 \mu\text{F}$; $U_0 = 3.5 \text{ kV}$; $L = 4 \mu\text{H}$; $L_M = 2,8 \mu\text{H}$; $\rho = 5 \text{ ohm}$ (length of cable 40 m); $I_1 = 300 \text{ A}$; $I_2 = 285 \text{ A}$; $I_3 = 15 \text{ A}$. Measuring resistances in the primary and secondary IT respectively 0.155 and 0.140 ohms.

Fig. 2 gives the current oscillograss in the primary circuit IT and in inductive load L_M .

653

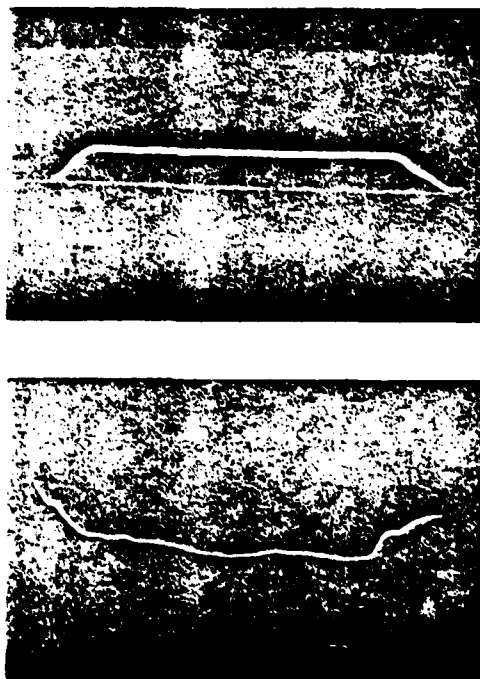


Fig. 2. Current oscillograms in inductive load (a) and in primary circuit of peak transformer (b).

The pulse duration in the inductive load (Fig. 2a) for the given parameters of circuit $\sim 2.5 \mu s$, in this case leading edge composed 250 ns and drop of current 300 ns.

An increase in the decay time in the current in comparison with rise time is explained by energy losses in measuring resistances, transmitting cable and ferromagnetic cores. Oscillations in plateau of impulse/momentum/pulse in the inductive load did not exceed $\pm 50\%$. The small flat ejection of current in plateau of impulse/momentum/pulse in the primary circuit IT (Fig. 2b) is caused by the full/total/complete magnetic reversal of the cores of chokes/throttles L_1 and L_2 .

REFERENCES

1. K. N. Myznikov, V. M. Tatarenko. Preprint IVPE, 67-10, 1967.
2. Design study on the fast ejection system of channel "A" Serpuchov 70 GeV proton synchrotron (February, 1969). CERN, 1969.
3. N. Van Breugel, J. Goni and E. Kuiper. Pulse generators for delay line deflectors, NFA/Int., 65-28, 1965.

DOC = 80069212

PAGE 45

4655

4. L. A. Meyerovich, I. M. Vatin, E. P. Zaytsev, V. M. Kandykin.
Magnetic pulse generators. M., Soviet radio, 1968.

46. Special features/peculiarities of the construction of the power-supply system of the electromagnet of the rapid booster of proton synchrotron.

G. A. Gusev, A. I. Konstantinov, A. G. Roshal', P. M. Spevakov, A. M. Stolov, A. A. Tunkin.

(Scientific research institute of the electrophysical equipment in L. V. Efremov).

A comparatively small supply of magnetic energy of the electromagnet of rapid booster and the considerable power of its power-supply system determine the advisability of use/application for the targets of the diagrams in question, in which occurs the energy exchange between capacitor bank and electromagnet. Diagrams of this type had extensive application and steels by conventional for the power-supply systems of electronic synchrotrons. However, during the direct use of the technical solutions, used in these diagrams, for the power-supply systems of rapid booster is not considered the series/row of the special features/peculiarities of its work as injector-accelerator. As is known, during the use/application of a rapid booster the duration of injection occupies the essential part

of the operating cycle of main accelerator. For shortening of the duration of injection it occupies the essential part of the operating cycle of main accelerator. For shortening of the duration of injection it is expedient to increase the frequency of the work of booster, which is limited first of all by the difficulties of the realization of powerful/thick high-frequency accelerating system at a high speed of the rearrangement of frequency. Certain compromise between these two facts can be achieved/reached during the appropriate construction of the power-supply system of the electromagnet of booster.

In the generally accepted resonance power-supply systems of the electromagnets of accelerators the curve of a change of the magnetic field has symmetrical form, as a result of which approximately/exemplarily the half the booster duration is nonoperative. In connection with this it is expedient to create system with the asymmetric form of curve with the increased duration of the section of the increase of field and the reduced duration of decrease, and also with the leading edge, which has on a large part of the section, close to the linear. With this form of curve in comparison with the symmetrical can be abbreviated/reduced the duration of injection without an increase in the maximum power of system of hf accelerator or with the retention/preservation/maintaining of the time of injection are

facilitated the requirements for the system of hf acceleration.

In the principle the asymmetric form of the curve of a change of the magnetic field can be obtained by different methods, including during the use of capacitors as the source of reactive power by means of the commutation of current by the controlled valves/gates in the circuit of electromagnet or the use/application of multifrequency resonant circuit, in which the inductance of electromagnet enters as one of the elements/cells of this contour/outline. Fig. 1 shows some versions of diagrams with the commutation of circuit current of electromagnet. A deficiency/lack in these diagrams is the need for use/application in power circuits of the power-supply system of a large quantity of power controlled valves/gates with the total power, which exceeds the reactive power of power-supply system, which with the general/common/total complication and the rise in price of system reduces the reliability of the work of setting up.

More advisable is the diagram with multifrequency resonant circuit, in which the desirable form of the curve of the current of electromagnet is created by the appropriate selection of resonance frequencies and by excitation in the contour/outline of oscillations with the prescribed/assigned amplitudes and by phases for each frequency. As an example Fig. 2 shows some versions of the schematics of three- and two-frequency resonant circuits of the power-supply

systems of electromagnet. It is possible to show that during the use of a comparatively simple two-frequency contour/outline, adjusted into the resonance for the fundamental and double frequency, can be obtained an essential improvement in the form of the curve of a change in the magnetic field.

Page 157.

Thus, with the voltage on the electromagnet, which has the form

$$U = U_0(\cos \omega t - 0.3 \cos 2\omega t),$$

the maximum speed of the increase of magnetic field decreases 1.45 times in comparison with the sine voltage of fundamental frequency with the same amplitude of the magnetic field of the electromagnet (see Fig. 3).

For the diagram the supplies with two-frequency resonant circuit (Fig. 2a) of resonance conditions can be written in the form

$$\begin{aligned} \frac{1}{C_1} + \frac{\alpha}{\alpha-1} \frac{1}{C_2} &= \frac{1}{\beta}, \\ \frac{1}{2C_1} + \frac{2\alpha}{4\alpha-1} \frac{1}{C_2} &= \frac{2}{\beta}, \end{aligned}$$

where

$$\alpha = \omega^2 L_2 C_2; \quad \beta = \frac{1}{\omega^2 L_H}.$$

Equations contain three parameters C_1 , C_2 and α , which gives the

660

possibility to optimize system according to the conditions of the minimum of reactive power of capacitor banks. Solution to the system of system gives

$$C_1 = \beta \frac{1}{4\alpha}, \quad C_2 = -\beta \frac{\alpha}{(\alpha-1)(4\alpha-1)}$$

The limits of possible values α are determined by condition $0.25 < \alpha < 1$. The corresponding calculations according to the conditions of the minimum of reactive power of capacitor banks determine optimum value $\alpha_{opt} = 0.3$. The realization of diagram with the two-frequency contour/outline with the optimum relationships/ratios of the parameters requires an increase of the reactive power of battery 1.54 times in comparison with the single-frequency contour/outline, which is technically justified in connection with an increase in the effectiveness in the work of system.

For the presentings between amplitudes and phases of the oscillations of harmonic components can be used both impulse circuits the supplies of active power and special inverter. In the first case is necessary the generation of two systems of the impulses/moments/pulses, shifted in the time in such a way, that would be the most separate possible regulating of amplitudes and phases of each harmonic or supply of contour/outline impulses/moments/pulses in two different sections of diagram. During the use/application of an inverter the latter must provide voltage with the necessary composition of frequencies, that can be

achieved/reached, n with the aid of asymmetric output transformer of inverter and corresponding filter.

One of the special features/peculiarities of the power-supply system of the electromagnet of booster is also the possibility of applying an alliteration-sacr-ters mode of its operation. In this case can be obtained essential savings on the flow rate of electric power. Task this can be solved due to the commutation power circuits of power-supply system or by the use/application of the mode/conditions, during which periodically is excited resonant circuit before beginning injection and is de-energized in the interval between the operating pulses. The first method, apparently, is not advisable due to the decrease of the reliability of system, but in the second case becomes complicated the task of guaranteeing high stability of amplitude and form of a charge of the magnetic field in the period of injection.

AD-A089 303

FOREIGN TECHNOLOGY DIV WRIGHT-PATTERSON AFB OH
TRANSACTIONS OF THE ALL-UNION CONFERENCE (2ND) ON CHARGED PARTI--ETC(U)
JUL 80 A L MINTS, A A KOMAR, A A VASIL'YEV

F/G 20/7

UNCLASSIFIED

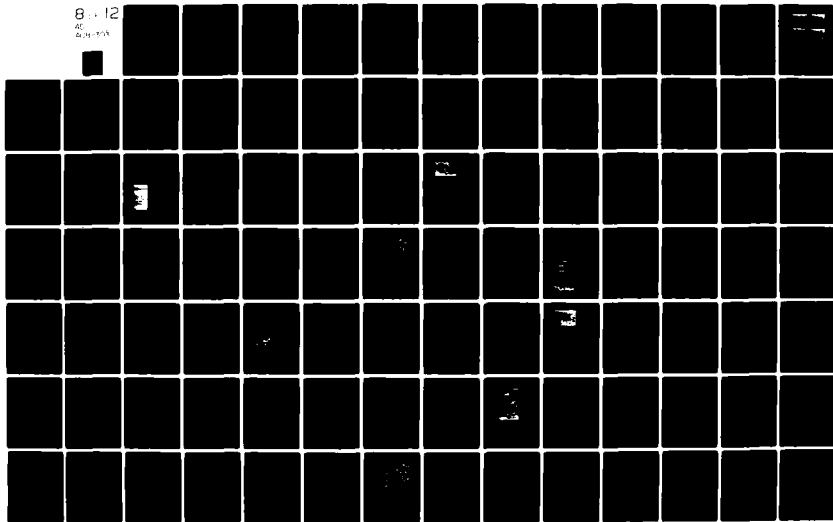
FTD-ID(RS)T-0692-80

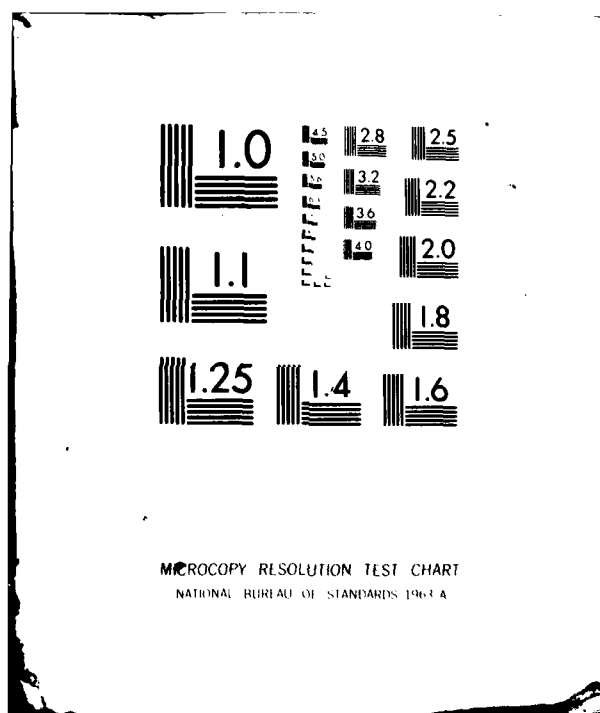
NL

8-12

AC

20-100





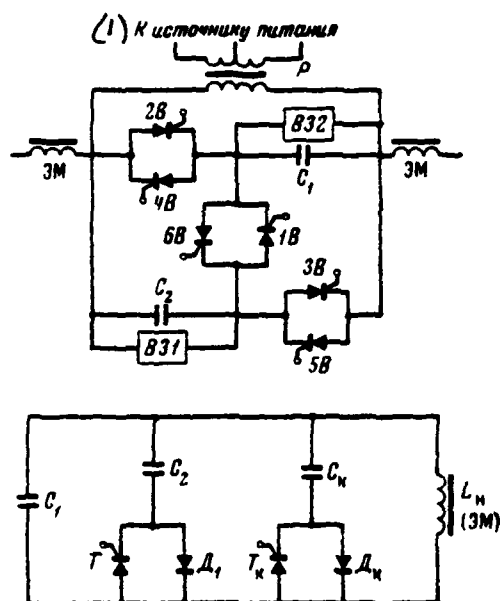


Fig. 1. Schematic diagram of supply with the commutation of capacities/capacitances.

Key: (1). To the power supply.

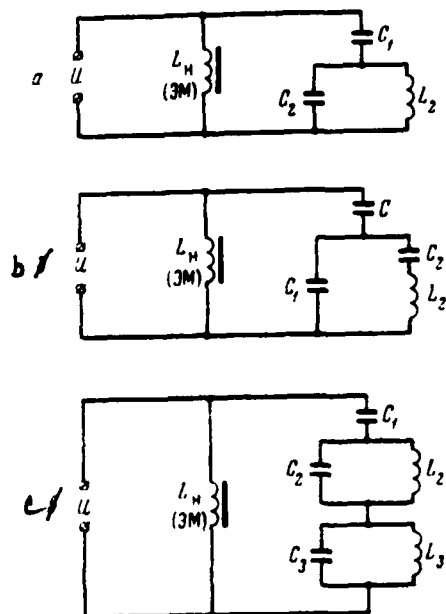


Fig. 2. Equivalent resonance diagrams. a, b) two-frequency system; c) three-frequency system.

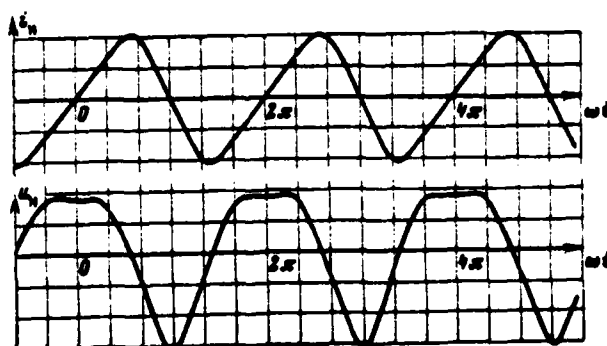


Fig. 3. Curves of alternating current component and voltage of magnet winding with two-frequency supply.

Page 158.

The analysis of the transient processes of exciting resonant circuit showed the possibility of the realization of intermittent service during which the ohmic losses decrease approximately doubly, with an insignificant increase in the cost/value of power equipment, and simultaneously is provided the necessary stability of mode/conditions. For decreasing the effect of delay, introduced by the system of active power, on the building up of oscillations in the contour/outline is provided for the special mode/conditions, during which occurs preliminary energy storage in its passive elements/cells (inductance of the cathode choke/throttle of inverter or the charging choke of the storage capacity/capacitance of impulse circuit). For formation of the process of exciting the contour/outline it is expedient to apply program control system with the appropriate feedback.

Fig. 4 gives the curves of currents and stresses of the power-supply system of the electromagnet of booster during the intermittent duty.

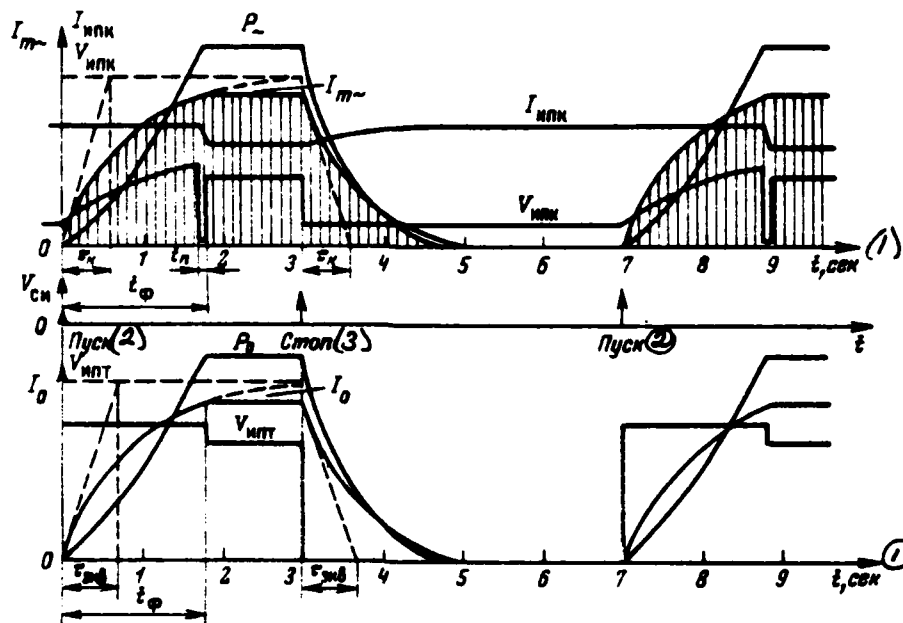


Fig. 4. Curves of current and stresses of the power-supply system of electromagnet of booster during the intermittent duty. I_m - amplitude of the alternating current component in the contour/outline; I_{unk} - current of the source of the makeup of contour/outline; V_{unk} - voltage of the source of the makeup of contour/outline; V_{cu} - synchronizing pulses; t_0 - rise time of impulse/momentum/pulse; I_0 - the constant component of current in the contour/outline; V_{unt} - voltage of the source of direct current; τ_k - time constant of contour/outline on the envelope of oscillations; τ_0 - time constant of the load circuit of direct current; P_{\sim} - power of losses from the alternating current

component; P_0 - power of losses from the constant component.

Key: (1). s. (2). Launching/starting. (3). reams/feet.

Discussion.

V. V. Ivashin. Why you do consider that for the power-supply system of booster - this typically pulse setting up - is expedient the use/application of a continuous power-supply system, but not pulse, constructed on the thyristors?

A. M. Stolov. The use/application of continuous systems is more profitable from the point of view of their reliability.

Page 159.

^{47.}
~~47.~~ System of forming of the flat/plane part of the pulse of the magnetic field of proton synchrotron IFVE.

Ya. V. Kornakov, V. M. Kofman, G. S. Lyapichev, N. S. Rezchikova, A. G. Roshal', P. M. Spevakova, A. M. Stolov.

(Scientific research institute of the electrophequipment in. D. V. Efremov).

A. I. Vagin, Yu. ^{S.} ~~Glukhov~~ Glukhov, V. P. Kuz'min.

(Radio engineering institute of the AS USSR).

V. V. Pletnev, O. N. Radin.

(Institute of high-energy physics).

For the realization of the slow conclusion/output of secondary particles from the proton synchrotron on 70 GES IPVE was developed formation system of the flat/plane part of the impulse/momentum/pulse of the magnetic field of the basic electromagnet of accelerator. Shaping of the flat/plane part of the impulse/momentum/pulse of the field of electromagnet is accomplished/realized by a method of reducing the voltage of converters due to the control of the firing angle of valves/gates. In this case increase the pulsations of rectified voltage. For decreasing the pulsations of magnetic field was developed the passive filter, which ensures the decrease of the pulsations of the voltage of the fundamental frequency of converter approximately/exemplarily 50 times and making it possible obtain satisfactory transient process with a change in the modes/conditions of the work of the system of the excitation of electromagnet.

The examination of the possible versions of the execution of the system of the depression of pulsations with the use of known filter components/links showed the inadequacy of their direct use/application for stated problem, since the condition of the aperiodicity of transient process caused the limitation of filtration

factor or considerable power losses in the attenuating impedances, and the use of a tuned filter was unacceptable due to the large range of a change in the slip of the main aggregates/units of power-supply system. As the solution was proposed the schematic of filter, depicted in Fig. 1.

In this diagram for obtaining the necessary transient responses of filter with the limited losses in the attenuating impedance of R is utilized symmetrical buffer capacitor bank C_1 whose capacity/capacitance considerably exceeds the filtering capacity/capacitance C_2 .

Filtration factor k_Φ for the diagram in question can be written in the form

$$k_\Phi = \sqrt{\frac{\frac{R^2}{(R^2\omega^2C_2^2+1)^2} + \left[\omega L - \frac{R^2\omega^2C_2(C_1+C_2)+1}{\omega C_1(R^2\omega^2C_2^2+1)}\right]^2}{\frac{R^2}{(R^2\omega^2C_2^2+1)^2} + \left[\frac{R^2\omega^2C_2(C_1+C_2)+1}{\omega C_1(R^2\omega^2C_2^2+1)}\right]^2}} \quad (1)$$

The transient process of changing the voltages on the magnet winding is determined by the roots of the characteristic equation

$$p^3 + \frac{1}{RC_2} p^2 + \frac{C_1+C_2}{LC_1C_2} p - \frac{1}{RLC_1C_2} = 0. \quad (2)$$

The analysis of transient process showed that the required characteristics of filter can be provided with the real roots of equation (2), two of which are equal to each other.

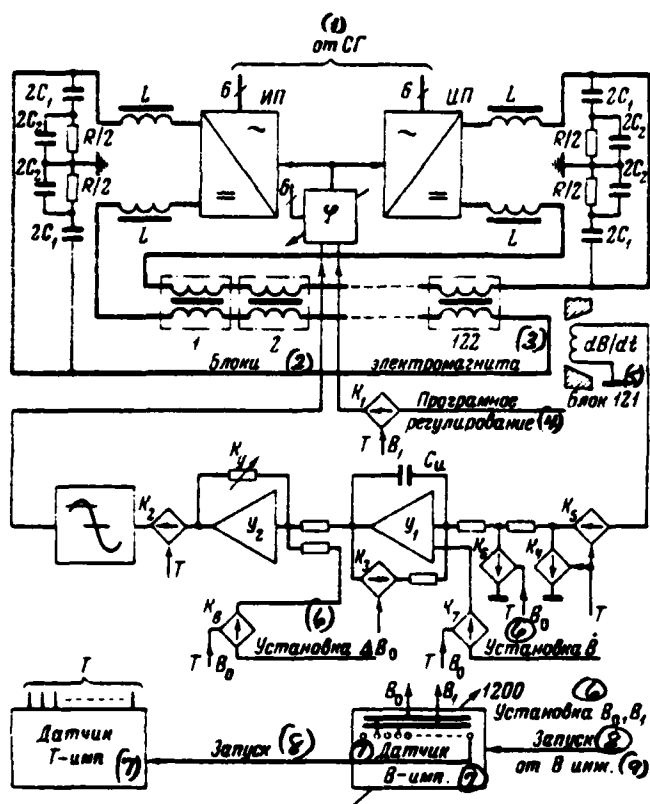


Fig. 1. Block diagram of power circuits, units of stabilization and control of the system of the excitation of the electromagnet of proton synchrotron IPVE.

Key: (1). from. (2). Blocks/modules/units. (3). electromagnet. (4). Program control. (5). Block. (6). setting up. (7). Sensor imp. (8). starting/launching. (9). from in Eng.

In this case the transient process of the establishment of voltage on the electromagnet upon the start of power-supply system is described by the expression

$$u_m = u_0 \frac{C_1 + C_2}{LC_1 C_2} \left\{ \frac{\tau}{\beta \alpha^2} + \frac{\beta - \alpha}{\beta(\alpha - \beta)} e^{-\beta t} + \left[\frac{\tau - \alpha}{\alpha(\alpha - \beta)} t + \frac{2\alpha\tau - \alpha^2 - \beta\tau}{\alpha^2(\alpha - \beta)} \right] e^{-\alpha t} \right\}, \quad (3)$$

where α and β - roots of equation (2) and $\tau = \frac{1}{R(C_1 + C_2)}$.

Connection/communication between the value of roots α and β and the parameters of filter can be written in the form

$$RC_2 = \frac{1}{2\alpha + \beta}, \quad \frac{C_1}{C_2} = \frac{2(\alpha + \beta)^2}{\alpha\beta}; \quad (4)$$

$$LC_2 = \frac{1 + \frac{1}{\tau} \frac{\beta}{\alpha}}{(\alpha + \beta)^2}.$$

From the conditions of limiting the duration of the transient process of the establishment of voltage on the magnet winding by time $t = 25-40$ ms were obtained the values of roots and on the basis (4) and (1) were determined the parameters of the filter $L = 26 \cdot 10^{-3}$ H, $C_1 = 2500$ μ F, $C_2 = 150$ μ F, $R = 6.8$ ohms.

Fig. 2 gives the oscillograms of current and voltage of electromagnet during the use of a filter with the parameters indicated. The start of filter made it possible to lower the

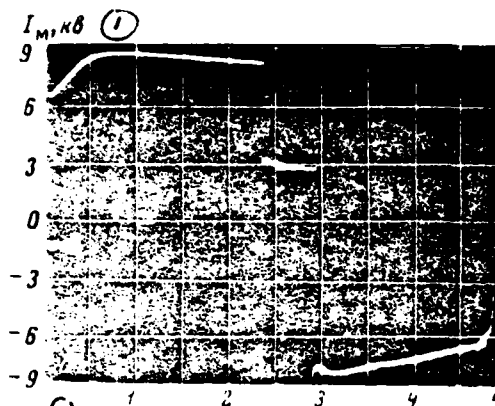
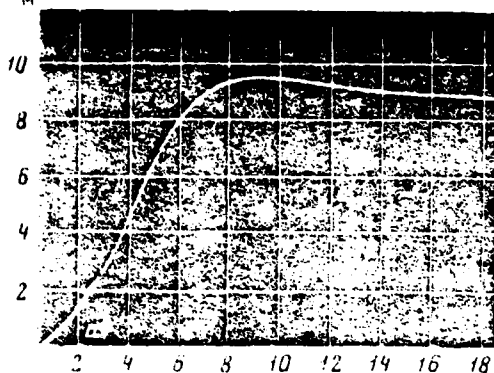
pulsations of the field of electromagnet by the frequency of 600 Hz to $\frac{\Delta H_{\omega}}{H_{max}} \approx 10^{-6}$.

One of the serious problems, which appear with the resolution of the task of reducing the pulsations of magnetic field, is the depression of low-frequency harmonic components of field, the caused by the absence of a precise symmetry of work converters. As follows from the oscillogram Fig. 2d during the use/application of the described filter the depression of pulsations 600 Hz it proved to be so/such considerable that primary meaning acquire the pulsations with the frequencies substantially lower than fundamental conversion frequency. Taking into account the high value of the high degree of symmetry of impulses/momenta/pulses, that control converters with shaping of the flat/plane section of the impulse/momentum/pulse of magnetic field, was developed the special system of the generation of driving pulses. It is the device/equipment, which consists of the generator of primary impulses/momenta/pulses, which has at the output the united in one channel sequence of 12 impulses/momenta/pulses with the repetition frequency 600 Hz. Control of stage of pulse with the control is accomplished/realized in one phase-shifting device/equipment in the form of the stagnation blocking oscillator, through which is passed the sequence of all 12 impulses/momenta/pulses. The final cascade/stage of device/equipment is the distributor of the out of phase impulses/momenta/pulses, made on the thyristor triggers.

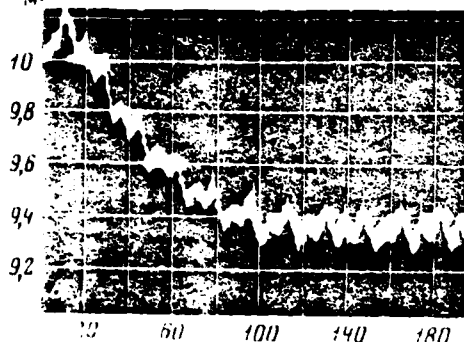
DOC = 80069213
 U_M, kV (1)

PAGE →

673



U_M, kV (1)



t, msec (2)

I_M, kA

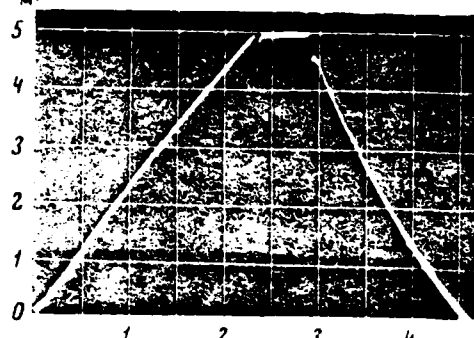


Fig. 2. Oscillograms of current and voltage of magnet winding upon the start of filter a) the transient process of the establishment of voltage upon the start of power-supply system; b) voltage and current of electromagnet with shaping of the flat/plane part of the impulse/momentum/pulse of magnetic field; c) the voltage of transient process in the beginning of shaping of the section of the flat/plane part of the impulse/momentum/pulse.

Key: (1). kV. (2). ms.

The use/application of this device/equipment provides the maintenance of the high degree of symmetry of driving pulses with the control. In this case the intervals between the igniting impulses/momenta/pulses are determined almost exclusively by the phases of the primary impulses/momenta/pulses, supplied by the voltage of the auxiliary generator, connected with the shaft of main generator. As showed investigations, with the pulsing of converters and deceleration of the rotation of aggregates/units appear the distortions of the voltage of auxiliary generator, the leading to the asymmetry of primary impulses/momenta/pulses. For the liquidation of the asymmetries of primary impulses/momenta/pulses is necessary taking special actions.

For guarantessing the required high stability of the flat/plane part of the impulse/momentum/pulse of magnetic field is developed the special automatic control system (SAR), which affects the diagram of control of converter in the function of the divergence of magnetic field at the pulse apex from the assigned magnitude. In accordance with the special features/peculiarities of task of SAR it has variable/alternating structure. The rearrangement of structure is accomplished/realized from the discrete/digital sensor of magnetic field and timer device/equipment. As the measuring element of control

system is utilized the induction sensor and the integrator, which is operational amplifier y_1 , included by feedback through capacitor/condenser C_n (Fig. 1).

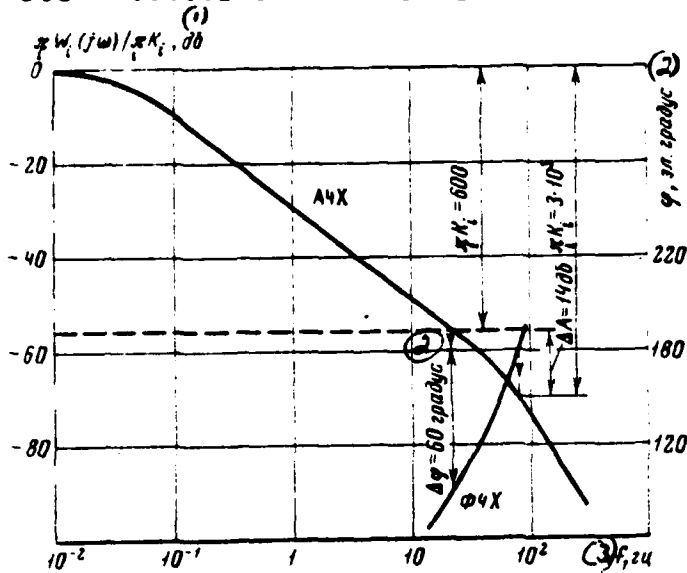


Fig. 3. Frequency characteristic of the extended reaction circuit of the stabilization system of the flat/plane section of the impulse/momentum/pulse of magnetic field.

Key: (1). dB. (2). el. degree. (3). Hz.

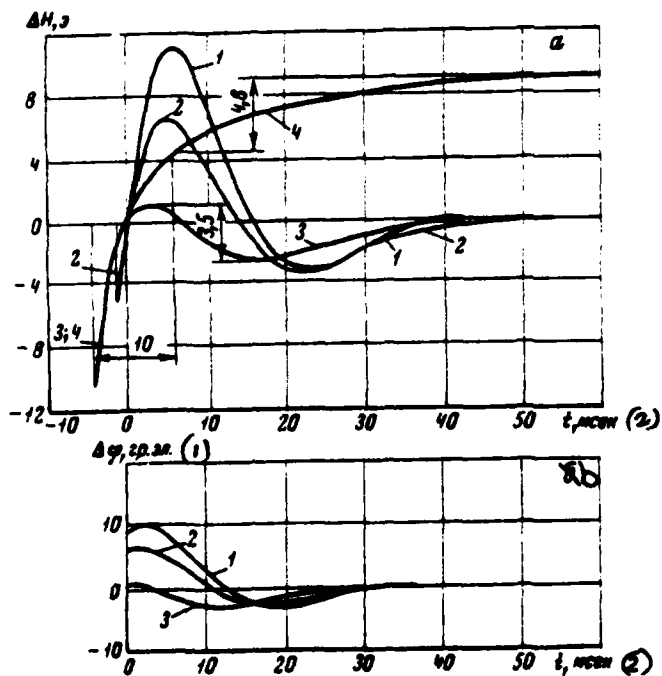


Fig. 4. Surge characteristics of establishment of magnetic field in the beginning of shaping of flat/plane part of impulse/momentum/pulse; obtained on AVH during simulation of prevention/advance of program signal with respect to field of closing/shorting 1 - prevention/advance 100e; 2 - the same, 200e; 3 - the same, 300e; 4 - the same, 300e with simultaneous feed to entrance of amplifier γ_2 of supplementary signal.

Key: (1). gr el. (2). ms.

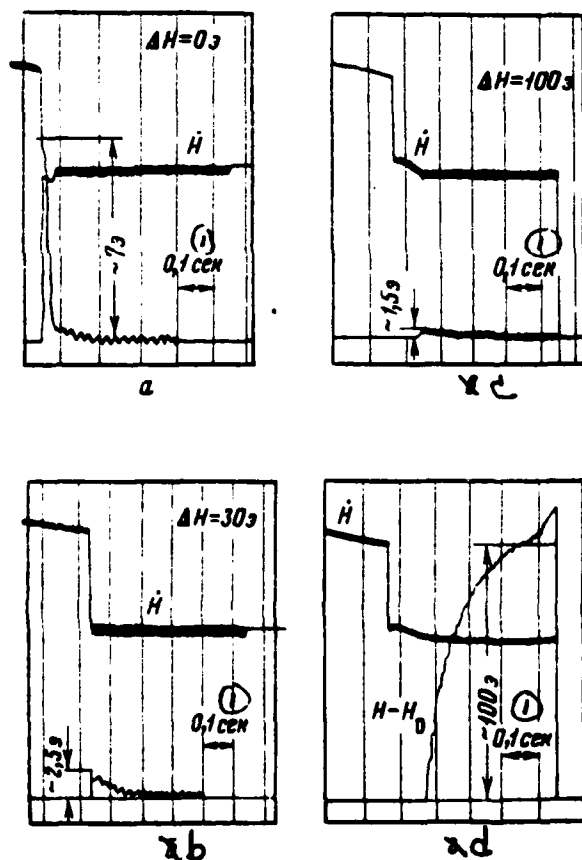


Fig. 5. Oscillograms of transient processes of magnetic field in the beginning of shaping of flat/plane part of impulse/momentum/pulse with work of system of excitation of electromagnet. a,b,c) in the looped system on the magnetic field with the different values of lead/anticipation of program signal; d) in the system without the feedback on the field.

Key: (1). s.

Page 162.

During the pause between the impulses/momenta/pulses of magnetic field is conducted the automatic correction of the drift of amplifier and capacitor discharge C_n with the aid of key/wrench k_3 . Agreement of integrator with the entrance of amplifier γ_2 . For the purpose of an increase in the precision/accuracy of control and decrease of the dynamic range of elements/cells SAR, besides reverse connection/communication, is used the circuit of program control, which directly affects the diagram of control of converter.

Fig. 3 depicts the frequency characteristics of the extended reaction circuit (valid, due to the presence in circuit of converter, only for the frequency band $f(60-120 \text{ Hz})$). The overall efficiency of amplification SAR in this characteristic $\sim 3 \cdot 10^3$ and frequency of

excitation ~ 80 Hz, which makes it possible to obtain high statistical precision/accuracy and duration of transient control less than ~ 80 ns.

For the optimization of the process of transition to the flat/plane part of the current pulse were investigated on AVN two methods of the correction: the lead/advance of the introduction of program signal and the inclusion/connection of supplementary constant stress U_{AB} on the entrance of amplifier γ_2 simultaneously with closing/shorting of feedback. Fig. 4 gives the results of investigation. As it follows from Fig. 4b, the range of the firing angle of valves/gates in this case does not exceed 15 el. deg. The oscillograms of the transient process of the establishment of the field of electromagnet are given in Fig. 5. Tests showed that the system in the range of energies 20-76 GeV provides the following parameters: the duration of area/site to 1.5 s, the duration of the transient process of 20-80 ns, the field nonuniformity on the pad ± 1 Oe, the recurrence of the level of area/site ± 40 Oe, the total amplitude of the pulsations of field 0.5 Oe, pulsations of field with the frequency of 25 Hz 0.25 Oe, with the frequency of 50 Hz ~ 0.1 Oe and the frequency of 600 g-0.01 Oe.

Discussion.

G. I. Kugushev. Are such the possibilities of applying the sensors of period on the shaft of the feeding aggregate/unit?

A. M. Stolov. Sensors on the shaft of generator to apply difficultly due to the high requirements for them on the mechanical precision/accuracy.

48. On the possibility of using the principle of self-balanced field in the proton synchrotrons.

I. P. Karabekov, M. A. Martirosyan, Yu. R. Nazaryan.

(Yeravan physical institute).

In the electromagnets of proton synchrotrons due to the large slope/transconductance of the leading edge of the feeding impulse/momentum/pulse appear the unsteady processes, which lead to the considerable azimuthal asymmetry of field in the beginning of acceleration. For the weakening their effects on the process of shaping of the accelerated beam and possible reduction in the field of injection into magnet blocks usually introduce supplementary fading, and with the aid of the capacities/capacitances, connected to the blocks/modules/units, accomplish/realize the specific equalization current distribution on the perimeter of electromagnet. The values of capacities/capacitances and impedances are selected of special law [1], which is expressed by the function of the parameters of the blocks/modules/units of electromagnet and form of the spectrum of the feeding impulse/momentum/pulse.

¹I. A. Monoszon, et al. PTE, 1962, No. 4, p. 168.

Basic the expression, which is determining the value of variable component of magnetic flux Φ_{ns}^* in the strictly prescribed/assigned region of clearance S of each separate block/module/unit, connected with the system of self-balancing (Fig. 1), which consists of N of magnet blocks, for the case of arbitrary current distribution takes the form

$$\Phi_{ns}^* = J_1 \xi(n) R_n + \frac{J_1 X_2 \left[\sum_{i=1}^N \xi(i) - \xi(n) \right] - J_1 \xi(n) X_{1n}}{X_{1n} + X_2 + \omega L_{sn}} R_n.$$

Here J_1 - current, which flows along inducing winding of the first block/module/unit, to which is connected the power supply;

$\xi(n)$ - arbitrary law, defined as J_i/J_1 , when the circuit of self-balancing is extended; R_n - proportionality factor between the value of magnetic flux in S region and the current, which flows along inducing winding of block/module/unit: $|X_{1n} = \frac{U_{2n}}{J_1 \xi(n)} - \omega(L_{mn} \omega^2 - \frac{1}{C_n})| U_{2n}$ - voltage on the corrective winding when it is extended; L_{mn} - inductance of the magnetization of the n block/module/unit; C_n - stray capacitance of block/module/unit; $X_2 = \frac{1}{\sum_{i=1}^N \frac{1}{X_{1i}} - \frac{1}{X_{1n}}}$; L_{sn} - leakage inductance of the corrective winding of the n block/module/unit. In equation (1) value r_n - the effective resistance of secondary winding of block/module/unit - is omitted, since for the natural vibration frequencies of blocks/modules/units relation $|r_n|/|X_{1n}| \sim 10^{-5}$.

For magnet blocks with the relationship/ratio of a number of turns of basis and corrective windings, equal to one, $\omega L_{sn} \ll X_{1n}$. After expansion (1) according to degrees ωL_{sn} and representation $R_n = R_0 + \Delta R_n$, where R_0 - average/mean value $\frac{\Phi_{si}}{J_i \xi(i)}$, we will obtain

$$\Phi_{ns}^* = J_1 R_0 \left\{ \frac{X_2}{X_{1n} + X_2} \sum_{i=1}^N \xi(i) + \frac{\Delta R_n - \omega L_{sn}}{X_{1n} + X_2} \times \right. \\ \left. \times \left[\frac{X_2}{X_{1n} + X_2} \sum_{i=1}^N \xi(i) - \xi(n) \right] \right\}. \quad (2)$$

With $N \gg 1$, when $X_2 \ll X_{1n}$ even with comparatively large divergences X_{1i} , relation $X_2/X_{1n} = 1/N$. Then (2) it can be rewritten in the form

$$\Phi_{ns}^* = J_1 R_0 \left\{ \frac{1}{N} \sum_{i=1}^N \xi(i) + \frac{\Delta R_n - \omega L_{sn}}{X_{1n}} \times \right. \\ \left. \times \left[\frac{1}{N} \sum_{i=1}^N \xi(i) - \xi(n) \right] \right\}. \quad (3)$$

From (2) and (3) it is evident that for absolute self-balancing with the arbitrary form of current distribution and the arbitrary amounts of deflection ΔR_n and $\Delta \omega L_{sn}$ for each block/module/unit it is necessary to have a range of selection X_{1i} , making it possible to compensate for divergence ΔR_n and $\Delta \omega L_{sn}$. This range it is easy to determine from the relationship/ratio

$$\frac{\omega L_{s0}}{X_{1n}} = \frac{\Delta R_n + \omega(L_{s0} + \Delta L_{sn})}{X_{1n} + \Delta X_1}, \quad (4)$$

whence

$$\Delta X_1 = X_1 \frac{\Delta R_n + \Delta \omega L_{sn}}{\omega L_{s0}}. \quad (5)$$

Expression (5) makes it possible to determine a quantity of supplementary turns of the corrective winding and to select the parameters of the controlling element/cell, on the basis of technological precisions/accuracies ΔR_i and $\Delta \omega L_{Si}$. However, due to by the frequency of dependence X_{1i} a strict satisfaction of condition (2) is possible only at one frequency at which is carried out the compensation for the divergences of the parameters of blocks/modules/units. Therefore absolute self-balancing is possible only for the electronic synchrotrons. For the proton machines azimuthal heterogeneity at the high frequencies will be determined in essence by value

$$\Delta \Phi_{ns} = J_1 R_0 \frac{\omega L_{Sn} [X_{1n}(f) - X_{1n}(f_0)]}{X_{1n}(f) X_{1n}(f_0)} \times$$

$$\times \left[\frac{1}{N} \sum_{l=1}^N \xi(l) - \xi(n) \right], \quad (6)$$

where f_0 - frequency, at which is realized the selection of the parameters according to (2). For the process of self-balancing at the low frequencies a substantial limitation is the ohmic resistance of the corrective winding. In this case the equation, which is determining the value of magnetic flux in the n block/module/unit, takes the form

$$\Phi_{ns}^* = J_1 R_0 \left\{ \frac{1}{N} \sum_{l=1}^N \xi(l) + \left(\frac{\Delta R_n + \omega L_{Sn}}{X_{1n}} - \frac{1}{2} \frac{r_n^2}{X_{1n}^2} \right) \times \right.$$

$$\times \left. \left[\frac{1}{n} \sum_{l=1}^n \xi(l) - \xi(n) \right] \right\}, \quad (7)$$

where r_n - value of the ohmic resistance of the circuit of the corrective winding. For the compensation for the divergences of values r_i from one block/module/unit to the next it is necessary to provide the supplementary range of control, equal to

$$\Delta X_1 = X_1 \frac{\Delta r_n}{r_{cp}}. \quad (8)$$

Then the full/total/complete value of the required range of control ΔX_1 must be equally

$$\Delta X_{1max} = X_1 \left(\left| \frac{\Delta R_n}{R_0} \right|_{max} + \left| \frac{\Delta \omega L_{sn}}{\omega L_{s0}} \right|_{max} + \left| \frac{\Delta r_n}{r_{cp}} \right|_{max} \right). \quad (9)$$

From (7) it is evident that in the case when

$$\frac{1}{2} \frac{r_n^2}{X_{1n}^2} = 1, \quad (10)$$

value of flow $\Phi_{ns}^* = J_1 R_0 \xi(n)$, i.e. the process of self-balancing is absent. From (10) value f_{kp} for the prescribed/assigned magnetic system is equal

$$f_{kp} = \frac{1}{\sqrt{2}} \frac{r_n}{2\pi L_{mn}}. \quad (11)$$

The process of self-balancing for the pulse magnetic systems was investigated experimentally on nine magnet blocks with the plane-parallel poles, supplied by the voltage pulse with parameters

$\tau_n = 180$ ns and $\tau_{\phi p} = 20$ μ s. The parameters of magnet blocks are given in the table.

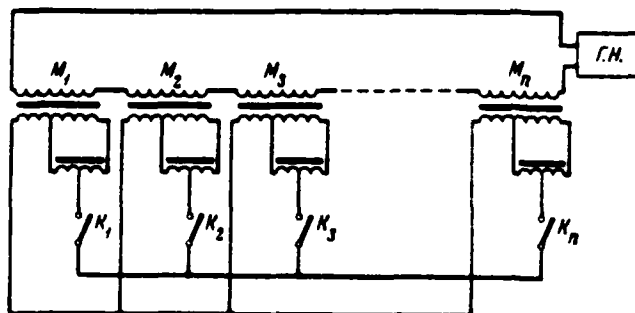


Fig. 1. Circuit diagram of magnet blocks into the system of self-balancing.

Page 164.

Magnetic system was preliminarily balanced at the frequency of 50 Hz with precision/accuracy 0.10/o. The measurement of the average/mean value of field in the blocks/modules/units was made with the aid of the air-core coil, adjusted into the strictly prescribed/assigned region of blocks/modules/units. For evaluating the correctness of the obtained relationships/ratios the magnetic system tested in the range of the frequencies of the feeding voltages from 50 Hz to 20 kHz. In Fig. 2 dotted line showed current distribution in magnetic system $\xi(t)$ for the different frequencies with the cutoff/disconnection of all blocks/modules/units from the circuit of self-balancing. Solid lines showed current distribution at the same frequencies, but after the inclusion of blocks/modules/units

into the circuit of self-balancing. Fig. 3 shows variation $X_{10}/X_{11} = \varphi(t)$, i.e. the degree of mutual disagreement X_{10} of the blocks/modules/units which must lead to the scatter of the value of magnetic fluxes according to (6).

(1) Параметры	(2) Номер блока								
	1	2	3	4	5	6	7	8	9
Z_m , МГН ⁽³⁾	26,2	25,1	23,1	23,1	21,1	26,2	24,6	21,8	24,4
Z_s , МГН ⁽³⁾	1,8	1,64	1,61	1,5	1,78	1,4	1,49	1,5	2,24
Z_i , Ом ⁽⁴⁾	0,60	0,602	0,502	0,475	0,490	0,473	0,465	0,456	0,60
R_0 , Вт/А ⁽⁵⁾	$8,5 \cdot 10^{-5}$	$8,5 \cdot 10^{-5}$	$7,6 \cdot 10^{-5}$	$7,6 \cdot 10^{-5}$	$7,0 \cdot 10^{-5}$	$8,5 \cdot 10^{-5}$	$7,95 \cdot 10^{-5}$	$7,15 \cdot 10^{-5}$	$7,75 \cdot 10^{-5}$

Note. $C_n \sim 4200$ pF for all blocks/modules/units.

Key: (1). Parameters. (2). Number of block/module/unit. (3). mH. (4). ohm. (5). Wb/A.

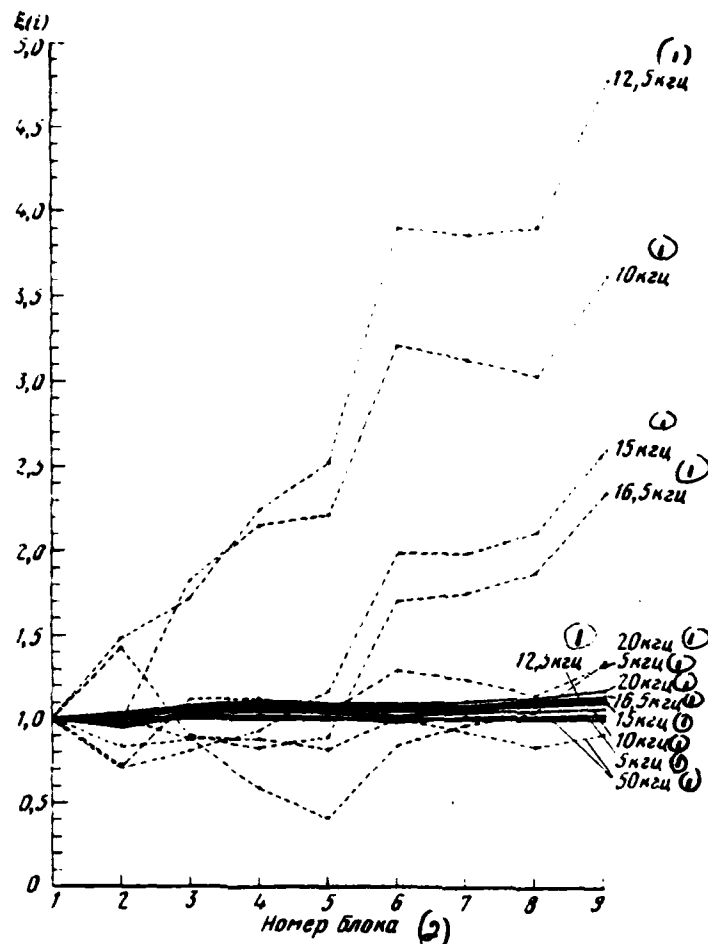


Fig. 2. Current distribution in magnet blocks depending on frequency.

Key: (1). kHz.; (2) Number of block.

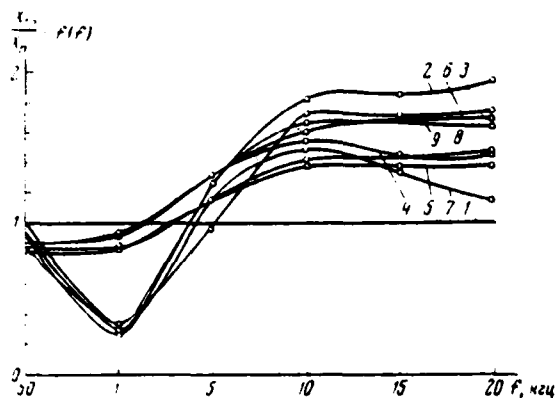


Fig. 3. Dependence of mutual disagreement X_{11} of blocks/modules/units on frequency (1-9 - number of blocks/modules/units).

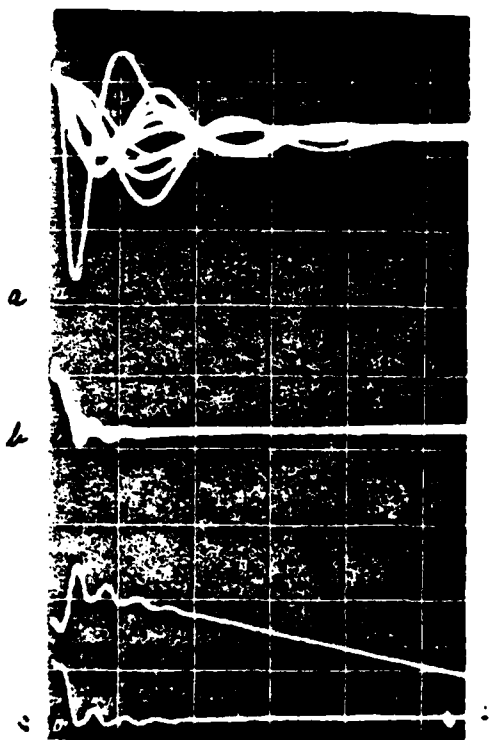


Fig. 4. Oscillograms of transient processes in usual magnetic system (a) and in system of self-balancing (b, c).

Page 165.

The calculations of the degree of flattening of flux at the different frequencies with precision/accuracy 2-3o/o (precision/accuracy of determination $\times 10$) coincide with the results of measurements, shown in Fig. 2. Fig. 4a shows the oscillogram of transient processes in the separate blocks/modules/units in the usual circuit diagram of blocks/modules/units. For the clarity all oscillograms are combined. The depression of transient processes in the same system, connected with the circuit of self-balancing with the invariability of value and shape of the feeding pulse, it is shown in Fig. 4b. In Fig. ^{4c} ~~4b~~ are shown the form of the derivative of field in one block/module/unit (lower curve) and the form of the current, flowing in the general/common/total circuit of primary windings. From the oscillograms evidently both depression of the amplitudes of transient processes and shortening the time of their existence and considerable decrease of the azimuthal asymmetry \bar{H}_0 in the self-balanced system. Furthermore, field in the block/module/unit repeats the form of the current, which flows in the primary winding. The introduction of self-balancing to the investigated magnetic system made it possible to increase the dynamic range of the utilized values of field H_{max}/H_{min} from 43 to 150.

In conclusion it should be noted that value f_{kp} for the contemporary proton accelerators close to the values of ~ 0.03 Hz. In the experimental installation frequency f_{kp} was equal to ~ 3 Hz. Estimations show that for the accelerator with $r_{\delta n} = 0.01$ ohm and $L_{m\delta n} = 0.03$ H for the duration of acceleration cycle $\tau = 1.5$ s, for the lowest frequency, equal to ~ 0.15 Hz, the value of the magnetic flux \bar{H}_0 in all blocks/modules/units will differ from the mean arithmetic value of flows in the unbalanced system for $\sim 50\%$.

49. The magnetic system of P-M cyclotron with a three-dimensional/space variation in the field.

Yu. G. Alenetskiy, S. B. Vorozhtsov, N. L. Zaplatin, L. K. Lytkin.

(Joint Institute for Nuclear Research).

At present in many laboratories of peace/world are conducted the investigations, connected with the reconstruction of acting synchrocyclotrons [1]. In the J.I.N.R. (USSR), just as in Columbian University (USA) and SREL - Virginia (USA), is intended to improve synchrocyclotron, after introducing three-dimensional/space variation and growing middle magnetic field, which does not reach, however, isochronal dependence [2-4].

In this work are given the results of shaping of the magnetic field of the model of the magnetic system of P-M cyclotron with a three-dimensional/space variation in the field the J.I.N.R. (setting up P) with the similarity factor 5.22. The simulation of the field of magnetic system (Fig. 1 and 2) was conducted for the confirmation of the selected basic parameters which were discussed in work [5], for refining the configuration of spiral and circular shims and

determination of the topography of magnetic field after a working radius, which made it possible to solve the questions, connected with the beam extraction from accelerator chamber.

Requirements for the magnetic field are presented in works [6.7]: a) a drop/jump in middle magnetic field $H(r)$ must be fulfilled with the precision/accuracy 200 e; b) in the central zone is necessary, that $0 \leq \Delta H \leq 8$ e, where ΔH - divergences of middle field from that required; c) allowance for the gradient of middle field changes with radius $|\Delta \frac{dH}{dr}| (2.3-11)$ Oe/cm for $M=12-51.7$ cm respectively (here are given below the sizes/dimensions of model); d) in the zone of the conclusion/output of particles it is necessary to satisfy the condition $|\frac{\Delta H_0}{H_0}| < 0.06$ and $|\Delta \frac{d\varphi_0}{dr}| < 5 \cdot 10^{-3}$ rad/a where H_0 - amplitude of fundamental harmonic, and φ_0 - phase of its maximum; e) the required flutter focusing must be provided, beginning with $r=3$ cm; f) lowest harmonics in center $\frac{H_1}{H} < 10^{-3}$, $\frac{H_2}{H} < 5 \cdot 10^{-3}$.

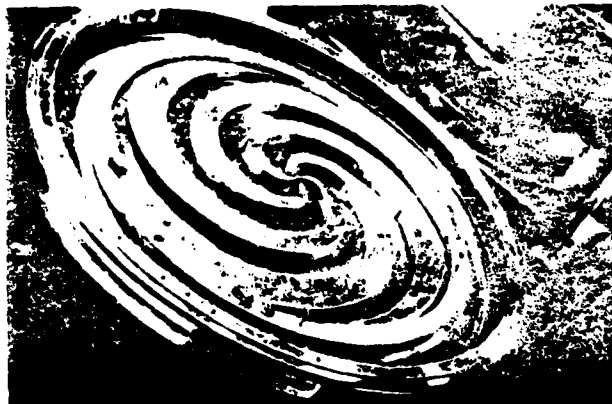


Fig. 1. Form of the pole piece of the model of magnetic system.

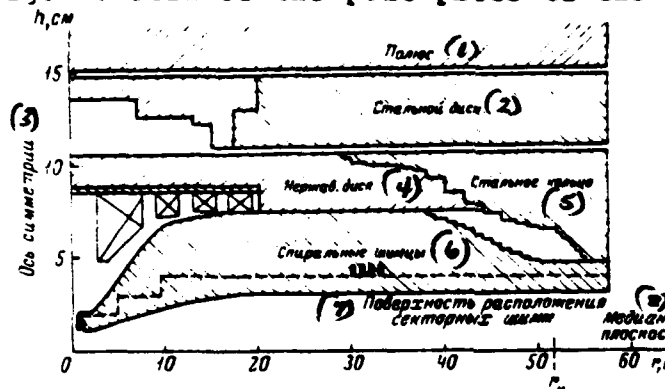


Fig. 2. Design concept of magnetic system with elements/cells of thin shimming.

Key: (1). Pole. (2). Steel disk. (3). Axis of symmetry. (4). stainless disk. (5). Steel ring. (6). Spiral shims. (7). Surface of location of sector shims. (8). Median planes.

Page 166.

The measurements of magnetic field on the model were made with

the aid of automated measuring bench [8] at 144 evenly distributed in the circumference points for each radius. The results of measurements were recorded with the aid of the perforator with the continuous displacement of the sensor of Hall magnetometer. The experimentally obtained accuracy of the measurement of middle field $H(r)$ comprises $1.5 \cdot 10^{-4}$, and the amplitude of basic harmonic $5 \cdot 10^{-4} H(r)$. Processing obtained information was performed on the computers SDS-1604A.

As a result of the calculations conducted and experiments on the model of magnetic system was shaped the field, represented in Fig. 3.

It is evident that $\Delta H_{\text{max}} = \pm 70$ e, $\Delta H_{4\text{max}} = 300$ e, $\left| \Delta \frac{d\varphi}{dr} \right| \leq 4.6 \cdot 10^{-3}$ rad/cm and the required variation is created, beginning with $r = 2.9$ cm.

During the calculation according to the analytical expressions of the natural frequencies of particles (Fig. 4) for required field $Q_x(H_r)$, $Q_y(H_r)$ and for actually created middle field $Q_x(H_p)$, $Q_y(H_p)$, and also the index of an increase in created field $n = r/H \frac{dH}{dr}$ it turned out that $\Delta n/n$ is found in the allowances for $r = (24 \pm r_k)$ cm, where $r_k = 51.724$ cm and values $Q_x(H_p)$, $Q_y(H_p)$ satisfy the stated requirements in entire range of radii.

Divergences ΔH and connected with this character of curves

$\frac{\Delta n}{n}(r)$, $Q_{(x)}(H_p)$, $Q_y(H_p)$ in the central zone must be corrected with the aid of the elements of the thin correction: current windings and sector shims (see Fig. 2). The experimental precision/accuracy of the simulation of magnetic field reached close to to maximally the possible $\Delta H_{\text{req}} = (30-40) \text{ e}$, determined by the geometric errors for production and assembly of elements/cells model.

The possibilities of current windings were evaluated by the method of calculation by the method of least squares of the required ampere-turns for compensation $\Delta H(r)$ and $\Delta \frac{dH}{dr}$. In the center the windings weakly act on the gradient of middle field and are suitable only for small ($\pm 30 \text{ e}$) changes in field level.

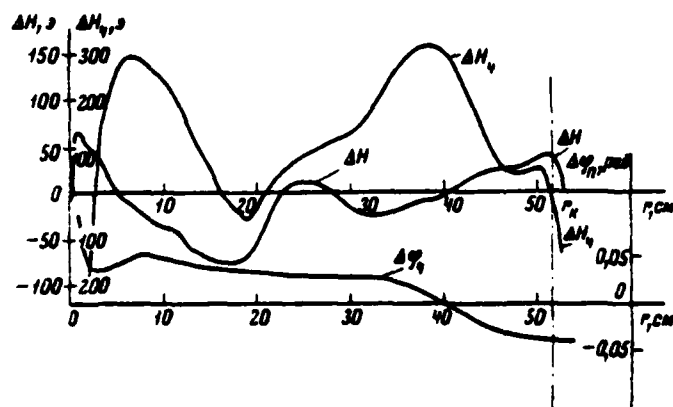


Fig. 3. Divergences of the shaped characteristics of field from the required dependences.

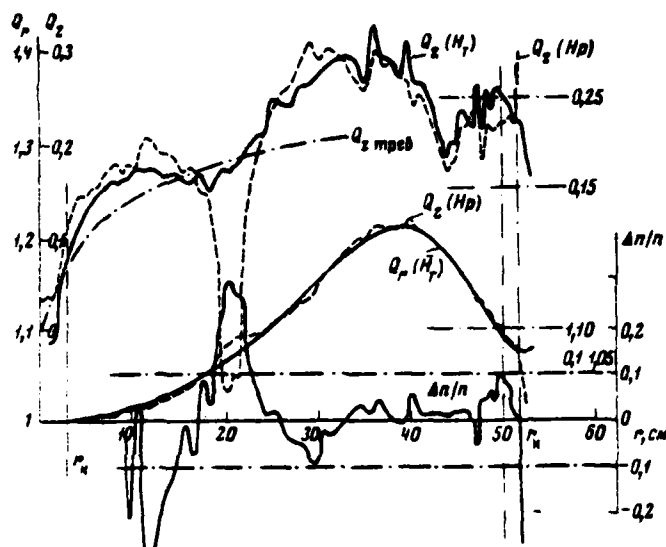


Fig. 4. Natural frequencies of particles and relative deflection of index of increase in shaped field.

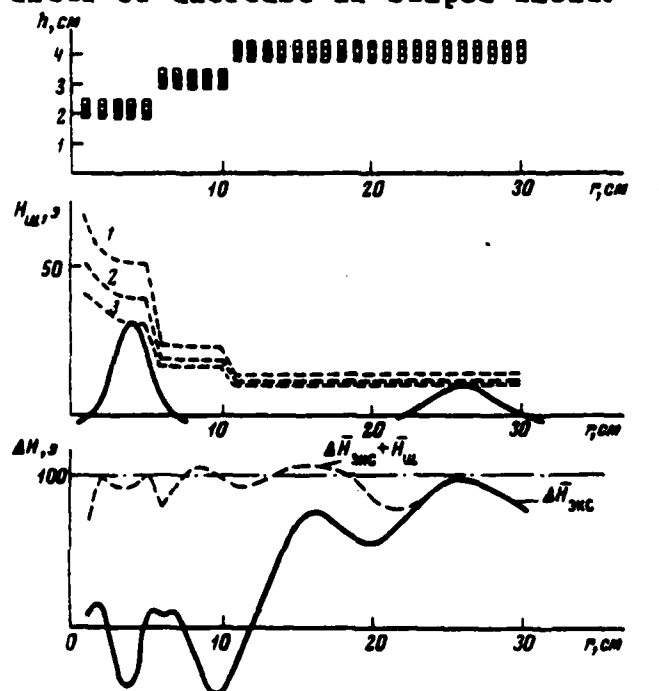


Fig. 5. Calculated shimmering of middle field with the aid of sector shims.

Page 167.

The optimum set of sector shims for the compensation for the level of field 100 e (Fig. 5) was located by the method of calculation on the computers by the cut-and-try method. The shims, which proved to be necessary for compensation $\Delta H(v)$, in Fig. 5 are shaded. In the middle part of the figure are given field distributions for different layers of sector shims. With exception of separate outshoots, connected with the measuring errors of field to the model, the divergences of field in the region of shimming do not exceed 18 e.

Thus, is shown the possibility of designing of the magnetic field of accelerator with the prescribed/assigned allowances.

REFERENCES

1. H G Blosser. IEEE Trans. on Nucl. Sci., 1969, NS-16, N 3, p.405.
2. A. A. Glazov et al. Preprint the J.I.N.R., 9-3951, Dubna, 1968.

3. R Cohen ~~and others~~. *AND OTHERS*. IEEE Trans. on Nucl. Sci., 1969, NS-16, N 3, p. 421.
4. H Kia, D Lavine and M Reiser. Internat. Conf. on Cycl., Oxford, 1969.
5. S. B. Vorozhtsov, N. I. D'yakov, N. L. Zaplatin. Preprint the J.I.N.R., 9-4517, Dubna, 1969.
6. V P Dmitrievsky ~~and others~~. *AND OTHERS*. Internat. Conf. on Cycl., Oxford, 1969.
7. Yu. G. Alenitskiy, S. B. Vorozhtsov, N. L. Zaplatin, L. K. Lytkin. Preprint of the J.I.N.R. the "simulation of the magnetic system of P-M cyclotron with a three-dimensional/space variation in the field". Dubna, 1970.
8. V. N. Anosov, Yu. N. Denises, P. T. Shishlyannikov. Preprint the J.I.N.R., 10-4930, Dubna, 1970.

50.

Pulse generator in power 1.5-2 GWT on the magneto controlled valves/gates.

L. L. Danilov, V. N. Pankin, G. I. Silvestrov.

(Institute of nuclear physics of SO AN USSR).

The contemporary development of pulse technology in the field of obtaining of strong magnetic fields (100-200 kOe) requires the creations of current generators of the reactive power into several gigawatts in the range of the pulse durations from several ten microseconds to several milliseconds. Thus, for optics of the conversion of positrons on rotary-focusing magnets of complex VEPP-3 [1] and meson channel on the parabolic lenses for the neutrino experiment in IPVE [2] (pulse fields ~120kOe) is required generator with reactive power 1.5 GW for the duration of pulse 100-200 μ s. Fundamental during the development of such generators is a question about the switching device/equipment and its maximum pulse parameters - dielectric strength, peak inverse anode voltage and maximum pulse current.

The use of industrial valves/gates in the mode/conditions of overload with respect to the pulse current allows in the limited range of the pulse durations to commutate reactive power on the order of 5 MW for the silicon ones (VKDU-150), 10 MW for the mercury TR 80/16) valves/gates with $\tau=0.7-1.5$ ms and 10 MW for hydrogen valves/gates (TGI1-2500/35) with $\tau=1-5$ μ s. The wish to expand the range of durations in the region 50-500 μ s (where mercury-arc rectifiers virtually do not work, but the reliability of the operation of silicon ones sharply falls) leads to the considerable decrease of the commutated reactive power. For example, for TGI1-2500/35 with $\tau=100$ μ s reactive power is 20 MW [3]. This leads to the need for the series-parallel start of a large quantity of valves/gates.

In IYAF of SO AN USSR is created the nonstandard gas-discharge valve/gate, controlled with the aid of the magnetic field over a wide range of the pulse durations from 50 μ s to 2 μ s [4]. Further development of this instrument made it possible to create the valve/gate which was capable to commutate reactive power into 1 GW in required for our purposes interval of the pulse durations. Instrument is conditionally named "Magutron" - the magneto controlled thyatron. In it is used series circuit of the storage capacities/capacitances, divided by valves/gates, with one supply of power and one stabilization system.

Fundamental oscillator circuit is given in Fig. 1. With the work of the load the generator is asymmetric relative to ground point series circuit of two storage capacities/capacitances, divided by valves/gates, with the total by effective stress $2U_0$. With the charge to voltage U_0 from one power supply storage capacities/capacitances are connected in parallel. For the optimum agreement of generator with the inductive load is used the peak transformer with a small ($\sim 4-5$ mH) leakage inductance and the current in secondary winding of the order of one megampere.

For the short-term stabilization of the amplitude of current in load and compensation for the slow departures/attendance of the parameters of generator and load in the time is applied the special diagram, which ensures voltage regulation on the storage capacities/capacitances with the precision/accuracy better $\pm 10^{-3}$ [5].

For eliminating the effect of the time/temporary instability, connected with the instability of the ignition of valves/gates ± 1 μ s, in the load is formed/shaped the current pulse flat-topped with precision/accuracy $\sim 0.10/0$ in the limits of ± 10 μ s [3]. The starting/launching of generator is accomplished/realized from the standard diagram of the ignition through matching cable transformer

(Tr2). As the load of the generator of ignition serve control windings by valves/gates.

Page 168.

Regeneration occurs through the recharging diodes D_1-D_{1+} .

Since the cathode of valve/gate M_1 is located under high voltage, then for the protection of amplitude from the possible breakdowns on the gas-filled gap is developed special vacuum decoupling.

The oscillography of the current pulses of control and operating current is accomplished/realized with the aid of the non-inductive low-resistance shunts and the Rogowski loop. A voltage drop across the grounded valve/gate was determined with the aid of the in parallel connected compensated divider with the supporting/reference stabilatron tubes.

The construction/design of Magutrons, which work in the oscillator circuit, is given in Fig. 2. Electrodes are made from the stainless steel in the form two long -80 cm of the cylinders with a diameter -20 of cm, isolated/insulated between themselves by discharge gas-filled gap -10 mm. Instrument is filled by low-pressure

hydrogen $\sim 10^{-1}$ - 10^{-2} torr. Inleakage and evacuation of hydrogen are conducted symmetrically according to entire diameter of the ends/faces of instrument. On the ends/faces the electrodes smoothly convert/transfer into the current input; the commuted current of working contour/outline is fed symmetrically. Cathode is made thin-walled (~ 1 mm). On the external surface of cathode are cut the helical flutes in which is placed the control winding, isolated/insulated from the cathode. The taking place on the winding pulse current creates in the working clearance the magnetic field of control. The initiation of the arc discharge in the instrument is accomplished/realized with the aid of the glowing discharge of high (~ 5 A/cm²) current density.

With the considerable range of instrument important becomes the creation of such conditions for the discharge, under which would work entire/all surface of electrodes, situated under the control winding. Such conditions are created by both the construction/design of control winding and by circuit solution - use/application of a saturating core device.

Double winding creates the alternating axial helical magnetic field of control, which with its correct polarity forces the discharge to move in the necessary direction. Saturating core devices (Dr1, Dr2) make it possible to tighten the duration of the glowing

discharge to the period, sufficient for the ionization of entire discharge gap and even distribution of discharge all over surface of electrodes, and the steady tightening of current with its approach to zero at the end increases time by the reionization of discharge gap and thereby it contributes to an increase in the peak inverse anode voltage of instrument.

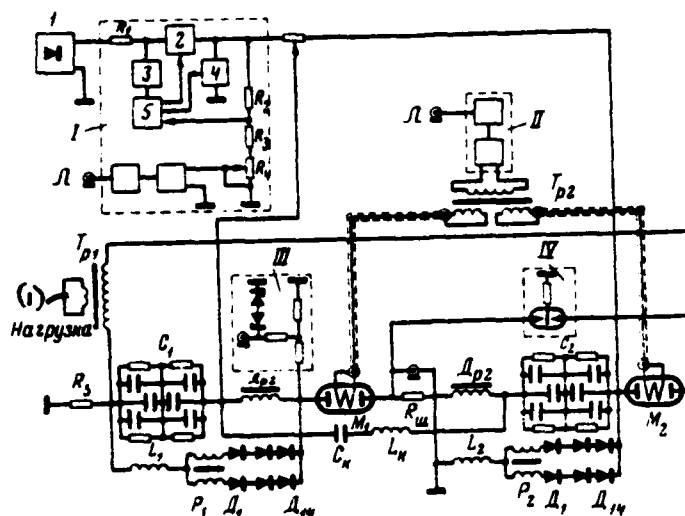


Fig. 1. Pulse generator circuit. 1 - rectifier; 2 - antihunting circuit; 3 - generator of magnetic ignition; 4 - voltage divider; 5 - vacuum decoupling; C_1 , C_2 - storage capacity/capacitance; M_1 , M_2 - valve/gate; Dr_1 , Dr_2 - saturating core device; R_1 - charging resistor; R_{sh} - instrument shunt; D_1 , D_2 - recharging diodes; L_1 , L_2 - recharging inductance; R_2 - reactor of pulse; $C_k L_k$ - correction circuit of the pulse apex; Tr_1 - matching transformer; Tr_2 - transformer of ignition; R_5 - decoupling resistor.

Key: (1) - Load.

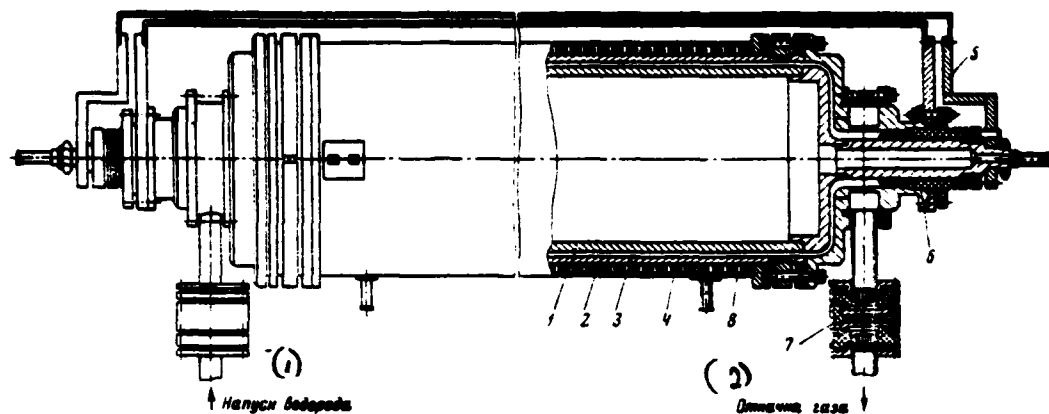


Fig. 2. Construction/design of magneto controlled valve/gate 1 - anode; 2 - cathode; 3 - discharge gap; 4 - control winding; 5 - current input; 6 - insulator; 7 - vacuum decoupling; 8 - jacket of cooling.

Key: (1). Allowance of hydrogen. (2). Evacuation of gas.

Page 169.

Fig. 3 and 4 give the time graphs of work of generator and the control characteristic magnetron. For the reliable prolonged work of generator preliminarily is conducted aging/training $\sim 2 \cdot 10^6$ the impulses/moments/pulses of the newly prepared valves/gates by the currents of density ~ 8 of A/cm² by a minimum quantity of reverse breakdowns. This current density makes it possible to exclude the interruptions/discontinuities of current and pinching of arc. In this

case the symmetry of current inputs makes it possible to drive away the discharge to that or other side along the electrodes. Further aging/training is done in the medium of hydrogen.

The characteristic parameters of a good work of valve/gate they are: 1) a quantity of reverse breakdowns is not more than 0.1o/o; 2) the step of the glowing discharge with a voltage drop into 300-350 in; 3) the stability of the firing point of discharge $\sim 1 \mu\text{s}$; 4) magnetron type control characteristic; 5) the stability of vacuum.

Are at present carried out experimental investigations and is achieved/reached the reliable work of generator for the duration of pulse $\sim 100-200 \mu\text{s}$ (the reactive power of $\sim 1 \text{ GW}$) on one magneto controlled valve/gate with the maximum pulse parameters: dielectric strength $\sim 20 \text{ kV}$; peak inverse anode voltage is not less than 10 kV , maximum pulse current 100 kA .

210

DOC = 80069213

PAGE 409

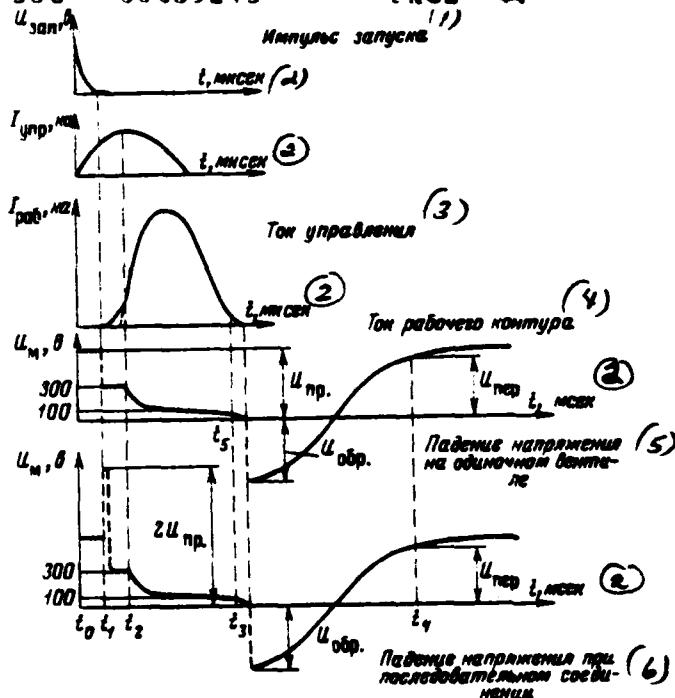


Fig. 3. The temporary/time performance records of generator t_0 - the moment/torque of the starting/launching of the generator of ignition; t_1 - firing point of valve/gate; t_2 - moment/torque of transiting the glowing discharge in the arc; t_3 - moment/torque of the approach of current and zero and the emergence of inverse voltage on the valve/gate; t_4 - moment/torque of the termination of overcharging began the charges of storage capacity/capacitance; t_1-t_2 - step of the glowing discharge; t_2-t_3 - arc discharge; t_3-t_4 - duration of overcharging; t_3-t_5 - delay of choke/throttle.

Key: (1). Trigger pulse. (2). μ s. (3). Control current. (4). Current of working contour/outline. (5). Incidence/drop on single valve/gate. (6). Voltage drop with series connection.

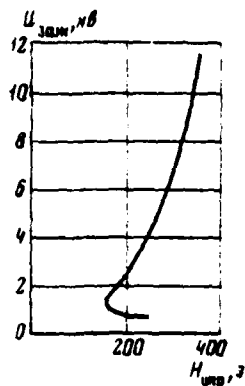


Fig. 4. Control characteristic of magutron for $(pd)_{N_2} = 2.10 \pm \text{torr} \cdot \text{cm}$
 $((pd)_{N_2} = 2.10^{-2} \text{ torus. cm})$.

Key: (1). kV.

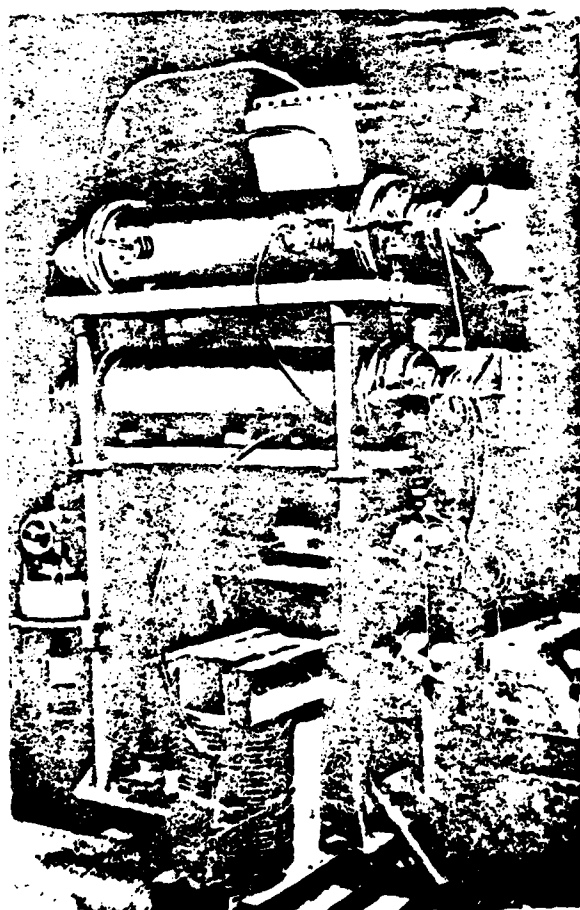


Fig. 5. General view of block/module/unit of magutrons.

Page 170.

Use/application of two magneto controlled valves/gates in diagram examined above made possible to obtain pulse generator of reactive power -1.5 GW (voltage on the valves/gates ± 9 kV, current 80 kA).

The standard circuit solutions of the commutation of magutrons (parallel connection) make it possible to create the reliably working generator of reactive power on the order of 2 GW. The general view of the block/module/unit of series-connected magutrons is represented in Fig. 5.

The distinctive special feature/peculiarity of valve/gate with the cold cathode lies in the fact that its valve properties do not depend on the polarity of electrode voltage. This makes it possible to create generator of the train of the impulses/momenta/pulses of different polarity, utilizing only one instrument. Promising is also further increase in the parameters of valves/gates of such type due to an increase in effective area of electrodes.

Further development and improvement of powerful/thick

valves/gates will significantly expand the possibilities of the impulse circuits of supply and will make it possible with their use/application to raise the technical parameters of many electrophysical devices/equipment.

REFERENCES

1. T. A. Vsevolozhskaya et al. (see present coll. ., Vol. 1).
2. D. L. Danilov et al. ZhTF, 1970, Vol. XXXVII, V. 5.
3. B. P. Bayanov et al. PTE, 1968, No 5.
4. B. P. Bayanov et al. Transactions of All-Union Conference on the charged particle accelerators. Vol. 1. of M., VINITI [All-Union Institute of Scientific and Technical Information], 1970, page 283.
5. A. P. Baydak et al. see present coll. vol. /

51. Electron analogue of cyclic accelerator with the ultrapowerful leading magnetic field.

A. V. Gryzlov, V. S. Panasyuk, V. M. Ryzhkov, A. A. Sokolov, Ya. M. Spektor, V. M. Stepanov.

(All-Union scientific research institute of optico-physical measurements).

The use/application of ultrapowerful magnetic fields on the order of 1 MG and more makes it possible to reduce to a minimum the sizes/dimensions of cyclic accelerator with the prescribed/assigned final energy of particles. In this case compactness and small cost/value of accelerator are reached due to its one-time action, since the pressures, which correspond to fields, considerably exceed the limit of the strength of metals. Under these conditions they resort to the explosive technique of obtaining ultrapowerful magnetic fields [1-3]. Are known two methods of obtaining the fields of 1 MG with the aid of explosion [2]: the compression of the magnetic flux, included in the conducting shell (generators of the type of MK-1), and the excitation of single-turn magnetic systems by explosive-magnetic current generators (generators of the type of

MK-2). First method to expediently apply mainly for the betatron action of particles, by the second - for the high-frequency.

If in the usual pulse cyclic accelerators the energy content of magnet determines the type of magnetic system and limits in the final analysis intensity and energy of accelerator, then for the energy possibility of explosive-magnetic generators it makes it possible to utilize although more energy, structurally/constructurally simplest types of magnetic systems with the sizes/dimensions of aperture, compared with the radius of curvature of the orbit of particles. This can considerably simplify the construction/design of accelerator and increase its intensity, which is extremely important for the accelerators of single action. It is obvious that in similar accelerators the systems of injection, capture, acceleration and issue of particles must be maximally simple and adequate to the magnetic system of accelerator on the sizes/dimensions and the cost/value.

From the possible fields of application of explosive-magnetic accelerators, first of all, should be noted clashing beams. As is known,, other conditions being equal, with an increase in the magnetic field quadratically increases the density of beams and the ratio of a number of useful interactions to the background. Besides this, characteristic for the explosive-magnetic accelerators very

rapid energy gain gives the possibility to accelerate the short-lived particles. These facts make it possible to hope that similar accelerators are, apparently, one of the most adequate/approaching devices/equipment for the realization of fundamental experiments for clashing meson beams.

Is given below the description of electron analogue of one of the possible versions of the accelerator, designed for the use of an explosive-magnetic generator of the type of MK-2. The supply of model is accomplished/realized from capacitor bank.

Fig. 1 gives the schematic of model. accelerator, it is shaped from within so that in the internal cavity of turn is formed/shaped the magnetic field, analogous in form to the field of usual adiabatic trap with the stopper coefficient approximately two. Turn is connected through the commutating discharger/gap to capacitor bank with the aid of the busbars/tires. Simultaneously the cavity of turn is utilized as cavity resonator for obtaining the high-frequency accelerating electric field. For this purpose to the ends/faces of the turn through insulating plates are superimposed the thin metallic plates, which close ends/faces in the high frequency. With the aid of the coupling loop cavity resonator are excited the high-frequency oscillations of the type H_{111} , whose electric field E_{111} , perpendicular \perp to the magnetic field of the accelerator (see Fig. 1) and is utilized

for the particle acceleration.

Page 171.

Tungsten cathode and opening/aperture in the lower plate form the electron gun, which injects along the axis/axle of accelerator electron beam with the energy ~ 100 eV, which ionizes residual gas in the near-axial region of accelerator. Upper and lower plates are found under the negative potential relative to housing, forming in the presence of magnetic field trap for the electrons, which additionally increases ionization in the near-axial region. With satisfaction of resonance conditions the electrons from this region are seized into the accelerative mode/conditions. The discharge/break of the accelerated particles is accomplished/realized to a target-target. The ends/faces of turn are closed by cover/cap and exhaust branch pipe, made from fiberglass. Fig. 2 gives the photograph of accelerator in the assembled form.

Let us give the fundamental principles, which characterize work of the accelerator. In spite of the complicated profile/airfoil of cavity resonator, we will use for simplification of the formula of the frequency of cylindrical cavity during the oscillations of the type H_{111} for the case when the length of cylinder is considerably more than its radius R [4]:

$$\omega_0 = 1,84 \frac{c}{R} . \quad (1)$$

Upon the high-frequency acceleration for resonant particle $\omega = v/r$ (where v - speed of resonant particle, r - a radius) it must coincide with the frequency ω_0 of accelerating field (condition of synchronism). Hence, taking into account (1), we have

$$r = \kappa \beta R, \quad (2)$$

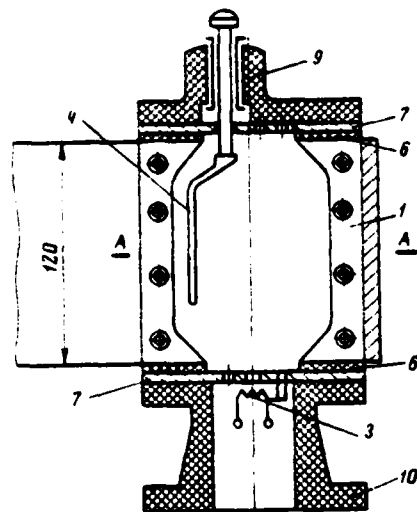
where $\kappa = 0.543$. Thus, the orbit of accelerating resonant particle must be the turned/run up spiral with the radius, proportional β and to those asymptotically approaching with $\beta \rightarrow 1$ and $r = \kappa R$. A similar trajectory, obviously, can be provided only with an increase in the leading magnetic field in accordance with the expression

$$\beta E = e H r, \quad (3)$$

where the leading field H we consider for simplicity uniform. From equations (2) and (3) we obtain

$$E = \kappa e H R . \quad (4)$$

719



(1) Section A-A

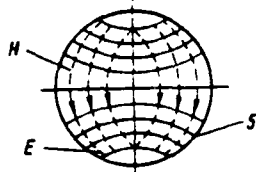
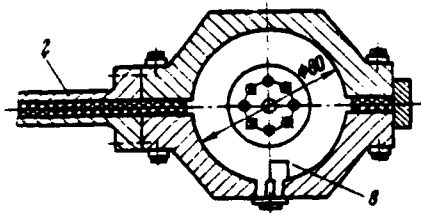


Fig. 1. The schematic of electron analogue of accelerator. 1 - electromagnet - resonator - vacuum chamber; 2 - busbar/tire for the connection to capacitor bank and discharger/gap; 3 - tungsten cathode; 4 - target - target; 5 - schematic of the lines of force of the electrical and magnetic field of wave H_{111} in plane AA; 6 - insulating plates; 7 - metallic plates of blocking HF capacitors/condensers; 8 - coupling loop with HF the generator; 9 -

cover/cap from the fiberglass; 10 - exhaust branch pipe from the fiberglass.

Key: (1). Section.

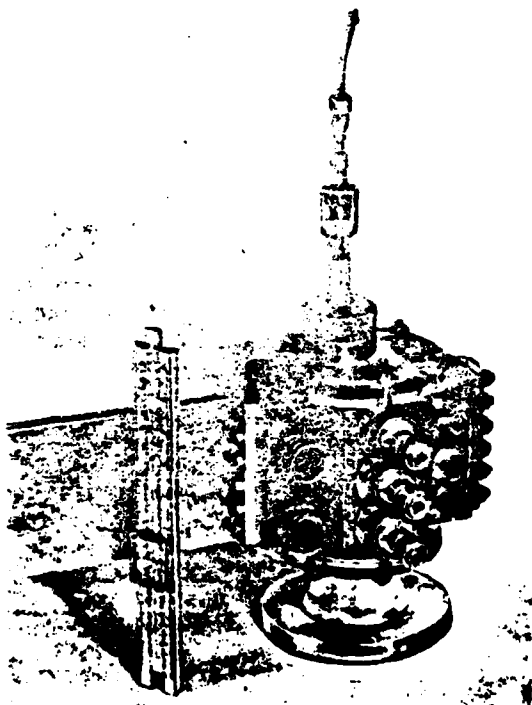


Fig. 2. Accelerator in assembled form.

Page 172.

Since $E = E_0 + W = M_0 c^2 + W$, that of expression (4) follows that acceleration for this type of particles it is possible, beginning only from certain value of the magnetic field

$$H_0 = \frac{M_0 c^2}{2eR}, \quad (5)$$

with which the cyclotron frequency of the rotation of nonrelativistic particle it is compared with the frequency of accelerating field. From equations (2), (4), (5) and relationship/ratio $\beta^2 = 1 - (\frac{E_0}{E})^2$ we find a change of the radius of resonant particle in the function of the leading field H:

$$r(H) = r_0 \sqrt{1 - \left(\frac{H_0}{H}\right)^2}. \quad (6)$$

From that presented it is evident that entire cycle of acceleration consists of two modes/conditions - synchrotron and preliminary, analogous synchro-cyclotron. a radial-phase equation of motion of particles in this mode/conditions proves to be the same type, as in the synchro-cyclotron [5]. For the uniform magnetic field it takes the form

$$\frac{\pi E_0}{\omega_s^2} \frac{d^2 \varphi}{dt^2} = eU (\cos \varphi - \cos \varphi_s). \quad (7)$$

In contrast to the usual equation here $\omega_s = \frac{eH}{Mc}$ and $U = \pi \delta r$, where M - relativistic mass of particle and δ - intensity/strength of high-frequency electric field.

Experiment was conducted as follows. For the check of the value of the intensity/strength of high-frequency electric field the accelerator was first adjusted to the cyclotron mode/conditions. The

period of oscillations of magnetic field was equal to 110 μ s was shifted to the apex/vertex of sinusoid. The emission current of gun was established/installed equal to 1 mA. With the aid of the preliminarily graduated photomultiplier, arranged/located above the cover/cap, was measured the medium energy of the quanta of bremsstrahlung from the target, which is located near the axis/axle of accelerator. On the basis of formula for the maximum energy, which for our case takes form $W_{max} = 0.228^{2/3}$ keV, we find $E \approx 500$ V/cm. Is further created the necessary building up leading magnetic field for accelerating the relativistic energy. Fig. 3 gives the oscillograms of the curve of magnetic field, radio-frequency voltage and impulse/momentum/pulse of bremsstrahlung from target on the terminal radius, passed through the copper wall turn (thickness of 3 cm) and recorded by the photomultiplier, directed tangentially toward the orbit. The basic parameters of model are given below.

Kinetic energy of electrons on the terminal radius $r=1.75$ cm... of 2 MeV.

Maximum induction of magnetic field at the center.... 4.8 kg.

Duration of acceleration cycle 2 μ s.

Electric intensity. 500 V/cm.

Wavelength of the accelerating electric field... of 11 cm.

The authors express appreciation to O. A. Val'dner for the kindly furnished possibility for the work in the high-frequency laboratory and to V. G. Tel'kovskiy for the aid in the organization of experiment.

REFERENCES

1. Ya. P. Terletskiy. ZhETF [ЖЭТФ - Journal of Experimental and Theoretical Physics], 1961, t 32, page 1396.
2. A. D. ^{KA}Sagarov. UFN 1966, Vol. 88, No 4.
3. J W Shearer et al J Appl. Phys., 1968, N 4, p 2102.
4. S. Raso, J. Uinneri. Fields and wave in contemporary radio engineering. M., 1950.
5. A. A. Kolomenskiy, A. M. Lebedev. Theory of cyclic accelerators. M., Fizmatgiz, 1962.

Discussion.

V. G. Davidovskiy. Did investigate you fatigue of metals with the intermittent loads, created by field 5 MHz?

V. S. Panasyuk. As it was already said in the report, we investigated the model of the accelerator of one-time action. Model works on the electrons in the low fields.

Ya. Skhvabe. To what maximum energy do intend you to construct accelerator?

V. S. Panasyuk. the predicted following step/pitch - construction of the accelerator of protons to energy Q of 5 GeV.

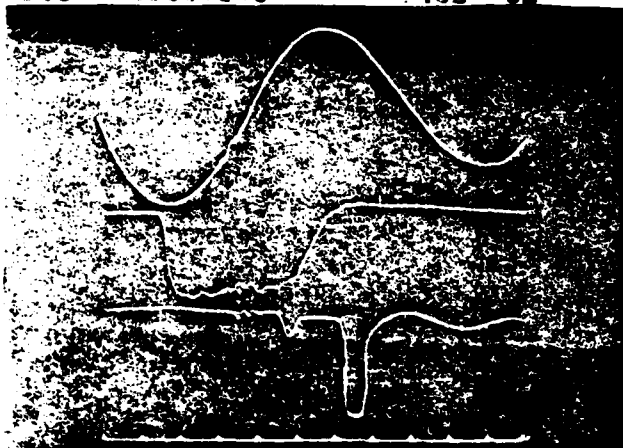


Fig. 3. Oscillograms of the impulse/momentum/pulse of magnetic field (1), impulse/momentum/pulse of radio-frequency voltage (2) and impulse/momentum/pulse of braking γ - study (3). Interval between the markers 1 μ s.

Page 173.

52

~~52~~. Use/application of the kickers with the fields 120 kOe in the unit of the conversion of accumulator/storage VEPP-3.

T. A. Vssavolozhskaya, T. E. Vecheslavova, L. L. Danilov, V. N. Karasyuk, G. I. Silvestrov, E. M. Trachtenberg.

(Institute of nuclear physics of SO AN USSR).

At present is developed interest in the creation of the reliably working devices/equipment with the pulse magnetic fields 100-200 kOe. However, in experimental nuclear physics propagation received solenoidal type only multiturn systems with uniform magnetic field [1, 2]. These devices/equipment possess convenient geometry for the perception of considerable dynamic loads, supply. Furthermore, it must be noted that the range of fields indicated did still not find use/application in optics of the transportation of the charged/loaded particles and accelerative technology.

In the work are examined created in IYaf SO AN in connection

with optics of the conversion of positrons on the setting up VEPP-3 [3] the single-turn pulse rotary-focusing magnets with the field 120 kOe and the prescribed/assigned permanent gradient.

The rational design of such systems must satisfy the series/row of the requirements, which concern strength, hardness and selection of the material of the current carrying busbars/tires: high thermal conductivity and heat capacity, acceptable strength characteristics and life. Essential are also the problems of the creation of contacts to the high current densities and heat abstraction, which separates in the conductors. Furthermore, the work of magnets is connected with the large frequency of cycles of minimum life on the order of millions of cycles.

The parameters of the kickers one of which focuses electrons to the converter M_1 and, etc. accumulate the converted positrons M_2 , they are given below:

	M ₁	M ₂
(1) Равновесный радиус, см.	12,5	7,5
(2) Угол поворота, град	63	45
(3) Показатель спада поля η	0,5	0,5
(4) Фокусное расстояние, см	25,4	20,6
(5) Энергия частиц, Мэв	450	225
(6) Высота шин, см	5	8
(7) Радиальная апертура, см	1,6	2
(8) Максимальное поле, кэ	120	120
(9) Максимальный ток, ка	860	1000
(10) Индуктивность, мкГн	0,05	0,03
(11) Длительность, мксек	120	100
(12) Энергия магнитного поля, кдж. .	18,5	15
(13) Частота повторения импульсов, Гц	5	5
(14) Средняя мощность тепловых потерь, кВт	18,5	15
(15) Тепловой напор, Вт/см ²	80	85

Key: (1). Equilibrium radius, cm. (2). Angle of rotation, deg. (3). Index of field slope. (4). Focal length, cm. (5). Energy of particles, MeV. (6). Height of tire, cm. (7). Radial aperture, cm. (8). Maximum field, kOe. (9). Maximum current, kA. (10). Inductance, μ H. (11). Duration, μ s. (12). Magnetic energy, kJ. (13). Frequency of repetition of impulses/moments/pulses, Hz. (14). Average/mean power of heat losses, kW. (15). Thermal pressure head, W/cm².

The construction/design of electronic magnet is represented in Fig. 1. In magnet opening the external and internal current carrying busbars/tires are shaped in the form of ellipsoids of revolution. On the ends/faces the shaping smoothly converts/transfers into the high flat/plane current inputs with the developed contact surface. For shaping of fringing field current distributing and that commutates busbars/tires with rectangular input and outlets for the transmission

of particles have the special shape, repeating the geometry of the current carrying busbars/tires on the ends/faces. Busbars/tires with exception of contact places are covered with insulator from epostek. Experiments in the investigation of contacts showed the lack of promise of the creation of contacts to the current density of full/total/complete operating field - on the order of 100 kA on 1 cm of height of tire: due to the large thermal and dynamic loads is observed the sparking of contacts after several thousand impulses/moments/pulses.

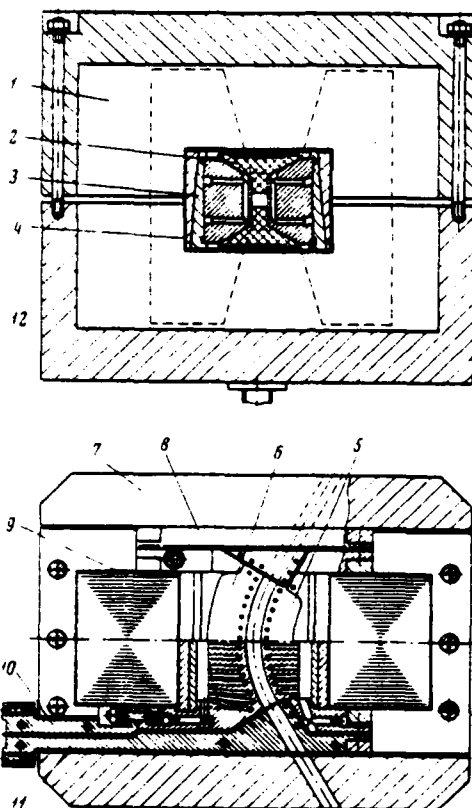


Fig. 1. Pulse magnet in the field 120 kOe. 1 - power banding made of transformer steel; 2 - apostek basing and simultaneously power inserts/bushings; 3 - power wedges; 4 - insulator; 5 - internal shaped busbar/tire; 6 - external shaped busbar/tire; 7 - power cover/cap; 8 - commutating busbar/tire; 9 - insulation/isolation of magnetic circuit; 10 - current input; 11 - current-conducting busbar; 12 - channels of cooling.

In the construction/design in question contact surfaces are strongly developed, which makes it possible to decrease the current density 3-4 times. In this case we proceed from the fact that the impedance of contact transition does not depend on the area of the overlap of the contacting electrodes and is determined by the full/total/complete force, created by bolted joints. The width of contact joint should not be taken more than three skin-layers, but height is determined by the arrangement/position of the necessary number of bolted joints. Furthermore, where this is possible, is necessary to abstract/remove the heat, which separates in the contact resistance directly in the place of contact, which makes it possible reliably to work at the current densities on the order of 30 kA on 1 cm of length.

As the material of busbars/tires is utilized the chromium bronze BrKh-0.5, which has after the special heat treatment (hardening/quenching, improvement) Brinell hardness on the order of 120 ones.

Radial fixation of busbars/tires is provided by expostek inserts/bushings, prepared from the glass-fiber cloth, saturated with epoxy resin by the method monolith. In this case the fiber stress is

selected perpendicular to the acting force.

The busbars/tires, assembled together with the inserts/bushings, are inserted into the banding, which is the laminated magnetic circuit in the rigid housing, and they are confined with the aid of two pairs of the steel hardened/tempered wedges, isolated/insulated from the magnetic circuit. The effort/force, developed with wedges, somewhat exceeds the force, created by magnetic pressure. From magnet ends current distributing and that commutates busbars/tires are tightly forced against the ends/faces of the current carrying busbars/tires by two power covers/caps with the openings/apertures for wiring of bundle. The use of the laminated magnetic circuit, besides the guarantee of the necessary for hardness construction/design due to the limitation of return flow, increases the effectiveness of magnets (we define it as relation H_{max}/I_{max} by 15-200/o. This method of fixation of the current carrying busbars/tires makes it possible to create the construction/design in which the prestressed parts under the effect of one and the same alternating load have higher safety factor on the destruction, which guarantees their large life. With the work the joint between the insert/bushing and the knowingly rigid busbars/tires is not opened and the value of maximum peak voltage does not exceed yield point. Thus, from the condition of the nondeployment of the joint of the prestressed construction/design, maximum peak voltage $G_{max} = G_0 + K\delta_{un}$.

where $k = \frac{1}{1+C_j/C_w}$ is determined by the relation of the hardnesses of insert/bushing (C_j) and the busbars/tires (C_w), and static stress from preliminary loading $\sigma_0 \approx \sigma_{0um}$, where σ_{0um} - amplitude of voltage under the effect of the impulse/momentum/pulse of magnetic pressure. When $\frac{C_j}{C_w} \approx 6$ variable component σ_{max} has a value of order 150/o from σ_0 , which substantially raises the service life of the material of parts. However, in magnet opening material works on the full/total/complete dynamic stress. It is known [4] which for calculating the dynamic stresses with the pulsating load is sufficient to know dynamic-response factor $k = 2 \sin \frac{\pi}{2} \frac{\tau_u}{\tau_0}$. This allows at the known value of half-period τ_0 of the natural oscillations of system to fit such duration of the pressure impulse of magnetic field, for which the dynamic stresses will be less than static ones. Thus, with $\tau_0 = 400 \mu s$, $\tau_u = 100 \mu s$ in the region of aperture $\sigma_{0um} \approx 0.75 \sigma_0$.

Characteristic for the single-turn systems is the fact that the energy loss to the effective resistance of conductors is defined as $W_R/W_H \approx 2.8 \cdot 10^{-4} \frac{\sqrt{p\tau}}{\Delta R}$, that for BrKh-0.5 ($\rho = 2 \cdot 10^{-6}$ ohm.cm) and $\tau_u = 100 \mu s$ and $\Delta R = 2$ cm compose ~20o/o.

In the given construction/design is accepted the special "porous" system of cooling: water drives away itself through the system of the channels of cooling in such a way that the heat is removed/taken virtually in that place where is separated/liberated

basic power. This reduces to the minimum the temperature differential on the metal. During the skin processes the heating per pulse

$\Delta T = 4.8 \cdot 10^{-8} I^2 \frac{1}{C \tau}$ does not depend on the pulse duration and composes $\sim 30^\circ\text{C}$. Steady temperature of $\sim 100^\circ\text{C}$ with the expenditure/consumption of water ~ 100 l/min.

To shaping of field in the aperture of iron free systems (distribution n according to a radius and according to the height) significantly is manifested relative change in the radius $\Delta R/R$ and ratio of height of tire to radial aperture $\frac{z}{\Delta R}$. Furthermore, height of tire determines even and the effectiveness of magnet.

The generatrices of the current surfaces of busbars/tires, which form field in magnet opening, we are given in the form of ellipses $\frac{z^2}{\xi^2} + \frac{\rho^2}{\xi^2 - 1} = \alpha^2$, where α is defined by an equilibrium radius and an index of "n" as $n = \frac{R_0^2}{R_0^2 + \alpha^2}$. Values ξ for each of the surfaces are found from condition $\rho^2_{z=0} = \alpha^2(\xi^2 - 1)$.

With the sufficiently high busbars/tires field component in the aperture take form $H_z = \text{const} \frac{\text{ch } v}{\text{ch}^2 v - \sin^2 u}$, $H_p = -\text{const} \frac{\text{tg } u \cdot \text{sh } v}{\text{ch}^2 v - \sin^2 u}$, where $\sin u = \frac{S_1 - S_2}{2\alpha}$, $S_1 = \sqrt{(\alpha + z)^2 + \rho^2}$, $S_2 = \sqrt{(z - \alpha)^2 + \rho^2}$, so that when $z=0$ H_z depends on a radius as $H_z = \frac{\text{const}}{\sqrt{\rho^2 + \alpha^2}}$ and nonlinearity on the edge of aperture $A_0 \sim \pm 1$ cm with $R_0 = 7.5$ cm gives the contribution in field $\sim 10^{-3} H_z(R_0)$.

The limitation of busbars/tires on the height is conducted by surface with the generatrix in the form of hyperbola $\frac{x^2}{\eta^2} - \frac{p^2}{1-\eta^2} = a^2$, where value η is determined by height of tire. Surface with such generatrix is equipotential for the field in the aperture, thanks to which the field distortion due to the limitation of height of tire proves to be minimum at their prescribed/assigned height. At the selected height of tire the disturbance/perturbation of the index of a field slope on the edge of aperture $A_z = \pm 1$ cm composes (according to the calculations) 100/o.

Page 175.

Essential for the optical properties of magnet is the contribution of the fringing fields of input and outlets (in the end ones the commutating and current-conducting busbars whose width it is compared with the length of magnet) into the integral of field along the length of magnet. Their effect was studied in the model and it was discovered, that the commutation of busbars/tires accepted with the use/application of end shields provides sufficiently good shaping of fringing fields, so that integral of the field along the length of magnet is linear on R and on z with precision/accuracy -30/o.

Thus, it is possible to expect that the use of the described magnets for the particle focusing in the unit of conversion will ensure the collection of positrons in calculated phase volume [3].

The supply of magnets is accomplished/realized from the pulse generator with reactive power 1.5 GW on magneto controlled valves/gates [5]. For agreeing the load with the generator is utilized cable type peak transformer with the transformation ratio 10 and a small leakage inductance on the order of 4 nH (see Fig. 2).

At present magnets are tested on $2.5 \cdot 10^5$ impulses/moments/pulses in the mode/conditions 100-120 kOe. Substantial changes in the state of the current carrying busbars/tires and epostek insert/bushing it is not observed. Fig. 3 depicts the positron magnet, established/installed on the complex for the assembly.

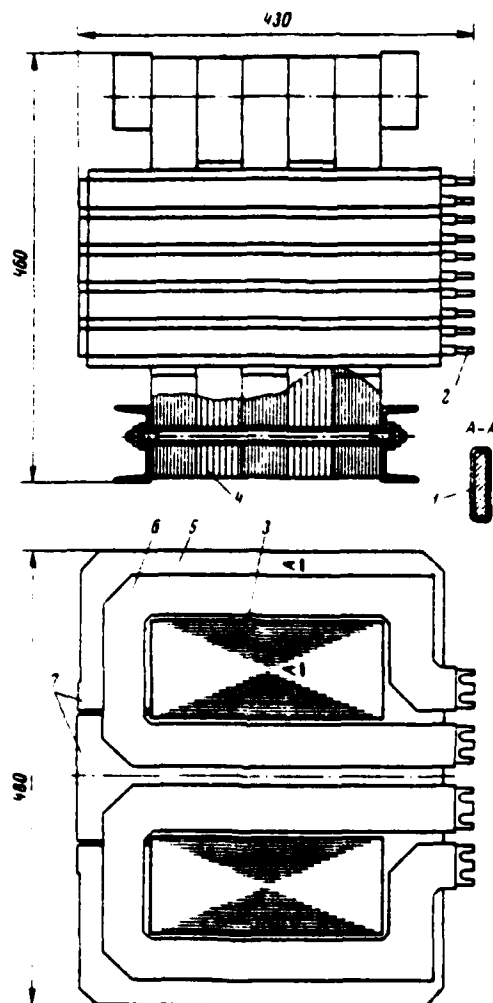


Fig. 2. Peak transformer. 1 - insulation/isolation of primary winding; 2 - introductions/inputs of primary winding; 3 - insulation/isolation of magnetic circuit; 4 - composite magnetic circuit; 5 - turn of secondary winding; 6 - flat/plane turn of primary winding; 7 - low-induction output of secondary winding.

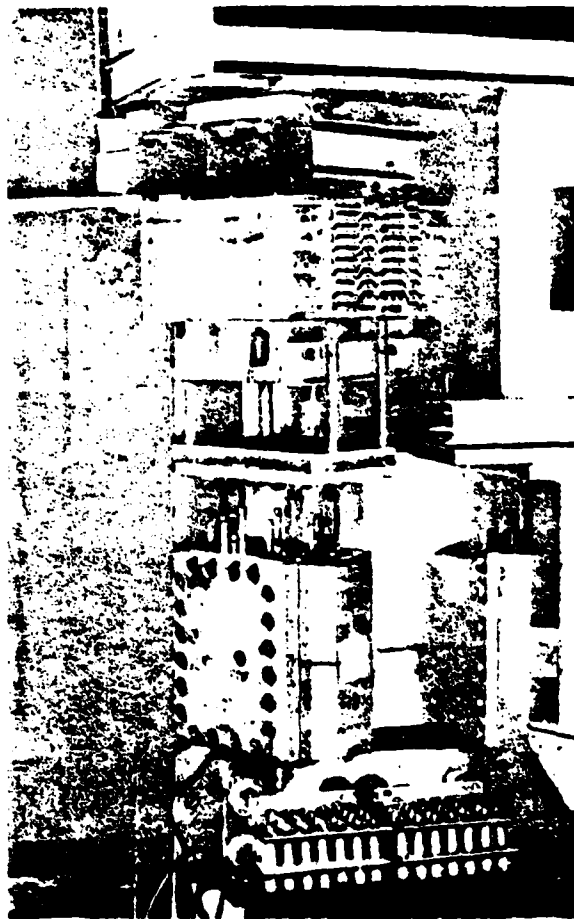


Fig. 3. Magnet with the transformer on the complex.

REFERENCES

1. V. V. Akhmanov et al. setting up for obtaining the pulse magnetic fields by intensity/strength to 150 kOe, utilized in the physical experiments on the synchrocyclotron LYaP of J.I.N.R. PTE, 1965, No 4.

2. V. K. Makar'yani. The kicker on 70 kOe PTE, 1970, No 1.

3. T. A. Vsevolozhskaya et al. Electron-optical channel VEPP-3. Transactions of All-Union conference on the charged particle accelerators, M., VINITI, 1970.

4. Ya. G. Panovko. Bases of the applied theory of elastic vibrations. M., 1957.

5. L. L. Danilov. See this coll., Vol. 1.

Page 176.

53. Hydraulic Systems with Electronic Control for Magnets of Beam Output.

V. Klok.

(Rutherford High-Energy Laboratory, England).

1. Introduction.

This report describes mechanisms used in beam output systems according to the Pichchioni [1] diagram on the "Nimrod" synchrotron. The large aperture of this accelerator makes it necessary to use large output systems with magnets weighing on the order of 1000 kg which must be moved 50 cm in around 0.5 s at a repetition frequency of 22 min⁻¹.

The working cycle of these mechanisms is shown in Fig 1. The size of the time interval between the injection plateau and the rapid cutoff of the beam is around 800 ms in the normal mode of the accelerator, which corresponds to energy of 7 GeV; however, the required time lag of 200 ms after injection and 50 ms before cut cutoff actually decrease the duration of the working cycle of the output magnet to 550 ms. At energies below 7 GeV, this time can be decreased to 400 ms.

Speeds of this order of magnitude require a peak power of around 114 kW, which

is transferred through the hydraulic actuating mechanism. The flow of oil to hydraulic piston has the maximum value of 5 l/s at a peak pressure of 206 bars, and during the production of these mechanisms there did not exist relay valves for the control of this level of flow. Therefore hydraulic power was created by pump with the slant, which has variable/alternating productivity.

2. Hydraulic mechanism.

Fig. 2 shows the mechanism of the system of conclusion/output in that form, in which it existed to the setting up to the accelerator. Hydraulic system is assembled on the bogie/carriage. Plunger is arranged/located from above and through the transmitting shaft is connected with the deriving/concluding magnet. Pump with the slant and homing/driving engine are established/installed under the bogie/carriage. The bogie/carriage moves over the rails, to which it is usually fastened with eight hydraulic jacks. Pumps at the end/lead supply pressure to the basic pump and to the terminals. The deriving/concluding magnet lies/rests on shaft butt end, which speaks in favor of the cover/cap of jacket, and rests on the rails within the vacuum volume. The feeding power is supplied to the mechanism

with the aid of the flexible connectors from the side the bogie/carriage through the water-cooled ducts above the construction/design and through the flexible tubes above the arch. In the lower part of the arch are arranged/located the rapidly disconnected connectors, which provide the rapid removal/distance of arch and magnet and can draw current to 14000 A. Shaft enters into the vacuum volume through labyrinth type three-stage multiplexing.

The supply of the control systems to check is accomplished/realized through 25- strand flexible cables which are visible in the foreground.

2.1. Diagram of control.

Due to the voltages in by inclination/slope disk the maximum acceleration of plunger is limited by value $5g$ (49 m/s^2), so that the ideal characteristic curve of mechanism must take the form, shown in Fig. 3. In this ideal curve both the acceleration and speed they reach the maximum allowed values for the minimum duration of working stroke/cycle. Fig. 3a illustrates two periods of uniform acceleration in the beginning and at the end of the working stroke/cycle, Fig. 3b show the period of constant velocity which in the minimum duration of working stroke/cycle would correspond to the peak output of pump. Fig. 3c shows the resulting curve of the dependence of displacement

on the time.

Fig. 4 gives the schematic of the control system. The error signal from the comparator passes through the dc amplifier to the relay valve whose exit flow is proportional to value and polarity of input current. The usually control current 10 mA creates the hydraulic flow of 0.7 l/s at the operating pressure of 206 bars. Relay valve moves performing pump piston with the slant.

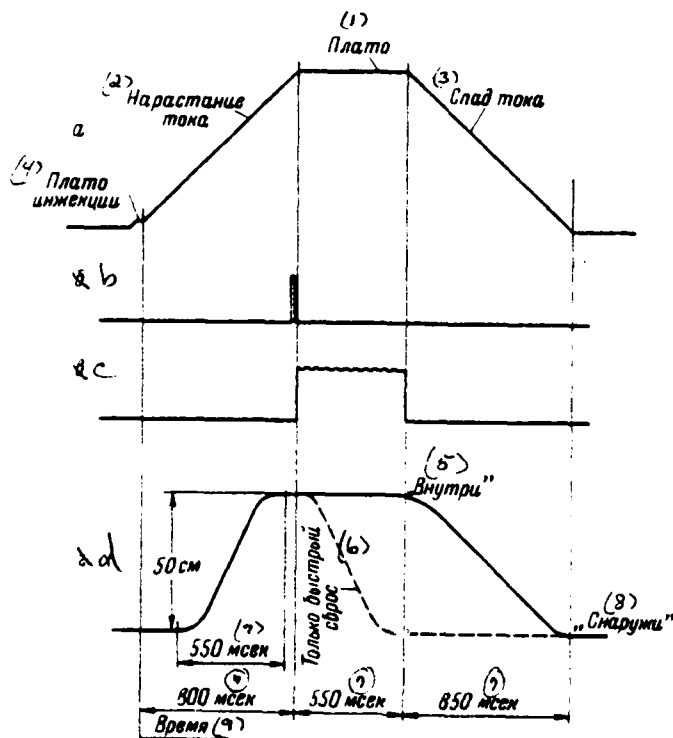


Fig. 1. The time characteristics of the work of the systems of the conclusion/output of accelerator "Mimrod". a) the program of the work of magnet; b) rapid discharge/break; c) slow discharge/break; d) the working stroke of the mechanism of the system of conclusion/output.

Key: (1). Plateaus. (2). Build-up/growth of current. (3). Decrease in current. (4). Plateaus of injection. (5). "inside". (6). Only rapid discharge/break. (7). ms. (8). "outside". (9). Time.

Page 177.

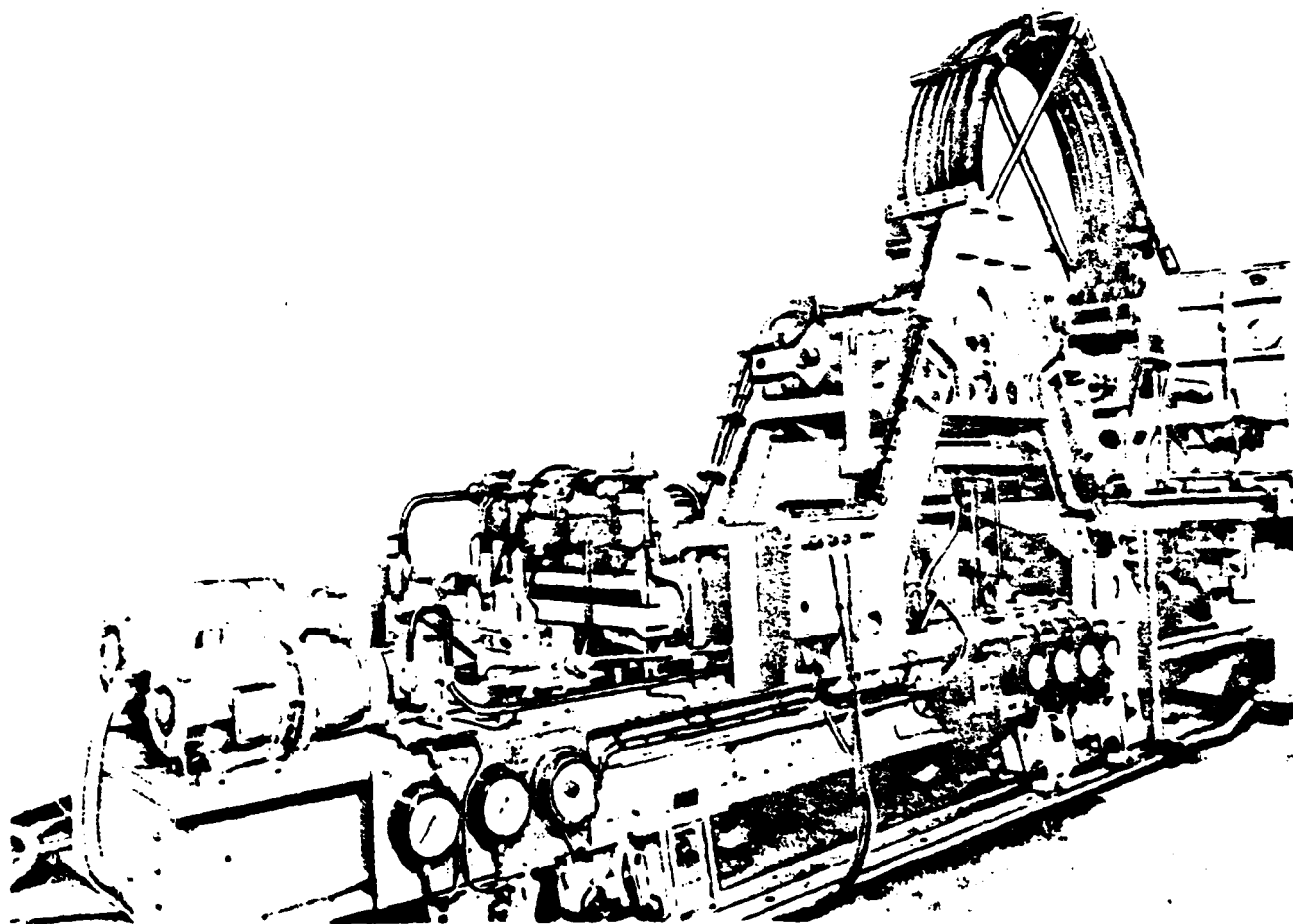


Fig. 2. Mechanism of system of conclusion/output ~~up~~ during tests.

MKP

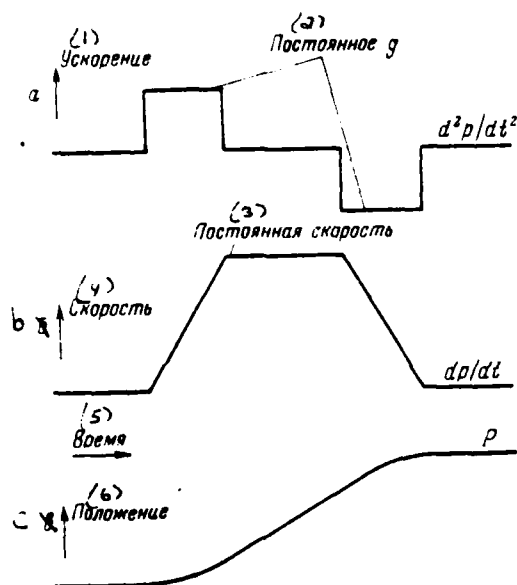


Fig. 3. Ideal forms of the impulses/moments/pulses of position, speed and the acceleration, utilized for the control of the mechanisms of the system of conclusion/output "nimrod".

Key: (1). Acceleration. (2). Constant. (3). Constant velocity. (4). Speed. (5). Time. (6). Position.

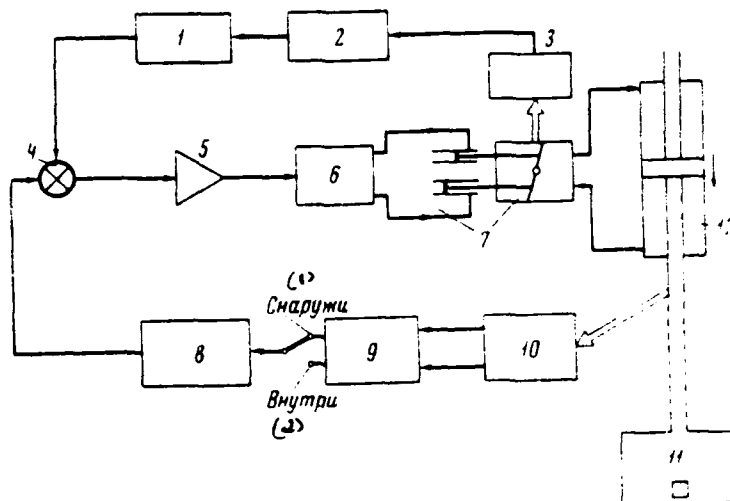


Fig. 4. Schematic of the control of the mechanisms of the system of conclusion/output "Mirod". 1 - zero adjustment and phase; 2 - the phase-sensitive rectifier; 3 - sensor of the angle of the slope of disk; 4 - comparator; 5 - dc amplifier; 6 - relay valve; 7 - pump with the slant, which has variable/alternating productivity; 8 - syncro generator; 9 - demodulator; 10 - position detector; 11 - magnet; 12 - plunger.

Key: (1). Outside. (2). Inside.

Page 178.

2.1.1. Pump with the slant.

The isometric projection of pump with the slant (Fig. 5) shows the disk which can be inclined in any direction under the effect of the pressure, created by the percussion of the pulling rods. The flow of oil from the relay valve moves performing plungers and, thus, turns slant to the necessary angle. On other end/lead of the pump is arranged/located the rotating cylindrical unit, powered through the shaft with the aid of the electric motor in power 45 kW. Within the cylindrical unit are established/installed eight pistons whose ends/leads are forced by springs against slant. During the rotation of cylindrical unit each piston moves over the surface of the slant which forces pistons to complete the forcing action, determined by the value of inclination/slope. In this case oil is supplied to the plunger through the plates with the openings/apertures, motionlessly established/installed at the end/lead of the rotating cylinder.

2.1.2. Reaction circuit.

In order to lock contour/outline, the position detector, installed on the slant, supplies feedback signal to the comparator. Sensor is actually the freely connected transformer with the movable iron core, excited by the stabilized sine voltage 24 V by the frequency of 3 kHz. The phase-sensitive rectifier converts the output signal of transformer into the direct current.

Null circuit introduces the compensating coefficient which removes the errors in position of zero, created by other elements/cells. For the stabilization of the contour/outline which possesses the characteristics of the second order, is utilized the phase balancer.

2.1.3. Position detector.

The signal of the position of plunger is obtained from the linear variable/alternating hybrid coil and are converted it into the direct current. This signal they convert with the aid of the synchro generator and through the reaction circuit supply to the comparator.

Fig. 6 shows the schematic of the position detector which has working stroke 50 cm. Transformer has primary winding by the length of 110 cm and two secondary with a length of 55 cm with turn ratio, equal to 1. The moving/driving core is the ferrite with a length of 55 cm and with a diameter of 13 cm, fastened/strengthened to the plunger and moved along the axis/axle within the framework/body of the windings of transformer. When ferrite core is located in position 1, on secondary winding 1 fall about 45 V, and on secondary winding by 2 - about 5 V. If core is located in position 2, these values transpose. The rectified output signals have saw-tooth form and are utilized for obtaining control signals for diagram in Fig. 7.

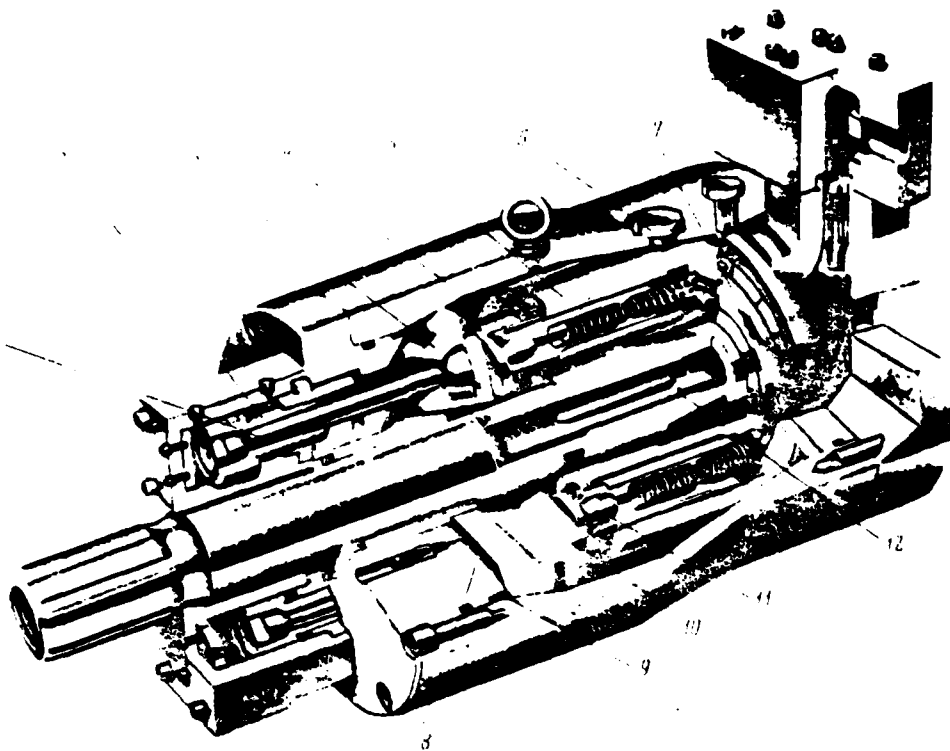


Fig. 5. The general view of pump with the slant of variable/alternating displacement (VW 20). 1 - pulling rod of disk; 2 - performing plunger; 3 - slant; 4 - pistons; 5 - rotating cylindrical unit; 6 - drain hole of housing; 7 - plate, which closes opening/aperture; 8 - hydrostatic holders; 9 - bearing of slant; 10 - slider-type plate; 11 - crosshead with ball bearing; 12 - slots/grooves for the connection of the second pump.

2.1.4. Synchro generator (Fig. 7).

The output signal, which enters the comparator, will be proportional to the speed of plunger. Signal must have the trapezoidal form (see Fig. 3b). The output sensor signal enters the amplifier with the variable/alternating amplification and cascade/stage 2, which is saturated on the high signal levels at the entrance. Cutoff point which corresponds to the beginning of delay/retarding/deceleration, is determined by the potentiometer of cutoff R8. Cascade/stage 2 normally works with diode D3 in the open state and, thus, has an amplification factor, equal to 1. The leading edge of signal is formed/shaped with circuit C2-R4, which creates exponential build-up/growth; however, in the process of delay/retarding/deceleration diode D4 disconnects this circuit.

Inertia leads to the delay of functioning and provides the non-linear acceleration of plunger, than this follows from the exponential waveform. In order to compensate for the effect of inertia in the process of delay/retarding/deceleration, to cascade/stage 2 is supplied the signal of direct connection/communication on the speed. This signal which is established/installed under the dynamic conditions, they obtain from the diagram, connected with cascade/stage 3. The beginning of the signal of direct connection/communication is determined by the diode

clamping circuit D1-R5, and its amplitude - by potentiometer R6.

Operating experience showed that due to the gap in the mechanical components/links, connected with the slant, appears the large his own "backlash". In order to bring together this effect to the minimum, the amplification of the controlling contour/outline they increase 10 times, utilizing a diagram with the large slope/transconductance. In proportion to the output signal of cascade/stage 2 drops, diode D3 finally is cut off and detaches the connected with it impedance of feedback R2. Beginning characteristics with the high slope/transconductance check by potentiometer R9. In practice this beginning is regulated, supplying to the mechanism the positive stopping effort/force, which does not call oscillations. The initial position of mechanism is established/installed by potentiometer R7, which is utilized also for the compensation for residual voltage 5 V at the end of the working stroke of sensor.

3. Work with the use of cybernetic control.

In order to ensure automatic scanning and recording of the given physical experiments on the accelerator, the control system they expand, switching on in it digital buffer device/equipment. The controllable/controlled/inspected parameters are the radial position of plunger, i.e. the position of the deriving/concluding magnet, and

radial position the bogies/carriages (position of bogie/carriage relative to the deriving/concluding magnet will affect working piston stroke).

3.1. Digital position detector.

The position detector, described in section 2.1.3, in this case cannot be utilized, since it records the motion of plunger only relative to bogie/carriage; it they replace by optical lattice [2] in length of course 1 a, which is established/installed outside the mechanism and is connected with the plunger with coupling rod. Lattice contains the three-channel optical system: two channels serve for determining of direction and difference count, and the third - for absolute measurement of zero. A counter of the type "upward-downward", calibrated completely in the values of an absolute radius, is actuated by the logical signals of direction from the lattice. Zero channel is utilized for discharge/break and launching/starting the counter in the middle of working stroke.

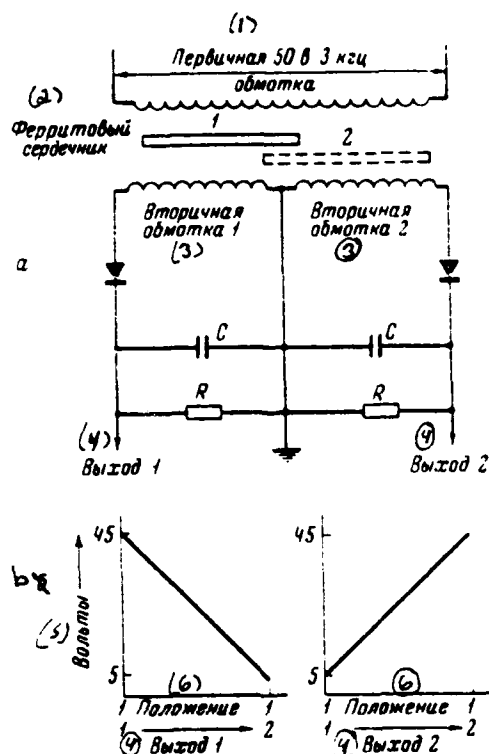


Fig. 6. 50 - centimeter sensor of linear position, utilized in the mechanisms of the system of conclusion/output of "Nimrod". a) the schematic of sensor; b) the shape of pulses from the outputs of sensor.

Key: (1). Primary 50 V of 3 kHz. (2). Ferrite core. (3). Secondary winding. (4). output. (5). Volts. (6). Position.

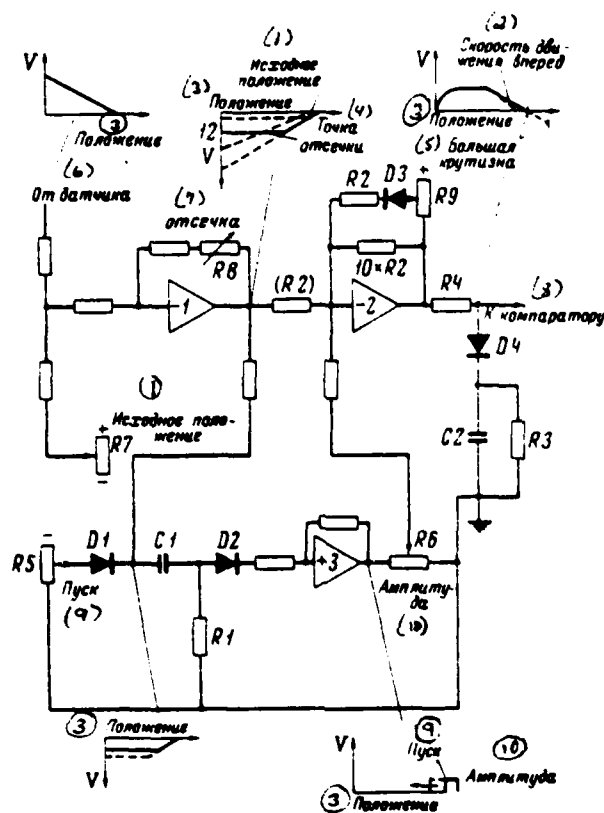


Fig. 7. Schematic diagram of syncro generator.

Key: (1). Initial position. (2). Speed forward movement. (3). Position. (4). Cutoff point. (5). Large slope/transconductance. (6). From sensor. (7). cutoff. (8). To comparator. (9). Launching/starting. (10). Amplitude.

This procedure makes it possible to reduce to to zero probabilities of the aberrations of the memory unit which can be caused by the disturbance/breakdown of optical path by dirt particles or by power losses. In the latter case for the cessation of the plunger before the collision with the mechanical end stops, which can lead to the damage of plunger, are utilized the circuits of blocking.

3.2. Combined analog-digital system.

The schematic of system is shown in Fig. 8. Lattice with the resolution 100μ sends signals to counter A - 4 - discharge binary decimal counter of "Up-down" whose normal count is changed from 2500 to 7500 for the positions of magnet "outside" and "inside" respectively. These values are conveniently utilized, since they permit implementation of scanning the limits of 25 cm in each direction and, furthermore, they correspond to four latter/last to significant digits of the absolute radius, which is determining the position of the deriving/concluding magnet, i.e. to radii from 1225.00 to 1275.00 cm.

The standard value of a radius obtains from computational device B), also, during the working stroke of magnet, which corresponds to position "inside", they compare with radius A, which are determining the position of magnet. Differential count (B-A) is converted into

the analog form with the aid of the polarized digital-analog converter to 12 bits. Then is obtained control signal as this described in section 2.1.4.

In order to exclude the shock about the end stops with a change in the standard radius, position of bogie/carriage (counter D) they continuously compare with a standard radius and the obtained difference utilize for moving of bogies/carriages to position $D=B$. Thus they do not allow/assume so that the end/lead of the working stroke, which corresponds to position "inside", would be nearer to the motionless end stop, than, for example, 0.5 cm. In order to ensure rapid control, admissibly to work in the range from 0.5 to 5.0 cm from the end stop, since this eliminates the need for each time moving bogie/carriage, what is very prolonged procedure.

For simplicity the monitor, which controls this operation/process, is not shown in Fig. 8, with exception of summator C, which provides the constant/invariable position of standard "outside" relative to bogie/carriage, i.e. at the given distance from the end stop "outside".

4. General/common/total principles of operation.

4.1. Use of electronic equipment.

AD-A089 303

FOREIGN TECHNOLOGY DIV WRIGHT-PATTERSON AFB OH
TRANSACTIONS OF THE ALL-UNION CONFERENCE (2ND) ON CHARGED PARTI--ETC(U)
JUL 80 A L MINTS, A A KOMAR, A A VASIL'YEV
FTD-ID(RS)T-0692-80

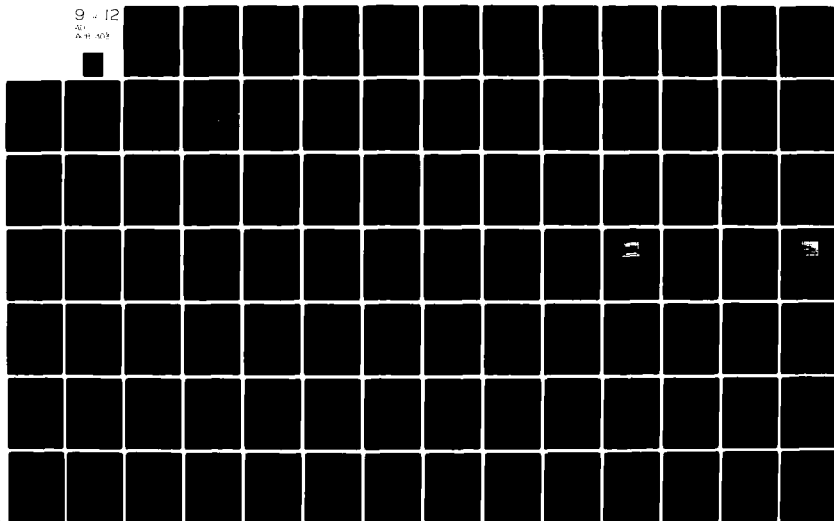
F/G 20/7

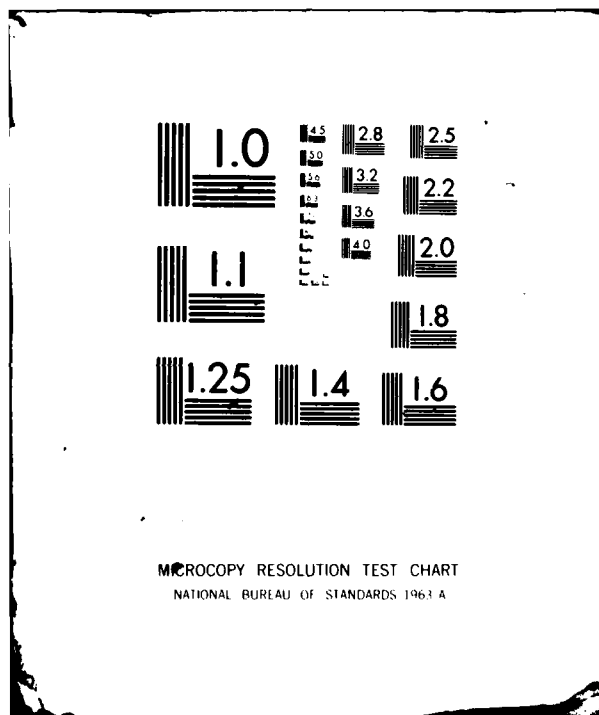
UNCLASSIFIED

NL

9 - 12

AD-A089 303





In the process of work of the accelerator the service personnel can determine malfunctions and accomplish/realize a repair, without resorting to specialists' aid, because of the use of electronic equipment for the indication of malfunctions and indicator lights in the circuits of blocking and logical diagram. In this case is applied the equipment with the safety devices and the auxiliary battery supply, which provides its normal functioning under the emergency conditions.

Are used extensively the interchangeable moduli/modules and the easily changeable mechanical elements/cells, which make it possible to reduce to a minimum accelerator shutdown. At the same time are taken measures for providing of personnel's safety for whom it is necessary to work on the potentially dangerous equipment of such type. Therefore equipment they place in such a way that all possible errors in the determination of malfunctions it would be possible to establish/install, without switching on main engine. If in the exceptional facts it is necessary to reveal the diagram of the checking of position is utilized auxiliary of control, which makes it possible to slowly move plunger from one end/lead to another. For this simply displace zero diagrams the controls.

If appears the danger of the pollution/contamination of the vacuum volume of "nimrod" by cooling water of the deriving/concluding magnet, the work of magnet is blocked by the devices/equipment, which ensure insulation/isolation of the vacuum volume of accelerator upon the appearance of a leak. Furthermore, continuously are checked expenditure/consumption and temperature of water in the deriving/concluding magnets. Special devices/equipment provide the instantaneous disconnection of high-current power supplies with the emergence of emergency conditions [3].

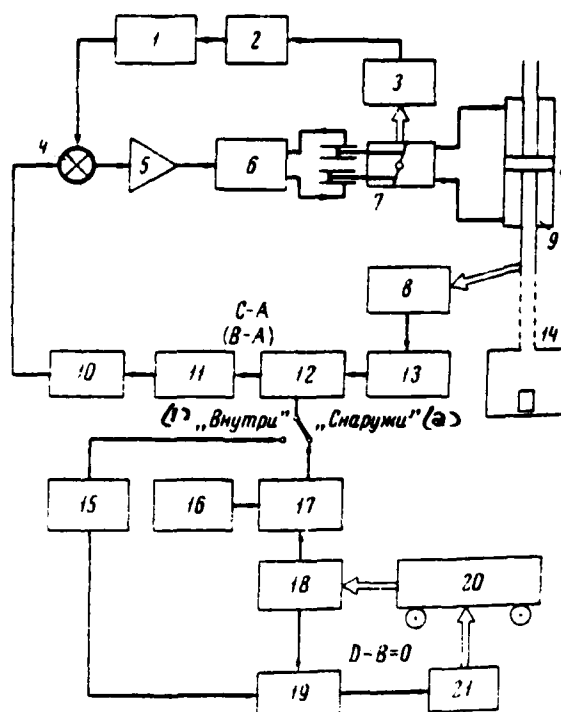


Fig. 8. Schematic of the combined system of control of mechanism. 1 - zero adjustment and phase; 2 - the phase-sensitive rectifier; 3 - sensor of the angle of the slope of disk; 4, 12, 19 - comparator; 5 - dc amplifier; 6 - relay valve; 7 - pump with the slant, which has variable/alternating productivity; 8 - optical lattice; 9 - plunger; 10 - synchro generator; 11 - digital-analog converter; 13 - counter A; 14 - magnet; 15 - setting up of radius B for the position "inside"; 16 - setting up of the length of working stroke; 17 - sumator C; 18 - position of bogie/carriage D; 20 - bogie/carriage; 21 - engine.

Key: (1). "inside". (2). "Outside".

Page 181.

4.2. Monitoring equipment.

Remote control of the work of four mechanisms, utilized on "Wiarod", accomplish/realize by a method of continuous measurement the durations of working stroke, acceleration and end position. Is possible also the visual testing of connections and moving parts with the aid of the television equipment; television camera is moved on the rails above the mechanisms.

4.3. Performing characteristics and reliability.

The precision/accuracy of the setting up of plunger depends on value of the backlash of pump with the slant, friction in the plunger and the zero sensitivity of relay valve. However, characteristic with the large slope/transconductance decreases the effective value of backlash and under working conditions during the prolonged operation were obtained the precisions/accuracies ± 0.5 mm.

In the latter/last 5 years two mechanisms fulfilled as a whole about $40 \cdot 10^6$ the operations/processes. In 1969 were

established/installed two additional mechanisms. At first utilized position detectors with the slipping contacts. Subsequently then they replaced with the described higher contactless pick-ups on alternating current, which since then reliably worked.

Later, when work became more stressed, breakages in the slant appeared as a result of the high required peak accelerations; in order to bring together them to the minimum, it was necessary to restrict the acceleration of plunger by maximum value $5g$ (49 m/s^2). Breakages were virtually completely removed after the setting up of pump with the smaller efforts/forces.

Preliminary information in 1970 until August shows that the systems of conclusion/output, switching on magnets and power supplies, worked with the total effectiveness of better than 950/o for the elongation/extent of 10^7 operations/processes. Two mechanisms, established/installed in 1969, fulfilled $2 \cdot 10^6$ the operating cycles between the capital repairs.

REFERENCES

1. D. A. Gray, M. R. Harold, B. H. C. Morgan, M. H. King, M. J. O. Connel.
"Extraction Techniques at Nimrod". See this coll., Vol. 1, page 000.
2. LIDA 35.12 Incremental Linear System, technical leaflet by Dr. Johannes Heidenhain, Traunreut, FRG.
3. F. S. Gilbert. "High Stability High Current Programmed Power Supplies For Nimrod Extraction Systems". Particle Accelerator Conf. Washington, 1969.

54. Formation of the magnetic cycles of intricate shape in the proton synchrotron ITEP.

I. P. Kleopov, G. I. Kugushev.

(Institute of theoretical and experimental Physics).

Depending on the character conducted on the accelerator ITEP of investigations in practice they are applied the cycles of various forms, beginning from the simplest cycle with the triangular graph/curve of current to the cycle with two areas/sites. The graphs/curves of current, which correspond to these cycles, are represented in Fig. 1a-d.

The practical implementation of these cycles required the solutions of series of problems, connected with the phase control of the valve converter: a) selection and development of the method of phase control; b) the development of the principles of the construction of the system of control and devices/equipment, entering it; c) the development of the schematic diagrams of all devices/equipment of system, their model studyings and experiments.

As a result of the analysis of the in principle possible methods of phase control, taking into account the accumulated experience of the operation of accelerator, was developed the method of the combined phase control. The essence of this method is illustrated by the diagrams Fig. 2 based on the example of the formation of compound cycle with two areas/sites. The impulses/momenta/pulses of phase control are generated by separate for each mode/conditions pulse generators: rectifying series - by generator GI-V; series 1 and P of area - GI-PL1 and GI-PL2; inverter series - GI-1. All pulse generators are 12- phase and controlled (open-closed). In the generator of the rectifying series GI-V are two synchronous 6- phase static phase-displacer, mixer, with the aid of which the impulses/momenta/pulses of rectifying series can be mixed on the phase. Remaining generators GI-PL1 GI-PL2 and GI-1 can be either phase-controlled (if necessary for the correction of the angles of control α_1 , α_2 and β), or not controlled on the phase (in the absence of the need for the correction of the angles of control). Cycle begins with the inclusion/connection of rectifying pulse train SV at the negative angle of regulation $-\alpha_0$ (see Fig. 1a). Through time/temporary interval $\Delta t_{\alpha_1} = 20-40$ ns is switched on the pulse train of the first area/site SPL1 with the angle of control α_1 . The presence of pulse train SPL1 does not interfere with the normal running of rectifying mode/conditions, since the impulses/momenta/pulses of series SPL1 lag on the phase behind the

impulses/momenta/pulses of series SV. Transition into the mode/conditions of the first area/site is conducted at the moment of time $t_{\alpha 1}$ by the displacement of the impulses/momenta/pulses of rectifying series SV in the direction of the positive angle of control $(-\alpha_0 \rightarrow +\alpha_0)$.

Page 182.

For the softening of transition into mode/conditions 1 of area/site the impulses/momenta/pulses of series SV are displaced gradually in time/temporary interval $\Delta t_{\alpha 1} = 10-30$ ms. The law of a change of angle $\alpha_0 = f(t)$ in time interval $\Delta t_{\alpha 1}$ is assigned by the program-time control unit of phase-displacer. In proportion to the displacement of the impulses/momenta/pulses of series SV proceeds gradual phase-by-phase transfer of control of valve converter from the pulse train SV on the series of the first area/site SPL1. Entire angular range of the displacement of the SV pulses does not exceed $100-110^\circ$. The pulses of series SV present over the entire length of the first platform does not interfere with the normal course of the first platform, since in the case, the condition $+\alpha_0 < \alpha_1$ is satisfied. The transition to the second rectifying mode is made at point in time $t_{\theta 2}$ by the shift of the rectifying SV pulse train in the direction of the negative angle of control $(+\alpha_0 \rightarrow -\alpha_0)$ in time interval $\Delta t_{\theta 2} = 10-30$ ms.

After transition into the second rectifying mode/conditions through time/temporary interval $\Delta t_{\alpha 1,2}$ the pulse train SPL1 is replaced by the pulse train of the second area/site SPL2 with the angle of control $\alpha_2 < \alpha_1$. Transition into the mode/conditions of the second area/site (at the moment of time $\Delta t_{\alpha 2}$ is accomplished/realized in time

interval t_{a2}) analogously with transition into the mode/conditions of the first area/site. Through time/temporary interval Δt_{00} after the beginning of the mode/conditions of the second area/site the impulses/moments/pulses of series SV are disconnected, and phase-displacer[shifter] of generator GIV are reset, which corresponds to the negative angle of regulation $(-\alpha_0)$. Transition into the inverter mode/conditions (at the moment of time t_u) it is conducted by the cutoff/disconnection of series SPL2 by the simultaneous inclusion/connection of the pulse train of the inverter mode/conditions of SI with the angle of control $\alpha_u = 180^\circ - \beta$ (β - the lead angle of the ignition of valves/gates in the inverter mode/conditions). Cycle is completed at the moment of time t_n by the cutoff/disconnection of inverter pulse train. Fig. 2b depicts the diagram of a change in the effective angle of control $\alpha_3 = f(t)$, while Fig. 2c gives the graph/curve of the current of valve converter in the cycle with two areas/sites. With the formation of cycles with the simpler graphs/curves of current (Fig. 1a-c) the method remains the same, but drop out these or other functional components of control. The method of control presented possesses the series of the important advantages, the main thing from which is the possibility of obtaining the full/total/complete functional decoupling, i.e. the full/total/complete freedom of any rearrangements of separate devices/equipment and components/links of system, it is independent of each other. Furthermore, this method in the difference, for

example, from the method of the single series of driving pulses [1] makes it possible to sharply lower requirements for the symmetry of phase-shifters providing in this case the very high precision/accuracy of control in the modes/conditions of areas/sites. The described method of phase control is realized by the authors on the proton synchrotron ITEP. The block diagram of the control system is represented in Fig. 3. Control of pulse generators GI-V, GI-PL1, GI-PL2 and GI-1 (commutation of generators and control of stage of pulse) is conducted by the appropriate electronic devices, arranged/located in the unit of control (BU).

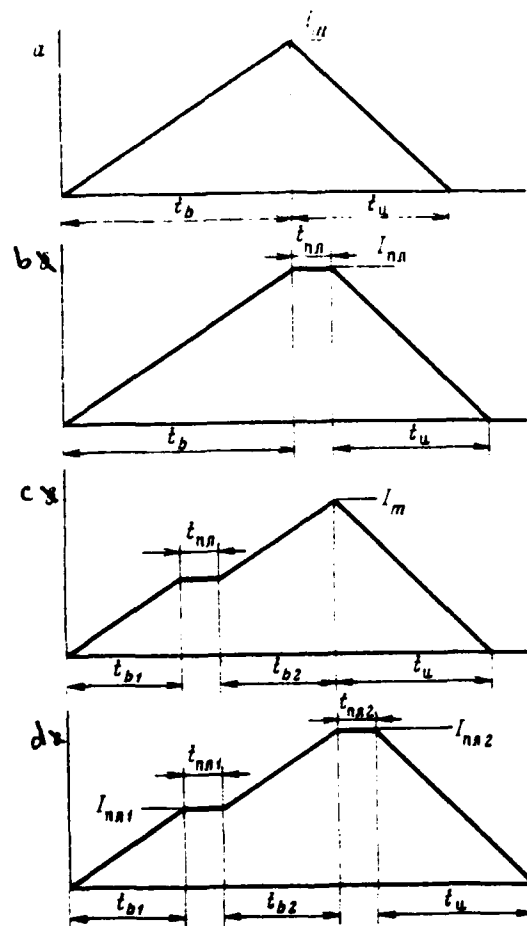


Fig. 1. Graphs/curves of current during the cycles of various forms.

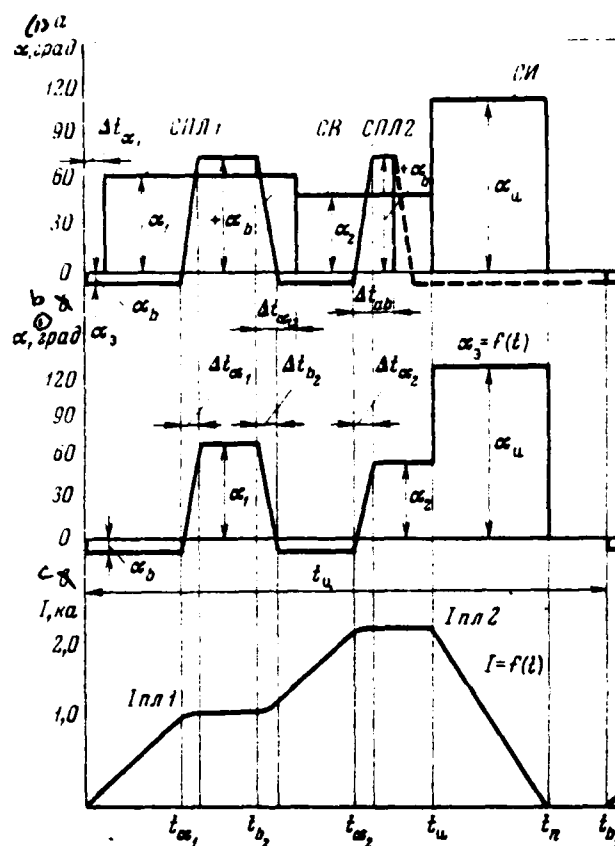


Fig. 2. Diagrams of phase control. a) - the diagram of the commutation of the pulse generators of phase control; b) the effective angle of control; c) the current of valve converter.

Key: (1) . deg.

In the unit of starting impulses/moments/pulses (BSI) are placed the generators of starting pulses of the mode switch and device/equipment of their synchronization. The initial angles of regulating pulse generators are established/installed by the phase shifters, arranged/located in the unit BFI, and the phases of starting impulses/moments/pulses are assigned by the phase shifters of unit BFS. In the unit of relay automation (BRA) are arranged/located the relay devices/equipment of protection, blockings, signaling and logic. The external commands (VK) of sensors and program-time devices/equipment of accelerator are introduced into the unit BSI. In the units of the peak transformers of BIT 1 and BIT 2 impulses/moments/pulses of generators GI-PL1 and GI-PL2 are converted into the narrow peak impulses/moments/pulses. Two hexaphase groups of output pulses BI-1S and BI-2S, shifted relative to each other the angle $\pi/6$, are put out with the devices/equipment of the formation of the igniter impulses/moments/pulses of the valve converter, constructed according to the schematic of two bridges, connected in parallel through equalizing reactors [2]. The control system allows for the possibility of the formation of the basic magnetic cycles of any given in Fig. 1 form during their alternation with the cycle of triangular form for the biomedical targets, which has the relatively small amplitude of current. Fig. 4 depicts the oscillogram, which corresponds to this mode/conditions, during the basic cycle with two areas. The control system is constructed completely on the

semiconductor devices with sufficient supplies according to the coefficients of their loads, that provides the mean time of failure-free operation not less than 3000 hour. Experience of permanent operating confirmed the effectiveness of the selected method of phase control and the high reliability of system. Some characteristics of the system of phase control are given below.

Asymmetry of static phase-shifters with the range 100-110 deg ... is not more than 1-2 deg.

Asymmetry of the impulses/moments/pulses of the generators of areas/sites GI-PL1 and GI-PL2 ... is not more than 0.1 deg.

Asymmetry of the impulses/moments/pulses of the generator of inverter mode/conditions ... is not more than 1-2 deg.

The duration of rectifying modes/conditions $t_{b1} + t_{b2}$... is not more than 1.3 s.

The duration of the mode/conditions of areas/sites t_{n1} and t_{n2} ... is not more than 0.35 s.

The duration of inverter mode/conditions ... is not more than 0.65 s.

Duration of the programmed rotations of impulses/moments/pulses by static phase-shifters $\Delta t_{\alpha 1}, \Delta t_{\beta 2}, \Delta t_{\alpha 2} \dots$ 10-40 ms.

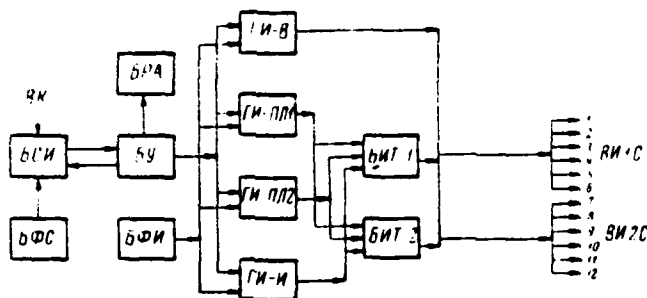
Range of regulating the phase of the driving pulses of the rectifying series ... of 100-110 deg.

Value of the negative angle of regulating in rectifying mode/conditions ($-\alpha_{\beta}$) ... 10-15 deg.

Limits of the angle of regulating in the modes/conditions of the areas/sites ... of 60-85 deg.

Slope/transconductance of the driving pulses ... of 100-200 V/deg.

The initial lead angle of the ignition of valves/gates in inverter mode/conditions (β) ... is not more than 40 deg.

[illegible]

Key: (1). Basic cycle. (2). kV. (3). s. (4). Scales. (5). kA/mm. .
(6). kA/s. mm. (7). kA/s. (8). s/mm. (9). kA. (10). Medical cycle.

REFERENCES

1. A. A. Smirnov, A. V. Doroshenko, D. P. Kalaykov, L. N. Belyayev.
The semiconductor circuit of control of valve converter. PTE, 1970,
No 1.
2. N. A. Monoszon, A. M. Stolov, M. A. Gashev, P. M. Spevakova et al.
Power-supply system of the electromagnet of proton synchrotron on 7
GeV. PTE, 1962 No 4.

Page 184.

55. Measurement of the static and dynamic parameters of materials with the nonrectangular loop of hysteresis.

L. Z. Barabash, P. I. Lebedev, L. N. Plyashkevich.

(Institute of theoretical and experimental physics).

During the design of the resonators of the accelerating stations with the rearrangement of frequency arises the question about the monitoring of the uniformity of the ferrite filler of resonators.

Usually in the resonators are applied large-size ferrite circuits with a volume of into hundreds of cubic centimeters, in their properties which differ from the small ferrite rings. At the values of HF induction in ferrite one hundred and more gauss for measuring the parameters of large-size ferrite cores are required Q - meters by power into several kilowatts.

For measuring the static and dynamic characteristics of large-size ferrites usually are utilized powerful/thick tuned amplifiers, and measurements are accomplished/realized on the

oscillograph, which introduces the element/cell of subjectivity. We proposed the method of measurement both of the static and dynamic parameters of ferrites based on the method of pulse impulsing in the contour/outline, which contains the measured object (ferrite, ferroelectric dielectric etc.) with subsequent processing of the results of measurements by digital computer technology.

The measurement of a number of impulses/moments/pulses (periods) for the calibrated interval of time determines the average/mean value of frequency and, consequently, also μ core in the range from \tilde{B}_{u_N} to $\tilde{B}_{u_N+\tau}$. Reference point can be shifted/sheared in the time for determining the dependence $\mu(\tilde{B})$.

Since quality Q depends substantially on \tilde{B} - high-frequency induction in the ferrite, it is expedient to measure Q as energy loss during one oscillatory period, i.e. to measure the amplitude of two adjacent oscillatory periods. Dying oscillations from the contour/outline are supplied to the amplitude discriminator which is regulated so as to a number of impulses/moments/pulses it would increase per unit, and is measured voltage difference. By a consecutive change in the level of discrimination it is possible to measure dependence $Q(\tilde{B})$. For increasing the accuracy of measurements is summarized the count for several cycles.

Dynamic characteristics are measured analogously. Ferrite will magnetize according to the prescribed/assigned law, and at the moments of time, which correspond to the specific values of current, are measured μ , Q and dependences $\mu(\tilde{B}, t, d\tilde{r}/dt)$ and $Q(\tilde{B}, t, d\tilde{r}/dt)$.

For the resonators of the accelerating stations of the reconstructed proton synchrotron ITEP are selected the ferrite circuits, which consist of 6 bars 150x90x20 mm. Three glued/cemented bars form U-shaped half-chain. The characteristics of each bar (to the cementing) measure in the statics and the dynamics: the characteristics of semiring - only in the statics. For the measurements of static bars is utilized the circuit, which consists of two bars (one standard) and two inserts/bushings 30x20x20 mm; for measuring the dynamic characteristics are utilized two such circuits (3 bars of standard ones) with the magnetizing winding of the type of eight. Value μ is determined from the formula

$$\mu = \frac{1}{4\pi^2 L_0 C p^2} = \frac{l \tau^2 10^8}{1,6 \pi^3 n^2 S C N^2},$$

where l - average/mean length of magnetic line of force in the ferrite; S - section of ferrite core; τ - time of measurement; n - number of turns; C - capacity/capacitance of contour/outline; N - number of impulses/moments/pulses.

During the replacement of one bar (half circuit)

$$\Delta\mu = 2 \frac{\Delta N}{N} \mu.$$

Hence it is apparent that the precision/accuracy of the measurements μ of bar with $N=100$ composes 40/o.

Precision/accuracy measurements Q determine by the equation

$$\Delta Q = Q \frac{Q}{\pi} \left(\frac{\Delta \delta_u}{u_N} - \frac{\delta_u}{u_N} \frac{\Delta u}{u_N} \right) \frac{1}{1 + \frac{\delta_u}{u_N}},$$

where $\delta_u = u_N - u_{N+1}$; $\Delta \delta_u$ - error in measurement δ_u ; Δu - the error in measurement u_N . With $\Delta u = \pm 3 \cdot 10^{-3}$ and $\Delta \delta_u \pm 10\%$ $\Delta Q = 12\%$. The accuracy of measurements can be increased, if measurements are conducted for several periods, for example, to $u = 0,75 - 0,5 u_{ампл}$. However, in this case it is necessary to know dependence $Q(\tilde{B})$ for the measured ferrite.

The given procedure can be used for measuring the static and dynamic characteristics of the ferroelectrics and other materials with the nonrectangular hysteresis loop. Method is convenient both for the detailed laboratory investigations and for the mass measurements in the plant conditions, since it does not require the qualified personnel for check and rejecting the articles.

Page 185.

56. To shaping of field in the electromagnets of the type of "window frame".

V. D. Borisov, L. N. Vaulin, M. I. Doynikov, A. S. Simakov, A. S. Sudarushkin.

(Scientific research institute of the electrophysical equipment in D. V. ~~Y~~ Efremov).

An electromagnet of the type of "window frame" is carried to the class of implicit-pole magnetic systems [1, 2], which are characterized by the very weak dependence of field distribution in operating region of electromagnet on the degree of saturation of iron. The field coils of a comparatively low altitude of rectangular cross section with the small "escape of end connections" allow/assume the use/application of magnetic screens [3] for localization and linearization of the fields of scattering. Certain increase of the power in such electromagnets in comparison with the salient pole ones is completely redeemed by the noted earlier advantages, and also by the large effectiveness of the use of a region of field because of the high degree of its uniformity virtually in the entire zone

between the coils. The construction/design of electromagnet is characterized by simplicity and absence near operating region of the intensely saturated sections of the magnetic circuits which could lead to the inadmissibly large field distortions. The latter are detected only with inductions B , close to the saturation induction of iron; however they to a considerable extent can be corrected, and the interval of the variation in the induction is expanded with the aid of the special openings/apertures in magnetic circuit [1, 4], located near the clearance of electromagnet on the edges of its operating region.

The optimization of the parameters of intra-jugular openings/apertures (their sizes/dimensions and position) is conducted, as a rule, it is experimental as a result of very labor-consuming searches on the models. In spite of the intense development of the methods of mathematical simulation, publication according to the studying calculation procedures in connection with the case in question are absent.

In the present report are discussed the questions, connected with the determination with the calculated method of the parameters of the corrective openings/apertures. A definite interest also can present proposition on the supplementary correction of field and regulating of the optical parameters of electromagnet with the aid of

the turns with the current, placed in the intra-jugular openings/apertures.

Basic difficulty during the use/application of numerical methods to the electromagnets of the type "window frame" with the corrective openings/apertures of the magnetic circuit consists of the need for the account of local and simultaneously small effects with the sufficiently high precision/accuracy. If in this case operating speed and working storage of computers are small, and the use of auxiliary storage on any reasons is inexpedient, it is necessary to search for supplementary systematic possibilities for accelerating of count and obtaining of the required precision/accuracy. In this case such possibilities consisted of the combination of through and separate grids, and also in the use/application of a multistage grid.

For obtaining the zero distribution of vector potential A was utilized through grid with the single algorithm in all its nodes/units. Algorithm was obtained under the assumption of the piecewise constant distribution of magnetic permeability ($\mu = \text{const}$ in the limits of each mesh [5]), and the ineterational process was accomplished/realized according to the method of over-relaxation [6]. A full/total/complete quantity of nodes/units was limitedly on top, and the sizes/dimensions of iron considerably exceeded the sizes/dimensions of air region; therefore the step/pitch of through

grid was compared with the latter, so that the finite-difference approximation of differential equations in air gap proved to be very approximate.

Since the effect interesting is small and connected with the saturation of iron, asserts itself the representation of full/total/complete field in the form of the sum, which consists of ground field ($\mu=$) and small addition. This target answer the successive approximations, which consist of the successive solution of Dirichlet problems that relatively modified of scalar and vektor potentials respectively in the "window" of magnet (linear task) and in the magnetic circuit (nonlinear task) with the mating of the solutions along the contour/outline of "window" by means of the assignment of boundary conditions upon transfer to the nonlinear task from the distribution of the normal component of induction B_n and upon transfer to the linear task - from the distribution of the tangential component of the intensity/strength of field H_τ [7, 8]. In this case the effects of the saturation of iron project/emerge in an explicit form, namely under the boundary condition of linear task (when $\mu=$ $H_\tau=0$), and are eliminated the existed previously inaccuracies, caused by approximate solution of Neumann's task.

Near the corrective openings/apertures in view of the local character of field distortions it is necessary to have a grid with the sufficiently low pitch. One should also note that in each region the following after each other approximations/approaches differ virtually little; therefore basic time will be spent on the calculation of first approximation, if we each time memorize the obtained array of the unknown function in order to only refine it taking into account the changed boundary conditions during the determination of the following approximation/approach. Mating of the boundary-value problems conveniently carrying out with multiple steps/pitches of grid in both regions.

On the basis of these considerations transition to the successive approximations preceded two-fold reduction of the step/pitch of grid with the simultaneous decrease of the global region. On its new boundary was assigned obtained earlier on the through grid with the step/pitch $h=0.5$ cm distribution λ , which subsequently remained constant/invariable. Fig. 1 depicts the section of magnet; dotted line isolated the region, in which were conducted successive approximations. The multiplicity of the step/pitch of separate grid is equal to unit.

On the computers "Minsk-2" is made the large series of calculations for different sizes/dimensions, positions and number of

corrective openings/apertures. The series/row of results is represented in Fig. 2 and 3. In the case of "large" opening/aperture the field proves to be virtually uniform ($<0.10/o$) all over width of operating region up to inductions $B_0 = 21,6$ kg. Apparently, analogous field can be obtained also with smaller openings, but arranged/located it is nearer to the clearance (see [4]). For calculating this version it is necessary to additionally reduce the step/pitch of grid, that virtually it is possible to carry out only on the computers of higher class.

In the calculations was utilized the dependence $\mu(B)$ for steel 3 [9]; the duty factor of magnetic circuit took as the equal to 0.97. According to Fig. 3, the calculated and experimental data are in satisfactory qualitative and quantitative agreement.

If the effect of openings/apertures proves to be insufficient or, on the contrary, too great, supplementary correction can be conducted with the aid of the turns with the current, arranged/located both on the poles and within the openings/apertures. In the first case will be required smaller current, but for placement of turns it is necessary to provide the place in operating region, which will lead to an increase in its height with all ensuing/escaping/flowing out consequences.

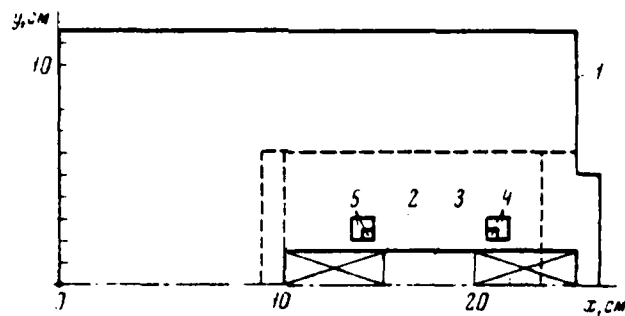


Fig. 1. The cross section of electromagnet. 1 - magnetic circuit; 2 - coil; 3 - operating region; 4 - corrective opening/aperture; 5 - supplementary turn with the current.

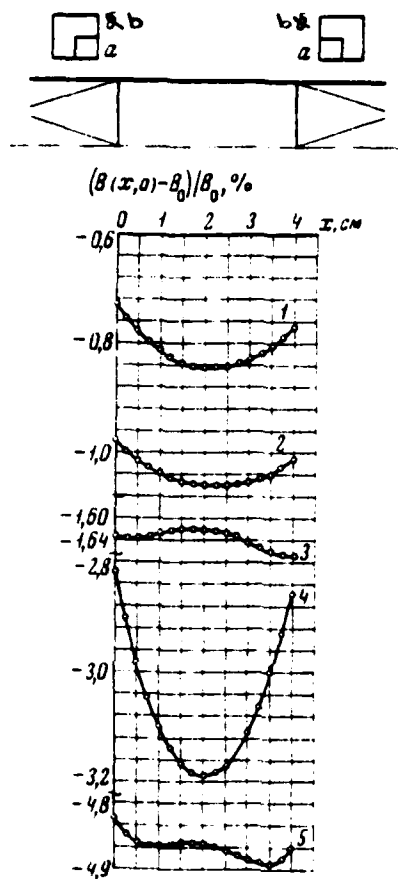


Fig. 2. Field distribution in the median plane for two types of the corrective openings/apertures. 1 - without the openings/apertures; 2 - with the openings/apertures and; 3 - with openings/apertures b (for curves 1-3 $B_0 = 18.40 \text{ kg}$); 4 - without the openings/apertures; 5 - with openings/apertures b (for curves 4-5 $B_0 = 22.5 \text{ kg}$) x - calculation data without taking into account duty factor.

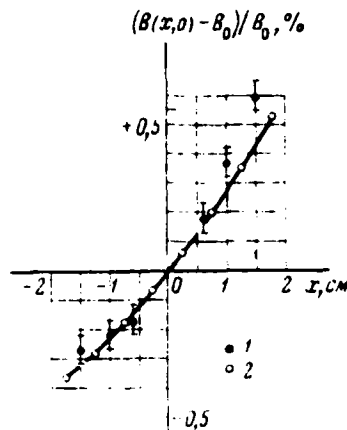
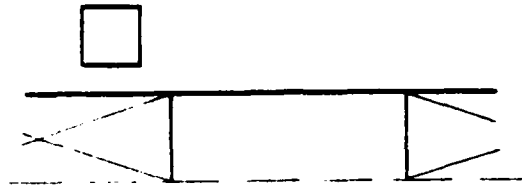


Fig. 3. Field distribution in the median plane. 1 - experimental data; 2 - calculation data on the through grid with consideration the duty factor ($B_0 = 18$ kg).

Page 187.

Intra-jugular turns with the current are less effective; however structurally/constructurally this version is simpler. On the possibilities admitted through the openings/apertures in the magnetic circuit turns it is possible to judge by Fig. 4, in which are represented some results of calculation. If necessary these turns

make it possible directly on the effect to produce the compensation for the defects of production, and also the correction of the integral characteristics of magnet. Loading supplementary turns is not connected with any complications of computational program; the duration of count actually remains the same.

In conclusion the authors express gratitude to the colleague of IPVE K. P. Myznikov for the great organizational assistance while conducting of calculations on the computers.

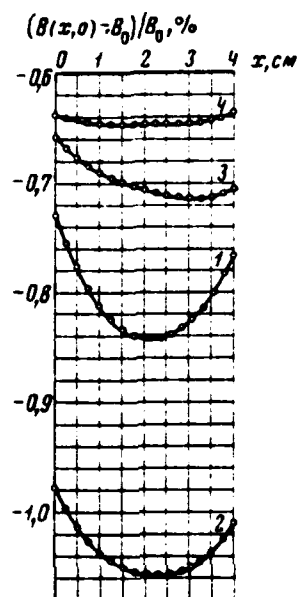


Fig. 4. Field distribution in the median plane depending on the current strengths in the corrective openings/apertures: 1 - without the openings/apertures and the currents; 2 - with the openings/apertures, $j_1=j_2=0$; 3 - with the openings/apertures, $j_1=j_2=0.12j$; 4 - with the openings/apertures, $j_1=0.18j$ $j_2=0.75j$; j - current density; $B_0 = 18.48$ kg; X - calculation data without taking into account duty factor.

REFERENCES

1. Status of the Argonne 12.5 GeV Zero Gradient Synchrotron. Particle Accelerator Div. Staff. International/inter conf on the accelerators, Dubna, 1963. M., Atomizdat, 1964, page 187.
2. R.R. Wilson. Proc. Sixth Internat. Conf. on High Energy Accelerators. Cambridge, 1967, p.210.
3. K.G. Steffen. Internat. Conf. on High Energy Accelerators, Brookhaven, 1961, p.347.
4. K.Holm a, K. G. Steffen. Proc. Internat. Sympos. Magnet Technol. Stanford, 1965, p.146.
5. P. Coneus, Proc. Internat. Sympos. Magnet. Technol. Stanford, 1965, p. 164.
6. N. I. Doynikov, A. S. Sinakov. ZhTF, 1969, 39. page 1463.
7. J.H. Dorst. Proc. Internat. Sympos. Magnet Technol. Stanford, 1965, p.182.
8. N. I. Doynikov, A. S. Sinakov. the transactions of All-Union conference on charged particle accelerators. Vol. 1. VINITI, 1970, page 319.
9. N. I. Doynikov, S. N. Konarova, A. S. Sinakov. Preprint the J.I.N.R., R13-4134, Dubna, 1968.

57. Nuclear stabilizer of magnetic field with the discrete/digital stabilization system and control of frequency of autodyne detector NMR.

Yu. N. Denisov, P. T. Shishlyannikov.

(Joint Institute for Nuclear Research).

The nuclear stabilizers of stationary magnetic fields provide under laboratory conditions the maximum stability of the magnetic field of electromagnets and, in spite of the relative complexity of equipment, is found an increasing use in the technology of accelerators, magnetic analyzers and so forth [1, 2].

In the laboratory of the nuclear problems of Joint Institute for Nuclear Research are developed several types of the nuclear stabilizers of magnetic field, which are characterized by in essence the method of stabilization of the frequency of transverse exciting high-frequency magnetic field [3, 4].

In the proposed report is examined the nuclear stabilizer of magnetic field with the specialized system of setting up and

frequency fixing, designed for the work with the autodyne detector NMR, in which the rearrangement of frequency is accomplished/realized by varicaps [5]. The absence of the power drive usually utilized in the sensor NMR of air capacitors substantially expands operational possibility of stabilizer, since sensor can be arranged/located, also, in the almost inaccessible places of the clearance of electromagnet.

Page 188.

The block diagram of the nuclear stabilizer of magnetic field is shown in Fig. 1, the system block diagram of setting up and frequency fixing of autodyne detector NMR of stabilizer is given in Fig. 2.

The principle of the operation of the diagram of installation and frequency fixing is based on the periodic comparison with standard time interval T_0 of time T_n , necessary for the filling of the register of calculating decades/ten-day periods S_4 0-10* with adjusted by volume with A impulses/momenta/pulses, which follow with adjustable frequency f_n . Equality these times is established/installed and is supported by the effect through the feedback loops on the parameters of the oscillatory circuit of autodyne detector NMR. The volume of the register of calculating decades/ten-day periods changes by means of the preliminary discharge/break of decades/ten-day

periods not into the zero state, but to number $A' = 10^6 - A$. If we select

$$T_0 = 93950 \text{ } ^{(1)} \text{ мксек,} \quad (1)$$

Key: (1). μs .

then when a preliminary frequency division is present, f_x 40 times (decade/ten-day period to 100 MHz and two-digit binary dividers on 10 MHz)

$$A = 2348,75 \text{ } ^{(1)} \text{ (МГц),} \quad (2)$$

Key: (1). MHz.

On the other hand,

$$B(\text{mG}) = 2348,75 \cdot 10^{-5} \cdot f_x, \quad (3)$$

i.e. value A will track the magnetic field in the adzes.

The counter of reference frequency with a maximum volume of 10^3 and with the feedback to 6470 impulses/moments/pulses starts triggers T1-T6 in such sequence, that in the presence of reference oscillator on 1 MHz the channels of the final adjustment of error are blocked only with the observance of the relationship/ratio

$$T_x = 93950 \text{ } ^{(1)} \text{ мксек,} \quad (4)$$

Key: (1). μs .

moreover the channel of the rough final adjustment of error is sensitive to the detuning the channel of a precise final

$$\left| \frac{\Delta f_x}{f_x} \right| > 4 \times 10^{-3},$$

adjustment - to detuning $\left| \frac{\Delta f_x}{f_x} \right| > 2 \times 10^{-4}$ and the channel of the fine adjustment of frequency - to $\left| \frac{\Delta f_x}{f_x} \right| > 1 \times 10^{-5}$. The channels of the final adjustment of error are made on the identical diagram the logic of work of which is illustrated by time/temporary diagram for its basic elements/cells in Fig. 3.

Reference point T_x is assigned by the translation/conversion of trigger into the working order which corresponds to the opening of the valve/gate V1, gating pulses with frequency $10^{-1} \times f_x$ on counter with the adjustable volume. The end/lead of reading T_x is fixed/recorded with filling of this counter. Trigger T5 will twice change its state through 93930 and 93970 μs relative to the moment/torque of the beginning of filling of counter with the adjustable volume, i.e. trigger T5 will shape the pair of the impulses/moments/pulses, arranged/located on both sides from $T_0 = 93950 \mu s$ on the "temporary/time distance" 20 μs .

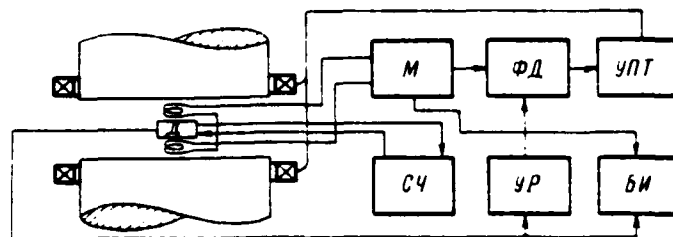


Fig. 1. Block diagram of the nuclear stabilizer of magnetic field. M - modulator; PD - the phase discriminator; SCh - frequency regulator; UR - tuned amplifier; BI - display unit; UPT - dc amplifier.

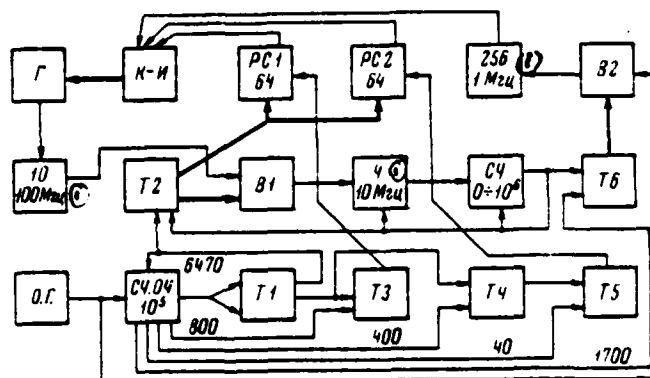


Fig. 2. System block diagram of setting up and frequency fixing (frequency regulator). OG - reference quartz oscillator on 1 MHz; S.Ch.O.Ch. - counter of reference frequency; T - static trigger; V - valve/gate; SCh - counter with an adjustable volume of; RS - bidirectional counter; G - external generator; 10 (100 MHz), 4 (10 MHz), 256 (1 MHz) - counters of 10, 4 and 256 with the indication of maximum operating speed; k-I - converter code-voltage.

Key: (1) . MHz.

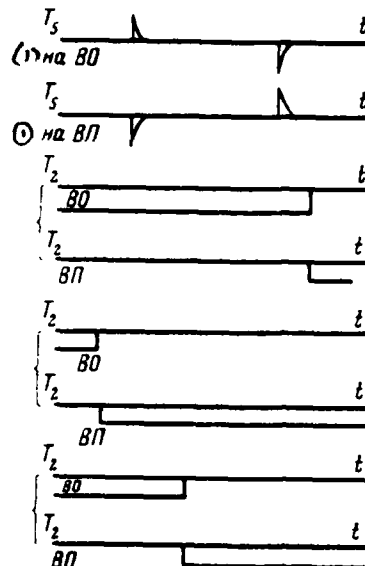


Fig. 3. Constitution diagram of the elements/cells of bidirectional counter with different relationships/ratios of the current and prescribed/assigned values of frequency. VP - direct count gate; VO - valve gate of reverse count.

Key: (1) . on.

Page 189.

These impulses/moments/pulses enter the entrance of the reversible sixfold charged binary counter PS2, the mode/conditions of work of which is assigned by the state of the trigger T2, which forms interval T_2 (Fig. 4). From the time/temporary diagram Fig. 3 follows

that with $T_x < 93\,930\ \mu\text{s}$ in the counter RS2 the code of a number it decreases, with $T_x > 93\,970\ \mu\text{s}$ - it increases also with $93\,930\ \mu\text{s}$ $< T_x < 93\,970\ \mu\text{s}$ both impulses/momenta/pulses T5 are blocked by the valves/gates of straight/direct (VP) and reverse (VO) count, i.e. the code of a number in RS2 does not change. Thus, counter S2 is sensitive to a relative change in the time on

$$\left| \frac{\Delta T_x}{T_x} \right|_{93\,950} \approx 2 \cdot 10^{-4}.$$

Channel S1 is sensitive to $\left| \frac{\Delta T_x}{T_x} \right| > 4 \cdot 10^{-3}$, since RS1 it is started pulses (T3), by those by symmetrically arranged/located relative to end/lead T_x at a distance of $400\ \mu\text{s}$.

Registers RS1 and RS2 control digital relay rheostat-converters "code-voltage", connected in series. The use/application of this schematic of converter is caused by the fact that function $f_x(u_y)$ substantially nonlinear (Fig. 5), and for the linearization of function $f_x(n)$, where n - code of a number of bidirectional counter, dependence $u_y(n)$ must be quadratic.

The fine adjustment of frequency is accomplished/realized with the aid of the counter to 256 [6], which controls the digital potentiometer, voltage from which is supplied to the separate varicap, connected through small amount of capacitance (10 pF) to the contour/outline of autodyne detector.

The range of the stabilized frequencies for the system examined is 1-100 MHz, which provides the work of the stabilizer of magnetic field from the lower limit of the work of sensor NMR (50 MTL) to 2.35 T. The "step/pitch" of the rearrangement of magnetic field is equal to 10 μ T.

Regulating unit (UPT) of nuclear stabilizer provides the maximum current 3A of both signs in the corrective windings with the impedance to 10 ohms.

Stabilization factor in the magnetic field is equal to ~ 100 . The lasting precision/accuracy of the stabilization of field comprises $\pm 2 \cdot 10^{-3}$. Transit time at any other value of magnetic field within one sub-range ($\frac{B_{\max}}{B_{\min}} \approx 1,4$) is not more than 2 min. Because of the absence of air capacitor with the power drive the interferences, connected with the microphonics, virtually are absent.

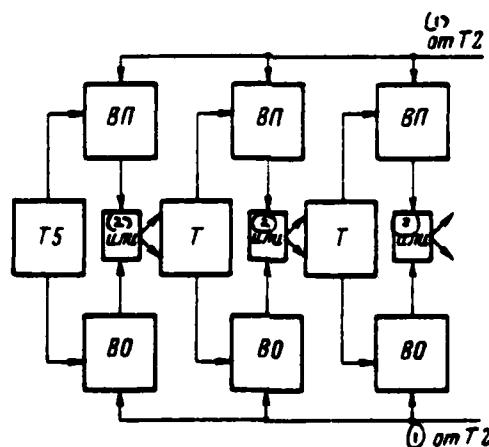


Fig. 4. Block diagram of reversible counter.
Key: (1). from. (2). or.

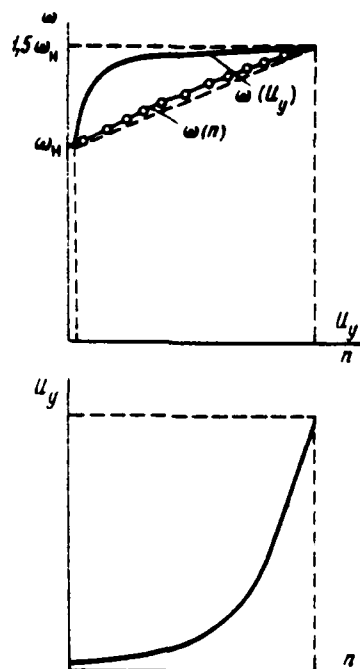


Fig. 5. Required dependence $U_y(n)$ for the linearization of dependence $\omega(n)$.

REFERENCES

1. A. Lashe. Nuclear induction. IL, 1963.
2. G. P. Melnikov, V. I. Shergbatykh. Transactions of fifth scientific and technical conference on nuclear radio electronics. T. 1. GOSATOMIZDAT, 1962, page 207.

3. L. V. Vasil'yev, Yu. N. Denises. Preprint the J.I.N.R., No 1463, Dubna, 1963.

4. L. V. Vasil'yev, Yu. N. Denises, S. A. Iwaszkiewicz et al. Preprint J.I.N.R., No 2459, Dubna, 1965.

5. Yu. N. Denises, S. A. Iwaszkiewicz. Preprint the J.I.N.R., No 13-3218, Dubna, 1967.

6. Yu. N. Denises, A. G. Komissarov, V. I. Prilipko. PTE, 3, 107, 1966.

Page 190.

58. Semiconductor circuit of control of the valve converter of Dubna proton synchrotron.

L. N. Belyayev, A. Z. Leshchenko, D. P. Kalmykov, A. A. Smirnov.

(Joint Institute for Nuclear Research).

The increased requirements from the side of physical experiment, expressed in the increase precisisions/accuracies of cutoff and maintenance of magnetic intensity in limits of $\pm 0.05-0.10\%$ during 400-500 ms at the level 8-12.8 kOe, the creation of mode/conditions with two areas/sites in the field current of the electromagnet of accelerator and the need of guaranteeing the conditions for the normal work of the equalizing reactors of converter in the complicated modes/conditions of the work of power-supply system led to the development in 1967-1968 the qualitatively new schematic of the control of the valve converter of Dubna synchrophasotron on 10 GeV.

Fig. 1 gives the functional diagram of this device/equipment. In this device/equipment and in the diagrams of development of NIIEPA (Leningrad), is used the vertical principle of control. However, in contrast to the known diagram the block of rectifying impulses/moments/pulses and the block of impulses/moments/pulses for the control of converter in the mode/conditions "current platform" is replaced by the 12-channel phase-shifting device/equipment PS. Developed by this device/equipment impulses/moments/pulses depending on the value of the control voltage, put out by device/equipment UPR2 (along line 1) change phase in the range $\alpha=0.160$ deg. el.

The work of converter VP in the rectifying mode/conditions with different angles of regulating, the translation/conversion of converter from the rectifying mode/conditions into the mode/conditions of "arcs/sites current" and vice versa, and into the inverter mode/conditions are also accomplished/realized by impulses/moments/pulses of the phase shifter on the smallest level of displacement on the thyristors of the schematic of the ignition of the valves/gates of converter SP. This displacement is determined by the device/equipment UPR1, which is given the time parameters of the operating cycle of power-supply system.

The programming of the form of the field current and respectively magnetic field in the clearance of the electromagnet of

accelerator EM in the process of particle acceleration is accomplished/realized with the aid of the device/equipment UFR2.

This device/equipment upon transfer of converter from one mode/conditions to another changes the exit voltage of comparison for the diagrams of the phase converter abruptly, but smoothly during 20-30 ms, in this case the cessation of current by the valves/gates of converter at this time does not cease.

In the process of the translation/conversion of the converter of power-supply system into the inverter operating mode the phase of output pulse by phase shifter PS changes to such moment/torque, what control pulses, developed by the block of inverter peak transformers BIPT, begin first to ignite the thyristors of the diagram of ignition - SP. After this on the command of device/equipment UFR2, put out along line 2, the device/equipment UFR1 changes bias voltage in the schematic of the ignition of the valves/gates of converter SP up to such value, that the thyristors of this diagram can subsequently be ignited only by the impulses/pulses of the block of inverter peak transformers BIPT.

In the dwelling periods when converter with the aid of the device/equipment UFR1 is blocked, device UFR2 is transferred into the initial state with the aid of the sensor of current zeros DNT (along line 3).

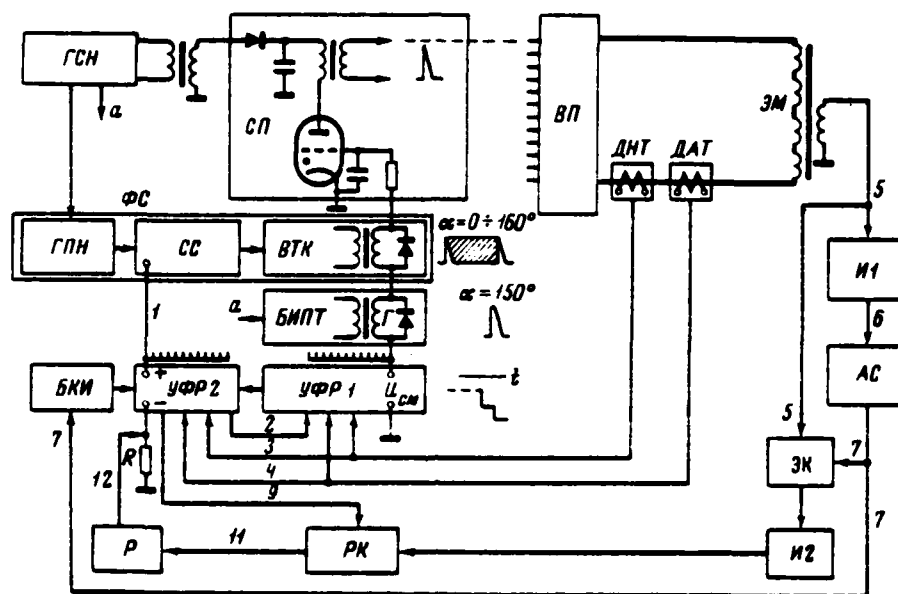


Fig. 1. Functional diagram of peak-generator of Dubna proton synchrotron with a steady change in the phase of driving pulses.

Page 191.

The developed by it voltage of comparison corresponds in this mode/conditions to such value, that the phase of output pulses of phase shifter PS corresponds to the unguided rectifying mode/conditions of the work of the converter of power-supply system VP.

In the case of the emergence of emergency nodes the

devices/equipment of the protection of converter, acting on device/equipment UFR1, transfer/translate converter into the inverter mode/conditions without the steady transition or cut off it (depending on the character of emergency process).

For the translation/conversion of converter into the mode/conditions of the "area/site of current" was used the integral sensor of the level of the magnetic field of RF equipment for the accelerating system of accelerator, which consists of integrator I1 and amplitude selector AS. The output pulse, which appears at the specific level of magnetic field (precision/accuracy $\pm 0.10/c$), enters the block of command impulses - BK1, where it is amplified and, acting on UFR2 (along line 7), is transferred/translated converter with the mode/conditions of the "area/site of current". Simultaneously this impulse/momentum/pulse switches on electronic gate EK of integrator I2.

By the reciprocal pulse of voltage (along line 9) on the period of the duration of the mode/conditions of the "area/site of current" is switched on the relay key/wrench RK, with the aid of which exit voltage from integrator I2 (along line 10) is connected to the entrance of the level regulator of field R. The exit voltage of regulator is supplied (along line 12) to resistance B and respectively into the comparison circuit of the phase shifter of

peak-generator, forming the closed into the ring control system.

Fig. 2 gives the oscillograms of magnetic intensity in magnet gap of accelerator N (lower oscillogram) and its derived \dot{N} (upper oscillogram) during the work of the converter of power-supply system in the mode/conditions of the "area/site of current" at the level 12.8 kOe together with the schematic of regulator.

The divergence of magnetic intensity from the prescribed/assigned level does not exceed ± 1 Gs. All devices/equipment of peak-generator are carried out on the semiconductor devices. The most critical node/unit of peak generator is the phase shifter - PS which encompasses sawtooth generator GPH, diode-regenerative comparison circuit SS and exit forming cascade/stage on the thyristor VTK (see Fig. 1).

The schematic of device/equipment and the linear diagram of voltages in the diagram, which elucidate its work, are given on Fig. 3.

In the oscillator circuit of saw-tooth voltage is utilized the initial section of the exponential increase of the voltage of capacitor C1, connected through resistor R₂ to the source of voltage U_{CT} . Diode commutator (diodes D1 and D2) synchronizes the beginning

DCC = 80069215

PAGE 807

of charge of capacitor with the voltage of the generator of the supply of its own targets of converter GSN (see Fig. 1). The saw-tooth voltage through diode D3 is supplied into diode-regenerative comparison circuit SS.

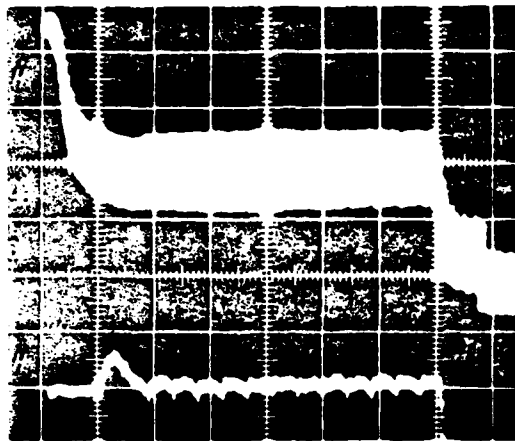


Fig. 2. Oscillograms of magnetic intensity N (lower) and its derivative \dot{N} (upper) into magnet gap of accelerator. Scales: time - 1 cm = 50 ns; N - 1 cm = 2 Oe; \dot{N} - 1 cm = 1.5 kOe/s.

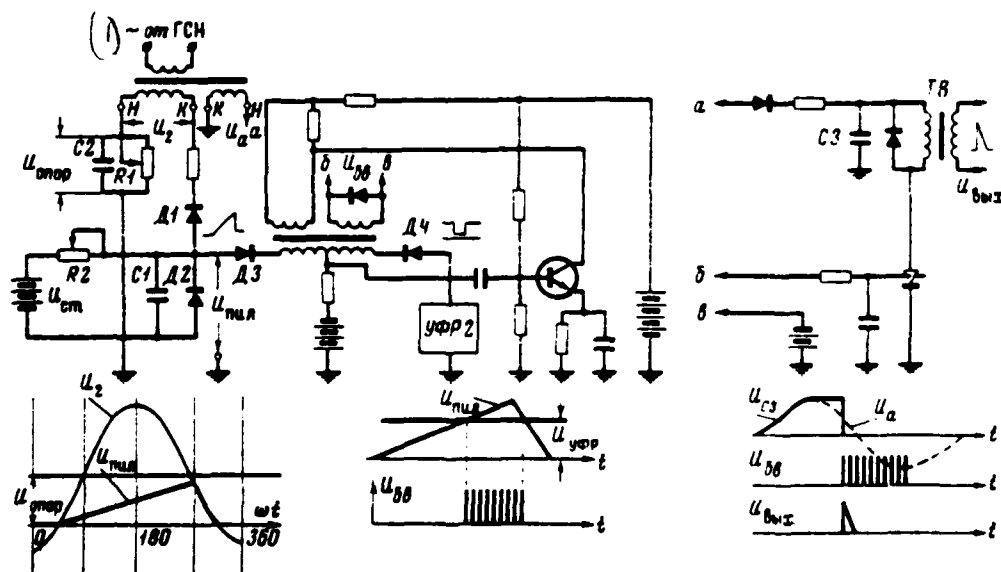


Fig. 3. Electrical circuit of phase shifter.

Key: (1). from.

Page 192.

As soon as this voltage it will achieve the value of the voltage, put cut by the device/equipment of phase regulating UPR2, diode D4 is cut off, and diagram begins to work as usual blocking oscillator, starting by the first impulse/momentum/pulse the thyristor of exit shaper. Capacitor C3, being discharged through the winding of output transformer of TV and the thyristor, induces in secondary winding impulse/momentum/pulse (one during the period). By this impulse/momentum/pulse the control circuit of the ignition of the valve/gate of converter.

Repeated tests in the static behavior showed that the appearing in 6-8 hours of continuous operation mutual changes in the phases of driving pulses do not exceed ± 0.1 el. deg in entire range of the angles of regulating from 0 to 160 el. deg with a change in the temperature of surrounding air from 15 to 40°C.

Device/equipment UPR2 consists of three-position trigger on the thyristors and reference-voltage source¹.

FOOTNOTE ¹. A. A. Smirnov, A. Z. Deroshenko, D. P. Kalmykov, L. N.

Belyayev. Semiconductor system of control of valve converter. PTE, 1, January-February of 1970, pages 165-167. ENDFCOINCTE.

Conclusion.

The use/application of peak-generator examined in the schematic of the control of the converter of Dubna synchrotron ensured with the latter new possibilities.

1. Are realized complicated modes/conditions of work of power-supply system with one and two areas/sites in field current of electromagnet of accelerator as, for example, mode/conditions, characterized by oscillograms of rectified voltage (upper oscillogram) and current of converter (lower oscillogram) on Fig. 4.

2. Appears possibility of considerable decrease of power of interbridge equalizing reactors.

3. Is conducted dynamic discharging of shafts of dynamoelectric power supply units of converter.

4. Appears possibility of stabilization of rectified voltage of converter for realization of prolonged braces of emitted beam of nonenergetic particles.

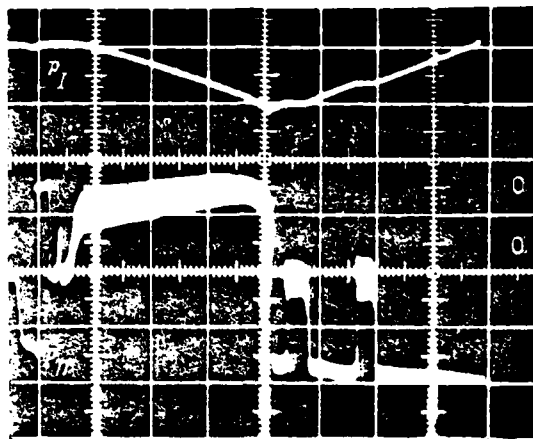


Fig. 4. Oscillograms of rectified voltage u_d (upper) and the current of the load of converter I_d (lower) in the complex operating mode.

The scales: time - 1 ss=1 s; u_d - 1 cm = 5 kV; I_d - 1 cm = 10 kA.

59. Calculation of the three-dimensional fields of iron free magnets.

L. R. Zakharov, R. A. Meshcherov, Ye. S. Mironov.

(Radio engineering institute of the AS USSR).

During development and design of accelerators to superhigh energy very promising is the use of superconducting iron free magnets [1, 2]. Precomputation and selection of the initial parameters of such magnets is conducted usually employing the simplified procedure. Calculation is based on assumptions of the fact that in the limits of separate magnet block the field does not depend on longitudinal coordinate [3-5]. In the accelerators to high energies are utilized rectangular magnet blocks by length into several meters. The at the same time cross section of accelerator chamber and, therefore, the transverse sizes/dimensions of operating region of magnet do not exceed 10-15 m. Therefore in the larger part of magnet block the character of the distribution of the field in the first approximation, of the same and in the rectilinear magnet of infinite extent.

During the detailed calculations of the motion of the

charged/loaded particles in the fields of real magnets it is not possible to be limited to the simplified procedure, it is necessary to calculate the distribution of magnetic field on the basis of the entire length of magnet block, and also cut of the block.

In the radio engineering institute of the AS USSR are developed/processed the iron free superconducting coil electromagnets with the pulse field. At the initial stage is provided for the production and the investigation of the model of dipole type superconducting block.

The winding of magnet is formed/shaped from a large number of turns, which have characteristic "saddle-shaped" form.

Page 193.

A number of turns is determined by the assigned magnitude of field and by the permissible current density. Winding is divided into the series/row of layers. The schematic image of one layer of winding is given in Fig. 1. For the illustration is given only one fourth layer, the arranged/located on the surface circular cylinder of radius R . From the figure it is evident that in each turn it is possible to isolate three characteristic sections: rectilinear (I), to circular (II) and transient (III). The rectilinear parts of the turns of each

layer are placed on the generatrices of cylinders with the density, which is changed according to the law $\sim \cos \alpha$, which approximately corresponds to a change in the current density according to the law of $j \sim \cos \alpha$, necessary for the creation of uniform field. The location of circular and transition sections on the edges of winding was selected in essence according to the design considerations.

To obtain the solution of the problem about field distribution in this magnet is analytically impossible; therefore was developed the program of the calculation of magnetic field with the aid of the digital computers.

During the use of most universal algorithms [6] all current conductors of winding are broken down into segment elements of the previously selected length. Field at the particular point of observation is determined by the method of the addition of the fields of segment elements in accordance with Biot-Savart's law. For achievement of high precision/accuracy of calculation it is necessary to select the segment elements of a comparatively small length, which leads to a considerable increase in the "machine" time. Nevertheless during the calculation of field at observation points, distant behind the segment elements at the distances, compared with their length, appears inadmissibly large error. In this case for shortening of the count time the straight portions of turns were not divided/marked off

in the segment elements, and the components of field from these sections were determined by the method of calculation according to the formulas for the rectilinear conductors of finite length. Curvilinear sections (II and III in Fig. 1) were divided/marked off in the segment elements, moreover in the program was provided for the possibility of decreasing the lengths of segment elements during the determination of field at observation points, which are located in immediate proximity of the current conductor in question. Thus at all points of the field was maintained/withstood the requirement of the smallness of the length of segment element in comparison with the distance of observation point.

With the aid of the comprised program is calculated field of one of the versions of a dipole type magnet block. Fig. 2 gives the graph/curve, which illustrates the degree of a difference in the field from the uniform with $x=0$, $z=0$. From the graph/curve it follows that on the larger part of the aperture of magnet block field close to the uniform. Residual/remnant heterogeneity is explained mainly by the fact that in some layers the latter/last turn with $z \rightarrow R$ was withdrawn, since the radius of bending of its transient part proved to be less than 1 cm. (Superconducting cable it can be damaged, if we it bend on the radius less than 1 cm). This heterogeneity can be removed by the introduction of correction into the law of the distribution of conductors. Sharp decrease H_z in immediate proximity of the winding is explained by the effect of the discreteness of winding.

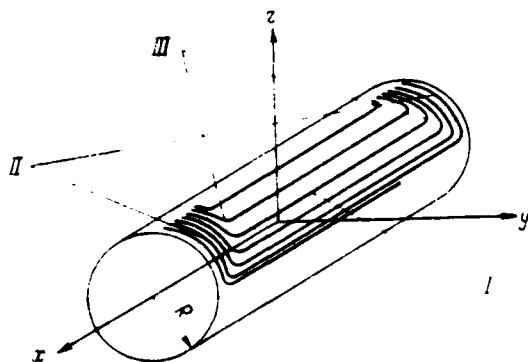


Fig. 1.

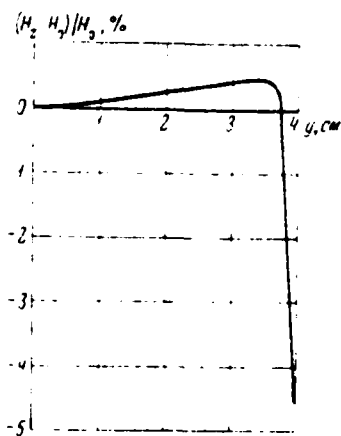


Fig. 2.

Fig. 1. Location of turns in one layer of winding of magnet block (dynes quadrant).

Fig. 2. Relative deflections of vertical component of field H_z from field at the center of magnet H_0 ($R_1 = 4$ cm).

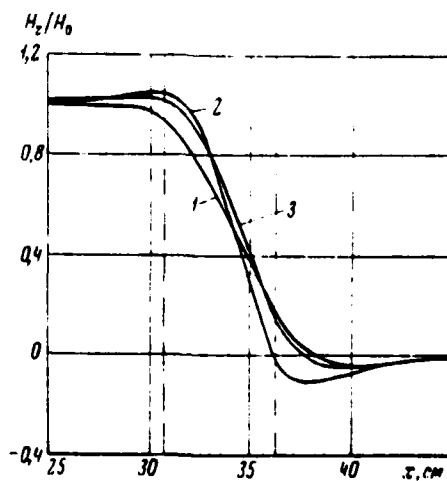


Fig. 3.

Fig. 3. Character of field change in end part of magnet block with different y and z . 1 - $y=0$, $z=0$; 2 - $y=0$, $z=3$; 3 - $y=3$, $z=0$.

Page 194.

Fig. 3 gives graphs/curves $\frac{H_z}{H_0}(x)$ with different y and z for the end part of magnet block. By broken lines are shown beginning and end/lead of the end part of the winding where are arranged/located the circular and transition sections of turns.

The examined in this work calculation procedure it is proposed to utilize first of all for determining the optimum construction/design of the end parts of the winding, which ensure such form of field on the edges of magnet, with which the disturbance/perturbation of particle motion due to the edge effects would be minimum.

It should also be noted that the procedure of a precise calculation of field gives the possibility to critically analyze the results of the measurements of the magnetic field of the prepared superconducting coil electromagnets. According to the degree of a difference in the results of measurements from calculation data it is possible to find not only about the precision of manufacturing magnet, but only and about the strength of possible "idle" currents in the superconducting cable cores of the winding of magnet, caused by the magnetization of the superconductor of the II kind.

REFERENCES.

1. P.F. Smith, J.D. Lewin. Nucl. Instr. and Methods, 1967, 52, N 2, p.298.
2. A. A. Vasil'yev, A. I. Izergach, R. A. Mesharov, Ye. S. Mironov, A. G. Zeldovich. UP international conference on the accelerators. Yerevan, 27 August-9 September, 1969.
3. R.A. Beth. Proc. Second Internat. Conf. on Magnet Technol. Oxford, 1967, p. 135.
4. R. A. Meshchercv, Ye. S. Mironov. Transactions of All-Union conference on charged particle accelerators. M., 9-16 October, 1968. Vol. 1 VINITI, 1970, page 605.
5. J.P. Blewett. Proc. 1968 Summer Study on Superconducting Devices and Accelerators. Part III, p. 1042.
6. A.A. Halacsy, G. Clark, J. Dunks. Proc. Second Internat. Conf. on Magnet Technol. Oxford, 1967, p.61.

60. CALCULATIONS OF IRON FREE MAGNETS WITH "THICK" WINDINGS FOR ACCELERATION TECHNOLOGY.

V. G. Davidovskiy.

(Institute of nuclear physics of SO AN USSR).

In connection with the development of technology of superconductors and the transition to the accelerators to super-high energies increasingly wider will be used iron free magnets. During their construction it is useful to know the ideal forms of the windings, which form prescribed/assigned stationary plane field, and some characteristics of such systems. Thin windings were examined in [1]; however, are virtually interesting "thick" windings.

Let us examine shaping of the plane of field $H_0(r, \varphi)$ with the potential

$$A(r, \varphi) = - \sum_{n=1}^{\infty} \frac{b_n r^n}{n} \left(\frac{r}{r_0} \right)^n \cos(n\varphi + \psi_n) \quad (1)$$

in the circle which is tightly surrounded by the long current carrying conductors, perpendicular to the plane of circle (forming winding). The value of current density j is permanent over entire section of winding, full current is equal to zero. The forming

winding is surrounded by the screen (iron ($\mu=\infty$) or current - the shielding winding) whose internal boundary is the circumference, concentric with the boundary of the region of shaping (Fig. 1). Everywhere lower upper sign relates to the case of iron screen, lower - current. The potential of the field between the forming and shielding windings let us write in the form:

$$A_{\text{npom}}(r, \varphi) = \sum_{n=1}^{\infty} \left\{ \frac{d_n}{n} \left(\frac{r_0^{n+1}}{r^n} \right) + \frac{c_n}{n} \left(\frac{r^n}{r_0^{n-1}} \right) \right\} \cos(n\varphi + \psi_n). \quad (2)$$

In the case of current screen we consider that there is no field cut of the system.

"Thin windings". If the "thickness" of winding $\Delta(\varphi) = r(\varphi) - r_0 \ll r_0$, then winding it is possible to consider "thin" and to consider as current layer. We obtain

$$c_n = \pm \frac{(r_0/r_2)^{n+1}}{1 \pm (r_0/r_2)^{2n}} r_0^{n-1} b_n, \quad d_n = \frac{1}{1 \pm (r_0/r_2)^{2n}} r_0^{n-1} b_n,$$

the equation of the "thin" forming winding

$$-\frac{j_2(\varphi)}{j} \frac{\Delta(\alpha, \varphi)}{r_0} = \frac{1}{\frac{2\pi}{c} j r_0} \sum_{n=1}^{\infty} \frac{1}{1 \pm \left(\frac{r_0}{r_2}\right)^{2n}} r_0^{n-1} b_n \times \cos(n\varphi + \psi_n)$$

and, in the case of current screen, the equation of the "thin" shielding winding

$$\frac{j_2(\varphi)}{j} \frac{\Delta_2(\alpha, \varphi)}{r_0} = \frac{1}{\frac{2\pi}{c} j r_0} \sum_{n=1}^{\infty} \frac{(r_0/r_2)^{n+1}}{1 - (r_0/r_2)^{2n}} \times r_0^{n-1} b_n \cos(n\varphi + \psi_n),$$

where by $j(\phi)$ and $j_s(\phi)$ - piecewise constant alternating functions $|j(\phi)|=j$ and $|j_s(\phi)|=j_s$. We introduced the parameter of thickness which is conveniently defined as $\alpha = b_p \gamma_0^{p-1} / (\frac{2\pi}{c} j \gamma_0)$, where b_p - coefficient most substantially of multipoles in expansion (1), which characterizes the amplitude of the forced/shaped field with its prescribed/assigned configuration.

Page 195.

Setting to zero right sides (3) and (4), we determine the position of points on circumferences γ_0 , in which the "thickness" $\Delta(\alpha, \phi)$ of winding turns into zero, and direction of flow is changed by the reverse. We will call these points nodal. From (3) and (4) it follows: 1) the external boundaries of the forming windings form single-parametric family $\gamma(\alpha, \phi)/\gamma_0 = 1 + \Delta(\alpha, \phi)/\gamma_0$, having the nodal points, which lie on the boundary of the region of shaping (it is analogous for the shielding windings); 2) the position of nodal points ϕ_n on circumference γ_0 (for the current screen - on circumference γ_1) is determined exclusively by field pattern and does not depend on its amplitude. Nodal points divide/mark off windings into the separate

elementary parts, directions of flow in two adjacent parts are mutually reverse. The position of the nodal points of pure/clean multipoles is obvious from the symmetry.

In the case of "thin" winding the thickness $\Delta(a, \theta)$ is proportional a .

"Tolstoy" of winding. Conclusion/output 1) and 2) are valid for the windings of any thickness. Therefore, after determining the position of nodal points from the equation of "thin" windings (3) and (4), we know the separation of the winding of arbitrary thickness into the elementary parts. It is easy to show that the potential of field within this any part is given by the expression

$$A_n(r, \varphi) = A_0(r, \varphi) - \frac{\pi}{c} j [r^2 - r_0^2 - 2r_0^2 \ln(r/r_0)], \quad (5)$$

where $A_0(r, \varphi)$ - potential of the formed/shaped in the circle field. Upon transfer to the adjacent elementary part of $j \rightarrow -j$. With the current screening the potential of field within the shielding winding analogously is expressed as the potential of intermediate region (2):

$$A_{2n}(r, \varphi) = A_{n\text{pot}}(r, \varphi) + \frac{\pi}{c} j_2 [r^2 - r_2^2 - 2r_2^2 \ln(r/r_2)]. \quad (6)$$

Potentials (5) and (6) automatically satisfy boundary conditions respectively on circumferences r_0 and r_2 . In the case of iron screen boundary condition on the iron gives $c_n = d_n(r_0/r_2)^{n+1}$. Utilizing (5) and (2), let us write the boundary conditions on the external boundary of forming winding $r(\varphi)$

$$H_{0r}(r(\varphi), \varphi) = \sum_{n=1}^{\infty} d_n \left\{ (r_0/r(\varphi))^{n+1} + (r_0/r_2)^{2n} \times \right. \\ \left. \times (r(\varphi)/r_0)^{n+1} \right\} \sin(n\varphi + \varphi_n), \quad (7)$$

$$H_{0\varphi}(r(\varphi), \varphi) + \frac{2\pi}{c} j(\varphi)(r(\varphi) - r_0^2/r(\varphi)) = \\ = \sum_{n=1}^{\infty} d_n \left\{ -(r_0/r(\varphi))^{n+1} + (r_0/r_2)^{2n} (r(\varphi)/r_0)^{n+1} \right\} \times \\ \times \cos(n\varphi + \varphi_n).$$

this is the equation of "thick" forming winding with the iron screen, they determine $r(\varphi)$ and the totality of coefficients d_n .

It is analogous in the case of current screen, writing/recording boundary conditions on the external boundary of the forming winding and condition for the disappearance of field on the external boundary of the shielding winding, we obtain the system of equations of "thick ones" the forming and shielding windings. This system determines $r(\varphi), r_s(\varphi)$ and the totality of coefficients c_n, d_n .

The obtained equations of "thick" windings are conveniently solved by the numerically following iterative process. Let during the solution of system (7) on some iterative loop be obtained totality d_n and sequence of points $r(\varphi_p)$ on the unknown boundary of the forming winding. Next iterative loop consists of the determination of new totality d_n , in the best way in the root-mean-square sense of satisfying the first equation system (7) on the sequence of points $r(\varphi_p)$. Utilizing this new totality d_n , from second equation (7) we

determine the refined sequence of points $r(\varphi_p)$. Process rapidly converges. Fig. 2-6 illustrate some of obtained results [2].

The power lines of magnetic field have centers, which lie within the elementary parts of the winding. The position of centers qualitatively characterizes the "half-thickness" of winding and can be elementarily determined from (5), since in the center field is equal to zero. The centers of quadrupole winding are located at points with $r_u = r_0 / \sqrt{1+\delta}$, where $\delta = VH / (\frac{2\pi}{c} j)$. Consequently, $VH < \frac{2\pi}{c} j$, moreover equality is reached in the limit of infinitely thick winding.

Elliptical region. The determination of the forms of the winding of those forming the prescribed/assigned field with potential $A_0(r, \varphi)$ (1) in the elliptical region with the semi-axes (a, b) in the presence of the screen (iron or current) whose internal boundary is a confocal ellipse with the semi-axes (A, E), can be conducted in perfect analogy with the case of circular region.

The position of the nodal points of the forming winding is determined from the equation of "thin" winding ($a > b$):

$$-\frac{j(\eta)}{4} \Delta(\eta) = -\frac{1}{\frac{2\pi}{c} j \frac{a+b}{2}} \sum_{n=1}^{\infty} b_n \frac{a+b}{2} \frac{1}{a^2 \sin^2 \eta + b^2 \cos^2 \eta} \times \frac{8\pi n}{2^n n},$$

825

where

$$S_{\Phi n} = \sum_{k=0}^{k \leq n/2} \binom{n}{k} (n-2k)(a+b)^{n-2k} (a^2 - b^2)^k \times$$

$$\times \left(\frac{1 \pm \left(\frac{A-B}{A+B} \right)^{n-2k}}{1 \pm \left(\frac{a+b}{A+B} \right)^{2(n-2k)}} \cos \Phi_n \cos (n-2k) \eta - \right.$$

$$\left. - \frac{1 \pm \left(\frac{A-B}{A+B} \right)^{n-2k}}{1 \pm \left(\frac{a+b}{A+B} \right)^{2(n-2k)}} \sin \Phi_n \sin (n-2k) \eta \right).$$

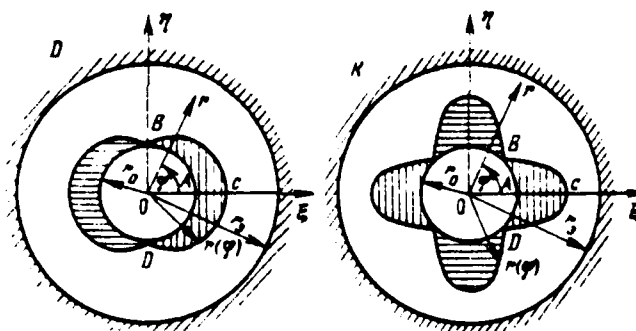


Fig. 1. Qualitative forms of dipole and quadrupole magnets with the iron screens. The parts of the windings with the mutually opposite currents are covered with mutually perpendicular shading.

826

Page 196.

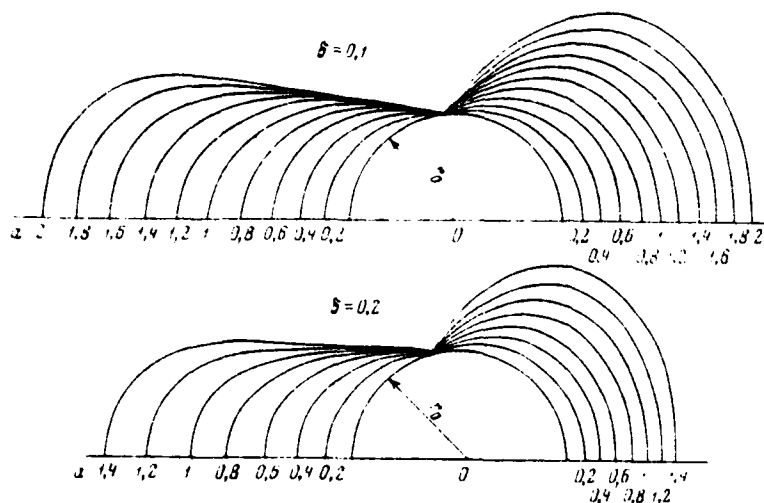


Fig. 2.

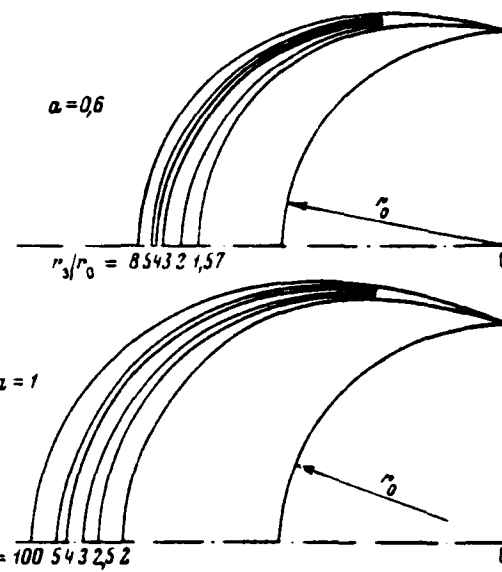


Fig. 3.

Fig. 2. Forms of unshielded windings, which form superposition of dipole and quadrupole fields with horizontal plane of symmetry.

$$\delta = (r_0 \nabla H) / H_0, \quad \alpha = H_0 / \left(\frac{2\pi}{c} j r_0 \right)$$

Fig. 3. Forms of dipole windings with iron screen. About each curve is shown the corresponding position of screen $\alpha = H_0 / \left(\frac{2\pi}{c} j r_0 \right)$

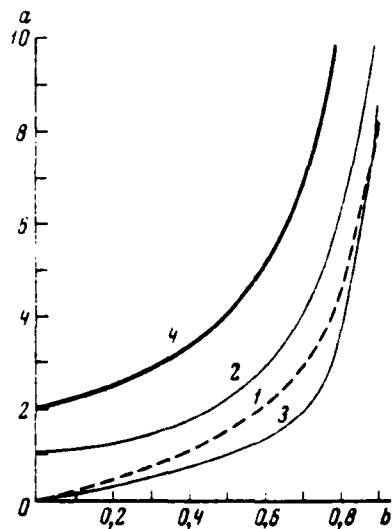


Fig. 4.

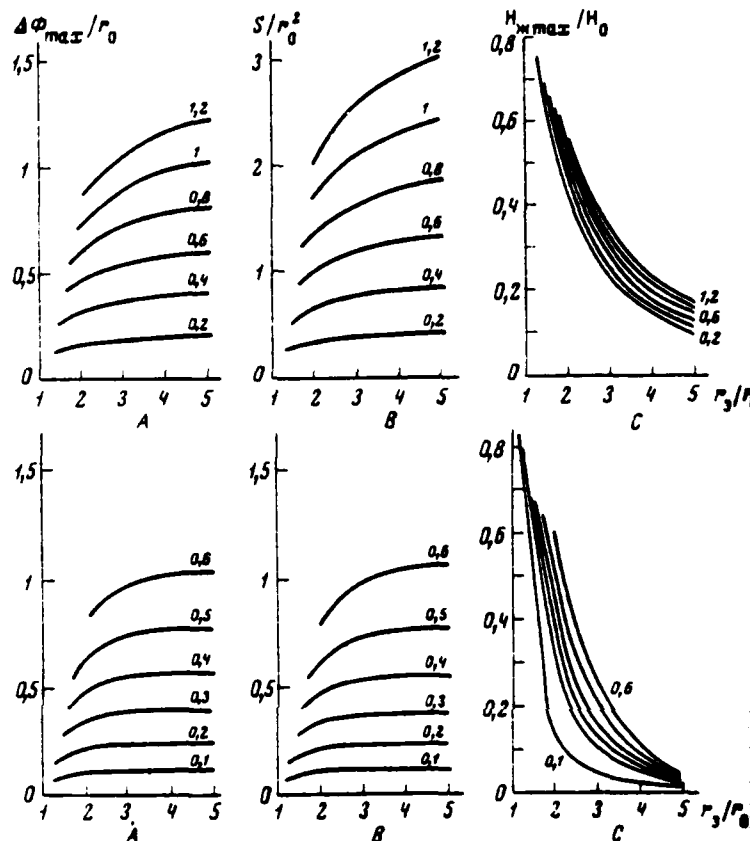


Fig 5.

Fig. 4. Unshielded quadrupole magnet. Area of one "ear/eye" of winding S/r_0^2 (1), magnetic energy in the metal of winding W_{MET}/W_0 (2), out of magnet W_{MOP}/W_0 (3) and total energy W_{TOTAL}/W_0 as the functions $b = \nabla H / (2\pi/c)$ ($W_{TOTAL} = W_0 + W_{MET} + W_{MOP}$, $W_0 = (\nabla H)^2 \cdot r_0^2 / 16 -$

energy of field in the region of shaping).

Fig. 5. Dipole magnet with iron screen (upper series/row) and quadrupole magnet with iron screen (lower series/row): Δ - maximum thickness of winding $\Delta\phi_{\max}/\nu_0$; E - area of one "ear/eye" of winding S/ν_0^2 ; C - maximum field on iron H_{\max}/H_0 (in the case of quadrupole $\nu_0 \nabla H$ is marked H_0) - function of position of screen ν_0/ν_0 . About each curve of upper series/row is shown the value of parameter $a = H_0 / (\frac{2\pi}{c} j \nu_0)$, about the curves of lower series/row - value of parameter $b = \nabla H / (\frac{2\pi}{c} j)$

Page 197.

Connection/communication of elliptical (ξ, η) and Cartesian coordinates (x, y) : $d = \sqrt{a^2 - b^2}$,

$$x = d \operatorname{ch}(\xi - \beta) \cos \eta, \quad y = d \operatorname{sh}(\xi - \beta) \sin \eta,$$

$$\beta = \ln\left(\frac{\sqrt{a^2 - b^2}}{2}\right), \quad \xi_0 = \ln\left(\frac{a+b}{2}\right).$$

Potential of field within the parts of the forming winding:

$$A_m(\xi, \eta) = A_0(\xi, \eta) - \frac{2\pi}{c} j e^{2\beta} \left\{ \operatorname{ch} 2(\xi - \beta) - \right. \\ \left. - \operatorname{ch} 2(\xi_0 - \beta) + \cos(2\eta)(1 - \operatorname{ch} 2(\xi - \xi_0)) - \right. \\ \left. - 2(\xi - \xi_0) \operatorname{sh} 2(\xi_0 - \beta) \right\}.$$

Analogous relationships/ratios it is easy to write, also, for the shielding winding.

Examining the position of the centers of quadrupole winding, we obtain, that if the axes/axles of field are turned on 45° relative to the axes/axles of ellipse, then $VH \leftarrow \frac{2\pi}{c} j \times 2/(1+a/b)$, but if they are directed along the axes of ellipse, then $VH \leftarrow \frac{2\pi}{c} j \sqrt{1 - \left(\frac{a-b}{a+b}\right)^2}$, moreover equalities are reached in the limit of infinitely thick windings.

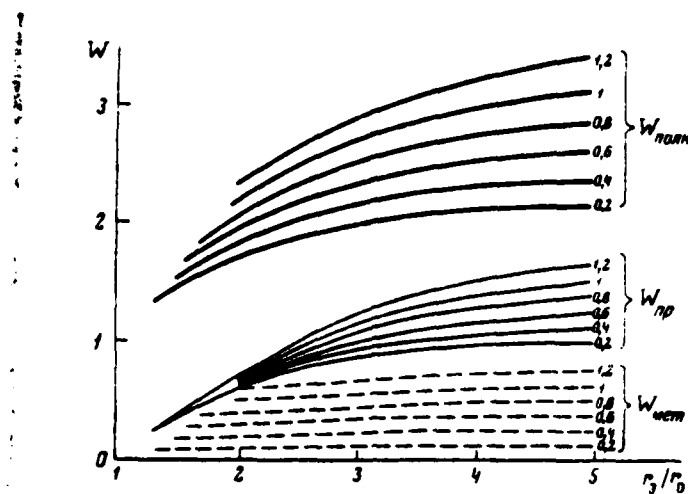


Fig. 6. Dipole magnet with the iris screen. Energy of field in the metal of winding $W_{\text{мет}}$, is the region between the winding and screen W_{np} and total energy of field $W_{\text{пульн}} = W_0 + W_{\text{мет}} + W_{\text{np}}$ in units W_0 ($W_0 = H_0^2 r_0^2 / 8$ - energy of the formed/shaped in the circle field) as the functions of the position of screen. About each curve is shown the value of parameter $a = H_0 / (-\frac{2\pi}{c} j r_0)$

REFERENCES.

1. R. A. Beth. IEEE Trans. Nucl. Sci., Ns-14, 386, 1967.
2. V. G. Davidovskiy. Preprint No 40, IYAF of SO AN USSR, 1970.

61. Calculation of magnetic field in the magnets with the sections/cuts.

V. P. Papadichev.

(Physical institute im. P. M. Letedev of the AS USSR).

Magnets with the sections/cuts found wide acceptance in the accelerative technology. As examples it is possible to indicate the magnetic systems of synchrotrons, which switch on sectors and straight sections, sector magnets of isochronal cyclotrons [1-4], of circular F-M cyclotrons, microtrons with the sectional magnet, etc. However, similar systems are used for the spectrometers, the analyzers and the separators of particles, and also in the circuits wirings and beam focusing.

In these all cases the significant role plays edge effect, i.e., the form of field about the boundary magnet-gap/interval. For example, with the narrow sectors such characteristics, as the "effective width" of sector and flutters, strongly depend on air-gap clearance of magnet and location of winding. In other cases (rings, circuits of wiring) edge effects change effective length of magnets and lenses and can be reason the nonlinearity of field and

aberrations.

However, the methods of calculation [5] used utilize a sufficiently rough approximation of "sharp" edge, i.e., edge effect is not considered. Usually this is made experimentally, and the creation of the field of complex configuration is connected with the simulation of several versions of magnet, which requires long time for conducting the precise measurements on the models.

Page 198.

In the present report are presented results [6, 7] of a more precise calculation taking into account the edge effect and the effect of the location of winding on the form of field during the arbitrary excitations of the adjacent blocks of magnet. This makes it possible to sharply reduce the volume of measurements during the simulation.

For the calculation is utilized the method of conformal mappings. Strictly speaking, it is applied when magnetic permeability of the material of poles is infinitely great and field flat/plane. The first condition usually is satisfied well, since in the systems, intended for the creation of field with the high precision/accuracy, iron is far from the saturation. Second condition is not necessary: comparison with the experiment on the circular F-M cyclotron (KF) [6]

and the cyclotron with sectioned magnetic system of the Lebedev physics inst. [8] shows that the calculation is valid with a good precision/accuracy (it is better than 10/o) and in the case of three-dimensional nonuniform fields. This is connected with the fact that a change of the parameters of magnet in the dependence on a radius can be considered as "disturbance/perturbation" in two-dimensional problem. In the system with the iron the effect of disturbances/perturbations rapidly decreases with the removal/distance from the perturbation source, and the azimuthal form of field is determined with a good precision/accuracy by the form of the section of magnet on the given radius.

1. Field at edge of poles. The geometry of poles, for which were carried out the calculations, it was shown in Fig. 1A. With the aid of Schwarz-Christoffel's integral is located the function, which reflects the prescribed/assigned region on plane $z=x+iy$ to half-plane $\text{Im} \zeta > 0$. Then for the case of the different excitations of blocks are conducted linear-fractional transformations, establishing the necessary correspondence of boundaries. In the presence of conductors with the current near operating region (Fig. 1b) is utilized the expression of potential for the conductor above plane $\text{Im} \zeta = 0$.

For the case of Fig. 1A (conductors with the current at points $x \rightarrow \infty$ and $y \rightarrow \infty$) the dependence of the vertical component of

magnetic intensity on axis/axle x for three cases of exciting the adjacent blocks is given in implicit form (field within the excited block far from edge $z=1$)

$$\frac{x}{h} = \frac{2}{\pi} \left(\operatorname{arctg} \frac{f_1}{\mu} + \mu \operatorname{arctg} f_1 \right), \quad (1)$$

$$\frac{x}{h} = \frac{2}{\pi} \left[\operatorname{arctg} \frac{1}{\mu} \sqrt{(1+\mu^2)f_2^2 - \mu^2} + \operatorname{arctg} \sqrt{(1+\mu^2)f_2^2 - \mu^2} \right], \quad (2)$$

$$\frac{x}{h} = \frac{2}{\pi} \left(\operatorname{arctg} \frac{f_3}{\mu} + \mu \operatorname{arctg} f_3 \right), \quad (3)$$

$$f_3 = \frac{1}{2} \left(f + \sqrt{\frac{f^2 + \mu^2}{1 + \mu^2}} \right),$$

where $\mu = h/H$, $2h$ - vertical, $2H$ - horizontal the pole gaps; f_1 - field during the opposite excitation of the adjacent blocks ($V_1 = V_4 = +V$; $V_2 = V_3 = -V$); f_2 - field during the identical excitation of adjacent blocks ($V_1 = V_3 = +V$; $V_2 = V_4 = -V$); f_3 - field during the excitation of one right block ($V_1 = +V$; $V_2 = -V$; $V_3 = V_4 = 0$). Fig. 2 gives these dependences (curves 1, 2, 3) for $\mu = 0.835$.

235

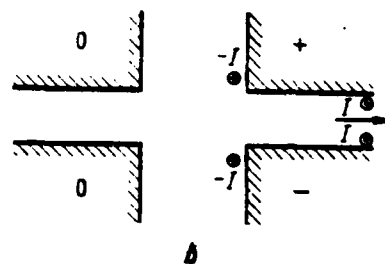
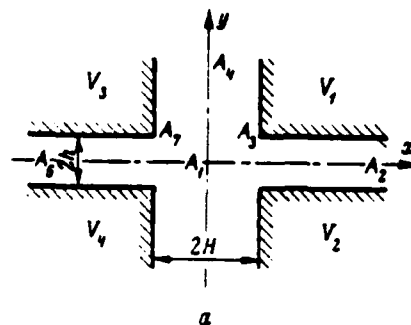


Fig. 1. Form of magnet poles, used for conformal mapping (a) and location of conductors with current of the I during the excitation of one block of magnet (b).

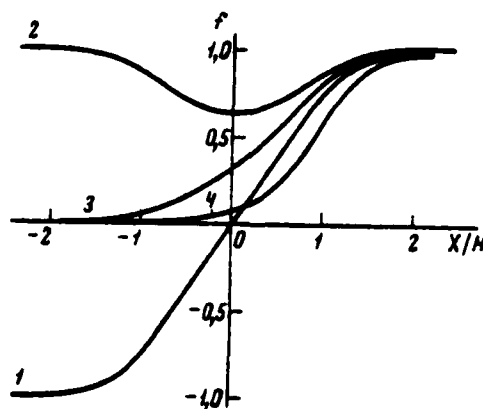


Fig. 2. Dependence of vertical component of magnetic intensity in median plane on coordinate x . 1 - corresponds to the opposite f_1 ; 2

836

- to identical (f_2) excitation of adjacent blocks; 3 - to excitation of one right block (f_3), 4 - field when conductor with the current is arranged/located in angle of Λ_3 . For all curves $\mu = h/H = 0.835$ (a "similar" region of annular F-M cyclotron of the Letedev physics inst.).

Page 199.

Asymptotic field expressions within excited block ($x/H > 1$) take the form:

$$\begin{aligned} f_1 \approx 1 - \epsilon_1 &= 1 - 2 \exp\left(-\frac{2}{\mu} \operatorname{arctg} \frac{1}{\mu} - \frac{\pi}{h} x\right), \\ f_2 \approx 1 - \frac{\epsilon_1}{1 + \mu^2}, \quad f_3 \approx 1 - \frac{2 + \mu^2}{2(1 + \mu^2)} \epsilon_1, \end{aligned} \quad (4)$$

but for f_3 within excited block ($x/H < -1$):

$$f_3 \approx \frac{\mu^2}{1 + \mu^2} \exp\left(-\frac{2}{\mu} \operatorname{arctg} \frac{1}{\mu} - \frac{\pi}{h} |x|\right). \quad (5)$$

Difference from the unit (or zero in the case (5)) $\epsilon < 10^{-4}$ with the deepening into the block on $x \approx (3-5)h$, which makes it possible to use the obtained results for the limited poles and, in particular, for the periodic structures.

2. Fields in periodic structures. In this case (Fig. 3) of function f they are represented in the form of Fourier series:

$$f = \sum_{k=0}^{\infty} a_k \cos \frac{2\pi}{L} kx, \quad (6)$$

where the origin of coordinates is shifted the middle of block, and L - period of the magnetic system (f_1 contains only odd ones, and f_2 - even harmonics). The use of formula (2) makes it possible to find constant component (in the curve of Fig. 4, and it is depicted $a_0(\mu)/2$):

$$a_0 = \langle f_2 \rangle = 1 + \frac{\frac{4\mu}{\pi} \ln \frac{1+\mu^2}{\mu^2} - \frac{8}{\pi} \operatorname{arctg} \frac{1}{\mu}}{L/H}. \quad (7)$$

The knowledge of the sum of the squares of harmonics makes it possible to connect frequencies of betatron (for the cyclotron with sectioned magnetic system) with the geometric parameters of magnet). Calculations give:

$$\phi_1 = \sum_{k=0}^{\infty} a_{2k+1}^2 = 2 \frac{L/H - \frac{4}{\pi} (1+\mu^2) \operatorname{arctg} \frac{1}{\mu}}{L/H}, \quad (8)$$

$$\phi_2 = \sum_{k=1}^{\infty} a_{2k}^2 = 2 \frac{L/H - \frac{8}{\pi} \operatorname{arctg} \frac{1}{\mu}}{L/H} - 2a_0^2, \quad (9)$$

$$\phi_3 = \sum_{k=1}^{\infty} a_k^2 = \frac{L/H - \frac{4}{\pi} (2+\mu^2) \operatorname{arctg} \frac{1}{\mu}}{L/H} - \frac{a_0^2}{2}, \quad (10)$$

where formula (8)-(10) correspond to (1)-(3). Fig. 4b (curve 6) gives the dependence of fluxer $\phi_2/2a_0^2$ on μ . The obtained formulas easily are generalized to the case when gaps/intervals have different width, and adjacent blocks different width and excitation.

3. Effect of conductors with current. If is excited one block and conductor is arranged/located at point $z=x+iy$ (Fig. 1b), to which corresponds point C on half-plane $\operatorname{Im} \zeta > 0$, then field equal

$$f_4 = f_3 \frac{CC^* - \frac{C+C^*}{2} \left(1 - \frac{f_1}{f_2}\right)}{\left(1 - C - \frac{f_1}{f_2}\right) \left(1 - C^* - \frac{f_1}{f_2}\right)}, \quad (11)$$

where α is determined from (1), C^* - value complex conjugated, C which is determined from the relationship/ratio:

$$\frac{\alpha}{H} = \frac{2i}{\pi} \left\{ \mu \operatorname{arctg} \left[\mu \frac{1-C}{\sqrt{(1-C)^2 - (1+\mu^2)}} \right] + \operatorname{arctg} \left[\frac{1-C}{\sqrt{(1-C)^2 - (1+\mu^2)}} \right] \right\}. \quad (12)$$

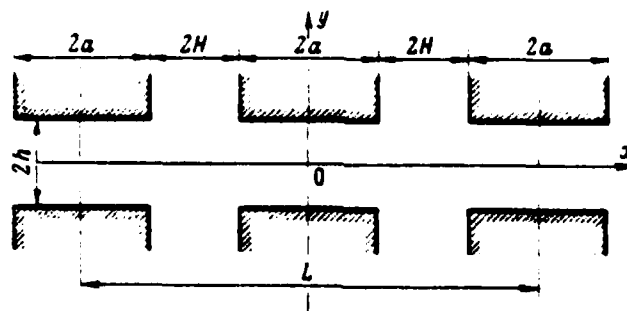


Fig. 3. Geometry of magnetic system for the periodic structures ($2a$ - the width of blocks, $2H$ - the distance between blocks $L=4(a+H)$ - the period of magnetic system).

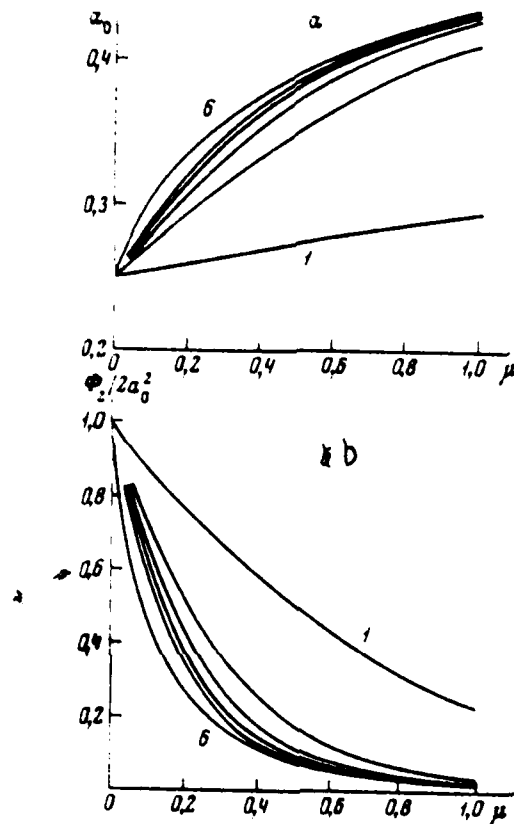


Fig. 4. Dependence of constant component of field on $\mu = h/H$ at different height of conductor with current from middle coordinate plane of conductors ($z = h + iy$ and $z^* = H - iy$) (a) and flutter $\phi_2 / 2a_0^2$ from μ in different positions of conductor with current (b). 1-6 correspond to the consecutive values of $y/h = 1, \dots, 5, \dots$. Parameter $x = L/4H = 2$, which corresponds to the equal extents of blocks and gaps/intervals.

Page 200.

At point $z=x-iy$ is arranged/located the conductor with the same current. Inverse currents are found in point A_2 ($x \rightarrow -$, Fig. 1A). Fig. 4a and 4b gives dependences a_0 and $\phi_2/2a^2_0$ on μ with the different value y/h - location of conductor on the boundary of block A_3A_4 . Curved change with increase in y/h from 1 (conductor in angle of A_3) to shows the possible range of changes a_0 and $\phi_2/2a^2_0$ in the magnet in different positions of the winding (approximation/approach of "sharp" edge gives with $L/4h=2$ $a_0=0.25$ and $\phi_2/2a^2_0=1$ independent of μ and y/h). During the location of windings of deeper $(3-5)h$ from the horizontal plane their effect on the form of field it is possible to virtually disregard and to use formulas (1)-(10). For the extended winding the field is calculated by the addition of fields from the separate conductors.

The obtained formulas were used for the calculations of the azimuthal form of field in circular F-M cyclotron [6, 7] and cyclotron with sectioned magnetic system [8] and became a good agreement with the experiment. Fig. 5 gives calculated curve and experimental points for the geometry of circular F-M cyclotron with sharply nonuniform field along radius ($\sim r^{1/2}$). A difference in the calculation from the experiment does not exceed 0.50/c and, apparently, it is connected in essence with the measuring errors.

DOC = 80069215

PAGE ~~48~~ 841

Calculation by this method of field in the region of the shaped pole of circular F-M cyclotron of the Lebedev physics inst. made it possible to simplify production and to immediately obtain necessary pole-piece configurations [9].

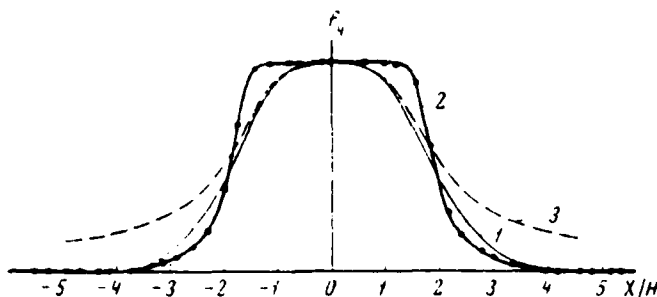


Fig. 5. Dependence of magnetic field f_v on the azimuth in the measurement on the bench. 1 - $\mu=0.835$; 2 - $\mu=0.293$. Curve 2 considers the small proximity effect of winding to operating region. Points in curves 1 and 2 correspond to experimental data, their size/dimension - to measuring errors. Curve 2 - calculated field in the approximation/approach of "one" block (second is extended to infinity, i.e., $H \rightarrow \infty$, $\mu \rightarrow 0$, $\mu H = h$). It is evident that the presence of the adjacent unexcited block leads to a sharper field slope.

REFERENCES.

1. E.M. Moroz, M.S. Rabinovich. Proc. CERN Symposium, 1950, 1, 547.
2. I. Ya. Barit et al. Preprint the Lebedev physics inst., 1969, No 15.
3. A.A. Glasov et al. Nucl. Instr. and Methods, 1969, 70, 274.
4. J.A. Martin. IEEE Trans. Nucl. Sci., 1969, 16, Part 1, 797.
5. M.M. Gordon. Ann. Phys., 1968, 50, 571.
6. V. A. Papadichev. Short communications/reports in physics, 1970, No 4, 61.

DCC = 80069215

PAGE

84³

7. V. A. Papadichev. Preprint of the Lebedev physics inst., 1969, No 69.

8. V. N. Kanunnikov. Preprint of the Lebedev physics inst., 1969, No 21.

9. V. N. Kanunnikov, A. A. Melomenskiy, V. A. Papadichev. Short communications/reports in physics, 1970, No 2, 18.

Page 201.

Session V.

COLLECTIVE METHODS OF ACCELERATION.

62. Collective ion accelerator - new instrument in physics of elementary particles.

V. P. SARANTSEV

(Joint institute of nuclear research).

Let us pause briefly at the state of matters for the creation of the accelerator, which uses electron rings, in the different laboratories of peace/world. If we characterize position on the whole, then it is necessary to say that the procedure of obtaining electron rings is completely mastered. At present are solved questions of obtaining rings with the maximum electron density. For this is constructed a whole series of new devices/equipment and installations. In the laboratories which dealt, until now, by obtaining small clusters for the collective acceleration, occurred

upheaval in the ideology of experiment in favor of annular formation/education. In recent years are published several propositions on obtaining of circular clusters by the methods, different from the usual compression, proposed by our group. However, there are no serious investigations both experimental ones and theoretical ones up to now using these methods and therefore it is difficult to speak about advantages and deficiencies/lacks in one or the other methods. Plans/layouts for near future provide for such investigations, and to the following conference, apparently, it will be possible to make a selection of optimum compressor. Briefly let us pause at these plans/layouts.

It is known that already one-and-a-half^{years} ago Kristolfilos made propositions on obtaining of circular clusters in the static compressor. The essence of this proposition is reduced to the fact that the ring in the period of its formation passes two three-dimensional/space diverse stages of compression, on one of which occurs in essence the acceleration of electrons in the ring, and on the second - bringing/finishing circular cluster to a necessary radius; during the first stage are satisfied usual betatron conditions for field 2:1. At present is conducted the preparatory work, which foresees the possibility of using the magnetic system "astro-on" for formation and accelerating the electron rings. It is assumed that the work on the acceleration will begin to be carried

out from in the spring of 1971.

In 1971 questions of obtaining and accelerating the circular clusters it is proposed to investigate in one more American laboratory in the University of Maryland. Until the present time this research group was occupied by obtaining and studying the bundles of electrons of cylindrical type, applying the method of the adiabatic compression of electron spiral in the longitudinal magnetic field of stopper configuration; to this group it was possible to obtain compact electronic formation/educations. In the final state of compression electronic small cylinder had sizes/dimensions 0.4×4 of cm. However, the difficulties, connected with the retention of this cluster upon the acceleration, in practice do not make it possible it to utilize for purposes of the collective acceleration of high intensity. At present occurs the technical rearmament of group - group obtains electronic direct voltage accelerator on energy 4 MeV with the current 10 kA. There occurred change and directions of investigations. Is outlined transition to obtaining and study of circular clusters. The formation of cluster is intended to conduct in the static magnetic field, which has at the output magnetic mirror. The formed in the magnetic field spiral from the electrons with the ispiement to the plug is grouped into the ring. As show calculations, to obtain small sizes/dimensions of the section of ring thus is difficult. Direct voltage accelerator, which is intended to

utilize in these experiments, gives the large scatter of particles on the energies, and this even more impedes obtaining the parameters of ring. Nevertheless experiments are designed for obtaining in the ring of 10^{13} electrons and it is more.

Let us pass to the state of matters and the nearest plans/layouts in the laboratories, which work on the usual diagram of obtaining circular cluster. Large successes achieved in last year the group, which works in Garching (FRG). Utilizing an electron accelerator of direct action, this group obtained in the compressor the ring of electrons by diameter on the order of 7 cm. The special feature/peculiarity of the compressor, created with this group, is the rapid time of compression of ring (9 μ s). This is reached because of the use of a single-turn single-stage winding of pulse field. The total number of electrons in the ring is small ($\sim 10^{10}-10^{11}$). In this is guilty first of all the electron accelerator, which has the high energy scatter of particles. The use of a single-stage system of compression also affects the process of capture and, therefore, to a number of seized particles. At present is accomplished/realized transition to the usual version of the three-stage compression. This gives the possibility to decrease the sizes/dimensions of ring and to increase the total number of electrons in it.

As is shown experiment of the use of direct voltage accelerators for obtaining the circular clusters, such accelerators cannot compete with the induction ones and without an essential improvement in the qualities of beam, apparently, they cannot be utilized for obtaining the circular clusters with the large proper fields. Basic laboratories dealt by development and creation of the more effective injectors which would make it possible to obtain electric ion clusters with the effective intensity/strength of field $\sim 10^7$ V/cm. This it is possible to achieve first of all due to a considerable increase in the intensity of the electron accelerators, and also due to the decrease of the perveance of launching/starting the electrons of these accelerators.

The solution of precisely these questions composed the basis of the scientific program of the group of Berkeley. This group achieved the great successes in the formation of electron rings. However, further progress of the investigations of this group was restrained by two basic reasons: a) the electron accelerator which was utilized by this group as the injector, it possesses sufficiently high perveance, which impedes obtaining circular cluster with the optimum parameters; b) insufficient vacuum in compressor ($6 \cdot 10^{-7}$ mm Hg) does not make it possible to conduct the acceleration of cluster due to

destructive resonance effect $Q_{\gamma} = 1$.

At present in practice are completed works on the creation of new electron accelerator. This is betatron type linear accelerator. Use as basic material of the inductors of this accelerator of ferrite gives possibility due to shortening of the duration of pulse (30 ns) to increase substantially peak power and to accelerate electronic currents ~ 1000 A. Transition to the field emission cathode substantially improves the quality of the accelerated beam. Characteristics indicated above of accelerator in conjunction with a small scatter of particles on energies ($\Delta E/E \sim 0.5\%$) will make possible to obtain in annular cluster $\sim 3 \cdot 10^{13}$ electrons. This ring is possible to use for accelerating the protons with the average/mean strength of field to $5 \cdot 10^6$ V/cm.

The works, conducted by group in Dubna, passed in two main trends: investigation on the model of collective accelerator and investigations, connected with the creation of separate elements/cells and systems of future accelerator. The basic task which was solved on the model of accelerator, was the adjustment of the separate elements of setting up for the acceleration in the ring α - particles. This adjustment was dictated the need of studying the behavior of those accelerated α - particles in the ring about different accelerations of ring. Experiments must be conducted at

different speeds of circular cluster. These investigations will make possible to correctly determine requirements for the precision/accuracy of the maintenance of accelerating field, which is extremely important in the first stages of acceleration for the times of acceleration, compared with the time of the oscillation of ions within the electronic potential pit. If this is transferred to the appropriate energies of the accelerated ions, then this corresponds to energies 1-4 MeV/nucleon. To conduct such investigations on the ions of heavy elements is difficult. Thus, for the ions of nitrogen, for which were conducted the first experiments on the acceleration in the ring, it is possible to select the nuclear reactions according to which it is possible to determine the intensity of accelerated ions. However, the thresholds of these reactions lie/rest sufficiently high (3-4 MeV/nucleon) and therefore it is impossible to investigate entire region of energies with the aid of nitrogen ions. α - particles were selected because all possible nuclear reactions with them in the interesting us range of energies are well studied on the cyclotrons. During the preparation of installation for the acceleration α - particles we proceeded also from the fact that after conducting of the necessary measurements it would be possible to sufficiently rapidly switch over to the acceleration of protons.

Preparation of installation included two basic tasks: shaping of the magnetic field of the corresponding configuration and obtaining

more fine vacuum. The rearrangement of magnetic field encompassed the creation of the necessary three-dimensional/space gradient in the section of the conclusion/output of circular cluster. In order to ensure the possibility of the control of accelerating voltages both as a whole in the section of conclusion/output and in the individual sections, along the length of acceleration it was introduced additionally the dash of turn in by current. The current through these turns can be regulated, changing the time of the start of the intercepting discharger/gap. Such changes in the diagram made it possible to ensure a steady change in the gradient of the magnetic field, which accelerates the annular cluster. As showed the measurements of magnetic field, this system of conclusion/output will make possible to accelerate α - particle in the range of energies from 1 to 10 MeV/nucleon.

Transition to the acceleration α - particles required improvements in the vacuum in the chamber/camera of compressor 2-3 times. This is dictated first of all by the need to limit the content of the ions of residual gas. For guaranteeing the necessary pressures in the chamber/camera was improved the system of vacuum evacuation. Besides usual system were introduced additionally two turbomolecular pumps of the type TMN-200.

For further acceleration of circular cluster is provided for the

system of resonators with appropriate modulation of magnetic field along the length of acceleration. As the accelerating element of system is selected the coaxial cavity. For the final selection of constructing/designing this resonator were carried out the investigations, connected with the work of resonator in the pulse magnetic field, and also the investigations of high-frequency discharge. On the basis of these investigations is made the selection of constructing/designing this resonator. Resonator is made from the stainless steel with thin copper coating of internal surface.

Important for the model of accelerator is the agreement of time of flight the electron ring of the clearance of resonator with the phase of high-frequency oscillations. For guaranteeing the necessary precision/accuracy of agreement is selected the system of consecutive bunching of rings, which consists of three resonators. As showed calculations, this system can ensure agreement into 90% of cases, i.e., with $\sim 320^\circ$ on the phases of accelerating voltage.

The second direction of the works of group encompassed the investigations, connected with the creation of separate elements/cells and systems of the future accelerator. These investigations provided for the creation of the new injector of electrons, cryogenic accelerating section and the selection of the optimum configuration of compressor.

Linear induction accelerator at the present time - fundamental set, which makes it possible to obtain the monoenergetic relativistic charged particle beams of the large intensity.

Page 203.

Work experience with similar type accelerator showed the possibility of designing of accelerator with the substantially larger intensity of the accelerated particles without the essential complication of systems. On the contrary, as showed the investigations of sampled-data system, the accelerating part can be simplified. The investigations of different commutators showed that most adequate/approaching for the accelerator are the thyratrons of the type TGI-1 2500/50, which for the duration of pulse 10^{-7} s are capable of drawing current ~ 12 kA.

A basic question during the creation of this accelerator is a question of the selection of material for the core of the accelerating element/cell - inductor. Obvious is the fact that this material must possess very small specific conductivity. In another case due to the strong surface/skin effect, called by eddy currents, the volume of ferromagnetic material, necessary for producing the

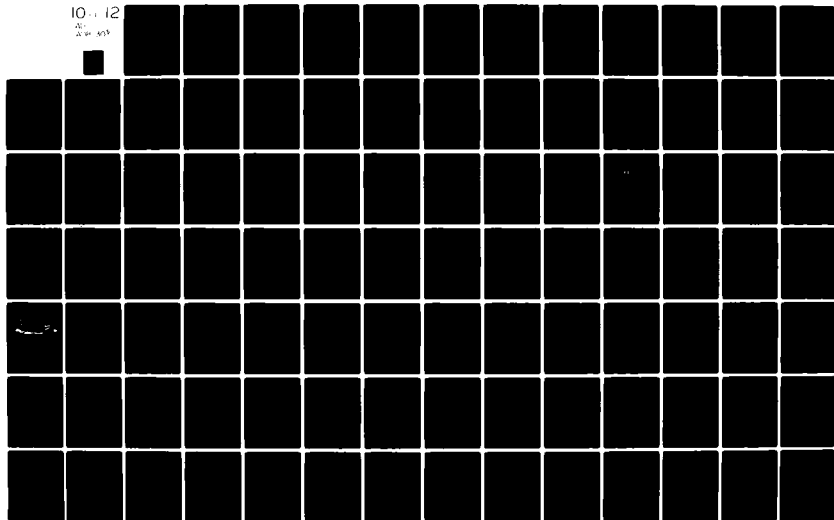
AD-A089 303

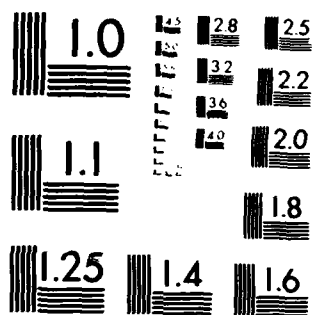
FOREIGN TECHNOLOGY DIV WRIGHT-PATTERSON AFB OH F/G 20/7
TRANSACTIONS OF THE ALL-UNION CONFERENCE (2ND) ON CHARGED PARTI--ETC(U)
JUL 80 A L MINTS, A A KOMAR, A A VASIL'YEV
FTD-ID(RS)T-0692-80 NL

UNCLASSIFIED

10-12

AD
A089 303





MICROCOPY RESOLUTION TEST CHART
NATIONAL BUREAU OF STANDARDS-1963-A

inductor, would prove to be large. Experiments showed that for the durations of operating pulse 30-40 ns the most adequate/approaching material is ferrite. However, the low value of the saturation induction of ferrite superimposes supplementary requirements for the primary impulse/momentum/pulse, namely to its duration. For shortening of the pulse duration in the diagram is utilized the saturation of ferrite core. The section of ferrite is selected in such a way that with the given amplitude of current saturation would begin after time t_{HMT} , after which automatically occurs the shunting of load and voltage on it rapidly drops to zero. In order to avoid the losses of beam due to the low-power electrons, which are formed at the leading impulse front, necessarily reasonably possible shortening of front. For this is used the system of the aggravation of front with the aid of the coaxial line, filled with ferrite. During the use of a cut of coaxial dimension line 38x24x7.5 mm and by length of 70 cm was obtained the impulse/momentum/pulse with the front 5 ns for the duration of the front of launched pulse 70 ns. This made possible completely to forego the special preliminary impulse shaping and to be restricted to the use of a simply storage capacity/capacitance.

The described above investigations became the basis of the created at present accelerator.

Basic parameters of the accelerator:

energy of the electrons of ~3.5 MeV.

Maximum pulse current of 2000 A.

Duration of the main pulse of 20 ns.

Pulse repetition rate of 50 Hz.

Scatter of particles on the energies $\Delta E/E \sim 10\%$.

The mock-up of the accelerating system is fulfilled in the form of the system of the superconducting resonators, placed into the longitudinal magnetic field 20 kg, created by the superconducting windings. For the purpose of selecting of the material of resonators were carried out experiments on the investigation of the skin drag of superconductors of the 2nd kind under the influence on them of magnetic field 20 kg. The results of these works give grounds to speak today about the possibility of designing of the superconducting resonators, operating in the magnetic fields, with the quality $>10^6$. For obtaining the high values of quality it is necessary to conduct the studies of the effect of different treatments of the surface of resonator on the quality. At present are conducted investigations on

the application of the superconducting coatings on the resonator with the use of the glowing discharge. Experiments with the pure/clean superconductors it became the encouraging results. In detail the results of investigations on the cryogenic accelerating section will be represented in the separate report.

In the latter/last part of the report to me it would like to dwell on the question of the use of a collective accelerator for the physicist of elementary particles. This question frequently is raised on different conferences and many they frighten the completely new conditions for the work of physical equipment. Contemporary physical experiments in the method of conducting can be divided into two groups. In some equipment records everything, which through it passes without any preliminary selection. In others - the equipment works in the controlled mode/conditions, i.e., it records only some events which are selected/taken by special starting system, disregarding the large part of passing through not "uninteresting" particles. Usually without the preliminary selection are studied the processes, which go with the relatively large cross section, for example, the formation/education of resonances, elastic scattering, total cross sections. In the unguided mode/conditions works the equipment in neutrino experiments due to the smallness of the interaction cross section of neutrino. The controlled mode/conditions of the work of experimental installations is applied in the case of the

investigation of rare reactions or search of rare particles. For example, in the experiment of Yu. Prokoshkin's group on the searches of the antinuclei of helium for recording five nuclei through the detectors were passed $2 \cdot 10^{11}$ pi-mesons.

Collective accelerator is characterized by the fact that in it it is difficult to realize the expanded in the time discharge/break of the accelerated particles on the target. The methods of the temporary selection on this accelerator are unacceptable.

The basis of the procedure of experiment on this accelerator must be track detectors.

In order to encompass entire class of the experiments which are conducted on the contemporary accelerators, track detectors must make it possible to carry out experiments at least with the same particle fluxes, as at present. Let us examine the possibilities of such detectors.

Filmless spark chambers/cameras, proportional wire chambers/cameras and streamer chambers/cameras make it possible to simultaneously record to 100 tracks. The operating speed of these instruments is such, that they allow/assume synchronous working with the accelerator at the frequency of messages to 10^6 imp./s. Thus,

comparatively easily can be realized the experiments in which the particle fluxes reach 10^5 or $2 \cdot 10^{11}$ particles in 500 hours of work of the accelerator. (Collective accelerator it can operate at a frequency of 10^3 Hz.).

Under these conditions of the work of experimental installation the function of the selection of events is transferred from experimenter's equipment to the computer. The analysis of development of computational technology shows that, apparently, into the next five years it is possible to rely on the creation of the machines, which make it possible to treat this quantity of information. By such form, track electronic engineering will make it possible to optimally utilize possibilities of collective accelerator and to effectively conduct research in its beams. Furthermore, accelerator opens/discloses completely new possibilities in the analyses of the properties of neutrino. Will appear the possibility of designing of the monochromatic beams of neutrino ($\Delta E/E \sim 10\%$).

Page 204.

This fact not only makes it possible at the qualitatively new level to carry out all neutrino experiments, but also offers the possibility of the setting up of the experiments which in principle cannot be carried out without the monochromatic neutrinos. An example

of this experiment can be B. Poptekorvo's proposition about the search of strong $\nu-\nu$ interaction.

In conclusion we it is desirable to express large gratitude those all sent propositions according to possible experiments on the accelerator and especially V. A. Sviridov, who actually based the systematic possibility of the setting up of these experiments.

63. Some questions of the theory of the acceleration of ions by the scanning of electron beam.

A. A. Kolomenskiy, I. M. Logachev.

(Physical institute in. P. M. Lebedev of the AS USSR).

Recently much attention attract the collective methods of acceleration. Among them is separated/liberated the method of accelerating the ions, seized in relativistic electron rings and moved together with them [1]. Are known other methods of the collective acceleration when the use/application of rings it is possible to avoid. Idea of one of such methods in the form of the diagram of moving foci was expressed already long ago (see [2], and also [3]). This diagram it is possible generalize, being based on the achievements in the creation of high-current electron beams and by considering the displacement (scanning) of this focused beam as whole.

The task of this work is the study of some problems of particle dynamics with the scanning of beams for accelerating the ions.

Let us examine the simplest in principle possible diagram of the

acceleration of ions by the scanning of the electron beam (see Fig. 1). From point 0 comes high-current electron beam with the circular cross section. Electrons with total energy $E_e (\gamma \frac{E_0}{m_e c^2})$ after the passage of the focusing system move in the direction OV, forming current I. The electron beam with the aid of the deflection system is moved as whole in transverse direction CD. At point C occurs the admission (capture) of the ions which are carried off by the field of electron beam and are accelerated in direction D. The curve ODB is an instantaneous photograph at the given instant of the position of the particles of the beam, which left the deflection system at the different moments of time.

Envelope of particles of electrons taking into account the Coulomb forces is described by the equation:

$$\frac{d^2 r}{dx^2} = \frac{2A}{r}, \quad (1)$$

where r - radius of beam in section x ; $A = \frac{8 \cdot 10^{-5} I}{\gamma^2}$; I - beam current in amperes; γ - relativistic factor. The solution of this equation is the following expression, which gives connection/communication between the longitudinal coordinate x and a radius of the beam

$$x = \frac{r_0}{\sqrt{A}} e^{-\frac{A}{r_0^2}} \int_{\sqrt{\frac{A}{r_0^2}}}^{\sqrt{\ln \frac{r}{r_0} + \frac{A}{r_0^2}}} e^{z^2} dz, \quad (2)$$

$$r_0 = r|_{x=0}, \quad \alpha_0 = \left. \frac{dr}{dx} \right|_{x=0}.$$

If beam is focused, then at a distance

$$y_0 = \frac{r_0}{\sqrt{A}} e^{-\eta_0^2} \int_0^{\eta_0} e^{z^2} dz, \quad \eta_0^2 = \frac{\alpha_0^2 r_0^3}{2.4 \cdot 10^{-4} I} \quad (3)$$

from the focusing system will be located "sausage node" or crossover with the radius

$$r_{min} = r_0 e^{-\eta_0^2} \quad (4)$$

Electric field on the edge of beam in the region of sausage node is determined by the expression

$$E = \frac{80 I}{r_0} e^{-\eta_0^2} \left(\frac{6}{cm} \right), \quad (5)$$

where I - beam current in the amperes; r_0 - radius of beam in the centimeters.

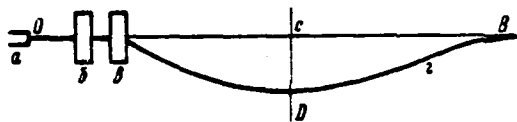


Fig. 1. Diagram of the acceleration of ions by the scanning of electron beam. a) the high-current accelerator; b) focusing system, c) the deflection system; d) electron beam.

Page 205.

Upon the acceleration of ions due to their shifting (scanning) together with the electron beam it cannot be allowed/assumed so that the displacement would occur with too high an acceleration, since as a result of the action of the inertial forces ions from the beam can be lost. If we are restricted to nonrelativistic case $E_i \leq \frac{E_{i0}}{3}$, where E_{i0} - rest energy of ion, then the allowable acceleration is determined by the inequality

$$a \leq \frac{e \mathcal{E}}{M_i}. \quad (6)$$

Taking into account (6) maximum energy to which it is possible to accelerate ions in cut 1, will be determined by the expression

$$E_i = 60 I \frac{\ell}{\tau_0} e \tau_0^2 (\text{eV}). \quad (7)$$

Dependence E_z on I for the different values α_0 and at the prescribed/assigned value γ it is shown in Fig. 2. The straight line AB is determined by the locus of extrema $\frac{\partial E_z}{\partial I} = 0$ and it corresponds to condition $\eta_0 = 1$. For us is of interest region $I \leq I_0$ or $\eta_0 \geq 1$. The decrease of a radius of beam with the prescribed/assigned current leads to an increase in the effective electric field and, therefore, to the possibility of accelerating the ions to the high energies. However, value r_{min} must be bounded below by certain value r_0 , $k < 1$ in order to ensure the necessary phase volume upon injection and during capture of ions into the accelerative mode/conditions. In this case $\eta_0 = \sqrt{2\pi k}$, to what in Fig. 2 corresponds the straight line EF. Requirement on r_{min} limits from above the field of energies to which it is possible to accelerate the ions

$$E_z \leq \frac{60 \ell I}{r_{min}} \quad (8)$$

For the realization of scanning it is necessary that the longitudinal sizes/dimensions of beam Y_0 (distance from the focusing system to "stretching") would be more than its transverse sizes/dimensions. Moreover, the theory of the electron beam is constructed on the assumption about its paraxiality. In accordance with this we set the following limitation

$$\frac{Y_0}{r_0} = \frac{1}{\sqrt{A}} e^{-\eta_0^2} \int_0^{\eta_0} e^{z^2} dz \gg 1. \quad (9)$$

The optimum value of current, which corresponds to maximum energy of the accelerated ions, is equal to

$$I \sim 1.7 \cdot 10^4 \left(\frac{r_0}{y_0} \right)^2 \Phi^2(\sqrt{-\ln k}) \gamma^3(\alpha), \quad (10)$$

$$E_i \sim \frac{\ell}{r_{\min}} \left(\frac{r_0}{y_0} \right)^2 \Phi^2(\sqrt{-\ln k}) \gamma^3(M\theta), \quad (11)$$

where

$$\Phi(z) = e^{-z^2} \int_0^z e^{t^2} dt.$$

The scanning of electron beam is accomplished with the aid of the magnetic or the electrical of the rotary systems whose parameters should be selected, on the basis of the optimum conditions for acceleration. As showed calculations for the computers, the motion of ions with angular shifts of beam in limits of 30° occurs virtually on the straight line, parallel to the direction of scanning, but to the initial thermal velocities of ions do not have in this case a noticeable effect. This can make it possible to manage without supplementary devices/equipment for the focusing of ions, although this question requires supplementary investigation. In order to ensure the maximum permissible or magnetic field of rotary systems according to the law:

$$H = \frac{1.7 \cdot 10^4}{h} \sin \frac{\alpha t^2}{2} (2c), \quad \alpha = 10^{16} \text{ ccm}^{-2}$$

$$\varepsilon = \frac{2.5 \cdot 10^{22}}{h} t^2 \left(\frac{6}{\text{cm}} \right),$$

where h - significant dimension of the deflection system in the centimeters.

For brevity we do not give formulas and are limited to the table of values γ , I , E_i for specific case $r_0 = 5$ cm, $r_n = 0.1$ cm, $\psi_0 / r_0 = 25$, $z = 40$ cm.

γ	2	4	6	8	10	15
I, a	20	150	500	1250	2500	8000
$E_i^{(1)}, \text{MgB}$	0.5	4.0	15	35	65	200

Key: (1) - MeV.

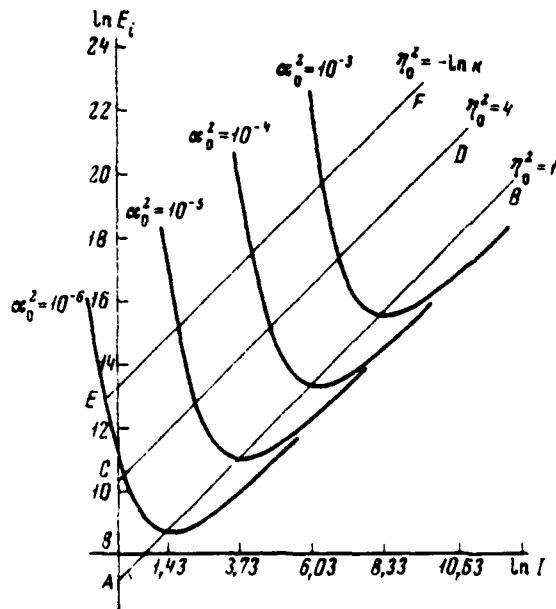


Fig. 2. Dependence $\ln E_i$ on $\ln I$ with $\gamma=10$.

Page 206.

As can be seen from table, for increasing in energy and intensity of the accelerated ions it is necessary to simultaneously increase the values of the current of electrons and their energy (factor γ).

In conclusion let us note that for the application of method of scanning it is necessary to overcome numerous difficulties. However, scanning has the definite advantages, and first of all the fact that

drops off the necessity of the use/application of a complicated compressor and entire system for formation and maintaining of rings and guarantee of their stability.

REFERENCES

1. V.I. Veksler et al. Proc. 6th Internat. Conf. on High Energy Accelerators, Cambridge, 1967, p.289; Атомная энергия, 1968, 24, 317.
2. H. Alfven, O. Wernholm. Arkiv Fys., 1952, 5, N 12.
3. R.B. Johnson. Sympos. on Electron Ring Accelerators, UCHL-18103, Berkeley, 1968, p. 219.

Discussion.

M. S. Rabinovich. What method of the creation of overwinding mode you do utilize with the scanning of electron beam?

I. I. Logachev. First, much here depends on the beam which we will have. Depending on its properties are selected the methods of focusing. Secondly, here is not proposed a concrete scheme, but only method of acceleration.

I. V. Chuvilo. What you can say about the effect of nonparaxiality of electronic and ionic component on the final result of your calculations?

I. I. Logachev. This was not examined?

I. V. Chuvilo. But this can lead to the resonances.

I. I. Logachev. Question of resonances to some degree opened. We do not have this closed system as in the relativistic rings where the same electrons always coexist with the ions. The electrons are carried out by beam. With the ions each time are contacted new portions of electrons.

A. A. Kolomenskiy. I would want to make the following observations in connection with questions of I. S. Rabinovich and I. V. Chuvilo. Focusing of electron beam and creation of necessary overvinding node (crossover) can be obtained with the aid of more or less usual electron-optical systems, in particular, with the aid of the magnetic quadrupole lenses. Special requirements it is necessary to present as electron source in the sense of its homocentricity and exitance. For our estimations we tried to take the values of the parameters, already achieved/reached in the experiment. For example, electron density in the stretching node corresponds so that in the electron rings, rate of rise of magnetic field in the deflection system and sizes/dimensions of the region of field approximately/exemplarily reached correspond to parameters, which characterize the work of injectors in the acting storage machines and, etc.

64. Study program, connected with the development of the accelerator of electron rings in Berkeley ¹.

FOOTNOTE ¹. Work is financed by the U.S. Atomic Energy Commission.
ENDFOOTNOTE.

J. M. Peterson, V. V. Chash, A. A. Garren, D. Keef, G. R. Lambergson,
L. J. Laslett, V. A. Perkins, A. M. Sessler.

(Lawrence radiation laboratory, California university, USA).

I. Introduction.

In the beginning of 1968 in radiation laboratory named after Ernest O. Lawrence of California university in Berkeley was created group for studying the new method of accelerating the ions with the aid of the rings, which consist of relativistic electrons. The idea of this acceleration was advanced and developed by Veksler, Sarantsev and by other scientists in Dubna. [1]. The first results of the work of group were reported for I. All-Union conference on charged particle accelerators in Moscow in 1968. In this report the authors make the survey/coverage of further works and study program.

II. Experiments in obtaining of dense electron rings.

The target of the first large experiment was formation and compression of the electron rings of large density. At the disposal of the authors, fortunately there was the source of relativistic electrons with the large intensity, namely, astro-n - linear induction accelerator with the energy of the particles of 3.5 MeV and the current 400 A.

The axial and radial sections of used in the work experimental installation [2] by the name "Compressor-2" are shown in Fig. 1. The "weakly-focusing" magnetic field is provided by three pairs of the pulse windings, arranged/located outside the ceramic vacuum chamber/camera. Winding 1 serves for the retention of the injected beam with energy of 3.5 MeV on radius 19 cm and after-acceleration and its compression to the radius with which the following winding can continue compression.

Page 207.

This process continues until is obtained the beam with a radius of 3.5 cm and by energy 18 MeV.

Fig. 2 shows changes in the time of a radius of beam, kinetic

energy, magnetic field and field index $n = -\frac{R}{B_z} \frac{dB_z}{dR}$ in ring in a 500-millisecond cycle of compression.

The field index n is the very important parameter, since is determined the possibility of the emergence of the resonance instability of beam. Usually beam becomes unstable, when axial and radial frequencies of betatron Q_z and Q_r (number of betatron oscillations per revolution) are connected with the relationship/ratio:

$$aQ_z + bQ_r = c,$$

where a , b and c - small integers, which depend on the means of the disturbance/perturbation of the magnetic field, which calls the instability of beam. In view of the fact that of frequency of betatron Q_z and Q_r are determined by the index of a field slope n , namely, $Q_z^2 = 1 - n$ and $Q_r^2 = n$, then, obviously, at some values of n (5/9, 4/9, 9/25, 1/4, 1/5, 1/9, etc.) are possible resonances with a strong increase in the sizes/dimensions of beam, if occurs the corresponding nonlinearity or the distortion of magnetic field and if resonance passes sufficiently slowly. During the experiments with "Compressor-2" for achievement of necessary compression it proved to be necessary to select the mode/conditions of change n only for the initial section of the cycle of compression (with a large radius of beam), when distortions of magnetic field were maximum. After this selection n the injected beam was compressed almost without the

DOC = 80069216

PAGE

893

losses. Ring density proved to be equal to about $4 \cdot 10^{12}$ electrons and it was limited faster to injector, than by some effect in the compressor.

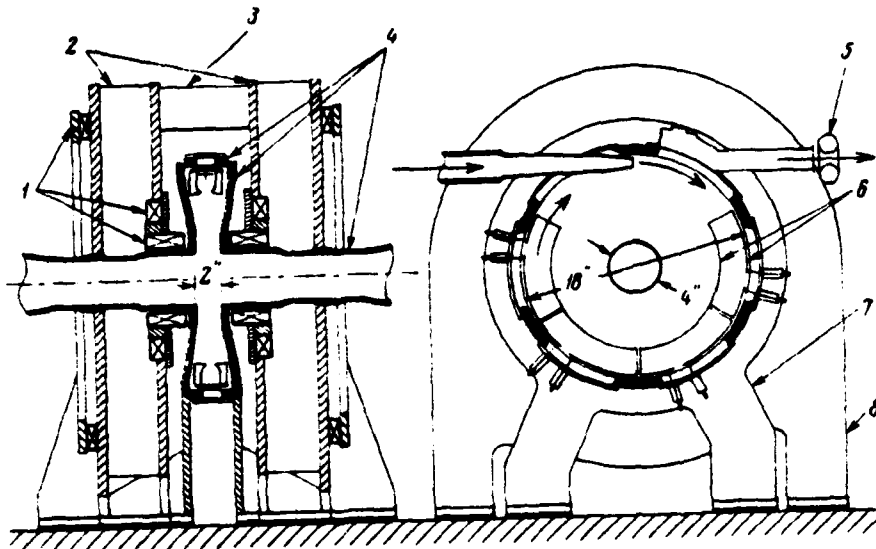


Fig. 1. The longitudinal and cross sections of installation "Compressor-2": 1 - winding 1, 2 and 3; 2 - frames, which support windings; 3 - spacer, frames; 4 - ceramic vacuum chamber/camera (bore of 45.7 cm); 5 - monitor of the injected beam; 6 - deflecting electrodes; 7 - support of vacuum chamber; 8 - support of windings.

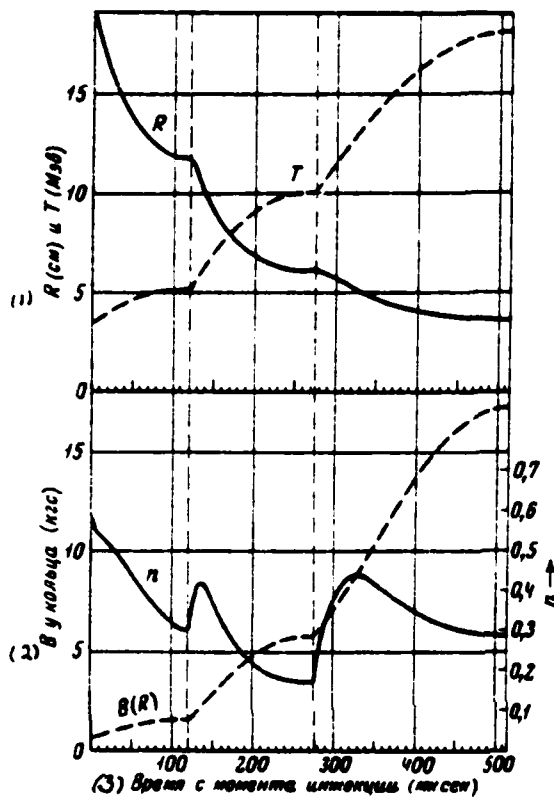


Fig. 2. Change in parameters during cycle of compression upper curves: radius of ring (cm) and kinetic energy of electrons (MeV). Lower curves: the index of magnetic bump (right axis/axis of ordinates) and magnetic field strength in the ring (left axis/axis of ordinates, kg).

Key: (1). R (cm) and T (MeV). (2). V in ring (kg). (3). Time from moment/torque of injection (μs).

Page 208.

With the work it was observed no essential effects of space charge, with exception of the useful mechanism of self-engagement, which occurs with the currents are above 50 or 75 A. Ring remained stable during several milliseconds, which was limited only to a change in the magnetic field, which brings finally to value $Q_{\gamma} = 1$, when beam became unstable and was lost. Were observed also the effects of ionic focusing. For the filling of ring with ions into the chamber/camera with the aid of the rapid-action valve was admitted a small quantity of gas. The introduction of ions caused earlier resonance onset $Q_{\gamma} = 1$.

With the energy 18 MeV the synchrotron radiation of ring very bright and can be photographed for explaining spatial distribution of electrons within the ring. Measurements showed that the density is distributed according to the law of Gauss, and the rms values of an inside radius of rings were 1.6 and 2.3 mm, which will agree with the results of the measurements, carried out by the sound method. On the basis of geometric dimensions and quantity of electrons in the ring was calculated the maximum value of the electric field of 12 MeV/m, which is already of interest from the point of view of the acceleration of ions. It must be noted that this intensity can be achieved/reached without the special difficulties and, apparently, it

is not axiaua.

III. Experiments in the acceleration of ions.

The following task of our group consisted of the acceleration of the electron ring, loaded with ions. It was necessary to form a ring, to load with its several percentages of hydrogen ions and to accelerate from to the energy into several MeV at the length of 0.5 m with the aid of the magnetic field. The experimental installation for conducting these works, named "Compressor-3", it is shown in Fig. 3.

Basic differences in this installation from "Compressor-2" consist of the following:

1) winding by 3 was replaced by the solenoid, in which was accelerated the ring;

2) winding 1 was modified in order to reduce to a minimum a variation in the decrease in magnetic field n on the first several centimeters of compressor.

Primary attention during the design of "Compressor-3" was given to the translation/conversion of the compressed ring from the magnetic potential pit into the accelerating solenoid, in which the

magnetic field is actually constant. In this case it is necessary to ensure supplementary focusing in order to avoid, first of all, the vertical flaring of ring ($Q_z=0$), and in the second place, its radial instability with approximation/approach Q_r to unity. The accelerated positive ions favor focusing in both directions, but the focusing forces with the light ion load are insignificant. Focusing by image with the aid of the conducting cylinder of the type of "squirrel wheel" [3] is more effective and more advisable: it increases frequency of axial betatron Q_z and it decreases the frequency of radial moving aside resonance Q_r 1.

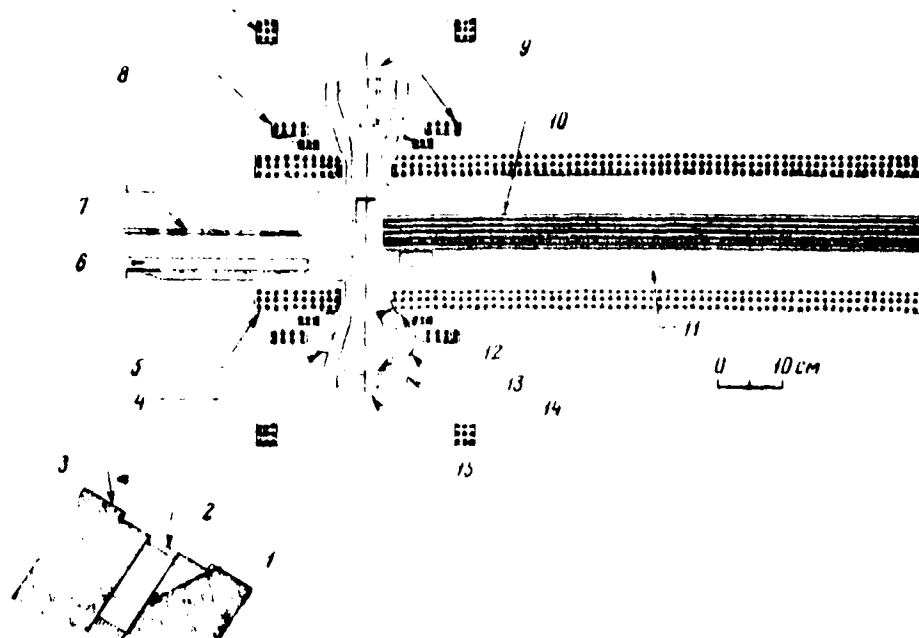


Fig. 3. View of the cross section of installation "Compressor-3".

1 - phototube; 2 - plastic scintillator; 3 - detector of X-radiation;
 4 - magnetic measuring turn; 5 - winding by 3; 6 - admission valve; 7
 - moving reflecting probe; 8 - winding 1, 2, 2A; 9 - moving
 collector probe; 10 - cylinder; 11 - moving collector probe; 12 -
 deflecting windings; 13 - loop antenna; 14 - corundum vacuum
 chamber/camera; 15 - sapphire windows for SHF or synchrotron
 radiation.

The attempt to accelerate ions was not crowned with success because in "Compressor -3" could not shape the rings with the necessary parameters. Thus, we did not succeed in even attempting to accelerate ions in the well shaped ring within the time, which was isolated to group for the work with the accelerator astro-W. The authors encountered two difficulties, first of which was the sharply pronounced effect of negative mass. With the increase of the current of the injected beam approximately/exemplarily to 150 A the radial breadth of ring increased to the value, which corresponds to 100/o energy spread, which strongly decreased electron density in the ring. The effect of negative mass occurred due to the unexpectedly small energy spread in the beam, obtained from the injector which was completely altered within the time between two experiments. While the energy spread in the injector during the experiments with "Compressor-2" was approximately 0.50/o, in the new injector it did not exceed 0.20/o. For measuring the energy scatter "Compressor-3" was utilized as magnetic analyzer. Since the threshold of negative mass changes as $(\Delta p/p)^2$, the results of measurement indicate that in "Compressor-3" the threshold is considerably lower than in "Compressor-2".

The second difficulty, which set during the experiment

"Compressor-3", was axial beam blowup and loss of its larger part due to the single-particle resonances. The loss of particles in essence occurs with $n=0.5$ (i.e. when $Q_y - Q_z = 0$). The system of windings permitted implementation of an injection with $n < 0.5$, but attempt of work in this region led to the considerable losses of beam in the presence of resonances $n=9/25$ and $n=1/4$. These resonances became apparent also during the experiments with "Compressor-2", but then they brought less than uneasiness/unrest, since the form of magnetic field was different.

IV. Program of the works, being conducted at present.

The reasons for the instabilities which they met during the experiment with "Compressor-3", now are sufficiently well studied, and into construction of installation introduced the necessary changes. In order to get rid of the instability, called by the effect of negative mass, first of all, it is proposed to supply on the path of bundle foil of variable/alternating thickness, which will ensure a sufficient instantaneous energy spread. The instabilities, which appear as a result of the resonances of single particles, are excluded by the change in the form of magnetic field, which decreases the second by third derived fields ($\frac{d^2 B_z}{dR^2}$ and $\frac{d^3 B_z}{dR^3}$), causing resonance $n=0.5$. Furthermore, the decrease of the azimuthal distortions of magnetic field will exclude resonances $n=9/25$ and $n=1/4$. All these

changes in the construction/design of installation are checked in the recently initiated new experiments with the compressor. In winter 1970-1971 we proposed to derive and to accelerate the loaded with ions electron rings.

V. Equipment of new injector.

For the more systematic execution of our program of works in the course of the latter/last several months in Berkeley is installed new injector-accelerator. This linear induction accelerator with the energy 4 MeV and maximum current 500 A in the principle is similar/such to injector. Astro-M, but has smaller duration of impulse/momentum/pulse (from 30 to 40 ns) and smaller repetition frequency of the accelerating cycles (1 Hz), which simplifies and reduces the cost of its creation. The construction/design of injector is modular: it consists of seventeen resonators which by driving pulses by the duration of 40 ns from the forming lines of Bloembergen. On the clearance of each resonator the voltage is equal to 0,25 MV. Fig. 4 shows one of the resonators. Inductive cores are made from ferrite, but not of the convoluted metallic strip/film, as this was done earlier. Resonators are not only partly the injector, but also serve as models for testing the possibility of their use/application for accelerating the electron rings in the accelerator to the high energies. Below this question will be examined in more detail.

Our electron gun about new accelerator, shown on Fig. 5, consists of five such resonators, arranged/located adjacent to each other.

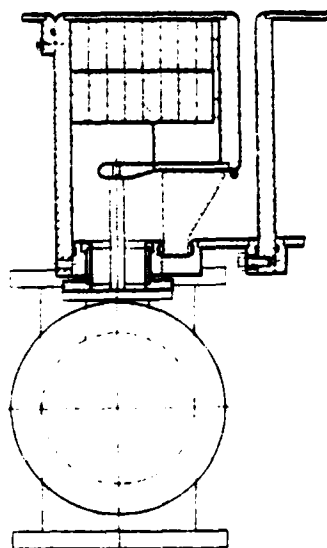
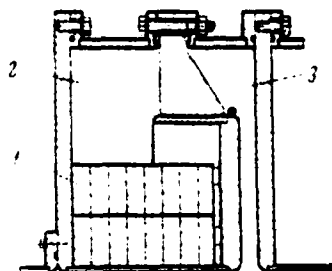


Fig. 4. Means of the cross section of the resonator of linear induction accelerator. 1 - ferrite; 2 - oil; 3 - vacuum.

Page 210.

They are connected by means of the central conducting rod which

terminates in the fifth resonator and holds the emitting cathode. The voltage of cathode is, thus, the sum of voltages of five resonators is 1.25 MV.

This accelerator is assembled and successfully tested on the energy up to 2 MeV, and now is used in the experiments with compressor. Until now, were utilized only the cathodes with the autoelectronic emission, although the electron gun makes it possible to apply thermionic cathodes. Cathodes with the autoelectronic emission were selected due to their simplicity and up to the present time show satisfactory results.

The maximum current, obtained from these cathodes, comprised more than 1000 A with the acceptable time of the service (more than $2 \cdot 10^5$ impulses/moments/pulses). The density of beam in the phase space is sufficient for shaping of electron rings. Instantaneous energy scatter is not still accurately measured, but it is known that it is less than 0.50/o.

The schematic of the arrangement/position of injector and research equipment is shown in Fig. 6. Installation for formation and accelerating the electron rings is prepared for the assembly in the experimental hall at the end of the location for the injector.

VI. Prospects for further experiments.

We continue to optimistically estimate the possibilities of applying the accelerators of electron rings for accelerating the ions both to the averages and to the high energies. Very encouraging are the results, obtained by the group of Sarantsev in Dubna [4]. The analysis of the technical and economic aspects of this problem, carried out in Berkeley, also yielded positive results.

Recently we investigated the possibility of constructing the proton accelerator with the electron rings to the energy of 60-100 GeV [5, 6].

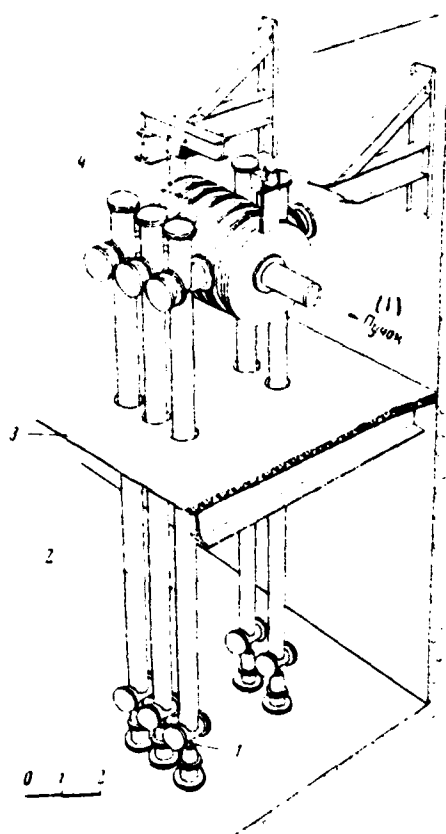


Fig. 5. The schematic of five-resonator electron gun. 1 - discharge gap; 2 - line of Bloembergen; 3 - flooring; 4 - the accelerating cavities with the pulse supply, loaded with ferrites; 5 - beam, scale figure gives in the meters.

Key: (1). Beam.

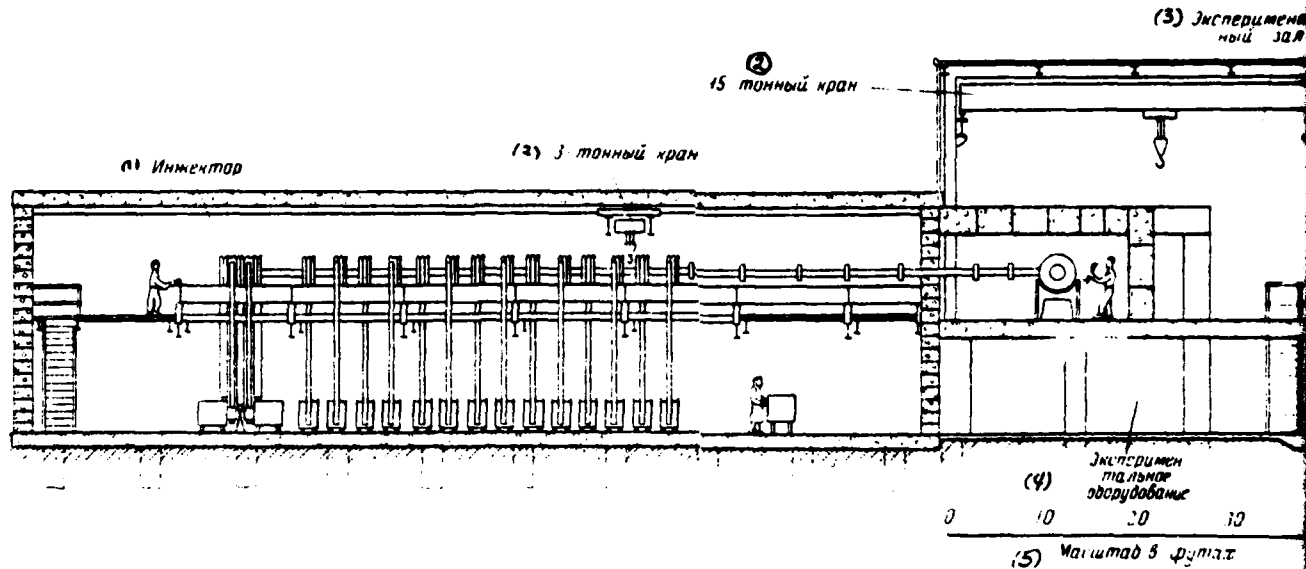


Fig. 6. Drawing of linear induction accelerator and location for the experiments with the electron rings.

Key: (1). Injector. (2). 3 - ton/grand tap/crane. (3). Experimental hall. (4). Research equipment. (5). scale in feet.

Page 211.

This machine must consist of compressor, 320-meter accelerating section with the resonators and 160-meter section with the magnetic acceleration. Both types of the accelerating sections are shown in Fig. 7.

First type section consists of the series/row of the resonators, loaded with inductance of the same type, as in the injector-accelerator (Fig. 4). The average/mean value of external accelerating field, created by resonators, is 5 mV/m. Between the resonators are arranged/located the superconducting windings, providing the solenoidal leading field 30 kg. Although a radius of the electron rings of order 2-3 cm, a span channel in the resonators have a radius of 19 cm. This is made for the purpose of the decrease of electromagnetic energy loss due to the interaction between the electrons and the accelerating structure. Energy loss changes as the square of a quantity of electrons in the ring and limits the quantity of electrons which for this machine composes $3 \cdot 10^{13}$ electrons to the ring. This effect impedes the use of the focusing cylinder which can sharply increase energy loss. Energy loss, furthermore, caused axial defocusing of electrons in the ring; however, latter/last investigations showed that this the effect was small and does not set substantial limitations on the parameters of accelerator [7].

In the version in question electron ring creates the electric field of 500 MeV/m and it is loaded with 0.50/o of protons. The set of energy by protons in the resonator section composes approximately/exemplarily 125 MeV/m, so that total energy after the

passage of 320-meter section reaches 40 GeV. The average/mean rate of acceleration of protons in this section corresponds only to fourth of maximum voltage of electric field in the ring. This is done for decreasing the polarizational effects within the ring. In the first section the electric ion rings holds only ionic focusing. Therefore there is a danger in the instability of rings when the centers of positive and negative charges are strongly mixed relative to each other. The self-consistent solution of this problem is not yet found.

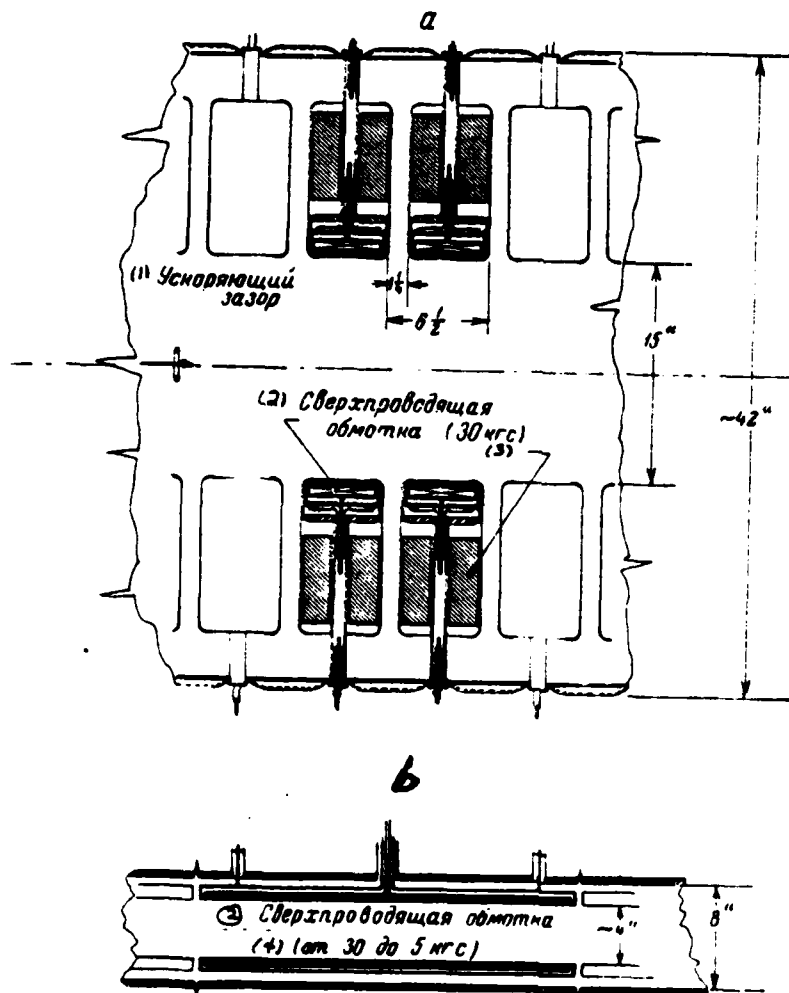


Fig. 7. Drawings of two types of the accelerating sections (sizes/dimensions are given in inches). a) resonator section; b) section with the magnetic acceleration.

Key: (1). Accelerating clearance. (2). Superconducting winding. (3). kg. (4). from 30 to 5 kg.

Page 212.

The latter/last section of the accelerator with a length of 150 m with the collapsible/dropped along the axis magnetic field is the slightly expanding toward the end superconducting solenoid. Here protons increase their energy approximately/exemplarily two times, reaching 80 GeV toward the end of the section. In this section effective accelerating field is equal to the half maximum electric field in the ring (but not $1/4$ as in the first section), since here ring is focused by cylinder and the polarization of ions and electrons does not threaten the completeness of ring.

On the parameters of electron rings are superimposed sufficiently strict limitations. Besides the limitation, connected with the radiation losses during interaction examined above of ring with the resonators, it is necessary to ensure the stability of ring during entire process of its shaping and acceleration. A quantity of electrons in the ring must be lower than the thresholds of instability of the type of negative mass, instability due to the final conductivity of walls and due to transverse incoherent space-charge effect. All these conditions strongly limit the possibilities of design. The interesting solution is proposed by

Pellegrini [8] the method of compressing the ring due to the use of a mechanism of synchrotron radiation. Unfortunately, this the process of compressing the ring due to the radiation/emission requires the time of the order of several milliseconds. Are possible other simpler versions of compressor. Below are presented typical parameters of one of the versions.

Energy of the injection of 8 MeV.

Radius of injection 50 or 100 cm.

Final energy of 12 MeV.

Terminal radius 2 or 3 cm.

Final small radius of the ring of 0.1 cm.

Initial scatter along the impulses/momenta/pulses
0.4-1.0o/o.

Final scatter along the impulses/momenta/pulses 0.7-1.0o/o.

Number of electrons in the ring $(1.5-3) \cdot 10^{13}$.

Although above we spoke about the accelerator as 80-GeV, it is necessary to remember that in such machines actual output energy strongly depends on the value of the load of electron ring by ions and on the characteristics of ring itself. With the same construction/design of the accelerating sections final energy can be 100 GeV at average/mean intensity $5 \cdot 10^{12}$ protons per second (repetition frequency 100 Hz), or 60 GeV at intensity $2 \cdot 10^{13}$ protons per second (there is assumed, of course, optimum mode/conditions is each time).

The given by us estimate of the cost of this accelerator to the energy 80 GeV was based on the experience of laboratory in the construction of the superconducting coil electromagnets, linear induction accelerators and elements/cells of usual accelerators. We arrived at the conclusion that for obtaining the protons of high energies the cost/value of the construction of accelerator with the electron rings is considerably less than usual synchrotron.

The acceleration of large ions with the aid of the electron rings, of course, is considerably simpler than the acceleration of protons. Heavy-ion accelerator can consist only of compressor and section with the expanding magnetic field. It has small sizes/dimensions, it is comparatively simple and in it do not act limitations, connected with the electromagnetic losses in the

resonator accelerating section.

Keeping in mind entire that outlined above, it is possible to arrive at the conclusion that the idea of electronic circular accelerator is very promising and is expedient its intense further development. In the implementation of the programs of the development of the accelerator of electronic rings in the Lawrence radiation laboratory participated colleagues' large group, including E. J. Lofgren, J. B. Rechen, R. U. Allison, D. George, A. Entlis, L. Smith, A. U. Lyuchcho, K. Pellegrini, K. Bove, A. Nakau, J. M. Hauptmann, E. K. Khartvig, A. Faltens, H. D. Lancaster, U. R. Baker, F. Velker, R. G. Nemets, K. D. Payk, U. U. Salisig, R. T. Eyveri, Kh. P. Hernandez, J. R. Menegetti.

REFERENCES

1. V.I. Veksler et al. Proc. 6th Internat. Conf. on High Energy Accelerators, Cambridge, 1967, p. 289.
2. D. Koef et al. Phys. Rev. Letters, 1969 22, 558.
3. G. V. Dolbilov et al. Transactions of the 7th international conference on the charged particle accelerators high-energy. T.P. Iss. AS ARM SSR, Yerevan, 1970, page 535.
4. V. P. Sarantsev. The transactions of the 7th international conference on the charged particle accelerators high-energy. T.P. Iss. AS ARM SSR, Yerevan, 1970, page 440.

5. ERA Group at LRL. Conceptual Studies for New Technology Proton Accelerators (50-100 Gev.). LRL Internat. Report ERAN-108, April, 1970.
6. C. Boyer and C. Pellegrini. LRL Report UCRL-19892, June, 1970.
7. E. Keil, C. Pellegrini and A.M. Sessler. LRL Report UCRL-20069, Oct. 1970.
8. C. Pellegrini. LRL Report, UCRL, 19815, May 1970.

Discussion.

V. N. Tsytovich. Which the reason for the construction of new injector? Is connected this with the need for excluding the instabilities which were observed in your first experiments?

J. Paterson. We now construct our own injector in Berkeley since that injector, which we wanted to utilize, was intended for Livermore and it is very loaded. This is main reason. Furthermore, we want so that this accelerator would possess necessary to us special features/peculiarities, in particular, if we speak about the effect of negative mass, then energy spread proves to be very narrow, and we have a series/row of ideas on increase of this scatter. One of these ideas is reduced to an increase in the area of filament emission.

V. N. Tsytovich. Was observed difference in the character of the instability of ring under conditions when it was found close to walls (at the initial stage), also, at the end of the compression?

J. Peterson. All basic instabilities were observed at the initial stage when a radius of ring was large. Upon transfer to a small radius we did not have instability. At this point the ring could exist sufficiently for long, and we held its ~ 20 ns, moreover duration was limited only to a decrease in the charge in the line.

V. N. Tsytovich. How did change of radiation/emission of ring with a change in the parameters of the injected electrons and, in particular, the energy spread?

Page 213.

J. Peterson. We observed a whole series of emission frequencies, in particular, cyclotron frequency. Radiation/emission continues during 15-20 ns. furthermore, were observed wavelengths up to 3 cm; in this case, if was increased energy spread, decreased the intensity of radiation/emission at these wavelengths.

P. R. Zenkevich. How much approximately/exemplarily electrons were injected into the chamber/camera and how much it did remain after compression?

J. Peterson. In the first experiments we led current to 150 mA upon 3-4 reverse injections. in this case maximum effectiveness reached

1/3. According to our estimations, toward the end of the compression the losses did not exceed 20o/o. This in a good experiment, and in the poor - remained about 10o/o.

I. M. Kapchinskiy. There are estimations of the emittance of electron beam?

J. Peterson. As a rule, emittance of the injected beam was 0.07 cm. mrad. However, the admittance of the system of injector composed approxisately/exemplarily the half this value. Therefore we could not take entire beam.

A. A. Vorobyev. Cannot lecturer give explanations about the final goals of program?

J. Peterson. Generally to speak about this is possible much. We would want to construct in Berkeley accelerator on 80 GeV; however, for this we thus far do not have means.

65. Synchronous radiation/emission and formation of rings in the accelerators with electronic rings.

K. Pellegrini

In the accelerators with the electron rings hope to obtain high rate the accelerations of ions $\frac{dE_i}{dz}$. In order to hold ions within the ring, is required high electric field E_H , whose value is determined by the relationship/ratio

$$\frac{dE_i}{dz} < eE_H Z.$$

For the ring with the cylindrical section and the even distribution of electrons within this cylinder the field, which holds ions, is proportional

$$eE_H \approx \frac{N_e}{aR},$$

where N_e - quantity of electrons, a , R - small and large radii of ring.

Distilling rate of energies by ions is proportional to the following expression

$$\frac{dE_i}{dz} \approx \frac{eE_{ex}}{f + \frac{E_e}{E_i}},$$

where E_{ex} - the applied field, which accelerates ring; f - ratio of a quantity of ions to a quantity of electrons; E_e, E_i - energy of

electrons and ions.

If ring is formed by means of the magnetic up to now, energy of electrons and radii of ring depend on their values at the moment of injection as follows:

$$R = \frac{R_0}{B^{1/2}}, \quad \alpha = \frac{\alpha_0}{B^{1/2}}, \quad E = E_0 B^{1/2}.$$

Here index "0" noted the initial values of values, and B is a relation of the finite and initial values of magnetic field.

It is clear that with a decrease of radii of ring and an increase in the confining field increases energy of electrons and, thus, is geared down of the set of energy by ions.

It is interesting to examine the possibility of the use of other processes for the formation of electron rings with other laws of value change in the process of compressing the rings which would make it possible to improve the characteristics of accelerator. For example, it is possible to compress ring in the magnetic field so that the value of field in the electron orbit and the magnetic flux through the section of ring would change independently of each other. An example of this class of compressors is the static compressor in which with the decrease of a radius of ring the energy of electrons remains constant. In this article attention is given to the possibility of using the effect of synchrotron radiation. In this

case decrease the energy of electrons and the radius of ring, and the field, which holds ions, and dialing rate by them energies grow/rise.

Let us examine the electrons, which move in the magnetic field with the permanent gradient, characterized by index of decay n . In this case a change of the large radius of ring in the course of time is described by the expression:

$$\frac{R}{R_0} = \left\{ 1 - \frac{2}{3} \frac{r_e c}{(m_0 c^2)^3} \frac{3n-1}{1-n} \frac{E_0^3}{R_0^2} t \right\}^{\frac{1}{3n-1}},$$

where R_0 , E_0 - initial values of a radius and energy, r_e - classical radius of electron, S - speed of light, m_0 - rest mass of electron.

Page 214.

Energy of electron changes according to the law

$$\frac{E}{E_0} = \frac{R^{1-n}}{R_0},$$

and energy spread is determined by the expression:

$$\frac{\Delta E}{E} = \left(\frac{\Delta E}{E} \right)_0 \left(\frac{R}{R_0} \right)^{1-3n}.$$

Usually the insignificant effect of quantum fluctuations in this case is not considered. Synchrotron radiation affects the amplitude of betatron oscillations less than to the energy spread, and a change in the amplitude of betatron oscillations occurs in essence due to

the adiabatic fading:

$$\frac{b}{b_0} = \left(\frac{R}{R_0} \right)^{\frac{n}{2}}.$$

Let us note that with satisfaction of condition $n < 1/3$ the energy spread in the course of time decreases, and the amplitude of betatron oscillations changes little.

Thus, with the aid of only one synchrotron radiation it is not possible, apparently, to strongly decrease a small radius of ring.

It is possible, however, to expect that the combined use of different methods of compressing the ring, for example, of static compressor and supplementary compression due to the synchrotron radiation, completely can give rise to of rings with very large magnitude of confining field, on the order of 1 GeV/m.

Let us note that the time, necessary for a sufficient decrease of a radius of ring caused by the radiation/emission, can be sufficiently large, for example, order of tens of milliseconds. In this case appears the problem, connected with the process of the ionic load of ring, since for maintaining the quantity of admixtures/impurities in the ring in the permissible limits it is necessary to support in the chamber/camera vacuum not less than 10^{-11} torr.

Discussion.

A. N. Lebedev. Under all whether conditions it is possible to disregard the effect of the fluctuations of radiation/emission?

K. Pellegrini. No, this it is possible to disregard not always, but to the specific values of wave energy. However, in all practical cases with which we deal, quantum fluctuations can be disregarded/neglected.

A. A. Vorobyev. There are whether the energy estimations of the examined in the process work of compression?

K. Pellegrini. We carried out the estimations which showed that this method makes it possible to obtain the high values of confining fields, it removes different instabilities, makes it possible to increase energy of injection, without increasing substantially final energy. So that this method, in our opinion, it possesses the doubtless advantages. Only problem is the problem of vacuum. As far as particle losses are concerned, then such estimations we did not make.

A. A. Kolomenskiy. We examined the influence of radiation effects on the dynamics of electron relativistic rings. The general/common/total conclusion/output are analogous to that which were made by Dr. K. Pellegrini; however, there are disagreements, which can prove to be essential in practice. First, relative to the effect of energy spread. Since the effective electronic field in ring $\delta \sim [R(\alpha + \beta)]^{-1}$ depends on the disturbance/perturbation of instantaneous radius $\rho_g = R(1-n)\frac{\Delta E}{E}$, but it is not direct from $\Delta E/E$, then it is necessary to superimpose the requirement of compression on ρ_g , which leads to condition $n < 2/3$, and not $n < 1/3$ as in the report to Dr. Pellegrini.

In the second place, in the report is utilized the law of fading the amplitude of radial oscillations in the form $\alpha \sim R^{n/2}$, which, corresponds to usual adiabatic fading. The influence of radiation damping here Dr. Pellegrini disregards. However, calculation gives for the radiation damping result $\alpha \sim R^{\frac{n}{2}}$, in the precision/accuracy which coincides with the adiabatic. Therefore the full/total/complete dependence of amplitude on a radius takes form $\alpha \sim R^n$, but not $\alpha \sim R^{n/2}$, as it is given in the report.

66. State of works on the project of the accelerator of electron rings Karlsruhe.

G. Dustman, V. Khaynts, G. Germann, P. Kapp, G. Kraut, L. Shteynbok, L. Tsernial'.

(Institute of experimental nuclear physics of the center of nuclear research and university of Karlsruhe, FRG).

Device/equipment of accelerator into a general state of works.

The program of works on the accelerator of electron rings in Karlsruhe has as a goal testing special components and by the method, developed/processed in connection with the predicted in the future construction of heavy-ion accelerator.

As the electron gun is utilized the produced by industry electron source with the autoelectronic emission. After it is arranged/located the three-meter line of the transportation of electrons with the quadrupole lenses, which makes it possible to investigate the effects of space charge and to arrange the detecting devices/equipment, which is very important from the point of view of the transportation of intense charged particle beams.

Page 215.

Ring is formed in the process of three-stage moderately rapid compression. The moderately rapid cycle of compression was selected on the basis of general/common/total technical concept, placed as the basis of the project of accelerator. In comparison with the rapid compression it possesses the advantage that it imposes lower requirements on the precision/accuracy of starting/launching and synchronization of equipment. In comparison with the slow compression more easily are fulfilled the requirements, which concern vacuum and lifetime of ring. From the point of view of the stability of ring very important value have tolerances on field errors of compression coils. This question is examined below in more detail.

Equipment for accelerating the ions is found in the production. Here is involved the special source of molecular beams, intended for loading of rings, and constructed specially for the accelerator of electron rings, and also the rapid system of expansion.

The general view of the installation is shown in Fig. 1.

Besides the mentioned above works are conducted also the

developments of compression chamber/camera. Several versions constructions/designs with the use of different materials were examined from the point of view of fulfilling such requirements as neutral behavior in the pulse magnetic fields, guarantee of fine vacuum, high mechanical strength and universality in the sense of experimental possibilities, and also cost/value and possibility of production by industry. It was explained that at the stage of experiment to the load of rings by ions it is expedient to utilize cheap and universal chamber design from the epoxy ring with the lateral covers/caps from the special glass. Vacuum tightness of chamber/camera is provided with the aid of screw ferrules. Several chambers with a diameter of with 50 cm with axial flanges for the expansion ducts and without them they were tested with the vacuum to 10^{-6} torus. More fine vacuum can be obtained with the rings from the stainless steel. Special surface treatment and the decrease wall thickness to 1 mm made it possible to lower the distortion of the field index on a radius of injection to the value, lying beyond the limits of errors of measurement. The best magnetic and vacuum properties expect to receive for the one-piece/entire construction/design chambers/cameras with the expansion rings (from oxide of aluminum), which is developed/processed together with industry. this inconvenient and expensive chamber/camera it is proposed to utilize not earlier than will be completed the experimental investigations of the stages of compression and loading

of rings, which require a change in parameters and means of diagnostics. Continued also the work above the electronic injector, prepared with industry. Injector gives current of approximately 6000 A, the energy of electrons lying/resting at the range from 1 to 2.3 MeV during 30 ns. In the case of such intense beams important role play the effects of space charge; they assume that precisely these effects near the cathode and on the way of acceleration lead to the fact that useful beam in compressor is only several percentages of the intensity of entire useful beam. The investigations of autoelectronic emission from different cathodes and change in the potentials along the way of acceleration must lead to an increase in the intensity of useful beam. These investigations are conducted in parallel with the basic experiment on the second installation.

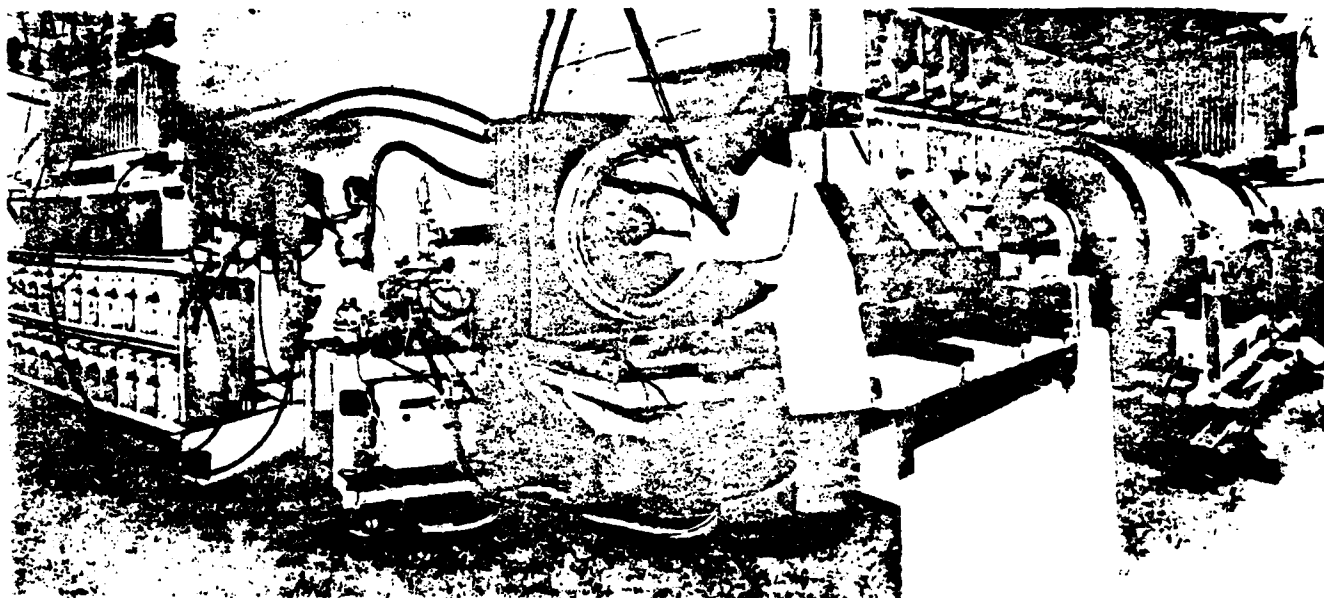


Fig. 1. Experimental accelerator of electron rings in Karlsruhe.

Characteristics of the supply of power and switches: voltage 30 kV, power 3x50 kVA, pulse frequency 1 Hz, switching elements - spark clearances. Characteristics of compressor: currents 10, 20 and 30 kA, maximum induction of approximately 22 kg, radius of injection 23.5 cm. Characteristics - line of the transportation of the beam: the length of 3 m, the focusing elements/cells - 6 quadrupole lenses and 2 solenoids. Characteristics of the injector: the generator of Marx and electron source with the autoelectric emission; energy of electrons 2.2 MeV, current 6 A, the effective length of impulse/momentum/pulse of approximately 5 n s.

Page 216.

Optimization of field in Helmholtz's powerful/thick coils.

Single-particle betatron resonances are very essential the process of formation of electron ring in the compressor. They are caused by the disturbances/perturbations of magnetic field, which have different origin. One of the possible reasons for these disturbances/perturbations is the structure of the very winding of Helmholtz's high-current high-voltage coils. Due to the high currents is required the considerable section of conductor; high voltage of supply leads to the need for ensuring durable radial and axial insulation/isolation. Because of this, and also due to the need for jumpers unavoidably appear the disturbances/breakdowns of azimuthal symmetry. Fortunately, the system of Helmholtz's coils consists of two separate coils. It is possible to show that in the case of two identical coils, arranged/located on both sides from the median plane, the error for total magnetic field in this plane, created by both coils, strongly they depend on the azimuthal shift/shear Δ of one coil relative to another (angle of their rotation relative to

common axis), for example, the shift/shear between the positions of points of connections. Thus, if the errors for the field of one coil, caused by unavoidable inaccuracies in the production, prove to be too great, it is possible to attain the considerable decrease of the errors for the resulting field of two coils, rotating one of them relative to another around the common axis.

As an example it is possible to indicate the results of the study of the errors for the total field of the coils of two different constructions/designs in their median plane. Both systems of coils have parameters, indicated below:

The basic parameters of the coils:

The mean radius of the coil ... 360 mm.

Median axial distance between the coils ... 620 mm.

Diameter of the conductor (round cross-section) ... 10 mm.

Number of turns in the coil ... 6.

Number of layers in the coil ... 2.

Thickness of insulation/isolation between the turns (axial) ... 3 mm.

Thickness of the lamination insulation (radial) ... 4 mm.

The only difference between them is the form of transition between two layers of turns. One of the coils, the so-called coil "with the sharp transition", has the radial connection between the layers (two layers on three turns). The construction/design of second type coil ("with the gradual transition") provides steady transition on a radius between two layers, for the elongation/extent of one ~~full~~/total/complete turn. From the design considerations the axial distance of this turn from the adjacent is necessary to increase in comparison with the usual.

Curves in Fig. 2 and 3 depict the errors for field in the function of azimuthal angle θ (value $\theta=0$ is selected arbitrarily). In the figures are shown the relative deflections of field $\Delta B_z/B_z$ on the circumference of the arbitrarily selected radius of 22.5 cm in median plane (index z designates axial component). Curves in Fig. 2 depict the errors for the field of separate coils of both types. In Fig. 3 (on the increased 10 times scale) are given accumulated errors for the field of the pair of coils in the function of azimuthal angle Δ , to which is turned one coil relative to another. Are given data only

for the vicinity of optimum angle Δ . Generally speaking, accumulated errors it is considerable (to ten times) more than for the optimum values Δ . It is evident that for both constructions/designs of coils is a specific optimum value Δ . Is possible also the analogous optimization, for example, of gradient errors.

Load of rings by ions.

For the correct work of the accelerator of electron rings is required completely specific load of rings by ions. Was developed device/equipment for loading of ring by the pulse molecular beam, selected, so that it is possible to less disrupt the vacuum in the compression chamber/camera.

The installation diagram is shown in Fig. 4.

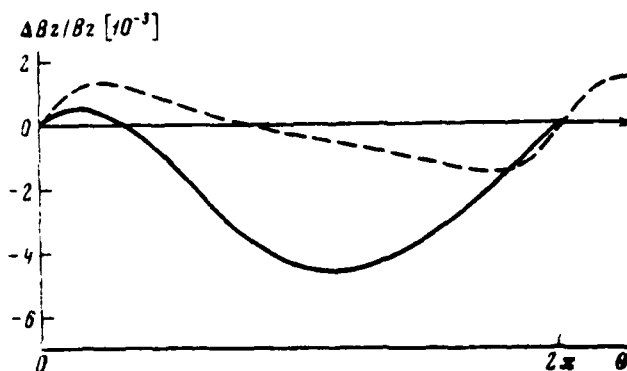


Fig. 2. Errors for the field of single coils with the "continuous transition" (solid line) and with the "sharp transition" (dotted line).

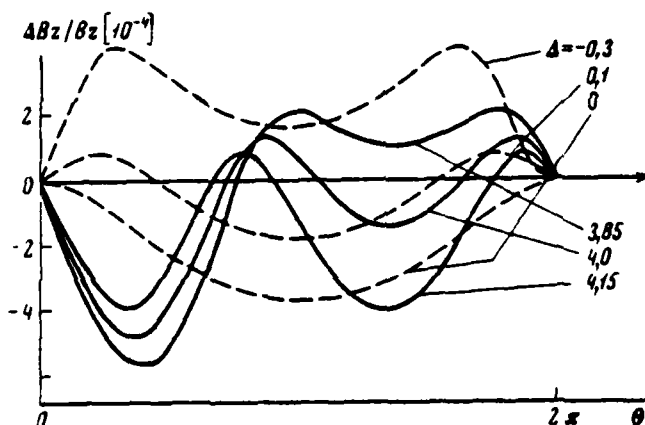


Fig. 3. Errors for total field of pair of coils with "continuous transition" (solid lines) and with "sharp transition" (dotted line) in vicinity of optimum value of angle of relative rotation Δ .

We required so that the fraction/portion of load due to the molecules of residual gas in vacuum compression chamber would not exceed 100/o of the full load. Hence it follows that the partial pressure H_2 must be less than $2 \cdot 10^{-8}$ torr; the partial pressures of other gas, for example CO_2 or H_2O , must be still less than by approximately order. In order to satisfy these requirements, were developed two constructions/designs of vacuum chambers in which can be achieved/reached the vacuum above 10^{-8} torus.

1) One-piece/entire chamber/camera from oxide of aluminum.

2) Ring made of the stainless steel with the glass parts on viton multiplexing.

For the evacuation of chambers/cameras are utilized turbomolecular and cryogenic pumps.

The source of molecular beam is arranged/located at a distance of approximately 1 m from median plane of compressor in order not to distort magnetic field. The density of the flow of molecules, necessary for loading of rings, is determined by the sizes/dimensions of the compressed ring and duration of loading (about 100 μs). It

must be order $10^{16}-10^{17} \text{ cm}^{-2} \text{ s}^{-1}$ (depending on the rate of molecules and their ionization cross section). The intensity of usual molecular beam of the furnace several orders below. However, the method, which uses a supersonic flow through nozzle, makes it possible to comparatively easily obtain such intensities.

The gas, utilized for obtaining the molecular beam, is located in the cylinder at a high pressure (for example 3 atm(abs.)). With the aid of the pulse quick-operating magnetic valve this cylinder periodically is connected with the vacuum to the short time intervals (1-2 ms). In the expanding section of nozzle occurs the adiabatic expansion of gas. The significant part of the energy of thermal agitation converts/transfers into the energy of the ordered motion of molecules, as a result of which is formed/shaped supersonic flow. The center section of this flow is discharged into fine vacuum through the diaphragm of special form (limiter). The second diaphragm (collimator) is intended for maintaining the difference in the static pressures between the ultrahigh vacuum in the compression chamber/camera and vacuum 10^{-3} torus in the chamber/camera between the nozzle and the limiter. The chamber/camera of collimator is evacuated by diffusion pump to vacuum 10^{-6} torus.

The important effect, which facilitates an increase in the intensity to the necessary level, is the partial condensation of

molecules in the process of the adiabatic expansion of gas in the nozzle. In this case are formed the groups of the large number of molecules (to 1000, depending on the gas pressure in the cylinder). For obtaining this effect some gases (for example hydrogen) it is necessary to cool to the temperature of liquid nitrogen. The axial velocity spread in the condensed beam is only several percentages, and the transversing speeds of them also are very small. Therefore even at large distances the beam retains sharp profile. By a somewhat different installation, used in the first measurements, were obtained good profiles of beam at a distance to 40 cm.

The third, ring stop forms/shapes the circular beam whose sizes/dimensions correspond to the sizes/dimensions of electron ring. The results of two measurements of the profile/airfoil of such beams are given in Fig. 5.

For our purposes are necessary the clusters with the duration of approximately 100 μ s, the synchronized with the cycles compressions. This is accomplished/realized with the aid of the rotary disk, located in the chamber/camera of collimator.

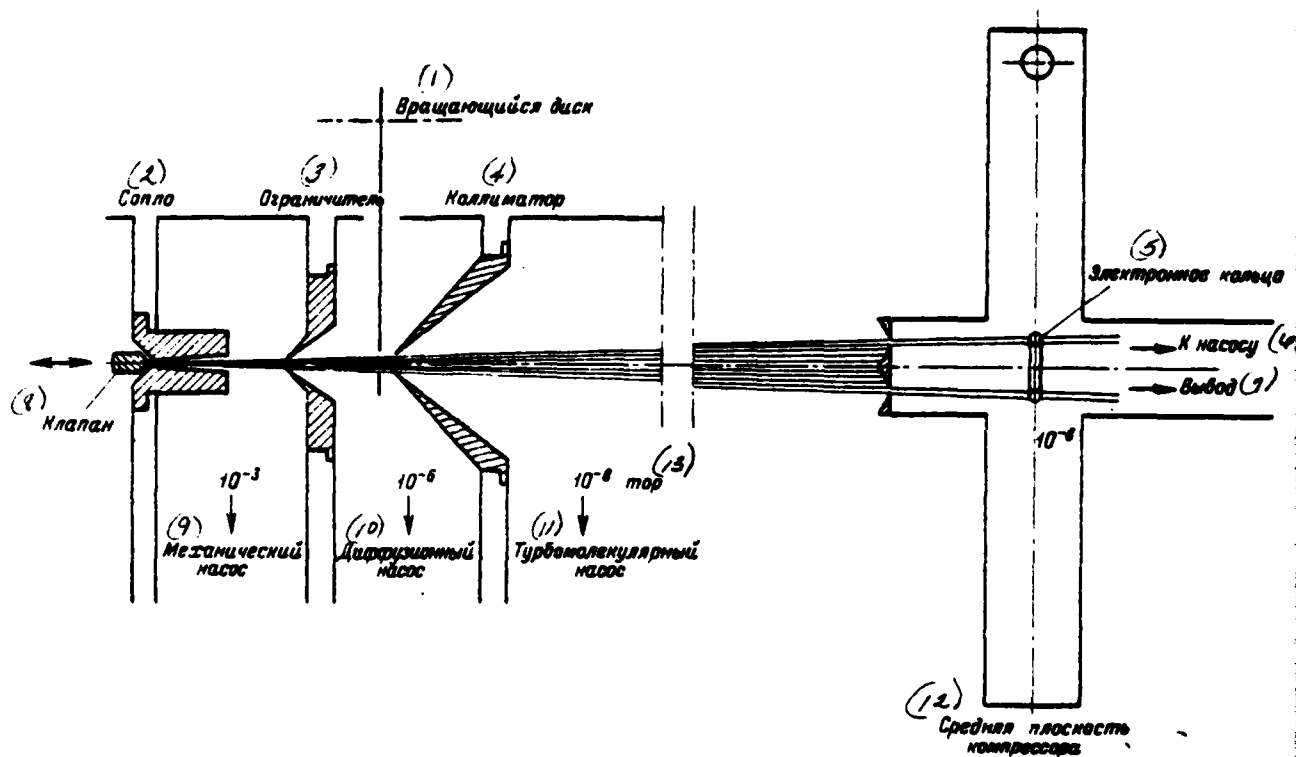


Fig. 4. Source of molecular beam.

Key: (1). Rotary disk. (2). Nozzle. (3). Limiter. (4). Collimator. (5). Electron ring. (6). To pump. (7). Conclusion/output. (8). Valve. (9). Mechanical pump. (10). Diffusion pump. (11). Turbomolecular pump. (12). Median plane of compressor. (13). torus.

Page 218.

Disk cuts from bundle the necessary clusters with the duration of 100

μs; the remaining part of the molecules of beam is evacuated by diffusion pump. Disk makes it possible to also ensure the synchronization of the feed of clusters. In summary the described device/equipment made it possible to charge ring by the completely specific form, without disrupting vacuum in the compression chamber/camera. The degree of loading can be changed by the method of changing the storage pressure. This method is suitable for all gaseous substances.

System of conclusion/output and acceleration of rings, loaded with ions.

During the first stage of the development of the accelerator of electron rings it is proposed to utilize acceleration by magnetic field. A change of the magnetic field in the space and the time must satisfy the following conditions:

- 1) a sufficient focusing in the period of loading;
- 2) rapid passage through the resonances during the conclusion/output;
- 3) the decrease of magnetic field in accordance with the properties of ring.

In order to ensure certain flexibility of construction/design at the stage of experiments, is expedient to use a system of coils, individual parts of which can be rapidly demounted and replaced.

In order to obtain the required form of magnetic field in the first approximation, the third compressor stage was changed: its one half was replaced by the long massive coil (solenoid) with the uniform coil/winding. This construction/design ensured the high mechanical strength of coil, since it is located under the action of intense magnetic forces. In order to satisfy three enumerated above conditions, into the massive coil placed supplementary coils with the small currents (on which act only small magnetic forces). These coils are accomplished/realized the correction of magnetic field in the region of the determination of ring in accordance with the physical requirements.

The construction/design proposed is shown in Fig. 6. The forming coil, arranged/located within basic solenoid, forms the thin layer, which consists of the separate sections with the independent supply, which makes it possible to change the form of the collapsible/dropped section of field in accordance with the properties of ring. Nearest of all to median plane of compressor is arranged/located the focusing coil, which amplifies the focusing action of basic solenoid at the end of the cycle of compression.

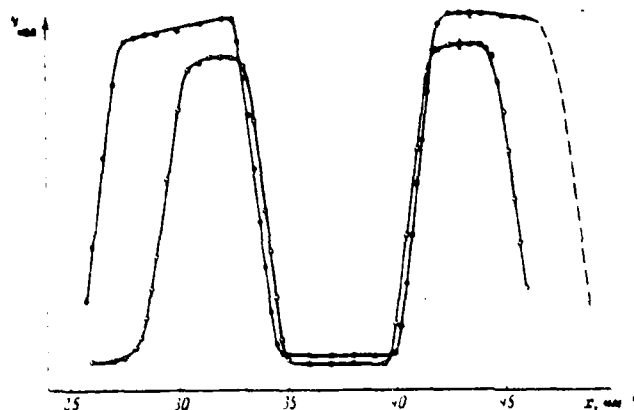


Fig. 5. Profile/airfoil of beam.

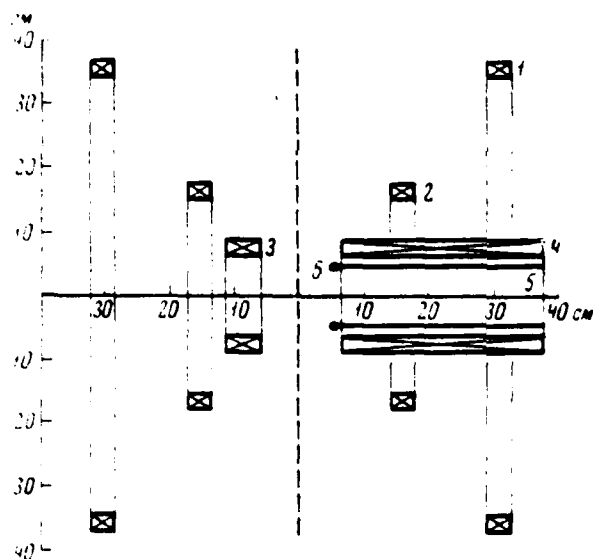


Fig. 6. System of coils of accelerator of electron rings. 1 - coil of first stage; 2 - coil of the second step/stage; 3 - coil of the third step/stage; 4 - main solenoid; 5 - forming coil; 6 - focusing coil.

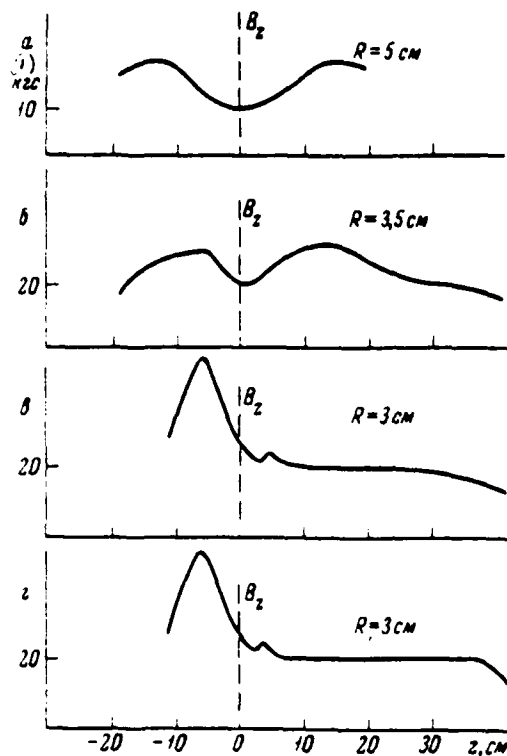


Fig. 7. Axial field distribution for successive moments of time. a) in the beginning of the third stage of compression; b) during the third stage of compression; c) at the end of the third stage of compression; d) before the conclusion/output.

Key: (1) . kg.

Page 219.

Fig. 7 shows the distribution of magnetic field in this installation

for the series/row of consecutive time intervals. The first graph/curve depicts magnetic field in the beginning of the third stage of compression, the second - during the third stage of compression. During this period the ring has already been driven out from the median plane. On the third graph/curve is shown the distribution of magnetic field after the termination of the third stage of the compression when is switched on focusing field. During this period the ring must be charged by ions; simultaneously the field of basic solenoid is changed by correspondingly with the aid of the corrective coils and acquires the form, shown on the fourth graph/curve.

Fig. 8 gives dependence of I on the time for different currents. Indices correspond to the numbers of coils in Fig. 6.

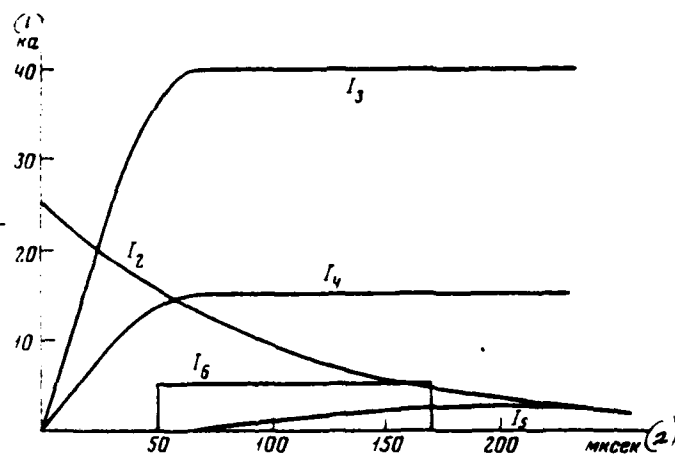


Fig. 8. Dependence $I(t)$ for different coils.

Key: (1) . kA. (2) . μ s.

67. Resonances of connection/communication of transverse vibrations of two circular beams.

P. R. Zenkevich, D. G. Koshkarev. (Institute of theoretical and experimental physics).

In the system, which consists of two beams of different particles, each of the beams can play with respect to a different role of "external force", creating the acting on the second beam disturbances/perturbations of middle field, to quadratic nonlinearity, etc. In the literature [1, 2] is examined the dipole two-bundle instability ("snake"), which appears when the oscillations of beams change the acting on them middle fields. It is obvious that besides dipole ones, in the two-bundle systems they are possible and the resonances of higher order, which correspond to the oscillations of the gradient of quadratic nonlinearity, cubic nonlinearity, etc.

We conducted theoretical studies of resonances. The procedure of this study will be in detail described in the work which at present is prepared for print. In this report are briefly described the used models and is given the summary of the obtained results. Furthermore, are examined the limitations, which superimpose two-bundle

instabilities on the parameters of the accelerators of electron-ion rings.

For the investigation of resonances are used two models: 1) the model of bundles with the density, the constant over the section; 2) the model of "strip/tape" bundles with the permanent density in the phase space; for calculating the electric fields in this model was utilized the one-dimensional equation of Poisson.

With the aid of the first model were obtained and investigated dispersion equations for the resonances of the first and second orders. For studying the simultaneous resonances of arbitrary order is used the model of "strip/tape" bundle and the apparatus of kinetic equation. The comparison of the results, obtained with the aid of both methods, showed that the error for "strip/tape" model is not too great.

Basic obtained results:

1. General condition of the two-bundle resonance

$$mQ_{1y,1} + nQ_{2y,1} = k, \quad (1)$$

where m, n, k - integers, Q_1 and Q_2 - "betatron" frequencies of the first and second beams.

2. In coaxial beams appear only "even-even" and "odd-odd" resonances (m and n respectively, both even and both odd).

3. In presence of polarization can appear "even-odd" resonances; estimations show that their increments several times less.

4. Increment and width of dipole resonance for electron-ion ring (δ_{11} and $\delta\omega_{11}$) are determined by formulas:

$$\delta_{11} = 0,5 \sqrt{\frac{Q_1^2 Q_u}{Q_3}}, \quad \delta\omega_{11} = 2\delta_{11}. \quad (2)$$

δ_{11} is increment in units of betatron frequency. Here Q_1 - "betatron frequency" of electron motion in the field of ions with the absence of external focusing; $Q_3^2 = Q_1^2 + \lambda^2$ - betatron frequency of external focusing; Q_u - betatron frequency of oscillations of ions.

5. Results, obtained for quadrupole resonances, are given in Table 1.

Page 220.

For standard electron-ion rings $Q_{1u} = Q_{qu}$, $Q_{1s} \neq Q_{qs}$. Therefore usually is sought the "single-/mono-dimensional-didimensional" resonances (size/dimension of electron ring is sought according to one degree of freedom, the size/dimension of ion - in terms of two

degrees of freedom).

6. From table for quadrupole resonances it is evident that increment of "crossed" resonance ($2Q_{yu} + 2Q_{y, -k}$) is three times less than increment of one-dimensional resonance.

7. Results, obtained for increments of "one-dimensional" resonances of arbitrary order with the aid of strip/tape model, are given in Table 2.

8. Basic conclusion/output from table: a) increments rapidly fall in proportion to removal/distance from principal diagonal ($m=n$): b) increments of resonances, arranged/located on principal diagonal, fall as n^{-1} ; c) width of resonance bands for these resonances falls as n^{-2} .

9. Landau damping stabilizes all instabilities with number n , for which

$$n \geq \left[\frac{\delta_n^2}{\langle \Delta Q_u \rangle \langle \Delta Q_y \rangle} \right]^{1/4} \quad (3)$$

so when $\delta_n = 0.15$, $\langle \Delta Q_u \rangle = \langle \Delta Q_y \rangle = 0.02$ all instabilities with $n \geq 2.7$ are stabilized by Landau damping.

Let us examine the limitations which superimpose two-bundle

instabilities on the parameters of the accelerator of electron-ion rings.

Let us assume that Landau damping suppressed all resonances, except dipole and quadrupole. It is obvious that for the stability it is necessary to select operating point out of the resonance bands. It is possible to show that when $\delta_{||} = 0.15$ the correctly following relationship/ratio:

$$E \cdot N_u = 5 \cdot 10^{14} \gamma \left(\frac{a}{R} \right)^3 \left(1 + \frac{\lambda^2}{Q_z^2} \right), \quad (4)$$

where E - accelerating field in MeV/m; N_u - number of ions; a/R - ratio of a small radius of ring to the large. Let us note that with change $\delta_{||}$ permissible value EN_u varies in proportion to $(\delta_{||}/0.15)^4$.

From formula (4) it is evident that value EN_u more strongly is limited by that degree of freedom, on which is weaker external focusing. In the real electron-ion ring the focusing in the axial direction is very small ($\lambda_z = 0.05$). In the figure in plane $Q_{zu}, Q_{z\pi}$ is depicted the curve, which corresponds $\delta_{||} = 0.15$ and $\lambda = 0.05$. To the centers of three stability regions correspond points with the following values of the frequencies:

- 1) $Q_{zu} = 0.16$, $Q_{z\pi} = 0.16$, $Q_z = 0.15$;
- 2) $Q_{zu} = 0.7$, $Q_{z\pi} = 0.07$, $Q_z = 0.043$;
- 3) $Q_{zu} = 1.3$, $Q_{z\pi} = 0.055$, $Q_z = 0.032$.

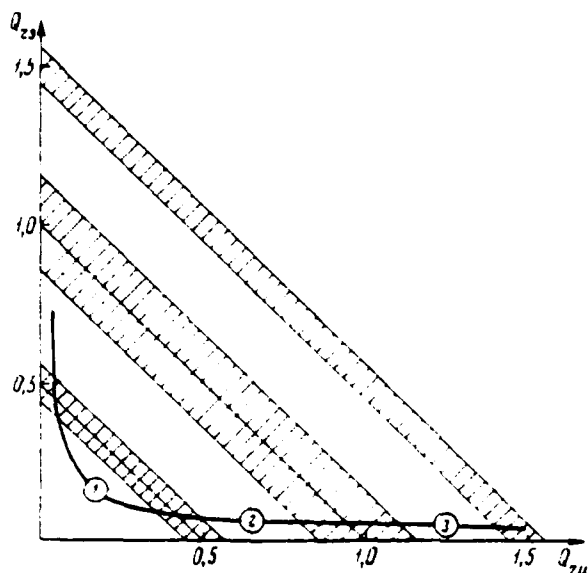
Table 1. Summary of results about the resonances of the 2nd order.

Тип резонанса (1)	Условие реализации (2)	Инкремент (3)	Ширина (4)
(5) Симметричный двумерный	$Q_{y3} = Q_{z3}; Q_{zu} = Q_{yu};$ $2Q_y + 2Q_u = k$	1	0,5
(6) Одновременный, несвязанные колебания	$Q_{y3} \neq Q_{z3}; Q_{zu} \neq Q_{yu};$ $2Q_{y,z} + 2Q_{u,y,z} = k$	0,75	0,375
(7) Одномерно-двумерный	$Q_{y3} \neq Q_{z3}; Q_{yu} = Q_{zu};$ $2Q_{y,z} + 2Q_u = k$	0,78	0,39
(8) Асимметричный двумерный	$Q_{y3} = Q_{z3}; Q_{zu} = Q_{yu};$ $2Q_y + 2Q_u = k$	0,5	0,29
(9) Двумерный, несвязанные колебания	$Q_{y3} \neq Q_{z3}; Q_{zu} \neq Q_{yu};$ $2Q_{y,z} + 2Q_{u,z,y} = k$	0,25	0,125

Key: (1). Type of resonance. (2). Condition of realization. (3). Increment. (4). Width. (5). Symmetrical two-dimensional. (6). Simultaneous, free oscillations. (7). Single-/mono-dimensional-didimensional. (8). Asymmetric two-dimensional. (9). Two-dimensional, free oscillations.

Table 2. Resonance increments of arbitrary order.

m	n				
	1	2	3	4	5
1	1	0	0,115	0	0,012
2	0	0,41	0	0,100	0
3	0,115	0	0,25	0	0,007
4	0	0,100	0	0,18	0
5	0,012	0	0,007	0	0,15



Page 221.

At prescribed/assigned values γ, N_0 and R the pair of the values of betatron frequencies completely determines the basic parameters of electron-ion ring: n_u , E , and α . The results of calculating these parameters at $\gamma=50$, $R=5$ cm and $N_0=10^{14}$ are given in Table 3.

The intensity of ions, led in the table, can be somewhat improved with increase δ_u , but only by the value of the considerable stiffening of allowances.

From the table it is evident that with the weak external

focusing it is difficult to obtain the accelerator of electron-ion rings, the exceeding proton synchrotron simultaneously both in the intensity of the accelerated beam and on an energy gain per the unit of length.

In conclusion let us note that the creation of the strong external focusing of electron ring according to both degrees of freedom would make it possible to substantially improve the intensity of the accelerated beam in the accelerator of the electron-ion rings.

REFERENCES

1. G. I. Budker. Atomic energy, 1956, 5, 9.
2. B. V. Chirikov. Atomic energy, 1956, 19, 239.

Discussion.

N. S. Dikanskiy. Why decrement of dipole instability does not depend on a number of particles? Indeed it is proportional to root from the frequencies.

P. R. Zankovich. Root of frequencies $\sim (N_u N_s)^{1/4}$, since each of the frequencies $\sim N^{1/2}$. In the presence of external focusing the increment

somewhat falls. But on z one should consider that there is no external focusing.

A. N. Lebedev. Is it possible to draw from your report the conclusion that the large part of the region of parameters, selected now for the creation of ring, is in actuality prohibited?

P. R. Zenkevich. Within the framework of this theory (I emphasize that here there is an even more disputable/more debatable question about the effect of radiation/emission) was actually/really obtained the conclusion/output that obtaining field strengths greater than 200 MeV/m is virtually impossible. Estimates of the frequency for the existing accelerators show that they lie in the first region, i.e., their frequencies obviously do not exceed 0.1. Thus, we cannot say that this contradicts the theory.

Table 3. Parameters of accelerators of electron rings.

N , points	N_u/N_g	n, cm^{-3}	a, mm	$E, \text{MeV/m}$	N_u
1	$2.4 \cdot 10^{-2}$	10^{12}	10	48	$2.4 \cdot 10^{+12}$
2	$1.00 \cdot 10^{-4}$	$2 \cdot 10^{13}$	2.2	200	$1 \cdot 10^{10}$
3	$1.6 \cdot 10^{-5}$	$7.0 \cdot 10^{13}$	1.2	380	$1.6 \cdot 10^9$

Key: (1) . point. (2) . MeV/m.

68. Progress in the creation of the accelerative section of ring accelerator.

N. G. Anishchenko, N. I. Balalykin, V. A. Vasil'yev, Yu. S. Derendyaev, A. G. Zeldovich, M. K. Zeldovich, Yu. V. Muratov, N. B. Rubin, A. A. Sabayev, V. P. Saraitsev, Yu. I. Smirnov, V. G. Shabratov, Yu. A. Shishov.

(Joint Institute for Nuclear Research).

As the probable prototype of the accelerating system of collective linear ion accelerator in Dubna is developed/processed the cryogenic high-frequency accelerative section of ring accelerator [1].

Section (Fig. 1) consists of four superconducting (SP) accelerating cavities, SP of the solenoids, which create the controlling longitudinal magnetic field, and separate cryogenic systems for cooling of resonators and solenoids. The working length of section is 1.6 m. Section must make it possible to simulate the case when middle accelerating field for the ions ~ 2 MV/cm, and it is calculated on heat losses 30-35 W/m. The power of hf generators ~ 6

kW/a must be supplied with different porosity (depending on the operating modes) up to continuous mode/conditions.

In the past after Yerevan conference year scientific research works in connection with the creation of the accelerating section conducted on five to main trends:

a) continued the investigations of SHF-resistors of second-order superconductors for the purpose of selecting of the adequate/approaching coating material of the internal surfaces of resonators. In this case in accordance with the actual conditions in the ring accelerator the measurements of SHF impedances were conducted in the presence of the external magnetic field, directed both in parallel and it is perpendicular to the surface being investigated. Magnetic field strength exceeded the value of the first critical field;

b) was developed/processed installation for the application of SP coatings on the resonators under maximally "pure/clean" conditions and were accomplished/realized the test depositions of SP films on model installation;

c) were studied the methods of designing of the magnetic field of the required configuration with the aid of of SP windings.

Page 222.

Are prepared and tested model solenoid and test corrective coils;

d) were developed/processed the parts of the system of thermostatic control;

e) continued theoretical and calculated works on the finding of current distribution in the windings for the creation of the prescribed/assigned magnetic field.

1. Study of HF impedances of superconducting surfaces. For the investigations was used the procedure, presented in [1, 2]. Experiments were conducted in the range 500 MHz on the coaxial half-wave resonators, made from alloys of the type niobium-zirconium and niobium - titanium, with low levels of HF fields.

The superconducting resonator it is accepted to characterize by coefficient of increase in quality F , by the equal to the relation of quality of SP resonator Q_c and the quality of analogous copper resonator Q_M at a room temperature $F = Q_c / Q_M$.

Was investigated group of SP materials with different mechanical and thermal methods of the surface treatment. For some samples/specimens of the factors of quality Q three times less in the cross field to 10 kOe in the comparison with the case of zero-field. The great incidence/drop in coefficient Q was obtained by the equal to 5. Extrapolation of the obtained values for the transverse floor/sax $B=2$ T with $T=1.8^\circ\text{K}$ gives $Q=600-1000$. For the comparison it should be noted that the factor of quality in the external longitudinal field $B=2$ T and $T=1.8^\circ\text{K}$ was obtained equal to 2000.

Subsequently it is proposed to conduct the measurements of the HF impedance of superconductors in the high-frequency fields of average/mean power.

2. Application of superconducting coatings. In the process of perfecting the method of obtaining SP coatings, described in [1], was developed the ionic method, which makes it possible conduct process at a pressure of the residual gases $P=1-5 \cdot 10^{-6}$ torus, which contributes to obtaining the films more pure in the chemical composition. The rate of formation of film in this case is different, depending on the kind of material, and it is considerably higher in comparison with other methods. Thus, for instance, for Nb the rate of formation of film is two orders higher than during the thermal evaporation. For the purpose of the adjustment of the

modes/conditions of obtaining of SP coatings and debugging of the thermally loaded noles/units of electron-beam gun was conducted the deposition of SP on different samples/specimens made from copper: ribbon 180x4x1.1 mm, plate 180x50x1.5 mm, the tube with a diameter of 3 mm, with length of 300 mm (external surface was sprayed), tubes with a diameter of 30 mm, with length of 200 mm (was spray-coated internal surface) and other samples/specimens of more intricate shape. It is necessary to note that the obtained coatings do not require the subsequent mechanical treatment to the surface finish. The latter depends only on the class of the purity/finish of backing and corresponds to it.

The check of the thickness of film was performed by quartz resonator. Fundamental crystal frequency $f=500$ kHz, the frequency coefficient $N=1690$.

For the static investigations of the superconducting properties of the plotted/applied niobium were utilized copper sample/specimen 180x4x0.1 mm, thickness of the film of niobium ~ 5 μ m. According to the taken volt-ampere characteristic of the sample/specimen there was determined critical current $I_{kp} = 34$ A which in the recalculation gives current density $\sim 1.7 \times 10^5$ A/cm². this corresponds to the critical field of niobium.

3. Superconducting solenoids. The leading magnetic field 20 kOe is created by the solenoid of rectangular cross section. The required uniformity of field 0.150/o in the ion guide is provided due to the selection of currents in 96 corrective coils. Are studied two versions of the windings of solenoid: from completely stabilized strip/film (see the Table), from the internally stabilized conductor.

In the first case is provided for the short-term heating of windings for the release from those induced during the creation of the field of eddy currents, as is done in the solenoid of chamber/camera VEVS [3]. In the second case is expected the rapid fading of the induced currents due to the joining of filaments with the step/pitch approximately 30 nm.

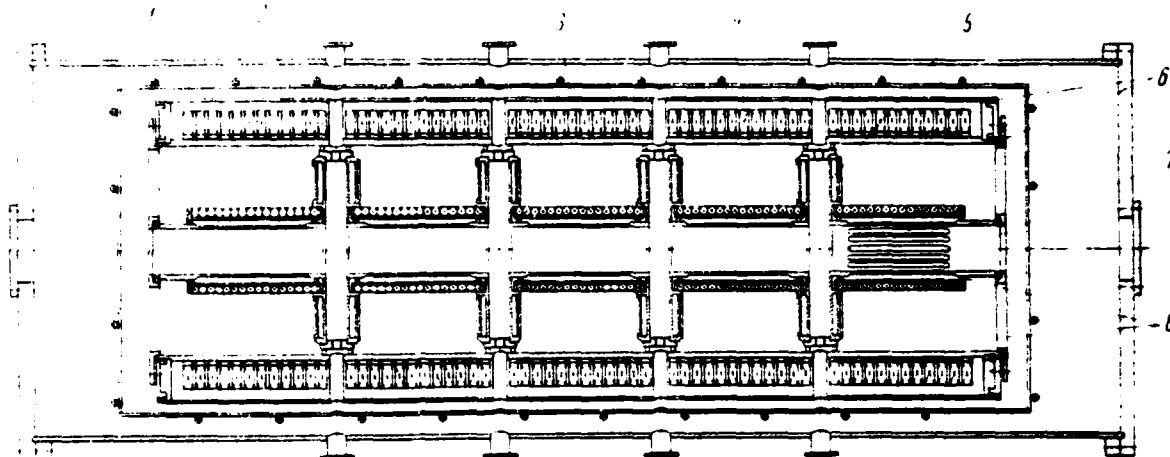


Fig. 1. Cryogenic high-frequency accelerative section of ring center.
1 - vacuum envelope; 2 - nitric screen (78°K); 3 - superconducting solenoid of longitudinal magnetic field; 4 - superconducting corrective coils; 5 - resonator; 6 - helium cryostat; 7 - perforated focusing ducts; 8 - steel fulcrum balls.

Page 223.

For the final adjustment of construction/design and technology of the production of solenoid, and also testing of the devices/equipment of guarantee by liquid helium, power delivery and evacuation of stored energy is prepared and tested superconducting magnetic system with the solenoid with a bore of 35 cm [4]. In this solenoid is achieved/reached the intensity/strength of field 25 kOe with the current in the completely stabilized strip/film 1.8 kA.

To the corrective coils is presented the series/row of the stringent requirements: 1) maximum current density in the winding -2.10^4 A/cm^2 ; 2) independent feed of all coils; 3) a precise reproduction of the strength of field with one and the same current.

There are tested the coils of the niobium-zirconium wire ϕ 0.25 mm (in the brass coating). However, their critical currents were obtained low and had large scatter. Therefore it is decided to pass on the coil from the cable with the internal stabilization (see tables).

For the supply of coils and solenoid are created semiconductor sources on nominal currents 100 and 5000 A.

The emergency evacuation of stored energy it is proposed to produce to the arc-suppression lattice of the automatic field damper. In this case the process continues with constant stress on the ends/leads of solenoid; therefore the time of evacuation is five times less than with the use of constant active discharge resistor (without taking into account actively connected with winding of the solenoid of contours/outlines). The guarantee of a rapid conclusion/output of energy is especially important in the case of

applying the conductors with the internal stabilization, that possess by an order high current densities, than completely stabilized.

4. System of thermostatic control. With the system of thermostatic control of section are connected liquefier by productivity about 80 l of liquid helium in the hour and two containers, established/installed above the section.

The schematic diagram of installation is shown in Fig. 2. Helium is compressed by compressor K up to a pressure of $P_1=30$ atm (tech), it passes through counterflow heat exchangers of I-IV, bath of liquid nitrogen, stabilizing liquid helium bath C_1 and three $T_1=5^\circ\text{K}$ enter into the expanded ejector E.

After ejector helium falls into container C_2 with temperature $T_2=4.5^\circ\text{K}$. Liquid helium from container C_2 of one's own accord/by gravity enters the lower points of the cryostats of section, gaseous is -particle into return flow of liquifier, partially - for cooling of the electric leads of solenoid and coils. Furthermore, occurs throttling/choking liquid from container C_2 into container C_3 , which has $T_3=1.8^\circ\text{K}$. Here also occurs the gravity circulation of superfluid helium through the resonators; vaporized helium is exhausted by ejector. Bath C_1 serves for the maintenance of permanent temperature before the ejector.

Diagram with the ejector makes it possible to forego the extremely bulky pumps for the evacuation of helium and reduces the sizes/dimensions of heat exchangers.

5. Calculations of currents of corrective coils. For maintaining the radial size/dimension of ring in the accelerating system is utilized longitudinal magnetic field ~ 2 T. The condition of accelerating of rings under the action of constant force requires the creation of special periodic modulation of this field.

Current distribution, which create the required magnetic field was calculated on the computers with the use of minimization of functional [5]

$$\chi^2 = \sum_{i=1}^N \left(\frac{B_i - B_i(r_i, z_i, I_j)}{\Delta B_i} \right)^2,$$

where B_i - required function of parameters I_i at points

$r_i, z_i, B_i(r_i, z_i, I_j)$ - function at fixed/recorded parameters I_j at points

r_i, z_i, I_j - unknown currents in 96 corrective coils; ΔB_i - accuracy of maintaining of magnetic field at points r_i, z_i .

The basic parameters of superconducting solenoid and corrective coils.

	(1) Соленоид	(2) Катушка
(3) Напряженность магнитного поля	20 кэ	0 - 4 кэ
(4) Внутренний диаметр по обмотке	60 см	1,7 см
(5) Внешний диаметр	72 см	21 см
(6) Длина	240 см	1,7 см
(7) Рабочий ток	2100 а	0 - 70 а
(8) Плотность тока в обмотке	2670 а/см ²	0 - 2,10 ⁴ а/см ²
(9) Запасенная энергия	1,1 Мдж	785 дж
(10) Сечение провода	2 x 25 мм ²	φ 0,5 мм
(11) Индуктивность	0,5 Гн	0,32 Гн

Кэу: (1). Solenoid. (2). Coil. (3). Magnetic intensity. (4). Bore on winding. (5). Outer diameter. (6). Length. (7). Operating current. (8). Current density in winding. (9). A/cm. (10). Stored energy. (11). MJ. (12). J. (13). Section of lead/duct. (14). Inductance. (15). H.

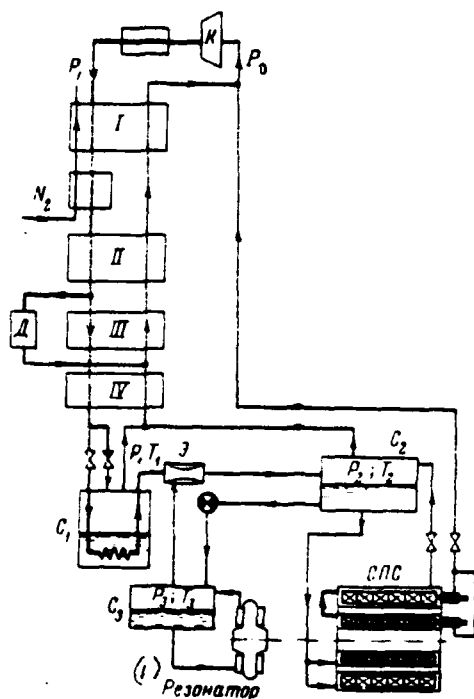


Fig. 2. Schematic diagram of thermostatic control of section of ring accelerator.

Key: (1). Resonator.

Page 224.

REFERENCES

1. N. G. Anishchenko et al. Preprint J.I.M.R. P9-4722, Dubna, 1969.

2. N. B. Rubin. et al. Preprint J.I.N.R. P8-4785, Dubna, 1969.
 3. European bubble chamber. CERN Courier, 1970, 10, N 2.
 4. N. G. Anishchenko et al. Preprint J.I.N.R. 8-4882, Dubna, 1969.
 5. S. N. Sokolov, I. N. Silin. Preprint J.I.N.R., D-810, Dubna, 1961.
 69. Theoretical and experimental studies on the creation of intense waves in the electron beams.
- G. G. Aseyev, A. P. Klyucharev, G. G. Kuznetsov, N. S. Repalov, B. G. Safronov, N. A. Khizhnyak.

(Physiotechnical institute of AS UkrSSR, Kharkov).

The study of the behavior of the beams of charged particles and plasma in space-periodic fields is of interest in many respects. In particular, the passage of the electron beam through the longitudinal electrostatic field can be accompanied by instability on the longitudinal waves, if is satisfied the condition [1] $v_{on}/L - kf_{on}$, where k - integer; v_{on} - rate of beam; L - three-dimensional/space period of electric field; f_{on} - Langmuir frequency of the beam. In the case when $k=1$, must occur the rapid increase of the strength of the field

between the clusters of electrons, which in the principle can be used for the particle acceleration. The consequence of resonance at multiple frequencies ($k > 1$) is the amplification of the initial level of the longitudinal oscillations of beam.

In the case of the passage of the charged/loaded particles through the plasma, placed into the spatial-periodic electric field, there can appear specific effects. The presence along the axis/axis of this system of the periodic sequence of points with the extrema of potential can lead to the capture of plasma near these points. With the passage of the beam through this plasma there is possible, in particular, the resonance on the seized particles which is realized with the coincidence of the frequencies of wave and natural of the seized particles. In this case is feasible the heating of any of the components of plasma.

The purpose of this work is experimental detection and investigation of the conditions of the instability of the electron beam, passing through the external electrostatic field. The latter was created by plate system, shown schematically in Fig. 1. The period of system was selected equal to 3.1 cm, number of periods is equal to 10. the calculations conducted and the experiments showed that the potential between the centers of openings/apertures in the plates is approximately $0.3 U_0$, where U_0 - voltage, supplied to the

plates. Stationary electron beam passed through opening/aperture to plates and it fell to the collector/receptacle. The leading longitudinal magnetic field were approximately 800 e. In the experiments were measured the relative level of hf-radiation/emission of beam and its frequency spectrum at the output from the electric field.

Fig. 2 gives the dependences oscillation level on current I_k , of accelerating voltage of beam U_n and voltage between plates. They all have resonance character.

The initial level of HF radiation/emission under conditions for our experiments was created by beam itself. As it proved to be, in the absence of plates at the specific values of current and rate of beam in it is excited certain oscillation spectrum, located in 50-200 and 3000-4000 MHz regions. In this series of preliminary experiments we did not study an important question about the nature of these oscillations. For purposes of this work essential is only the presence of certain initial level of the oscillations of beam.

In Fig. 3 by crosses and small circles are plotted the experimental values of current and accelerating voltages of beam, which correspond to maximum of the amplitude of the oscillations of beam in the absence of the plates of electric field. Cherayys point

in this figure correspond to the maximum of the amplitude of oscillations depending on rate and density of beam and voltage on the plates. In this case the level of the oscillations by more than two orders of magnitude exceeds the initial level of the oscillations of beam.

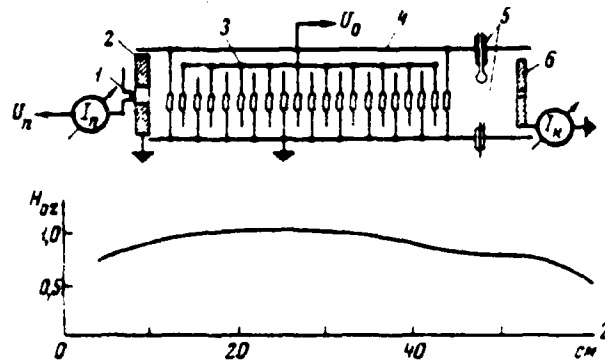


Fig. 1. Installation diagram. 1 - cathode; 2 - anode; 3 - plates, which create electric field; 4 - vacuum chamber; 5 - probes; 6 - collector/receptacle of bundle. Below - the distribution of magnetic field along the axis/axle of system.

Page 225.

Unbroken curves correspond to computed values of current and rate of beam which were obtained from the resonance condition. Experimental points agree sufficiently well with the calculation for case of $k=2$.

The resonance dependence of the amplitude of oscillations on the value of the electric field (see Fig. 2b), apparently, it can be explained by change in the average speed of the beam between the plates and by subsequent disruption/separation of resonance. If we rate/estimate this change from Fig. 2b, then it will be in complete

AD-A089 303

FOREIGN TECHNOLOGY DIV WRIGHT-PATTERSON AFB OH F/G 20/7
TRANSACTIONS OF THE ALL-UNION CONFERENCE (2ND) ON CHARGED PARTI--ETC(U)
JUL 80 A L MINTS, A A KOMAR, A A VASIL'YEV
FTD-ID(RS)T-0692-80

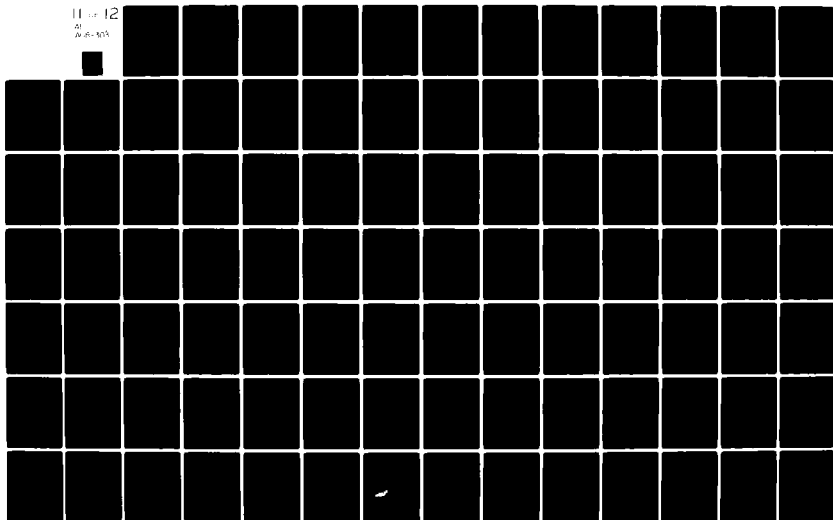
UNCLASSIFIED

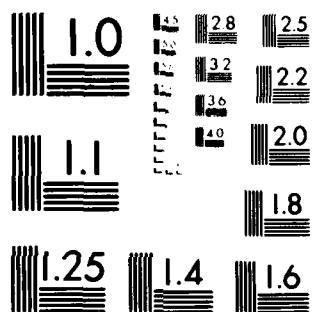
NL

11 of 12

21

AD-A089 303





MICROCOPY RESOLUTION TEST CHART
NATIONAL BUREAU OF STANDARDS-1963-A

agreement with the half-width of resonance in the rate of beam in Fig. 2c.

The scatter of points in Fig. 3 characterizes the reproducibility of results, precision/accuracy of the measurement of the parameters, and also degree of the conformity of one-dimensional theoretical model to the actual conditions for experiment. For the purpose of an improvement in reproducibility of results before the measurements was carried out prolonged conditioning of system by the beam of maximum power. This made it possible to also avoid the masking of studied resonance by the breakdown-preceding and breakdown phenomena and connected remove/take by different forms of cluster-plasma instabilities [2].

In the case of insufficiently fine vacuum in the region of electric field with the passage of beam can be excited the oscillations with the frequency of 0.7-1.0 MHz which virtually depends on magnetic field, it increases with an increase in the beam current and decreases with increase of the mass of residual gas.

The amplitude of these oscillations increases with an increase in the electrical field between the plates (see Fig. 4). Under these conditions the amplification of MF oscillations of beam is difficult to judge, since occurs scattering of hf oscillations at the low

frequency. It was discovered, that with external MF modulation of beam at the entrance into the electric field the signal from the probe at the output from it has the fixed/recorded frequency, which coincides with the frequency of modulator in the case of the absence of electric field. During the imposition of this field are excited the L.F. of oscillation, and the monochromatic signal of modulator "will be dispersed" into the spectrum, individual lines of which are shifted to frequency of LF oscillations. This phenomenon substantially impedes the study of the amplification of hf oscillations of beam under our experimental conditions. More effective from this point of view can be pulsed mode.

The experiments conducted make it possible to make the following conclusions:

1. Spatial-periodic electric field under conditions, close to the resonance ones, leads to amplification of the initial level of hf oscillations of beam.

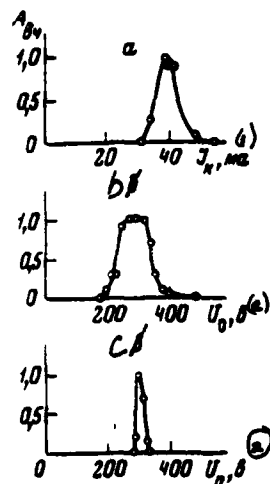


Fig. 2. Dependence of the amplitude of hf radiation/emission on the parameters of beam and value of electric field a) $U_n = 300V$, $U_0 = 300V$; b) $U_n = 300V$, $U_0 = 40$ mA; c) $U_0 = 300$ V, $I_k = 40$ mA.

Key: (1). mA. (2). V.

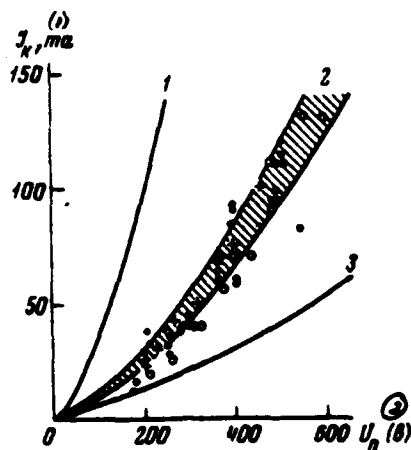


Fig. 3. Experimental points and theoretical dependences of beam current on accelerating voltage under resonance conditions.

1-3 - correspond to resonance on the first, second and third harmonics of Langmuir frequency of beam. Lower curve for the second harmonic is calculated for the cathode whose area to 200/o is lower than geometric area of the cathode, used in the experiment. Remaining curves are calculated with the use of a geometric area of cathode.

Key: (1). mA . (2). V.

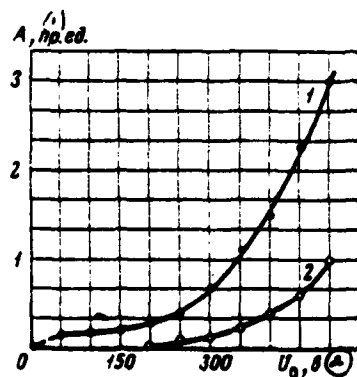


Fig. 4. Dependence of amplitude L.F. of oscillations on value of electric field 1 - ten periods; 2 - three periods. Conditions $U_m = 600$ V, $I_m = 180$ mA.

Key: (1). lin. unit. (2). V.

2. Dependence of amplitude of oscillations on current, accelerating voltages of beam, and on value of electric field has resonance character.

3. Experimental values of current and accelerating voltages of beam, which correspond to maximum oscillation level in presence of electric field, completely satisfactorily will agree with calculation for case of $k=2$.

4. In the case of insufficiently fine vacuum in plasma are excited L.F. of oscillations, which mask effect of amplification of hf oscillations.

REFERENCES

1. N. S. Repalov, N. A. Khizhnyak. ZhTF, 1966, 36, 219.
2. Ya. B. Faynberg. Atomic energy, 1961, 11.350.

Discussion.

V. N. Tsytovich. Was reached nonlinear mode/conditions at modulation of beam?

N. S. Repalov. We did check, emerge we against the nonlinear mode/conditions. Theoretically it is obtained, which for the output to the nonlinear mode/conditions is sufficient 10 periods. Therefore were carried out the following experiments. We changed a number of plates, to which was supplied the voltage (others grounded). Was removed/taken the curve of the dependence of the amplitude of HF-signal on effective length of acceleration. It turned out that we emerge to the mode/conditions when amplitude is saturated. This, of course, does not mean that mode/conditions are nonlinear, nonlinearity could be judged by the fact that the wave which in this case was obtained, it carried Riemann character, since we already have the harmonics, which were placed well in the Riemann of wave. Thus on the only the basis/base I can say that we seemingly would emerge to the nonlinear mode/conditions.

V. N. Tsitovich. Was investigated the stability of bright to the clusters beam?

N. S. Repalov. No, it was investigated neither experimentally nor theoretically.

A. L. Kolomenskiy. What prospects for your method for coherent acceleration of ions?

N. S. Repalov. If we utilize the very powerful/thick beam which is already now (100 kA on 100 kV of voltage) and if it is possible to modulate it, then we will attain 50-100 kV/m. At high energies us, of course, expect the difficulties. The fact is that with the increase of intensity appears the plasma, which fills trap, which are obtained along the axis/axle in the presence of periodic potential, and interaction of beam with this plasma can bring to various kinds to instabilities. Therefore we intend to operate in pulses, until plasma is formed, and, thus, to remove this effect. The formation/education of dense plasma leads to the fact that in proportion to motion to the parametric resonance about which I spoke, must be oscillation buildup of the defined level. This occurs not always. When appears plasma, first occurs the amplification of oscillations, and then monochromatic spectrum begins to be dispersed, are formed three-wave interactions at this frequency, and the amplification of oscillations is broken away.

70. To a question about the acceleration of ions by electron ring in the ~~collapsible/dropped~~ ^{DECAYING} magnetic field.

I. N. Ivanov, E. A. Perel'shteyn, V. P. Sarantsev.

(Joint Institute for Nuclear Research).

In the collective linear ion accelerators as the accelerating cluster is utilized electron ring. During the conclusion/output from the adhesive the ring is accelerated in the collapsible/dropped magnetic field. In the accelerator, calculated for the acceleration of protons to the superhigh energies, the stage of acceleration in the magnetic field is preliminary. As show calculations, upon the acceleration in the collapsible/dropped field of the electron ring, loaded with large ions, the latter can acquire energy to 10 MeV/nucleon and this is sufficient for physical experiments.

In this work is examined the problem of confinement of ions in potential well of the electronic rings upon its acceleration in the collapsible/dropped magnetic field. In this case are accepted the following assumptions:

- electron ring considers toroid the round cross section; the ratio of a small radius a to the large radius R of toroid satisfies inequality $a/R \ll 1$;

- total mass of all ions considerably less than the total mass of electrons;

- polarization of the accelerated ion-electrical ring is considered small, and the form of electronic cluster remains constant/invariable upon the acceleration;

- by effect of the field of ionic component to the electronic cluster is disregarded;

- prior to the beginning of acceleration ions in the electronic cord are monoenergetic and have an energy E_0 , and the function of the distribution of ions takes the form

$$f = \frac{N_0}{2\pi^2 a^2} \psi(x_0) \delta(E - E_0), \quad (1)$$

where N_0 - number of ions in the ring before the acceleration; E - energy of ion; $\psi(x_0)$ - certain function from the coordinate of the ion (see below).

- the gradient of magnetic field in the laboratory system is constant, the rate of ring in the direction of acceleration is considered nonrelativistic.

The basic parameters of the problem following:

the frequency Ω of ion in potential well of the electronic cord

$$\Omega^2 = \frac{2v_e mc^2 Z}{M a^2 A}; \quad v_e = \frac{N_e}{2\pi R} \frac{e^2}{mc^2}, \quad (2)$$

where N_e - number of electrons in the cord; M , m masses of the rest of ion and electron; e Z , A - charge of ion and its atomic weight respectively;

the value of acceleration in the laboratory coordinate system:

$$w_0 = -\frac{e\beta}{m\gamma} \frac{R}{2} \frac{\partial \bar{H}_2}{\partial x}; \quad \gamma = (1 - \beta^2)^{-1/2}, \quad (3)$$

where β - ratio of the velocity of the rotation of electrons in external magnetic field H_2 to the speed of light; $\bar{H}_2 = \frac{2}{R^2} \int_0^R H_2 x dx$ - time of acceleration t which is possible to connect with a length of accelerating circuit of $L = w_0 t^2 / 2$.

The accepted by us approximations/approaches make it possible to

replace the field, which acts on the ion from the side of electron ring, with the field of the straight/direct electronic cord of round cross-section, to introduce coordinates x and z - the divergence of ion from the center of cord, and in the system, connected with the accelerating cord, to write the equations of motion of ion in the form:

$$\begin{aligned} M\ddot{z} &= Mw(t) + e\mathcal{E}_z, & z(0) &= z_0, & \dot{z}(0) &= \dot{z}_0, \\ M\ddot{x} &= e\mathcal{E}_x, & x(0) &= x_0, & \dot{x}(0) &= \dot{x}_0. \end{aligned} \quad (4)$$

In formula (4) \mathcal{E}_z and \mathcal{E}_x - the components of the electric field of cord ($\mathcal{E} = -\text{grad}\Phi$), and acceleration w is the function of time, which makes it possible to consider the moment/torque of the beginning of the acceleration of cord. We will place

$$\begin{aligned} (1) \quad w &= w_0 \delta(t), \\ \text{rue } \delta(x) &= \begin{cases} 1 & x \geq 0, \\ 0 & x < 0. \end{cases} \end{aligned} \quad (5)$$

Key: (1). where.

This form of time dependence $w(t)$ simplifies calculation and is not fundamental for the final results. Let us find first constant of motion of system (4):

$$\begin{aligned} \frac{\dot{z}^2 + \dot{x}^2}{2} &= -w_0 z - \frac{e}{M} \Phi + E_0, \\ \frac{e}{M} \Phi &= \Omega^2 \left[\frac{z^2}{2} \delta(a-z) - a^2 \ln \frac{a\ell^{-1/2}}{z} \delta(z-a) \right], \\ \ell^2 &= x^2 + z^2; \quad \ell = 2, 718 \dots, \quad E_0 = \frac{\Omega^2 a^2}{2} + w_0 z_0 \delta(t). \end{aligned} \quad (6)$$

Let us examine potential energy of ion U in the field of cord. From

equations (6) it follows

$$U = w_0 z + \Omega^2 \left[\frac{z^2}{2} \theta(a-z) - a^2 \ln \frac{a \ell^{-1/2}}{z} \theta(z-a) \right]. \quad (7)$$

Function U has extrema in plane $x=0$: when $|z_{\min}| < a$ at point $z_{\min} = -\frac{w_0}{\Omega^2}$ function U is minimum

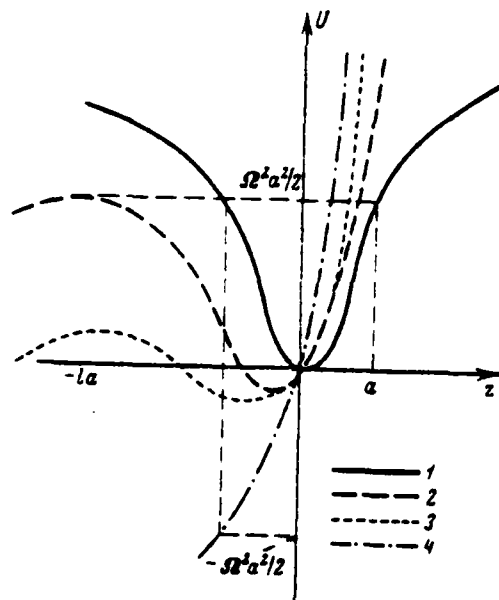
$$U_{\min} = -\frac{w_0^2}{2\Omega^2}, \quad (8)$$

and when $|z_{\max}| > a$ at point $z_{\max} = \frac{\Omega^2 a^2}{w_0}$ the maximum of function U

$$U_{\max} = \Omega^2 a^2 \ln \frac{\Omega^2 a^2 \ell^{-1/2}}{w_0}. \quad (9)$$

Figure gives form U in plane $x=0$ for different z . From the figure one can see that when $w_0 < \Omega^2 a \ell^{-1/2}$ the acceleration does not affect the motion of ion, pit for the ion remains.

When $\Omega^2 a \ell^{-1} < \omega_0 < \Omega^2 a$ value U_{\max} becomes less than the wave energy of the ion



Potential energy $U_{(0,z)}$ for different accelerations

$$1 - W_0 = 0; 2 - W_0 = \Omega^2 a \ell^{-1}; 3 - \Omega^2 \ell^{-1} < W_0 < \Omega^2 a; 4 - \Omega^2 a$$

E_0 , but when $\omega_0 > \Omega^2 a$ pit does not exist. By proceeding from the picture of the strain of potential pit, it is possible to write the conditions with executing of which the ion remains in the electronic cord. We will consider that function $\psi(z_0)$ describes these conditions. Since E_0 for $t \geq 0$ is function z_0 [equation (6)], then solve system (4) let us find $z_0[z(t), \dot{z}(t)]$:

$$z_0 = z \cos \Omega t - \frac{z}{\Omega} \sin \Omega t - \frac{W_0}{\Omega^2} (1 - \cos \Omega t). \quad (10)$$

It is now easy to find a number of ions at the moment of time t from the formula

$$N = \int f dz dx dy dz = \frac{N_0}{\pi^2 a^2} \int \frac{\delta(x_0^2) \psi(z_0) dz dx dy}{x_0} -$$

$$- \frac{x_0^2}{2} = \frac{z^2}{2} + w_0 \left(z + \frac{w_0}{\Omega^2} \right) (1 - \cos \Omega t) +$$

$$+ \frac{w_0 z}{\Omega} \sin \Omega t + \frac{\Omega^2 (x^2 + z^2 - a^2)}{2}. \quad (11)$$

Page 228.

Let us examine two acceleration modes:

1. $w_0 < \Omega^2 a$, $\Omega t > 2\pi$. From figure it is clear that for this time in cord will remain ions with $E_0 < U_{\max}$. From (6) and (9) let us find that this condition is satisfied for the ions with origin coordinate

$$-a < z_0 < a \frac{\Omega^2 a}{w_0} \ln \frac{\Omega^2 a}{w_0} e^{-1/2} = a v. \quad (12)$$

From (12) is determined form $\psi(z_0)$:

$$\psi(z_0) = \delta(z_0 + a) \delta(a v - z_0). \quad (13)$$

Producing integration in (11), taking into account (13) we will obtain

$$N/N_0 = 1/2 + v \sqrt{1-v^2} + \frac{1}{\pi} \arcsin v. \quad (14)$$

Table gives numerical calculations according to formula (14).

$\alpha = \frac{\Omega^2 a}{w_0}$	$y = \begin{cases} v = \alpha \ln(\alpha e^{-1}) \\ u \end{cases}$	$\frac{1}{2} + y\sqrt{1-y^2} + \frac{1}{\pi} \arcsin y$
1,01	-1,000	0,000
1,10	-0,9952	0,00020
1,30	-0,9589	0,00496
1,50	-0,8918	0,02220
1,70	-0,7979	0,05082
1,90	-0,5905	0,10305
2,10	-0,5419	0,17272
2,30	-0,3843	0,26150
2,50	-0,2093	0,36775
2,71	-0,0083	0,49474
	0,17	0,60142
	0,37	0,73006
	0,57	0,84213
	0,77	0,93613
	1,00	1,0000

Let us note only that $|v| < 1$. From condition $v=1$ is located the minimum acceleration, upon which, according to (13), all ions are held in the cord.

II. $w_0 > \Omega_0^2 a$, $\Omega t < 2\pi$. We will consider that in this mode/conditions remain all ions whose coordinate at any moment of time $x < a$. Hence

$$\psi(z_0) = \sigma(\Omega^2 - z^2) \quad u(t)$$

$$N/N_0 = \sigma(1+u) \left[\frac{1}{2} + u \sqrt{1-u^2} + \frac{1}{\pi} \arcsin u \right], \quad (15)$$

$$u = 1 - \frac{w_0}{\Omega^2 a} (1 - \cos \Omega t).$$

Key: (1) . and.

In the table are contained the results of calculations $\frac{N}{N_0}(u)$ also for this acceleration mode. If u is positive for $w_0 > \Omega^2 a$ when $\Omega t < \pi$, and for $\Omega t > \pi$ when $w_0 < \Omega^2 a$. Formulas (14) and (15) together with the table give response/answer to stated problem within the limits of the model accepted.

In conclusion it is possible to note the following: the assumption about the energy homogeneity of ions in the beginning of acceleration can be considered unessential. It is possible to generalize results, after introducing into the function of distribution (1) dependence $N_0(E_0)$ and to integrate final results on E_0 :

during the short times of acceleration it is possible to carry out $w_0 > \Omega^2 a$, at a cost of the losses of certain quantity of ions:

it is possible to carry out acceleration mode of two stages: the first $w_0 < \Omega^2 a$ and $\Omega t > 2\pi$, by the second - $w_0 > \Omega^2 a$, and $\Omega t < \pi$. In this case by N_0 in formula (15) should be understood N from formula (14).

Page 229.

71. Numerical investigation of the radiation instability of the charged/loaded relativistic rings in the nonlinear mode/conditions.

A. G. Bonch-Osmolovskiy, Ya. P. Zhidkov, V. G. Makhon'kov, V. M. Tsytovich, V. G. Shchinov.

(Joint institute of nuclear research).

In connection with the development of the collective method of acceleration [1] high value will have stability problem of the relativistic charged/loaded rings. Latter/last investigations [2, 3] showed that one of the most dangerous instabilities of such rings is the radiation instability. For the ring in the free space (which usually occurs under conditions for experiment) this instability carries hydrodynamic character and it is characterized by the increment:

$$\gamma_n = n^{2/3} \bar{\omega} \sqrt{\frac{\gamma}{\gamma}},$$

where n - number of the azimuthal harmonic of disturbance:

$\bar{\omega} \approx c/R$, γ - "linear electron"; γ - relativistic factor of particles; R - radius of ring.

With the sufficiently large energy scatter the instability has a threshold, connected with Landau damping, determined by formula $\Delta\omega_{kp} \approx \bar{\omega} n^{1/2} \sqrt{\frac{3}{8}}$, where $\Delta\omega_{kp}$ - the threshold value of the scatter of frequencies of revolution.

Under the assumption $\nu/\gamma \ll 1$, $a/R \ll 1$, $n \ll R/a$ it is possible to obtain [3] nonlinear equations for the evolution of the disturbances/perturbations

$$\frac{\partial \psi_n}{\partial t} + i n \alpha w \psi_n + \sum_{n_1} \sigma_{n-n_1} \frac{\partial \psi_{n_1}}{\partial w} \int \psi_{n-n_1}(w_1) dw_1 = 0, (1)$$

where $\psi_n(w, t)$ - harmonic of the distribution function; w - moment of momentum of particles,

$$\alpha = \frac{d\omega}{dw} \approx \frac{\omega - \bar{\omega}}{w}, \quad \sigma_n = -\frac{0.52\pi e^2}{c} \bar{\omega} |n|^{1/3}.$$

The analytical investigation (see [3]), carried out in limiting cases far and near from the threshold, makes it possible to qualitatively rate/estimate maximum energy of fluctuations and indicates the possibility of the establishment of nonlinear steady state.

By the purpose of this work are the numerical investigation of the evolution of initial disturbances, the described system of equations (1), and the searches of nonlinear steady state.

2. Numerically was solved system of 22nd equations (1), i.e., $n_{max}=10$, with the following initial data:

$$\psi_0(0, w) = \frac{N}{\sqrt{2\pi} w_0} \exp\left(-0.5 \frac{w^2}{w_0^2}\right), \quad (2)$$

where $\psi_n(0, w) = i \frac{G_n A_n \psi_0'}{k_n + \alpha n w}$; w_0 - initial scatter; A_n - low numerical coefficients, which characterize amplitude distribution of initial disturbances according to n .

Expressions (2) can be obtained from equations (1) disregarding by nonlinear terms, if is fulfilled dispersive relationship/ratio. The selection of such initial conditions provides initial evolution in accordance with the linear theory. With arbitrary initial data functions ψ_n in the process of count take the form (2) after some time.

As is known, the selection of stable difference diagram for the equations, which contain derivatives in terms of two variable/alternating, is far not trivial task. In our case the solution of equations (1) was carried out by the method of prediction/forecast and correction [4], as a result the utilized implicit flow chart of numerical calculation proved to be stable during the appropriate selection of the step/pitch of integration for

the time. The program, written in the language CERN - FORTRAN, was realized on BESM-6 of J.I.N.R.

3. At first was investigated linear stage of development of instability. Were selected the following parameters, which are of practical interest for the collective method of the acceleration:

$$R=5\text{cm}, N=10^{13}, \sqrt{\frac{J}{I}}=1/15, A_n=10^{-4}+10^{-5};$$

a) for the hydrodynamic limit

$$\frac{\langle w \rangle}{w_0} = \frac{m R c}{w_0} = 100.10;$$

b) near the threshold

$$\frac{\langle w \rangle}{w_0} = 2 \div 5.$$

Fig. 1 depicts the graphs/curves of the amplitudes of fields depending on time for $n=1$ and 10 for case of a). It is evident that the curves have oscillating character and are

approximately/exemplarily described by relationship/ratio $e^{\Gamma_n t} \cos \Omega_n t$;

Γ_n increases with increase of n . Numerical values Γ_n, Ω_n will well agree with the data of linear theory [2]. Is most interesting case b) near from the threshold where the development of instability significantly affects Landau damping. The corresponding results are represented in Fig. 2. Depending on the selection of the value of initial scatter the curves have different character. Thus, when

$\frac{\langle w \rangle}{w_0}$ - all harmonics build up, but also by the increment, considerably smaller than the hydrodynamic, moreover increment decreases with the number of harmonic. When $\frac{\langle w \rangle}{w_0} = 3$ long-wave harmonics build up, and short-wave attenuate.

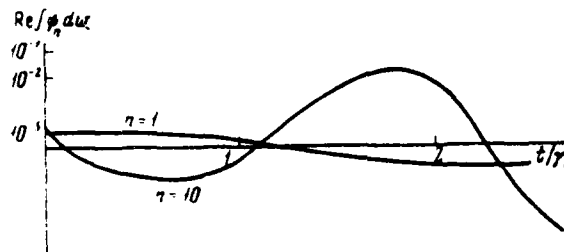


Fig. 1. Amplitudes of fields $n=1$ and 10 in the linear conditions when $\frac{\langle W \rangle}{W_0} = 100$.

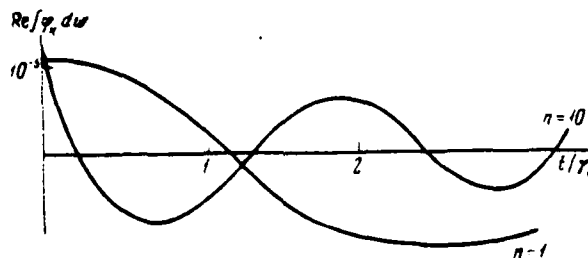


Fig. 2. Amplitudes of fields for $n=1$ and 10 in linear conditions when $\frac{\langle W \rangle}{W_0} = 3$.

Page 230.

Finally, when $\frac{\langle W \rangle}{W_0} = 2$ all harmonics attenuate, which also will agree well with the conclusion/output of linear theory.

4. Let us switch over to research of dynamics of development of radiation instability taking into account nonlinear terms. Since the increments are great when $\frac{\langle W \rangle}{W_0} = 10$, it is of interest to investigate

precisely this case. Initial conditions were selected in the form (2) (Fig. 3), so that the maximum energy of disturbance/perturbation was concentrated in the middle part of spectrum ($n=5$). In the process of count standardization $\int \psi_0 d\omega$ was retained with an accuracy to 1%.0.

Fig. 4 depicts the graphs/curves of the evolution of electric fields 1, 5, 8 and 10 harmonics at the nonlinear stage, from which it is evident that occurs sharp of shift of phases and transformation of vibrational energy kV the region small n . Total vibrational energy $\sum |E_n|^2 n^{1/2} / 4\pi$ at the nonlinear stage undergoes a series of oscillations with the consecutive stabilization and the destabilization, reaching the permanent average/mean level to two orders smaller than the maximum, evaluated theoretically [3]. Fig. 5 and 6 depict the evolution of the averaged of the orbit function of distribution ψ_0 and harmonics ψ_n .

From Fig. 5 it is evident that the nonlinear processes lead to blurring ψ_0 with the small decrease of the medium energy of electrons, so that effective scatter stops the order of threshold value.

REFERENCES

1. V.I. Veksler et al., Proc. 6th Internat. Conf. on High Energy Accelerators, Cambridge, 1967, p.289.
В.И. Векслер и др. Атомная энергия, 1968, 24, 317.

2. A. G. Bonch-Broslovskiy, E. A. Perel'shteyn, V. N. Tsytovich. Transactions of VII international conference on the charged particle accelerators high-energy. T. P. Yerevan, Iss. AS ARM SSR, 1970, page 579; preprint J.I.N.R., E9-4751. Dubna, 1969.

3. A. G. Bonch-Broslovskiy, V. N. Tsytovich. Nonlinear theory of the radiation instability of relativistic circular beams. M., transactions of the Lebedev physics inst., 1970.

4. D. Mak-Kraken, U. Dorn. Numerical methods and programming on FORTRAN. M., publishing house "Mir", 1969.

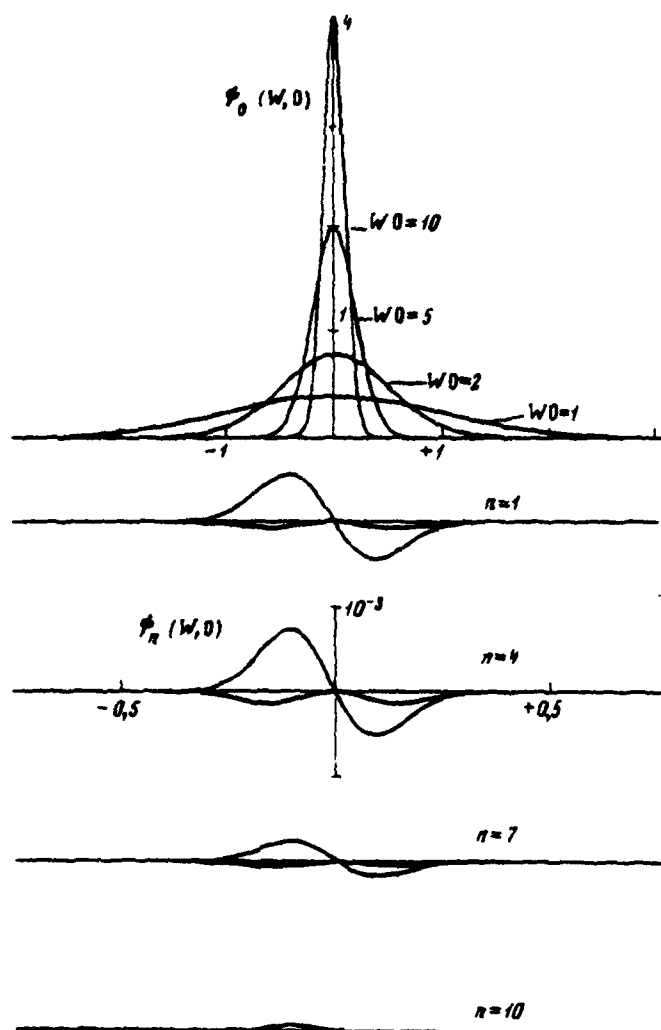


Fig. 3. Initial data for ϕ_0 and ϕ_n . Here $\frac{\langle W \rangle}{W_0} = 10$, where W_0 - initial scatter.

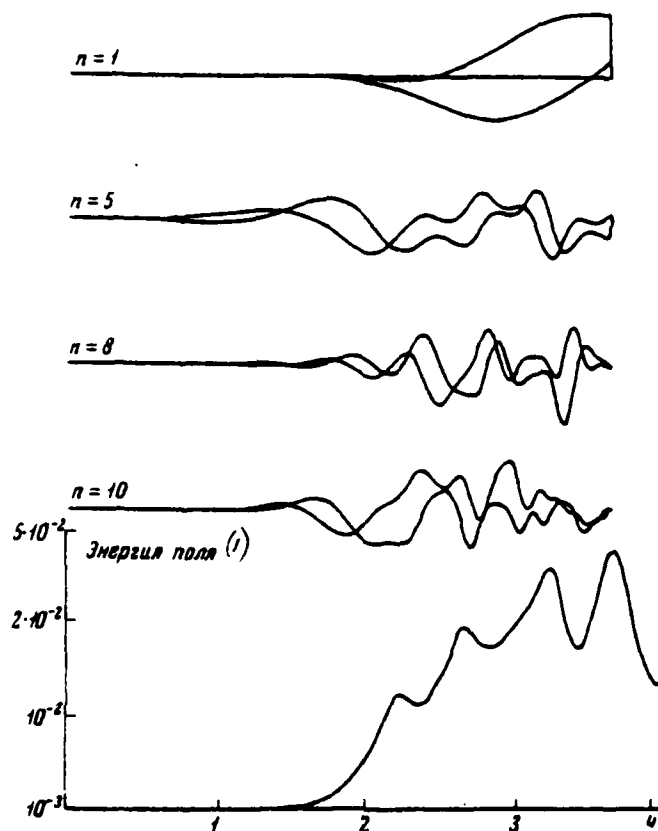
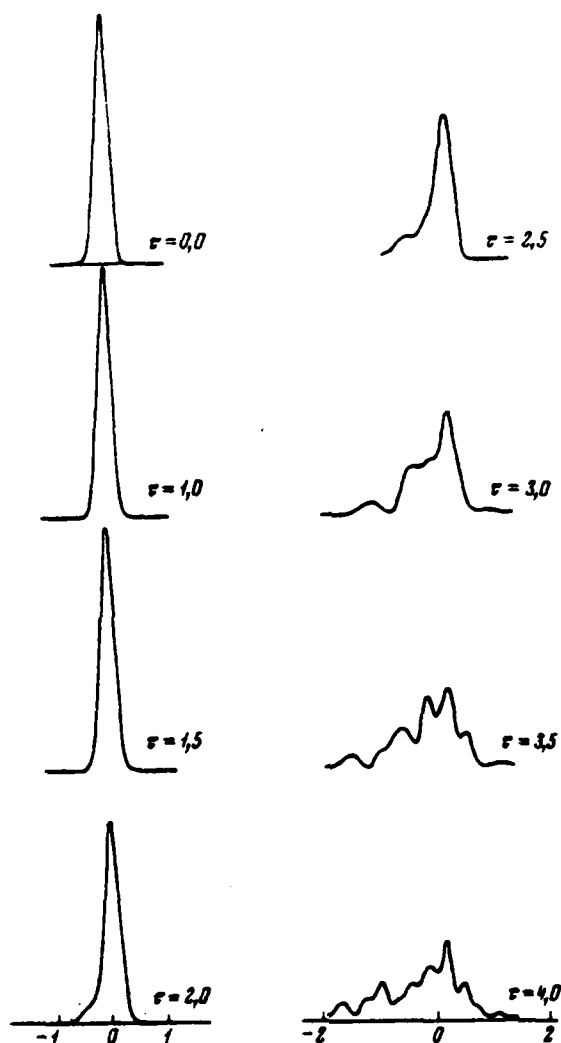


Fig. 4. Graphs/curves of the evolution of electric fields and total energy of disturbance/perturbation in the time.

Key: (1). Energy of field.

Page 231.

Fig. 5. Nonlinear theory, evolution Ψ .

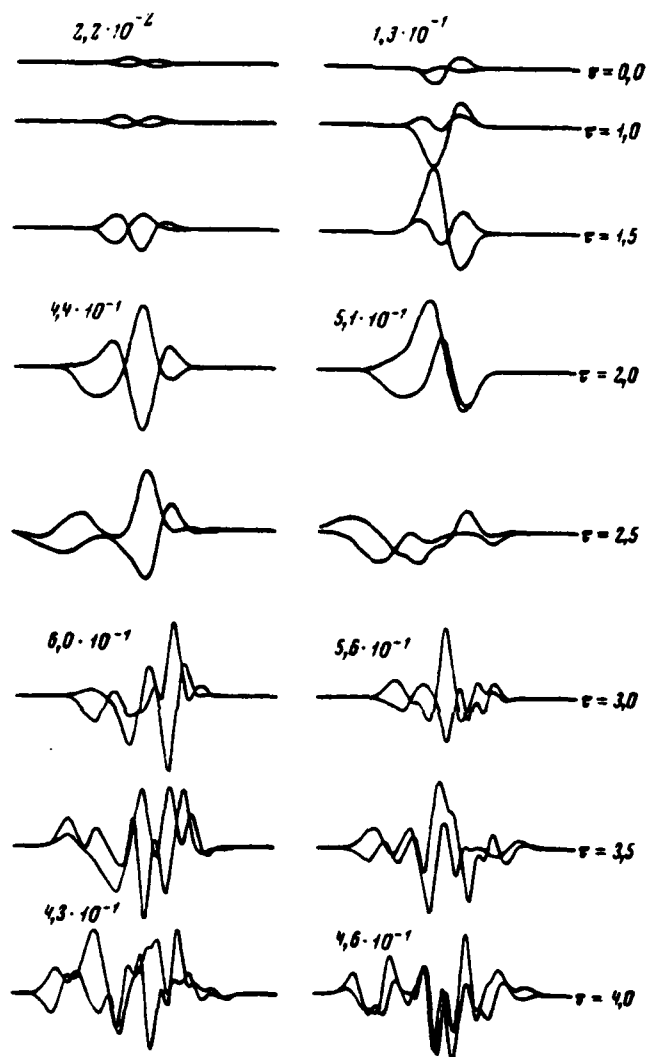


Fig. 6. Evolution of the harmonics of the entire function of distribution Ψ_n

72. Some questions of the design of linear coherent heavy-particle accelerator to low energies.

O. A. Bal'ner, V. A. Vorontsov, S. A. Pukshin, O. N. Popov.

(Moscow physical engineering institute).

This work is the continuation of the investigations, initiated in works [1-2] on the creation of universal coherent ion accelerator is based on the use of a static magnetic field for shaping of electron ring, capture of ions and for after-acceleration of ring, loaded with ions, in the collapsible/dropped magnetic field. The installation consists of solenoid with the prescribed/assigned form of the distribution of the longitudinal component of magnetic field along the axis, linear accelerator of electrons and ionic source. According to the character of a change in the longitudinal component of magnetic field solenoid it is possible to divide into three parts. In the first part the field rapidly increases, on second section the magnetic field is virtually constant, in the third part the value of the longitudinal component of magnetic field decreases with the distance. Electrons of the linear accelerator are injected into the solenoid at angle to the axis/axle of magnetic field in the form of

short cluster by the duration of less than nanosecond. On the section of the increasing magnetic field it occurs the decrease of the longitudinal velocity of clusters, in consequence of which decreases the size/dimension of cluster lengthwise. Near the starting point, which corresponds to maximum magnetic intensity, is formed the similarity of the electron ring with a small cross section and the radius, equal to a radius of the tubular ion beam which is introduced into the solenoid parallel to its axis/axle. The longitudinal velocity of ring in the region of starting point close to the rate of ions, here occurs the capture of ions into the electron ring. The loaded by ions ring is accelerated in the section of the collapsible/dropped magnetic field due to the conversion of the part of the energy of rotational electron motion into the energy of axial motion. On this principle is projected/designed the model of accelerator for testing the idea of the acceleration of ions proposed by collective method.

The length of solenoid is selected equal to 1 m with the maximum value of the longitudinal component of magnetic field B_z 1.17 T. As the injector of electrons is intended to use the linear accelerator of electrons with $W=10$ MeV and $I_{umr}=15$ A. Cluster contains 10^{11} electrons, durations of pulse $1 \cdot 10^{-9}$ s. Repetition frequency of electronic rings 100 MHz. The diameter of cluster is less than 1 cm. The pulse current of protons from the ionic source in

the form of tubular bundle with the mean radius of 3 cm is equal to 0.5 A with the energy of protons 50 keV.

A basic question with the method of the formation of electron ring proposed is the effect of the parameters of cluster and form of magnetic field to the possibility of formation of electron ring and to the capture of protons. Calculations showed that the deviation of the rate of ring at starting point from the proton velocity must not exceed 100% with the realization of capture in a described below manner. The analysis of the single-particle model of the formation of ring in the static magnetic field showed the possibility of formation/education at the starting point of the electron ring with a radius of 3 cm. The section of ring has ellipsoidal form with the longitudinal size/dimension $2a$, equal to 1 mm and with transverse size/dimension $2c$, equal to 1 cm. In this case is necessary obtaining energy spread $\Delta\epsilon/\epsilon$ it is less than 10% and angular divergence $\Delta\theta$ it is less than $3 \cdot 10^{-4}$ rad. The effect of energy scatter with different average/mean gradients of magnetic field to the longitudinal velocity of ring at starting point is shown in Fig. 1. The selection of the form of magnetic field and the length of the section of the increasing magnetic field also affect shaping and longitudinal velocity of ring at starting point. Investigation of the formation of ring with different average/mean gradients of magnetic field thus far showed the expediency of the selection of the average/mean gradient

of the magnetic field of 50 G/cm. The length of the section of shaping of ring L_c and the angle of injection φ between the direction of the injected electrons and the axis/axle of magnetic field are selected taking into account the possibility of obtaining the longitudinal size/dimension of ring $2a$, equal to 1 mm. The value of the section of shaping of ring is equal to 10 cm, the angle of injection is equal to 70° . The time of the formation of ring is (3-5) $\cdot 10^{-9}$ s. It should be noted that a question about the formation of electron ring in the static magnetic field was examined by other authors [3, 4].

At the end of the section of shaping during braking of electron ring in the magnetic field occurs the capture of protons. The possibility of capture is caused by the presence of the inertial forces in systems of the rings whose action during the specific selection of the rate of braking leads to the fact that total energy of proton in the system of ring becomes negative. In parameters examined above of electron ring proves to be possible the capture of protons from the region in the form of torus by section $0.4-0.6 \text{ mm}^2$ by the radius, equal to a radius of electron ring. With the section of the tubular proton bundle $18-20 \text{ cm}^2$ and current 0.5-1 and a quantity of sized protons is equal (to 6-8) $\cdot 10^7$. The length of the section of capture is 0.7-1.2 cm. The acquisition time is equal (2-4) $\cdot 10^{-9}$ to s. The inertia principle of capture imposes heavy demands on

the rate of ring at the starting point whose divergence from the proton velocity must not exceed 100/o. This limitation can be reduced by the grouping of proton beam at starting point, which simultaneously leads to an increase in the quantity of seized protons.

From the starting point the loaded with protons electron ring accelerates in the collapsible/dropped magnetic field. Upon the acceleration of ring its longitudinal size/dimension increases due to space-charge effect, kinematic divergence, scatter in the longitudinal velocities. was evaluated the divergence of ring under the action of Coulomb forces without taking into account the effect of ionic component. The longitudinal size/dimension of ring increases 20-30 times for time $(70-100) \cdot 10^{-9}$ s. However, during capture of the necessary number of ions space-charge effect of electrons on the longitudinal divergence can be considerably reduced.

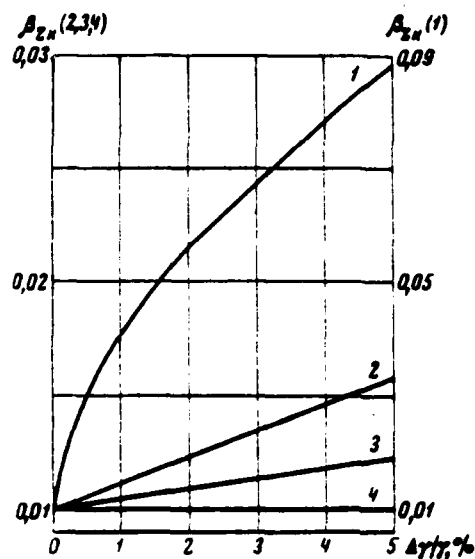


Fig. 1. Graph/diagram of the dependence of the rate of ring at starting point β_{zk} on the scatter of beam on energy $\Delta\gamma/\gamma$ at the point of injection with different gradients of magnetic field. 1, 3, 4 - correspond to gradients 500, 50 and 100 G/cm; 2 - correspond to the parabolic dependence of the derivative of magnetic field and to the average/mean gradient of the magnetic field of 50 G/cm.

Page 233.

Kinematic divergence is connected with the fact that the end-points of ring pass starting point at different moments of time. For the determination of the possibility of decreasing the effect of kinematic divergence are examined two cases: I) at starting point is located ring with the round cross-section with a diameter of 1 mm, which corresponds to injection into the solenoid of the cluster with the sizes/dimensions of $2a = 1 \text{ cm}$, $2b = 1 \text{ mm}$; II) at starting point is located ring with elliptical cross section $2a = 1 \text{ mm}$, $2b = 1 \text{ cm}$, which corresponds to injection into the solenoid of cluster with the round cross-section with a diameter of 1 cm. Fig. 2 shows a change in the strength of the field of ring along the accelerating section of magnetic field for these two cases. In the case of 1 decrease of the effect of kinematic divergence is connected with the decrease of size b . In the case II the effect of kinematic divergence can be reduced with satisfaction of condition $a \ll b$ at the entire length of the accelerating part of the solenoid. The time of acceleration is $50-100 \cdot 10^{-9} \text{ s}$ at the length of the section of acceleration 80-100 cm. For eliminating the longitudinal divergence is necessary effective

longitudinal focusing in the section of the collapsible/dropped magnetic field. Under realization condition for focusing is possible the acceleration of protons to the energies 0.3-0.5 MeV with the current of protons $I_{\text{pump}} = 10$ mA. At present is conducted the study of space-charge effect and betatron oscillations on the compression and the longitudinal velocity of ring at starting point, is revealed/detected effect of the parameters of ring, rate of its braking in the magnetic field and interactions of proton beam with the ring to a quantity of seized protons and a possibility of their further acceleration, are examined the possibilities of applying the different methods of the longitudinal focusing of ring. Further increase in the effectiveness in the acceleration is connected with an increase in the beam current and a decrease of the diameter of the section of ring. Thus, for instance, an increase of the quantity of electrons in the ring to $(2-5) \cdot 10^{11}$ and the simultaneous decrease of diameter the sections of ring to 3-5 mm make it possible to rely on an increase in the final energy of protons to 3-8 MeV with current $I_{\text{pump}} = 10-20$ mA.

REFERENCES

1. O. A. Val'ner. Transactions of VII international conference on the charged particle accelerators high-energy. Vol. 2. Yerevan, publ. ARM SSR 1970, p 547.

2. O. A. Val'dner. coll. "Accelerators", Atomizdat, 1970, iss. 12, page 4.

3. R. Berg et al. Phys. Rev. Let., 1969, 22, N9, 419.

4. R. Berg, H. Kim and M. Reiser. IEEE Trans. on Nucl. Sci., 1969, NS-16, 3, 1043.

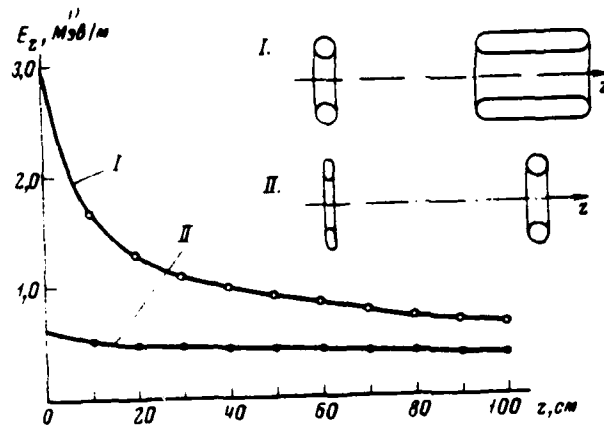


Fig. 2. Graph/curve of a change in the electric intensity E_z of ring along the accelerating section.

Key: (1). MeV/m .

Page 234.

73. Motion of the charged/loaded relativistic ring in the corrugated magnetic field.

K. A. Reshetnikova.

(Joint Institute for Nuclear Research).

Is examined the motion of the thin azimuthally symmetrical

charged/loaded ring in the periodic along by the variable/alternating z magnetic field. Vector potential of the field:

$$A'_\varphi = \frac{\bar{H}_2 r'}{2} (1 + \alpha \sin k' z'). \quad (1)$$

Here α - depth of modulation of field; $k' = 2\pi/\lambda'$; λ' - three-dimensional/space period of the magnetic field (prime shows that the values relate to the laboratory coordinate system). Initial conditions with the entrance of ring into the corrugated field are such:

$$t=0, \quad r' = r'_0, \quad z' = 0, \quad v'_r = 0, \quad v'_\varphi = v'_{\varphi 0}, \quad v'_z = v'_{z0} = c.$$

In the coordinate system, which moves with the constant velocity, equal to the initial longitudinal velocity of ring, for (1) we have:

$$A_\varphi = \frac{\bar{H}_2 r}{2} (1 + \alpha \sin \psi). \quad (2)$$

Here

$$\psi = \omega t + k z, \quad k = k' \gamma_{z0}, \quad \omega = k v'_{z0}, \quad \gamma_{z0} = \frac{1}{\sqrt{1 - \beta_{z0}^2}}.$$

The intensities/strength of electromagnetic field, which correspond to potential (2), will be:

$$\begin{aligned} E_\varphi &= -\frac{\alpha r \omega}{2c} \bar{H}_2 \cos \psi, \\ H_r &= -\frac{\alpha r k}{2} \bar{H}_2 \cos \psi, \end{aligned} \quad (3)$$

$$\bar{H}_2 = H_2 (1 + \alpha \sin \psi).$$

Was solved first the task about the motion of single particle in the fields of form (3) without taking into account the effect of the proper field of the charged/loaded ring. Is proved the invariance of value $\gamma(\frac{E}{\omega} + \beta_z) = \text{const}$, which gives the single bond of energy of particle

with its longitudinal velocity. Equations of motion with the aid of the law of conservation of the generalized azimuthal impulse/momentum/pulse and mentioned invariant are reduced to the system of two equations whose solutions are found with Krylov-Bogolyubov's method [1].

After constructing the solution in the single-particle approximation/approach, they passed taking into consideration of the effect of the proper fields of the charged/loaded ring both static, and caused by motion in the applied field. The potentials, which describe the proper field of the charged/loaded ring, are decomposed/expanded in the series/row on curvature [2] from series expansion parameter $\frac{L}{r} \ll 1$ and on the delay at the harmonic dependence of rate on the time and the arbitrary value kr . Here α - radius of the section of the ring; r - large radius of ring; $L = 2\pi \frac{R_1}{\alpha}$. When $\frac{R_1}{kaL} \ll 1$ the effect of delay can be disregarded/neglected.

Are introduced the coordinates of the divergence of particles from the center of section of ring: $x_1 = r - r_0$, $x_2 = z - z_0$. The motion of the center of section is known from the single-particle approximation/approach. For diverging the coordinates from the center are obtained the equations in which is carried out the averaging on the rapid oscillations under the conditions: $\alpha \ll 1$, $\omega \gg \omega_H$, where ω_H - Larmor frequency.

As a result is obtained the following system of equations for the slow variable/alternating:

$$\frac{d^2 \bar{x}_1}{dt^2} + \left[\omega_H^2 - \omega_p^2 \left(\frac{1}{\gamma_H^2} + \frac{\alpha^2 \beta_{\psi H}^4}{8} \right) \right] \bar{x}_1 = 0, \quad (5)$$

$$\frac{d^2 \bar{x}_2}{dt^2} + \omega_p^2 \left[\frac{\alpha^2 \beta_{\psi H}^4}{8} \left(L k^2 a^2 + \frac{k^2 a^2}{2} - 1 \right) - \frac{1}{\gamma_H^2} \right] \bar{x}_2 = 0. \quad (6)$$

Here

$$\gamma_H^2 = \frac{1}{1 - \beta_{\psi H}^2},$$

$$\omega_H^2 = \left(\frac{e \bar{H}_z}{m_0 c \gamma_H} \right)^2, \quad \omega_p^2 = \frac{e^2 N}{\pi r_H a^2 m_0 \gamma_H},$$

where N - number of electrons in the ring; γ_H - initial value γ . As can be seen from (5), focusing in the radial direction is provided by the uniform magnetic field. Condition of radial focusing usual:

$$\omega_H^2 > \omega_p^2 \left(\frac{1}{\gamma_H^2} + \frac{\alpha^2 \beta_{\psi H}^4}{8} \right). \quad (7)$$

Condition of longitudinal focusing from (6)

$$\frac{\alpha^2 \beta_{\psi H}^4}{8} \left[\left(L + \frac{1}{2} \right) (ka)^2 - 1 \right] > \frac{1}{\gamma_H^2}. \quad (8)$$

Into the condition of longitudinal focusing a number of particles

does not enter, potential well depth depends on $r_{2H} (k - k' r_{2H})$.

Focusing lengthwise - quadratic effect in the value of variable field, caused on the one hand by a change in the energy of particle external δ_p - by field in that selected to the moving/driving coordinate system, with another - by the action of radiation proper field 3, proportional to a number of particles and to the acceleration of ring with figurative sign $(\frac{e^{(p\omega)}}{c} - \frac{1}{c} \frac{\partial A_3}{\partial t} \sim -iN)$. Radiation field is called here the part of the proper field of cluster, caused by its acceleration.

The action of these two factors leads to the appearance of the standing wave relative to the center of the section of ring whose frequency is equal to zero. Appears the usual mechanism of focusing on the standing wave whose value is determined by relation δ/λ . Wave amplitude $\delta \sim i - M_1$, where M_1 - component of applied field, in this case $M_1 \sim r_{2H}$. At the same time the wavelength of field in the selected system of coordinates $\lambda \sim \frac{1}{r_{2H}}$. Therefore relation $\frac{\delta}{\lambda} \sim r_{2H}^2$, potential well depth increases as r_{2H}^2 .

The integration of equations of motion in general form on the computers confirmed the presence of stable oscillations relative to center at the values of the parameters, under satisfying conditions (7), (8).

Thus, during the motion of the charged/loaded relativistic ring in the corrugated magnetic field in the coordinate system, which moves together with the ring, appears potential well on the radiation wave and the wave of applied field, which changes energy of particles, that brings with increase δ_1 and supplementary compression lengthwise. From the condition of confinement of ions in the ring in the case when the frequency of the effect of field is much more than frequency of ionic, we will obtain: $\alpha < k' a \gamma_1^2$, the value of modulation of field does not depend on a number of electrons in the ring and can increase with increase δ_1 .

REFERENCES

1. N. M. Bogolyubov, Yu. A. Mitropol'skiy. Asymptotic methods in the theory of nonlinear vibrations. M., State Technical Press, 1955.
2. E. A. Perel'shteyn, O. I. Yarkova. Preprint J.I.N.R. 2351, Dubna, 1965.
3. I. Ye. Tamm. The transactions of the Lebedev physics inst., Vol. XVIII. Publishing house of the AS USSR, 1962, p 3.

Page 235.

74. Calculation of the phase volumes of the electric ion clusters and beams in the collective accelerator and questions of separation.

M. L. Iovnovich, N. B. Rubin, V. P. Sarantsev.

(Joint Institute for Nuclear Research).

For the experimental use of protons, accelerated to the high energies by the collective method of acceleration [1], it is necessary to determine the scatter of protons on the impulses/momenta/pulses and the phase volume of proton cluster. These values were evaluated at work [2]. For refining these estimations let us examine the motion of protons in the electronic cluster in the process of combined acceleration. Protons are formed in the process of the ionization of the atoms of hydrogen in the circular cluster of relativistic electrons with the sufficiently low speeds, compared with the rates of the atoms of hydrogen. The formed proton tests/experiences the action of the electrical and magnetic field of electronic cluster, and also external magnetic field, along which is accelerated the cluster. Let us examine circular cluster with a number of electrons less than 10^{10} , and by the small radius a , such smaller than the large radius R_0 .

In this case for the estimations it is possible to disregard proper magnetic field in comparison with the external, and also curvature of ring. As a result we come to the task about the motion of protons in the cylindrical electron stream, perpendicular to axis/axis of which (axis/axis Oy) is directed the external uniform magnetic field of value H_0 (along the axis/axis Oz). In the system of the rest of electronic cluster the equations for the transverse motion of proton take the form:

$$\ddot{x} + \omega_0^2 x - \Omega \dot{y} = 0, \quad \ddot{y} + \Omega \dot{x} = 0. \quad (1)$$

where $\omega_0^2 = \frac{2\pi e^2 n}{M}$; $\Omega = \frac{e H_0}{Mc}$; n - electron density; M - mass of proton. As the initial conditions let us accept $x=x_0$, $y=0$, $\dot{x}=\dot{y}=0$. Integrating second, and then first equation (1), we will obtain for the coordinates and the rates:

$$x = x_0 \frac{1+q \cos \omega t}{1+q}, \quad y = x_0 \frac{q(\omega t - \sin \omega t)}{(1+q)^{3/2}},$$

$$\dot{x} = -x_0 \omega_0 \sqrt{\frac{q}{1+q}} \sin \omega t, \quad \dot{y} = 2x_0 \frac{\Omega q}{1+q} \sin^2 \omega t, \quad (2)$$

where $\omega^2 = \Omega^2(1+q)$; $q = \omega_0^2/\Omega^2 = 2\pi M c^2 n/H_0^2$.

For the electric ion cluster $q \gg 1$ in question. In this case expression (2) takes the following form:

$$x = x_0 \cos \psi, \quad y = x_0 q^{-1/2} (\psi - \sin \psi),$$

$$\dot{x} = -\omega_0 x_0 \sin \psi, \quad \dot{y} = 2x_0 \Omega \sin^2 \frac{\psi}{2}, \quad (3)$$

where $\psi = \omega_0 t$.

The time during which the proton velocity reaches maximum, is much less than the storage time and acceleration of protons. With the aid of expressions (3) it is possible to find the scatter of protons by transverse pulses in the laboratory coordinate system:

$$\Delta p_x = 2M\omega_0 a, \quad \Delta p_y = 4M\Omega a. \quad (4)$$

Expression for the emittance of the cluster of the protons

$$\varepsilon = \frac{\Delta p_x \Delta p_y s}{p_0^2}, \quad (5)$$

where p_0 - longitudinal impulse/momentum/pulse of proton, equal for ultrarelativistic motion $Mc\gamma$, s - the maximum cross-sectional area of ring, in the case in question accepts the form

$$\varepsilon = \frac{32\pi R_0 a^3 \omega_0 \Omega}{c^2 \gamma^2}. \quad (6)$$

For the cluster with a number of electrons $5 \cdot 10^{13}$, $H_0 \approx 2 \cdot 10^4$ e, $\gamma \approx 10^3$ we obtain $\varepsilon \approx 5 \cdot 10^{-2}$ (mm. mrad)². The comparison of the obtained emittance of the accelerated beam with the emittance of strong-focusing accelerator to this same energy shows that this of the value of one order.

Besides the emittance the important characteristic of the beams, obtained on the accelerators, is their temporary/time extent and

respectively "fill factor".

The length of the impulse/momentum/pulse τ of the accelerated particles in the collective accelerator is very small. For the energy of protons 1000 GeV $\tau \sim 10^{-14}$ s. This structure of beam has its advantages and deficiencies/lacks. Advantages become apparent in all experiments with the neutrino, and also in a number of cases with the work with the bubble and spark chambers/cameras. The works in which by a traditional method are utilized the counters and the coincidence circuits, here require special developments.

Experiments with bubble chambers require preliminarily the separations of the beams of secondary particles. This task is generally very complicated with such energies. However, the beams, which can be obtained with the aid of the collective accelerator, are most been adequate/approached for this purpose in view of their small axial extent. The diagram of separation is simple. Frequencies with the identical impulses/momenta/pulses and the differing masses after the flight/span of the specific basis L are radiated lengthwise in certain distance ΔL due to the difference in the rates. Further is arranged/located high-frequency device-separator, which deflects/diverts particles from the axis/axle. If we take $\Delta L = \lambda/2$, where λ - wavelength in the separator, then the particles of different masses differ from axis/axle in opposite directions, i.e.,

will occur their separation. The basis

$$L = \lambda \frac{(pc)^2}{E_{02}^2 - E_{01}^2}, \quad (7)$$

where E_{01} , E_{02} - rest energy of the types of the particles in question (for example, see [3]), p - particle momentum.

Page 236.

For example, for isolation/evolution K - mesons from π - mesons with $\lambda \approx 3$ cm and $pc \approx 500$ GeV we obtain $L \approx 30$ km, and for the antiprotons - $L \approx 7.5$ km,

For shortening of the overall sizes of separative system it is possible to force secondary particles to move over the closed trajectories in the magnetic field. Let us take for an example weakly-focusing type magnetic system with superconducting coil electromagnets and time-constant magnetic field $H \approx 60$ kOe. For $E \approx 500$ GeV radius of circular path $R \approx 280$ m. During the appropriate collimation of secondary beams it is possible to have an amplitude of betatron oscillations $a_\beta \approx 1$ cm. Let us examine two versions.

1. Particles of different masses, rotating in magnetic system, diverge along azimuth. If we further rapidly decrease by the small

magnetic field strength, then the fallen behind particle will not repeat the trajectory of front/leading particle, and they will be derived from the ring in the different directions. It is possible to make more simply: after the conclusion/output of particles along one trajectory to utilize a usual separator.

2. After particle injection in ring are switched on accelerating high-frequency elements/cells. Then with the passage by particles in the ring of path $2L$ useful particles during the appropriate selection of the phase of accelerating field obtain the addition of energy and they will pass to a larger radius, and particles with another mass will remain on a previous radius. Shift/shear by a radius is determined by formula $\frac{\Delta R}{R} = \frac{1}{1-n} \frac{\Delta E}{E}$, where n - index of magnetic field; $\Delta p/p \approx \Delta E/E$, E - energy. With $\Delta R \approx 5$ cm, $n=2/3$, $\Delta E/E \approx 6 \cdot 10^{-3}$ speed for K - mesons ≈ 37 , for antiprotons ≈ 8 . The useful particles, isolated on a radius from the unnecessary particles, are derived/concluded further from the ring.

It should be noted that the intensity of decaying particles will decrease at the large mean free paths examined. The ring in question can be used also as storage system for the protons, the antiprotons and for the realization of their collision, or as the device/equipment, which stretches proton beam in time [2].

REFERENCES

1. V. I. Wexler et al. Atomic energy, 1968, 24, 317.
 2. D. Keyser. Sympos. on Electron Ring Accelerators, UCRL - 18103, Berkeley, 1968, p 79.
 3. V. I. Kotov, V. V. Miller. Focusing and separation throughout the masses of high energy particles. Atomizdat, M., 1969.
 75. Steady state of electron ring in the external magnetic field.
- S. Budnyan, Ye. I. Zhidkov, I. M. Ivanov, E. A. Perel'shteyn.
- Joint institute of nuclear investigations).

In the collective method of acceleration as those accelerating are utilized the proper fields of charged/loaded bunches of particles [1]. Their own forces, which act on the particles in the system, are compared in value with the external, mathematical models of such formation/educations they are the particular decisions of the self-consistent system of equations of Vlasov.

Here is examined the model of stationary circular cluster - model of Yarkovoy [2-4]. The function of particle distribution in the phase space is selected in the form of function from two constants of motion. The first - total energy - the consequence of the stability of system, the second - the generalized moment of momentum - the consequence of azimuthal symmetry. Total energy, and also generalized moments/torques are selected identical for all particles of one type α and equal to respectively $H_{0\alpha}$ and $M_{0\alpha}$. The use of this distribution function reduces to the system of nonlinear two-dimensional integral equations for kinetic energies E_α and azimuthal particle momenta $p_{\phi\alpha}$, depending on coordinates r, z in the cylindrical coordinate system. It is impossible to find the decision of the obtained system in general form. In many interesting physical cases it is difficult to obtain even approximate solution. ^RIn this work, on one of the examples, is investigated the possibility of applying the numerical method of decision, analogous developed in [5], to the system of equations of the model in question.

1. Us interests steady state of ring of electrons in weakly-focusing type external magnetic field with index of decrease n . We will consider as the given ones parameters $H_0 = mc^2\gamma_0$, H_0 , n , and also r_0 and $p_{\phi 0} = mc\eta_0$ - respectively a radius of equilibrium orbit and an azimuthal impulse/momentum/pulse of lone electron (in the absence of its own forces), $\alpha = \frac{2e^2 N}{ES}$, where N - total number of particles in

the ring; e, m - charge and mass of electrons; E - kinetic energy of electron, averaged over the section of the ring whose area is equal to S^1 .

FOOTNOTE 1. Selecting thus the basic parameters, we simplify the system of equations of model. It is possible instead of τ_0, p_{y0} to assign the appropriate values taking into account its own forces, and instead of n - total number of electrons N . This will not produce the need for changing the method of numerical solution which we utilize.
ENDFOOTNOTE.

Page 237.

The system of the integral equations of the model of Yarkovoy in our case takes the form:

$$\gamma = -\frac{e}{4\pi} \int_S G_p(z, z', z, z') \gamma(z', z') dz' dz + \gamma_0, \quad (1)$$

$$\eta = -\frac{e}{4\pi} \int_S G_A(z, z', z, z') \eta(z', z') dz' dz + \quad (2)$$

$$+ \eta_0 \left[1 + \frac{1}{2} (1-n) \frac{(z-z_0)^2}{z_0^2} + \frac{n}{2} \frac{z^2}{z_0^2} \right].$$

L - boundary of the region s - is assigned by the functional equation

$$\gamma^2 - \eta^2 - 1 = \Phi(z, z) = 0. \quad (3)$$

In formulas (1) - (3) value $\gamma = \frac{E}{mc^2}$, $\eta = \frac{p_y}{mc}$, the function

$$G_p = \frac{4}{\sqrt{(z+z')^2 + (z-z')^2}} K(\kappa), \quad (4)$$

but

$$G_4 = \frac{4}{\sqrt{(z+z')^2 + (z-z')^2}} \left[\left(\frac{2}{k^2} - 1 \right) K(k) - \frac{2}{k^2} E(k) \right], \quad (5)$$

where K and E - complete elliptic integrals;

$$k^2 = \frac{4rr'}{(r+r')^2 + (z-z')^2}.$$

2. Following work [5], let us introduce continuous parameter t changing in interval $0 \leq t < \infty$, and auxiliary system of equations which converts/transfers in (1)-(3) with $t \geq t_1$, $0 \leq t_1 < \infty$.

We will consider that boundary $L=L(t)$ let us define $R=R(t)$ as the radius-vector of arbitrary point on L .

The means of equations (1)-(2) let us leave without the changes, and instead of (3) let us require

$$\frac{d\Phi_L}{dt} = \frac{dR}{dt} \text{grad} \Phi_L = -\Phi_L, \quad \Phi_L = \Phi(R) \quad (6)$$

with the initial conditions $L(t=0) = L_0$, $\Phi_L(t=0) = \Phi_{L_0}(r(t=0), \varphi(t=0))$, where $r(t=0)$ and $\varphi(t=0)$ - respectively the decision of equations (1)-(2), in which region s is limited by L . From many directions in which it is possible to deform $L(t)$ at each point of boundary in accordance with (6), let us select the direction, normal to $L(t)$:

$$e_t(R) \frac{dR}{dt} = 0, \quad (7)$$

where $e_t(R)$ - vector, tangent to L .

System of equations (1), (2), (6), (7) determines the motion of boundary with a change in parameter t , moreover from (6) it follows that $dR/dt=0$ when $\Phi_1 = 0$, the motion of boundary ceases with execution (1)-(3) and the decision of auxiliary system of equations coincides with unknown with the cessation of boundary $\alpha(t)$. Let us note that the decision of system (1), (2), (6), (7) with $t > t_1$, if it exists and is singular, must not depend on selection α_0 and direction of strain.

3. Decision of system (1), (2), (6), (7) was made on computers. Was selected the initial region $s=s_0$ and were numerically solved equations (1), (2) by the method of replacing the integral equations by the system of algebraic linear equations. Simultaneously were located $\Phi_{\alpha 0}$ and $q_{\alpha 0}$. Equations (6), (7), solved relative to dR/dt , were replaced by finite-difference and were calculated values $R(t_1)=R(r)$, which correspond to the new region s_1 . Then entire course of calculations was repeated with use s_1 and so forth. Obtained thus decision of system must converge to precise with $r \rightarrow 0$.

For the final adjustment of algorithm and explanation of the precision/accuracy of calculations was at first solved the system of equations (1), (2) disregarding by the effect of curvature in nuclei (4) and (5). This corresponds to the determination of the stationary

form of electronic cord. It is clear that this task must be azimuthal symmetrical over the section, and therefore the dependence of physical quantities from the azimuth is connected with the miscounts. Besides in addition to this, as it follows from work [3], there is a dependence of energy and impulse/momentum/pulse on the coordinate of particle over the section of cord. Fig. 1 given the section of cord (circle by a radius $a=0.76$, $x=83$) gives values γ at different points of section. From it it is evident that the maximum difference γ at points on outer circumference is equal to 0.0005, and the difference between value γ in the center of cord and on outer circumference 0.01. Hence, in accordance with [3], it is possible to make the conclusion about the precision/accuracy of the determination of a radius of the section of cord $\sim 1\%$.

It is possible to trace the dependence of discrepancy $\Phi(\gamma, z)$ on initial conditions γ_0, z_0 . So for $a=0.76$, $\gamma_0=5$ and $z_0=4.80$ we obtain $\Phi=-0.1$, for $z_0=4.82$ we have $\Phi=0.02$. This means that when $4.80 < z_0 < 4.82$, radius $a=0.76$ is true decision.

1005

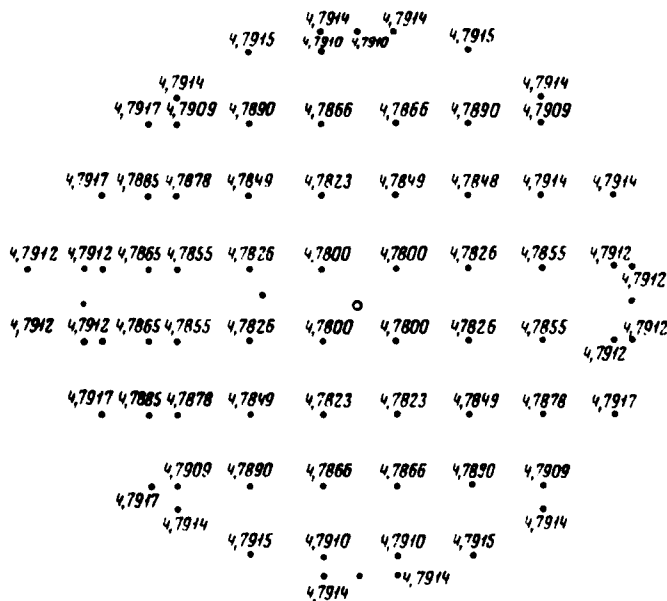


Fig. 1. Dependence of γ on the coordinates over the section of cord.

Page 238.

Finally, were made calculations for the ring with a large radius of $r_0=30$ ($x=0.83$). In this case in (4) and (5) were considered the terms, which give corrections for curvature. The form of section is given in Fig. 2.

The obtained results give grounds to consider that the algorithm of decision presented will make it possible to find the self-consistent form of the electronic cluster of large density, and also steady-state solution for the two-component systems.

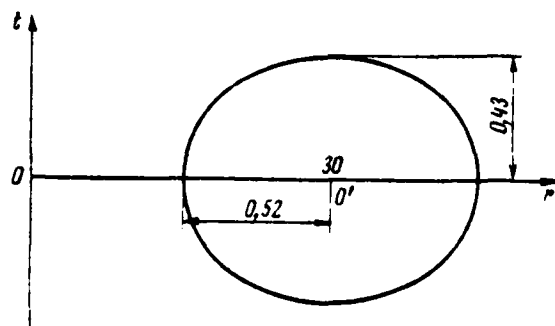


Fig. 2. Form of the section of electron ring for $x=0.83$, $r_0=30$, $\gamma_0=5$.

REFERENCES

1. V I Veksler et al. Proc. 6th Internat. Conf. on High Energy Accelerators, Cambridge, 1967, p 280, and also preprint J.I.N.R. 9-3440-2, Dubna, 1967; "Atomic energy", 1968, 24, 317.
2. O. I. Yarkovoy. ZhTF, 1962, XXXII, 1285.
3. O. I. Yarkovoy. Preprint J.I.N.R. 2182, Dubna, 1965.
4. E. A. Paral'shteyn, O. I. Yarkovoy. Preprint J.I.N.R. 9-4423, Dubna, 1969.
5. Ye. P. Zhižkov, I. V. Puzynin. ZhVM and MF, 1967, 7, No 5, 1086.

Page 239.

Session VI.

SUPERCONDUCTING ELEMENTS OF ACCELERATOR.

76. Study program of Rutherford laboratory for superconducting proton synchrotron.

N. D. Vest.

(Rutherford laboratory, England).

This report contains the short survey/coverage of works on the creation of the project of the superconducting proton synchrotron for the Rutherford laboratory. Will be here touched upon only some basic investigations, and detailed survey/coverage can be found in recently published article [1].

Study of the degradation of windings.

The important problem, which appears during the design of the superconducting coil electromagnet, is the creation of winding,

capable of maintaining high current densities without a change in its characteristics. Despite the fact that the basic reason for the degradation of windings (jumps of magnetic flux) is removed during the use of multicore cable [2], it is necessary also not to allow such mechanical effects as heating windings due to the internal friction in the conductors, that appears with the displacements of the turns of coil. For dealing with the data by the phenomenon it is possible to secure windings, pouring by their suitable for this purpose substances. Unfortunately, it is discovered, that the coils, saturated, for example, with epoxy resin, nevertheless undergo wear and degradation. The part of our experimental program was dedicated to the investigation of this problem with the aid of several coils, supplied by direct current.

These coils in bore 12 cm and length of 40 cm, intended for applying as the pole windings the quadrupole, are wound by eighteenvein/eighteenstrand cable of niobium-titanium alloy. Now is manufactured a large number of the pole windings which are impregnated with different substances. The first nine such windings already underwent tests. Are given below the basic results of tests.

1. In unimpregnated current coils, attained in process of aging/training, is only 60-80% of current which succeeds in obtaining in short cut of this cable.

2. In coils, saturated with wax, current, equal in magnitude to current in short sample/specimen of cable, is obtained without aging/training. In this case occurs the splitting of wax, that, however, it does not affect the performance characteristics of coil.

3. Current in coils, saturated with epoxy resin without filler, can become very close in value to current in short sample/specimen of cable only after intense aging/training. In the sections of coil, strongly saturated by resin; is also possible the splitting, which leads to the subsequent change in the characteristics of coil.

4. In coil, resin-impregnated with admixture/impurity of powder-like quartz, does not occur splitting, but current reaches maxima value after brief aging/training. However, it is necessary to note that the cable, which was being utilized for the coil/winding of this coil, was previously processed by solder and it is unknown, as this influenced the obtained performance characteristics of coil.

Degradation and effects of agings/trainings of the coils, resin-impregnated, can occur on different reasons. For example, strain energy due to different local importance of the coefficient of the thermal expansion of the materials of coil upon the inclusion of

supply can be separated/liberated in the form of heat or produce the splitting of impregnant, which leads to the displacement of the turns of winding. Resolution of this problem consists in the use of such impregnants which either do not yield to splitting or the strain energy of which is small as, for example, from wax. Furthermore, it is possible to utilize resins with the admixtures/impurities which have the value of the coefficient of thermal expansion close to the value of the coefficient of the expansion of the material of conductor.

The use/application of resins with the fillers is most promising, although the high viscosity of such resins complicates the process of impregnation. Now tests different technology of the impregnation of coils and are investigated the properties of some other impregnating substances.

Development of the magnets of alternating current.

The considerable place in our program is assigned to the development of large high-current kickers for the proton synchrotron. Are now completed the first part of this work, connected with the investigation of the working characteristics of basic conductor on alternating current [2].

Page 239.

Lead testing, wound around the small coils, showed the operational stability of such conductors in the pulsed operation and confirmed the correctness of theoretical calculations magnitudes of losses with alternating current. Furthermore, now is studied the possibility of producing the cables, twisted from 216 strands basic conductor, which in the state to maintain currents on the order of 5000-10 000 A. For facilitating the process of coil/winding and improvement in density distribution of current in the cross section of cable was developed technology of obtaining cable with the square section. This technology eliminates the damage to insulation/isolation of cable.

In the present stage of experimental work are investigated the performance characteristics of the wound by cable coils of alternating current. Have already been begun the tests of entrance coils with the simple geometry for the dipole magnets. At the same time for the purpose of the final adjustment of construction/design is installed the large pulse dipole magnet with a length of 40 cm, also, in bore 10 cm. The coils for this magnet, which have sector windings [3] with the form of the end connections, proposed by Coupland [4], are wound by cable with the section 5 mm², twisted of 108 strands. Magnet must create magnetic field with the induction 5 T with the current 7000 A.

Is interesting the selected method of cooling the coils. Between the separate layers of conductors are placed the packing from the isolated/insulated copper conductors, that discharge heat to the channels with helium. These channels are placed between the sectors of coils. Coil is assembled by means of the connection of a large number of separate windings. One experimental winding, wound by copper wire, is already prepared. With its aid will be checked technology of the process of coil/winding and is investigated the effect of the mechanical cooling stresses. The production of the superconducting windings will be begun immediately after into the laboratory will be supplied lead/duct.

During the development of magnet it is very important to study different possible versions of the geometry of coils and precision/accuracy of the execution of coil/winding, which would ensure the necessary quality of magnetic field [5]. Special interest causes the problem of obtaining the optimum form of the cross section of coil with the given size/dimension of conductor. Practical investigations switch on also stability measurements of the sizes/dimensions of coil during its cooling. These measurements are conducted on the accurately wound non-superconducting models of coil.

Design of accelerator.

Target of the leading investigations - to replace the working in the laboratory accelerator with the energy of particles to 7 GeV with the new superconducting proton synchrotron. It is possible, however, to hope that these investigations will be useful during the design and of other machines, which use the superconducting coil electromagnets.

The basic requirement of design consists of obtaining of particles with the final energy 25 GeV with the mean radius of machine 28 m. The selection of a radius of this value is caused by the size/dimension of the existing location. Special attention it was necessary to give to the optimum use of the available area. This requirement determined the selection of magnetic structure with the separation of the functions of its separate elements/cells. For long straight section, intended for injection and beam extraction, it was possible to place in the location, after foregoing the series/row of confronting after each other rotary magnets. On the liberated place it is possible to establish/install the magnets for the rapid beam deflection and other instruments. Magnetic structures with the combination of the functions of separate elements/cells can, however, also be utilized in the accelerators. This is achieved by arrangement/position on the magnets of dipole and quadrupole

windings. The absence of connection/communication between such windings makes it possible to excite from independently of each other, making control of machine the same of flexible, as in the case magnetic system with the separation of the functions of separate elements/cells. The supplementary savings of place is achieved by the arrangement/position of the larger possible number of magnets in one general/common/total cryostat for the maximum decrease of the surface of cryostats. This becomes possible in such a case when elements/cells, such, for example, as correcting, are made in the form of the supplementary superconducting winding on background magnet, and other components, for example the beam-position sensors, they can work within the cryostat. Furthermore, especially for the machines of small diameter, it is necessary to develop the compact frontal windings of magnet, since in this case due to the effect of the sagging of floor/sex many elements of magnetic structure must be small according to the sizes/dimensions.

Among many other questions of the design of accelerators, which deserve discussion, special attention during the development of the construction/design of magnets must be paid to the guarantee of the required characteristics of magnetic field, the adjustment of magnets and their shielding from the external magnetic fields.

Other investigations.

Besides the mentioned above works, by us is carried out the study of cryogenics and materials which will be required during the construction of proton synchrotron [6]. Keeping in mind the future superconducting synchrotrons to the very high energies, especially attentively one should relate to the use of the superconducting installations for the energy storage, which, possibly, are the resolution of the problem of the supply of powerful/thick magnets. Now is discussed the possibility of the construction of the prototype of such installations. Theoretical questions of the superconducting installations for the energy storage examine recently published article [7].

REFERENCES

1. P. F. Smith. Particle Accelerators, July, 1970.
2. M. N. Wilson, C. R. Walters, J. D. Lewin, P. F. Smith, A. N. Spurway. Rutherford Lab., preprint RPP/A73, 1969.
3. J. H. Coupland. Nucl. Instr. and Methods, 1970, 78, 181.
4. J. H. Coupland. Rutherford Lab. Internal Report, RHEL M, 179, 1969.
5. J. H. Coupland. 3rd Magnet Technol. Conf. Hamburg, 1970.
6. B. Cover. Rutherford Lab. internal Report, RHEL M 177, 1969.
7. P. F. Smith, J. D. Lewin. Particle Accelerators, July 1970.

Page 241.

77. The superconducting coil electromagnets with the iron screens.

Yu. P. Batakov, N. I. Doynikov, A. G. Zhikhareva, N. A. Monoszon, G. V. Trokhachev, G. F. Churakov.

(Scientific research institute of the electrophysical equipment in. D. V. Efremov).

During the creation of strong magnetic fields with the aid of the superconducting and cryogenic magnets difficulties presents the account of the final thickness of winding, and also effects of the saturation of iron.

The calculation of the effect of iron screen and the correction of this effect it is comparatively simple to satisfy, if screen is arranged/located comparatively far [1], in the region where the

induction lower than saturation induction of iron. However, for decreasing the necessary number of ampere turns of winding the screen should be arranged immediately behind winding [2] in spite of its strong saturation. In this case the effect of iron will pronounce both at the level and on the form of field, and for its determination will have to resort to relaxation method [3, 4].

Under conditions for the strong saturation of iron the task of determining the field proves to be substantial nonlinear which extremely impedes the use/application of analytical methods and analog models. Actually the only method of decision in the sufficiently general/common/total formulation of the problems of nonlinear magnetostatics is the net point method which effectively can be realized only on the computers.

The purpose of this work is the examination of the procedure of shaping of fields taking into account the nonlinear properties of environment and the calculation of the superconducting dipole magnet with the iron screen.

Assume in circular tube domain of radius r_0 (Fig. 1) it is necessary to create the plane-parallel magnetic field of intensity/strength H_0 . Its vektor potential has only one component $A_z = A_z(r, \varphi)$. In the occupied by current region the vektor potential can

1018

be represented in the form [5]

$$A_{e\tau} = A_i - \frac{\pi j}{c} (\tau^2 - 2\tau_0^2 \ln \frac{\tau}{\tau_0}), \quad (1)$$

where j - permanent over the section of winding current density.

The effect of environment can be described by the assignment of the distribution of the tangential component of the intensity/strength of field H_τ along the outer duct $\rho(\varphi)$ current region. Expression for distribution $H_\tau|_{\tau=\rho(\varphi)}$ lengthwise $\rho(\varphi)$

$$H_\tau|_{\tau=\rho(\varphi)} = \frac{\rho}{\sqrt{\rho^2 + (d\rho/d\varphi)^2}} \left[-\frac{\partial A_i}{\partial \tau} \Big|_{\tau=\rho} + \frac{2\pi j \tau_0}{c} \left(\frac{\rho}{\tau_0} - \frac{\tau_0}{\rho} \right) \frac{d\rho/d\varphi}{\rho \sqrt{\rho^2 + (d\rho/d\varphi)^2}} \frac{\partial A_i}{\partial \varphi} \Big|_{\tau=\rho} \right]. \quad (2)$$

is simultaneously the equation, which are determining $\rho(\varphi)$.

In the case of uniform field $H_y = H_0$; $A_i = -H_0 \tau \cos \varphi$, and equation (2) for the first quadrant is reduced to the form

$$f(v) = \left[\sin v - k \left(\frac{\rho}{\tau_0} - \frac{\tau_0}{\rho} \right) \right] \frac{\rho}{\sqrt{\rho^2 + (d\rho/d\varphi)^2}} - \frac{\cos v d\rho/d\varphi}{\sqrt{\rho^2 + (d\rho/d\varphi)^2}}, \quad (3)$$

where

$$k = \frac{2\pi j \tau_0}{H_0}; \quad v = \frac{\pi}{2} - \varphi; \quad f(v) = \frac{1}{H_0} H_\tau(v) \Big|_{\tau=\rho}.$$

Fig. 2 depicts the configurations of winding, obtained during integration (3) under the assumption $\mu = \infty$, ($H_\tau|_{\tau=\rho} = 0$).

In general $H_\tau|_{\tau=\rho} \neq 0$, the calculation of magnet can be brought to the following procedure:

1. Is fulfilled approximate computation for estimation H_T .
2. From (2) is determined $\rho(\varphi)$, while from (1) - distribution A_e along internal contour/outline of iron, which makes it possible to tentatively determine thickness of screen.
3. Decision by relaxation method of exterior problem relatively A_e , determination $H_T|_{r,\rho} = \frac{1}{\mu} \frac{\partial A_e}{\partial n}|_{r,\rho}$ and return to point/item 2.

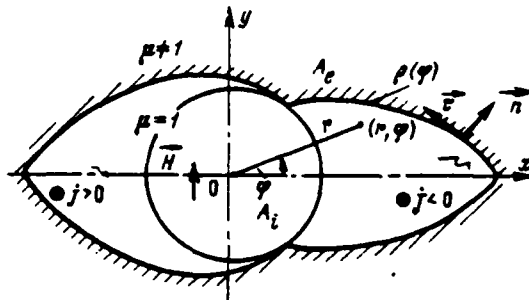


Fig. 1. Calculating a dipole superconductive magnet.

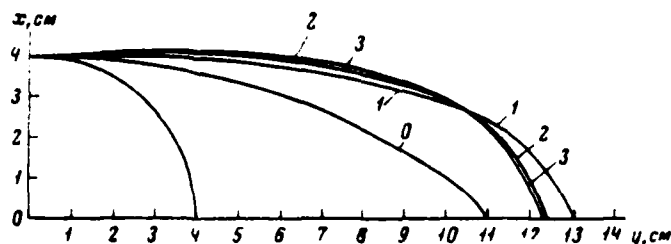


Fig. 2. The position of the outer duct of current region with the successive approximations: 0 - zero approximation; 1 - first approximation, etc.

Page 242.

4. In latter/last cycles is useful to include/connect finding of field in magnet opening on known ones $H_{\tau}|_{r,p}$ and configurations of winding; this calculation is conveniently carried out with use of modified potential [6].

The developed/processed superconducting dipole (Fig. 3, 4) has parameters $OA, r_0 = 4 \text{ cm}$, $H_0 = 50\,000 \text{ e}$, $j = 10^4 \text{ A/cm}^2$. The superconducting winding is made from the "thin" niobium-titanate superconductors in the copper matrix/lie, compounded of epoxy resin with the filler, which possesses high thermal conductivity. Winding is compounded together with the iron screen. For the best heat removal from interior inside the winding are embedded copper tubes, and the

surface, adjacent to the screen, will be bordered by the copper foil.

Screen consists of the "cold" part, located in the region of liquid-helium temperatures, and the "warm" part, arranged/located outside the cryostat.

This construction/design of magnet makes it possible to reduce the mass of the cooled material in comparison with the magnets whose screen is arranged/located within the cryostat, and in comparison with magnets, whose screen is arranged/located outside the cryostat, to decrease the necessary number of ampere turns of winding. Furthermore, during this construction/design the "cold" part of the screen is simultaneously stressed frame, which simplifies the attachment of winding.

Cryostat consists of two shells, between which is supported the vacuum. Between these shells are arranged/located the heat shields, cooled by liquid nitrogen. Heat shields and internal volume of cryostat rest on the heat-insulating supports.

For calculating the magnet with the aid of the computers to the region of the first quadrant of section (Fig. 3) was superimposed square grid with the step/pitch $h=1$ cm. A_0 along axis/axle oy and outer duct of iron it was assumed/set by equal to zero. The calculation of field in the iron was fulfilled by the method of over-relaxation [4].

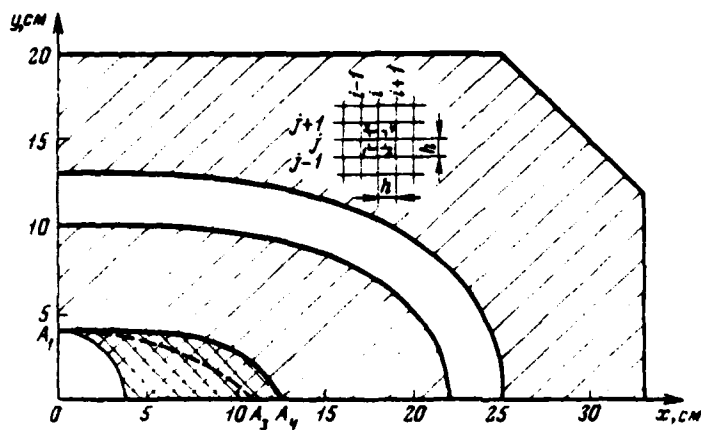


Fig. 3. First quadrant of the section of the dipole superconducting coil electromagnet with the iron screen.

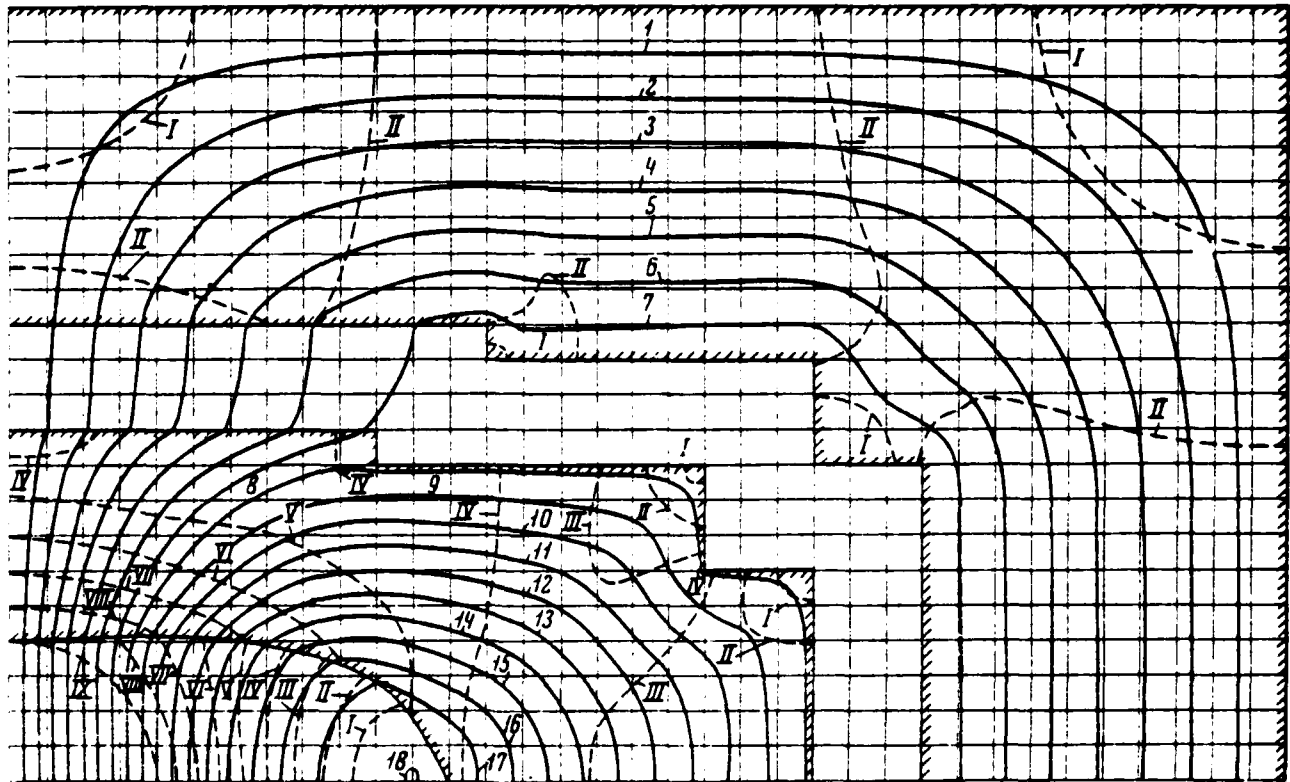


Fig. 4. Families of lines $A=\text{const}$ and $B=\text{const}$. a) $A \cdot 10^{-2}$ (kgf·cm): 1 - 0.2; 2 - 0.4; 3 - 0.6; 4 - 0.8; 5 - 1.0; 6 - 1.2; 7 - 1.4; 8 - 1.6; 9 - 1.8; 10 - 2.0; 11 - 2.2; 12 - 2.4; 13 - 2.6; 14 - 2.8; 15 - 3.0; 16 - 3.2; 17 - 3.4; 18 - 3.6; b) B (kg): I - 10 (1440), II - 15 (570); III - 20 (72); IV - 25 (8.8); V - 30 (3.8); VI - 35 (2.7); VII - 40 (2.2); VIII - 45 (2.0); IX - 50 (1.8). In the brackets are given the values for iron.

The program, which fulfills procedure indicated above of calculation, provided the determination of the boundary between the winding and iron - line A_1A_2 in Fig 3 (line A_1A_2 - the position of boundary with $\mu=0$). Count concluded, when the maximum distance between the subsequent and preceding/previous boundaries became less than 0.5 mm. A number of ampere turns of winding is equal to $5 \cdot 10^5$ A, which is approximately two times less than the number of ampere turns of the corresponding magnet without the iron screen.

Subsequently it is proposed to switch over to the irregular triangular grid with the smaller step/pitch, which ensures high precision/accuracy, especially during the calculation of boundary values in the curvilinear sections.

Calculations were performed on the computers BESM-4.

The authors are grateful to P. P. Shelonin and V. M. Staklyannikov for the aid in the organization of calculations and for the discussion of the number of questions of programming.

REFERENCES

1. M. A. Green. IEEE Trans. on Nucl. Sci., 1969, NS-16, N3, p 1082.
2. W. B. Simpson et al. IEEE Trans. on Nucl. Sci., 1969, NS-16, N3 p. 720.
3. P. Councus. Proc. Interat Sumpos. Magnet. Technol., Stanford, 1965, p. 164.
4. N. I. Doynikov and A. S. Simakov. ZhTF, 1969, XXXIX, page 1463.
5. N. I. Doynikov. Electrophysical equipment, iss. 6. Atomizdat, 1967, page 3.
6. R. Perin., S. VanderMaer. CERN 67-7, ISR Div., 1967.

Discussion.

V. G. Davidovskiy. Since in the magnets of the type iron in question it is substantially nonlinear element/cell, then this magnet can form/shape a good field only with the specific for this magnet value of field. Was examined the temporary/time dynamics of field with a change of the value of coil current?

N. I. Doynikov. This examination was not given.

V. G. Davilovskiy. In that case I want to say that, apparently, for the accelerators much more being adequate/approaching are the systems in which the screen is located at the considerable distance from the winding, there where there is no saturation, i.e., this system is good for the accumulator/storage where the field is constant, but not for the accelerator.

78. Some calculated and experimental data on the development of synchrotrons with stationary field on the energy 35-350 GES.

N. I. Doynikov, N. A. Monoszon, B. V. Rozhdestvenskiy, Yu. P. Sivkov, A. M. Stolov, G. V. Trokhachev.

(Scientific research institute of the electrophysical equipment in D. V. Yefremov).

In works [1, 2] was examined the possibility of designing of proton synchrotrons on the basis of the superconducting electromagnets with the stationary field, which are synchronously turned relative to equilibrium orbit. This system makes it possible

to change middle field in orbit with the supply of the superconducting windings by direct current.

In this case there is no need for in the powerful/thick system of the excitation of magnetic field, are eliminated the losses of alternating current in the superconductors, is simplified the construction/design of windings and cryostats, descend heat-input and decreases the power of refrigerators and liquefiers. A number of most important tasks, which are subject to decision during the creation of such synchrotrons, includes the stabilization of particle motion near the equilibrium orbits of double curvature and precise synchronous rotation of the superconducting electromagnets.

Are examined below some questions of particle dynamics, and also questions, connected with the realization of the synchronous rotation of electromagnets. On the basis of this examination are given two versions of the basic parameters of possible accelerators to the energy into ten and hundreds of GeV.

In the simplest magnetic structure consecutive electromagnets 1.2 (Fig. 1) are turned in opposite directions. In this case vertical field component is identical in all electromagnets and is equal to $B_z = B \cos \theta$, where B - value of field in the electromagnet. The radial component of field, directed in the consecutive units to opposite

sides, leads to the orbit perturbation in the vertical plane, which is changed in the process of particle acceleration. Fig. 2 shows the maximum value of the displacement of orbit depending on the length of electromagnets for two versions of accelerators at different lengths of free gaps/intervals - and different values λ - the ratio of maximum energy E_m to the energy of injection E_0 .

Beam focusing by the acceleration can be conducted by quadrupole lenses with the variable field. The energy, stored up in the magnetic field of lenses, many times of less than the energy, stored up in the field of rotary electromagnets. Therefore the power of the power-supply system of lenses is small.

Page 244.

The dual curvature of equilibrium orbit leads to connection/communication of vertical and radial betatron oscillations. Calculation with the aid of matrix procedure [3] shows that the effect of this connection/communication on the frequencies of betatron is unessential. Essential, however, proves to be a change in the frequency of vertical betatron due to a change of the curvature of orbit in the vertical direction.

A change in the phase of betatron oscillations for one period

with an azimuthal length of $2\psi_0$ is determined by the relationships/ratios

$$\cos \mu_1 = 1 - 2 \frac{R_0^2 \psi_0^2}{f_1 f_2} - 8 \psi_0^2 + 2 R_0 \psi_0 \left(1 - \frac{8}{3} \psi_0^2 \right) \left(\frac{1}{f_1} - \frac{1}{f_2} \right), (1)$$

$$\cos \mu_2 = 1 - 2 \frac{R_0^2 \psi_0^2}{f_1 f_2} - 8 \tan^2 \psi_0 - 2 R_0 \psi_0 \left(1 - \frac{8}{3} \psi_0^2 \tan^2 \psi_0 \right) \left(\frac{1}{f_1} - \frac{1}{f_2} \right),$$

where R_0 - radius of curvature of orbit (at the end of the cycle of acceleration), f_1 , f_2 - focal lengths of the lenses, which focus on a radius and on the vertical line.

In formulas (1) and (2) are omitted the terms with the degrees of value $(\psi_0 \tan \psi_0)$ from the fourth and it is above.

For the compensation for dependence Q_2 on ψ it is necessary to regulate values $1/f_1$ and $1/f_2$. Figure 3 gives the dependence $1/f_1$ and $1/f_2$ on the energy of protons for a number of elements/cells of periodicity $N=25$ ($Q_2 = 5.25$).

For maintaining the constancy f_1 and f_2 the currents in the lenses must vary in proportion to particle momentum, i.e., as $B \cos \psi$. Dependence f_1 and f_2 on energy E requires the more complicated law of a change in the current, but, as can be seen from Fig. 3, in essence, at the initial stage of acceleration. This makes it possible to create dependence f_1 and f_2 on the energy with the aid of comparatively low-power compensators.

Possibly also the use/application of the quadrupole lenses with the stationary field, in which a change of the average/mean gradient is conducted analogously with electromagnets due to synchronous rotation [2].

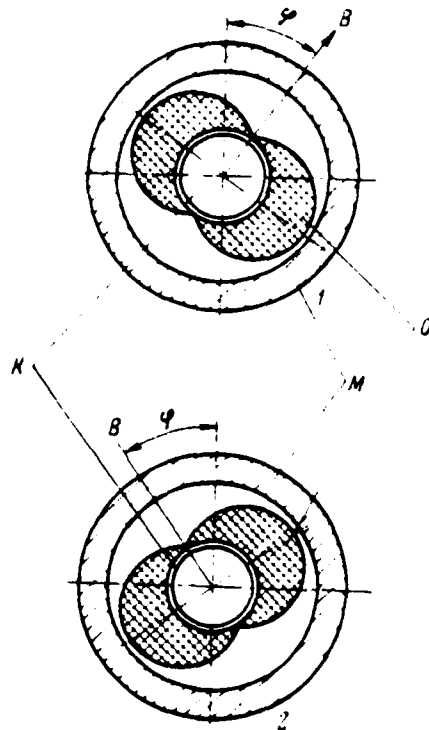


Fig. 1. Synchrotron with the rotary electromagnets: K - chamber/camera; O - winding; M - magnetic screen.

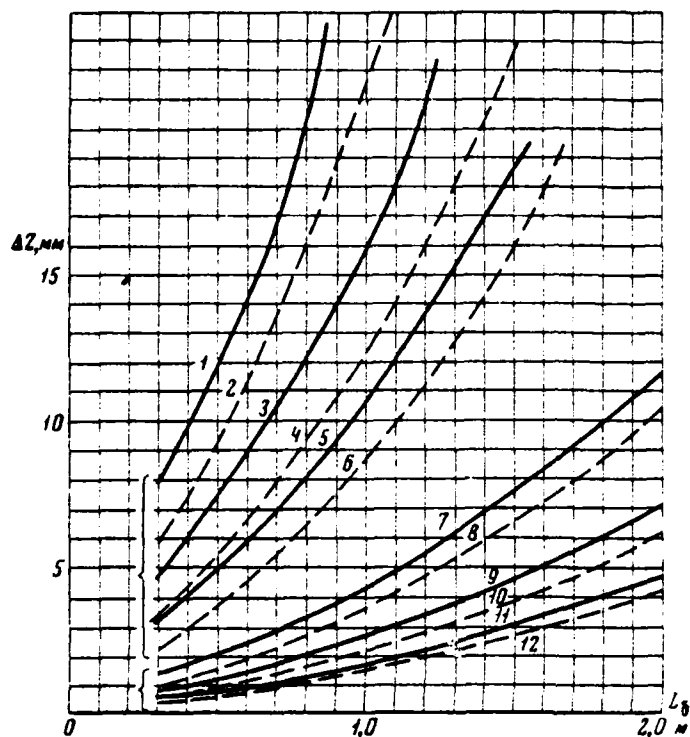


Fig. 2. Dependence of vertical orbit perturbation $\pm \Delta Z$ on length of unit of electromagnet L_g . 1-6 - they correspond to orbit circumference 250 m; 7-12 - correspond to orbit circumference 1500 m. For curves 1, 2, 7, 8 - $1/\lambda = 0.15$; for curved 3, 4, 9, 10 - $1/\lambda = 0.25$; for curves 5, 6, 11, 12 - $1/\lambda = 0.35$. Unbroken curve $l_{np} = 0.4$ m, broken $l_{np} = 0.3$ m.

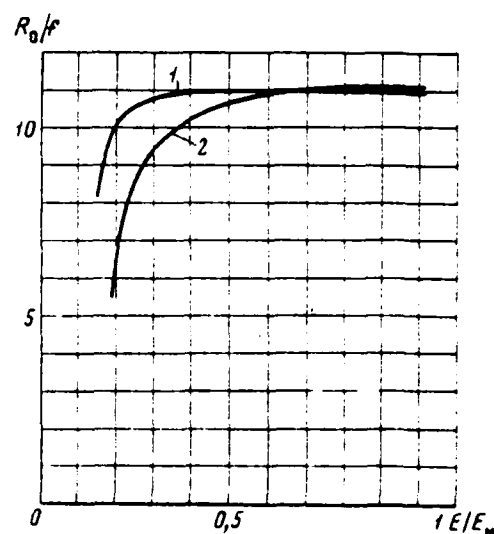


Fig. 3. Dependence of focal lengths of quadrupoles from energy of protons: 1 - lenses, which focus on radius; 2 - lenses, which focus on vertical line.

Page 245.

The use of such lenses leads to the additional constraint of vertical and radial oscillations.

As noted above, one of the important tasks, which appear during the creation of the accelerators, based on the described principle, is the development of the devices/equipment, which ensure with the high precision/accuracy the synchronous rotation of a large number of elements/cells, arranged/located at a great distance. Allowance for the lack of synchronisation of rotation changes during the operating cycle approximately is inversely proportional to energy of accelerated particles [2]. With $\lambda=7$ it composes in the beginning of cycle value $(1-2) \cdot 10^{-4}$ and at the end of cycle -10^{-3} .

As is known, tasks of this type in the principle can be solved with the aid of the servo synchronous electric drive, which is the energy source and simultaneously creates the necessary synchronising torque, which appears during the disagreement/mismatch of the angles of driving elements. In application to the case in question when it is necessary to create the regular oscillations of magnetic systems in the limits of preset angles, smaller 2π , the use of this principle requires the use/application of drive, calculated not only for the power of energy losses during the oscillations, but also to the

reactive power, necessary for acceleration and braking of electromagnets and reducers.

In connection with this it is of interest to examine the drive, based on the use of mechanical oscillatory systems.

Fig. 4 depicts the diagram of a similar drive with the pendulum.

Before beginning operating cycle pendulum, it is rigid with that bound to the turned electromagnet, it is deflected to the initial angle α_0 and is held in this position with the aid of the special fixers with electromagnetic control. At the moment of injection the system starts up also through half-period, after being deflected in the opposite direction, it is held in it with the aid of the fixers. With this middle field it varies from its initial value to maximum. Fixation of electromagnets in the maximum field makes it possible to carry out a slow conclusion of the particles of any duration.

The period of oscillations of the system in question is approximately equal to

$$\tau = 2\pi \sqrt{\frac{l}{g} \left(1 + \frac{J}{m l^2} \right)},$$

where l, m - length and mass of pendulum; τ - moment of the

inertia of electromagnet. Divergence from the synchronism of motion is determined by differences in the period of the natural oscillations of separate electromagnets, asynchrony of the beginning of motion Δt and by difference in the idle braking moments/torques. Idle braking moments are caused by energy losses to bearing friction and against the air and to the magnetic reversal of steel of magnetic screens. They lead to damping of oscillations which can be compensated by the method of the pulling of pendulums with their approach to the end positions with the aid of the electromagnets or in any other manner. Estimations show that with $\Delta t = 10^{-4}$ s the use/application of usual ball bearings and high-alloyed transformer steel for magnetic screens will ensure the necessary allowances for the displacement angle. For the experimental check of the effect of friction on the synchronism of the motion of pendulum drive is prepared the model (Fig. 5), on which are confirmed the estimations indicated higher than.

Is given below the table of the possible parameters of two accelerators with the different energy levels.

1036

Предельная энергия	35 Гэв	310 Гэв
Энергия инжекции	10 Гэв	50 Гэв
Максимальная индукция	6 тл	6 тл
Число бетатронных колебаний	4,25	5,25
Число пар/квадрупольных линз (периодов)	22	24
Длина одного электромагнита	0,88 м	1,4 м
Длина промежутка между магнитами	0,34 м	0,30 м
Длина укороченного магнита	0,65 м	1,0 м
Длина квадруполя	0,7 м	1,1 м
Апертура линзы	φ 50 мм	φ 50 мм
Градиент поля в линзе	4000 э/см	4000 э/см
Число длинных промежутков	4	4
Длина длинных промежутков (между соседними квадруполями)	4,5 м	31,25 м
Общее число:		
электромагнитов нормальной длины	80	704
укороченных электромагнитов	80	88
квадрупольных линз	44	48
Общая длина орбиты	250 м	1500 м
Апертура камеры	φ 65 мм	φ 65 мм
Энергия, запасенная в магнитном поле сверхпроводящего магнита	$3,4 \cdot 10^7$ Дж	$3,8 \cdot 10^8$ Дж
Энергия, запасенная в поле линз	$1,5 \cdot 10^5$ Дж	$2,5 \cdot 10^5$ Дж
Время ускорения	1 сек	2 сек
Прирост энергии за оборот	36 кв	1200 кв
Мощность питания магнетронного электроприбора	10 квт	100 квт

Key: (1). Maximum energy. (2). GeV. (3). Energy of injection. (4). Maximum induction. (5) T. (6). Number of betatron oscillations. (7). Number of pairs of quadrupole lenses (periods). (8). Length of one electromagnet. (9). Length of gap/interval between magnets. (10). Length of shortened magnet. (11). Length of quadrupole. (12). Aperture of lens. (13). Field gradient in lens. (14). Number of long gaps/intervals. (15) e/cm. (16). Length of long gaps/intervals (between adjacent quadrupoles). (17). Total number. (17a) electromagnets of normal length. (17b) the shortened electromagnets. (17c) quadrupole lenses. (18). General/common/total orbit circumference. (19). Aperture of chamber/camera. (20). Energy, stored up in magnetic field of superconducting coil electromagnet. (21). Energy, stored up in field of lenses. (22) J. (23). Time of acceleration. (24) s. (25). Energy gain per revolution. (26) kV. (27). Input power of pendulum electric drive. (28) kW.

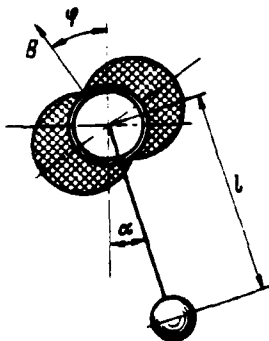


Fig. 4. Schematic of pendulum mechanism.

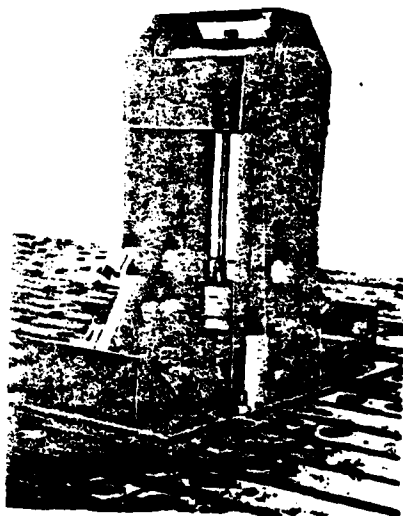


Fig. 5. Model of pendulum mechanism.

Page 246.

REFERENCES

1. M L Goos. IEE Transaction on Nucl. Sci., N 16, 1969, N 3, p 1061.
2. N. I. Doynikov. et al. Superconducting synchrotron on the basis of magnetic systems with the stationary field. Report at the VII international conference on the accelerators. Yerevan, 1969.
3. E Courant and H Snyder. Ann. Phys., 1958, 8, 1-48.

Discussion.

B. N. Samoilov, will be such losses in the superconducting winding, connected with the motion windings of one dipole in the field of another?

How is connected pendulum with the winding and as it is solved a question with the heat-input concerning the pendulum and the mechanical suspensions of winding?

N. A. Monoszon. There are no coil losses, since dipoles are spread from each other on the orbit. Problem now is not studied not in order to answer your second question.

V. Khaynts. Will be such the effects of sextupole and octupole harmonics due to the fringing fields during the rotation of the system of magnets? Did estimate you this effect?

N. A. Monoszon. It is obvious that the edge effects will lead to the appearance of harmonics, which are changed in the time, and for their compensation it is necessary to use the system, supplied by current according to the specific program.

A. A. Kolomenskiy. What does give the basic contribution to very close tolerance $\sim 10^{-4}$ for the synchronization of the fluctuation of separate magnets?

N. A. Monoszon. Basic contribution is connected with the fact that at the level of weak vertical field, which turns particles, there is even a strong field, turned at angle, let us say, to close ones to 90° . The small error in the rotation leads to the large disturbances/perturbations. In connection with this in this system it is not possible to obtain this high value of the ratio of maximum energy to the energy of injection as in the usual synchrotrons.

P. A. Vodop'yanov. What is more preferable at today's stage of development - synchrotron with the variable field or accelerator with the movable magnets?

N. A. Monoszon. The complexity of problem requires performing work in all directions. Up to now there is nowhere virtually yet working on alternating current superconducting coil electromagnet of considerable volume. For the large accelerators are characteristic large coil currents; therefore there is a problem of current inlets. Since energy density is proportional H^2 , then during the use of large fields appears the problem of the creation of powerful/thick power-supply system. In the system with moving magnets this question is removed/taken.

A. I. Dzergach. In this system is unavoidable the transition from the motionless container with liquid helium to the movable. Will not mixing helium lead it to the heating?

N. A. Monoszon. We did not carry out investigations on the effect of the displacement of reservoirs, but mixing during the fluctuation will be limited.

Page 247.

79. Developments for the cryogenics and the superconducting coil electromagnets.

P. Arendt, Kh. Brekhv, I. Yerb, M. Fessler, G. Khartvig, V. Khaynts, K. P. Yungst, V. Maurer, G. Merle, G. Bis, V. Shauer, I. Von. Schaewin, P. Tichovski, A. Ulbricht.

(Institute of experimental nuclear physics, FRG).

1. Introduction.

Those superconducting are magnetic pulse current they acquire important value for the future accelerators (proton synchrotrons). The magnets of direct current give the possibility to create short channels for the rapidly decomposing particles, the shielding and forming magnetic fields, which detect devices/equipment, magnets with the large solid angle are magnetic, the powerful/thick fields created in the large volumes. The cost/value of the operation of large

experimental magnets of direct current substantially descends in the comparison with the usual magnets, which have water cooling and iron magnetic circuit.

The economical generation of the strong magnetic fields ($> 5 \text{ T}$) in the superconducting pulse dipole magnets makes it possible to decrease a radius of synchrotron approximately 3-4 times in the comparison with the usual accelerators, which gives the considerable savings of capital investments to the buildings, the tunnels, the experimental halls, etc.

The superconducting proton synchrotrons to the high energies are more compact, and, possibly, less expensive than usual accelerators. This in particular is correct for the accelerators with the highest energy at the low repetition frequencies and during the cycles of acceleration with the prolonged flat/plane apex/vertex.

Before applying this new technology in such large installation as proton synchrotron, it is necessary to conduct vast works on resolution of the basic problems, connected with the superconducting devices/equipment; will be examined below only some of them: the hysteresis losses in the superconductors, the phenomena, which appear during the cooling, field distribution and reproducibility of field, characteristic and fatigue of materials, radiation questions,

accumulation and distribution of the large magnetic energy (by approximately order it is higher than in the comparable usual devices/equipment), work with the large volumes of liquid helium, which is found in the diverse containers, the complex of actions for safety and control systems and, etc. In this article are described works, carried out on the superconducting and cryogenic magnets in the institute of experimental nuclear physics - center of nuclear research in Karlsruhe, target of which was the use of superconducting pulse magnets on the phase of the transformation of large (300 GeV) European accelerator (CERN II). During the use of combination of the superconducting and usual magnets the present project of accelerator on 300 GeV decomposes to two stages of construction. During the first stage will be completed the circular tunnel with a radius of 1100 m. In order to obtain energy 200 GeV in the accelerator with the divided functions, will be established/installed only the focusing magnets and the part of all necessary dipole magnets. Between two deflecting magnets is left the gap/interval 12 m (Fig. 1), which it is possible to establish/install new magnets. During the first stage of construction (about 3-4 years after beginning) it will become clearly, sufficiently they moved research works on the pulse superconducting coil electromagnets so that it would be possible to establish/install the superconducting coil electromagnets into these gaps/intervals. It is considered it real to raise energy of accelerator to 600 GeV. The second stage encompasses the alteration

of all usual magnets to those superconducting. Magnet openings are determined by the requirements of injection and by a structure of accelerator on 300 GeV; as the injector is utilized the existing proton synchrotron of CERN. The construction/design of accelerator encompasses the system of the focusing and defocusing magnets of 108 blocks, the structure FCI0, 6 large straight sections by value Q27, 75 in both transverse directions. Necessary aperture of beam is 10.2 cm in the horizontal and 4 cm in the vertical direction.

It is necessary to test magnets in system (after their individual testing), which consists, let us say, from the half-period of synchrotron CERN II, or on the model of accelerator with the energy of particles in the range GeV. This system of magnets must satisfy the following conditions:

1. Magnets must have the size/dimension of aperture rise time of field and duration of the flat/plane apex/vertex, compared with appropriate data of the real magnets of accelerator CERN II.

2. For systematic study of effects of nonlinearity (edge/boundary of field, divergences of fields in different magnets, aberrations, etc.) simulating system must be sufficiently flexible so that it would be possible to bring about a change. The effect of different allowances can be investigated, changing the parameters of

AD-A089 303

FOREIGN TECHNOLOGY DIV WRIGHT-PATTERSON AFB OH
TRANSACTIONS OF THE ALL-UNION CONFERENCE (2ND) ON CHARGED PARTI--ETC(U)
JUL 80 A L MINTS, A A KOMAR, A A VASIL'YEV

F/S 20/7

UNCLASSIFIED

FTD-ID(RS)T-0692-80

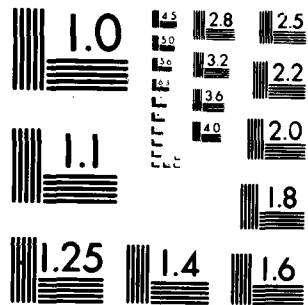
NL

12 - 12

2 - 12

6 - 12

END
DATE
FILMED
10 80
DTIC



MICROCOPY RESOLUTION TEST CHART
NATIONAL BUREAU OF STANDARDS 1963 A

beam independent of other errors and obtaining the appropriate corrections.

3. Final energy of model of accelerator must be found in the range several GeV. System must be suitable for the interesting experiments on the high energies, such, as the acceleration of deuterons.

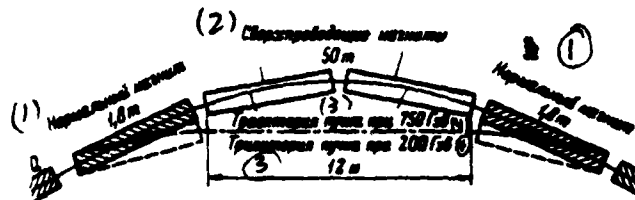


Fig. 1. Diagram of the structure of accelerator (CERN II) with the superconducting coil electromagnets.

Key: (1). Normal magnet. (2). Superconducting coil electromagnets. (3). trajectory of beam with (4). GeV.

Page 248.

The magnets, created for the model of accelerator, will have nominal length of approximately one or two meters. One of the most important tasks will be the association of several magnets in such a way, that would be obtained the long blocks (6-7 m) without deterioration of the properties of beam.

II. Survey/coverage of achievements and tasks.

At the present stage of the developments of the superconducting coil electromagnets it is possible to begin the creation of larger magnet system in order to accumulate experience, necessary for the

construction of the large accelerator, such as CERN II. Is briefly described below the wide circle of the problems, confronting developers of magnet.

1. Slow conclusion/output and necessary for precision/accuracy fields of magnets. Slow beam extraction with the use of a resonance method is feasible only in the case of substantially linear field distribution in the ring of basic magnet. This means that for the projected/designed European accelerator on 300 GeV the relative error for field $S = \Delta B/B$ in the median plane (extent 4... 5 cm) must be less 1.5×10^{-3} . This is reflected in Fig. 2a and 2b of those showing radial phase plane along the azimuth of the location of septum in one of the structures of magnet in question. Graphs/curves are obtained as a result of miscounting on computers [1] of the passage of four particles through each element of ring and fixation of their coordinates after each revolution. In the case of the resonance of the third order the reference coordinates are located near the origin of the coordinates of phase plane. The error for field is less 1.5×10^{-3} , caused by the sextupole component (Fig. 2b) in the deflecting magnets, it does not substantially affect the process of conclusion/output. An increase in the error for field up to 2.5×10^{-3} (Fig. 2b) retains full/total/complete stability. particles remain within the limits of the acceptance, which corresponds to the position of septum in 3 cm from the closed orbit, and therefore they

cannot be satisfactory brought out. The highest multipole components in field expansion, which give the same error for field, are less essential than sextupole term [2]. In the case of the introduction to correction of the closed orbit the change in the value of field from one magnet to the next, equal to 0.5×10^{-3} , can be admissibly from the point of view of calculation/output and shift of orbit. Unconditionally this is planned.

2. Joule losses and properties of conductors. One of the targets of use/application cryogenic or superconducting accelerator is a reduction in the losses. They appear in the superconductors, in the supports/bases of superconductors, in metal construction (if the same are) and in the metallic cavities. The magnets of the prototype of synchrotron are designed for the work in the strong fields (nominally, let us say, 4-5 T). Losses in the composite/compound conductors are predicted by theory correct within error limits for measurements up to the diameters of 10 μ m. Are achieved the essential successes in two different areas: Joule losses can be lowered by the method of the creation of thin-core twisted composite/compound conductors, and the current density of superconductors can be substantially with the values, achieved/reached several years ago. The dependences of critical current of short conductors on the applied field, perpendicular to conductor, for the majority of those produced by industry Nb-Ti - conductors are given in Fig. 3. Is at

DOC = 80069219

PAGE

5
1050

present attained the general/cooling/total current density of coil about 2.5×10^8 A/m² in the field 5 T. With such data the duty factor of coil is approximately 0.25, which is connected with the construction/design of cooling channels and cable.

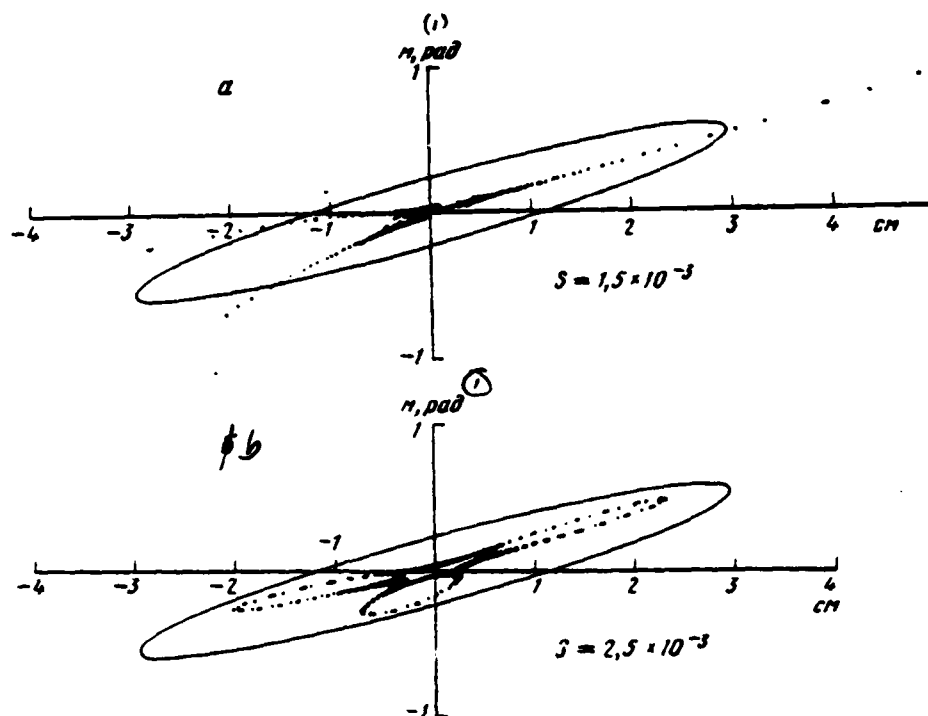


Fig. 2. Phase plane for the first septum (S - value of septum) a) $S = 1.5 \cdot 10^{-3}$; b) $S = 2.5 \cdot 10^{-3}$.

Key: (1). rad.

Page 249.

During the excitation of coil conductor affects the considerable Lorentz force, which under the conditions of the absence of support and reinforcement substantially exceeds the limit of the strength of superconductor. Were investigated two methods of fixation of coil:

the reinforcement of conductor with the aid of the structural support and the impregnation of coil with appropriate resins. Experiments with the saturated coils of flow it did not become satisfactory results as a result of the nonuniformity of the coefficients of the thermal expansion of composite/comound conductor and resin. Conductor is subjected to aging/training and deterioration of properties in the course of time.

The measurements of heat transfer in the uptakes, lowered in helium, by the length of 0.4 m and in height of clearance 1.0, 1.5, 2.0 mm with the width of 40 mm came to light/detected/exposed transition from the nuclei forming to the film boiling with $\Delta T = 0.3 - 0.4^\circ K$, while the corresponding heat fluxes lay/rested in the range $0.12 - 0.17 \text{ W/cm}^2$. The thermal conductivity of the superconducting coils, impregnated with epoxy resin, perpendicular to cheeks composed $2 \times 10^{-3} \text{ W/cm}^2 \text{ } ^\circ K$ at a temperature $4.5^\circ K$. With such data the height of the separate saturated sections was selected as being equal to 0.5 cm so that the increase in the temperature in one section would comprise about $0.1^\circ K$ or less. Thus, section with the highest temperature in the saturated coils will have a temperature by $0.4 - 0.5^\circ K$ higher than in the volume. Under such conditions in the magnets, which use conductors with the filaments $10 \text{ } \mu m$, is attained the build-up of the field of 1.8 T/s. The at present saturated coils are more preferable than the reinforced unimpregnated ones.

3. Losses of alternating current in exteriors of magnet. With a change in the magnetic field with the discussed speeds (5T/3 s for the filaments 10 μ m) in all "inactive" metallic parts occur Joule losses, moreover such parts can be accessories, supporting structures, metallic bandings, also, in particular the Dewars. Some structural parts must be made from the high-strength metals, in particular, made of the nonmagnetic stainless steel in which can occur the eddy current losses. Although specific resistance of stainless steel with reduction of temperature from 300 to 4.2°K decreases only twice, the total induced losses are sufficiently great, and must be considered then. The measures adopted consist in the exception/elimination, if it is possible, all parts from the high-strength metals both the use of strips/films from unidirectional glass-thermosetting resin (semihard) and the use/application of high-strength nonmetallic structural materials.

The preliminary design of Dewar of coil is box type construction/design, in which the forces between coil and target of closing/shorting flow (iron framework) are received by the flanges, arranged/located on the ends/leads of the separate sections of Dewar. Glass-epoxy Dewar must have the impenetrable cladding, which prevents, or de-gassing of epoxy resin into the vacuum space.

4. Study of irradiation. The superconducting coil electromagnet undergoes the effect of radiation for a number of reasons:

- a) displacement of atoms;
- b) the generation of secondary particles near the slots or the collimators.

The effect of irradiation and characteristic of magnets with the continuous operation they are of considerable interest and they are at present investigated by the method of irradiating the small coils by deuterons with the energy 50 MeV with 4-5°K.

The effect of electronic, neutron, proton and deuteron radiation on characteristic J_c - B_c of second type superconductors, such as NbTi and Nb₃Sn, is studied by several researchers [3-7]. During irradiation descend T_c and H_c . J_c changes; however, a precise forecast of changes J_c is difficult. In some materials, such as the diffuse films Nb₃Sn, the density of critical current increases approximately six times during irradiation by protons with the energy 3 MeV. In NbTi the density of critical current even descends. *As an increase in J_c depending on the radiation dose* It does not occur uniform all over coil, but it is the local phenomenon. Characteristic

$J_c - B_c$ of conductor changes in the local region, so that it comes into more brittle or, is more precise, more sensitive to "flux jumps" of state. Temporary/time external or internal disturbances/perturbations can give rise to of "normal" zone, since the support/base is also subjected to the effect of radiation [8]. The weakest coupling link in the coil - interturn insulation in particular if for the impregnation of coils are utilized organic materials. "normal" zone can lead to the short circuit between the turns (due to the charring of insulation/isclation), the shift of energy distribution according to the coil and finally to the destruction of magnet. At low temperatures the behavior of organic insulation somewhat is improved [9]; however, this it is insufficient for the guarantee of the reliable operation of filaments during the existing constructions/designs, if we do not undertake preventive measures and not to create new systems.

5. Distance, passed by reverse magnetic. by flow. The location of iron framework on the coil, its form and effect on field distribution is very important for the work of magnet. Iron framework can be placed in immediate proximity of the coil and it must be cooled to the temperature of liquid helium. Theoretical studies show that in this case the contribution in the field, connected with the iron, is maximum, and the screening of field is effective; however, if the form of framework is selected incorrectly, occurs the

distortion of field in working aperture [10]. The advantages of this solution consist in the fact that to Dewar are not transferred the forces as a result of the relative attitude of coil and framework, or in the fact that Dewar can be prepared in essence from the nonmagnetic stainless steel when only the part of magnet opening must be made either from the bellows with the low losses of alternating current or from nonmetallic filamentary structure. A deficiency/lack in this diagram consists of the large consumption of helium for the cooling and the iron losses due to hysteresis and eddy currents which are summarized with the losses in the superconducting coil on alternating current, and they must be compensated by the cooling medium.

If iron framework is arranged around Dewar, the contribution in the field due to the iron is small, the forces, caused by the eccentric location of coil and iron framework and transferred to Dewar, they can become considerable; however, descends the effect of iron on distortion of field. The losses of alternating current in the iron at a room temperature are unessential. At present in Karlsruhe are investigated both solutions. Iron near the coil is applied in the dipole from high-purity aluminum, whereas iron around Dewar is planned/gilded to apply in the superconducting dipole magnet.

6. Cryogenic magnets. Strips/films from high-purity aluminum possess low losses and can be of interest for the use/application in low-frequency cryogenic magnets [11], and also as the supports/bases for the multi-fibrous superconductors, the current busbars/tires and other cryogenic uses/applications. Are especially interesting losses at a temperature of liquid hydrogen; aluminum strips/films with the coefficient of residual/remnant specific resistance $RRR=10^4$ in the strips/films ($RRR=\rho(300^\circ K)/\rho(4.2^\circ K)$) are discharged by industry and are utilized in Karlsruhe in the dipole coil with a length of 0.4 m. Although the measurements of reluctance at a temperature of liquid hydrogen came to light/detected/exposed, that the losses of alternating current in the coil by approximately order of magnitude are higher than in the comparable superconducting coils at a temperature of $4.2^\circ K$, the use/application of aluminum strips/films can be very expediently at frequencies when losses in the superconductors become excessive.

III. Those superconducting are magnetic.

At present test two types of magnets:

a) the superconducting dipole magnets of alternating current;

b) the superconducting quadrupole magnets of direct current.

Are given below some most important the results of tests in two directions indicated.

1. Superconducting dipole magnets of alternating current. For the purpose of the construction of the pulse superconducting coil electromagnet of accelerator were carried out the series of preliminary tests with the coils of different sizes/dimensions with the accumulated energy of field to 2 kJ. In parallel to the experiments, conducted on the multiple composite/compound conductors, are made theoretical studies on the losses of alternating current in the superconductors.

During the theoretical derivation of the magnitude of losses of alternating current in the magnet was used the model of critical state of Bins. With the aid of the program of the computers losses of alternating current in the coil were obtained by the method of subdivision of volume of coil to a large number of the trace elements, for each of which affected stationary field. Taking into account the addition of losses from the eddy currents in the support/base theoretical values will agree with the experimental data

with precision/accuracy 200/o up to the thread diameters 13 μ m [12].

In accordance with the selected type NETI dependence J_c-B (see Fig. 3) was assumed to be linear, hyperbolic or exponential. Fig. 4 gives the calculated losses for the diol magnet with a length of 1 m and field 5 T (aperture 8x11 cm). Losses to the cycle are given in the dependence on $J_0 B_0 d$, where J_0 and B_0 - characteristic the parameters of relationship/ratio $J(B)$, and d - diameter of separate filament [13].

Dotted lines show the dependence of current density on $J_0 B_0 d$ in the superconductor for different thread diameters, under the assumption that for the field 5 T attains the critical value of the current of short sample/specimen in the filament.

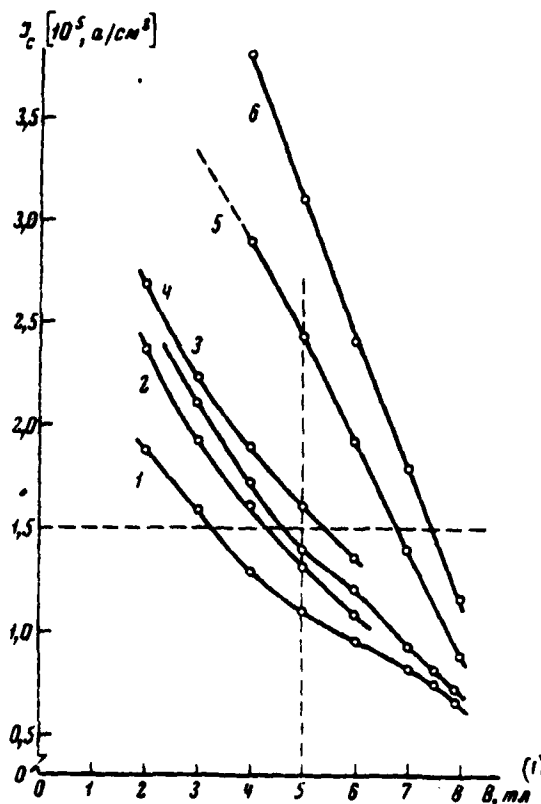


Fig. 3. Characteristics (J_c - B) of short sample/specimen for the samples/specimens of conductor from NETi.

1 - "AIRCO" 0.5 mm, 13 μ ; 2 - "INI" 0.2 mm, 4 μ ; 3 - "AIRCO" 0.5 mm, 24 μ ; 4 - "INI" 0.5 mm, 48 μ ; 5 - "VAC" 0.5 mm, 34 μ ; 6 - "VAC" 0.18 mm of 12 μ (short sample/specimen).

Key: (1). ml.

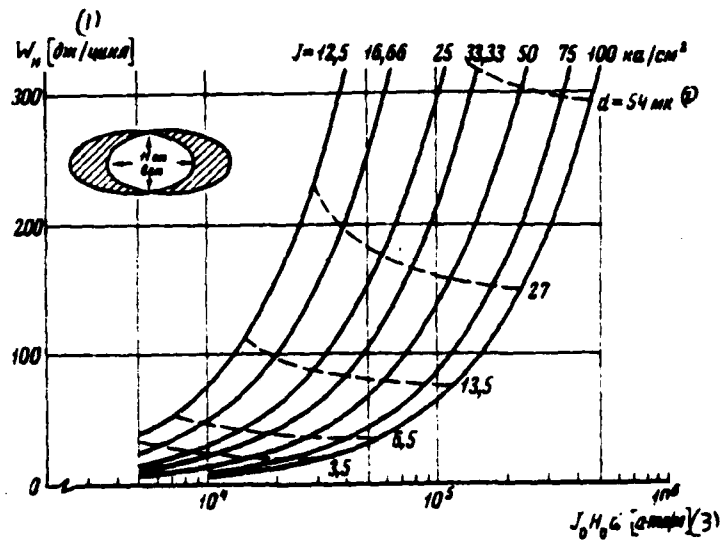


Fig. 4. Hysteresis losses on alternating current for the superconducting dipole with a length of 1 m.

Key: (1). J/cycle. (2). μ . (3). A·cm/m.

Page 251.

A reduction in the losses of alternating current as a result of an increase in the current density is insignificant. However, an increase of the general/commen/total current density in the coil to the possible attainable limit unconditionally decreases a quantity of that required for the magnet of the conducting material, decreases the overall sizes of coil and decreases the accumulated energy of field. The preliminary project of the superconducting dipole magnet

is given in Fig. 5. Working magnet opening is cooled. The aperture of winding is 8x11 cm, moreover around Dewar is arranged/located the iron framework with an internal diameter of 40 cm; it is assumed that in this case Dewar is made on the glass-epoxy basis. Cross section coils approximate two intersecting ellipses. The actual device/equipment of coil and the sizes/dimensions of separate sections are obtained as a result of miscalculation of program on the computer, which optimized each element/cell on the criterion of the minimum error for field with a given number of sections.

Calculations show that for the depicted magnet the field nonuniformity in the limits of broken small circle ($d=6\text{cm}$) comprises $\Delta B/B=2 \times 10^{-4}$. The relative error for field, introduced by the displacement of washer on 0.1 mm in the horizontal direction, is approximately 6×10^{-4} , which by itself superimposes severe limitations on the allowances of coil, the precision/accuracy of coil/winding, and also the precision/accuracy of the support of coil. The magnetomechanical forces, which affect the conductor of dipole by length 1m, are approximately 9×10^4 kg and therefore in order for the conductor not to move impregnation with appropriate thermal-reactive resins is necessary.

Main problem at present composes selection of corresponding resins, which coincide in the coefficient of thermal expansion with the conductor. The construction/design of the support of coil

consists in essence of nonmetallic high-strength bandings and strips/films of glass cloth and epoxy resin.

Fig. 5 shows the device/equipment of winding with the tangential channels for the cooling, with which can arise the specific problems with the cooling. In Fig. 6 represented yes-no decision with the uptakes, which gives good values of heat transfer.

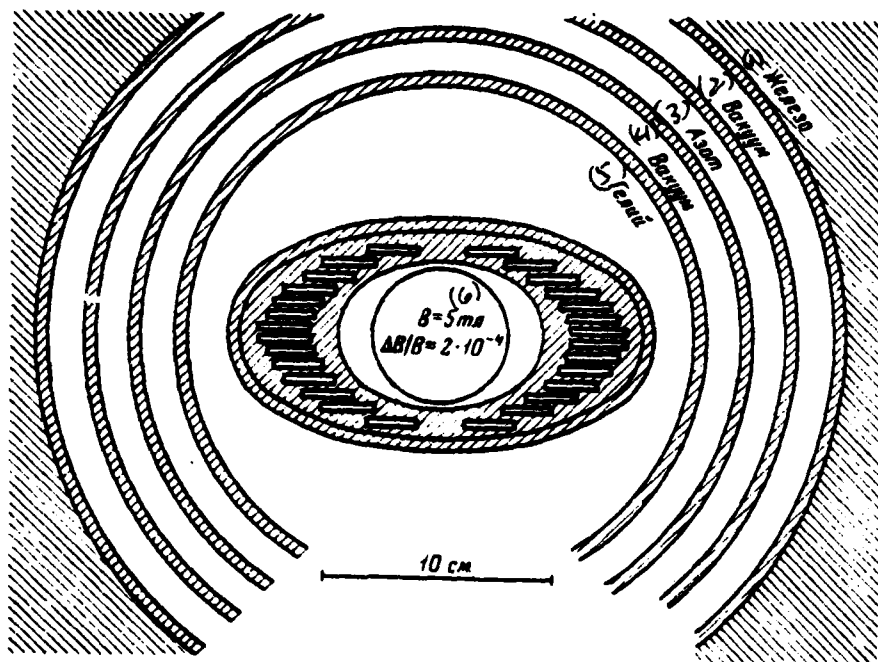


Fig. 5. Diagram of the dipole, which works in the mode/conditions of the changing magnetic field (field 5.54 T, current density 50 kA/cm², aperture 8x11 cm², vacuum chamber cold).

Key: (1). iron. (2). Vacuum. (3). Nitrogen. (4). Vacuum. (5). Helium. (6). sl.

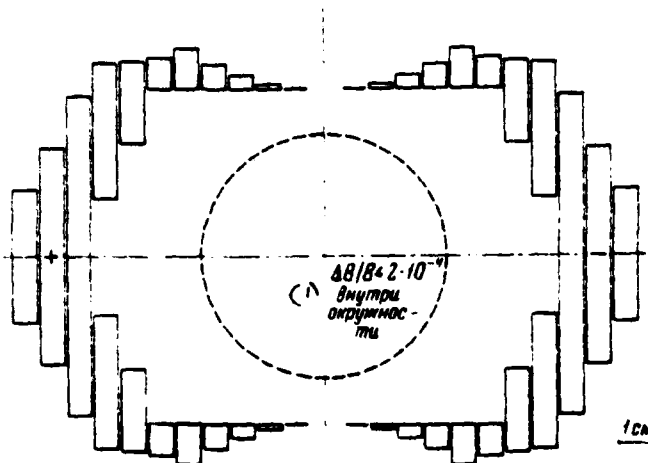


Fig. 6. Calculated on the computers configuration of the dipole, which ensures fields 5, 36T at the current density 50 kA/cm².

Key: (1). Inside periphery.

Page 252.

Calculation on the computers the uniformity of field in the circle with a diameter of 6 cm is compared with the values, obtained in Fig. 5. Much attention is specific to the outputs of the coils which substantially affect the uniformity of field. If the outputs of coil are angled at 90° to the longitudinal axis, straight/direct (parallel to longitudinal axis) sections have equal length, the integral of field ($\int B dz$) on the working aperture of coil will be constant.

For studying methods of coil/winding and hermetic

sealing/pressurization/sealing is prepared the series of test dipole windings. Was created full-scale model from copper (by the overall length of 1 m), analogous to device/equipment in Fig. 5, target of which was the study of pressure the allowances of coil for field distribution. During the use of square isolated/insulated conductors from solid copper of the fluctuation of the thickness of separate sections did not exceed $\pm 70 \mu\text{m}$.

Due to different mechanical properties of composite/compound superconductors and copper, and also for obtaining the close tolerances, at present is made the series of sections from the composite/compound multiple superconductors, saturated with corresponding thermosetting resins.

2.
1 Superconducting quadrupole of direct current.

For the investigation of characteristics of the large superconducting coil electromagnet for the channel of the transportation of beam and for obtaining data on the optical properties (first and second order) to the short-term and long-term behavior of coil was developed and constructed [14] the quadrupole with a length of 1 m with the uncooled internal opening/aperture ($\phi 12 \text{ cm}$). Coils coiled by strip/film Nb_3Sn with a width of 1.5 cm and with a thickness of 0.15 mm, plated from both sides by the copper

bands with a thickness of 0.05 cm. Conductor they cooled on the edges.

Magnet placed horizontally into Dewar, which has static losses of the heat (magnet and Dewar) of 5.8 l/h, whereas total losses with excited magnet comprised 6.2 l/h of helium.

During cooling of quadrupole was supplied liquid nitrogen for cooling of magnet and its external parts down to $\sim 80^\circ\text{K}$. Within the cooling time, which was 2 hours, were used approximately 110 l of liquid nitrogen. The gradual evaporation of liquid nitrogen and final evacuation are carried out in 1.5 hours. The temperature of magnet comprised in this case about 100°K . Cooling down to 4.2°K and filling of helium container are carried out in 2.5 hours with the flow rate of 220 l of liquid helium. The weight of all cooled parts was about 220 kg. Helium container accommodates 60 l of liquid helium.

When magnet was excited, they will achieve critical current 990 A, which corresponds to the field gradient of 37.2 T/m, whereas calculated value was 1300 A, ensuring 50 T/m. With the calculated current the field in conductor would be 3.9 T (bore of coil is 15.5 cm).

In Fig. 7 data of short sample/specimen for Nb_3Sn is given in

the shaded region, whereas measured critical currents lie/rest considerably lower than the expected values for the short sample/specimen.

Coil has a good support and hardly it is possible to expect that the displacements of conductor can cause premature transition into the normal state, which testifies about the degradation of conductor. Up to now it was not observed the phenomena of aging/training.

It is not possible to definitely indicate the reasons for the smaller value of the measured gradient. The unstable work of conductor can be also caused by the poor characteristics of the heat transfer of coil. Two- and three-dimensional calculation of field came to light/detected/exposed the component 2.7 T of field with 990 A, perpendicular to width Nb_3Sn of belt in the region between the adjacent poles at the ends/leads of the coil. In the fields it is above 2 T, perpendicular to the width of belt, belt from Nb_3Sn becomes unstable [15, 16]. The field gradient, measured in the radial direction, is constant in the region of aperture of the uncoupled magnet with an accuracy to 10^{-2} .

Field measurements along the longitudinal axis of quadrupole revealed periodic changes in the field $\Delta B/B = 2 \times 10^{-3}$ Fig. 8a, b). The distance between the maximum divergences $\Delta B/B$ corresponds to the

location of armature made of the stainless steel, which is located with the gaps/intervals 6.5 cm. The error for field can be caused by local distortion of coil; however, it is possible to also carry due to the specific ferrimagnetic austenitic behavior of the stressed stainless steel at a temperature of 4.2°K [17].

IV. Cryogenic magnets.

One of the materials which today have the best cryogenic characteristics for the use in the magnets, is aluminum. During the use of such technological processes as electrolysis and zone improvement, it is possible to obtain the coefficient of end resistance on the order of several ten thousands. It is possible to obtain copper of the same frequency as aluminum; however, its magnetic resistance grows/rises with the field linearly, whereas in the high magnetic fields in aluminum observed the effects of saturation.

In the process of studying the applicability of conductors from Al in the pulse cryogenic magnet were carried out the measurements of the behavior of specific resistance in the small wound by belt (12x0.3 mm²) sections with an internal and outer diameter of with respect 4 and 12 cm. Belts were insulated by foil Khostafan¹.
FOOTNOTE ¹. Khostafan - trade mark of foil from the polyethylene terephthalate of firm "Kalle-AG". ENDFCCTNCTE.

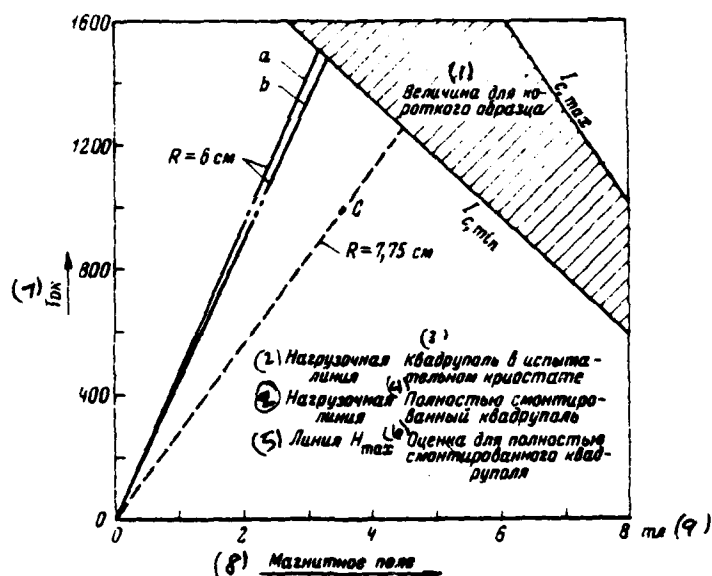


Fig. 7. Characteristics of the developed in Karlsruhe quadrupole in diameter 12 cm.

Key: (1). Value for the short sample/specimen. (2). Load line. (3). Quadrupole in experimental cryostat. (4). Completely installed quadrupole. (5). Line. (6). Estimation for completely installed quadrupole. (7). Current. (8). Magnetic field. (9). ml.

Page 253.

With this configuration the measurements were carried out for the diverse belts in the range of residual resistances $1600 \leq R_{RR} \leq 11700$ at temperatures 4.2 and $20.4^\circ K$. For the high-purity belts with thickness $d=0.3$ mm the size effect is evident. Correction of size

effect for completely diffuse surface/skin scattering ($\rho=0$) it is calculated according to the theory Sondheimer [18]

$$\rho_{\text{лентил}} = \rho_{\text{объемный}} \frac{\Phi(d/l, \rho)}{d/l} \quad (1)$$

During the calculations for the mean free path of electrons l was utilized the averaged on several experiments value ρ volumetric of $l=7 \times 10^{-12}$ ohm cm². Integral $\Phi(d/l, \rho)$ is obtained from the numerical calculations of Dvorak, etc. [19]. With such numbers the coefficient of residual/remnant specific resistance $RRR_{\text{объемный}} = 11700$ decreased in the case of belt 0.3 mm to $RRR_{\text{лентил}} = 8000$.

According to the law of Mattissen, specific resistance is obtained, summarizing the independent from the temperature residual/remnant part and its con part, proportional T^5 :

$$\rho(T) = \rho_n + \rho_d \cdot T^5 \quad (2)$$

Residual/remnant specific resistance is obtained from electron scattering on the defects, and internal resistance - from an electronic-phonon interaction. Latter/last part is virtually negligible at a temperature of 4.2°K. From Fig. 9 it is evident that both effects are not dependent, and the law of Mattissen is disrupted. Is given the dependence of a difference in specific resistances $\rho(20.4^\circ\text{K}) - \rho(4.2^\circ\text{K})$ according to several experimental results [11, 20, 21] or the coefficient of residual/remnant specific resistance. Interaction between the phenomena of dispersion increases proportional to the concentration of defects.

According to Kohler, a relative change in specific resistance

$$\Delta\rho/\rho = [\rho(B,T) - \rho(0,T)]/\rho(0,T)$$

is function only B/ρ . A change in specific resistance can be written in the form:

$$\frac{\Delta\rho}{\rho} = \frac{\alpha(B/\rho)^2}{1 + \beta(B/\rho)^2},$$

where α and β - constant of material. Divergences from Kohler's law, based on the isotropy of the processes of scattering, were revealed for the functions of temperature and impurity content both for polycrystalline Al [11, 20] and for single crystals [21, 22]. Fig. 10 gives the dependence of a relative increase in specific resistance on the magnetic field strength. In the measurements of the authors of article are given the values of proper field, which compose in the rough approximation the half the central field of coil, and intended for the comparison with measurements in the short samples/specimens. Very satisfactory quantitative agreement testifies about a considerable increase in magnetic resistance with an improvement in the purity/finish. In the fields, which exceed 3 T, were observed the effects of saturation. The measurements of Fickett [20] came to light/detected/exposed even linear part of the curve reluctance in the field 4 t.

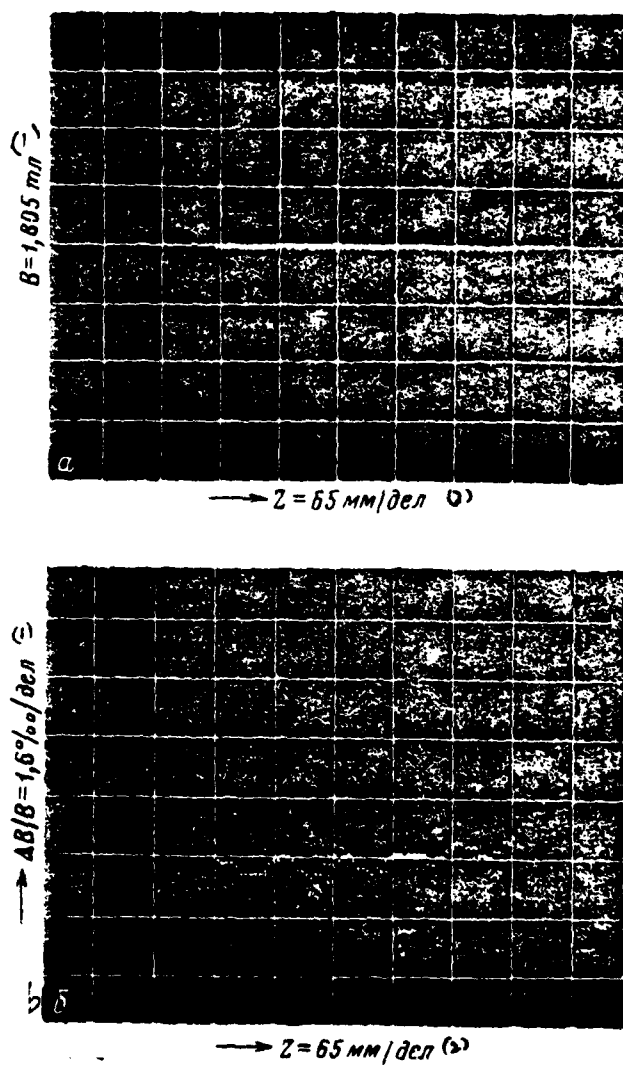


Fig. 8. Magnetic bump along the line, parallel to Z-axis on radius $r = 4.95 \text{ cm}$ in the region between adjacent poles ($J = 950\text{a}$) (a), the heterogeneity of field the same, but with an increase 32 times.

Key: (1). ml. (2). mm/div.

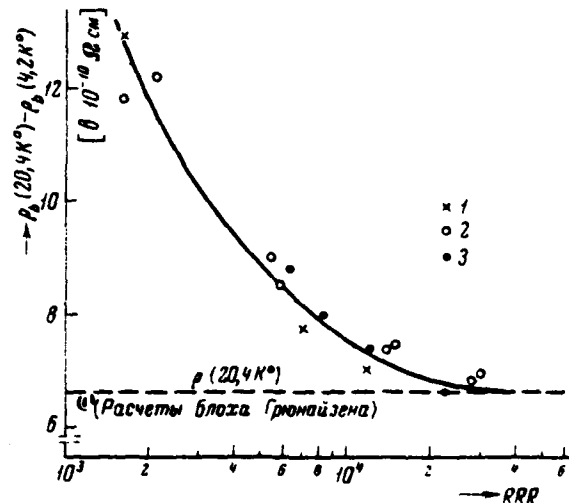


Fig. 9. Divergences from the law of Mattissen for aluminum. The experimental values $\rho(20.4K) - \rho(4.2K)$ depending on the residual/resonant relation of resistances (RRR)

1 - on data of this work; 2 - on data of Pickett; 3 - according to the data of Boroviki, etc.

Key: (1). (Calculations: Grueneisen's law).

Page 254.

Fig. 11 gives temperature changes in the reluctance and effective coefficient of specific resistance $R_{\text{ленты}}(B, T)$ for different values of the surface finishes, investigated at

temperatures 4.2 and 20°K.

Measurements on the single crystals of specific angular directions between crystallographic axis/axis and applied field determined the effects of saturation for several directions, but for other directions the anomalous absence of saturation of reluctance is not thus far yet understood. Possibly, are combined several phenomena of such, as an electronic-phenomenon small-angle scattering [23], magnetic breakdown for the specific directions of crystal [24] or generation of "collar" channels into Brillouin's adjacent zones [25], with which of the mechanisms of conductivity are eliminated the electrons.

The anomalous behavior of specific resistance causes interest still and because aluminum can be used in the magnets at a temperature of liquid hydrogen. Thus necessarily more systematic experimental study, mainly on the study of the dependence of reluctance on the temperature and the admixtures/impurities. For this purpose are prepared the measurements in the short samples/specimens for the tests under conditions, expected in the magnet with strong field.

In parallel to investigations in the short samples/specimens is constructed the magnet in the form of window frame (Fig. 12), which

is designed for obtaining of field 4 T in the aperture $4 \times 5 \text{ cm}^2$ at the length of 40 cm. With the belt, which has $R_{\text{eff}} = 10000$, will be used aluminum foil by section $8 \times 0.3 \text{ mm}^2$, insulated by surface/skin oxide of aluminum with a thickness of 5 μm . Are successfully completed tests on the coil/winding of saddle-shaped coils. Experimental cryogenic magnet works with different cryogenic temperatures and at frequencies of pulses for which will be calculated total losses.

The extrapolation of reluctance in the field 4 T on the basis of those carried out of earlier measurements shows that at 4.2°K it is possible to expect the loss 160 W of direct current, and at 20.4°K - losses 1000 W of direct current. These values correspond to gain of total power 7 times in 4.2°K and 13 times with 20.4°K, if we assign the effectiveness of cooler with respect to the ideal thermodynamic effectiveness, which comprises 0.15 with 4.2°K and 0.3 with 20.4K.

1077

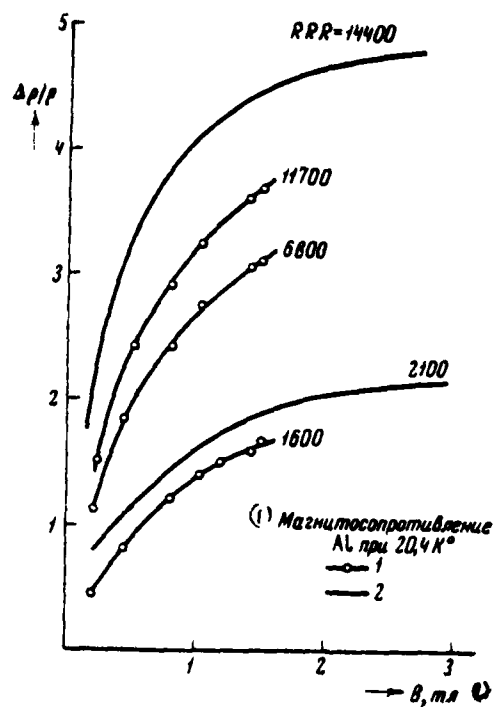


Fig 10. Magnetic resistance of aluminum at 20.4K^o.
1 - according to data of this report; 2 -
according to data of Fickett.

Key: (1). Magnetic resistance of Al at 20.4K^o.

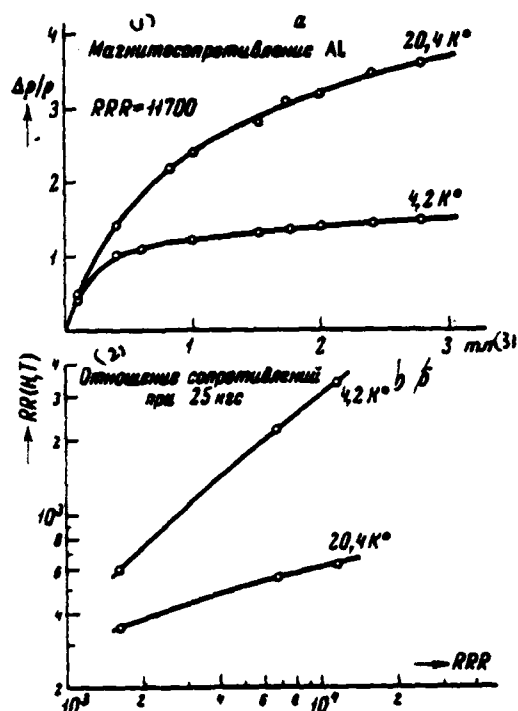


Fig. 11. The measurement of winding impedance a - and relative increase of resistance in the dependence on the central field for 4.2 and 20.4°K and belt with the value of the residual/resonant relation of resistances = 11.7. 10^3 ; b - effective relation of winding impedances with the value of central field in 2.5 T depending on the value of the residual/resonant relation of resistances RRR for 4.2 and 20.4°K.

Key: (1). Magnetic resistance. (2). Relation of resistances with 25 kg. (3). ml.

Page 255.

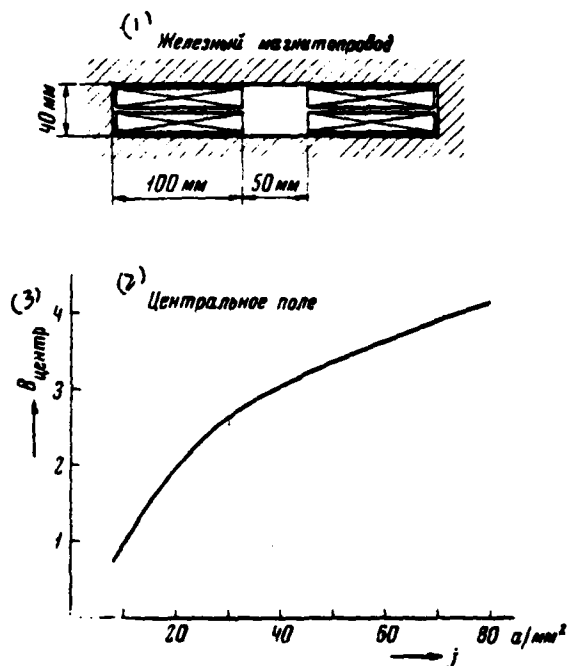


Fig. 12. Central field of experimental magnet with aluminum windings. This magnet with a length of 40 cm will have uptakes for the cooling. Iron magnetic circuit (outer diameter -60 cm) is cooled together with the wound from the belt windings.

Key: (1). Iron magnetic circuit. (2). Central field. (3). center.

REFERENCES

1. J. Erb and G. Merle. KFK 3.69 26 (1969), Karlsruhe.
2. J. Erb, G. Merle to be published.
3. H.J. Bode. K. Wohleben. Z. angew. Phys., 1969, 27, 92.
4. G.W. Cullen. R.L. Novak. J. Appl. Phys., 1966, 37, 3348.
5. H.T. Coffey, E.L. Keller, A. Petterson, S.L. Autler. Phys Rev., 1967, 155, 355.
6. H. Ullmaier. Z. angew. Phys., 1969, 26, 261.
7. C.P. Bean, R.L. Fleischer, P.S. Schwartz, H.R. Hart. J. Appl. Phys., 1966, 37, 2218.
8. H. Brechna, Proc. 1968. Brookhaven Summer Study, Part, 1968, 111, 1011.
9. E.E. Kerlin, E.T. Smith. FZK, 1966, 290.
10. J. von Schaeven, H. Brechna. To be published.
11. W. Schauer, W. Specking, P. Turowski. Proc. 3rd Magnet. Technol. Conf. Hamburg, 1970.
12. K.P. Jüngst, G. Krafft, G. Ries. Proc. 3rd Magnet Technol. Conf., Hamburg, 1970.
13. G. Ries. BSG Notiz, 1970, 7019, KFZ-Karlsruhe.
14. N. Fessler, G. Bogner, H. Kuckuck, D. Kullmann. Proc. 3rd Magnet Technol. Conf. Hamburg, 1970.
15. M.N. Wilson. Rutherford Lab., 1969, RPA A 73.5.
16. H. Brechna. SLAC TN, 1970, 10, 1.
17. D.C. Larbestier, H.W. King. Cryogenics, 1970, 10, N 1, 110.
18. E.H. Sondheimer. Advanc. Phys., 1952, 1, 1.
19. F. Dworschak, W. Sassin, J. Wick, J. Wurm, KFA Jülich, 1969, Jül-375-FN.
20. R.F. Fickett. NBS Boulder, Col. to be published.
21. E.S. Borovik, V.G. Volotskaya, N. Yu, Fogel. Sov. Phys. JETP, 1964, 18, 31.
22. Y.N. Chiang, V.V. Emerenko, O.G. Shevchenko. Sov. Phys. JETP, 1970, 30, 1040.
23. A.B. Pippard. Proc. Roy. Soc., 1968, 305A, 291.
24. R.J. Balcombe, R.A. Parker. Philos. Mag., 1970, 21, 533.
25. R.A. Young. Phys. Rev., 1968, 175, 813

Discussion.

V. G. Davidovskiy. Which the maximum value of field on the surface of iron screen?

V. Khaynts. 40 kg for the latter/last development of aluminum magnet. For the developed superconducting magnet - only 20 kg, so that it is not saturated.

V. G. Davidovskiy. Such the ratio of full/total/complete magnetic energy in the system to the energy of field in the useful aperture of accelerator?

V. Khaynts. Approximately half of the energy is expended on the energy is expended on the winding of the magnet, and half on the aperture.

V. G. Davidovskiy. Did you try to optimize this relationship depending on the radius of the screen and thickness of the winding?

V. Khaynts. Yes.

N. V. Kovalev. Request in more detail to describe that it was observed in stressed austenitic steels at liquid-helium temperatures.

V. Khaynts. We do not know exactly what occurs in these steels under such conditions and they were astonished, after clashing with the effect which we now have. Is necessary the study of this effect subsequently. But this is the indication that it is not possible to utilize the stainless steel in such devices/equipment close to the working aperture.

P. A. Vodop'yanov. In what relationship/ratio they are located through your estimations of loss in the aluminum and superconducting

windings at frequencies on the order of 1 Hz?

V. Khaynts. Relative losses at a temperature of liquid helium will be approximately 5 times more in the aluminum magnets, than loss in those superconducting, where are utilized conductors in thickness of veins/strands 5-10 μ m. At the present moment/torque aluminum magnets are too poor for their use.

Page 256.

80. Program of works on the creation of the superconducting coil electromagnets in Saclay.

G. Bronk.

(Saclay, France).

Introduction.

In recent years they will achieve the considerable progress in obtaining of the superconducting materials and designing the magnets. At present a large number of the superconducting coil electromagnets, intended for the work in the continuous duty, is located in the stage of construction. The kickers thus far are located on the stage of design, but there is a clear prospect for their practical use in the near future. In many works it is noted [1], that the use/application of the superconducting coil electromagnets in high-energy physics is of large interest, since they have the best characteristics, smaller

dimensions, smaller power consumption, etc.

The work on the superconducting coil electromagnets, conducted in the laboratory of division "Saturn", concerns both the their use/application in the continuous duty for the detectors and elements of the systems of the transportation of beam and development and construction of the kickers for the synchrotrons.

Lenses of systems for the transportation of beam (O.G.A.).

After the successful tests of the construction/design of magnet BIM (length of 1 m, induction 4T, stored energy 10 MJ) in 1969, was constructed the doublet of quadrupole lenses, which ensures a noticeable increase in the intensity of the beam of the secondary pions, created in the experimental zone of accelerator by proton beam with the energy 3 GeV. The expected gain in comparison with the usual quadrupole lenses, attained as a result of applying the superconducting materials, is proportional to an increase in the angular acceptance and is equal to four. However, such is the relation of maximum fields in both cases.

Optical considerations and studies of particle trajectories led to the conclusion that it is necessary to utilize an elliptical aperture and different field gradients. However, for simplification

in the construction/design of quadrupole lenses was selected the circular shape of apertures. The values of the basic parameters of lenses are given in Table 1. The two-dimensional pictures of field and current distribution are obtained by two methods: by the method of resolution in the Fourier series the field of coils with the permanent current density [2] and as a result of analytical and numerical calculations of the field, created by the current, flowing through the polygonal ones section [3]. The three-dimensional pictures of field are calculated with the aid of the program, based on bih-savart's law, and the contribution to the field gradient, given by iron screen, is obtained as a result of calculations according to the program, which is the modification of program "HARE" [4]. The cross section of coils is shown in Fig. 1, and field distribution for both quadrupoles ^{Fig} - 2.

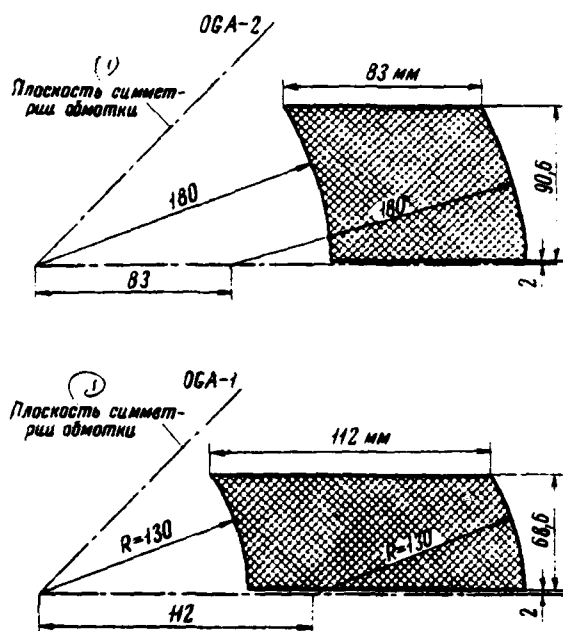


Fig. 1.

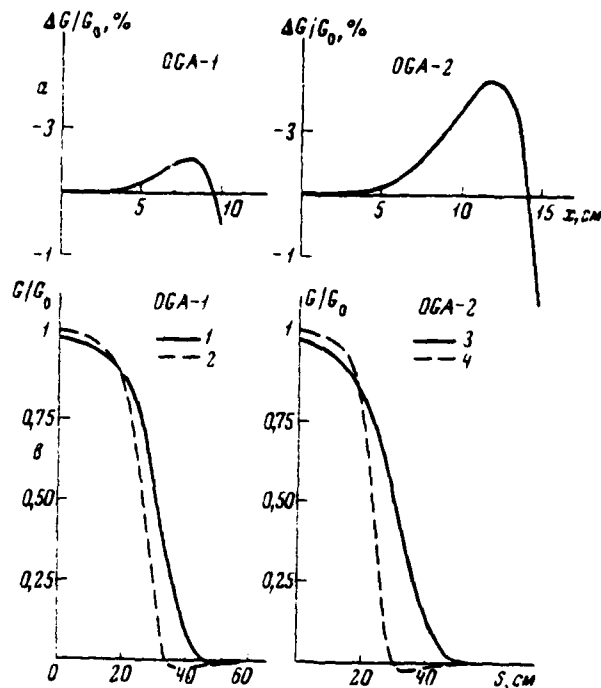


Fig. 2.

Fig. 1. Cross section of windings of quadrupole.

Key: (1). Plane of the symmetry of winding.

Fig. 2. Field distribution of quadrupole. a) change in the gradient in a radius in the central plane; b) change in the gradient lengthwise from the quadrupole: 1 - $x=0$; 2 - $x=10$ cm; 3 - $x=0$; 4 - $x=15$ cm.

Page 257.

The basic parameters of magnets are selected taking into account the technological possibilities, which existed in the period of design and determined the construction/design of magnet (stabilized by copper superconductor, interwoven from the thin wires of the diameters of 100μ). It was more lately explained that the possibilities of contemporary industrial technology make it possible to improve the magnetic characteristics of doublet. For example, an external radius of the first quadrupole is reduced with 31 to 24.2 cm, and average/mean current density is increased by 250/o. Are given below the values of the parameters of the new construction/design of quadrupole.

Basic parameters of the quadrupole lenses:

parameter O.G.A. 1 O.G.A. 2.

Useful radius, m 0.10 0.15.

Inside radius of coil, m 0.13 0.18.

External radius of coil, m 0.242 0.263.

Maximum field gradient, t/m 35 23.

Maximum induction, t 4.64 4.18.

Magnetic length, m 0.68 0.67.

General/common/total current density, A/cm² 10220 10350.

Maximum current, A 1.175 1.150.

Stored energy, MJ 0.70 0.83.

Longitudinal length, m 0.84 0.84.

The overall length of conductor, m 4x1130 4x1145.

Bore of screen, m ... 1.45 1.45.

Thickness of screen, m 0.09 0.09.

Thickness of end plates, m 0.03 0.03.

The conductor of rectangular cross section (2.35×2.35^2 mm) is prepared from large number (37x37) of the twisted filaments in diameter approximately 40μ , included in the matrix/die from copper, moreover the relation of the sections of copper and superconducting material is equal to 3.6. The film of epoxy resin with a thickness of 50μ serves for the isolation of conductors from the housing, and cooling coil is provided by channels for helium with width 0.6 mm, arranged/located between the layers. When selecting of the form of coil/winding by the ends/leads of the poles are accepted the special precautionary measures for the purpose of ensuring the ease/lightness of coil/winding and at the same time preserving by free aperture. The made selection provides the constancy of the length of all turns and a minimum number of turns in each layer. As is shown trajectory calculation, obtained field distribution, shown in Fig. 2, is completely acceptable.

Cryostat is shown in Fig. 3, where is represented the diagram of the layout of entire installation. Cylindrical tank for helium is placed eccentrically relative to the axis/axle of coil in order to ensure the possibility of access to the reservoir for helium with a capacity/capacitance of 140 l, established/installed higher than the level of coils. The electrical protection of coils is provided by the device/equipment which records transition into the normal state and is accomplished/realized the removal/distance of stored energy with

the effectiveness of more than 990/o.

during November 1970 were set many parts of installation (cryostat, screen, supply of power and strut), whereas the conductor of new construction/design still is located in the stage of production. Immediately at the termination of tests the doublet of quadrupole lenses will be established/installed in the experimental zone for its testing under working conditions.

Investigations on the use/application of the superconducting coil electromagnets in the pulsed operation.

As is well known, with field changes in the superconducting material appear the energy losses, moreover the value of these losses is the function of the intensity/strength of field, geometry of coil, sizes/dimensions of conductor and its construction/design [5]. The superconducting coil electromagnet for the synchrotron must create the field of order 6T in the zone by width on the order of 10 cm and lengths several meters and operate on a pulsed basis during pulse repetition after every 4-5 s. As it follows from the theory, under such conditions the diameter of thin wires from the alloy of titanium-niobium must be order on the order of 2-4 μ , and the step/pitch of their joining - about 1 mm.

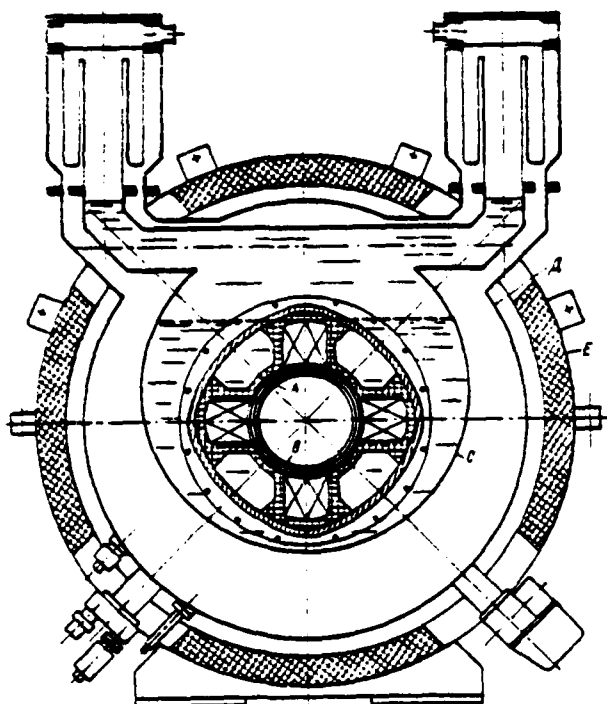


Fig. 3. The general view of the quadrupole

2) A - внутренняя стенка криостата	08A1	08A2
3) B - гелиевый танк	Φ 200	300 мм
4) C - гелиевый танк	Φ 238	338
5) D - внешняя стенка криостата	Φ 1010	
6) E - экран	Φ 1350	
	Φ 1630	

Key: (1). Inside wall of cryostat. (2). B - helium tank. (3). C - helium tank. (4). D - external wall wall of cryostat. (5). E - screen.

For testing the theory is carried out a very large number of experiments. The superconducting windings, prepared from the thin wires in diameter from 300 to 8 μ by different producers in Europe and USA, were used for producing more than 35 solenoids with the bore of 20 mm, outer diameter of 90 mm, and length of 90 mm, which create field by intensity/strength 6T in the center of coil. The relation of the sections of copper and superconductor was changed in the limits from 1 to 6. The pulsed source of supply permitted implementation of cycles with the frequency one impulse/momentum/pulse within the time from 2 to 15 s.

Experimental data are compared with the theoretical values of the losses which are obtained by the method of calculations with the use of a calculated picture of field and theoretical expressions for the losses.

Generally speaking, the ratio of the measured values of losses to computed values lies/rests at the range from 1 to 2 and does not depend on the diameter of thin wires, if it exceeds 0 μ , when the step/pitch of winding on is small in comparison with the critical length, to the corresponding period of the increase of the field (see Fig. 4). It is more precise, the basic results of experiments can be presented as follows.

The degradation, defined as the relation of the experimental value of current upon transfer into the normal state to its theoretical value, was determined as a result of experiments with a slow increase of the current and in the pulsed operation. With the slow increase of current this relation always ranged from 1 to 0.9 with exception of the case of the braid/cover, for which it was obvious that some conductors were torn/broken. In the pulsed operation it turned out that this relation depends on cooling and mechanical stresses in the winding. With a good cooling of coils - (channels for helium with a width of 1 mm or copper heat withdrawals with a diameter of 0.2 mm) and mechanical stresses in the winding (5 kg/cm²) the degradation of energy was approximately the same as with the slow increase of current. In other cases it was on the order of 0.3 (see Fig. 5).

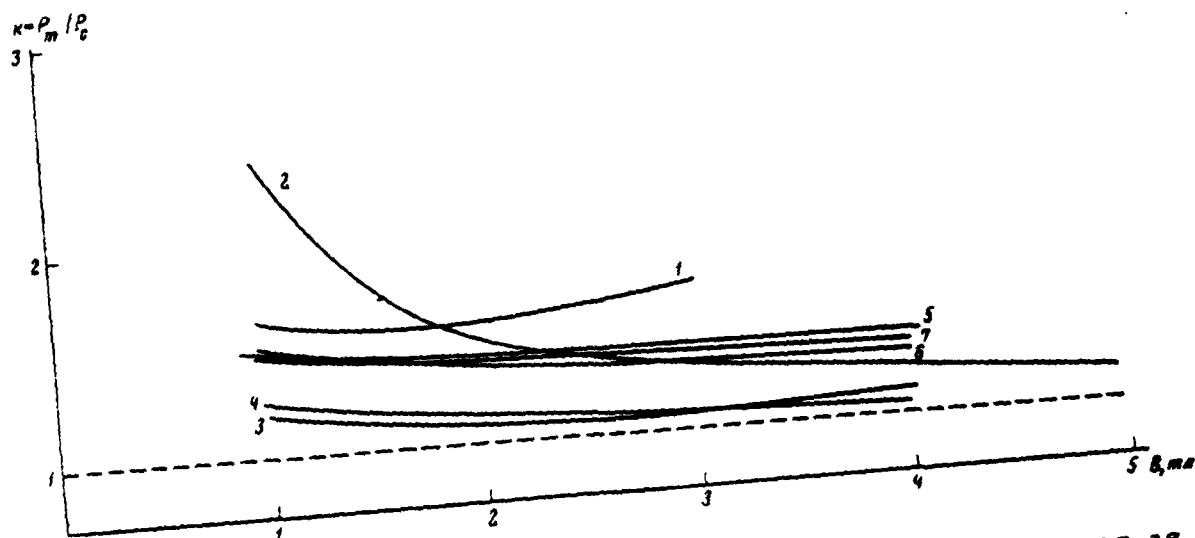


Fig. 4. Ratio of the measured losses to the calculated losses as the function of field. 1 - cable of 210 conductors (10x3x7), diameter of strands 36 μ [CPTH]; 2 - cable of 28 conductors (4x7), diameter of strands 97 μ [CPTH]; 3 - strip/film of 288 conductors; diameter of strands 48 μ [CPTH]; 4 - multiple conductors (61), diameter of strands 28 μ [INI]; 5 - multiple conductors (1045), diameter of strands 12 μ [INI]; 6 - multiple conductors (400), diameter of strands 7.5 μ [Supercon]; 7 - multiple conductors (1045), diameter of strands 6.6 μ [INI].

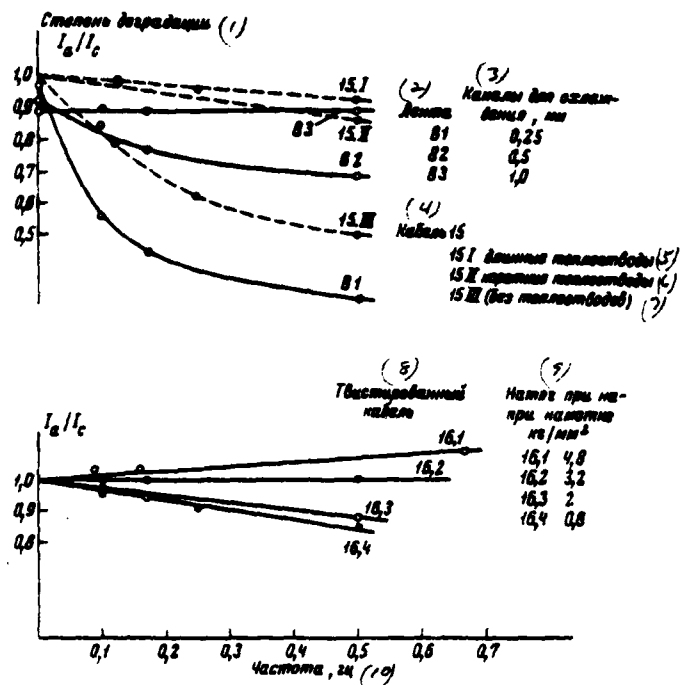


Fig. 5. Dependence of the degree of degradation on the cooling and on the interference with the coil/winding.

Key: (1). Degree of degradation. (2). Strip/film. (3). Channels for cooling, mm. (4). Cable. (5). long heat withdrawals. (6). short heat withdrawals. (7). (without heat withdrawals). (8). Twisted cable. (9). Interference with press to coil/winding kgf/mm². (10). Frequency, Hz.

As is shown experiment, with the diameter of thin wires it is more than 6.6μ the behavior of losses corresponds to the predictions of the theory. For the isolated/insulated thin wires and the thin wires in the copper matrix/die, twisted in the step/pitch it is less than the critical, losses are proportional to the diameter of the monofilaments of the superconductor (see Fig. 6).

It was discovered, that under conditions indicated above of loss do not depend on frequency the washing of winding. However, when the relation of the step/pitch of entanglement toward the critical value ranges from 1 to 4, it was discovered, that the losses grow/rise with an increase in the frequency.

Cooling by noticeable form affects the measured losses: the better the cooling, the lower the loss. As in the case of effect on the legradation, the windings, wound with large mechanical stresses, detect the considerably best properties (see Fig. 7).

Design of synchrotron.

Results relative to lead loss, prepared from the thin wires of a small diameter, proved to be sufficiently encouraging in order to

begin the design of dipoles and quadrupoles for the synchrotron. However, up to now there does not exist the magnets of sufficient sizes/dimensions which would be tested in the horizontal position. From the solenoids of small sizes/dimensions, prepared for material testing, it is still far to the full-scale magnet of synchrotron.

During the design of such magnets it is necessary to accomplish of the series/row of conditions.

To the form of coil it must provide uniform field and low value of stored energy.

The conductor, prepared from the correctly interwoven filaments with diameter several microns, must be calculated for currents on the order of thousands of amperes.

Must be provided the very rigid construction/design of coil for obtaining small allowances.

Are necessary also a good cooling, the careful account of dynamic forces, the shielding, the helium cryostat, designed for the pulsed operation.

Form of coil.

From the theory are known the section of winding and the form of its edges, necessary, in order to obtain a good topography of field.

Speaking in general terms, are possible two approaches with the design of winding. In the first case they attempt to satisfy the stated above requirements, whatever practical difficulties. In the second case, keeping in mind the simple method of coil/winding, they attempt to find the form of coil which would satisfy the stated technological requirements.

It is obvious, the difference between the two approaches indicated is not very great, since in any event it is necessary to search for a compromise between the requirements of theory and the practical possibilities.

In the laboratory of division "Saturn" it is solved as far as possible to simplify technology of coil/winding in order to decrease the cost/value of the production of coil. This path leads to certain increase in the dimensions, since deteriorates the uniformity of field; however, becomes all more obvious, that in any event the inaccuracy of production must lead to the same result, even when selecting of the form of coil in accordance with the requirements of theory.

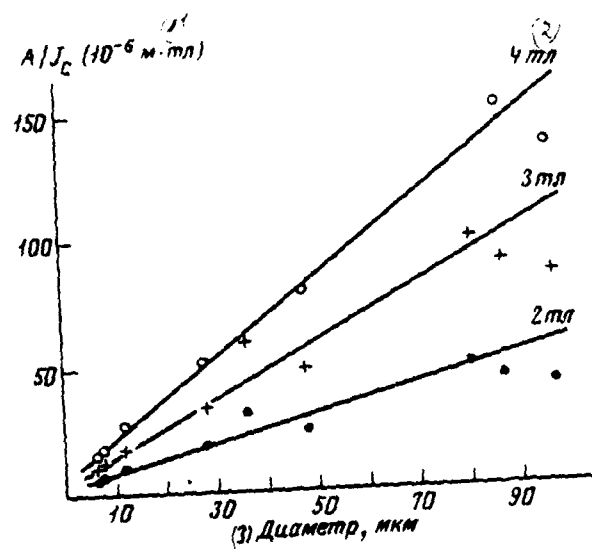


Fig. 6.

Fig. 6. Dependence of measured losses on diameter of strands.

Key: (1). $m \cdot T$. (2). T . (3). Diameter, μm .

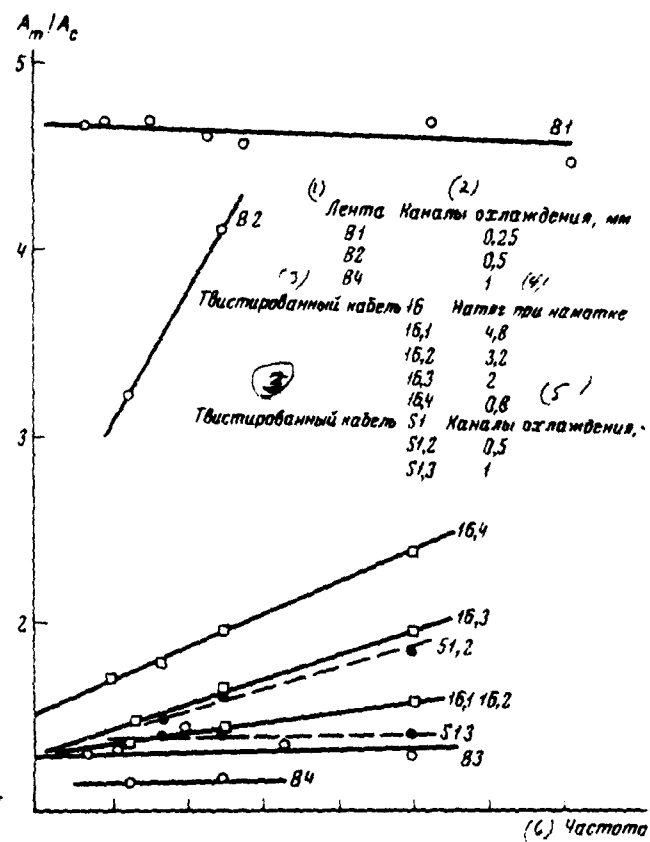


Fig. 7.

Fig. 7. Dependence of measured losses on cooling and interference with coil/winding.

Key: (1). Strip/film. (2). Channels of cooling, mm. (3). Twisted cable. (4). Interference with coil/winding. (5). Channels of cooling, mm. (6). Frequency, Hz.

Page 260.

Coil/winding and cooling.

Taking into account the importance of a good cooling which was noted above, during the design of coils were provided for the cooling channels for helium or metallic (copper) heat withdrawals. The ends/leads of such heat withdrawals, which use for removing the heat from the center of coil, were submerged in liquid helium.

Copper heat withdrawals are very promising, since they make it possible to obtain more compact winding: in this case it is not necessary to take the special measures, which ensure the regular arrangement of heat withdrawals as in the case of cooling channels for helium.

During the use of heat withdrawals it is necessary to impregnate coil in order to ensure a good thermal contact between heat

withdrawals and layers of conductor. Detailed designed investigations led also to the conclusion that the impregnation plays positive role in the process of coil/winding, it impedes the displacement of turns and raises the mechanical strength of winding. At present is developed/processed technology of impregnation. The circuit of investigations lies in the fact that to establish/install, what must be the optimum characteristics of binder and as it will behave during the cooling, during the prolonged operation in the pulsed operation and under the effect of radiation.

Is prepared a large number of dipole magnets of small sizes/dimensions for the investigation of their behavior with the coil/winding (in particular at the ends/leads) and developing the best impregnation operation with the coil/winding, which ensures the prescribed/assigned allowances.

Iron screen.

It is obvious that the magnets of synchrotron must be protected/surrounded by the iron screens, which ensure the absence of the distortions of the field, which perturbs the effects of the field to other instruments and the uncontrollable forces. There are two methods of designing the iron screens.

Iron is arranged/located in the cryostat. In this case is provided a maximum increase in the strength of field and the ease/lightness of the compensation for magnetic loads. Deficiencies/lacks in this method of resolution of problem are an increase in the sizes/dimensions in the cryostat, the disturbances of the uniformity of magnetic field as a result of the effects of saturation and mainly the high hysteresis losses, which lead to the heat liberation which must be driven out at a temperature of liquid helium. From a practical point of view high losses on hysteresis make this decision unacceptable.

Iron out of the helium cryostat. This construction/design is more complicated as a result of the need for the compensation for loads, created by magnetic forces through walls of cryostat. Since the screen is arranged/located further from the magnet, it cannot seize more than 10-15% ground field in the majority of the practical cases; in this case the effects of saturation will be absent. All magnets, prepared in the laboratory, have the iron screen, arranged/located out of the cryostat.

Cryogenics.

When is utilized classical metallic cryostat and repetition period of cycles it composes several seconds, main difficulty in this

region is connected with the eddy currents.

Therefore simple resolution of problem lies in the fact that to utilize the cryostat, prepared from the nonmetallic material, although it is possible to utilize a metallic cryostat, if it is possible to use any crafty method of reducing the losses (for example, the corrugated ducts made of the stainless steel).

Experimental dipole magnet.

For the practical familiarization with the problems, which appear during the construction of the magnet of synchrotron, which works in the pulsed operation, and developing the methods of their resolution it was decided to prepare the experimental dipole magnet which would differ from the final construction/design of magnet in essence only in terms of sizes/dimensions.

Was designed the winding, which creates field with the induction 6 T in the center of the aperture with a diameter of 10 cm.

The aperture indicated somewhat less than it will be required for the magnet of synchrotron, and the magnetic length of coil (50 cm) is considerably lower than necessary. The basic parameters of this magnet are shown below:

Bore of coil, cm 10.

Outer diameter of coil, cm 24.

Field, created by coil without the screen, T 5.5.

Field in the presence of screen, T 6.

General/common/total current density, A/cm² 15000.

Magnetic length of dipole, cm ... 50.

Stored energy, kJ 280.

Number of turns 1000.

Sizes/dimensions of belt, mm 5x1.5.

Length of belt, m ¹⁶⁰⁰~~16000~~.

Maximum current strength, A 1500.

Losses in the superconductor per cycle, J (with the diameter of strands 10 μ) 100.

Operating mode:

the period of the increase of current, s 1.2.

the period of the drop of current, s 1.2.

the period of the constant value of current, s 4.0.

Iron screen

diameter,
bore \sqrt{cm} ... 56.

outer diameter, cm 98.

material - plate from low-carbon steel by thickness, mm
1.5.

Page 261.

Cryostat (metallic cryostat, prepared from the corrugated ducts made of the stainless steel for the depression of the eddy currents

the wall thickness of core tubes, mm 6.

the wall thickness of external ducts, mm 30.

static losses, W 6.

Calculated additional losses due to eddy currents during
mode/conditions indicated above, W 1.5.

The general view of magnet and cryostat is shown in Fig. 8.

Contemporary state of works.

Testings of magnet are noted for autumn 1971. Is at present
ordered conductor and soon it is proposed to order cryostat.
Coil/winding is one of the most complicated technological
operations/processes; therefore was carried out a large number of
tests on full-scale models with the copper conductor, that has the
same sizes/dimensions, as the belt, which contains superconductor.

Conclusion.

The basic goal of the investigations, which were being carried out in the laboratory of division "Saturn" as the laboratory, connected with high-energy physics, consisted of ensuring the possibility of producing the superconducting coil electromagnets for the accelerators and other auxiliary magnets, in particular, the elements of the system of the transportation of beam and magnets, which are the part of the detectors. In the valueless time it is obvious that there does not exist the serious problems, connected with the use of the superconducting coil electromagnets in the constant duty. As far as magnets are concerned, designed for the pulsed operation, then is very probable that for their practical use will be required the even many-year works. However, all research groups, which work above the resolution of this problem, are completely confident in the final success. It is necessary to consider that the construction/design of future accelerators can differ from contemporary. In particular, the high values of the energy, stored up in the magnet and the scattered in the superconductor power, can create tendency toward the development of accelerators with the larger duration of cycle [6]. However, the only one of the directions of wide study program which will be required for the successful decision of stated problems.

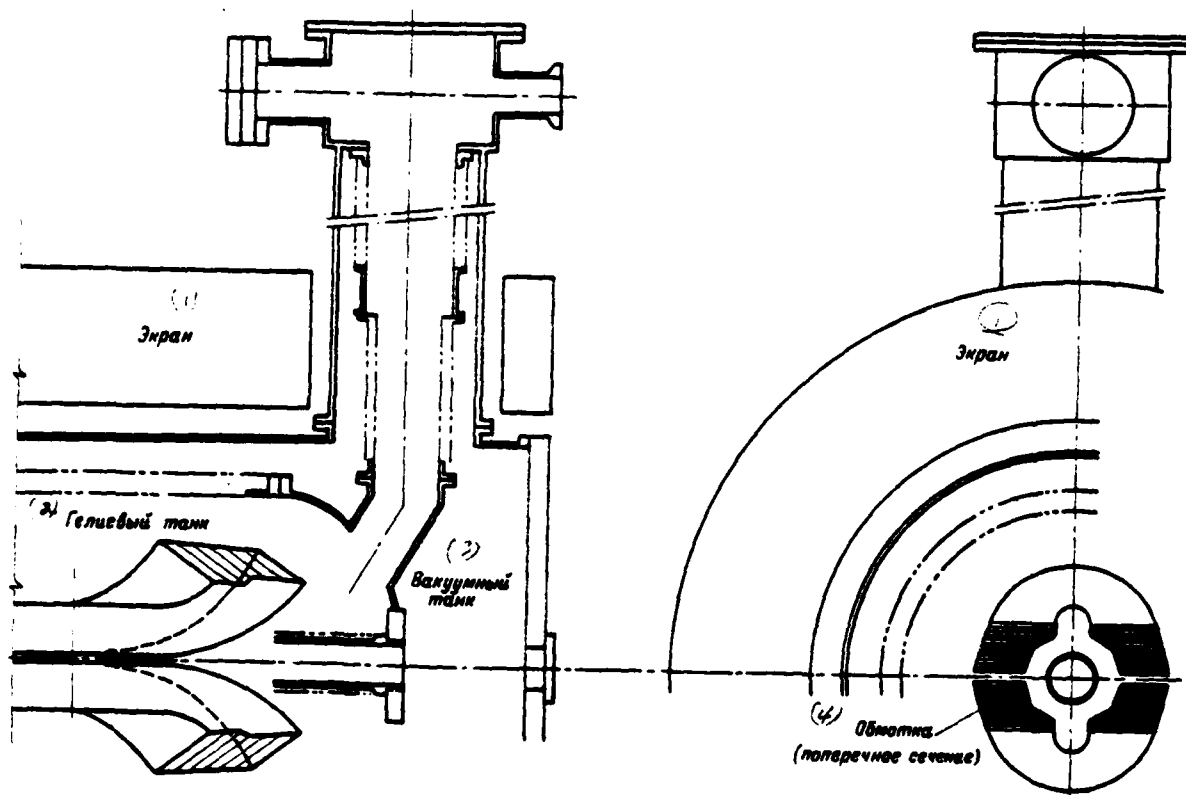


Fig. 8. The general view of dipole.

Key: (1). Screen. (2). Helium tank. (3). Vacuum tank. (4). Winding (cross section).

REFERENCES.

1. 1. Proceedings of the 3-rd international conference on magnet technology. Hamburg, May 1970.

2. G. Bronca, J.P. Pouillange. CEN SACLAY Internal Report: SEDAP 67-01, December 1967.
3. R.A. Beth. J. Appl. Phys., 1966, 37, N 7.
4. R. Perin, S. Vander Meer. CERN/67-7, March 1967.
5. G. Bronca, I. Hlasnik, C. Lefrancois, J. Perot, J.P. Pouillange. Proceedings of the 3-nd international conference on magnet technology. Hamburg, May 1970.
6. G. Bronca, R. Levy-Mandel, G. Neyret, J. Parain. Particle Accelerators, vol. 1, N 3, p. 187, July, 1970.

Discussion.

N. Vest. Were impregnated the windings of direct-current quadrupole?

If not, then as are held conductors in the winding?

What current density in the winding?

G. Bronk. The windings of quadrupole were not flooded, but they were cooled with the aid of the channels, formed by packing. As far as effects are concerned mechanical, winding is sufficiently durable due to the stretching of conductor, and when its winding on is completed and four windings are assembled together, then there is a special device/equipment, which will reliably hold down/retain them. We hope not to have essential troubles due to the displacements.

The current density which we expected, is equal to 11 kA/cm².

Page 262.

81. Development and investigation of the combined conductors with the thin superconducting veins/strands.

A. I. Kostenko, N. A. Monoszon, G. V. Trokhachev.

(Scientific research institute of the electrophysical equipment in.
D. V. Yefremov).

V. V. Baron, Ye. M. Savitskiy, V. A. Frolov

(IMET - Institute of Metallurgy in. A. A. Baykov] of the AS
USSR in. A. A. Baykova).

At present special interest cause the multiple combined conductors with the thin superconducting veins/strands. The use/application of such conductors makes it possible to raise average/mean current density in the windings of the superconducting coil electromagnets to $(3-5) \cdot 10^4$ A/cm² and to create the superconducting coil electromagnets, which work on alternating current. In the present report is described the method of producing the multiple combined conductors with the thickness of those

superconducting strands to 30 μ , and are also represented the results of their investigation both in the form of short samples/specimens and with the coil/winding into the solenoids, which have the varied conditions for cooling.

Method of production.

The production of the combined conductor was conducted by the method of the combined plastic deformation of the superconducting niobium-titanate alloy, placed into copper die. The rods of niobium-titanate alloy, installed into the special mount/mandrel, were heated in the atmosphere of argon to temperature of 700°C, were inserted into the copper matrix/die and was conducted pressing. The temperature of the container of press in this case was approximately 400°C. Heating the niobium-titanate rods before the pressing contributed to the best cohesion/coupling of alloy with the copper matrix/die. The selection of temperature conditions during the pressing provided the most advantageous relationship/ratio of the resistances to deformation of superconducting alloy and copper.

As the superconducting material there was selected the alloy of niobium with 60o/o of titanium.

The composite rods with a diameter of 25-30 mm, obtained after pressing, were further worked by rolling in the grooved rolls with

the subsequent dragging to the wire $\phi 0.3$ mm.

For increasing the density of critical current was applied the heat treatment of the combined conductor at the intermediate diameter at a temperature of 450°C for 2-4 hours. Intermediate diameter was selected from the condition that the strain with the dragging to the final diameter composed 50-60%.

For the research works on alternating current were prepared the samples/specimens of the three-component combined conductors, which consist of those superconducting strands in the titanium shell, placed into the copper matrix/die.

For producing the three-component conductors was applied the method of dual pressing, which consists in the fact that the multiple rods with the titanium matrix/die, obtained by the method pointed out above, were inserted into the copper matrix/die and underwent repeated pressing. Further technological process did not differ from process for the two-component combined conductors.

Characteristics of short samples/specimens.

The results of the measurements of the dependence of critical current in the short sample/specimen on the external magnetic field

are given in Fig. 1 and 2. As can be seen from given data, the characteristic feature of the volt-ampere characteristic of the investigated samples/specimens is smooth running in the initial segment of a curve of transition in normal state, which can be explained by the presence in the superconducting strands of stable resistance region.

Page 263.

With thermal loads $q \sim 0.8 \text{ W/cm}^2$ is observed the abrupt transition of sample/specimen into the normal state, which, apparently, is connected with the crisis of heat emission. The average density of critical current in the field $\sim 50 \text{ kg}$ composes $3-4 \cdot 10^4 \text{ A/cm}^2$ with thicknesses of the superconducting strands in the range $(30-90) \text{ }\mu$.

For the analysis of stability of the superconducting current in the developed combined conductors is used the procedure, which made it possible to determine the maximum value of the superconducting current when flux jumps are present. The test specimen in the form of the bifilar wound coil is established/installed in the solenoid, which creates pulse magnetic field duration $(40-150) \cdot 10^{-6} \text{ s}$ in amplitude $100-150 \text{ a}$.

With the aid of the pulse magnetic field in the sample/specimen

was excited flux jump and was determined the maximum threshold value of the superconducting current, which does not lead to uncontrollable spread of normal phase.

The contrarily connected induction coils, arranged/located inside and out of the sample/specimen, made it possible to record flux jumps which did not lead to the appearance of a normal phase.

External magnetic field was created with the aid of the superconducting solenoid. Measurements showed that while for the single niobium-titanate conductor $\varnothing 0.32$ mm with copper coating with a thickness of 0.04 mm the threshold current in the field 20 kg comprised 16A, and critical current - 270A, the degradation of the current of the combined conductors with 19 superconducting veins/strands in thickness from 35 to 80 μ m virtually was not manifested.

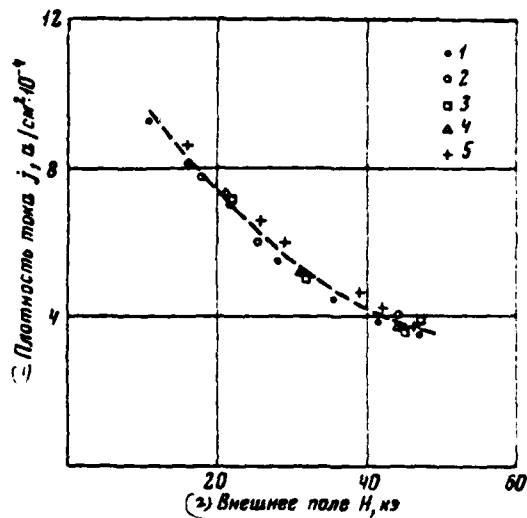


Fig. 1. Dependence of the density of critical current on the applied field for the samples/specimens of 19-strand conductors of different outer diameter. 1 - $\phi 0.3$ mm; 2 - $\phi 0.4$ mm; $\phi 0.5$ mm; 4 - $\phi 0.6$ mm; 5 - $\phi 0.8$ mm.

Key: (1). Charge of current. (2). Applied field H, kOe.

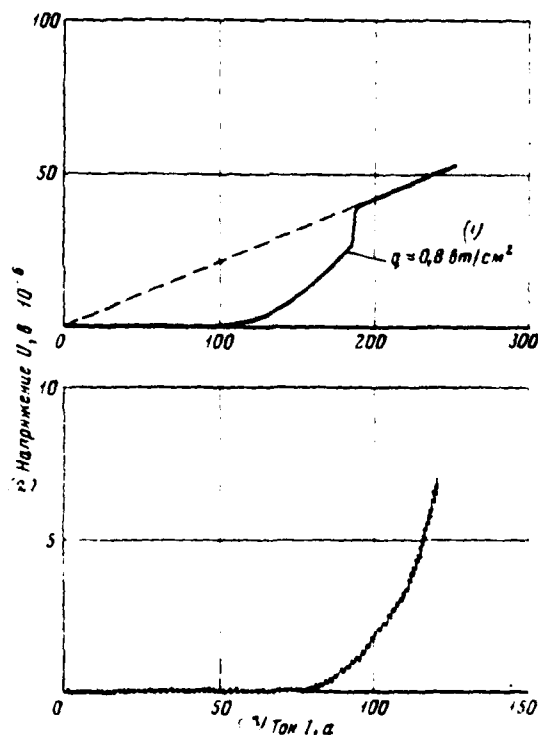


Fig. 2.

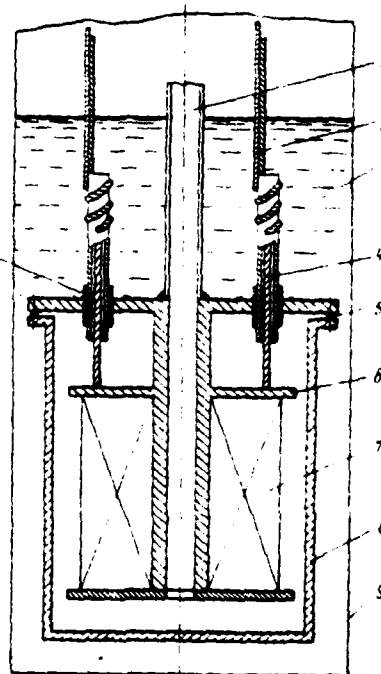


Fig. 3.

Fig. 2. Volt-ampere characteristics of combined conductor with a diameter of 0.5 mm with 37 superconducting veins/strands with a thickness of ~ 40 ($H=24$ kOe).

Key: (1). W/cm^2 . (2). Voltage. (3). Current.

Fig. 3. Tester of solenoid in vacuum. 1 - duct for the vacuum evacuation; 2 - current inputs; 3 - liquid helium; 4 - current

inputs; 5 - vacuum multiplexing from the indium; 6 - copper framework/body of solenoid; 7 - winding of solenoid; 8 - vacuum envelope; 9 - internal wall of cryostat; 10 - ceramic insulator.

Page 264.

Testing the combined conductors with the coil/winding into the solenoids.

From the conductor #0.3 mm with 19 niobium-titanate veins/strands was prepared with the method of joining the semivein cable, from which the was wound the solenoid. The length of conductor was equal to ~600 m. Was measured the current of the junction of solenoid into the normal state during its insertion into liquid helium, and also during the placement of solenoid into the vacuum.

Tester of solenoid in the vacuum is shown in Fig. 3. During testing of solenoid in the vacuum the solenoid was cooled due to the thermal conductivity through the copper framework/body whose upper part had a contact with liquid helium. The junction of superconductor with the current inputs was found in liquid helium. Measuring circuit and results of the tests of solenoid in liquid helium and in the vacuum are given in Fig. 4.

As it follows from given data, in both cases with the accuracy of measurements is reached the current of short sample/specimen and the curve of transition into the normal state in the initial section has steady character.

Fig. 5 gives the results of the tests of solenoid from 19-strand conductor with a diameter of 0.8 mm and by the thickness of those superconducting strands $\sim 90 \mu\text{m}$. The winding of solenoid is saturated with the epoxy travelling compound with the filler, which possesses high thermal conductivity. The length of the combined conductor was 350 a. As can be seen from given data, the degradation of current is not observed.

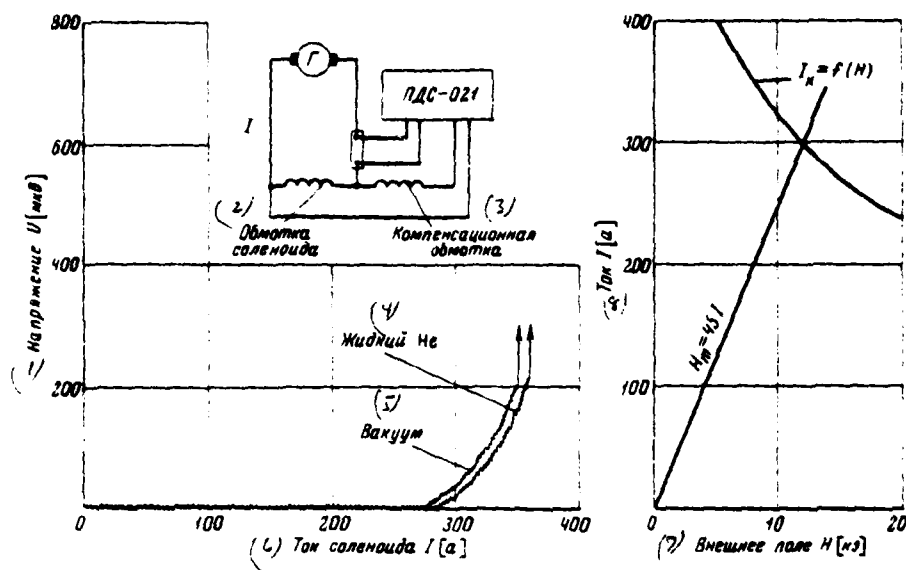


Fig. 4. Measuring circuit and results of the tests of solenoid in liquid He and in the vacuum.

Key: (1). Voltage U [μV]. (2). Winding of solenoid. (3). Pole face winding. (4). Liquid. (5). Vacuum. (6). Current of solenoid. (7). External field. (8). Current.

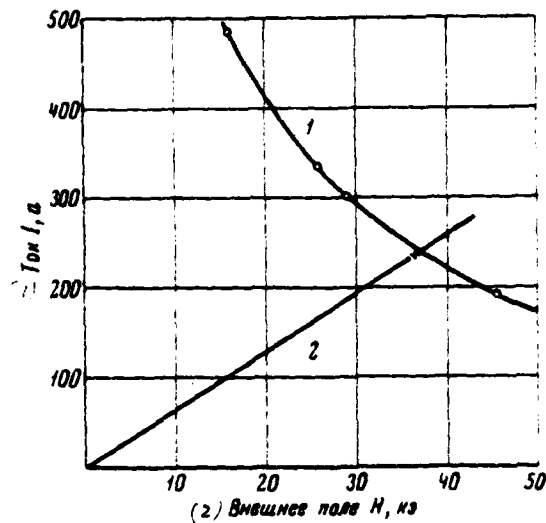


Fig. 5. Results of the tests of the solenoid, saturated with the epoxy trowelling compound. 1 - dependence $I_k = f(H_k)$; 2 - dependence of the maximum value of magnetic intensity on the winding of solenoid from the current; x - transition point into the normal state.

Key: (1). Current. (2). External field H , kOe.

Discussion.

B. N. Sinoilov. Correctly whether I understood that the current density in the superconductor of this cable was equal to $4 \cdot 10^4$ A/cm². Which duty factor?

A. I. Kostenko. This is average/mean current density for entire section of cable. Duty factor was order 300/o.

Page 265.

82. Calculation of the losses in the superconductors and the kind in the pulse magnetic field.

L. I. Greben', Ye. S. Mironov.

(Radio engineering institute of the AS USSR).

The impedance of the superconductors (SP) of the II kind in the magnetostatic field is equal to zero; however, in the variable field which occurs in the magnets of synchrotrons, in superconductors of II type appear the losses. In work [1] it was shown that with some assumptions the power of losses in the superconductor was proportional to the critical density of current SP, to its transverse size/dimension and rate of the build-up/growth of magnetic induction. However, in many real cases, in particular, in the accelerators in which the magnetic field in the process of acceleration changes over wide limits, the adopted assumptions are not fulfilled. In connection with this were carried out the present more detailed calculations of losses in SP.

For determination of losses in SP of the II kind, which is

located in the external pulse magnetic field, was used the model of critical state [2-4]. In this case it was considered that the density of critical current j_c , aimed in SP with a change in the magnetic flux, was connected with the local value of induction B with the relationship/ratio

$$j_c = \frac{\alpha}{B + B_0} \quad (1)$$

During the correct selection α and B_0 formula (1) approximates sufficiently well experimental dependences $j_c(B)$ of real superconductors of II kind in the range of inductions from 0 to 6-8 T. Expressions for the losses per unit volume SP are obtained for the sample/specimen (superconducting vein/strand of multicore cable) of the square section, placed into the transverse magnetic field whose lines of force are directed in parallel to one of the sides of square. With this geometry the distributions over the section SP of the current density, magnetic induction and electric field depend only on one coordinate. These distributions are obtained from the decision of the equations of Maxwell

$$\text{rot } \vec{H} = \vec{j}, \quad (2)$$

$$\text{rot } \vec{E} = - \frac{\partial \vec{B}}{\partial t} \quad (3)$$

together with equation (1). In equation (2) is not written the term, which corresponds to the current density of mixing. In view of the large density of critical current in SP of the II kind this is

completely justified. The account of the fact that the veins/strands have actually round, but not square section, gives the correction factor, which differs little from the unit.

Integrating the power of losses $\Delta P = j_c E \Delta V$ by the volume SP and on the time of a change in the magnetic induction from 0 to maximum value, we obtain magnitude of losses per unit volume SP for the half cycle of magnetization. During calculations it is expedient to break the amplitude range of variable/alternating magnetic induction into two parts: small inductions ($B < B_p$) and large inductions ($B > B_p$). The induction of penetration B_p - such the value of induction on the surface SP with which the power of losses becomes different from zero in entire volume of sample/specimen. In the case

$$B_p = -B_0 + \sqrt{B_0^2 + 4\mu_0 \alpha a}, \quad (4)$$

in question where $2a$ - transverse size/dimension of the superconducting vein/strand.

When $B < B_p$ the expression for the losses per unit volume SP with an increase in the induction from 0 to maximum value B_m takes the form

$$W = \frac{B_0^4}{\mu_0^2 \alpha a} F_1(\xi), \quad (5)$$

$$\xi = \frac{B_m}{B_0},$$

$$F_1(\xi) = \frac{3}{16} + \frac{\xi}{4} + \frac{\xi^2}{8} + \frac{3}{16} (1+\xi)^4 + \frac{(1+\xi)}{8\sqrt{2}} \sqrt{1+(1+\xi)^2} -$$

$$- \frac{(1+\xi)}{4\sqrt{2}} (1+(1+\xi)^2)^{3/2} + \frac{1}{8\sqrt{2}} \ln \frac{1+\xi+\sqrt{1+(1+\xi)^2}}{1+\sqrt{2}}. \quad (6)$$

In region $B > B_0$ with induction change from B_0 to B_m we have

$$W = \frac{B_0^4}{\mu_0^2 \alpha a} F_2(\eta, k), \quad (7)$$

where $k = \frac{\mu_0 \alpha a}{B_0^2}$, $\eta = 1 + \frac{B_m}{B_0}$ - dimensionless parameters, and

$$F_2(\eta, k) = \frac{\eta^4 - (1+4k)^2}{4} - k \frac{\eta^2 - (1+4k)}{2} \frac{\eta(\eta^2 - 2k)^{3/2}}{4} -$$

$$- \frac{k}{4} \left[\eta \sqrt{\eta^2 - 2k} - 2k \ln \frac{\eta + \sqrt{\eta^2 - 2k}}{\sqrt{1+4k} + \sqrt{1+2k}} \right] +$$

$$+ \frac{k}{4} \sqrt{(1+4k)(1+2k)} + \frac{\sqrt{(1+4k)(1+2k)^3}}{4}. \quad (8)$$

As an example were made numerical calculations according to formulas (5)-(8) for three values $2a$ - 250, 20 and 2 μ and for three curves $j_c(B)$, shown in Fig. 1. Curves 1 and 2 correspond to two concrete/specific/actual samples/specimens made from the alloy NbZr. Curve 3 depicts idealized case of dependence $j_c \approx \text{const}$. Curves $j_c(B)$ are selected in such a way that they all would intersect at one point with $B = 4$ T, $j_c = 10^5 \frac{\text{A}}{\text{CM}^2}$, by the being predicted operating point of the superconducting coil electromagnet.

Page 266.

The field of penetration will be greatest for the sample/specimen with the transverse size/dimension of 250μ , prepared from the substance, which corresponds to curve 1, and smallest - for the sample/specimen with the size/dimension of 2μ from the substance, which corresponds to curved 3. Fig. 2 gives dependence B_p on the transverse size/dimension of vein/strand for one of the alloys N8Ti.

When $B_m < B_p$ the losses per unit volume SP depend on B_m by approximately exponential form. Exponent $\sim 3-4$. When $B_m > B_p$ this dependence approaches logarithmic. The results of calculations are given in Fig. 3. Curves 1-1, 1-2 and 1-3 relate to the substance, which corresponds to curve 1 in Fig. 1, curves 2-1, 2-2, and 2-3 - to the substance, which corresponds to curve 2, and 3-1, 3-2 and 3-3 - to the substance, which corresponds to curved 3. On curves of 1-1, 2-1, 3-1 and 1-2 are noted by the small circle of the points, which correspond to the inductions of penetration. For other curves of the induction of penetration do not exceed 0.1 T , and in Fig. 3 they are not noted.

As can be seen from Fig. 3, with large inductions ($B_m > B_p$) the

losses are approximately proportional to the transverse size/dimension of the superconducting vein/strand. With the smaller inductions this law is not retained. Moreover, in certain cases of loss in SP with the larger transverse sizes/dimensions they prove to be smaller than in SP with the smaller transverse sizes/dimensions with identical dependence $j_c(B)$.

The important result of the calculations conducted is the fact that with the induction 4 T, with which all samples/specimens have the identical critical density of current, losses for the different samples/specimens are not identical with one and the same transverse size/dimension. Samples/specimens whose dependence $j_c(B)$ has larger lift with $B \rightarrow 0$, have large losses. This means that by the method of selection SP, which has weak increase j_c with the decrease of induction, it is possible to lower losses in SP magnet, retaining constant/invariable other characteristics of the superconducting coil electromagnet. Given calculations make it possible to interpret the character of the experimental dependences of quality and losses on the amplitude of magnetic induction and on the transverse size/dimension of conductors [5, 6].

Besides the given above calculations, were obtained the expressions for the power of losses in SP taking into account the transport current, flowing throughout the sample/specimen in

question, in regions $B_m < B_p$ and $B_m > B_p$. Integrating these expressions by the cycle time and the volume of SP of the winding in which B_m is a function of coordinates, it is possible to calculate losses in entire volume of the superconductor of any concrete/specific/actual magnet.

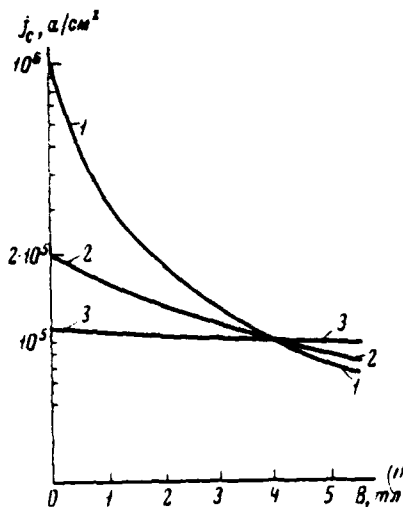


Fig. 1.

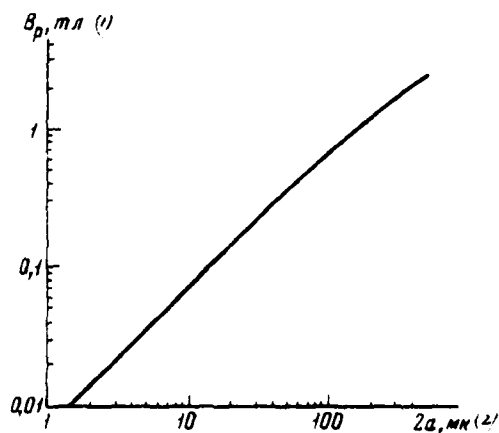


Fig. 2.

Fig. 1. Dependences of density of critical current on magnetic induction for different samples/specimens SP. 1 - $B_0 = 0.44$ T, $\alpha = 4.44 \cdot 10^9$ N/m³; 2 - $B_0 = 4$ T, $\alpha = 8 \cdot 10^9$ N/m³; 3 - $B_0 = 40$ T, $\alpha = 4.4 \cdot 10^{10}$ N/m³.

Key: (1) . T.

Fig. 2. Dependence of induction of penetration B_p on transverse size/dimension of superconducting vein/strand for case $\alpha = 1.2 \cdot 10^{10}$ of N/m³ $B = 2.134$ T.

Key: (1) . T. (2) . μ .

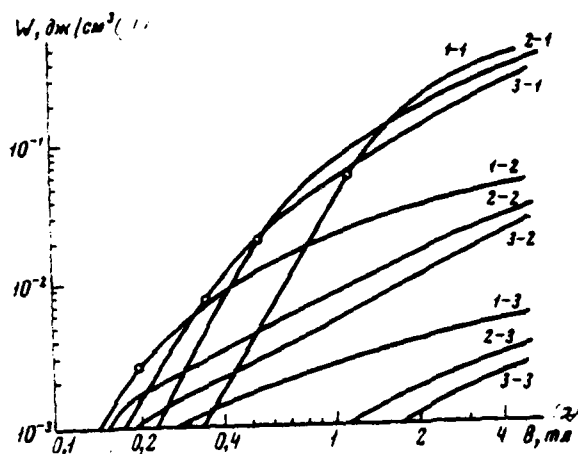


Fig. 3. The dependence of losses per unit volume SP 1 -
 1. 2-1. 3-1 - $a=125 \mu$; 1-2. 2-2. 3-2 - $a=10 \mu$; 1-3. 2-3. 3-3 - $a=1 \mu$.

Key: (1). J/cm^3 . (2). T .

REFERENCES.

1. P.F. Smith, J.D. Lewin. Nucl. Instr. and Methods, 1967, 52, 298.
2. C.P. Bean. Phys. Rev. Letters, 1962, 8, 250.
3. C.P. Bean, M.V. Doyle. J. Appl. Phys., 1962, 33, 3334.
4. Y.B. Kim, C.F. Hempstead, A.R. Strnad. Phys. Rev. Letters, 1962, 9, 306; Phys. Rev., 1963, 129, 528.
5. W.B. Sampson et al. IEEE Trans. on Nucl. Sci., 1969, NS-16, 3, 720.
6. W.B. Sampson et al. Proc. 6th Internat. Conf. High Energy Accelerators, Cambridge, September 1967 (CSETI, Springfield, Va, 1967), p. 393.
7. P.F. Dahl, G.H. Morgan, W.B. Sampson. J. Appl. Phys., 1969, 40, 2083.

Discussion.

P. A. Vodop'yanov. Was conducted the experimental check of results?

L. I. Greben'. Was conducted qualitative testing, agreement is.

P. A. Vodop'yanov. What are differences in your theory from the previously developed theory?

L. I. Greben'. Difference is in the fact that is in detail examined the region of small inductions, and, apparently, new result consists in the fact that with small inductions the thinner sample/specimen can possess large losses.

Page 167.

83. On the development of accelerators to the superhigh energies with the superconducting coil electromagnets.

R. L. Martin.

(Argon laboratory, USA).

The purpose of this work lies in the fact that to note most of from the point of view of the author of the advantage of the superconducting coil electromagnets in application to accelerators to the very high energies, namely, the possibility of maintaining the maximum magnetic field during limited time intervals without the energy consumption. If it would be possible to accelerate sufficiently intense beam, then the realization of prolonged beam (100 s and more) it would make it possible 3-4 times to decrease the porosity in experiments in physics of high energies in comparison with the values, achieved/reached on the contemporary proton accelerators, with all resultant important consequences.

On the basis of the general/common/total idea indicated when selecting of constructing/designing the accelerator, it is possible

to attain considerable savings, in addition to the savings, caused by the essential simplification the technological problems of the use/application of the superconducting coil electromagnets in the accelerative technology, which is expected in the near future. This is possible to achieve, utilizing comparatively slow acceleration mode (for example, by the duration of 10 s) and annular magnet of a large radius with a comparatively weak field, which has iron magnetic circuit and superconducting windings.

The power, necessary for exciting this magnet, will be directly proportional to the rate of the increase of field and to its maximum value for the prescribed/assigned final energy; with the approach indicated both these values can be substantially lowered/reduced. The analogously accelerating rf voltage directly proportional to the rate of the increase of field; with a larger radius of magnet it is possible to utilize a large number of high-frequency stations of smaller power. Parameters of both the systems indicated can be selected taking into account the porosity, not less than 100/o, which leads to the supplementary savings.

At the initial stages of the realization of accelerators with the superconducting coil electromagnets the use of iron for the creation of the basic configuration of the leading magnetic field considerably simplifies many technological problems, connected with

the use/application of the superconducting coil electromagnets for the creation of magnetic fields in the synchrotrons. To most significant from these problems, thus far not yet obtained the checked in practice decision, they relate the setting up of the superconducting coils with the high precision/accuracy, required in the synchrotrons, mechanical strength and stability of the position of coils under the influence of the considerable forces, which appear with the increase of field to of the maximum, the guarantee sufficient cooling, and finally, the possibility to maintain exclusively small allowances for the end sections. During the use of iron as the main factor, which is determining field pattern, the ways of resolution of technological problems are obvious and well known, the necessary field current is minimal, thanks to which significantly lower the forces, which act on the coils, and the necessities for the cooling (which are already small because of a small pulse repetition frequency); at the current density ¹⁰⁻²⁰ ~~12-10~~ kA/cm² the section of the iron core of magnet strongly it decreases in comparison with the magnets of contemporary synchrotrons with the same strength of field. Cooling iron down to the low temperatures facilitates the thermal insulation of coils and are decreased the requirements for the vacuum system, which during the operating mode indicated are very rigid. The totality of these factors makes it possible to obtain a comparatively inexpensive annular magnet, so that its replacement by new magnet with the higher field, which gets up to the agenda in proportion to

the perfection the of superconducting coil electromagnets technique, will not involve exorbitant expenditures/consumptions. Thus, the tendency of the creation of the accelerators, permitting an increase in both energy and intensity as a result of consecutive reconstruction, will be further developed. This idea was advanced in the radiation laboratory of Lawrence, is for the first time realized in the national laboratory of accelerators and it was continued by the Soviet project of the construction of accelerator on 1000 GeV and by the project of the construction of accelerator on 300 GeV in CERN.

Page 268.

The problem of the injection more than of 10^{14} protons for one second is solved. The colleagues of Argonne national laboratory hope to demonstrate in practice the possibility of its economical decision in the near future based on the example to the injection of negative hydrogen ions into the small synchrotron - injector with the high pulse repetition frequency. Successful resolution of this problem would make in practice possible creation of high-energy accelerator with the superconducting coil electromagnets, which works in the mode/conditions, shown in Fig. 1, and with the duration of pulse of more than 100 ns, that gives the accelerated beam intensity than 10^{12} protons per second. It is obvious, are possible some changes in the mode/conditions indicated, ensuring optimum conditions for

experiment.

The author assumes that although an increase in the intensity has the important value with the lower energies for the detailed investigation of the properties of the low-lying resonances and particles of the sufficiently small mass, and also during the study of the completely new regions of nuclear interaction, the decisive role belongs faster not to an increase in the intensity, but to an increase in the energy. The plan/layout of the construction of this machine will provide for the initial period of usual construction, which has as a goal possibly the more rapid achievement of in practice useful high energy, and following of in practice useful high energy, and the subsequent thirty-year period of improvement for the purpose of an increase both energy and intensity of the beam during which the reconstruction of accelerator will be accomplished/realized with the minimum expenditures, comparatively short interruptions in its use for the physical investigations. The program of improvement, calculated for the very prolonged period, can be stopped in any stage in such a case when the fundamental problem of nuclear forces will be finally it is solved. Otherwise the final goal of this direction in the development of accelerative technology completely can be the creation of the second accelerative ring, identical to the first and intersecting with it like the intersecting rings in CERN. Therefore this possibility must be from the very beginning taken into

consideration in the construction/design of accelerator. Initially this second ring will be it serves as the accumulator/storage of particles for main accelerator with the storage time, which amount to, possibly, by 100 s. In this way in neck ring completely it is possible to obtain intensity of 10^{15} protons per pulse. In this stage the second ring would be a precise copy of basis, but it would work in the constant duty at the level of the field of the injection of main accelerator. Subsequently the addition of pulse supply and high-frequency system, and also an increase in the power of cooling would make it possible to convert this ring into the accelerator, identical to the first, and to carry out experiments on clashing beams with the maximum energy intensity than 10^{15} protons in each beam.

It is obvious that the actual advantages and disadvantages in this concept from the point of view both technology and cost/value can be revealed only in the process of detailed study and development of the design of concrete/specific/actual accelerator. This investigation is not yet carried out. Thus far is proposed only the basic idea, which differs from the existing concept in the relation, which from the very beginning is intended to utilize the superconducting coil electromagnets taking into account their advantages, in particular for the promising accelerators on the energy it is more than 1000 GeV. If such accelerators are required for the resolution of the fundamental problems of nuclear forces, they must be constructed and the success of this enterprise can depend on economic factors to the larger degree than from any others.



Fig. 1. Proposed mode of a change in the magnetic field of accelerator with the superconducting coil electromagnets to the very high energies.

Key: (1). s.

Pages 269-273.

No typing.

DATA
FILM

0—